Mathematical modelling and simulation of the transmission, surveillance and control of human pathogens in healthcare settings

David Smith

université
PARIS-SACLAY

Mathematical modelling and simulation of the transmission, surveillance and control of human pathogens in healthcare settings

Modélisation mathématique et simulation de la transmission, la surveillance et le contrôle des agents pathogènes dans les milieux de soins

Thèse de doctorat de l'Université Paris-Saclay

École doctorale n° 570 : santé publique (EDSP)
Spécialité de doctorat : santé publique – biostatistiques
Graduate School : Santé publique
Référent : Université de Versailles-Saint-Quentin-en-Yvelines

Thèse préparée dans l'unité de recherche **CESP** (Université Paris-Saclay, UVSQ, Inserm) sous la direction de **Lulla OPATOWSKI**, professeur des universités, et sous la co-direction de **Laura TEMIME**, professeur des universités

Thèse soutenue à Paris, le 16 décembre 2021, par

David SMITH

Composition du Jury

Laurence MEYER PU-PH, Université Paris-Saclay	Présidente
Ben COOPER PU, University of Oxford	Rapporteur & Examinateur
Jean-Christophe LUCET PU-PH, Université de Paris	Rapporteur & Examinateur
Sonja LEHTINEN PhD, ETH Zürich	Examinatrice
Lulla OPATOWSKI PU, Université Paris-Saclay	Directrice de thèse
Laura TEMIME PU, Conservatoire national des arts et métiers	Co-directrice de thèse

THESE DE DOCTORAT

NNT : 2021UPASR029

université PARIS-SACLAY | ÉCOLE DOCTORALE Santé Publique (EDSP)

Titre : Modélisation mathématique et simulation de la transmission, la surveillance et le contrôle des agents pathogènes dans les milieux de soins

Mots clés : prévention ; infections nosocomiales ; antibiorésistance ; microbiote ; SARS-CoV-2 ; COVID-19

Résumé : Les infections associées aux soins sont le résultat de la dissémination d'une grande diversité de microorganismes pathogènes. Elles représentent un fardeau important de morbidité et de mortalité dans le monde. L'objectif principal de cette thèse était de développer de nouveaux modèles mathématiques afin de mieux comprendre les dynamiques de transmission des pathogènes dans ces milieux spécifiques et de proposer des mesures de contrôle et de surveillance adaptées. Je me suis spécifiquement intéressé aux bactéries résistantes aux antibiotiques et à SARS-CoV-2.
Dans un premier temps, un nouveau cadre de modélisation pour l'épidémiologie des bactéries résistantes aux antibiotiques a été formalisé. Celui-ci prend en compte des mécanismes d'interactions intra-hôtes entre le microbiote humain et des bactéries pathogènes, tel que la résistance à la colonisation et le transfert horizontal des gènes de résistance. La prise en compte de ces interactions permet d'expliquer comment un niveau de consommation intermédiaire d'antibiotiques maximise la sélection et la propagation des bactéries résistantes au niveau populationnel. Ce modèle a ensuite été appliqué à différentes espèces bactériennes pour évaluer l'impact potentiel d'interventions de santé publique sur le risque qui est leur est associé. Les résultats des simulations suggèrent une efficacité des mesures barrières pour prévenir la dissémination de *Staphylococcus aureus* résistant à la méticilline. En revanche, celles-ci se sont avérées inefficaces en ce qui concerne les Entérobactéries multirésistantes.
A l'inverse, les politiques antibiotiques, mais également les interventions ciblant la préservation du microbiote, étaient globalement efficace pour prévenir toutes les espèces pathogènes prises en compte.
Dans un second temps, j'ai analysé les simulations issues d'un modèle individu-centré pour investiguer comment les stratégies de surveillance pouvaient être optimisées afin de détecter et contrôler au mieux des épidémies de SARS-CoV-2 dans les hôpitaux de long séjour. Dans un contexte de pandémie précoce où l'accès aux tests était limité, les résultats ont montré l'intérêt du déploiement du dépistage de groupe, qui s'est avéré être la stratégie la plus efficace pour détecter des épidémies. Dans un contexte de pandémie ultérieur, j'ai montré l'intérêt du déploiement additionnel de stratégies de dépistage par des tests antigéniques et mis en évidence l'importance des délais entre les tests.
Ainsi, par le développement de modèles spécifiques, les travaux de cette thèse ont permis de mieux comprendre l'influence du microbiote sur le risque de transmission nosocomiale des bactéries multirésistantes dans les milieux de soin. Ils ont également permis de proposer des protocoles de surveillance optimisés pour détecter précocement et contrôler la dissémination de SARS-CoV-2 dans les milieux de long séjour dans un contexte de ressources sanitaires limitées.

Title : Mathematical modelling and simulation of the transmission, surveillance and control of human pathogens in healthcare settings

Keywords : nosocomial infection prevention, antibiotic resistance, microbiome, SARS-CoV-2, COVID-19

Abstract : Healthcare-associated infections are caused by a diversity of pathogenic micro-organisms, which together represent leading causes of global infectious disease morbidity and mortality. The objective of this thesis was to develop novel mathematical models to evaluate the transmission dynamics of antibiotic-resistant bacteria and SARS-CoV-2 in healthcare settings, and to provide evidence for the design and optimization of species-specific surveillance and control interventions.
First, a modelling framework for the hospital epidemiology of antibiotic-resistant bacteria was formalized. This framework accounts for within-host mechanisms of ecological interaction between the host microbiome and bacterial pathogens in the context of antibiotic exposure. Microbiome-pathogen interactions, including microbiome-induced colonization resistance and the interspecific horizontal transfer of antibiotic resistance genes, were found to underlie trade-offs in how antibiotics select for the epidemiological spread of resistance. In a simulation study using this framework, contact precautions were effective for prevention of colonization with methicillin-resistant *Staphylococcus aureus* but not multidrug-resistant Enterobacteriaceae, while antibiotic stewardship interventions and microbiome-targeted therapies were broadly effective across species.
Second, simulations from an individual-based SARS-CoV-2 transmission model were used to inform optimization of testing and screening interventions in long-term care facilities. In an early pandemic context, group testing (sample pooling) was the most efficient means to detect emerging outbreaks in resource-limited facilities, while hierarchical testing cascades were most effective given high testing capacity. In a later pandemic context, population screening using rapid antigen diagnostic testing was an effective but time-sensitive means to prevent nosocomial transmission.
Overall, work from this thesis represents a first step in understanding how the microbiome influences nosocomial transmission risk of antibiotic resistance, and provides evidence for optimizing SARS-CoV-2 surveillance in the context of limited and imperfect testing resources.

Maison du doctorat de l'Université Paris-Saclay
2ème étage aile ouest, Ecole normale supérieure Paris-Saclay
4 avenue des Sciences,
91190 Gif sur Yvette, France

Acknowledgments

I sincerely thank the members of my jury for their time and commitment in evaluating this work: Jean-Christophe Lucet and Ben Cooper, Laurence Meyer and Sonja Lehtinen.

I offer special thanks to my thesis supervisors. Lulla, you're a joy to work with. Your open mind and enthusiasm for new ideas inspire me to push further and explore deeper. Laura, you're positive, committed, rigorous; you pay attention to the details. Together, you're a fantastic team, and much more than any PhD student could ever really hope for. Thank you both for taking a chance on me, supporting me through time zones, and for setting positive examples of how to work and how to lead. I'm fortunate to have worked with you these past three years, and grateful for everything you've taught me.

Je tiens à remercier sincèrement William Dab, Didier Guillemot et Pascale Tubert-Bitter pour m'avoir accueilli dans vos laboratoires respectifs et les belles équipes que vous avez établies.

Merci à l'équipe MESuRS pour la bonne compagnie et tous les repas autour de la table familiale : Anne, Armiya, Cynthia, Frédérique, Kévin, Jérôme, Kamel, Karim, Hanaya, Hélène, les Isabelles, Morgane, Mounia, Narimane, Narimene, Oumou, Rania, Sofia, Tom, Yasmine, Hanifa (thank you for the memes), Pearl (for the coffee breaks) and Paul (for the good vibes).

Merci à l'équipe EMAE/B2PHI/PHEMI dans toutes ces itérations : ab-fab Annick, Anne, Bich-Tram, Christian, Elisabeth, Lamia, Marie, Samia, Solen (pour tous les conseils) et Laurence (pour toutes nos discussions et celles à venir). Je remercie Aleksandra, Anabelle, Anna, Antoine, Aurélien, Camille, Épiphane, Fanny, Félix, Florian, George, Hélène, Jeanne, Lara, Lénaig, Marion, Matthieu, Maya, Mehdi, Niels, Salam, Sophie et Wilfried. Et bien sûr je remercie Audrey (sans toi cette thèse n'existerait pas), Eve (pour ta bonne humeur), Mélanie (à très vite sur les pistes), Jonathan (bagarre !) et Lison (pour ne pas avoir dévoilé ma vraie identité… jusqu'à la fin).

Merci aussi à l'orchestre de la Pasteurale pour de bons moments de repas et repos. Merci également à d'anciens pasteuriens, Benedik, Nico, d'autres.

I would also like to thank previous mentors who were instrumental in preparing me for this thesis, in particular Nicole Mideo, Julie Robotham, Timo Smieszek and Koen Pouwels.

Merci aux financeurs de cette thèse (l'Agence national de la recherche et les Instituts de recherche

en santé du Canada, Doctoral Foreign Study Award 164263) et à l'EDSP et l'implication de ses représentants. Je remercie aussi Matthieu Sourdeval et Abigail Cahill pour deux super années d'enseignement de Montigny à Albion.

To friends in Europe, thank you for keeping me going: the dream team, the blue blox squad, Gabriel, Lucas, Sebastian, Mathilde, Paola, Rachael, Jules, Ophé, Clem. Merci à Léa et Nelly d'avoir supporté un coloc en thèse, and to Rébécca, the only diva of Deauville. Thank you to too many people from home, for visiting, keeping in touch, and keeping me updated. I love you all. And thank you of course to Mike.

My dearest thanks are for my family. The worst part about this thesis was doing it so far from you. To Duncan, to Ashley, to Laura. To Nolan and Addison, for all the joy you bring me, little do you know it. To another whose name I'll find out very soon. And to my parents, for everything.

This thesis is dedicated to Gran Joan.

Scientific output

Published and accepted articles

Research articles

- **Smith DRM**, Duval A, Pouwels KB, Guillemot D, Fernandes J, Huynh B-T, Temime L, Opatowski L. Optimizing COVID-19 surveillance in long-term care facilities: a modelling study. *BMC Medicine* **2020**; 18: 386. https://doi.org/10.1186/s12916-020-01866-6
- **Smith DRM**, Temime L, Opatowski L. Microbiome-pathogen interactions drive epidemiological dynamics of antibiotic resistance: a modelling study applied to nosocomial pathogen control. *eLife* **2021**; 10: e68764. https://doi.org/10.7554/eLife.68764
- **Smith DRM**, Duval A, Zahar J-R, the EMAE-MESuRS working group on SARS-CoV-2 modelling, Opatowski L, Temime L. Rapid antigen testing as a reactive response to surges in nosocomial SARS-CoV-2 outbreak risk. *Nature Communications* **[In press]**.

Commentaries and short reports

- Temime L, Gustin M-P, Duval A, Buetti N, Crepey P, Guilemot D, Thiébaut R, Vanhems P, Zahar J-R, **Smith DRM**, Opatowski L. A conceptual discussion about the basic reproduction number of severe acute respiratory syndrome coronavirus 2 in healthcare settings. *Clinical Infectious Diseases* **2021**; 72(1): 141-3. https://doi.org/10.1093/cid/ciaa682
- **Smith DRM**, Opatowski L. COVID-19 containment measures and incidence of invasive bacterial disease. *The Lancet Digital Health* **2021**; 3(6): e331-2. doi: https://doi.org/10.1016/S2589-7500(21)00085-6

Conference proceedings

- Duval A, **Smith DRM**, Guillemot D, Opatowski L, Temime L. CTCmodeler: An Agent-Based Framework to Simulate Pathogen Transmission Along an Inter-individual Contact Network in a Hospital. *International Conference on Computational Science* **2019**, 477-87. https://doi.org/10.1007/978-3-030-22741-8_34

Articles outside this thesis

- **Smith DRM**, Pouwels KB, Hopkins S, Naylor NR, Smieszek T, Robotham JV. Epidemiology and health-economic burden of urinary catheter-associated infection in English NHS hospitals: a probabilistic modelling study. *Journal of Hospital Infection* **2019**; 103(1): 44-54. https://doi.org/10.1016/j.jhin.2019.04.010
- Bouziri H, **Smith DRM**, Descatha A, Dab W, Jean K. Working from home in the time of covid-19: how to best preserve occupational health? *Occupational and Environmental Medicine* **2020**; 77(7): 509-10. http://dx.doi.org/10.1136/oemed-2020-106599
- Duchemin T, Bastard J, Ante-Testard PA, Assab R, Daouda OS, Duval A, Garsi J-P, Lounissi R, Nekkab N, Neynard H, **Smith DRM**, Dab W, Jean K, Temime L, Hocine MN. Monitoring sick leave data for early detection of influenza outbreaks. *BMC Infectious Diseases* **2021**; 21: 52. https://doi.org/10.1186/s12879-020-05754-5

Articles under revision

Articles outside this thesis

- Roselló A, Barnard RC, **Smith DRM**, Evans S, Grimm F, Davies NG, Deeny SR, Knight GM, Edmunds J. Impact of non-pharmaceutical interventions on SARS-CoV-2 outbreaks in English care homes: a modelling study. (Pre-print: https://www.medrxiv.org/content/10.1101/2021.05.17.21257315v1)

Articles submitted to pre-print servers

- **Smith DRM**, Duval A, Zarah J-R, Opatowski L, Temime L. Bringing COVID-19 home for Christmas: a need for enhanced testing in healthcare institutions after the holidays. *medRxiv* 2020. https://doi.org/10.1101/2020.12.18.20248460

Scientific conferences

Oral presentations

- Multispecies interactions as drivers of antimicrobial resistance dynamics. *Spread of Pathogens in Healthcare Institutions and Networks: a Modeling Conference* **June 2019**. Paris, France.
- Mass rapid diagnostic testing as a public health response to SARS-CoV-2 outbreaks in long-term are settings. *International Conference on Prevention & Infection Control* **September 2021**. Geneva, Switzerland.
- Microbiome-pathogen interactions drive epidemiological dynamics of antibiotic resistance: modelling insights for infection control. *Epidemics 8.* **December 2021**, Bologna, Italy.

Posters

- Multispecies interactions as drivers of antimicrobial resistance dynamics. *Mathematical models in Ecology & Evolution*. **July 2019**. Lyon, France.
- Multispecies interactions as drivers of antimicrobial resistance dynamics: a mathematical modelling study. *Epidemics 7*. **December 2019**. Charleston, USA.
- Mass rapid diagnostic testing as a public health response to SARS-CoV-2 outbreaks in long-term care settings. *Epidemics 8*. **December 2021**. Bologna, Italy.

Seminars and workshops

- Microbiome ecology and the epidemiology of antibiotic resistance: a mathematical model for antibiotic stewardship. *Journée Scientifique du Centre de recherche en Epidémiologie et Santé des Populations (Inserm)*. **November 2020**. Paris, France.
- Microbiome ecology and the epidemiology of antibiotic resistance: a mathematical model for antibiotic use and stewardship. *Microbial Diversity Workshop (Institut Pasteur)*. **February 2021**. Paris, France.
- Testing strategies for controlling SARS-CoV-2 spread in healthcare settings. *Modelling of Infectious Diseases Course (Institut Pasteur; Conservatoire national des arts et métiers)*. **May 2021**. Paris, France.

Table of Contents

List of figures

List of tables

List of abbreviations

- Ag-RDT: antigen rapid diagnostic test
- ARB: antibiotic-resistant bacteria
- BSI: bloodstream infection
- CDC: Centers for Disease Control and Prevention [United States of America]
- COVID-19: coronavirus disease 2019
- CP-KP: carbapenemase-producing *Klebsiella pneumoniae*
- CPI: close-proximity interaction
- ECDC: European Centre for Disease Control
- ECONI: Evaluation of Cost of Nosocomial Infection study
- ESBL: extended-spectrum beta-lactamase
- ESBL-EC: ESBL-producing *Escherichia coli*
- EU: European Union
- FNR: false-negative rate
- FPR: false-positive rate
- GI: gastrointestinal infection
- HCAI: healthcare-associated infection
- HCW: healthcare worker
- IBM: individual-based model
- IER: incremental efficiency ratio
- IPC: infection prevention and control
- LTCF: long-term care facility
- MDR: multidrug-resistant
- MRSA: methicillin-resistant *Staphylococcus aureus*
- ODE: ordinary differential equation
- PPE: personal protective equipment
- RTI: respiratory tract infection
- SARS-CoV-2: severe acute respiratory syndrome coronavirus 2
- SC: Susceptible-Colonized
- SIR: Susceptible-Infectious-Recovered
- SEIR: Susceptible-Exposed-Infectious-Recovered
- SSI: surgical site infection
- R_0: basic reproduction number
- RFID: radio-frequency identification device
- RT-PCR: reverse transcriptase-polymerase chain reaction
- TNR: true-negative rate
- TPR: true-positive rate
- UK: United Kingdom
- USA: United States of America
- UTI: urinary tract infection
- VRE: vancomycin-resistant Enterococci
- WHO: World Health Organization

Résumé en français

Les infections associées aux soins (IAS) font parties des événements indésirables les plus fréquents chez les patients hospitalisés et les résidents des établissements de soins de longue durée. Elles posent également un risque de santé au travail grave pour les soignants. Les IAS représentent un coût important de morbidité et de mortalité dans le monde avec un impact significatif sur les parcours de soins des patients. Elles entraînent des durées de séjour plus longues et font peser ainsi un lourd fardeau économique sur les individus, les établissements de soins et la société dans son ensemble. Bien que fréquentes, elles sont souvent évitables et constituent en cela une priorité de recherche et d'actions dans le cadre de la prévention des maladies infectieuses au niveau mondial. Malgré des progrès significatifs réalisés au cours des dernières décennies dans le contrôle des infections nosocomiales, de nouveaux défis de santé publique subsistent et apparaissent. Deux enjeux majeurs liés aux IAS se distinguent : la dissémination mondiale de bactéries multirésistantes aux antibiotiques et l'émergence soudaine de nouveaux agents pathogènes ayant une forte capacité de diffusion nosocomiale tel le SARS-CoV-2.

La modélisation mathématique est un outil puissant pour mieux comprendre l'épidémiologie des IAS et guider les interventions de santé publique visant à les contrôler. Cependant, ces nouveaux défis épidémiologiques nécessitent de nouvelles approches de modélisation. Une des limites à la compréhension de la diffusion de la résistance aux antibiotiques est la méconnaissance des principes clés de l'éco-évolution, notamment la compétition au sein de l'hôte entre les agents pathogènes bactériens et le microbiote. Dans le cas d'un virus émergent comme le SARS-CoV-2, ses caractéristiques épidémiologiques uniques, l'incertitude qui peut leur être associée au début d'une épidémie et les difficultés de détection et de surveillance dans les milieux de soin, posent des défis fondamentaux quant à la détection et le contrôle des épidémies nosocomiales.

Ce travail de thèse avait trois objectifs principaux : mieux comprendre les dynamiques de transmission et de risque épidémique de différentes espèces pathogènes, optimiser la surveillance des épidémies nosocomiales dans un contexte de ressources de dépistage limitées et enfin proposer des mesures de contrôles adaptées au mieux à différentes IAS et scénarios épidémiologiques. De nouveaux modèles mathématiques ont été développés afin de répondre à ces objectifs à travers deux axes de recherche principaux. Dans le premier, j'ai exploré d'une part les effets simultanés de l'écologie du microbiote et de

l'utilisation des antibiotiques sur la propagation des bactéries multirésistantes aux antibiotiques (BMR) et, d'autre part, leur influence sur l'efficacité des interventions de contrôle des IAS en milieu hospitalier. Dans le second axe de recherche, j'ai exploré la contribution des mesures de surveillance et d'isolement sur le contrôle et la propagation nosocomiale du SARS-CoV-2 dans les établissements de soins de longue durée.

A travers le premier axe de recherche, présenté dans le chapitre 4, j'ai développé un nouveau cadre de modélisation mathématique pour formaliser les dynamiques de colonisation des BMR. Ce cadre, basé sur des systèmes d'équations différentielles ordinaires, s'appuie sur l'incorporation progressive dans un modèle épidémiologique d'une gamme d'interactions écologiques ayant lieu au sein de l'hôte. Ces dernières incluent la compétition entre les souches d'une même espèces (sensibles et résistantes aux antibiotiques), la compétition inter-espèces entre le microbiote et les espèces pathogènes, ainsi que le transfert horizontal des gènes de résistance aux antibiotiques. Dans ce modèle, je prends également en compte la contribution de la dysbiose du microbiote sur la dynamique épidémiologique des BMR en milieu hospitalier, formalisant simultanément l'impact des antibiotiques sur la colonisation par des agents pathogènes et sur la stabilité du microbiote.

Par le biais d'une analyse numérique d'agents pathogènes théoriques, j'ai montré que deux mécanismes écologiques différents peuvent expliquer la sélection de la résistance par la consommation des antibiotiques : premièrement la compétition entre deux souches d'une même espèce de bactérie pathogène et deuxièmement la compétition entre cette espèce et le microbiote dans son ensemble. De manière intéressante, j'ai montré que ces mécanismes de compétition ont des conséquences distinctes pour différents indicateurs épidémiologiques. Alors que la compétition des souches tend à augmenter la proportion des souches résistantes aux antibiotiques dans la population, la compétition entre une BMR et le microbiote tend à augmenter l'incidence et la prévalence de colonisation aux BMR. Lorsque les antibiotiques provoquent à la fois une dysbiose et éliminent les souches sensibles, ils sélectionnent plus fortement la propagation de la résistance. Ces analyses révèlent également trois *trade-offs* distincts de sélection au-delà desquels l'exposition intermédiaire aux antibiotiques maximise la propagation des BMR. Dans l'ensemble, ce cadre théorique constitue une première étape clé dans la compréhension des impacts hétérogènes du microbiote de l'hôte sur la dissémination de la résistance aux antibiotiques dans les établissements de soins.

Dans le chapitre 5, ce cadre de modélisation a été appliqué à différentes espèces bactériennes afin d'évaluer les interactions écologiques intra-hôte en jeu et la manière dont celles-ci peuvent déterminer l'efficacité des interventions de santé publique visant à contrôler leur dissémination. Quatre des agents pathogènes nosocomiaux les plus fréquemment observés en milieu de soin à l'échelle mondiale ont été étudiés : *Clostridioides difficile*, *Staphylococcus aureus* résistant à la méthicilline (SARM), *Escherichia coli* producteur de BLSE (BLSE-CE) et *Klebsiella pneumoniae* producteur de carbapénémase (CP-KP). Pour chacune de ces BMR, les données disponibles dans la littérature scientifique ont été utilisées pour paramétrer un modèle spécifique. De plus, une procédure formelle de *expert elicitation (consultation d'experts)* a été réalisée : des entretiens avec des experts en microbiologie clinique et l'épidémiologie de l'antibiorésistance ont été menés pour qualifier et quantifier le rôle de la dysbiose sur l'épidémiologie des différentes espèces de BMR, et pour quantifier les coefficients d'interaction avec une échelle d'incertitude.

Une série d'interventions de santé publique a ensuite été implémentée et simulée pour évaluer leur impact respectif sur les dynamiques épidémiologiques des différentes espèces pathogènes, en fonction de leur contexte écologique spécifique. Les interventions évaluées étaient : les mesures barrières (*contact precautions*), les politiques antibiotiques (*antibiotic stewardship*) et la thérapie de guérison du microbiote (*microbiome recovery therapy*). Dans l'ensemble, les résultats suggèrent que les mesures barrières sont efficaces pour la prévention du SARM mais ont un impact limité contre les espèces entériques considérées. De plus, les interventions favorisant un équilibre du microbiote (les politiques antibiotiques et la thérapie de guérison du microbiote) étaient globalement efficace pour prévenir de la colonisation par toutes les espèces, avec un effet particulier pour *C. difficile* et les Entérobactéries. Dans l'ensemble, les résultats de ce premier axe de recherche permettent de mieux comprendre la propagation de la résistance aux antibiotiques dans les milieux de soin et l'influence des caractéristiques écologiques intra-hôtes spécifiques aux différentes espèces bactériennes et du microbiote sur l'efficacité des interventions de santé publique.

Dans le deuxième axe de recherche de cette thèse, j'ai investigué des stratégies de surveillance pour détecter et contrôler au mieux des épidémies de SARS-CoV-2, notamment dans le cadre d'hôpitaux de long séjour. A partir de simulations issues d'un

modèle individu-centré de transmission nosocomiale de SARS-CoV-2, j'ai développé un algorithme de calcul pour simuler une variété d'interventions de surveillance. Ces interventions incluent le dépistage systématique des personnes symptomatiques (qui était effectivement mise en place dans ces milieux pendant toute la première phase de l'épidémie), de dépistage de groupe (dit les tests poolés), et le dépistage systématique de toutes les personnes dans l'établissement. J'ai évalué l'efficacité de ces différentes stratégies selon différents scénarios épidémiologiques, notamment plusieurs scénarios d'introductions du virus dans l'hôpital (ponctuel ou régulier, via des soignants ou des patients) ainsi que différents niveaux de risque sanitaire (en fonction des mesures mises en place). Ce travail a été mené en deux parties distinctes.

Premièrement, dans le chapitre 7, des épidémies ont été simulées dans un contexte de pandémie précoce sans aucune mesure de contrôle de COVID-19 en place. Dans ce cas, l'efficacité des stratégies de dépistage ont été évaluées afin de comparer leur capacité à détecter des épidémies émergentes dans un contexte de disponibilité restreinte de test de réaction en chaîne par polymérase à transcription inverse (RT-PCR). Le dépistage de groupe s'avérait être la stratégie la plus efficace et la plus efficiente lorsque les tests disponibles étaient peu nombreux (<1 test/100 lits/jour), tandis que les cascades de tests, qui attribuaient les tests en fonction d'une échelle de priorité liés à des indications cliniques, étaient les plus efficaces lorsque la capacité en tests était élevée dans l'hôpital (>10 tests/100 lits/jour).

Deuxièmement, dans le chapitre 8, les épidémies ont été simulées dans ce même hôpital mais dans un contexte de pandémie ultérieure, en supposant qu'une gamme de mesures de contrôle de COVID-19 est déjà en place (distanciation sociale, port obligatoire de masque, vaccination). À l'aide d'une analyse contrefactuelle, le dépistage de la population à l'aide des tests antigéniques a été évalué pour sa capacité à prévenir la transmission de SARS-CoV-2 à la suite d'une soudaine augmentation de risque épidémique dans l'établissement (par exemple lié à un risque accru en communauté, un retour de vacances ou un retour de fêtes). J'ai montré qu'avec deux cycles de dépistage antigénique programmés, jusqu'à 75 % des infections nosocomiales pourraient être évitées, contre 64 % avec un seul cycle de dépistage, ou 47 % dans le cas de tests RT-PCR de routine. Un délai de 4 à 5 jours entre le premier et le deuxième tour de dépistage s'avérait optimal pour la prévention de la transmission, en raison de la nature variable dans le temps de la sensibilité du test. Le risque sous-jacent d'épidémie était le principal facteur du coût-

efficacité du dépistage. Ce facteur était plus important qu'au moment du dépistage (immédiat ou différé), le type de test (antigénique ou RT-PCR) ou sa cible (patients ou soignants). En effet, selon la gamme de mesures de prévention de COVID-19 déjà en place, les bénéfices médio-économiques du dépistage antigénique différaient par un à deux ordres de grandeurs (établissement vulnérable aux épidémies : >10 infections évitées/1 000 tests antigéniques utilisés ; établissement résilient aux épidémies : <1 infection évitée/1 000 tests antigéniques). Ces résultats suggèrent que les tests antigéniques à eux seuls seraient insuffisants pour éliminer le risque d'épidémie nosocomiale de SARS-CoV-2, mais que leur utilisation constitue néanmoins un élément utile et efficace dans le cadre des stratégies multimodales de prévention des infections. En revanche, l'intérêt médico-économique de dépister à grande échelle une population hospitalière déjà bien protégée contre des épidémies s'avère discutable.

En conclusion, à travers cette thèse, je me suis servi de diverses approches de modélisation mathématique pour étudier la transmission, la surveillance et le contrôle des agents pathogènes dans les milieux de soins. J'ai développé un nouveau cadre de modélisation combinant la dynamique populationnelle et des spécificités écologiques intra-hôtes pour mieux comprendre la manière dont les bactéries résistantes aux antibiotiques se propagent dans les hôpitaux. De plus, j'ai utilisé un modèle individu-centré détaillé pour simuler la dynamique de transmission de SARS-CoV-2 dans les établissements de soins de longue durée. Les deux modèles ont été appliqués à l'évaluation des interventions de surveillance et de contrôle. Cela a permis de mieux comprendre l'écologie au sein de l'hôte et ses conséquences sur l'efficacité des interventions, menant ainsi à proposer des pistes d'améliorations pour les optimiser. Ces résultats pourraient avoir une application directe en termes de programmes de contrôle des infections hospitalières. Ce travail souligne également l'utilité de la modélisation mathématique pour comprendre l'étiologie mécaniste des infections nosocomiales. Ces connaissances permettent d'éclairer les décisions de santé publique face aux menaces infectieuses, qu'elles soient bactériennes ou virales, résistantes ou non aux médicaments, anciennes ou nouvellement découvertes.

Introduction

Healthcare-associated infections (HCAIs) are leading causes of infectious morbidity and mortality, sources of significant economic burden, and pressing health security concerns. HCAI control is a global health priority, and is the focus of extensive public health campaigns from the World Health Organization (WHO) and other national and international health agencies. However, the multiplicity of these infections complexifies their epidemiology and control. Indeed, HCAI is an umbrella term encompassing a wide range of diseases, caused by a diversity of ecologically distinct micro-organisms, which differentially affect the heterogeneous populations that populate the planet's varied healthcare institutions. The greatest infectious threats facing healthcare settings today range from longstanding nosocomial pathogens that have been the focus of decades of prevention efforts (e.g. *Clostridioides difficile*), to increasingly antibiotic-resistant strains of common bacterial symbionts (e.g. carbapenemase-producing Enterobacteriaceae), to emerging zoonotic threats with pandemic potential (e.g. novel coronaviruses like SARS-CoV-2). In order to prevent HCAIs caused by such distinct pathogens, it is necessary to understand the precise intersection between the ecological characteristics of each underlying pathogen species, the pathophysiology of the disease(s) they cause, their epidemiology in the populations concerned, and the mechanistic impacts of potential control interventions.

Over recent decades, mathematical modelling has emerged as a powerful tool for the evaluation of public health measures for HCAI control. In describing the fundamental mechanisms of pathogen spread in healthcare settings, models can simulate the health and economic impacts of surveillance and control interventions, and inform optimization of strategies for infection prevention. This is particularly useful when the collection of empirical data is impractical, unethical or simply not possible. Recent advances in microbiology and surveillance have helped to provide clearer pictures of which organisms cause which infections, how they transmit, and with what consequences for human health. This has helped to improve the characterization of different nosocomial pathogens, allowing for the development of more representative models that better describe HCAI epidemiology. However, new modelling approaches are needed to respond to new and evolving public health threats, their distinct epidemiological characteristics, and the specific public health interventions that are available to control them.

The main goal of this thesis is to develop novel mathematical models for the nosocomial epidemiology of multidrug-resistant bacteria and SARS-CoV-2, in order to better understand how these pathogens spread in healthcare facilities, and to evaluate the efficacy and efficiency of surveillance and control measures. First, in Chapter 1 I provide a general overview of HCAI epidemiology and control, and in Chapter 2 I present a methodological summary of mathematical modelling as applied to infectious disease epidemiology. In Chapter 3 I define the specific research objectives of this thesis. In Chapter 4 I develop a novel transmission modelling framework describing the epidemiology of antibiotic-resistant bacteria in the context of within-host interactions with the microbiome, and in Chapter 5 I apply this framework to evaluate impacts of the microbiome on the efficacy of public health interventions for different pathogen species. In Chapter 6 I introduce the COVID-19 pandemic and its impacts on healthcare settings and HCAI, and apply an existing individual-based pathogen transmission model to SARS-CoV-2. In Chapters 7 and 8 I use this model to evaluate the efficacy and efficiency of surveillance and control interventions for SARS-CoV-2 outbreak detection and infection prevention in long-term care settings. Finally, in Chapter 9 I discuss the scientific contributions made by this thesis, and perspectives for future study.

Chapter 1. Healthcare-associated infections and their control

A healthcare-associated infection (HCAI) is any infection acquired in a healthcare facility, including hospitals, long-term care facilities (LTCFs), outpatient clinics, or any other clinical settings. HCAIs are among the most frequent adverse events experienced by hospital patients and LTCF residents, and are an important occupational hazard for healthcare workers.(Allegranzi et al., 2017; Institute of Medicine (US) Committee on Quality of Health Care in America, 2000; World Health Organization, 2011) HCAIs contribute significantly to the global burden of infectious morbidity and mortality, and are a source of great psychological stress for victims and their loved ones alike. They complicate care pathways, result in longer lengths of stay in healthcare facilities, and place great economic burden on individuals, healthcare institutions, and society as a whole.(Marchetti and Rossiter, 2013; Stewart et al., 2021c) Though common, they are often preventable, and are an important focus of global investment in infectious disease research and prevention.(Bates et al., 2009) However, despite significant progress in HCAI control over the last several decades, new challenges continue to arise, from the shifting epidemiology of HCAI in aging populations, to the global dissemination of antimicrobial resistance, to the sudden emergence of novel nosocomial pathogens.

In this Chapter, I first introduce the burden of HCAIs on a global scale. I proceed to describe the epidemiology of the principal types of HCAI and their risk factors, and provide a comprehensive overview of the diversity of human pathogens that cause them. I then introduce the unique public health challenge of antimicrobial resistance, including key ecological and evolutionary considerations. Finally, I provide a summary of contemporary public health interventions that are used to mitigate and prevent HCAIs.

1.1. Global burden

The burden imposed by healthcare-associated infection (HCAI) is a public health concern of global significance. In 2011, WHO published a systematic review and meta-analysis quantifying the global public health burden of HCAI. The definition of HCAI that they propose, which is used throughout this thesis, is:

> *An infection occurring in a patient during the process of care in a hospital or other healthcare facility which was not present or incubating at the time of admission. This includes infections acquired in the hospital, but appearing after discharge, and also occupational infections among staff of the facility.*(World Health Organization, 2011, 2002)

This definition has largely replaced traditional, narrower definitions of hospital-onset or nosocomial infection, which have been limited only to hospitals, only to patients, and only to infections both acquired and presenting during a single hospitalization event, which may account for as few as half of HCAIs.(Stewart et al., 2021b)

Here I distinguish between two types of HCAI burden: health burden and economic burden.

1.1.1. Health burden

The health burden of HCAI describes their negative impact on the health and wellbeing of individuals who experience infection. A range of international estimates of HCAI health burden are reported here using three classic epidemiological indicators: (i) HCAI **prevalence**, the proportion of a population infected at a given point in time, (ii) HCAI **incidence**, the rate of infection acquisition in a population, and (iii) HCAI **mortality**, the rate of death due to infection.

1.1.1.1. HCAI prevalence

Synthesizing data from 131 studies published between 1995 and 2010 across 23 high-income countries, WHO estimated that 1 in every 14 hospital patients will experience HCAI at some point during their hospital stay.(World Health Organization, 2011) Mean pooled HCAI prevalence was 7.6%, ranging from 3.6% in Germany to 12% in New Zealand. Estimated HCAI burden was even greater in low- and middle-income countries, although data were less reliable: across 276 studies, 1 in every 10 patients was estimated to acquire HCAI; and when only including studies of high methodological quality, this

increased to 1 in 6 patients. Mean pooled prevalence was 10.1%, ranging from 5.4% in Mongolia to 19.1% in Albania.

According to recent point-prevalence surveys, global HCAI burden appears to have remained relatively stable since the WHO report. In an ECDC point prevalence survey from acute care hospitals in Europe in 2016/17, pooled HCAI prevalence was 5.4—7.8% (among 310,000 patients in 1,209 hospitals across 28 countries); while in LTCFs, prevalence was 2.4—6.0% (among 117,000 residents in 2,221 LTCFs across 23 countries).(Suetens et al., 2018) Country-level hospital HCAI prevalence from the ECDC survey is presented in **Figure 1.1**. In a point prevalence survey from the USA in 2015, hospital HCAI prevalence was just 2.9—3.5% (among 12,299 patients in 199 hospitals across 10 states), a significant reduction from a previous survey in 2011.(Magill et al., 2018) Other recent estimates of hospital HCAI prevalence at the national level include: 3.7% in China in 2014/15,(Y. Chen et al., 2017) 7.4% in Japan in 2018,(Komagamine et al., 2019) 7.9% in Canada in 2017,(Mitchell et al., 2019) 8.2% in Ghana in 2016,(Labi et al., 2019) 8.4% in Pakistan in 2017/18,(Saleem et al., 2019) 9.9% in Australia in 2018,(Russo et al., 2019) 11.9% in Singapore in 2015/16,(Cai et al., 2017) and 12.3% in 2016 across a pooled sample from Brazil, Venezuela, Mexico and Colombia.(Huerta-Gutiérrez et al., 2019) Recent systematic reviews have further estimated 9.0% in Southeast Asia,(Ling et al., 2015) and 17.0% in Ethiopia.(Alemu et al., 2020)

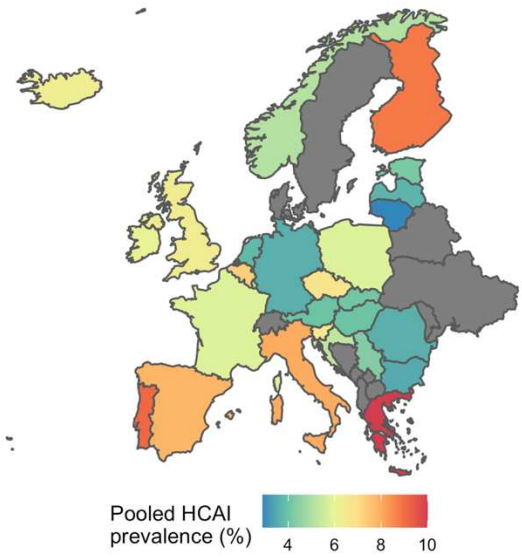

Figure 1.1. HCAI prevalence in Europe.

Pooled HCAI prevalence (the proportion of patients with at least one HCAI) in acute care hospitals in Europe in 2016/17, rendered for this thesis using ECDC point prevalence survey data.(Suetens et al., 2018) Data were unavailable for countries shaded in grey. Data from England are used for the United Kingdom.

1.1.1.2. HCAI incidence

Point prevalence surveys provide useful estimates of HCAI burden, but prospective longitudinal surveillance data are needed for robust estimation of HCAI incidence. Although methodologies like the Rhame & Sudderth method are widely used to calculate incidence from point prevalence data,(Rhame and Sudderth, 1981) validation studies suggest that such estimates are flawed: considerations like post-discharge onset and heterogeneous population- and individual-level risk factors make it difficult to reliably predict relationships between these distinct epidemiological indicators.(Gastmeier et al., 2001; Meijs et al., 2017) Further, longitudinal studies more reliably account for pathogens with seasonal or outbreak dynamics – as opposed to endemic pathogens with a stable background rate of infection – and can help to disentangle location of infection onset, and epidemiological risk factors associated with HCAI acquisition. Although comparatively rare due to time, cost and logistical considerations, some such studies do exist.

In the Evaluation of Cost of Nosocomial Infection (ECONI) study, a prospective one-year study from two Scottish hospitals beginning in April 2018, Stewart et al. reported 250 HCAIs per 100,000 acute occupied bed-days; in a full 1,000 bed hospital, this translates to approximately 2.5 new HCAIs per day.(Stewart et al., 2021b) Importantly, they identified trends not observable in point prevalence, including strong seasonality in HCAI – with highest rates in summer months, except for a peak in gastrointestinal HCAI in winter months – and a median 9-day length of stay until infection onset. Other HCAI incidence rates from prospective longitudinal studies include 1.1% from a four-year study in a hospital in China,(Han et al., 2021) approximately 5/1,000 patient-days over 2.5 years in a hospital in North Carolina,(Sickbert-Bennett et al., 2016) and 28/1,000 patient-days – an order of magnitude greater than the Scottish estimates – from a five-month study in a hospital in Ethiopia.(Ali et al., 2018)

1.1.1.3. HCAI mortality

Reliable estimates of HCAI mortality are notoriously difficult to ascertain. Infected individuals usually have comorbidities, and in hospital settings are generally already seeking care for other acute health problems or emergencies.(Allegranzi et al., 2017) HCAIs are also seldom reported as the primary cause of mortality on hospital records and death certificates.(Allegranzi et al., 2017) Nonetheless, using national surveillance data from 2002, Klevens et al. estimated that HCAIs result in an annual 99,000 deaths in USA hospitals.(Klevens et al., 2007) Relative to mortality rates reported by USA CDC in 2019,

this ranks HCAI as the seventh leading cause of death in the USA, following Alzheimer's disease but ahead of diabetes, and the leading cause of infectious mortality.(Kochanek et al., 2020)

In a report from ECDC from 2008, HCAIs were directly attributed to 37,000 deaths per year across EU member states, while contributing indirectly to an additional 110,000 deaths.(European Centre for Disease Prevention and Control, 2008) These figures contrast with findings from Cassini et al. from 2016, who estimated that HCAIs result in 90,000 deaths in Europe each year.(Cassini et al., 2016) Combined with estimates for HCAI-induced morbidity, this represents approximately 2.5 million disability-adjusted life-years annually due to HCAI, greater than the estimated health burden of all other infectious diseases combined (among the 32 included in the 2009-2013 Burden of Communicable Diseases in Europe study).(Kretzschmar et al., 2012; Mangen et al., 2013)

1.1.2. Economic burden

The economic burden of HCAI describes the financial costs that infection imposes on society. There are few reliable national estimates of the health-economic burden of HCAIs, and estimates across studies are rarely comparable due to different methodologies and cost definitions. In USA hospitals in 2013, Marchetti & Rossiter estimated annual societal costs of $96—$147 billion USD due to HCAI,(Marchetti and Rossiter, 2013) while in UK hospitals in 2021, Manoukian et al. estimated £0.3—£2.2 billion GBP in total health-economic burden.(Manoukian et al., 2021b) In both studies, cost estimates were further stratified into direct vs. indirect costs.

1.1.2.1. Direct costs

Direct health-economic costs are the ensemble of medical costs due to resource use that is completely attributable to a particular illness.(Kirch, 2008a) Excess direct costs associated with HCAI primarily result from extended inpatient length of hospitalization, often expressed as excess bed-days.(Manoukian et al., 2021b) However, HCAI-related direct costs result not only from initial hospitalization but also HCAI-related post-discharge healthcare use, including follow-up consultation at primary care providers, and readmission to hospital or other healthcare facilities. In the UK in 2018/19, direct costs in the 90 days post-discharge have been estimated at £1,004—£4,244 GBP per HCAI, increasing total cost by approximately 36%.(Manoukian et al., 2021a) Other than standard bed-day costs, HCAI-associated direct costs also include consumables like antimicrobial

agents, medical devices, and laboratory testing.(Manoukian et al., 2021b) More severe HCAIs contribute more to cost burden, particularly for patients treated in intensive care units (ICUs).

In a report from ECDC in 2008, direct hospital costs of HCAI in Europe were estimated at €7 billion/year,(European Centre for Disease Prevention and Control, 2008) while in a USA CDC report from 2009, direct costs were estimated to range from $28—$45 billion USD. Later, in 2013, Marchetti & Rossiter estimated that direct costs account for one-third to one-half of the health-economic burden of HCAI at $34.3—$74 billion USD, and that 72% of these are incurred during initial hospitalization.(Marchetti and Rossiter, 2013) Finally, in the UK in 2021, direct costs accounted for 55.5%—72.0% of total estimated health-economic burden, at £0.2—£1.2 billion GBP.(Manoukian et al., 2021b)

1.1.2.2. Indirect costs

Indirect health-economic costs are the combined value of lost economic output (e.g. due to impairment or disability to work) due to a disease or disorder, and can vary widely depending on the perspective taken.(Kirch, 2008b) In contrast to direct costs, for which costing or claims data are sometimes available, indirect costs are often more difficult to quantify. In the study by Marchetti & Rossiter, accounting only for lost wages due to incapacitation or premature death, annual indirect costs of HCAIs were estimated at $61.6—$72.6 billion USD. In Manoukian et al., indirect costs were defined as capital and overhead costs, and were estimated at an annual £0.1—£1 billion GBP. Overall, difficulty and inconsistency in quantifying the health and economic burden of HCAI relative to other diseases likely owes at least in part to its immense epidemiological heterogeneity.

1.2. Types of HCAI

HCAIs are traditionally grouped by the body system hosting the infection. Here I provide a brief overview of the epidemiology of the five principal types of HCAI and their principal risk factors. **Figure 1.2** depicts the mean hospital and LTCF prevalence of leading HCAI from the previously introduced ECDC point prevalence survey, and **Figure 1.3** shows a summary of risk factors for each infection as estimated from the ECONI study. Risk factors unique to each infection are highlighted below; other risk factors common across all or most HCAIs include older age, longer length of stay, emergency admission, socioeconomic deprivation and comorbidity (cancer, chronic renal failure, cardiovascular disease, diabetes).

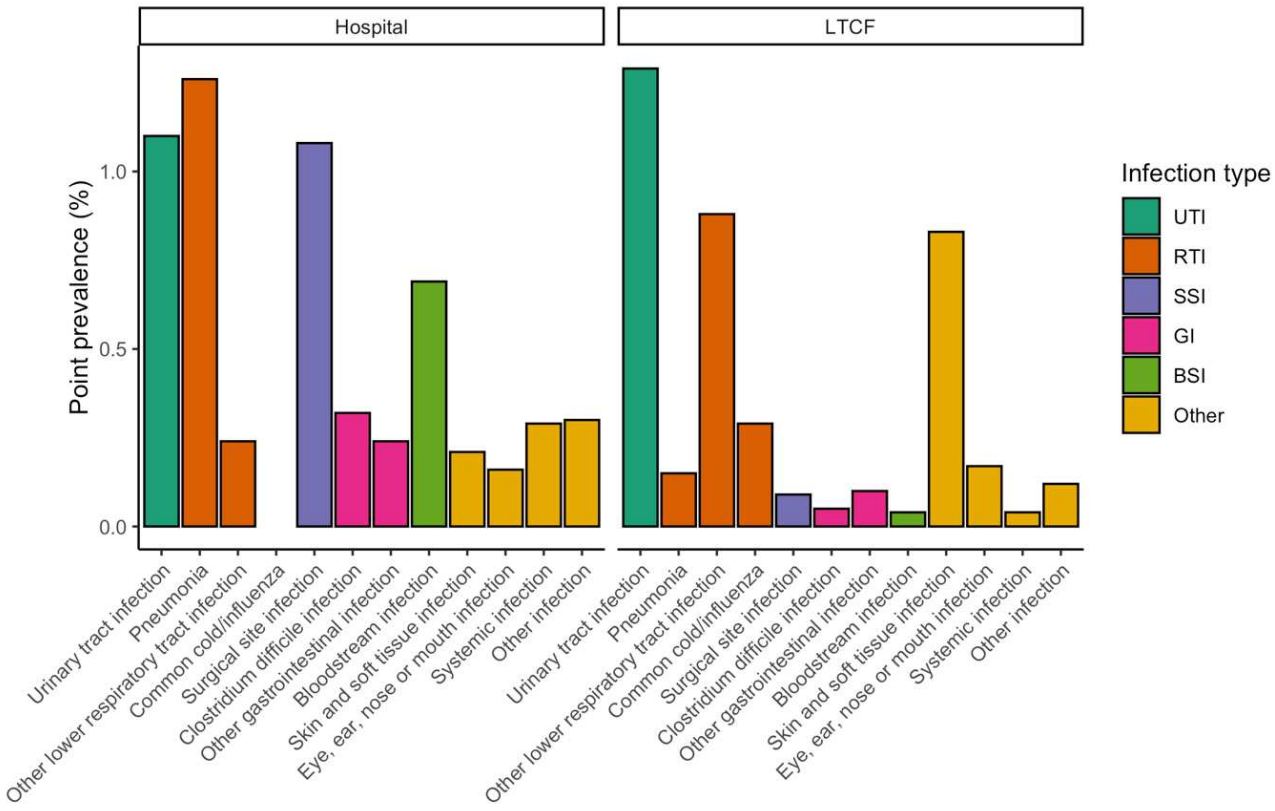

Figure 1.2. HCAI prevalence in Europe by type of infection.

Point prevalence of different types of HCAI, comparing acute care hospitals (left, % of patients infected) and LTCFs (right, % of residents infected). Prevalence estimates are pooled across all European countries contributing data to the 2016/17 ECDC point prevalence survey (rendered for this thesis using extracted data).(Suetens et al., 2018)

1.2.1. Urinary tract infection (UTI)

1.2.1.1. Epidemiology

Reports from WHO suggest that UTI is the most common nosocomial infection

worldwide.(World Health Organization, 2011, 2002) UTIs are predominantly caused by bacteria and some fungi, and a review of international studies estimated that two-thirds had endogenous origin (infection resulting from one's own microflora).(Iacovelli et al., 2014) In Europe, UTI was estimated to account for 18.9% of active HCAIs in hospitals and 32.0% in LTCFs, representing a combined annual 2.2 million infections.(Suetens et al., 2018)

1.2.1.2. Risk factors

Urinary catheterisation is the most important risk factor for nosocomial UTI, with 61.5% of UTIs observed to be catheter-associated in US hospitals.(Magill et al., 2018) Similarly, in Europe, 59.5% of patients with UTIs had a catheter inserted within 7 days of infection onset.(Suetens et al., 2018) In a recent modelling study, I quantified the health and economic burden of catheter-associated UTI in English hospitals.(Smith et al., 2019) Although women and girls are overall at greater risk of UTI, catheter-associated UTI is most prevalent – and most burdensome – in elderly men.(Iacovelli et al., 2014; Smith et al., 2019)

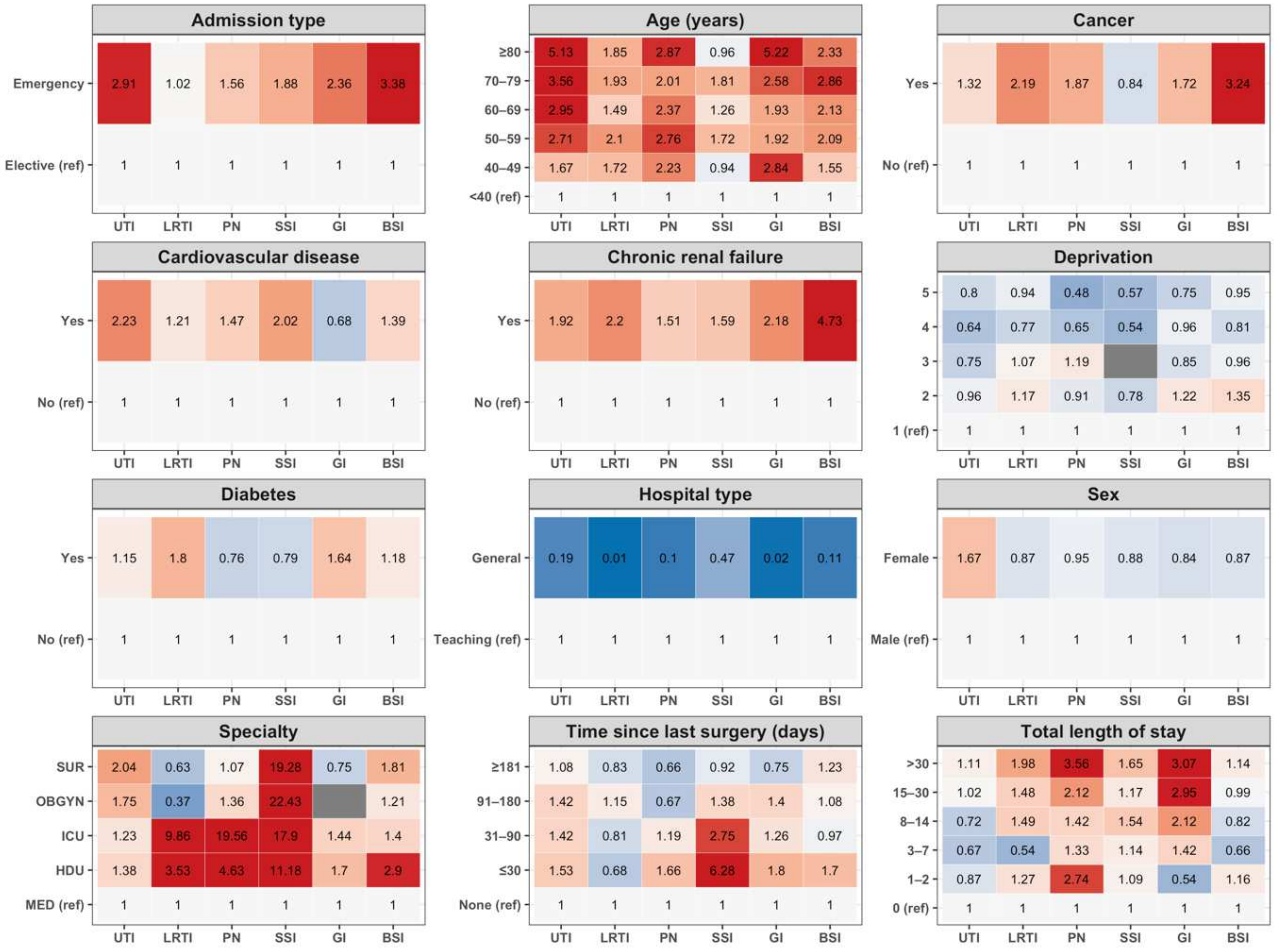

Figure 1.3. HCAI risk factors.

Adjusted risk ratios for hospital HCAI acquisition across a range of patient and care variables (panels). Figure was rendered for this thesis using data extracted from the ECONI study.(Stewart et al., 2021a) Estimates are based on a multivariate model including all variables. Note that LRTI and pneumonia (PN) are considered separately. Socioeconomic deprivation score ranges from 1 (most deprived) to 5 (least deprived). SUR=surgery, OGBYN=obstetrics and gynecology, ICU=intensive care unit, HDU=high-dependency unit, MED=medicine.

1.2.2. Respiratory tract infection (RTI)

1.2.2.1. Epidemiology

RTI is one of the most common HCAIs,(World Health Organization, 2011, 2002) and the most common infection acquired in ICUs and LTCFs.(Suetens et al., 2018; Vincent et al., 2009) In Europe, LRTIs (including pneumonia) accounted for 25.7% of active HCAIs in both hospitals and LTCFs, translating, like UTI, to approximately 2.2 million infections annually.(Suetens et al., 2018) RTIs are caused by a broad range of viruses, bacteria and fungi. However, robust RTI burden estimates are difficult to ascertain due to the wide range of infections classified as RTIs, high rates of non-symptomatic or pauci-symptomatic infection, and the intrinsic seasonality and epidemicity of a wide range of respiratory pathogens.(Manchal et al., 2020) Nonetheless, the morbidity and mortality imposed by

LRTIs alone may exceed all other HCAIs: in a modelling study, Cassini et al. estimated that pneumonia causes greater health burden than any other major HCAI when accounting for both years of life lost and years lived with disability.(Cassini et al., 2016)

1.2.2.2. Risk factors

The greatest risk factor for nosocomial LRTI is mechanical ventilation. In hospitals in the USA, 35.5% of hospital pneumonia cases were ventilator-associated,(Magill et al., 2018) and an estimated 10-40% of patients undergoing ventilation will develop ventilator-associated pneumonia within 48 hours of intubation.(Zaragoza et al., 2020) Likely owing to their typically mild nature, URTIs and their risk factors are comparatively understudied and poorly described in the literature.

1.2.3. Surgical site infection (SSI)

1.2.3.1. Epidemiology

WHO reports SSI as the second leading cause of HCAI in the USA, after UTI, and the third leading cause in Europe, after UTI and RTI.(World Health Organization, 2011) European data suggest that hospital SSI prevalence (18.3% of HCAIs) is similar to UTI (18.9%), but that SSI results in substantially fewer annual infections (520,000 vs. 870,000), explained by particularly long lengths of stay among patients with SSI.(Suetens et al., 2018) SSIs are often caused by endogenous microflora, and in particular bacteria and fungi residing on the skin, although contamination from nosocomial pathogens is also common.(Owens and Stoessel, 2008)

1.2.3.2. Risk factors

A surgery patient's probability of developing SSI varies widely from 0.5 to 15%, depending on the type of operation and their underlying pre-operative health.(World Health Organization, 2002) The principal risk factor across any operation is its duration, which scales with both the duration of potential contamination of the sterile site and the operation's complexity.(Cheadle, 2006; Lawson et al., 2013; Leong et al., 2006) A range of scoring systems for SSI risk have been developed, which all account for surgery duration and whether the operation is classified as dirty or contaminated.(Leong et al., 2006)

1.2.4. Gastrointestinal infection (GI)

1.2.4.1. Epidemiology

GI is caused by a diverse array of pathogens, including viruses, bacteria, protozoa and helminths, but the majority of GIs are self-limiting viral infections that last from 1 to 3 days.(Elliott, 2007; Payne et al., 2013) Healthcare-associated GI has historically garnered less attention than other HCAIs, largely overlooked by previous WHO reports on HCAI burden and prevention,(World Health Organization, 2011, 2002) and excluded from national nosocomial infection surveillance systems.(Spackova et al., 2010) However, increasing research focus and surveillance effort have been accorded to nosocomial GI in recent years.(Lopman et al., 2004; Wikswo et al., 2015)

In European hospitals, 8.9% of active HCAIs were GIs, corresponding to approximately 330,000 infections per year.(Suetens et al., 2018) By contrast, GI was estimated to be comparatively rare in long-term care settings, accounting for just 2.9% of HCAIs (164,000 annual infections). Yet, over eight years of surveillance in England and Wales, 27% of infectious gastroenteritis outbreaks occurred in hospitals and 28% in residential care facilities (primarily nursing homes);(Meakins et al., 2003) and over five years of surveillance data in the USA, just 4% of GI outbreaks occurred in hospitals versus 70% in LTCFs.(Wikswo et al., 2015) These conflicting data may to a certain extent reflect real differences in country-specific and time-varying GI epidemiology. They may also reflect incomplete data, inconsistent GI surveillance systems, and poor representativeness of point-prevalence data for seasonal infections causing sporadic outbreaks.

1.2.4.2. Risk factors

Overall GI risk is greater in older patients with longer hospital stays (**Figure 1.3**), although GI in the community is traditionally associated with children. In a retrospective analysis of medical records in the USA, approximately 9% of hospitalizations in children aged 1-4 were associated with gastroenteritis, compared to just 1.5% for adults.(Gangarosa et al., 1992) However, risks of severe disease and death were primarily borne by the elderly: the hospital gastroenteritis case-fatality rate was 3% for those over 80, but just 0.05% for those under five.

1.2.5. Bloodstream infection (BSI)

1.2.5.1. Epidemiology

In European hospitals, an estimated 10.8% of HCAIs are bloodstream infections, accounting for 375,000 infections annually. However, variation in case definitions, reporting standards, estimation methodologies and study populations has made BSI surveillance notoriously challenging.(Lin et al., 2010; Viscoli, 2016) In a review of population-based studies in North America and Europe, approximately 20-30% of BSIs were estimated to be hospital-acquired,(Goto and Al-Hasan, 2013) while LTCF-acquired BSI is comparatively rare.(Mylotte, 2005; Suetens et al., 2018) BSI has the highest case-fatality rate of any HCAI, estimated across a range of settings and methodologies at 12-32%, with substantially higher rates for nosocomial relative to community-onset infection.(Goto and Al-Hasan, 2013; Kontula et al., 2018; Lenz et al., 2012; Rodríguez-Baño et al., 2010; Søgaard et al., 2011) BSI was the 11th leading cause of death in the USA in 2019,(Centers for Disease Control and Prevention, n.d.) and has been estimated in a European modelling study to cause the greatest loss of life of any major HCAI.(Cassini et al., 2016) Epidemiological characteristics vary significantly across different pathogens,(Ani et al., 2015; Kontula et al., 2018; Wisplinghoff et al., 2004) and, as with many HCAIs, BSIs most often result from opportunistic infection caused by a patient's own endogenous flora.(Bennett MD et al., 2014)

1.2.5.2. Risk factors

Central venous and peripheral venous catheterization are the most important risk factors for nosocomial BSI.(Bassetti et al., 2016) Excluding infections with missing data, 39.6% of BSIs in European point prevalence were primary BSIs associated with vascular catheterization, 22.6% were non-catheter-associated primary BSIs, and 37.9% were secondary.(Suetens et al., 2018) The most common precursor infection for secondary BSI was UTI (29.3% of secondary BSIs), followed by GI (18.7%) and SSI (16.4%). In USA point prevalence, 73.1% of primary BSIs were central venous catheter-associated, and no secondary BSIs were reported.(Magill et al., 2018) This latter finding is consistent with the widely held belief that secondary BSI is under-reported, with diagnostic codes for primary, but not secondary infection often being the only ones entered into electronic medical records.(Goto and Al-Hasan, 2013) Further, BSI may go unnoticed as a cause of death in patients comorbid with terminal conditions like end-stage liver or kidney disease.

1.3. Nosocomial pathogens

HCAIs are principally caused by three distinct types of pathogen: bacteria, viruses and fungi. Here I introduce the most important nosocomial pathogens belonging to each of these groups, and comment on their ecology, transmission characteristics and epidemiology. There are no globally representative data describing exactly which pathogens cause which HCAIs, and their epidemiology varies through space and time, but a range of recent national and regional estimates are available. Some of the most comprehensive data come from the previously introduced ECONI study, which followed all patients across two Scottish hospitals and their combined 1,473 beds over a 12-month period.(Stewart et al., 2021b) The causative pathogen was microbiologically confirmed in 96.6% of 1,083 HCAIs, across a panel of 118 distinct species or taxonomic groups. These data are primarily used below to characterize HCAI aetiology, and are summarized in **Table 1.1**. Where relevant, comparisons are also made in the text to point prevalence surveys from the USA in 2015 (427 HCAIs, 70.3% microbiologically confirmed) and from ECDC in 2016/17 (19,626 HCAIs, 52.6% microbiologically confirmed).(Magill et al., 2018; Suetens et al., 2018) Further, geographical distributions of common pathogens are visualized in **Figures 1.4 – 1.5** using ECDC data from 2011/12. Although together these represent a substantial and relatively up-to-date sample, these estimates should nonetheless be interpreted as specific to particular high-income, Occidental contexts.

1.3.1. Bacteria

Bacteria are the leading cause of nosocomial infection, estimated in the ECONI study to account for 76.7% of HCAIs. Bacteria are ubiquitous, single-celled, prokaryotic microorganisms that reproduce asexually through binary fission. Estimates of the number of bacterial species on Earth range from approximately 1 million to over 1 billion,(Dykhuizen, 2005; Louca et al., 2019) but just 538 species have been identified as human pathogens, distributed across over 60 families.(Woolhouse et al., 2005) Bacteria are composed of an external peptidoglycan cell wall, a phospholipid membrane, and a cytoplasm typically containing a single DNA chromosome, and only in some species membrane-bound organelles.

In clinical settings, bacteria are classified based on how their cell walls react to Gram staining: Gram-positive bacteria have thicker cell walls with many layers of peptidoglycan that bind crystal violet stain, and are often capable of forming hardy, dormant structures

called endospores; while Gram-negative bacteria have a comparably thin cell wall, but a unique outer membrane that helps to protect them from external threats. Bacteria are further grouped according to their shape: most are spherical (coccus) or rod-shaped (bacillus), although some are spiral (spirillum), filamentous, box-shaped, and beyond. Bacteria are also widely classified according to their degree of resistance to common antibiotic agents, but this is introduced in the following section 1.4 of this Chapter.

Table 1.1. Leading pathogens causing different HCAIs.

Summary of findings from the ECONI study, a prospective longitudinal observational study reporting the microbiological causes of 96.6% of HCAIs in two Scottish hospitals in 2018/19. (Stewart et al., 2021b) RTI combines LRTI and pneumonia. Other *Enterococcus* spp. excludes *E. faecium* and *E. faecalis*. *Klebsiella* spp. combines *K. pneumoniae* and other *Klebsiella* species. *Candida* spp. combines *C. albicans* and other *Candida* species. Gram-negative cocci are excluded as individual species were not available. Table was compiled for this thesis using data extracted from Stewart et al.

HCAI			Pathogen		
	HCAI (%)	**Leading species (% of given HCAI)**		**Species (% of all HCAIs)**	**HCAI (top 5 rank)**
1.	**RTI (22.5%)**	Influenza (15.0%) *Staphylococcus aureus* (8.4%) *Candida* spp. (8.4%) *Escherichia. coli* (7.1%) *Klebsiella* spp. (7.1%)	**1.**	***Escherichia coli* (18.4%)**	BSI (1st) UTI (1st) SSI (3rd) RTI (4th) GI (5th)
2.	**UTI (21.9%)**	*Escherichia coli* (48.7%) *Klebsiella spp.* (9.4%) *Proteus mirabilis* (9.4%) Other *Enterococcus* spp. (9.0%) *Candida* spp. (7.3)	**2.**	***Staphylococcus aureus* (10.8%)**	SSI (1st) Other (1st) BSI (2nd) RTI (2nd)
3.	**BSI (18.7%)**	*Escherichia coli* (26.6%) *Staphylococcus aureus* (14.8%) *Klebsiella* spp. (9.8%) *Enterococcus faecalis* (8.6%) *Enterococcus faecium* (7.8%)	**3.**	***Klebsiella* spp. (6.9%)**	UTI (2nd) BSI (3rd) SSI (5th) RTI (5th)
4.	**GI (16.9%)**	Norovirus (39.8%) *Clostridioides difficile* (18.9%) *Enterococcus faecium* (8.2%) Coagulase-negative staphylococci (5.1%) *Escherichia coli* (5.1%)	**4.**	**Coagulase-negative staphylococci (6.3%)**	SSI (2nd) Other (2nd) GI (4th)
5.	**SSI (13.8%)**	*Staphylococcus aureus* (22.5%) Coagulase-negative staphylococci (15.7%) *Escherichia coli* (11.0%) *Enterococcus faecalis* (10.2%) *Klebsiella* spp. (6,4%)	**5.**	***Candida* spp. (6.0%)**	RTI (3rd) Other (3rd) UTI (5th)
6.	**Other (6.4%)**	*Staphylococcus aureus* (30.6%) Coagulase-negative staphylococci (22.6%) *Candida* spp. (11.3%) *Streptococcus* spp. (4.8%) *Enterococcus faecalis* (4.8%)	**6.**	**Norovirus (5.9%)**	GI (1st)

1.3.1.1. Gram-negative bacilli

Gram-negative bacilli are the primary causes of nosocomial infection, responsible for over one-third of all HCAIs (37.3% in ECONI) and approximately half of bacterial HCAIs (48.6%). Gram-negative bacilli cause all types of infections, including approximately three-quarters of UTIs (75.2%), half of BSIs (51.2%), and one-third of SSIs (31.4%). The

microbial ecology of HCAI-causing Gram-negative bacilli and their propensities for nosocomial transmission vary significantly from species to species. However, the most common threats belong to the family Enterobacteriaceae, which principally colonize the digestive tract as commensal symbionts, only relatively rarely causing opportunistic infection.

1.3.1.1.1. Escherichia coli

Among all species, *Escherichia coli* is the single leading cause of nosocomial infection in Europe (**Figure 1.4**). It has been estimated to account for 18.4% of HCAIs in Scotland, 16.1% across Europe, and 14.7% in the USA.(Magill et al., 2018; Stewart et al., 2021b; Suetens et al., 2018) The ECONI study reports it as the cause of approximately half of UTIs (48.7%) and one quarter of BSIs (26.6%), and an important cause of all other types of infection. Despite its high burden, the nosocomial transmissibility of *E. coli* is believed to be relatively low.(Duval et al., 2019a; Gurieva et al., 2018) *E. coli* is simply one of the most abundant Gram-negative bacteria of the human gut, and a key cause of infection is translocation from the colon to sterile sites like the urinary tract, for instance during urinary catheterization.(Garmendia et al., 2005; Jacobsen et al., 2008) However, not all *E. coli* strains are alike. While so-called extra-intestinal pathogenic *E. coli* strains are benign in the gut and only cause infection when translocated elsewhere, a distinct collection of other, rarer strains – including enteropathogenic, enterotoxigenic, enterohaemorrhagic, enteroaggregative and enteroinvasive *E. coli* – are highly virulent digestive pathogens, and important causes of potentially fatal GI associated with foodborne outbreaks.(Chen and Frankel, 2005; Yang et al., 2017)

1.3.1.1.2. Klebsiella *species*

After *E. coli*, *Klebsiella* spp. are the most common HCAI-causing Gram-negative bacilli, and the third overall cause of bacterial HCAI (**Figure 1.4**). *Klebsiella pneumoniae* is the leading species of concern, and high-risk epidemic clones – including a range of sequence types (STs) like ST11, ST442 and ST258 – have disseminated globally since the early 2000s.(Mathers et al., 2015; Pitout et al., 2015) *Klebsiella* spp. appear to spread more readily than other Enterobacteriaceae through inter-individual contact,(Duval et al., 2019a) and have been associated with large nosocomial outbreaks.(Hoenigl et al., 2012; Mollers et al., 2017; Shao et al., 2020; Sui et al., 2018) In Europe, acquisition of *Klebsiella* spp. and other Enterobacteriaceae has also been closely associated with international travel, highlighting difficulty in containing nosocomial introductions of gut-residing Gram-negative

bacilli in a globalized world.(Karampatakis et al., 2016; Ruppé et al., 2015)

1.3.1.1.3. Other Gram-negative bacilli

Other high-impact Gram-negative bacilli include *Proteus mirabilis* (2.7% of HCAIs), *Pseudomonas* spp. (2.1%), *Serratia marcescens* (1.7%), *Acinetobacter* spp. (0.4%) and other Enterobacterales (2.6%), including important pathogens like *Enterobacter* spp. and *Citrobacter* spp (**Figure 1.4**). Each of these has unique ecological characteristics that drive its nosocomial infection dynamics. For one example, *Pseudomonas* spp. are known to establish persistent colonies in sinks, pipes and drains, creating environmental reservoirs for spread in closed healthcare environments.(Ayliffe et al., 1974) For another, *Proteus* spp. are known for their adaptability and resilience across a wide range of hosts and environments, providing myriad sources for potential nosocomial introduction: *Proteus* spp. colonize the human digestive tract; are abundant in both domestic animals and livestock; have been isolated from wild animals ranging from mammals, birds and reptiles, to oysters, sandflies and cockroaches; and are found free-living across terrestrial, marine and freshwater environments.(Drzewiecka, 2016)

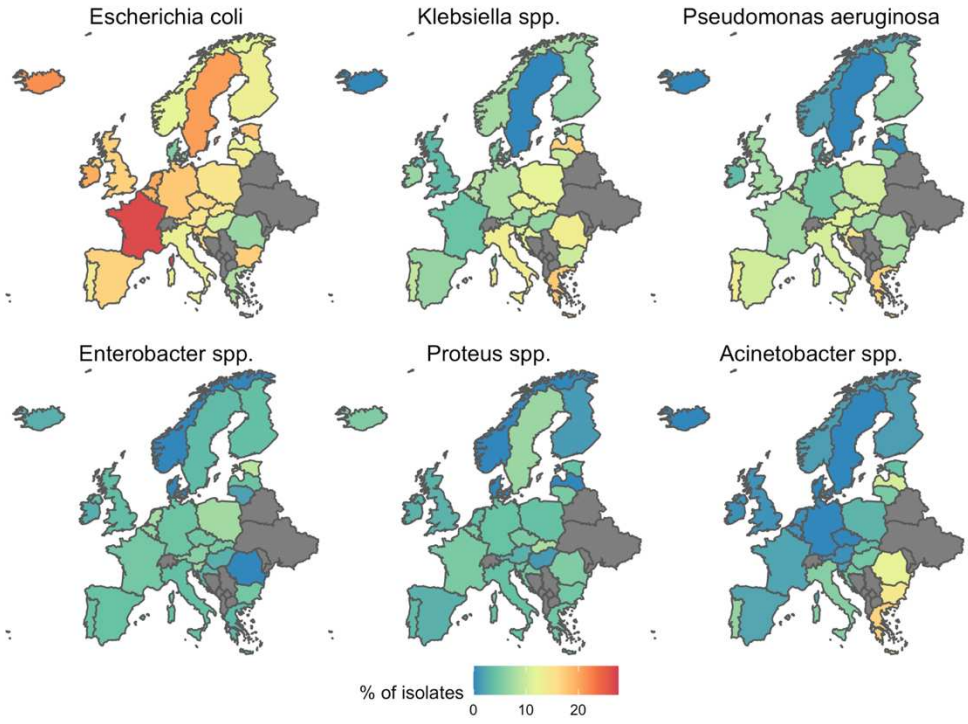

Figure 1.4. Gram-negative bacilli prevalence in Europe.

Gram-negative bacilli as a percentage of all HCAI isolates per country. Figure was rendered for this thesis using data extracted from ECDC surveillance from 2011/12.(Suetens et al., 2013) Data were unavailable for countries shaded in grey. Data from England are used for the United Kingdom.

1.3.1.2. Gram-positive cocci

Gram-positive cocci cause approximately one-third of HCAIs (32.1% in Stewart et al.) and an estimated 41.8% of bacterial HCAIs. Although they cause all types of infections, they are most strongly associated with SSI (56.4%), BSI (45.5%) and a large share of infections classified as other (66.1%), including skin, soft tissue, bone and joint infections. There are two main genera responsible for over 90% of HCAIs caused by Gram-positive cocci: *Staphylococcus* and *Enterococcus*.

1.3.1.2.1. Staphylococci

The characteristic nosocomial pathogen *Staphylococcus aureus* is the second-leading HCAI-causing species after *E. coli* (**Figure 1.5**). *S. aureus* is the principal cause of SSI (22.5%), the second-leading cause of BSI (14.8%), and a key driver of other HCAIs (30.7%). Unlike Gram-negative bacilli, the principal ecological niche of staphylococci is the skin, and *S. aureus* spreads readily on hands, medical equipment and textiles. Healthcare workers are key vectors for spread in hospital and long-term care settings, and have been estimated to have a 5.4% risk of acquiring *S. aureus* carriage on their gloves or gowns after contacting a colonized patient in a general hospital ward,(Nadimpalli et al., 2020) and 16.2% in the ICU setting,(O'Hara et al., 2019) with longer and more intimate types of contact increasing carriage risk. Beyond *S. aureus*, coagulase-negative staphylococci are also important causes of HCAI (6.3%) (**Figure 1.5**). This group includes a diverse range of nosocomial pathogens, like *S. epidermidis* and *S. haemolyticus*, both important causes of neonatal HCAI and infections linked to indwelling medical devices, and *S. saprophyticus*, a common cause of acute urethritis.(Becker et al., 2014)

1.3.1.2.2. Enterococci

Among *Enterococcus* spp., which altogether cause about 11.8% of HCAIs, two species predominate: *E. faecalis* and *E. faecium*. Enterococci are particularly associated with SSI, BSI, UTI and GI; their principal niche being the digestive tract, they have an outsized impact on GI relative to other Gram-positive cocci. Nosocomial infection by *E. faecium* is in particular associated with a subpopulation of globally disseminated clones that are rarely found in the community, and which have acquired a range of genetic elements favouring adaptation to healthcare settings.(Guzman Prieto et al., 2016) By contrast, HCAI-causing strains of *E. faecalis* are widely found in the community and animal reservoirs.(Guzman Prieto et al., 2016)

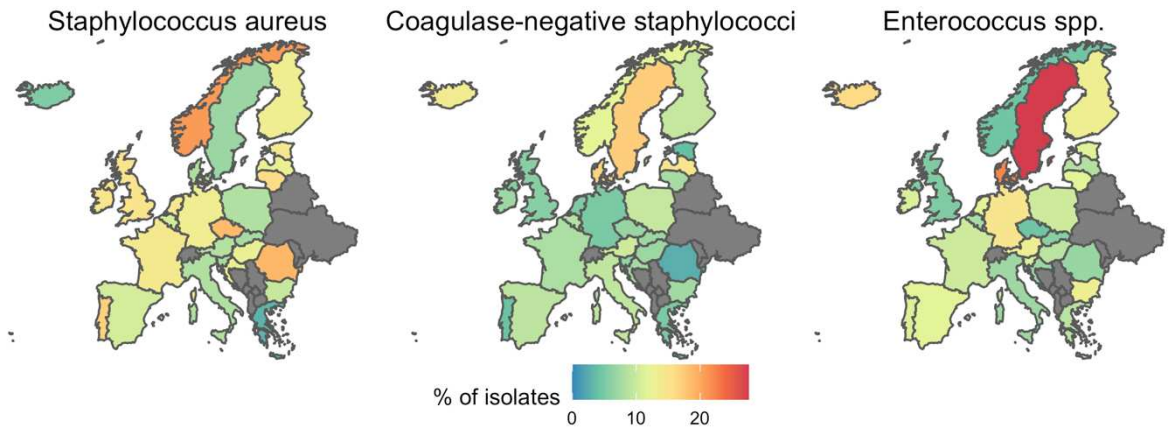

Figure 1.5. Gram-positive cocci prevalence in Europe.

Gram-positive cocci as a percentage of all HCAI isolates per country. Figure was rendered for this thesis using data extracted from ECDC surveillance from 2011/12.(Suetens et al., 2013) Data were unavailable for countries shaded in grey. Data from England are used for the United Kingdom.

1.3.1.3. Gram-positive bacilli

Relatively few nosocomial pathogens are Gram-positive bacilli. The most common is *Clostridioides difficile* (73.2% of HCAI-causing Gram-positive bacilli in Stewart et al.), a characteristic hospital pathogen and leading cause of nosocomial diarrheal disease. Pathogenic *C. difficile* strains produce a range of toxins, including enterotoxin and cytotoxin, and can cause life-threatening pseudomembranous colitis, colonic perforation and death.(Martin et al., 2016) Estimates of *C. difficile* burden – and hence Gram-positive bacilli burden – vary substantially across studies. *C. difficile* accounted for 2.8% of HCAIs and 18.9% of nosocomial GIs in the ECONI study, but 7.3% of HCAIs and 68.4% of GIs in ECDC point prevalence. By contrast, in USA point prevalence, *C. difficile* was the single leading cause of nosocomial infection, responsible for 15.5% of HCAIs and 72.5% of GIs. *C. difficile* surveillance is complicated by an important share of asymptomatic carriers, and only a minority of hospital infections are estimated to result from nosocomial transmission.(Baron et al., 2019; Martin et al., 2016) However, regardless of where acquisition occurs, nosocomial colonization and infection are strongly associated with disturbances to the intestinal microbiome, whether through antibiotic exposure, co-infection with other gastrointestinal pathogens, use of enemas or stool softeners, or other diarrheal events.(VanInsberghe et al., 2020)

1.3.1.4. Gram-negataive cocci and other bacteria

Gram-negative cocci are rare causes of HCAI, estimated to account for 3.4% of HCAIs in the ECONI study and just 0.3% in ECDC point prevalence. Although a range of pathogenic Gram-negative cocci of the genus *Neisseria* are common in the community, including *N.*

meningitidis and *N. gonorrhoeae*, these only rarely cause nosocomial infection.(Elias et al., 2006) Other bacterial pathogens that do not fit neatly into the above categories also cause nosocomial infection. These include, but are not limited to: (i) *Haemophilus influenzae*, a coccobacillary bacteria and relatively common cause of nosocomial RTI outbreaks;(Barreiro et al., 1995) (ii) *Legionella* spp., pleomorphic flagellated bacteria, which, although incapable of person-to-person transmission, trigger nosocomial outbreaks when disseminated by air conditioners, cooling towers and other contaminated water supplies in healthcare environments;(Roig et al., 2003) and (iii) *Mycobacterium tuberculosis*, a complex of respiratory bacilli impervious to Gram-staining, which represent common nosocomial pathogens, and leading causes of infectious mortality in low- and middle-income countries.(Collins and Blumberg, 2020; Genestet et al., 2020; Pai et al., 2006)

1.3.2. Viruses

Viruses are the second leading cause of nosocomial infection after bacteria, estimated in the ECONI study to account for 15.3% of HCAIs.(Stewart et al., 2021b) Viruses are submicroscopic infectious agents that lack even a rudimentary cellular structure. Each individual virus particle (virion) is composed simply of its *genetic material*, the strands of DNA or RNA that encode viral proteins, and a *capsid*, a protein coat that surrounds and protects its genetic material. Some viruses also have an *envelope*, an outer phospholipid layer.

Viruses are not free-living, and can only reproduce by entering a susceptible host cell and manipulating its metabolism to transcribe and replicate viral genes, assemble viral proteins, and ultimately propagate new virions. Human viruses are broadly classified by the structure of their genetic material: DNA viruses generally replicate within the cell nucleus, and RNA viruses in the cytoplasm. Although considered by only some scientists to be forms of life, viruses nonetheless reproduce and evolve through natural selection. Their taxonomy is particularly complex owing to unclear origins in the evolutionary history of life, but viruses can be grouped into distinct species, of which 219 have been identified as human pathogens.(Woolhouse et al., 2012)

1.3.2.1. Norovirus

Stewart et al. reported norovirus (*Norwalk virus*) as the leading cause of viral HCAI, accounting for one-third of viral HCAIs and 5.9% of all HCAIs. Norovirus is a principal

cause of acute gastroenteritis worldwide, particularly among children,(Koopmans, 2008) and accounts for an estimated 40.0% of nosocomial GIs. Spread through environmental or alimentary contamination, or through direct contact with infectious vomit or faeces, norovirus is highly infectious and transmits particularly easily in closed healthcare facility settings, sometimes as a result of asymptomatic carriage.(Greig and Lee, 2012; Sukhrie et al., 2012) Its infectious dose is also particularly low, highlighting the importance of hand hygiene and environmental decontamination in limiting norovirus spread.(Atmar et al., 2014)

1.3.2.2. Influenza

Influenza is the second leading cause of viral HCAI (3.0% of all HCAIs), the most common cause of healthcare-associated LRTI (15.0%), and an important cause of healthcare-associated pneumonia (5.2%). Its two principal species – influenza A (*Alphainfluenzavirus*) and influenza B (*Betainfluenzavirus*) – are both highly seasonal, and tend to co-circulate as they spread through winter months, driving global epidemics before receding again into the approach of summer.(Borchering et al., 2021) Significant progress has been made in nosocomial influenza control over recent decades, including reliable annual deployment of influenza vaccines, and use of rapid antigen tests for point of care case detection.(Maltezou, 2008) However, influenza nonetheless represents a significant nosocomial threat, particularly in the context of relatively low vaccine uptake among healthcare personnel, annual variability in vaccine effectiveness, and the unpredictable nature and pandemic potential of successive influenza seasons.(Vanhems et al., 2016)

1.3.2.3. Other respiratory viruses

Nearly all other endemic HCAI-causing viruses – including respiratory syncytial virus (*Human orthopneumovirus*, 1.3% of HCAIs), rhinovirus (*Enterovirus rhinovirus*, 1.1%), human coronaviruses (*Orthocoronavirinae*, 1.1%), parainfluenza virus (*Respirovirus* and *Rubulavirus*, 0.9%) and metapneumovirus (*Human metapneumovirus*, 0.8%) – principally or exclusively cause respiratory infections. By contrast to these estimates from the ECONI study, point prevalence surveys from the USA and ECDC reported, respectively, that only 1.0% and 0.5% of all HCAIs were caused by viruses. Such low estimates reinforce the beliefs that nosocomial viral infection is widely underreported, and that point prevalence surveys poorly characterize true nosocomial infection burden, particularly for seasonal viruses like norovirus and influenza.(Manchal et al., 2020; Vanhems et al., 2016) Data for rare and non-endemic viruses are likely even poorer, while novel threats like the

coronaviruses SARS-CoV-1 and SARS-CoV-2 continue to emerge and redefine which pathogens cause which HCAI.

1.3.2.4. Emerging viral threats

Over recent decades, a range of emerging viral zoonoses – infectious diseases that jump from animal reservoirs into human populations – have been closely linked to healthcare settings and nosocomial outbreaks. Although bacterial and fungal zoonoses also occur (e.g. brucellosis, leptospirosis, Q fever), these are comparatively rare and not discussed further.(Asante et al., 2019)

1.3.2.4.1. Viral haemorrhagic fevers

Among the most deadly emerging HCAIs are viral haemorrhagic fevers (VHFs), caused by a taxonomically diverse array of viruses. Case-fatality rates for some VHFs reach as high as 90%.(Fisher-Hoch, 2005) The most common is Lassa fever (*Lassavirus mammarenavirus*), originally acquired from multimammate rats but now endemic to West Africa, and estimated to cause thousands of deaths per year.(Richmond and Baglole, 2003) The first reported cases of Lassa fever occurred during a nosocomial outbreak in 1969,(Frame et al., 1970) while a well-documented outbreak in a tertiary care facility in Nigeria in 2018, responsible for 16 infections and 5 deaths among healthcare workers alone, demonstrates its ongoing potential for nosocomial spread.(Dan-Nwafor et al., 2019)

Less common but more deadly than Lassa fever, Ebola virus disease (*Zaire ebolavirus*) has spilled into human populations at least 20 times since its first identification in simultaneous outbreaks in 1976 in present-day South Sudan and Democratic Republic of the Congo. These outbreaks have repeatedly been associated with transmission between patients and personnel in healthcare facilities, and with healthcare workers that amplify spread back into the community.(Shears and O'Dempsey, 2015) The Western African Ebola outbreak of 2013-16, many times larger than all other Ebola outbreaks combined, demonstrated characteristic nosocomial transmission dynamics of zoonotic VHFs, with WHO estimating a total 874 healthcare worker infections and 509 deaths as of July 1, 2015.(World Health Organization, 2015)

Other, rarer zoonotic VHFs that have triggered nosocomial outbreaks include Marburg (*Marburg marburgvirus*),(Gear et al., 1975) Crimean-Congo VHF (*Crimean-Congo haemorrhagic fever orthonairovirus*),(Pshenichnaya and Nenadskaya, 2015) Bolivian VHF

(*Machupo mammarenavirus*),(Peters et al., 1974) the recently-discovered Lujo VHF (*Lujo mammarenavirus*) and Bas-Congo VHF (*Bas-Congo tibrovirus*),(Grard et al., 2012; Paweska et al., 2009) and Andes hantavirus (*Andes orthohantavirus*), the only hantavirus shown to spread through human-to-human transmission.(Martinez-Valdebenito et al., 2014) In a review of nosocomial risks posed by rare zoonotic diseases published in 2001, Weinstein et al. highlighted a number of other viruses not yet known to have caused nosocomial transmission but having theoretical potential to do so, including B virus (*Cercopithecine herpesvirus 1*), rabies (*Rabies lyssavirus*) and monkeypox (*Monkeypox virus*).(Weber and Rutala, 2001) Since, small nosocomial monkeypox outbreaks have been reported in Republic of the Congo,(Learned et al., 2005) Central African Republic,(Nakoune et al., 2017) and Nigeria.(Yinka-Ogunleye et al., 2019) Although this highlights that proactive outbreak preparedness may help clinicians to anticipate emerging zoonotic risks, the pathogens that are expected to pose serious public health threats in the future are not necessarily those that do. In 2001, few could have anticipated that novel zoonotic coronaviruses would become the great emerging nosocomial threats of the early 21st century.

1.3.2.4.2. Coronaviruses

Since the turn of the millennium, a trio of highly infectious zoonotic coronaviruses have spilled into human populations: *severe acute respiratory syndrome coronavirus 1* (SARS-CoV-1), introduced several times from civet cats in Guangdong, China between 2002 and 2004;(Wang et al., 2005) *Middle East respiratory syndrome-related coronavirus* (MERS-CoV), introduced tens to hundreds of times from dromedary camels, predominantly in Saudi Arabia since at least 2012; (Conzade et al., 2018) and *severe acute respiratory syndrome coronavirus 2* (SARS-CoV-2), introduced from an unknown origin in Hubei, China in late 2019. While SARS-CoV-1 has been contained since 2004, MERS-CoV infections have been observed every year since 2012, with the most recent infection reported to WHO in March 2021.(World Health Organization, 2021a) SARS-CoV-2 is the cause of the ongoing coronavirus disease 2019 (COVID-19) pandemic, with hundreds of millions of documented infections since the beginning of 2020, and counting.

These novel coronaviruses are all known to amplify in healthcare settings, whereby individuals that seek care for their disease trigger nosocomial outbreaks. For SARS-CoV-1 and MERS-CoV, most observed human-to-human transmission to date has occurred in hospitals. In a comparative analysis of hospitals clusters, 71% of MERS-CoV infections

and 58% of SARS-CoV-1 infections were estimated to have resulted from nosocomial transmission.(Chowell et al., 2021) Since widespread establishment of SARS-CoV-2 in community settings, only a relatively small share of total cumulative transmission is likely to have occurred in healthcare facilities. However, a rapid review of novel coronavirus outbreaks up to March 31, 2020 estimated that 44% of SARS-CoV-2 infections were acquired in hospital, similar to estimates for SARS-CoV-1 (36%) and MERS-CoV (56%), suggesting comparable intrinsic propensities for nosocomial transmission.(Q. Zhou et al., 2020) Nonetheless, these estimates may be biased by greater surveillance effort in healthcare settings than in the community, particularly early in the COVID-19 pandemic.

There are several reasons why these novel coronaviruses spread so well in hospital settings. First, by transmitting primarily through bio-aerosol droplets, classic nosocomial risk factors for respiratory pathogens play an important role, including dense concentrations of patients and staff with high rates of contact,(Reynolds et al., 2006) imperfect infection prevention measures like masking and isolation,(Seto et al., 2013) and inadequate ventilation systems that fail to eliminate, or even facilitate viral circulation through the air.(Li et al., 2005) Second, aerosolizing procedures required for patients undergoing respiratory distress, like bronchoscopy and intubation, increase risk of onward transmission.(de Wit et al., 2016) Third, all of these viruses can cause asymptomatic infection, and healthcare workers in particular have been identified as sources of silent infection, unknowingly transmitting the virus during contacts with their patients and other members of staff.(Grant et al., 2019; Rivett et al., 2020; Wilder-Smith et al., 2005) Fourth, within-host viral dynamics may also contribute: for SARS-CoV-1 and MERS-CoV, most patients have been shown to only begin shedding large amounts of virus well after symptom onset, at which point they are more likely to already be seeking care in healthcare environments.(de Wit et al., 2016)

1.3.3. Fungi

Fungi, although comparatively rare in healthcare settings relative to viruses and bacteria, are another important cause of nosocomial infection, estimated to account for 5.9–7.3% of HCAIs in Europe.(Stewart et al., 2021b; Suetens et al., 2018) Fungi are eukaryotic heterotrophs distinguished from plants and bacteria by the presence of chitin in their cell walls. Often multi-cellular, but sometimes single-cellular in the form of yeasts, fungi are represented by a tremendous diversity of morphological, ecological and genetic adaptations. Of an estimated 2.2 to 3.8 million species of fungi on Earth,(Hawksworth and

Lücking, 2017) 317 have been identified as human pathogens.(Woolhouse et al., 2005)

1.3.3.1. Candida *and* Aspergillus

Candida spp. are by far the most common cause of fungal HCAI (6.0% of HCAIs), the most noteworthy species being *C. albicans* and *C. auris*. *Candida* spp. are known to cause all types of HCAI, and are proportionally overrepresented causes of pneumonia (12.1%), other HCAI (11.3%), and LRTI (8.4%), but relatively rare causes of GI (2.6%) and BSI (2.0%). *C. auris* has in particular raised significant concern in recent years as an emerging nosocomial pathogen: discovered in Japan in 2009, it has since caused hospital outbreaks on all continents except Antarctica, is associated with invasive disease, is highly resistant to a range of antifungal compounds, and has proven capable of spreading in healthcare settings despite robust infection prevention and control measures.(Lone and Ahmad, 2019; Rhodes and Fisher, 2019) *Aspergillus* spp. are the other HCAI-causing fungi of note (0.7% of HCAIs), occasionally causing respiratory and surgical site infections, particularly in immunocompromised patients.(Suleyman and Alangaden, 2016)

1.3.4. Other pathogens

In the ECONI study, only 0.7% of HCAIs were caused by protozoa or other pathogens not classified as bacteria, viruses or fungi.(Stewart et al., 2021b) Protozoa are single-celled eukaryotes that lack a cell wall and which cause a range of important human diseases, including Chagas disease (*Trypanosoma brucei*), leishmaniasis (*Leishmania* spp.), toxoplasmosis (*Toxoplasma gondii*), and one of the most significant and burdensome of all: malaria (*Plasmodium* spp.). Yet most protozoa spread through arthropod vectors or contaminated water, and only rarely cause nosocomial infection. However, such pathogens can spread in the absence of vectors through, for example, mucous membrane contact, or through contaminated needlestick injury, blood transfusion or organ transplantation.(Lettau, 1991) Although these risks are likely much greater in endemic regions where prevalence is higher, several thousand cases of transfusion-related malaria have been reported in the USA since the first described case in 1911,(Bruce-Chwatt, 1974) while a recent case of unexplained nosocomial *P. falciparum* transmission in a German hospital highlights non-negligible risk, even in the absence of the pathogen's natural vector.(Gruell et al., 2017) Similarly, transfusion-related nosocomial transmission of viruses like HIV and hepatitis C virus have also had large impacts over the past several decades. Nevertheless, relative to the long list of other important healthcare-associated pathogens, such infections represent relatively rare exceptions.

1.4. Antimicrobial agents and antimicrobial resistance

Antimicrobial agents are chemical agents that kill microorganisms, impede their growth or stop their replication. These include: *disinfectants*, which are applied to inert surfaces (e.g. bleach); *antiseptics*, which are applied to living tissue (e.g. iodine, ethanol, chlorhexidine); and *anti-infectives*, which are introduced into the body to prevent or treat infection (e.g. antibiotics, antivirals, antifungals).

Each of these agents plays an important role in the fight against HCAI. Disinfectants are used for decontamination of healthcare settings, for instance on an operating table before surgery, or across a hospital ward after an infectious disease outbreak. Antiseptics are most often used locally on a patient's skin, for instance to reduce risk of contamination with their own flora during invasive procedures like catheter insertion. Finally, anti-infectives are used to treat patients for HCAI by ridding their body of the pathogen causing (or likely to cause) infection. The most widely used anti-infectives in healthcare settings, and an important focus of this thesis, are antibiotics.

1.4.1. Antibiotics

Antibiotics are critically important tools for treating and preventing bacterial infections and controlling HCAI. A recent ECDC point prevalence survey characterized hospital antibiotic use across 1,209 hospitals in 29 European countries in 2016/17. Notwithstanding substantial country-level heterogeneity – antimicrobial exposure prevalence ranged from 15.9% in Hungary to 55.6% in Greece – approximately one in three patients (32.9%) was estimated to receive an anti-infective agent during their hospitalization, of which 92% were antibiotics.(Plachouras et al., 2018) These estimates are presented in **Figure 1.6**, and are consistent with a similar global survey across 303 hospitals in 53 countries in 2015, which estimated that 35.5% of patients received at least one anti-infective agent (89.3% antibiotics).(Versporten et al., 2018) Both studies further estimated the share of antibiotic prescribing specifically for treatment and prevention of HCAI.

1.4.1.1. Antibiotic therapy and prophylaxis

Antibiotic chemotherapy describes the use of antibiotics for the treatment of an active infection. In ECDC point prevalence, therapy accounted for approximately 70% of hospital antibiotic use, 30% of which was for infections with hospital or LTCF onset. This translates to approximately one fifth (19.6%) of all hospital antibiotic use being for HCAI

therapy.(Plachouras et al., 2018) The estimate was somewhat greater in a global study: 25.2% of antibiotic use was estimated to be for HCAI therapy, ranging from 9.5% in Africa to 34.9% in Latin America.(Versporten et al., 2018)

Antibiotic prophylaxis describes the use of antibiotics for infection prevention. In ECDC point prevalence, prophylaxis accounted for 24.9% of all hospital antibiotic use.(Plachouras et al., 2018) For surgery patients, antibiotics are typically given 30 to 60 minutes prior to the first incision,(Cheadle, 2006) but the proportion of patients receiving only one antibiotic dose ranged from >60% in Scotland to <5% in Cyprus, highlighting important country-level differences in antibiotic prescribing practice even for standard procedures.(Plachouras et al., 2018) Overall estimates from the global sample were nearly identical, with prophylaxis accounting for 25.2% of hospital antibiotic use. Surgical prophylaxis was found to contribute to 71% of prophylaxis, versus 29% for general medical prophylaxis. In both studies, there was also extensive variation in exactly which types of antibiotics were prescribed and for which purposes.

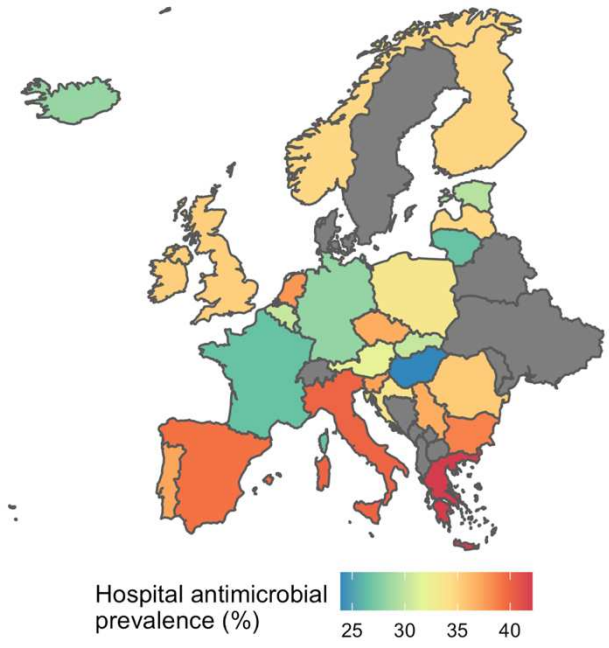

Figure 1.6. Antimicrobial prescribing prevalence in Europe.

Predicted antimicrobial prescribing prevalence (the proportion of patients receiving at least one antimicrobial) in acute care hospitals in Europe in 2016/17. Figure was rendered for this thesis using data extracted from ECDC surveillance.(Plachouras et al., 2018) Data were unavailable for countries shaded in grey. Data from England are used for the United Kingdom.

1.4.1.2. Types of antibiotics

The Anatomical Therapeutic Chemical (ATC) Classification System, a coding scheme developed by WHO for drug taxonomy, recognizes hundreds of different types of

antibiotics, which are distributed across 10 main groups (see **Table 1.2**). For some scientists, the definition of antibiotic includes only *natural antibiotics*, those that are isolated or derived from compounds occurring in nature. However, ACT also includes important synthetic compounds, such as sulfonamides, trimethoprim, and quinolones.

Table 1.2. Types of antibiotics

The ten groups of antibacterials for systemic use as defined by WHO, with characteristic examples.

ATC code	Name of group	Characteristic examples	Notes
J01A	Tetracyclines	- Doxycycline - Tetracycline - Tigecycline	
J01B	Amphenicols	- Chloramphenicol - Thiamphenicol	
J01C	Beta-lactam antibacterials, penicillins	- Ampicillin - Amoxicillin - Flucloxacillin - Piperacillin - Tazobactam	Subgroups include Penicillins with expended spectrum, Beta-lactamase-sensitive penicillins, Beta-lactamase-resistant penicillins, Beta-lactamase inhibitors
J01D	Other beta-lactam antibacterials	- Cefotaxime - Cefepime - Imipenem - Meropenem	Subgroups include Cephalosporins (1^{st}, 2^{nd}, 3^{rd}, 4^{th} generations), Monobactams, Carbapenems
J01E	Sulfonamides and trimethoprim	- Trimethoprim - Sulfamethoxazole - Co-trimoxazole	Synthetic
J01F	Macrolides, lincosamides and strepogramins	- Azithromycin - Clindamycin - Erythromycin - Pristinamycin	
J01G	Aminoglycoside antibacterials	- Amikacin - Gentamicin - Streptomycin	
J01M	Quinolone antibacterials	- Ciprofloxacin - Levofloxacin - Oxolinic acid - Temafloxacin	Synthetic, mostly fluoroquinolones
J01R	Combinations of antibacterials	- Azithromycin + fluconazole + secnidazole - Cefepime + amikacin - Ciprofloxacin + metronidazole	Excludes Combinations of penicillins (including with beta-lactamase inhibitor), Combinations of sulfonamides and trimethoprim
J01X	Other antibacterials	- Colistin - Fusidic acid - Linezolid - Metronidazole - Nitrofurantoin - Vancomycin	Includes Glycopeptides, Polymyxins, Steroids, Imidazole derivatives, Nitrofuran derivatives, Pleuromutilins, and Others

In ECDC point prevalence, the ranking of antibiotics used for HCAI treatment was:(Plachouras et al., 2018)

1. combined penicillin + beta-lactamase inhibitor (J01CR, 19.8%)
2. carbapenems (J01DH, 9.9%)
3. fluoroquinolones (J01MA, 9.4%)

Results were similar in the global sample:(Versporten et al., 2018)

1. combined penicillin + beta-lactamase inhibitor (J01CR, 24.8%)
2. fluoroquinolones (J01MA, 12.8%)
3. carbapenems (J01DH, 12.2%)

1.4.1.3. Biological mechanisms of action

Different types of antibiotics work via different biological mechanisms to either kill bacteria or halt their replication. The principal mechanisms of action are described below, including examples of prominent antibiotics that employ them.(Kapoor et al., 2017; Lewis, 2013; Theuretzbacher et al., 2020) However, it should be noted that the exact molecular targets and biochemical pathways of most antibiotics remain poorly understood, if not entirely undescribed.(Lewis, 2013)

1.4.1.3.1. Inhibition of cell wall synthesis

Some antibiotics work by inhibiting synthesis of peptidoglycan, the fundamental building block of the bacterial cell wall. In the presence of a bacterium's penicillin binding proteins (PBPs), peptidoglycan polymers normally form through *cross-linking* of underlying glycan strands and peptide chains. Antibiotics that bind to PBPs prevent cross-linking, impeding peptidoglycan synthesis. This disrupts maintenance of the bacterial cell wall and ultimately leads to lysis, the bursting of the cell. Antibiotics that work in this way include **beta-lactams** (e.g. **penicillins**, **cephalosporins**, **carbapenems, monobactams**) and **glycopeptides** (e.g. **vancomycin**).

1.4.1.3.2. Inhibition of protein synthesis

Like all living cells, bacteria make use of ribosomes to translate messenger RNA (mRNA) into proteins, a process known as mRNA translation or protein synthesis. Bacteria have a 70S ribosome composed of two ribonucleoprotein subunits: the 30S and 50S subunits. Antibiotics that bind to these subunits can disrupt or inhibit mRNA translation, impeding bacterial metabolism and leading to cell death. Antibiotics that target the 30s subunit include **aminoglycosides** and **tetracyclines**; those that target the 50s subunit include **macrolides**, **chloramphenicol** and **linezolid**.

1.4.1.3.3. Inhibition of DNA replication

DNA gyrase is a protein that manipulates the chromosome to facilitate both DNA replication and mRNA transcription. Bacterial DNA gyrase is distinct from the version found in eukaryotic cells, making it a safe pharmacological target. Antibiotics that target DNA gyrase lead to accumulation of double-stranded DNA breaks and interrupted DNA replication, ultimately causing cell death. These primarily include **quinolones** (e.g. **ciprofloxacin**, **oxolinic acid**).

1.4.1.3.4. Inhibition of folic acid metabolism

Folic acid metabolism is a fundamental metabolic pathway in bacterial cells, associated with DNA biosynthesis and the production of the vital electron donor NADPH. Different compounds target different steps in folic acid metabolism. These include **sulfonamides** (e.g. **sulfamethoxazole, sulfapyridine**), which inhibit the enzyme dihydropteroate synthase, and **trimethoprim**, which inhibits the enzyme dihydrofolate reductase. Such compounds can be used simultaneously to increase their bactericidal impact; the most common is a combination of sulfamethoxazole and trimethoprim known as **co-trimoxazole**.

1.4.1.3.5. Membrane permeation

Lipopolysaccharides form the outer membrane of Gram-negative bacteria. **Polymyxins** (e.g. **colistin**) are a unique class of antibiotics that, in binding to these molecules, result in detergent-like action that damages the outer membrane, increasing its permeability and killing the cell. However, these antibiotics are both neurotoxic and nephrotoxic, and are used relatively sparingly. Colistin is also an example of a “reserve” antibiotic, a classification from WHO designating an arsenal of last-resort antibiotics that should be saved only for targeted use against highly antibiotic-resistant organisms.(WHO Expert Committee on the Selection and Use of Essential Medicines, 2017)

1.4.2. Antibiotic resistance

Antibiotic resistance describes the ability of bacteria to resist the chemotherapeutic effects of a particular antibiotic compound. Resistance can be *intrinsic*, whereby bacteria naturally evade the toxic effects of antibiotics, such as through a protective outer membrane.(Cox and Wright, 2013) Resistance can also be *acquired*, whereby the emergence of previously undetectable resistance occurs, as an evolutionary response to natural selection imposed by use of those antibiotics.(Blair et al., 2015) Intrinsic and acquired resistances are not mutually exclusive, and acquired resistances can also accumulate, whereby a particular bacterium evolves to become multidrug-resistant (MRD), and in some cases even extensively drug-resistant (XDR) or totally drug-resistant (TDR), the latter describing a situation in which no effective treatment options remain.(Velayati et al., 2009) Such acquired multidrug-resistance is a particularly urgent public health challenge, as it renders once crucial therapies ineffective, limiting options for therapy and prophylaxis.

1.4.2.1. A brief history of antibiotic discovery and resistance

Humans have been using plants and fungi to treat infections for millennia, but the first explicit example of effective antibiotic chemotherapy dates to Paul Ehrlich's use of arsphenamine to treat syphilis in 1909.(Williams, 2009) Some years later in 1928 came Alexander Fleming's famous accidental discovery of the first naturally derived antibiotic. Upon returning from holiday to an uncovered culture plate of *S. aureus*, Fleming noticed that the fungus *Penicillium notatum* had cleared the bacteria wherever it grew. Penicillin would go on to become the first mass-produced antibiotic by the early 1940s, but not before bacterial resistance to penicillin was first reported, by Ernst Chain and Edward Abraham in 1940.(Abraham and Chain, 1988) The arms race between the discovery of new antibiotics, and the subsequent discovery of bacterial resistance to them, has been a recurring phenomenon for all major antibiotics introduced into clinical practice (**Table 1.3**). Yet antibiotic resistance long predates *Homo sapiens*, let alone Chain, Abraham, Fleming and Ehrlich.

Table 1.3. Timeline of antibiotic discovery and resistance.

Summary timeline for select antibiotics, when they were discovered to science, when they were introduced to clinical practice, and when resistance to that antibiotic was first observed. Lag to resistance describes the number of years from antibiotic discovery to first observation of resistance. Data adapted from Lewis.(Lewis, 2013)

Antibiotic	Year discovered	Year introduced	Year resistance observed	Lag to resistance
Beta-lactams	1928	1938	1940	12
Sulfonamides	1932	1936	1942	10
Aminoglycosides	1943	1946	1946	3
Tetracyclines	1944	1952	1950	6
Chloramphenicols	1946	1948	1950	4
Macrolides	1948	1951	1955	7
Glycopeptides	1953	1958	1960	7
Oxazolidinones	1955	2000	2001	4
Rifamycins	1957	1958	1962	5
Quinolones	1961	1968	1968	7
Streptogramins	1963	1998	1964	1
Lipopetides	1986	2003	1987	1

The evolution of resistance to antimicrobial compounds is not a modern or anthropogenic phenomenon: antibiotic resistance is ancient. Antimicrobial compounds are naturally occurring, and natural selection favours microbes that evolve mechanisms to overcome them. For instance, genetic elements conferring resistance to penicillins, tetracyclines, glycopeptides and aminoglycosides have been isolated from 30,000 year-old Canadian permafrost sediment.(D'Costa et al., 2011) Far more ancient still, whole genome sequencing of *Paenibacillus* isolated from Lechuguilla – a cave system in New Mexico severed from the surface over 4 million years ago – identified 18 chromosomal resistance

elements, providing evidence for the conservation of multidrug-resistance over the span of millennia.(Pawlowski et al., 2016) These are but two examples; the true extent of bacterial evolution of resistance to antibacterial compounds is immeasurable. However, the evolutionary mechanisms by which bacteria acquire antibiotic resistance are increasingly well described.

1.4.2.2. Evolutionary ecology of acquired resistance

Antibiotic resistance can be acquired through either genetic or phenotypic adaptation to antibiotic exposure. *Genetic resistance* describes changes to a bacterium's genetic material, which is a relatively stable and heritable means for bacteria to evade antibiotics. Conversely, *phenotypic resistance* (sometimes called *adaptive resistance*) describes either stochastic non-genetic heterogeneity in antibiotic susceptibility, or plastic responses to environmental stress; for instance, a bacterium's ability to alter its metabolism through modified gene expression to evade antibiotic effects. Phenotypic resistance is transient, reversible and far more difficult to recognize in clinical contexts than genetic resistance.

1.4.2.2.1. Genetic resistance : mutation

Bacterial genomes can change through a variety of mechanisms. The simplest are small-scale random point mutations, whereby a bacterium's genetic sequence is altered through substitution, deletion or insertion of a single base pair, typically resulting from errors made by polymerase proteins during DNA replication. Although such mutations occur at low rates (estimated across phyla at one mutation for every 10^7 to 10^{10} base pairs substitutions),(Westra et al., 2017) they can have a large impact on antibiotic susceptibility. For instance, in an experiment designed to mimic a naturally occurring bacterial niche, populations of wild-type *E. coli* exposed to ciprofloxacin developed resistance within 10 hours of antibiotic exposure, as a result of just four random point mutations.(Zhang et al., 2011)

Other more complex genetic mutations that can also lead to resistance acquisition include gene amplifications (duplications),(Sandegren and Andersson, 2009) transposition of extrachromosomal genetic elements into chromosomal DNA,(Devaud et al., 1982) and chromosomal rearrangements.(Hoeksema et al., 2018) If the mutated cell then reproduces, its mutations are transmitted *vertically* to its progeny. If those progeny are more evolutionarily fit than other cells in the population – that is, if they are better able to grow, reproduce and transmit, for instance due to an ability to resist antibiotics in a treated

patient – they will come to represent an increasing share of the population over subsequent generations through Darwinian selection, resulting in clinically observable genetic evolution of antibiotic resistance.

1.4.2.2.2. Genetic resistance : horizontal gene transfer (HGT)

Antibiotic resistance genes can also transmit *horizontally* through horizontal gene transfer (HGT), whereby a bacterium shares its genetic material with a neighbouring bacterium via one of three mechanisms.

1. **Transformation**: the release of naked DNA fragments from one cell and their subsequent uptake by another. Transformation of penicillin resistance genes across *Streptococcus pneumoniae* cells was observed as early as the 1950s.(Hotchkiss, 1951)
2. **Transduction**: the transfer of genes by a phage from one bacterium to another. For instance, phages have been shown to transduce tetracycline, chloramphenicol, macrolide, lincomycin and clindamycin resistance genes across *Streptococcus pyogenes* cells.(Ubukata et al., 1975)
3. **Conjugation**: the direct transfer of genetic material from one cell to the next via a pilus. This is the most widely studied, and purportedly the most common route of antibiotic resistance HGT.(Huddleston, 2014)

HGT is often achieved through the spread of *plasmids*, extrachromosomal genetic elements that replicate independently of the host chromosome, and which contribute to host metabolism through the production of plasmid-encoded proteins. There are two main plasmid categories: narrow-host-range plasmids (e.g. IncF), which typically only transfer between closely related species; and broad-host-range plasmids (e.g. IncA/C, IncL/M, IncN), which transfer more readily across species. Each poses unique clinical and epidemiological challenges. One example is IncF plasmids encoding CTX-M enzymes, which confer resistance to beta-lactam antibiotics, including late-generation cephalosporins. These highly antibiotic-resistant plasmids have spread quickly through various Enterobacteriaceae since the early 2000s, and have been associated with the global dissemination of high-risk epidemic clones of MDR *E. coli* (e.g. ST131) and *K. pneumoniae* (e.g. ST258).(Mathers et al., 2015) Another example is IncN plasmids encoding New Delhi metallo-beta-lactamase 1 (NDM-1), a carbapenem-degrading enzyme (carbapenemase) that has become perhaps the most common form of carbapenem

resistance in nosocomial settings worldwide since first reported in 2009.(Mathers et al., 2015)

1.4.2.2.3. Phenotypic resistance

Two bacteria with identical genes can vary in their susceptibility to antibiotics due to phenotypic resistance. This manifests in two principal ways.

Tolerance describes a slowed antibiotic kill rate of an entire bacterial population. A common mechanism is through the formation of a *biofilm*, a polymeric matrix of aggregated bacterial cells (e.g. an *E. coli* biofilm affixed to the bladder wall and causing UTI).(Schrader et al., 2020) Biofilms result in biochemical gradients that reduce towards their centre, with lower concentrations of oxygen and nutrients, lower metabolic rates and reduced antibiotic penetration further from the periphery, ultimately resulting in greater antibiotic tolerance of the bacterial population as a whole.(Crabbé et al., 2019)

Persistence describes a particular subset of a genetically identical population of bacterial cells that better survive antibiotic exposure, for example due to heterogeneous expression of genes encoding porins (bacterial membrane proteins that act as channels allowing molecules like antibiotics to enter the cell) or efflux pumps (proteins that actively remove chemicals from the cell).(Schrader et al., 2020) For *Salmonella enterica* experimentally exposed to antibiotics, reduced expression of the porin gene *ompC* was linked to increased resistance to kanamycin for certain persister cells, while efflux pump inhibition was linked to decreased resistance to nalidixic acid, demonstrating cell-to-cell variability in antibiotic resistance depending on pre-existing heterogeneity in gene expression.(Sánchez-Romero and Casadesús, 2014)

It is important to note that antibiotic resistance genes themselves – for example, a gene encoding a protein that degrades a particular antibiotic – can also vary substantially in their expression from one cell to the next. In other words, phenotypic and genotypic resistance can combine, whereby environmental factors modulate the expression of acquired resistance genes and their impact on resistance phenotypes.

1.4.2.3. Biological mechanisms of resistance

The total number of biological mechanisms resulting in antibiotic resistance has been estimated at over 6,000.(Bogaert and van Belkum, 2018) However, whether resistance is

genetic or phenotypic, the underlying mechanism can normally be described as one of three types. First, bacteria can prevent antibiotics from accessing their target by reducing intracellular antibiotic concentrations; second, they can directly modify the target of the antibiotic; and third, they can inactivate the antibiotic itself.(Blair et al., 2015) Below I provide characteristic examples of each.

1.4.2.3.1. Decreasing permeability

A bacterium's first line of defence against an antibiotic is to prevent it from entering the cell. A range of MDR Enterobacteriaceae – including clones of *E. coli* and *K. pneumoniae* – have reduced the permeability of their cell membranes to various antibiotics. This has been achieved both through phenotypic adaptation (downregulation of porin-encoding genes) and genetic adaptation (porin gene mutations that alter their shape).(Lavigne et al., 2013; Novais et al., 2012; Tängdén et al., 2013) Notably, a range of such adaptations have fostered resistance to carbapenems, and in the case of carbapenem-resistant *K. pneumoniae* have resulted in global dissemination of novel MDR clones associated with nosocomial spread.(Novais et al., 2012; Papagiannitsis et al., 2013; Poulou et al., 2013)

1.4.2.3.2. Increasing efflux

All bacteria contain efflux pumps capable of expelling chemical compounds from the cell, but some are more efficient than others for antibiotic removal.(Blair et al., 2015) Overexpression of efflux pumps is an example of phenotypic resistance, while recent evidence of a multidrug resistance efflux pump co-occurring with NDM-1 on an IncH1 plasmid isolated from *Citrobacter freundii* demonstrates potential for genetic acquisition of more effective efflux pumps, and synergistic interactions with other resistance genes.(Dolejska et al., 2013)

1.4.2.3.4. Protecting the target

Post-translational modifications can protect protein targets from antibiotics without the need for genetic mutations that could otherwise compromise protein function. In *M. tuberculosis*, methylation of the 16S ribosome subunit by *erm* genes adjusts the drug-binding site, reducing affinity for a range of antibiotics, including macrolides, lincosamines and streptogramins.(Blair et al., 2015; Kumar et al., 2014)

1.4.2.3.5. Inactivating antibiotics

Thousands of enzymes have been described that modify or degrade antibiotic compounds.

From a public health perspective, the most worrisome are the extended-spectrum-beta-lactamases (ESBLs), a diverse family of enzymes capable of hydrolyzing different types of beta-lactam antibiotics, including penicillins, monobactams and cephalosporins.(Blair et al., 2015) Many ESBL-producing Enterobacteriaceae in particular currently feature on lists of the greatest antibiotic resistance threats in the world today.

1.4.3. High-risk multidrug-resistant pathogens

The overall public health threat imposed by any particular antibiotic-resistant pathogen is a complex function of its epidemiological prevalence, its intrinsic virulence, and the number and efficacy of therapeutic options available for treatment. In 2008, Rice introduced the ESKAPE pathogens, a list of highly antibiotic-resistant nosocomial bacteria believed to pose the greatest risk to hospital patients worldwide:(Rice, 2008)

- E=*Enterococcus faecium*
- S=*Staphylococcus aureus*
- K=*Klebsiella pneumoniae*
- A=*Acinetobacter baumannii*
- P=*Pseudomonas aeruginosa*
- E=*Enterobacter* spp.

A composite index of the nosocomial burden of antibiotic resistance has been developed using ESKAPE pathogens, which pools the share of hospital isolates bearing phenotypic resistance to key antibiotics. These data are presented in **Figure 1.7**.

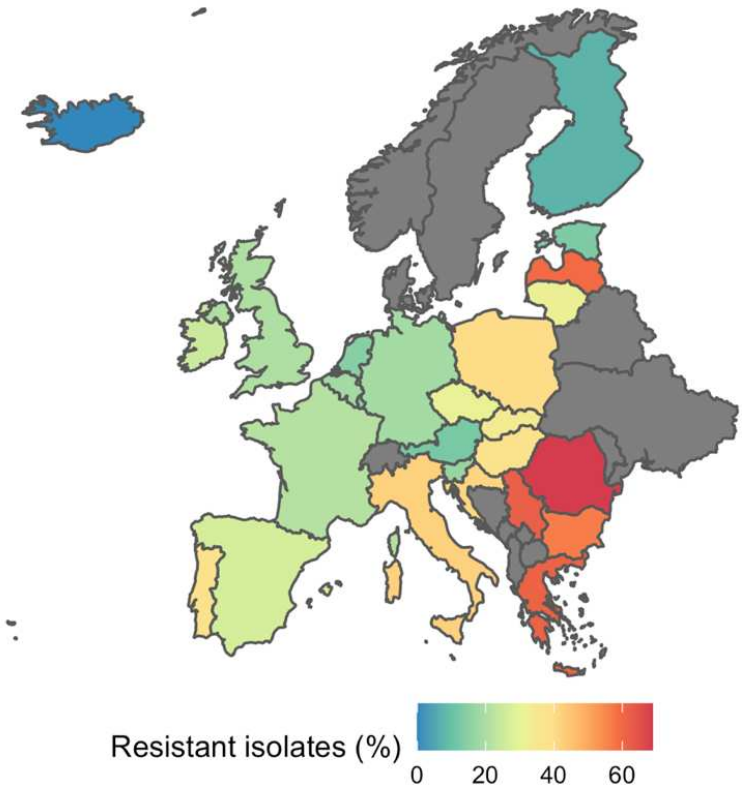

Figure 1.7. Antibiotic resistance prevalence in Europe.

Pooled resistance isolation rate (the pooled proportion of isolates of *S. aureus* resistant to methicillin, *E. faecium* and *E. faecalis* resistant to vancomycin, *E. coli* and *K. pneumoniae* resistant to 3rd-generation cephalosporins, and *P. aeruginosa* and *A. baumannii* resistant to carbapenems) in acute care hospitals in Europe in 2016/17, rendered for this thesis using data extracted from an ECDC point prevalence survey.(Suetens et al., 2018) Data were unavailable for countries shaded in grey. Data from England are used for the United Kingdom.

Later, in 2018, WHO published its global Priority Pathogens List. This list ranks the bacteria most urgently in need of new treatment options, due to their high rates of resistance, considerable public health burden and future epidemic potential. This involved synthesis of a range of previous lists from diverse institutions, collation of data from international antibiotic resistance databases, and a survey of 74 subject-matter experts.(Tacconelli et al., 2018) Key findings are summarized in **Table 1.4**, with a focus on evidence most relevant to healthcare settings, notably the all-cause mortality rate of infection, the excess hospital length of stay incurred by infection, and the resistance prevalence among isolates of that species. Most of the highest priority pathogens are Gram-negative bacilli resistant to carbapenems and/or third-generation cephalosporins, reflecting the few remaining treatment options for these pathogens. Overall, carbapenemase-producing Enterobacteriaceae are the bacteria of of greatest public health concern. Further, nearly all of the included bacteria are also important nosocomial pathogens, as reviewed in section 1.3. *A. baumannii* in particular – the highest priority of all – is almost exclusively isolated from nosocomial environments.(Antunes et al., 2014)

Table 1.4. WHO Priority Pathogens List

Summary of selected findings from WHO's Priority Pathogens List. Highest resistance burden lists the WHO-defined region with the highest reported resistance rate (proportion of isolates bearing the given resistance). Data was compiled using data extracted from Tacconelli et al.(Tacconelli et al., 2018) GNB=Gram-negative bacilli; GNC=Gram-negative cocci; GNCB=Gram-negative coccobacilli; GPC=Gram-positive cocci; GNS=Gram-negative spirilla or s-shaped; CR=carbapenem resistant; 3GCR=third-generation cephalosporin resistant; VR=vancomycin resistant; MR=methicillin resistant; ClaR=clarithromycin resistant; FQR=fluoroquinolone resistant; PNS=penicillin non-susceptible; AmpR=ampicillin resistant; NS=non-significant ; E Med = East Mediterranean

Rank	Species	Resistance	Category	All-cause mortality, % (95% CI)	Excess hospital LOS, days (95% CI)	Highest resistance burden	
						Region	Rate (95% CI)
1.	*Acinetobacter baumannii*	CR	GNCB	52 (45 – 59)	8.3 (4.6 – 12)	Africa	74 (72 – 76)
2.	*Pseudomonas aeruginosa*	CR	GNB	43 (33 – 53)	11.9 (5 – 19)	SE Asia	33 (32 – 34)
3.	*Escherichia coli*	3GCR	GNB	26 (16 – 36)	8.6 (4.5 – 12.8)	SE Asia	51 (34 – 68)
4.	*Klebsiella* spp.	3GCR	GNB	36 (26 – 45)	8.3 (2.2 – 14.4)	SE Asia	52 (33 – 70)
5.	*Klebsiella* spp.	CR	GNB	48 (40 – 55)	9.8 (6.9 – 12.7)	E Med	10 (1 – 27)
6.	*Enterobacter* spp.	3GCR	GNB	26 (7 – 46)	NS	Americas	37 (29 – 45)
7.	*Serratia* spp.	3GCR	GNB	29 (11 – 51)	/	Americas	33 (27 – 38)
8.	*Proteus* spp.	3GCR	GNB	37 (30 – 44)	17.5 (5.7 – 29.2)	Americas	40 (36 – 45)
9.	*Enterobacter* spp.	CR	GNB	54 (35 – 73)	NS	Africa	3 (2 – 4)
10.	*Escherichia coli*	CR	GNB	35 (5 – 65)	32 (11 – 54)	SE Asia	1 (1 – 2)
11.	*Providencia* spp.	3GCR	GNB	29 (21 – 37)	22	SE Asia	12 (9 – 16)
12.	*Enterococcus faecium*	VR	GPC	45 (35 – 54)	10 (6.6 – 14)	Americas	36 (20 – 52)
13.	*Staphylococcus aureus*	MR	GPC	30 (25 – 35)	5.1 (1.8 – 8.4)	Americas	44 (37 – 51)
14.	*Citrobacter* spp.	3GCR	GNB	<10	/	W Pacific	38 (31 – 45)
15.	*Morganella* spp.	3GCR	GNB	29 (21 – 37)	/	SE Asia	14 (12 – 16)
16.	*Helicobacter pylori*	ClaR	GNS	/	/	E Med	34 (25 – 44)
17.	*Campylobacter* spp.	FQR	GNS	<10	/	Europe	61 (60 – 62)
18.	*Salmonella* Typhi	FQR	GNB	6 (3 – 9)	NS	Europe	26 (24 – 28)
19.	*Neisseria gonorrhoeae*	FQR	GNC	/	/	SE Asia	95 (88 – 99)
20.	*Streptococcus pneumoniae*	PNS	GPC	18 (15 – 21)	NS	Africa	34 (18 – 53)
21.	Non-typhoidal salmonella	FQR	GNB	18 (7 – 30)	NS	E Med	15 (1 – 40)
22.	*Haemophilus influenzae*	AmpR	GNCB	12 (6 – 20)	/	SE Asia	43 (41 – 46)
23.	*Neisseria gonorrhoeae*	3GCR	GNC	/	/	Europe	2 (1 – 2)
24.	*Shigella* spp.	FQR	GNB	<10	/	Europe	10 (3 – 20)
25.	*Staphylococcus aureus*	VR	GPC	18 (15 – 21)	2.4 (0.5 – 4.3)	/	<10%

1.4.4. Antibiotic resistance in healthcare settings

Most antibiotic-resistant bacteria (ARB) are endemic and exist widely across community and healthcare settings. However, the public health challenges associated with resistance are arguably most urgent in nosocomial environments, where ARB cause large numbers of infections among particularly vulnerable individuals, and exacerbate the already large burden imposed by HCAI.

1.4.4.1. Increased burden

HCAIs caused by antibiotic-resistant bacteria result in greater health and economic burden than infections caused by antibiotic-sensitive strains of the same species, for several reasons.

1.4.4.1.1. Delays to effective therapy

Bacteria that resist first-line empiric therapy experience longer delays to appropriate treatment. This allows infection to aggravate in the interim, resulting in longer hospital stays, increased laboratory and treatment costs, and worse patient outcomes, including higher risks of mortality and ICU admission.(Schwaber and Carmeli, 2007) For outpatients, delays to effective treatment can also increase subsequent hospitalization risk. Infections that are not completely antibiotic-resistant but nonetheless tolerant also experience delays to completion of therapy and associated costs.

1.4.4.1.2. More toxic agents

A need for broader-spectrum or last-resort antibiotics may result in treatment with multiple antibiotics and/or with more toxic agents. One example is the use of colistin to treat carbapenem-resistant Gram-negative bacterial infection, leading to more, and potentially more serious side-effects than regular treatment, and greater pharmacy costs.(Falagas and Kasiakou, 2005)

1.4.4.1.3. Disruptions to care

The identification of high-risk ARB in healthcare facilities can trigger implementation of control measures, which can be expensive and potentially burdensome for resource-limited healthcare staff. In more extreme cases, ward closures and surgery cancellations in response to ARB outbreaks represent serious disruptions to the continuation of care for patients and staff alike.(Macrae et al., 2001)

1.4.4.1.4. Treatment void

Finally, in cases where no effective treatment options remain (e.g. for a TDR bacterium like colistin-resistant *A. baumannii*), patients may require surgical management, or may simply lack any treatment options whatsoever.(Friedman et al., 2016) This is the widely feared worst-case scenario of antibiotic resistance, whereby no tools remain to treat or prevent once easily cleared infections, placing patients at a high risk of severe complications and death.

1.4.4.2. Antibiotic selection

As a general rule, bacteria isolated from healthcare settings are more resistant to antibiotics than individuals of the same species isolated from the community. This has

been observed across all major HCAI-causing pathogens, including *E. coli*, *S. aureus* and *K. pneumoniae*.(Caneiras et al., 2019; Ferjani et al., 2015; Fey et al., 2003) Antibiotic-resistant HCAI are so common because healthcare settings generate strong selection pressure for antimicrobial-resistant organisms. Vulnerable patient populations, invasive procedures and high densities of inter-individual contact all facilitate the nosocomial transmission of resistant bacteria, but the main driver of resistance in healthcare-settings is antimicrobial use.(Chatterjee et al., 2018; Holmes et al., 2016)

There are a number of ecological mechanisms by which antibiotic use is proposed to select for the spread of ARB, although this remains a widely debated, contemporary focus of epidemiological reseaerch.(Knight et al., 2019) In 2002, Lipsitch & Samore proposed four such mechanisms, all consequences of ecological competition between drug-sensitive and drug-resistant bacteria presumed to overlap in their ecological niche:(Lipsitch and Samore, 2002)

1. **Survival advantage**: if a patient is co-colonized with both drug-sensitive and drug-resistant pathogen strains, antibiotics that effectively kill the sensitive strain afford a survival advantage to the resistant one, favouring its transmission.
2. **Relative prevalence**: antibiotics that successfully clear a drug-sensitive strain reduce its spread and ultimately its prevalence in the population relative to a resistant strain, shifting the competitive balance in favour of resistant bacteria.
3. **Increased susceptibility**: bacteria protect against colonization with other bacteria in their niche, such that patients are more susceptible to acquisition of a resistant strain subsequent to antibiotic clearance of a drug-sensitive strain.
4. **Increased load**: antibiotics favour the within-host outgrowth of resistant bacteria, leading to a larger population size, higher risk of invasive infection, and ultimately a higher transmission rate to other patients or environmental reservoirs. This may also favour a longer duration of carriage, extending potential for further onward transmission.(Niehus et al., 2020)

In the scientific literature, these mechanisms are widely used to explain antibiotic selection for the spread of resistance, but predominantly focus on ecological competition between competing strains of the same species (e.g. methicillin-sensitive vs. -resistant *S. aureus*).(Knight et al., 2019; Spicknall et al., 2013) However, there is increasing evidence for strong within-host competitive interactions between bacterial pathogens and other

constituents of the host microbiome.

1.4.4.3. The microbiome

The opportunistic bacterial pathogens introduced thus far in this Chapter represent only a small minority of the species comprising the human bacterial **microbiome** (the trillions of individual bacteria that collectively inhabit the human body). Primarily represented by a mixture of Bacteroidetes, Actinobacteria, Firmicutes and Proteobacteria, the intestinal microbiome has been revealed over the past several decades to be a fundamental determinant of human health. It provides support to development and homeostasis, facilitates core physiological processes like digestion, and protects against diseases ranging from colitis to cancer.(Bäckhed et al., 2005; Kamada et al., 2013b; Lynch and Pedersen, 2016; Round and Mazmanian, 2009; Roy and Trinchieri, 2017)

The microbiome can also protect against colonization with infectious bacterial pathogens, a phenomenon known as **colonization resistance**, limiting their capacities to establish colonies, grow, persist and transmit.(Bäumler and Sperandio, 2016; Buffie and Pamer, 2013) From the production of antimicrobial peptides to competition for limited nutrients, various biochemical mechanisms have been described by which microbiota protect their hosts – and themselves – from pathogen colonization. Among other examples: commensal taxa from Bacteroidia and Clostridia release volatile short-chain fatty acids that promote intestinal epithelial health and bolster colonization resistance;(Kim et al., 2017) various microbiota induce expression of cryptdins, a type of alpha defensin with antimicrobial properties that target both Gram-positive and -negative bacteria, as well as certain fungi and viruses;(Buffie and Pamer, 2013) and an overlap in the nutritional requirements of different *E. coli* strains may explain why mammalian hosts colonized with commensal biotypes are protected against enterohaemorrhagic biotypes.(Maltby et al., 2013) In this context, the microbiome is increasingly recognized not just as a reservoir of opportunistic pathogens and antibiotic-resistance genes, but conversely as a first-line of defence against colonization and infection with ARB, and more broadly as an important arbiter of individual and public health.(Wilkinson et al., 2021)

Links between microbiome ecology and bacterial epidemiology are perhaps most critical in the context of antibiotic selection for resistance. When prescribed appropriately, antibiotics target particular bacterial pathogens, but co-colonizing microbiota are also exposed.(Tedijanto et al., 2018) This can unintentionally destabilize healthy microbial

communities, resulting in **dysbiosis**, a state of population dynamic disequilibrium.(Bhalodi et al., 2019; Coyte et al., 2015; Dethlefsen and Relman, 2011) Microbiome dysbiosis is associated with reduced abundance and diversity of commensal bacteria, impaired host immune responses, and loss of colonization resistance, altogether increasing host susceptibility to ARB colonization.(Kim et al., 2017; Sorbara and Pamer, 2019; Zhang et al., 2015)

Antibiotic-induced dysbiosis may further result in elevated expression of antibiotic resistance genes, increased rates of horizontal transfer of resistance genes, and ecological release, whereby subdominant ARB are released from competition with other bacteria and grow out into dominant colonies (illustrated in **Figure 1.8**).(Doan et al., 2019; Letten et al., 2021; Ruppé et al., 2019; Stecher et al., 2013) These phenomena underlie increasing clinical recognition of microbiome dysbiosis as a key driver of ARB colonization and infection in healthcare settings.(Baggs et al., 2018; Prescott et al., 2015; Ravi et al., 2019) Accordingly, interventions facilitating microbiome health and recovery have been highlighted in recent years as promising means to control HCAI and limit the spread of resistance.(Pamer, 2016)

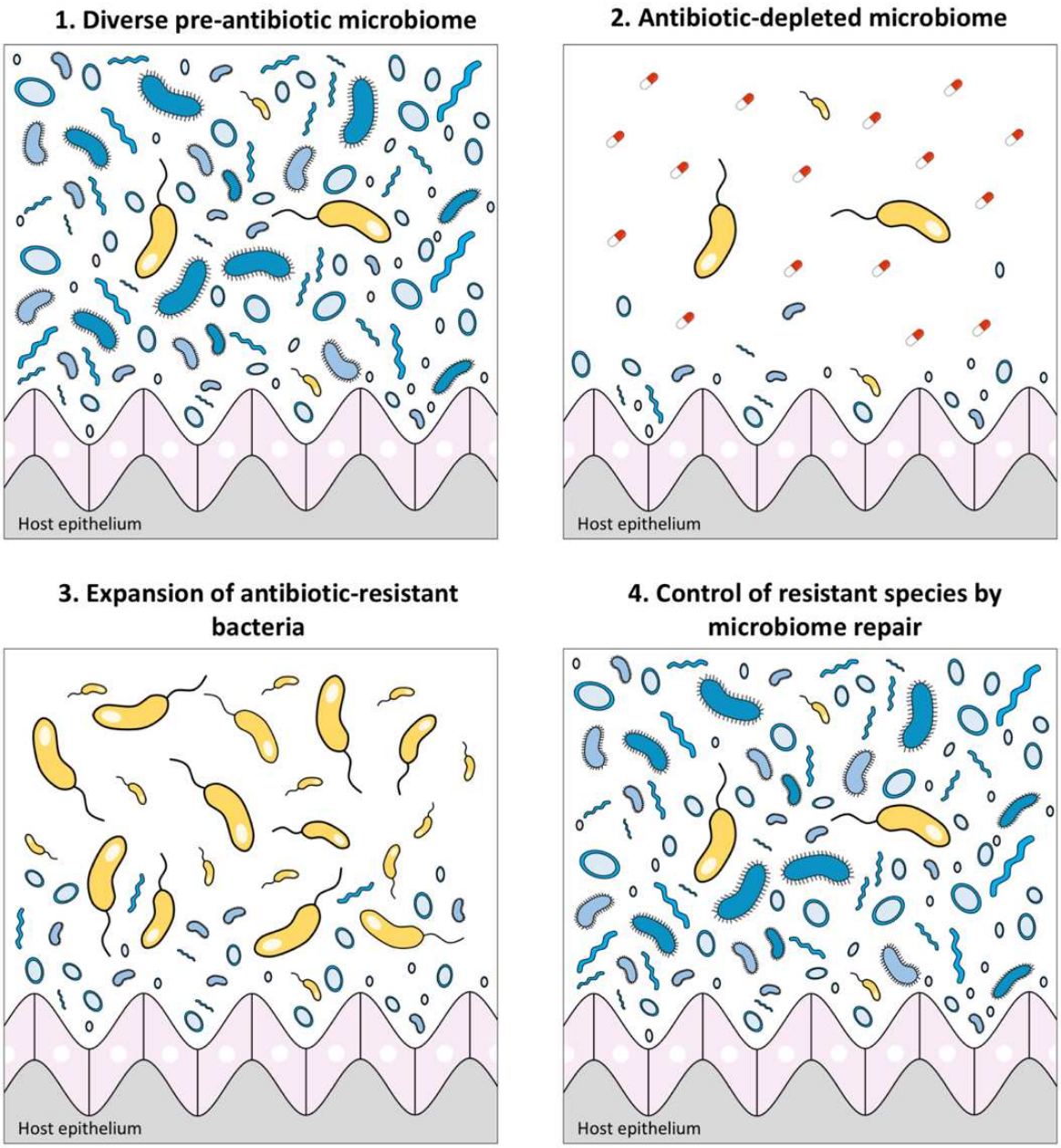

Figure 1.8. Microbiome dysbiosis illustration.

Illustration of how microbiota (blue bacteria) protect against outgrowth of an antibiotic-resistant pathogen (yellow bacteria) within the host (**1**), how antibiotics (red and white capsules) that cause microbiome dysbiosis can favour pathogen growth (**2** and **3**), and how microbiome repair can help control populations of resistant bacteria (**4**). Figure is inspired by Pamer.(Pamer, 2016)

1.5. Public health interventions for HCAI control

Well-designed public health interventions can prevent nosocomial transmission of high-risk pathogens, limit risk of endogenous infection, and at a broader scale reduce the societal burden imposed by HCAI.

1.5.1. Surveillance

Surveillance is a cornerstone of infectious disease control, and a necessary first step for outbreak detection and response. Epidemiological surveillance is defined as:

> *The systematic collection, analysis and dissemination of health data for the planning, implementation and evaluation of public health programmes.*(Thacker et al., 1988)

Surveillance can be **passive**, whereby a health system routinely detects and reports infections in a standardized way, or **active**, whereby public health professionals seek out infections, for instance through population surveys or case reviews, and often in conjunction with epidemiological field investigations. Whether passive or active, surveillance can be conceptualized as a circular process, in which surveillance efforts are in constant evolution to reflect the local epidemiological context (**Table 1.5**).

Table 1.5. Surveillance circularity

Surveillance: a circular process with four key steps. Adapted from WHO.(World Health Organization, 2002)

Step	Description
1. Implementation	- Define goals (e.g. surveillance of which population, pathogen, disease) - Define outcomes (e.g. prevalence, incidence, antibiotic resistance rate) - Set protocols for data collection and microbiological analysis
2. Feedback	- Analyze data - Interpret findings in broader context - Discussion of implications
3. Prevention	- Determine areas for improvement and actions required - Plan and implement corrective public health actions / interventions
4. Evaluation	- Assess impact of interventions on surveillance outcomes - Compare to other studies / institutions / contexts - Use findings to inform surveillance updates (back to step 1)

1.5.1.1. Surveillance assessment

Thacker et al. proposed a range of criteria by which public health surveillance programmes can be assessed.(Thacker et al., 1988) In the context of HCAI, these include:

- **Sensitivity**: the proportion of individuals with HCAI that are detected (true positive rate)
- **Specificity**: the proportion of uninfected individuals correctly identified as such (true negative rate)
- **Representativeness**: the extent to which the surveillance signal represents true HCAI burden in the population
- **Timeliness**: rapidity of the surveillance signal
- **Simplicity**: operational ease of the intervention
- **Flexibility**: ability for the intervention to accommodate operational changes or adapt to new purposes

1.5.1.2. Syndromic surveillance

Syndromic HCAI surveillance is the use of individual or population health indicators to detect potential nosocomial outbreaks. For instance, a hospital conducting syndromic influenza surveillance may track all reports of patients and staff experiencing febrile respiratory illness. The key advantage to syndromic surveillance is its timeliness, as it can trigger alerts before formal diagnoses are made, although sometimes with poor discriminatory power (low sensitivity, low specificity).

1.5.1.3. Testing and screening interventions

There are a wide variety of testing technologies available for infectious disease diagnosis. In this thesis, I discriminate between **testing interventions (passive surveillance)**, defined as the targeted use of diagnostic tests for individuals presenting with pre-determined indications (e.g. infection symptoms), and **screening interventions (active surveillance)**, the indiscriminate use of diagnostic tests across a population in order to detect any individuals potentially infected. Diagnostic tests can also be classified as **point-of-care tests**, bedside tests that provide results in a matter of minutes (e.g. rapid antigen tests), and **laboratory-based tests**, which are generally more sensitive and specific but less timely and more complex, requiring patient specimens to be sent to a laboratory for comprehensive microbiological analysis.

1.5.1.4. Surveillance administration

Public health surveillance requires coordination across a range of administrative levels, from individual healthcare institutions, to local health districts, to national or sub-national authorities. Most countries have their own particular surveillance systems and

corresponding legislation in place. In France, healthcare institutions are legally obliged to report HCAIs caused by multidrug-resistant bacteria using the electronic platform e-SIN: alerts are sent both to the local authority responsible for nosocomial infection surveillance (CPias) and to the regional health authority (ARS), who are then responsible for dispatching alerts to the national level (SPF).(Santé publique France, 2021a)

HCAI surveillance obligations vary not only by country, but sometimes by the type of pathogen or infection. In the USA as of 2013, 92% of sub-national authorities required reporting of primary healthcare-associated BSI in ICUs, compared to 54% for methicillin-resistant *S. aureus* (MRSA) infection and 51% for *C. difficile* infection.(Herzig et al., 2015) WHO, ECDC and other organizations also operate internationally collaborative surveillance networks and databases. For instance, WHO launched the Global Antimicrobial Resistance Surveillance System (GLASS) in 2015, which collects, analyses and disseminates global surveillance data on antibiotic resistance.

1.5.2. HCAI prevention and control

HCAI prevention has traditionally focused on infection prevention and control (IPC) interventions, which encompass the ensemble of public health strategies used to prevent nosocomial pathogen transmission and infection acquisition from the healthcare environment. These range from common-sense practices (e.g. handling sharps with care) to seemingly simple measures with significant operational obstacles (e.g. handwashing) to sophisticated biomedical interventions (e.g. use of antimicrobial-impregnated central venous catheters). Antibiotic stewardship and, more recently, microbiome-targeted interventions have also emerged as important tools for HCAI prevention. Here I list the most widely used HCAI control interventions, provide a table of suggested interventions for outbreak pathogens depending on their mode of transmission (**Table 1.6**), and provide a summary of common components of antibiotic stewardship interventions (**Table 1.7**).

1.5.2.1. Hygiene

Good hygiene practices help to remove carriage of potentially infectious microorganisms, preventing their introduction to sterile sites and transmission to other individuals. These include: (i) adherence to aseptic techniques, such as safe injection practices and application of antiseptic agents before insertion of indwelling catheters; (ii) sterilization of reusable medical equipment using appropriate thermal or chemical means, e.g. peracetic acid; (iii) efficient laundering services for uniforms, linens and other textiles;(Overcash and

Sehulster, 2021) and (iv) proper handwashing, a seemingly simple but operationally complex intervention, and a central pillar of worldwide HCAI and antibiotic resistance prevention campaigns.(Tartari et al., 2017)

Proper handwashing occurs prior to any patient contact, before aseptic procedures, after potential exposure to bodily fluids, and after touching a patient or any adjacent surfaces. WHO further defines multiple levels of handwashing technique depending on patient risk:(World Health Organization, 2002)

1. **Routine care** (low risk): simple handwashing with non-antiseptic soap.
2. **Antiseptic hand cleaning** (moderate risk): hygienic handwashing with antiseptic soap following guidelines.
3. **Surgical scrub** (high risk): hand and forearm washing with antiseptic soap for sufficient duration (3 – 5 minutes).

Proper handwashing is limited in practice by occupational challenges, including lack of handwashing infrastructure, understaffing, allergies or discomfort, and impractical recommendations. Diverse clinical trials have demonstrated efficacy of behavioural interventions for improving handwashing compliance,(Luangasanatip et al., 2015; Ofek Shlomai et al., 2015; Pittet et al., 2000; Teesing et al., 2020) but inadequate hand hygiene remains a central challenge in global HCAI prevention.(Allegranzi and Pittet, 2009)

1.5.5.2. Isolation and cohorting

Limiting inter-individual contact among and between patients and healthcare staff is an effective means to limit nosocomial transmission, especially during outbreaks of pathogens with high intrinsic transmissibility. These include pathogens that primarily spread through aerosols and/or respiratory droplets (e.g. SARS-CoV-2), and fomites (e.g. *S. aureus*).

Contact reductions can be achieved through patient **isolation**. This involves some or all of the following, depending on the infectious risk and resources available: (i) healthcare workers donning full personal protective equipment (PPE), including high-efficiency gowns, gloves and masks, (ii) contact precautions, i.e. limiting contacts only to those strictly necessary for provisioning of care, (iii) restriction of visitors, (iv) housing patients in private rooms, and (v) ensuring rooms have negative pressure and exhaust to the outdoors.

Contact reductions can also be achieved through **cohorting**. Patient cohorting involves clustering patients who are already infected by or colonized with the same organism into the same room, ward (e.g. ICUs for individuals colonized with MDR bacteria)(Rosenberger et al., 2011) or healthcare facility (e.g. tuberculosis or COVID-19 hospitals).(Jijón et al., 2020; Kang et al., 2020) Staff cohorting involves partitioning of healthcare staff to particular patients, to reduce the total number of patients that they contact, and the number of healthcare workers that any individual patient contacts. This can prevent staff from acting as transient vectors or sources of infection, both to patients and other staff.

Table 1.6. Interventions for HCAI outbreak control.

Infection prevention and control interventions implemented during a pathogen outbreak should reflect the suspected mode of transmission. Adapted from WHO.(World Health Organization, 2002)

Mode of transmission	Suggested intervention
1. Person-to-person (e.g. respiratory droplets)	- Patient isolation - Barrier precautions - PPE (e.g. gowns, face masks)
2. Hands / physical contact (e.g. fomites)	- Hand hygiene (e.g. audits, installation of alcohol-based hand rub dispensers) - Cohorting (infected individuals and/or healthcare workers)
3. Airborne	- Patient isolation with appropriate ventilation
4. Waterborne	- Assessment of water supply and liquid containers (and their replacement when necessary) - Use of disposable devices
5. Foodborne	- Elimination of the food at risk

1.5.2.3. Environmental decontamination

Regular decontamination of healthcare surfaces using disinfectants is standard practice, in particular for high-risk areas like ICUs and operating rooms.(World Health Organization, 2002) Environmental decontamination should also be prioritized during suspected nosocomial outbreaks of any pathogen, but particularly those known to transmit through fomites. For water sources contaminated by waterborne pathogens like *Legionella* spp. and *P. aeruginosa*, draining and disinfecting the apparatus, or full replacement may be necessary. Air filters should also be changed regularly, in particular for ducts connecting to ICUs or isolation rooms. More broadly, improved hospital architecture and design may help to limit environmental spread of HCAI, through reduced crowding, improved air flow, better handwashing accessibility, efficient processing of healthcare waste, and reduced occupational stress and fatigue among healthcare workers.(Cesario, 2009; Chaudhury et al., 2009; Dettenkofer et al., 2004)

1.5.2.4. Multimodal IPC interventions

Following James Reasons's *Swiss cheese model* of safety accidents,(Reason, 2016)

HCAIs are best prevented through successive layers of defences, barriers and safeguards: each individual IPC intervention is incomplete on its own, but together they accumulate to reduce HCAI risk. For this reason, HCAI interventions are often implemented as multifaceted infection control interventions, or *bundles*. A meta-analysis of trials from 2005 to 2016 estimated that, globally, 35-55% of all HCAIs are preventable by bundles, highlighting both that significant progress remains to be made in HCAI prevention, and that such progress is achievable.(Schreiber et al., 2018)

1.5.2.5. Antibiotic stewardship

In light of strong causal links between antibiotic consumption and the emergence and spread of high-risk MDR bacteria,(Chatterjee et al., 2018; Costelloe et al., 2010; Patel et al., 2008; Shen et al., 2012; Sun et al., 2012; Wind et al., 2017) the judicious use of antibiotics has become a public health priority for control of antibiotic-resistant HCAI. **Antibiotic stewardship programmes** are sets of interventional actions or policies that promote the responsible prescribing of antibiotics in order to limit negative consequences of their use, including the spread of antibiotic resistance. Stewardship programmes range from simple clinician education initiatives to complex, multimodal bundles combining simultaneous structural and behavioural interventions. A summary of common components of stewardship interventions is provided in **Table 1.7**.

In systematic reviews and meta-analyses, stewardship programmes have been associated with reduced total rates of antibiotic consumption, reduced rates of unnecessary and inappropriate prescribing, reduced use of restricted agents, reduced treatment duration, and reduced hospital length of stay, all without adversely affecting patient mortality.(Davey et al., 2017; Karanika et al., 2016) Critically, they have also proven effective for prevention of antibiotic-resistant HCAI. In a systematic review of trials of multimodal hospital antibiotic stewardship programmes, Baur et al. reported high efficacy for prevention of colonization and infection with high-risk MRB, including a 32% reduction for *C. difficile*, a 37% reduction for MRSA, and a 51% reduction for ESBL-producing Gram-negative bacteria.(Baur et al., 2017) Only recently has research into antibiotic stewardship begun to take into account potential additional benefits for the preservation of microbiome diversity and its ecological and immune functions.(Bogaert and van Belkum, 2018; Ruppé et al., 2018)

Table 1.7. Common antibiotic stewardship interventions.

Common components of antibiotic stewardship interventions, including supporting evidence from clinical trials in hospital settings. Data synthesized from WHO.(World Health Organization, 2021b)

	Intervention	Description	Supporting evidence (hospital setting)
1.	**Clinician education**	Provide knowledge on up-to-date practices and guidelines for judicious antibiotic use through lectures, workshops, webinars, email memos, telephone counselling, etc.	- Sustained reduction in annual prescribing rates (Doron and Davidson, 2011; Regev-Yochay et al., 2011)
2.	**Patient and public education**	Mass education campaigns (e.g. informal messaging) or direct clinician-to-patient education.	- Limited evidence outside of community setting or when not bundled with other interventions (Satterfield et al., 2020)
3.	**Local guidelines**	Institution-specific guidelines for management of common infections to reflect local epidemiology, access to diagnostic testing and drug availability.	- Increased appropriate antibiotic use (Hauck et al., 2004) - Increased narrow-spectrum antibiotic use (Neuman et al., 2012) - Early switch to oral from parenteral formulations (Carratalà et al., 2012)
4.	**Cumulative antibiograms**	Locally-adapted antibiotic susceptibility data for common pathogens	- Provide evidence for local emergence of resistance (Qadeer et al., 2016) - Allow better management of MDR infections (Liang et al., 2016) - Improve prescribing practice (Hsu et al., 2015)
5.	**Prior authorization**	Requires clinicians to obtain approval authorization from pharmacist / stewardship team for use of restricted antimicrobials	- Decreased use of restricted antibiotics, and reduction in resistance to restricted antibiotics (Chrysou et al., 2018) - Decreased inappropriate antibiotic use (Dassner and Girotto, 2018) - Reduced *C. difficile* infection (Feazel et al., 2014) - Reduced isolation of resistant bacteria (White et al., 1997)
6.	**De-labeling of spurious antibiotic allergies**	Performing dedicated allergy history-taking and skin testing for appropriate identification of antibiotic allergies	- Reduction in use of beta-lactam alternatives (J. R. Chen et al., 2017; Moussa et al., 2018) - Improved surgical prophylaxis (Moussa et al., 2018)
7.	**Prospective audit and feedback**	Review of antimicrobial use in individual patients and real-time recommendations to prescribers	- Increased antibiotic streamlining (Lukaszewicz Bushen et al., 2017) - Reduced total prescribing rates (Tamma et al., 2017) - Appropriate prescribing and reduced resistance rates (DiazGranados, 2012) - Reduced prescribing, duration of therapy and length of stay (Khdour et al., 2018)
8.	**Antibiotic time-outs**	Self-directed antibiotic reassessments, facilitated by structured reminders or conversations that prompt clinicians to reassess antibiotic prescription	- Decrease in inappropriate therapy (Thom et al., 2019) - Decrease in targeted antibiotic prescribing and *C. difficile* infection (Lee et al., 2014) - Increased early vancomycin discontinuation (Graber et al., 2015)
9.	**Dose optimization**	Pharmacy protocols, default dosing for commonly used agents, structured order entry	- Optimized vancomycin dosing based on common clinical variables (Crass et al., 2018) - Emerging evidence of benefits of weight-adjusted dosing (Polso et al., 2014)

1.5.2.6. Microbiome-targeted interventions

Beyond antibiotic stewardship – which, intentionally or not, preserves functionally important microbial symbionts and limits outgrowth of pro-inflammatory bacteria – a range of other interventions targeting microbiome diversity and function have been implemented as means of HCAI control.

1.5.2.6.1. Fecal microbiota transplantation

Fecal microbiota transplantation involves colonic transfer of healthy donor stool to patients indicated for transplant, for instance due to severe diarrheal disease. Fecal microbiota transplantation is already used to treat recurrent *C. difficile* infection, and is under investigation for multidrug-resistant Enterobacteriaceae decolonization.(Benjamin Davido et al., 2019; Kassam et al., 2013; Saha et al., 2019) However, its appropriateness for dysbiosis recovery in the absence of other clinical indications is unclear. Transplantation requires rigorous donor screening and close longitudinal follow-up, and cases of donor stool contaminated with toxicogenic and multidrug-resistant bacteria highlight non-negligible risks.(Gupta et al., 2021; Zellmer et al., 2021)

1.5.2.6.2. Probiotics

Probiotics are collections of live symbiotic bacteria, typically ingested orally, which are purported to boost microbiome diversity and function. *Lactobacillus GG*, a fermented probiotic milk product, has demonstrated efficacy for RTI prevention in clinical trials, and has been recommended for prevention of paediatric nosocomial diarrhea.(Hojsak et al., 2018, 2010) Although probiotic formulations and individual responses to them can vary greatly, and high-quality randomized trials are lacking, emerging evidence suggests efficacy of probiotics for prevention of ventilator-associated pneumonia and nosocomial *C. difficile* infection.(Bo et al., 2014; Shen et al., 2017)

1.5.2.6.3. Activated charcoal

A newly emerging microbiome-protective therapy is DAV132, an activated-charcoal product currently undergoing clinical trials. DAV132 is designed to deactivate antibiotics in the colon without compromising treatment efficacy. When co-administered with antibiotics by the oral route, DAV132 has been shown to absorb antibiotic residues in the colon and preserve the richness and composition of intestinal microbiota while maintaining systemic antibiotic exposure.(de Gunzburg et al., 2018, 2015; Pinquier et al., 2021) However, its impacts on HCAI and colonization or infection with antibiotic resistant bacteria have not yet been evaluated.

1.5.3. Decision-making for HCAI control

When deciding which HCAI control measures to implement – whether to reduce local resistance to a last-resort antibiotic, to curb a nosocomial outbreak of a novel respiratory

pathogen, or to achieve some other reduction in HCAI burden – decision-making should be founded upon best available scientific evidence. For medical interventions, randomized clinical trials are regarded as the best source of evidence. However, such data are often unavailable, and, in real-world settings, the kinds of questions answered by clinical trials (e.g. *How efficacious is intervention X in ideal conditions?*) do not necessarily provide answers needed for decision-making during public health crises (e.g. *How can available health-economic resources be optimally deployed to control pathogen Y?*), let alone for more fundamental questions about HCAI epidemiology (e.g. *How does intervention X affect the colonization dynamics of pathogen Y?*). In the absence of high-quality clinical data, mathematical modelling has emerged as a powerful tool to answer just such questions.

Chapter 2. Mathematical modelling of infectious disease epidemiology

A mathematical model is an abstraction of a complex system formalized by equations or computational algorithms. In the context of infectious disease epidemiology, a model generally represents a set of assumptions characterizing how a pathogen spreads or a disease manifests in a host population over time. Among other purposes, models are used to understand the ecology and transmission dynamics of pathogens, to inform biological experiments and clinical trials, to evaluate public health impacts of theoretical control interventions, and to make predictions about future disease burden under particular epidemiological scenarios.(Grundmann and Hellriegel, 2006; Opatowski et al., 2011) By distilling the inherent complexity of infectious disease dynamics into tractable systems with clear inputs and outputs, mathematical modelling acts as a crucial bridge between real-world epidemiology, which can be highly uncertain, and public health policy, which often requires urgent decision-making despite limited data.(Heesterbeek et al., 2015)

In this Chapter I introduce key concepts and methodological approaches for the mathematical modelling of infectious diseases. I then provide a series of illustrative examples of models tailored to different pathogens and epidemiological contexts, with a focus on considerations for the modelling of HCAI and antibiotic-resistant bacteria.

2.1. Modelling approaches

Simplifying the epidemiology of an infectious disease into a model requires carefully selecting the most relevant characteristics for inclusion. Simple or **parsimonious** models are preferred, which, as per Occam's razor, include only as few criteria as needed to describe the system. More intricate assumptions are required if a model is intended to reproduce more complex real-world dynamics, but each new assumption introduces additional sources of uncertainty, making it more difficult to disentangle cause and effect.(Opatowski et al., 2013) Building a model thus requires striking a balance between including enough information to accurately represent the system, while excluding extraneous information that limits tractability or muddles interpretation. Ultimately, the best model for any particular purpose depends on the specific research questions, the data and expertise available, and the underlying biology and epidemiology of the system under study.

2.1.1. Common characteristics of epidemiological models

Mathematical models of infectious disease epidemiology have several fundamental characteristics in common.(Kretzschmar and Wallinga, 2010) First, they are **dynamic**, meaning they account for how the quantities expressed by the model change over time, for instance how the number of infections in a population rises and falls as an outbreak waxes and wanes. This is in contrast to static models, which do not account for time and are unable to capture epidemic flux. Second, they are **mechanistic**, meaning they explicitly represent the biological mechanisms driving system dynamics. This is in contrast to phenomenological models, which reproduce empirical observations without describing the underlying causative processes. Finally, epidemiological models are by their nature **between-host** models that describe the spread of infection at the level of a host population (while nonetheless accounting for within-host phenomena; after all, infection inherently occurs within the host). This is in contrast to within-host infectious disease models, which explicitly describe within-host population dynamics – for instance, changing numbers of pathogen particles or immune cells over the course of infection – but which do not describe the epidemiology of the disease. **Nested** models can account for both, simultaneously describing both between-host and within-host population dynamics. This more complex approach has been particularly useful in the context of evolutionary epidemiology, and for certain pathogens with complex within-host life-cycles, like malaria parasites.(Greischar et al., 2019; Mideo et al., 2008) However, nested models remain

relatively rare among published models of HCAI and antibiotic resistance.(Birkegård et al., 2018; van Kleef et al., 2013)

2.1.2. Defining the host and pathogen

The first step in building a model is to define the pathogen and host population under study. In a review of mathematical modelling for HCAI control, Grundmann & Hellriegel (2006) identified three fundamental components needed for host and pathogen characterization:

1. **Pathogen natural history:** the underlying ecology of the pathogen under study, including its duration of colonization and/or infection.
2. **Pathogen transmission routes:** the different means by which the pathogen transmits and its implications for host acquisition. Common routes include direct transmission from other hosts, acquisition from the environment, or vectoring through intermediate hosts (e.g. healthcare workers).
3. **Host behaviour and demography**: the underlying changes that occur in the host population simultaneous to, but often independent of the pathogen's spread. These vary greatly depending on the scale of the model: at the level of a country, important demographic variables may be rates of birth, death and migration; at the level of a single hospital, patient admission and discharge are more relevant.

Aside from these fundamental characteristics, there is great heterogeneity in the structural assumptions and methodological approaches used in different infectious disease models.

2.1.3. Compartmental models

Compartmental models aggregate the host population into distinct groups depending on the states or characteristics of the individuals in that group (e.g. susceptible to infection, currently infectious, or recovered and immunized against re-infection). Within each compartment, individuals are assumed to have the same average characteristics, and interact and behave in a uniform manner.(Heesterbeek et al., 2015) Compartmental models are traditionally accompanied by **flow diagrams** that use arrows to illustrate how individuals move between compartments according to specific **rates** (e.g. rates of infection and recovery from infection). Examples of common compartmental models are provided in **Figure 2.1**.

Owing to its relative simplicity, compartmental modelling is the most common methodological approach. In a recent systematic review of antibiotic resistance models, 86% were compartmental.(Ramsay et al., 2018) Beyond infection status, hosts can also be aggregated into compartments describing their demographic traits (e.g. patient, healthcare worker), vulnerability to infection (e.g. high-risk, low-risk), prior medical exposure (e.g. vaccinated, unvaccinated), or any other variable or combination of variables that are epidemiologically relevant.(Opatowski et al., 2013)

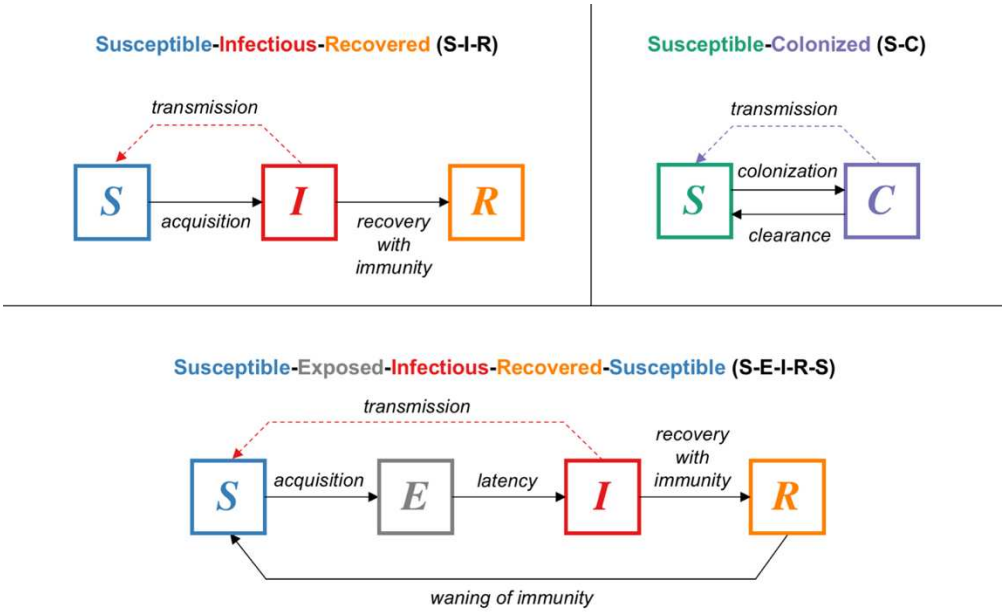

Figure 2.1. Compartmental model flow diagrams.

Flow diagrams for three classic transmission models: the S-I-R model (S=Susceptible, I=Infectious, R=Recovered) describing an infection that results in lasting immunity after recovery; the S-C model (S=Susceptible, C=Colonized) describing colonization and clearance of a pathogen that induces no immunity; and the S-E-I-R-S model (S=Susceptible, E=Exposed, I=Infectious, R=Recovered, S=Susceptible) describing an infection with a latent period prior to becoming infectious, and the gradual waning of immunity after recovery from infection. Solid arrows describe movement of individuals between compartments, while dotted lines indicate sources of transmission and not movement. In all models, only pathogen natural history and transmission are defined; in the absence of explicit terms describing host demography, the implicit assumption is a large, randomly mixing, demographically stable population.

2.1.3.1. Ordinary differential equations

Compartmental models can be written as systems of ordinary differential equations (ODEs) describing the number, density or proportion of individuals in each compartment as a function of time (**state variables**), with the movement of individuals between compartments per unit time described by transition rates (**parameters**).

The **S-I-R model** in **Figure 2.1** can be written as

$$\frac{dS}{dt} = -\beta \times S(t) \times I(t)$$
$$\frac{dI}{dt} = \beta \times S(t) \times I(t) - \gamma \times I(t)$$
$$\frac{dR}{dt} = \gamma \times I(t)$$

(eq 2.1)

where β is the rate of pathogen transmission, γ is the rate of recovery from infection, and S, I and R are interpreted as the number of individuals in the population who are Susceptible, Infectious and Recovered at a given point in time t. This model assumes host-to-host transmission because the risk of infection depends simultaneously on the prevalence of both susceptible and infectious individuals in the population; in the absence of either I or S, no new transmission can occur. (Note that, in ODE models, it is generally implicit that state variables are functions of time: terms t on the right hand side of ODE equations are henceforth omitted for simplicity.)

This classic model, and the underlying theory that ODEs can be used to represent the spread of infectious diseases, were first proposed in a series of papers by Kermack and McKendrick from the 1920s and 1930s.(Kermack and McKendrick, 1991a, 1991b, 1991c) Today, **Kermack-McKendrick theory** represents the foundation of mathematical epidemiology, and the basis of the transmission models presented in this thesis. However, adaptations of the original S-I-R model are needed to better describe the ecology of different types of pathogens and their particular epidemiological contexts. For instance, the **S-C model** is applicable to pathogens that tend to asymptomatically colonize their hosts without inducing host immunity (e.g. some bacterial symbionts), and can be written as

$$\frac{dS}{dt} = -\beta \times S \times C + \gamma \times C$$
$$\frac{dC}{dt} = \beta \times S \times C - \gamma \times C$$

(eq 2.2)

while the **S-E-I-R-S model** includes common characteristics of many common pathogens, including a rate of progression from latency (σ) and a rate of immune waning (ω), and can be written as

$$\frac{dS}{dt} = -\beta \times S \times I + \omega \times R$$
$$\frac{dE}{dt} = \beta \times S \times I - \sigma \times E$$
$$\frac{dI}{dt} = \sigma \times E - \gamma \times I(t)$$
$$\frac{dR}{dt} = \gamma \times I - \omega \times R$$

(eq 2.3)

2.1.3.1.1. Model analysis

Model analysis is a useful means to infer epidemiological insights about the system under study. For some models, **analytical solutions** can be derived for population-dynamic equilibria: mathematical expressions that symbolically describe the model's behaviour in the form of its steady-state outcomes. However, due to the non-linear structure of transmission models, explicit closed-form analytical solutions are often unavailable.(Keeling and Rohani, 2007) Alternatively, **numerical solutions** can be found using numerical integration, in which values for parameters and initial state variables are substituted into equations, and corresponding integrals are calculated over time using the Euler method, or more sophisticated algorithms like Runge-Kutte methods or Gear's method.(Keeling and Rohani, 2007) Time-varying change in state variable quantities – the number of individuals in each compartment – is referred to as a model's **dynamics**.

2.1.3.1.2. Epidemiological indicators

Model dynamics can be translated directly into basic epidemiological indicators or outcomes. The following are three examples used throughout this thesis. First, the sum of the number or proportion of individuals in each infected compartment (I for the S-I-R model, C for the S-C model, or $E + I$ for the S-E-I-R-S model) represents the **prevalence** of infection, the number or proportion of individuals infected at any given time. A pathogen can be described as **endemic** if it has non-zero prevalence and if this prevalence remains relatively stable over time. By contrast, a pathogen is **epidemic** if its prevalence tends to rapidly increase and decrease over time.

Second, integrating terms describing pathogen transmission (calculating the integrals $\int_{t_0}^{t_1} \beta \times S \times I \; dt$ for the S-I-R model and S-E-I-R-S model, or $\int_{t_0}^{t_1} \beta \times S \times C \; dt$ for the S-C model) represents infection **incidence,** the rate of infection acquisition over the period of time $t_1 - t_0$.

A third indicator that is of particular interest to epidemiologists is the pathogen's **reproduction number** (*R*), which describes the average number of secondary infections produced by an infected individual over the course of their infection. An outbreak can only occur or continue if, on average, each infection causes at least one new infection. In the S-I-R model, this can only occur if the rate at which an infectious individual causes new infections is greater than the rate at which that individual recovers,

$$\beta \times S(t) > \gamma$$

(eq 2.4)

and it follows that the average number of secondary cases produced by an infection at any time *t*, the **effective reproduction number**, is given by

$$R_t = \frac{\beta \times S(t)}{\gamma}$$

(eq 2.5)

and that the outbreak only continues if $R_t > 1$. If the population is fully susceptible (as in a naïve population before introduction of the pathogen, i.e. $S(0) = 1$) then this indicator is termed the **basic reproduction number**,

$$R_0 = \frac{\beta}{\gamma}$$

(eq 2.6)

and a newly introduced pathogen will only cause an outbreak if $R_0 > 1$. Since each of the models proposed above assumes the same transmission term and duration of infectivity, this same R_0 expression applies to each.(Bjørnstad et al., 2020; Keeling and Rohani, 2007)

2.1.3.1.3. Exponential growth

Provided that a novel pathogen has epidemic potential ($R_0 > 1$), its transmission in the absence of control measures is an inherently exponential process: infection risk scales with the prevalence of infectious individuals, so each new infection increases the risk of subsequent transmission (provided that the susceptible population is not immediately depleted, as is the case in all but the smallest populations). The reproduction number is also a useful indicator because it allows quantification of a pathogen's exponential growth rate (r_t) according to the formula

$$r_t = \frac{(R_t - 1)}{\tau}$$

(eq 2.7)

where τ is the average **generation time**, the mean duration between infection events in any infector-infectee pair.(The Royal Society, 2020) If $R_t < 1$, then r_t is negative and the outbreak is shrinking. Despite identical R_0 expressions for the models introduced above, the exposed period in the S-E-I-R-S model delays potential transmission events relative to corresponding S-I-R and S-C models, resulting in a longer generation time and lower exponential growth rate.

2.1.3.1.4. Non-linear population dynamics

Even for pathogens with identical infection durations and transmission rates, other differences in their life history – for instance, how they interact with their hosts, whether or not they induce immunity, and whether or not immunity is long-lasting – can fundamentally change their epidemiological dynamics. This is demonstrated for each of the models introduced so far, by numerically integrating each model using the same parameter set and initial state variable conditions. In the S-I-R model, as individuals recover from infection and acquire immunity, the pool of susceptible individuals dwindles, gradually limiting potential for new individuals to become infected and ultimately leading to **extinction** of the epidemic (**Figure 2.2A**). In the S-C model, due to the absence of immunity there is a continuous back-and-forth between susceptible and colonized compartments, such that the pathogen quickly becomes **endemic**, establishing itself at a steady population-dynamic equilibrium (**Figure 2.2B**). In the more complex S-E-I-R-S model, gradual replenishment of susceptible individuals through immune waning leads to **periodic fluctuations** with comparatively long delays until stable equilibrium states are reached (**Figure 2.2C**).(Bjørnstad et al., 2020) These examples illustrate that key indicators like R_0 and r_t, although useful, provide an incomplete representation of a pathogen's epidemiological trajectories.

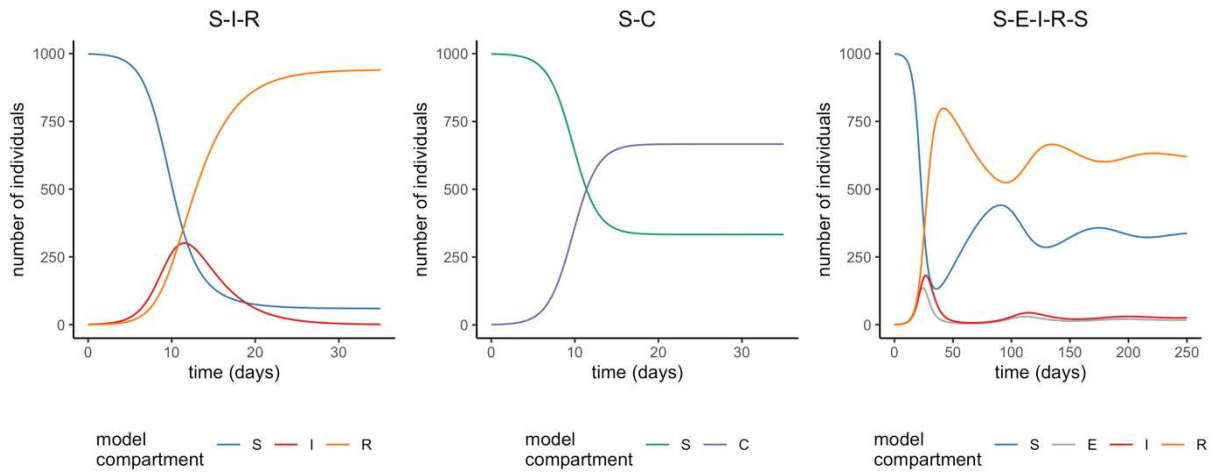

Figure 2.2. Epidemiological dynamics of compartmental models.

Epidemiological dynamics of the three compartmental models presented in **Figure 2.1**, assuming 999 susceptible individuals and 1 infected (or colonized) individual at $t = 0$, and identical parameter values ($\beta = 0.001, \gamma = 1/3$, and for the S-E-I-R-S model, $\sigma = 1/2, \omega = 1/70$). Models were solved through numerical integration using the function ode from the R package deSolve.

2.1.3.1.5. Density-dependent transmission

The models presented above assume **density-dependent transmission**: the probability of transmission increases linearly with the density of infectious individuals in the population. Underlying this assumption is a decomposition of the transmission rate,

$$\beta = c \times v$$

(eq 2.8)

Here, the rate of transmission per unit time is explicitly defined in terms of the number of contacts per individual and per unit time (c) and the probability of pathogen transmission per contact (v), such that the total number of contacts is an increasing function

$$c = k \times N$$

(eq 2.9)

depending linearly on the population density (N).(Begon et al., 2002) Density-dependent transmission maps intuitively to respiratory pathogens, for instance, in which a greater density of individuals in a fixed area leads to a higher rate of transmission.

2.1.3.1.6. Frequency-dependent transmission

An alternative assumption to density-dependent transmission is **frequency-dependent transmission**, in which interpretation of the transmission rate β is slightly modified. With frequency-dependent transmission,

$$\beta = n \times v$$

(eq 2.10)

where *n* is the number of contacts per individual and per unit time, which, unlike *c*, is assumed to be constant regardless of the density of individuals in the population.(Begon et al., 2002) This maps intuitively to sexually transmitted infections, in which an increasing density of individuals is unlikely to result in more sexual contacts and opportunities for transmission. In turn, the transmission function in the context of frequency-dependent transmission is divided by the population density N, as it is the proportion of infected individuals in the population that determines transmission risk per contact. For the S-I-R model introduced above, this equates to

$$\frac{dS}{dt} = -\beta \times \frac{S \times I}{N}$$
$$\frac{dI}{dt} = \beta \times \frac{S \times I}{N} - \gamma \times I$$
$$\frac{dR}{dt} = \gamma \times I$$

(eq 2.11)

In reality, this distinction between density and frequency dependence may not be clear-cut. Take HCAI-causing pathogens like methicillin-resistant *S. aureus* (MRSA) and vancomycin-resistant Enterococci (VRE), for instance. These bacteria spread extensively via contact with healthcare worker vectors, and it is not obvious whether – or how – the number of contacts that any given patient has with healthcare workers should change with an increasing density of patients in the hospital.

2.1.3.1.7. Heterogeneous contact behaviour

Whether density- or frequency-dependent, compartmental models assume homogenous mixing of individuals in each compartment. This results in so-called **mass-action transmission** whereby all susceptible individuals are equally likely to be infected by all infectious individuals. This assumption is potentially valid in large randomly mixing populations,(Bansal et al., 2007) but it is often more realistic to incorporate heterogeneity in contact behaviour and hence transmission rates between different types of individuals.

One way to account for such heterogeneity is to subdivide the population based on a demographic characteristic of choice (e.g. age, occupation) and introduce specific

transmission rates between the different subgroups. This is typically accomplished using a **WAIFW matrix** ("who acquires infection from whom"), in which the probability of an infectious individual in the jth column infecting a susceptible individual in the ith row depends on a demographically-stratified transmission rate $\beta_{i,j}$.(Vynnycky, 2010) Assuming that the intrinsic transmissibility of the pathogen is identical regardless of who is infected, heterogeneity in β can be interpreted as resulting from heterogeneity in *c* (the number of contacts per unit time, as defined above for density-dependent transmission).

For a hospital with different *c* between patients (*p*), healthcare workers (*h*) and ancillary staff (*a*), an illustrative WAIFW is,

$$\mathbf{WAIFW} = \begin{pmatrix} c_{p,p} = 1 & c_{p,h} = 8 & c_{p,a} = 0 \\ c_{h,p} = 8 & c_{h,h} = 4 & c_{h,a} = 2 \\ c_{p,a} = 0 & c_{h,a} = 2 & c_{a,a} = 3 \end{pmatrix}$$

(eq. 2.12)

describing a population in which patients have low rates of contact with one another ($c_{p,p} = 1$ contact/day), high rates of contact with healthcare workers ($c_{p,h} = 8$ contacts/day), and no contact whatsoever with ancillary staff ($c_{p,a} = 0$ contacts/day), while staff have overall similar contact rates with one another ($c_{h,h} = 4, c_{h,a} = 2$ and $c_{a,a} = 3$ contacts/day). With such a matrix, transmission between each sub-group remains a mass-action process, but the overall population is no longer assumed to mix homogenously. Accounting for such demographic heterogeneity in compartmental models has improved understanding of infectious disease dynamics, including spread of childhood diseases among school children, and efficiency of age-targeted vaccination strategies.(Babad et al., 1995; Bauch et al., 2007; Xiao et al., 2016) Further WAIFW matrix stratification can allow for contacts of different durations, types and intensities. However, an important limitation of this approach is that the number of model compartments increases exponentially with the number of host variables considered and their level of resolution, making it difficult to account for more than a select few sources of population heterogeneity, or a limited degree of granularity in demographic stratification.(Opatowski et al., 2013)

2.1.3.2. Stochastic models

ODE models are **deterministic**: there is a pre-determined relationship between model inputs and outputs. It follows that, for any given set of parameter values or state variable inputs, identical outputs result every time the model is evaluated. However, real infectious

disease dynamics are fundamentally **stochastic**: they are subject to random chance. By incorporating a degree of randomness, outputs from stochastic models are generally viewed as more realistic than outputs from deterministic models, especially in small populations where natural epidemic extinction is common and where a small number of chance events can have outsized impacts on overall dynamics. However, depending on a model's research goals, stochastic models are not necessarily better suited: ODEs produce the average expected behaviour of a system, and random chance may have a comparatively small impact on dynamics, particularly in large populations where stochastic and deterministic models produce similar outputs. Stochasticity may also muddle interpretation of results when using a model to better understand fundamental epidemiological mechanisms.(Heesterbeek et al., 2015)

There are a range of methods and algorithms that are used to describe compartmental epidemiological models as stochastic processes, which result in heterogeneous epidemic trajectories for the same fixed model inputs. Perhaps the most widely used stochastic models are Continuous-time Markov chains, which consider state variables as memoryless discrete integers, with incremental changes occurring according to a pre-defined probability matrix.(Allen, 2017) The Gillespie method is one example of a computational algorithm used to evaluate Markov chains.(Gillespie, 1977) **Figure 2.3** demonstrates the impact of stochasticity on dynamical outputs from the S-I-R model introduced above, comparing deterministic results from ODE integration with stochastic results obtained from 100 independent runs using the Gillespie algorithm (Direct method) from the R package gillespiaSSA.(Pineda-Krch, 2008) Beyond Markov chains, other stochastic modelling methods include the use of stochastic differential equations and Kolmogorov differential equations.(Allen, 2017)

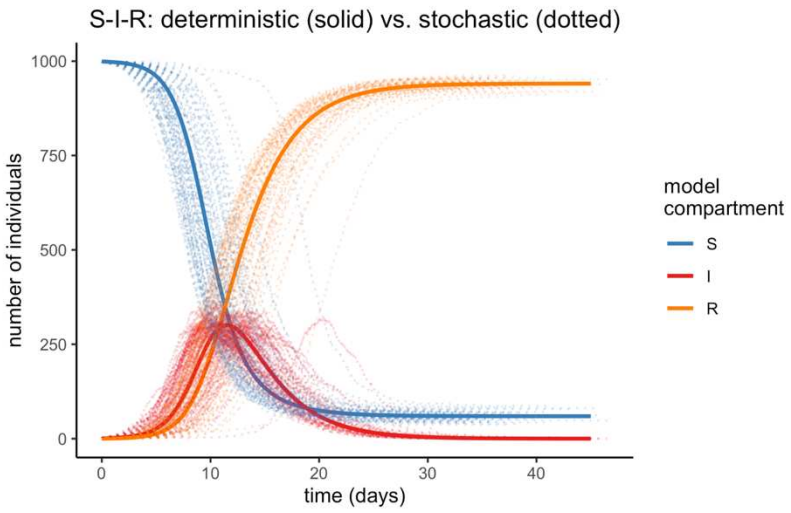

Figure 2.3. Stochastic vs. deterministic dynamics.

For a structurally identical S-I-R model ($\beta = 0.001, \gamma = 1/3, S(0) = 999, I(0) = 1, R(0) = 0, N = 1{,}000$), a comparison of deterministic outputs from numerical integration of ODEs (solid lines) and stochastic outputs from 100 independent runs of the Gillespie algorithm (dotted lines).

2.1.4. Individual-based models

Individual-based models (IBMs), also known as agent-based models, consider each individual in the model as a compartment unto themselves. Each unique agent can thus be represented by a limitless number of characteristics, allowing for individual-level heterogeneity at the levels of the host, the pathogen and the environment to be taken into account.(Willem et al., 2017) As a result, IBMs can include a far greater range of features than a typical compartmental model, from diverse infection risk factors, to gradated disease outcomes, to detailed host-pathogen interactions, to heterogeneous spatial structure, and beyond. With recent advances in computing power and increasing availability of high-resolution epidemiological data, individual-based approaches are increasingly used in infectious disease models.(Willem et al., 2017) However, IBMs also require a greater number of assumptions to inform this heterogeneity, are built upon more complex computational programmes, generally require substantially more time and resources to produce, and yield findings that may be more difficult to interpret.(Railsback and Grimm, 2011)

2.1.4.1. Dynamic contact networks

IBMs are not bound by assumptions of mass-action transmission. Simulating individual-specific contact behaviour and corresponding probabilities of transmission is a common goal of many epidemiological IBMs and can be accomplished through the use of dynamic contact networks. There has been a recent surge in the collection of inter-individual

contact data, whether from paper diaries or more sophisticated approaches like wearable electronic sensor devices.(Duval et al., 2018; Mossong et al., 2008; Vanhems et al., 2013) This has facilitated the advent of IBMs that simulate detailed contact networks to re-create observed contact patterns, resulting in more lifelike transmission dynamics and potentially more representative simulations of public health interventions that target human behaviour.(Assab et al., 2017) **Figure 2.4** illustrates an example of an IBM covering a small population of patients and healthcare workers in a healthcare facility with two wards, with arrows representing heterogeneous contact behaviour between individuals.

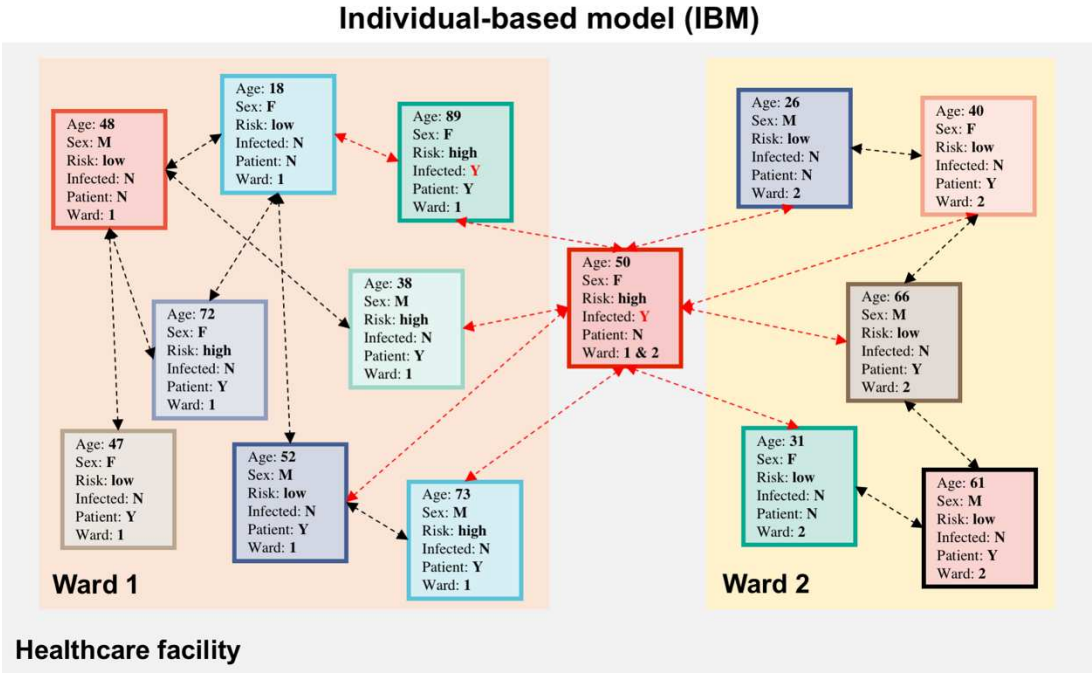

Figure 2.4. Individual-based model schematic.

Schematic of an individual-based model, where each square is an individual with his or her own unique characteristics: age (integer values), sex (male or female), infection risk (high or low), infection status (yes or no), patient status (yes for patient, no for member of staff), and hospital ward (1 or 2). Dashed arrows represent contacts between pairs of individuals aggregated over hypothetical unit-time, and are coloured red if they are infectious contacts that could potentially lead to pathogen transmission.

2.1.5. Parameterization and uncertainty

Parameterization is crucial in order to tailor a model to a specific pathogen and host population, but the parameter values used to inform epidemiological models are often imperfect or approximate due to the complexity of the underlying systems.(Keeling and Rohani, 2007) Even if a model is well-structured and appropriately captures the relevant biological mechanisms under study, inaccurate parameter values will result in false or misleading outcomes. Steps must be taken to ensure not only that a model is well parameterized, but that uncertainty associated with parameter inputs – and corresponding impacts on model outputs – are quantified.

2.1.5.1. Parameterization

2.1.5.1.1. Literature

Often the simplest means to parameterize a model is to find previous estimates from the scientific or grey literature. Reliable sources of parameter estimates include nationally representative population databases, multi-centre longitudinal studies, and systematic reviews and meta-analyses.

2.1.5.1.2. Expert opinion

In the absence of published estimates, subject-matter experts can be consulted to provide estimates for parameter values. Such estimates are inherently subjective and prone to a range of biases, but scientific consensus methodologies like **expert elicitation** have been developed that aim to facilitate collation of estimates from multiple experts while minimizing inherent biases.(Johnson et al., 2010b)

2.1.5.1.3. Model fitting and estimation

If relevant epidemiological data are available, parameters can be estimated directly. There are a broad range of potential techniques with different relevance depending on the types of data available, ranging from least-squares optimization, to maximum likelihood algorithms, to adaptive Bayesian approaches like Markov-Chain Monte Carlo, to emerging machine learning algorithms.(Bi et al., 2019; van Kleef et al., 2013)

2.1.5.2. Uncertainty

2.1.5.2.1. Epistemic vs. stochastic uncertainty

There are two main kinds of uncertainty that can drive heterogeneity in model outputs.(Marino et al., 2008) **Epistemic uncertainty** (also known as subjective, reducible, or type B uncertainty) results from incomplete knowledge about the system being modelled. Epistemic uncertainty is typically quantified using parameter distributions with high variance, from which distinct values are sampled randomly each time the model is evaluated. This results in heterogeneous model outcomes across model runs. **Stochastic uncertainty** (also known as aleatory, irreducible, or type A uncertainty) describes output uncertainty resulting from random chance, and is hence only relevant for stochastic models.

2.1.5.2.2. Sensitivity analyses

Sensitivity analysis is a quantification of the response of model outputs to uncertainty in model inputs (e.g. parameter variation).(Saltelli et al., 2000) **Probabilistic sensitivity analysis** (PSA) is considered a particularly rigorous approach, and is increasingly used in published models of HCAI transmission.(van Kleef et al., 2013) One of the most popular PSA methods in infectious disease modelling is the **Latin Hypercube sampling-partial rank correlation coefficient** method.(Marino et al., 2008; Wu et al., 2013) First, parameters are sampled from their assumed distributions without replacement using stratified Monte Carlo sampling, in which their distributions are divided into *N* equal probability intervals, ensuring more representative sampling of the full distribution than simple random sampling. Second, sensitivities of output states to variation in parameter inputs are calculated using linear regression models, after accounting for linear correlation between inputs and outputs. Other common PSA methods include simple visual inspection using scatter plots and the Morris and Sobol' methods.(Wu et al., 2013)

2.2. Modelling nosocomial pathogens in the healthcare setting

In the 1990s, mathematical modelling emerged as a novel methodology for the study of HCAI epidemiology, and has since become a major tool for the assessment of nosocomial control measures.(Grundmann and Hellriegel, 2006) Most models are tailored to specific healthcare settings and pathogens: in a systematic review, hospitals and ICUs were the principal setting for nearly all models, while **MRSA** was the most commonly studied organism (34% of studies), followed by VRE and generic ARB (both 16%).(van Kleef et al., 2013) Although they found that models for other nosocomial pathogens were relatively rare, a range of significant modelling studies have since been published for high-priority pathogens like ***C. difficile***,(Gingras et al., 2016) and **ESBL-producing Enterobacteriaceae**,(Bonneault et al., 2019; Domenech de Cellès et al., 2013; Kardaś-Słoma et al., 2017; Pelat et al., 2016) More recent systematic reviews have further characterized specific modelling contexts or approaches, including HCAI models using structured contact network data,(Assab et al., 2017) models focusing on health-economic evaluation,(Nelson et al., 2017) models of MRSA transmission in residential facilities,(Kwok et al., 2018) and HCAI models using system dynamics, discrete event simulation or agent-based approaches.(L. K. N. Nguyen et al., 2020)

2.2.1. Evaluating control strategies

Systematic reviews report that the primary focus of most HCAI models is evaluation of the epidemiological efficacy of **control interventions**.(L. K. N. Nguyen et al., 2020; van Kleef et al., 2013) The most widely studied interventions include hand hygiene, patient isolation, healthcare worker cohorting and antibiotic stewardship, followed by patient screening, vaccination and decolonization.(van Kleef et al., 2013) Such control measures can lead to significant changes in host **demography** (e.g. separating individuals through isolation), pathogen **transmission** (e.g. reduced host-to-host transmission rates through hand hygiene), or pathogen **life history** (e.g. reduced duration of bacterial colonization due to antibiotic treatment). Accordingly, the structure and parameterization of HCAI transmission models must reflect not only the specific biology of the HCAI and demography of the healthcare setting under study, but also epidemiological impacts of the interventions being evaluated.

2.2.2. A hypothetical HCAI modelling framework

Here I demonstrate how a mathematical model can be used to evaluate HCAI control

measures, through the example of a novel viral pathogen with frequency-dependent transmission. I adapt the S-I-R model presented above to represent a patient population in a hospital setting with a range of potential public health interventions measures in place.

2.2.2.1. Host demography

The main demographic consideration in hospital settings is **patient turnover** through a symmetric rate of new admissions and discharges, μ, which holds the total population size constant (i.e. assuming full bed occupancy). The community thus represents a source of potential infections – depending on the proportion of individuals **infected upon admission**, g_I – which can have a significant impact on epidemiological dynamics. Here, in the context of a novel pathogen, I assume no input of recovered individuals from the community, and no discharge of infectious or quarantined individuals from the hospital.

2.2.2.2. HCAI control interventions

Three distinct interventions are considered:

- **Hand hygiene**, which reduces the pathogen transmission rate by a proportion $\delta = 80\%$
- **Testing and isolating at admission**, in which a proportion $\kappa = 80\%$ of patients infected upon admission are sent to a quarantine compartment Q
- **Daily testing and isolation**, in which a proportion $\pi = 40\%$ of infected patients are tested daily and isolated in quarantine compartment Q for 10 days ($\rho = 0.1$)

2.2.2.3. ODEs

The S-I-Q-R model with these assumptions included is expressed as:

$$\frac{dS}{dt} = f_S - (1-\delta) \times \lambda \times S - \mu \times S$$
$$\frac{dI}{dt} = (1-\kappa) \times f_I + (1-\delta) \times \lambda \times S - (\gamma + \pi) \times I$$
$$\frac{dQ}{dt} = \kappa \times f_I + \pi \times I - \rho \times Q$$
$$\frac{dR}{dt} = \gamma \times I + \rho \times Q - \mu \times R$$

(eq. 2.13)

where the demography terms f_S and f_I expand to

$$f_S = (1 - g_I) \times \mu \times (N - I - Q)$$
$$f_I = g_I \times \mu \times (N - I - Q)$$

(eq. 2.14)

and the transmission rate is expressed as the frequency-dependent **force of infection** λ, which excludes quarantined individuals as they are assumed not to transmit,

$$\lambda = \frac{\beta \times I}{N}$$

(eq. 2.15)

In **Figure 2.5**, model dynamics are evaluated numerically for each intervention independently, demonstrating the prevalence of infection across each scenario. In **Figure 2.6**, cumulative infection incidence is reported over time for each intervention, and also when combining all interventions. Intervention **efficacy** can be calculated by comparing epidemiological outcomes with and without interventions, for instance reduction in pathogen prevalence or reduction in cumulative infection incidence. An example of the latter is provided in **Figure 2.6**.

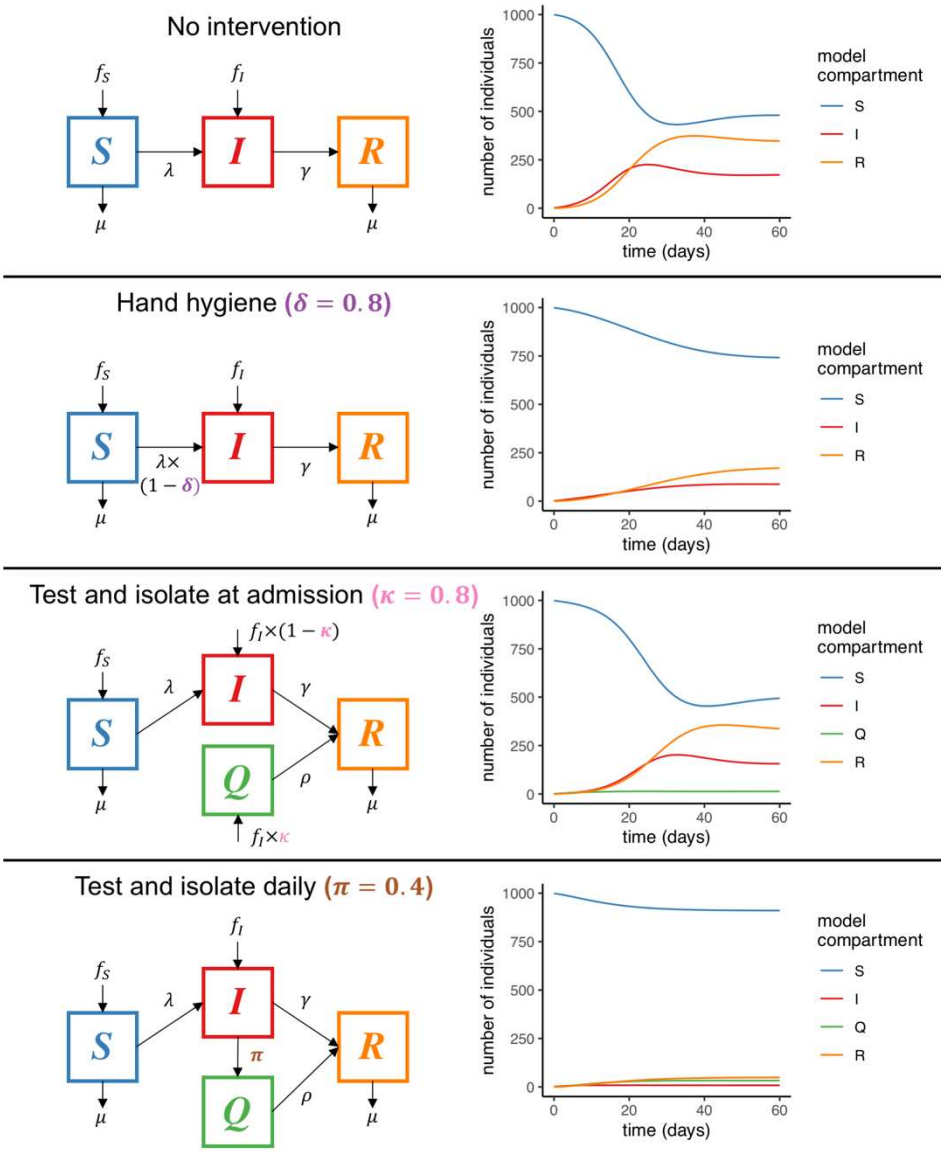

Figure 2.5. Illustrative HCAI models and dynamics.

Flow diagrams (left) and model dynamics (right) for four variations of the model in equation 2.13. In the absence of testing and isolation, the compartment Q is omitted. Identical initial conditions ($S(0) = 999, I(0) = 1, Q(0) = 0, R(0) = 0$) and parameter values ($\beta = 0.4\ \text{day}^{-1}, \gamma = 0.2\ \text{day}^{-1}, g_I = 0.02, \mu = 0.1\ \text{day}^{-1}$) are assumed for each evaluation. ODEs were solved numerically using the function ode from the R package deSolve.

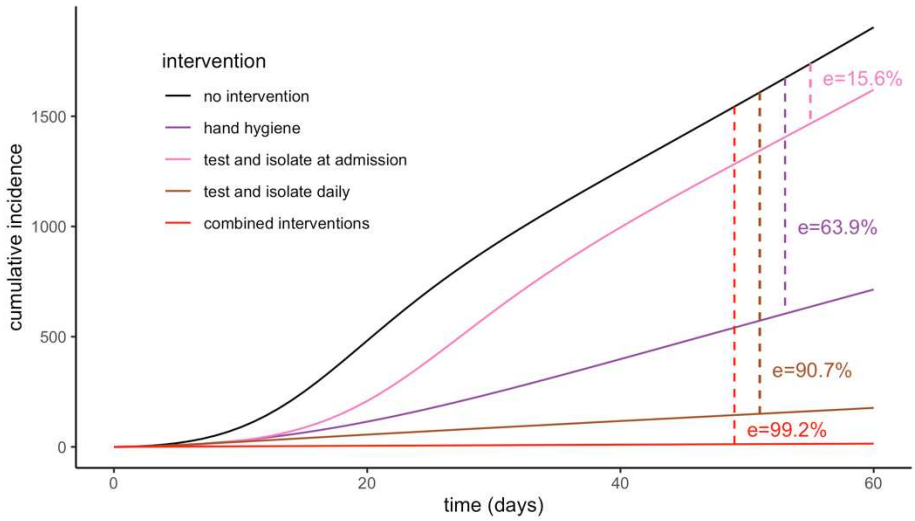

Figure 2.6. Demonstrating intervention efficacy.

The cumulative incidence of infection over time, corresponding to model dynamics simulated in **Figure 2.5**. In text, the efficacy of each intervention is reported as **e**, the proportional reduction in cumulative incidence relative to simulations with no intervention in place. For this model, daily testing and isolation is the single most effective intervention considered, while combined interventions prevent over 99% of infections.

2.3. Modelling antibiotic selection for resistance

Antibiotic resistance is a central focus of contemporary infectious disease modelling, and multidrug-resistant bacteria are the focal organisms of the vast majority of HCAI models.(Heesterbeek et al., 2015; van Kleef et al., 2013) In a review of findings and methodological approaches for ARB modelling, Opatowski et al. (2011) highlighted the importance of properly representing the mechanisms that drive resistance across scales. These range from biological characteristics of resistance at the genetic level (e.g. resistance mechanisms like horizontal gene transfer), to the bacterium's ecological dynamics within the host (e.g. competitive interactions with other organisms), to its epidemiological drivers at the host level (e.g. routes of person-to-person transmission). More recent reviews by Birkegård et al. (2018) and Ramsay et al. (2018) concur that mechanisms favouring the emergence and spread of resistance are fundamental considerations for most ARB models, and that evaluation of antibiotic stewardship interventions is a key motivation for their use.

2.3.1. Strain competition: a mechanism for antibiotic selection

To explain mechanistically how antibiotics drive the epidemiological spread of resistance, a classic modelling assumption is that selection results from intraspecific competition between at least one drug-sensitive strain C^S and one drug-resistant strain C^R.(Spicknall et al., 2013) The reasoning goes: strains of the same species occupy the same ecological niche, so colonization with one strain inhibits colonization with another. In turn, antibiotics that preferentially clear C^S render the within-host niche available to potential colonization with co-circulating C^R, indirectly favouring C^R spread through the host population. A simple two-strain exclusive colonization model (illustrated in **Figure 2.7**) can be written as:

$$\frac{dS}{dt} = f_S - (\lambda_S + \lambda_R) \times S + (\gamma + \mathrm{a}) \times C^S + \gamma \times (1 + c) \times C^R - \mu \times S$$
$$\frac{dC^S}{dt} = f_{C^S} + \lambda_S \times S - (\gamma + \mathrm{a} + \mu) \times C^S$$
$$\frac{dC^R}{dt} = \lambda_R \times S - (\gamma \times (1 + c) + \mu) \times C^R$$

(eq. 2.16)

This model assumes: (i) a rate of antibiotic clearance a that only affects the drug-sensitive strain, (ii) a fitness cost of resistance c that shortens the natural duration of colonization of

C^R relative to C^S, (iii) a distinct force of infection for each strain,

$$\lambda_{C^S} = \frac{\beta \times C^S}{N}, \lambda_{C^R} = \frac{\beta \times C^R}{N}$$

(eq. 2.17)

and (iv) that the drug-resistant strain is novel, and hence that there is input only of the drug-sensitive strain from the community, determined by the proportion of patients colonized upon admission g_{C^S},

$$f_S = (1 - g_{C^S}) \times \mu \times N$$
$$f_{C^S} = g_{C^S} \times \mu \times N$$

(eq. 2.18)

Under this model, an increasing magnitude of antibiotic use (higher a) leads to a greater prevalence of C^R, even though antibiotics have no direct impact on C^R in model equations. This is because each strain competes for limited hosts: the drug-resistant strain is at a survival disadvantage in the absence of antibiotics (due to supposed metabolic costs of expressing antibiotic-resistance genes), but is advantaged in the context of antibiotics that preferentially clear its drug-sensitive competitors, increasing the pool of susceptible patients that it can colonize.

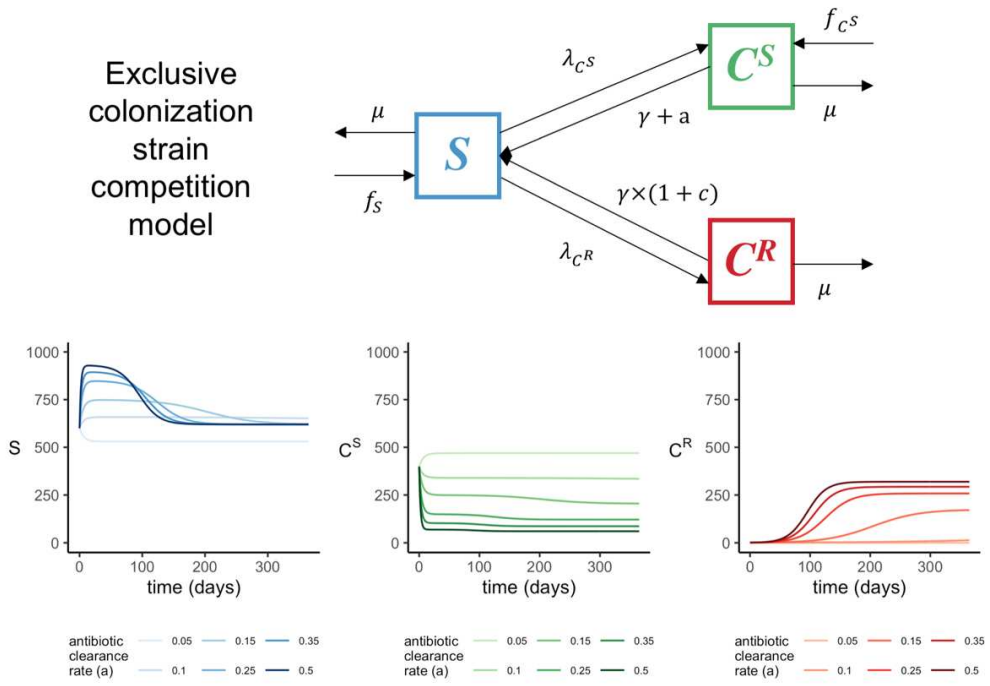

Figure 2.7. Exclusive colonization strain competition model.

A flow diagram (top) of a two-strain exclusive colonization strain competition model, and resulting model

dynamics (bottom), representing the number of individuals in each compartment in separate subplots. Line transparency represents the antibiotic clearance rate a, with more opaque lines corresponding to higher rates. ODEs were solved numerically using the function ode from the R package deSolve ($S(0) = 600, C^S(0) = 399, C^R(0) = 1$; $\beta = 0.2\ \text{day}^{-1}, \gamma = 0.02\ \text{day}^{-1}\ \mu = 0.1\ \text{day}^{-1}, c = 0.2, g_{C^S} = 0.3$).

2.3.2. Beyond strain competition

Most contemporary antibiotic resistance models are variants of this strain competition typology.(Blanquart, 2019; Spicknall et al., 2013) For instance, the 'mixed-carriage' model by Davies et al. demonstrates how intraspecific competition results in negative frequency-dependent selection for either of two competing strains, and provides a satisfying mechanistic explanation for widespread strain coexistence at the population level.(Davies et al., 2019) However, intraspecific strain competition is not the only mechanism by which antibiotic consumption can drive ARB spread (see Chapter 1.4.4.2), and may have limited relevance for certain species, settings and timescales.(Lipsitch and Samore, 2002)

Accounting for other forms of complexity in epidemiological models – from treatment intensity, to age-assortative contact behaviour, to hospital referral networks, to animal-human interactions, to genetic linkage between resistance and non-resistance genes – has helped to unravel the many, disparate forces that contribute to drive the spread of resistance.(Blanquart et al., 2018; Cobey et al., 2017; Colijn and Cohen, 2015; Donker et al., 2017; Lehtinen et al., 2017; van Bunnik and Woolhouse, 2017) However, contemporary work has stopped short of evaluating consequences of between-species competition on resistance epidemiology.(Davies et al., 2019) Yet for many ARB, including emerging high-priority multidrug-resistant bacteria like ESBL-producing Enterobacteriaceae, interactions with the host microbiome appear to be important mediators of nosocomial colonization dynamics.(Kim et al., 2017; Lerminiaux and Cameron, 2019; Pilmis et al., 2020) Indeed, an incomplete understanding of key eco-evolutionary principles – including within-host competition between bacterial pathogens and the host microbiome – has been highlighted as a limitation to the ability of mathematical models to predict future trends and inform decision-making.(Knight et al., 2019)

Chapter 3. Thesis objectives

This thesis aims at developing novel mathematical models to improve our understanding of HCAI epidemiology and to provide evidence informing optimal means of infection control. Three principal knowledge gaps are addressed in this work. First, there is a need to better understand how infection risk varies across pathogen species and population characteristics, and how different routes of transmission and forces of selection drive the epidemiological dynamics of diverse nosocomial pathogens in varied healthcare environments. Second, in order to ensure the timely detection of nosocomial outbreaks, there is a need to optimize infectious disease surveillance in the context of imperfect test sensitivity and limited testing capacity. Third, in order to reduce the overall burden of HCAI, there is a need to design better infection control strategies that respond to the particular ecological and epidemiological characteristics of targeted pathogens.

In this thesis I address these knowledge gaps through two principal bodies of work. First, I propose an ODE modelling framework for ARB that accounts for simultaneous impacts of antibiotic consumption on pathogen colonization and microbiome stability, in order to evaluate how microbiome dysbiosis contributes to the epidemiological dynamics of ARB in the hospital setting (**Chapter 4**). This framework is then applied in a Monte Carlo simulation study to evaluate how pathogen-specific differences in within-host ecological interactions drive the efficacy of public health interventions for ARB prevention (**Chapter 5).**

Second, I use individual-based modelling and counterfactual analysis to analyze how testing and control strategies limit the spread of SARS-CoV-2 in long-term care settings. This involves evaluation of surveillance in distinct pandemic contexts (introduced in **Chapter 6**). In an early pandemic context, with limited availability of reverse transcriptase-polymerase chain reaction (RT-PCR) tests and high outbreak vulnerability, surveillance interventions are evaluated for their ability to detect emerging nosocomial SARS-CoV-2 outbreaks (**Chapter 7**). Then, in a later pandemic context with availability of antigen rapid diagnostic testing and various alternative COVID-19 control measures, combined surveillance and isolation interventions are evaluated for their ability to prevent SARS-CoV-2 transmission (**Chapter 8**). Finally, these works are discussed in the context of their collective contributions to the scientific literature and relevance to public health (**Chapter 9**).

Chapter 4. Modelling within-host microbiome-pathogen interactions as drivers of epidemiological dynamics of antibiotic resistance

4.1. Introduction

Antibiotics are essential medicines for the treatment and prevention of bacterial infections, but their use selects for the spread of pathogenic ARB, and can inadvertently disrupt the host microbiome and its associated immune function.(Buffie and Pamer, 2013; Chatterjee et al., 2018; Kim et al., 2017) Within-host ecological interactions between co-colonizing bacteria can have important consequences for their colonization dynamics, which likely extend to influence the epidemiology of human pathogens in clinical settings.

Antibiotic-induced disruption of the host microbiome is a long-standing theory explaining how antibiotics select for the spread of resistance at both the individual and population levels,(Lipsitch and Samore, 2002) but most mathematical models consider just one species of bacteria at a time, under the traditional assumption that antibiotic selection for resistance results from intraspecific competition between co-circulating strains.(Blanquart, 2019; Ramsay et al., 2018; Spicknall et al., 2013) This simple framework has been particularly useful for bacteria like *Streptococcus pneumoniae* and *Staphylococcus aureus*, in which different strains – sometimes conceptualized as drug-sensitive vs. drug-resistant, or community-associated vs. healthcare-associated – are believed to be in close ecological competition.(Blanquart, 2019; Domenech de Cellès et al., 2011; Kardas-Sloma et al., 2011; Pressley et al., 2010; van Kleef et al., 2013) However, microbiome ecology remains largely absent from the epidemiological modelling of antibiotic resistance, (Assab et al., 2017; Birkegård et al., 2018; Blanquart, 2019; Niewiadomska et al., 2019) suggesting a need to better understand within-host competition between ARB and the host microbiome, its potential epidemiological consequences, and more broadly how antibiotics exert selection pressure on resistant bacteria.(Knight et al., 2019)

In this Chapter, I formalize a mathematical modelling framework for the epidemiology of antibiotic-resistant bacterial pathogens in the healthcare setting, accounting for the host microbiome, various within-host microbiome-pathogen interactions, antibiotic-induced microbiome dysbiosis, and consequences for the spread of antibiotic resistance. I use this

framework to demonstrate how different combinations of ecological interactions drive antibiotic selection for the spread of resistance, with heterogeneous impacts on classic epidemiological indicators and consequences for public health interventions.

4.2. Methods

I propose a series of five compartmental ODE models describing colonization dynamics of an antibiotic-resistant bacterial *pathogen*, denoted P^R, in the hospital setting. Each model accounts for different within-host ecological interactions between P^R and other bacteria, including intraspecific pathogen strain competition, interspecific microbiome-pathogen competition, and interspecific horizontal gene transfer (HGT). Expressions for the basic reproduction number (R_0) are derived and evaluated numerically, and ODEs are integrated numerically to calculate epidemiological outcomes. All models are evaluated over the same generic parameter space, to isolate impacts of model structure and assumptions on epidemiological outcomes, and hence to determine theoretical impacts of within-host ecological interactions on resistance epidemiology in the context of antibiotic use in the healthcare setting. R and Mathematica code for the equations and analyses described herein are available online at https://github.com/drmsmith/microbiomeR.

4.2.1. Model 1: Bacterial colonization in healthcare settings

I first propose a simple Susceptible-Colonized transmission model (**Figure 4.1**) representing a population of N hospitalized patients as either susceptible to colonization (S) or colonized (C^R) by P^R, the focal strain or species:

$$\frac{dS}{dt} = N \times (1-f) \times \mu - S \times (\lambda_R + \alpha_R + \mu) + C^R \times (\gamma_R + \sigma_R)$$
$$\frac{dC^R}{dt} = N \times f \times \mu + S \times (\lambda_R + \alpha_R) - C^R \times (\gamma_R + \sigma_R + \mu)$$

(eq. 4.1)

This model is adapted from classic colonization models of antibiotic-resistant bacteria introduced in Chapter 2,(Austin et al., 1997) includes no ecological interactions with non-focal bacteria, and reflects a suite of common assumptions relevant to the healthcare setting, detailed as follows.

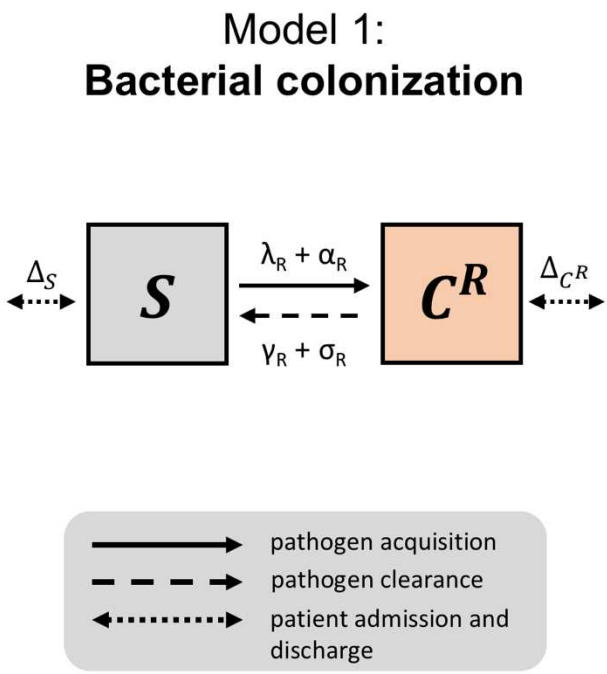

Figure 4.1. Model 1 flow diagram.

4.2.1.1. Patient demography

A constant population size is assumed ($N = 1$), balanced by a daily rate of hospital admission and discharge μ. The number of patients in each host compartment is expressed as proportions of the total population. The proportion of patients entering the hospital with particular characteristics g are given by admission fractions f_g. These are interpreted as representing prevalence of respective host types in the community (e.g. patients already colonized by the pathogen upon hospital admission), which are assumed to be stable over time and unaffected by hospital dynamics. For simplicity, in subsequent models demography terms are expressed as Δ_i for each model compartment i.

4.2.1.2. Pathogen epidemiology

Pathogen colonization can be acquired through dynamic patient-to-patient *transmission* according to the dynamic force of infection (λ_j) for any included strain j of the pathogen P^j. The force of infection is defined as the product of the pathogen's intrinsic transmission rate (β) and the prevalence of patients already colonized (C^j) with that strain, given by

$$\lambda_j = \beta \times \frac{C^j}{N} \qquad \text{(eq. 4.2)}$$

In hospital environments, pathogen colonization incidence also results from *endogenous*

acquisition (α_j). This subsumes alternative routes of acquisition not resulting from direct patient-to-patient transmission, and can include processes like translocation and within-host outgrowth of a subdominant/non-detectable/non-transmissible colony into a dominant/detectable/transmissible colony.(Archambaud et al., 2019; Bootsma et al., 2007; Duval et al., 2019a; Gurieva et al., 2018) This reflects the microbiological tenet that "everything is everywhere, but the environment selects".(de Wit and Bouvier, 2006) Lastly, in the absence of treatment, pathogen colonization is assumed to last for a duration $1/\gamma_j$ days, such that colonization is naturally cleared at rate γ_j day^{-1}.

4.2.1.3. Antibiotic-induced pathogen clearance

Pathogen colonization is also cleared by effective antibiotic treatment. Treatment efficacy is assumed to depend both on the distribution of antibiotics consumed in the hospital and on the intrinsic antibiotic resistance profile of the pathogen. This is expressed as

$$\sigma_j = \mathrm{a} \times (1 - r_j) \times \theta_C \quad \text{(eq. 4.3)}$$

where $\mathbf{a}$ is the hospital population's antibiotic exposure prevalence (the proportion of patients exposed to antibiotics at any time t), θ_C is the antibiotic-induced clearance rate (the rate at which effective antibiotics clear pathogen colonization), and r_j is the antibiotic resistance level (the proportion of antibiotics that are ineffective against that strain). Modelling the latter as a continuous proportion reflects that bacteria are not necessarily fully drug-sensitive ($r_j = 0$) nor -resistant ($r_j = 1$), but can range in their sensitivity to different antibiotics ($0 \leq r_j \leq 1$). The resistance level r_j is thus a model input interpreted as an overall measure of the pathogen's innate degree of resistance to the particular antibiotics to which it is exposed.

Antibiotic exposure is modelled independently of colonization status, reflecting high estimated rates of bystander selection for ARB, which predominantly colonize patients asymptomatically, are rarely detected and only opportunistically cause disease.(Tedijanto et al., 2018) Further, pathogen colonization is assumed not to be acquired endogenously among patients undergoing antibiotic treatment capable of pathogen clearance, such that

$$\alpha_j = \alpha' \times (1 - \mathrm{a} \times (1 - r_j)) \quad \text{(eq. 4.4)}$$

where α' is the baseline rate in untreated patients. All subsequent models build upon these assumptions.

4.2.2. Model 2: Introducing intraspecific strain competition

I next integrate intraspecific pathogen strain competition, as introduced in Chapter 2, into the above bacterial colonization model (equation 4.1). The resulting two-strain exclusive colonization model (**Figure 4.2**) is written as:

$$\frac{dS}{dt} = -S \times (\lambda_S + \lambda_R + \alpha_S + \alpha_R) + C^S \times (\gamma_S + \sigma_S) + C^R \times (\gamma_R + \sigma_R) + \Delta_S$$
$$\frac{dC^S}{dt} = S \times (\lambda_S + \alpha_S) - C^S \times (\gamma_S + \sigma_S) + \Delta_{C^S}$$
$$\frac{dC^R}{dt} = S \times (\lambda_R + \alpha_R) - C^R \times (\gamma_R + \sigma_R) + \Delta_{C^R}$$

(eq. 4.5)

where C^S and C^R denote patients colonized by a drug-sensitive strain P^S and a drug-resistant strain P^R, respectively. Strains are labelled as sensitive or resistant, but this should be interpreted as relative ($r_S < r_R$). For all parameters, subscripts *S* and *R* denote strain-specific rates, accounting for ecological differences between strains. Strain-specific levels of antibiotic resistance (r_S, r_R) drive strain-specific rates of antibiotic-induced clearance and endogenous acquisition (per equations 4.3 and 4.4), while the prevalence of each respective strain drives their forces of infection (per equation 4.2). To reflect potential metabolic costs associated with bearing the focal antibiotic resistance gene R,(Melnyk et al., 2015) we assumed that resistant strains P^R are naturally cleared at a faster rate than P^S, such that $\gamma_S < \gamma_R$. This is given by

$$\gamma_R = \gamma_S \times (1 + c)$$

(eq. 4.6)

where *c* is interpreted as the fitness cost of bearing the resistance gene R. Demography terms Δ_i expand to

$$\Delta_S = \mu \times ((1 - f_C) - S)$$
$$\Delta_{C^S} = \mu \times (f_C \times (1 - f_R) - C^S)$$
$$\Delta_{C^R} = \mu \times (f_C \times f_R - C^R)$$

(eq. 4.7)

where f_C is the proportion of newly admitted patients colonized with any pathogen strain,

and f_R the proportion of which bear the resistant strain.

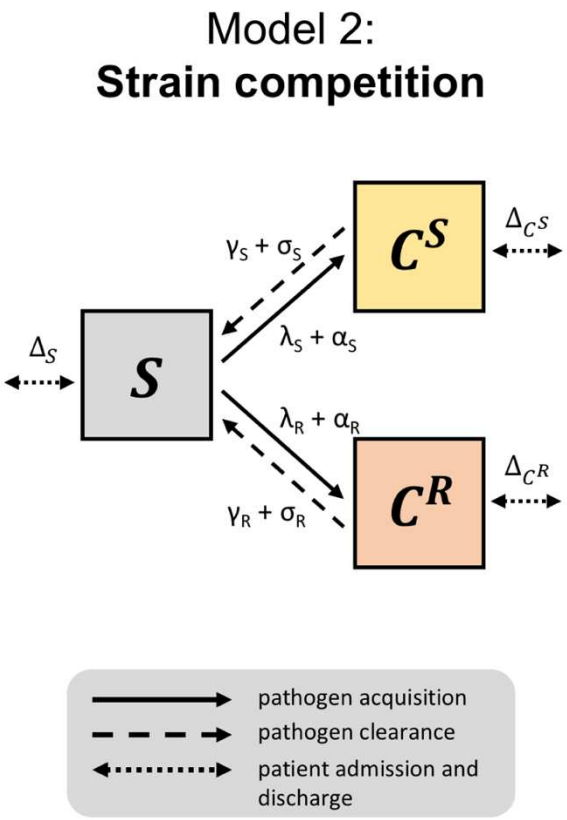

Figure 4.2. Model 2 flow diagram.

4.2.3. Model 3: Introducing interspecific microbiome-pathogen competition

I next propose a model in which (i) bacterial pathogens and commensal microbiota compete ecologically within the host, and (ii) antibiotic-induced microbiome dysbiosis disrupts these interactions, predisposing hosts to pathogen colonization. I consider three competitive within-host microbiome-pathogen interactions and conceptualize how they affect pathogen epidemiology (**Figure 4.3**).(Buffie et al., 2015; Hooper et al., 2003; Kamada et al., 2013a)

First, a stable microbiome can act as a barrier preventing introduced pathogens from establishing colonies. This *colonization resistance* (ε) is modelled as a reduced rate of pathogen transmission (β) to hosts with stable microbiota,

$$\beta_\varepsilon = (1 - \varepsilon) \times \beta$$

(eq. 4.8)

Second, co-colonizing bacteria can compete for space, nutrients and other limited resources within the host. In this case, antibiotics that reduce the density of potential

competitors may favour pathogen persistence. This *resource competition* (η) is modelled as a reduced rate of pathogen clearance (γ) among hosts undergoing dysbiosis,

$$\gamma_\eta = (1 - \eta) \times \gamma$$

(eq. 4.9)

Lastly, microbiome dysbiosis can favour the emergence or outgrowth of subdominant pathogen colonies, and this *ecological release* (ϕ) was modelled as an increased rate of endogenous pathogen acquisition (α) upon dysbiosis,

$$\alpha_\phi = \phi \times \alpha$$

(eq. 4.10)

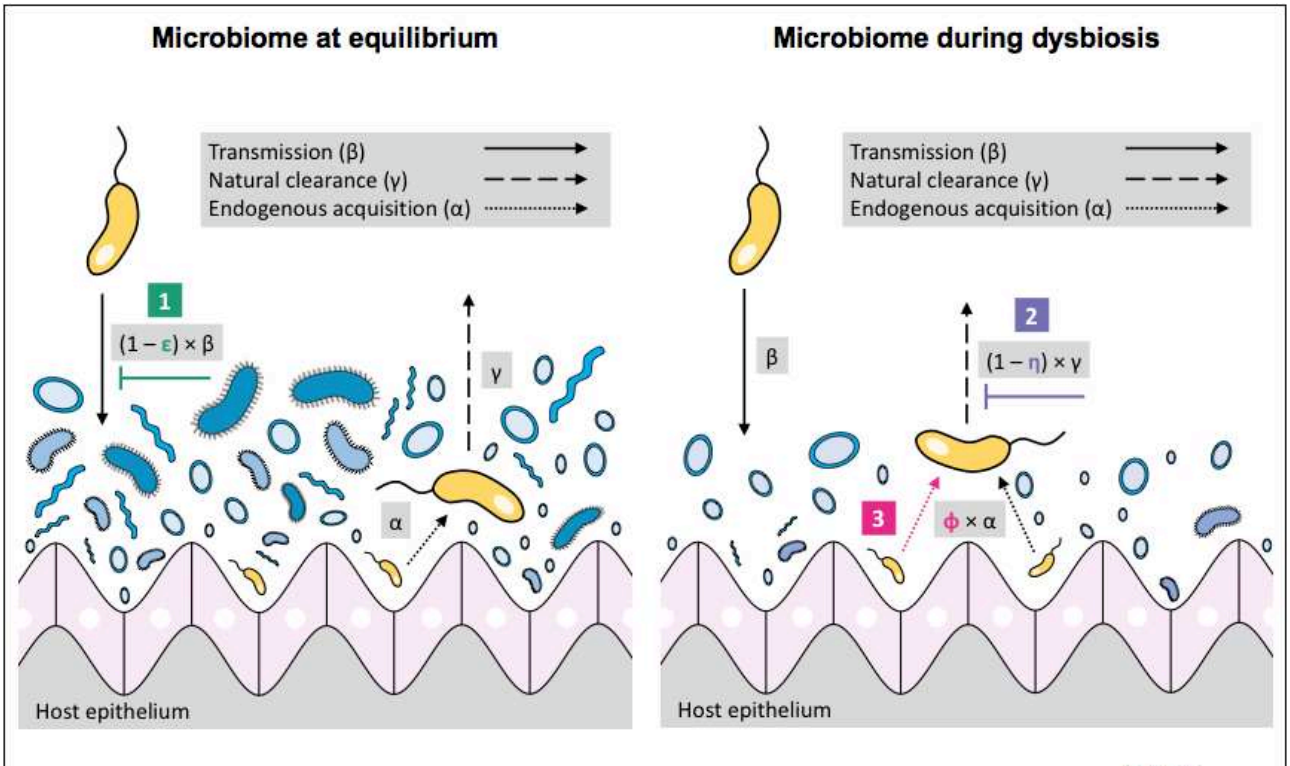

	Interaction	Interpretation	Example	Interval Base (min, max)
1.	Colonization resistance (ε)	Microbiota inhibit transmitted pathogen cells from establishing colonies	*Bacteroides* spp. produce angiogenins that inhibit *Enterococcus faecalis* colonies (Hooper et al., 2003)	0.5 (0.2, 0.8)
2.	Resource competition (η)	Loss of microbiota reduces competition, whether directly (e.g. more space and resources) or indirectly (e.g. reduced immune induction), facilitating pathogen persistence	Commensal *E. coli* compete with enterohaemorrhagic *E. coli* for organic and amino acids (Kamada et al., 2013a)	0.5 (0.2, 0.8)
3.	Ecological release (ϕ)	Loss of microbiota releases competition, frees up an ecological niche for subdominant pathogen emergence	*Clostridioides scindens* synthesize secondary bile acids that prevent outgrowth of subdominant *C. difficile* colonies (Buffie et al., 2015)	5 (2, 8)

Figure 4.3. Microbiome-pathogen interactions illustration.

Illustration of within-host ecological interactions between the host microbiome (blue) and a transmissible bacterial pathogen (yellow), and their impact on the pathogen's vital epidemiological parameters β (transmission rate), γ (clearance rate) and α (endogenous acquisition rate). To illustrate the latter: sub-dominant, non-transmissible colonies inhibited by microbiota are represented by small cartoon

pathogens, which can grow into dominant, transmissible colonies (large cartoon pathogens) via endogenous acquisition. Microbiome-pathogen interactions are assumed to differ between hosts with a stable microbiome at population dynamic equilibrium (left) and hosts experiencing antibiotic-induced microbiome dysbiosis (right). Interaction coefficients can be interpreted as terms explaining variation in host susceptibility to pathogen colonization, as depending on their recent history of antibiotic exposure. For interaction coefficient parameter values, broad intervals are assumed for the baseline analysis.

I integrate the microbiome, these three interactions, and antibiotic-induced microbiome dysbiosis into the single-strain model given by equation 4.1. The resulting 'microbiome competition model' (**Figure 4.4**) is given by

$$\frac{dS_e}{dt} = -S_e \times \left(\lambda_{R,\varepsilon} + \alpha_R + \sigma_m\right) + S_d \times \delta + C_e^R \times (\gamma_R + \sigma_R) + \Delta_{S_e}$$
$$\frac{dS_d}{dt} = S_e \times \sigma_m - S_d \times \left(\lambda_R + \alpha_{R,\phi} + \delta\right) + C_d^R \times \left(\gamma_{R,\eta} + \sigma_R\right) + \Delta_{S_d}$$
$$\frac{dC_e^R}{dt} = S_e \times \left(\lambda_{R,\varepsilon} + \alpha_R\right) - C_e^R \times (\gamma_R + \sigma_m + \sigma_R) + C_d^R \times \delta + \Delta_{C_e^R}$$
$$\frac{dC_d^R}{dt} = S_d \times \left(\lambda_R + \alpha_{R,\phi}\right) + C_e^R \times \sigma_m - C_d^R \times \left(\gamma_{R,\eta} + \delta + \sigma_R\right) + \Delta_{C_d^R}$$

(eq. 4.11)

describing colonization with a single pathogen strain across two host types: patients with a microbiome at dynamic equilibrium (subscript *e*) and those undergoing dysbiosis (subscript *d*). Antibiotics induce dysbiosis at a rate σ_m given by

$$\sigma_m = \mathrm{a} \times \theta_m$$

(eq. 4.12)

such that microbiome dysbiosis depends on both antibiotic exposure prevalence ($\mathbf{a}$) and the rate at which antibiotic exposure causes dysbiosis (θ_m). Accordingly, the same level of antibiotic exposure ($\mathbf{a}$) can have asymmetric effects on microbiome stability (via θ_m) and pathogen colonization (via $(1 - r_R) \times \theta_C$, as in equation 4.3). Dysbiosis can result in long-term changes to microbiome composition, but ecological function and population dynamic stability tend to recover in the days or weeks following antibiotic therapy,(Lozupone et al., 2012) represented here by microbiome recovery rate δ. However, microbiome stability is assumed not to recover among patients actively undergoing antibiotic treatment, such that

$$\delta = \delta' \times (1 - \mathrm{a})$$

(eq. 4.13)

where δ' is the baseline rate in untreated hosts. Lastly, demography terms Δ_i expand to

$$\Delta_{S_e} = \mu \times ((1 - f_C) \times (1 - f_d) - S_e)$$
$$\Delta_{S_d} = \mu \times ((1 - f_C) \times f_d - S_d)$$
$$\Delta_{C_e} = \mu \times (f_C \times (1 - f_d) - C_e)$$
$$\Delta_{C_d} = \mu \times (f_C \times f_d - C_d)$$

(eq. 4.14)

where f_d is the proportion of patients already experiencing antibiotic-induced microbiome dysbiosis upon hospital admission.

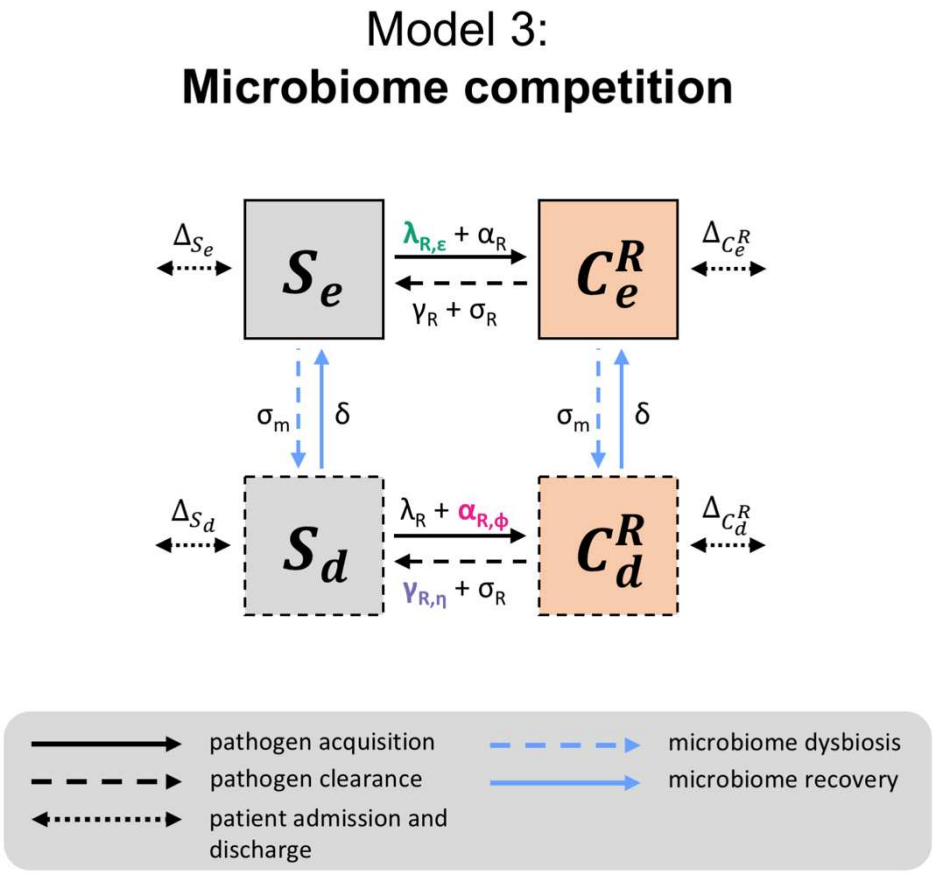

Figure 4.4. Model 3 flow diagram.

4.2.4. Model 4: Combined microbiome-strain competition

Strain competition and microbiome competition are not mutually exclusive: when combined in a two-strain "microbiome-strain competition" model, strains of the same species compete for hosts whose microbiota and history of antibiotic consumption influence susceptibility to colonization. Microbiome-pathogen interactions are assumed to be species- and not strain-specific, i.e. ε, η and ϕ apply equally to P^S and P^R. This fourth model (**Figure 4.5**) is given by:

$$\frac{dS_e}{dt} = -S_e \times \left(\lambda_{S,\varepsilon} + \lambda_{R,\varepsilon} + \alpha_S + \alpha_R + \sigma_m\right) + S_d \times \delta + C_e^S \times (\gamma_S + \sigma_S) + C_e^R \times (\gamma_R + \sigma_R) + \Delta_{S_e}$$

$$\frac{dS_d}{dt} = -S_d \times \left(\lambda_S + \lambda_R + \alpha_{S,\phi} + \alpha_{R,\phi} + \delta\right) + S_e \times \sigma_m + C_d^S \times \left(\gamma_{S,\eta} + \sigma_S\right) + C_d^R \times \left(\gamma_{R,\eta} + \sigma_R\right) + \Delta_{S_d}$$

$$\frac{dC_e^S}{dt} = S_e \times \left(\lambda_{S,\varepsilon} + \alpha_S\right) + C_d^S \times \delta - C_e^S \times (\gamma_S + \sigma_S + \sigma_m) + \Delta_{C_e^S}$$

$$\frac{dC_d^S}{dt} = S_d \times \left(\lambda_S + \alpha_{S,\phi}\right) + C_e^S \times \sigma_m - C_d^S \times \left(\delta + \gamma_{S,\eta} + \sigma_S\right) + \Delta_{C_d^S}$$

$$\frac{dC_e^R}{dt} = S_e \times \left(\lambda_{R,\varepsilon} + \alpha_R\right) + C_d^R \times \delta - C_e^R \times (\gamma_R + \sigma_R + \sigma_m) + \Delta_{C_e^R}$$

$$\frac{dC_d^R}{dt} = S_d \times \left(\lambda_R + \alpha_{R,\phi}\right) + C_e^R \times \sigma_m - C_d^R \times \left(\delta + \gamma_{R,\eta} + \sigma_R\right) + \Delta_{C_d^R}$$

(eq. 4.15)

where demography terms Δ_i expand to

$$\Delta_{S_e} = \mu \times ((1 - f_C) \times (1 - f_d) - S_e)$$

$$\Delta_{S_d} = \mu \times ((1 - f_C) \times f_d - S_d)$$

$$\Delta_{C_e^S} = \mu \times (f_C \times (1 - f_R) \times (1 - f_d) - C_e^S)$$

$$\Delta_{C_d^S} = \mu \times (f_C \times (1 - f_R) \times f_d - C_d^S)$$

$$\Delta_{C_e^R} = \mu \times (f_C \times f_R \times (1 - f_d) - C_e^R)$$

$$\Delta_{C_d^R} = \mu \times (f_C \times f_R \times f_d - C_d^R)$$

(eq. 4.16)

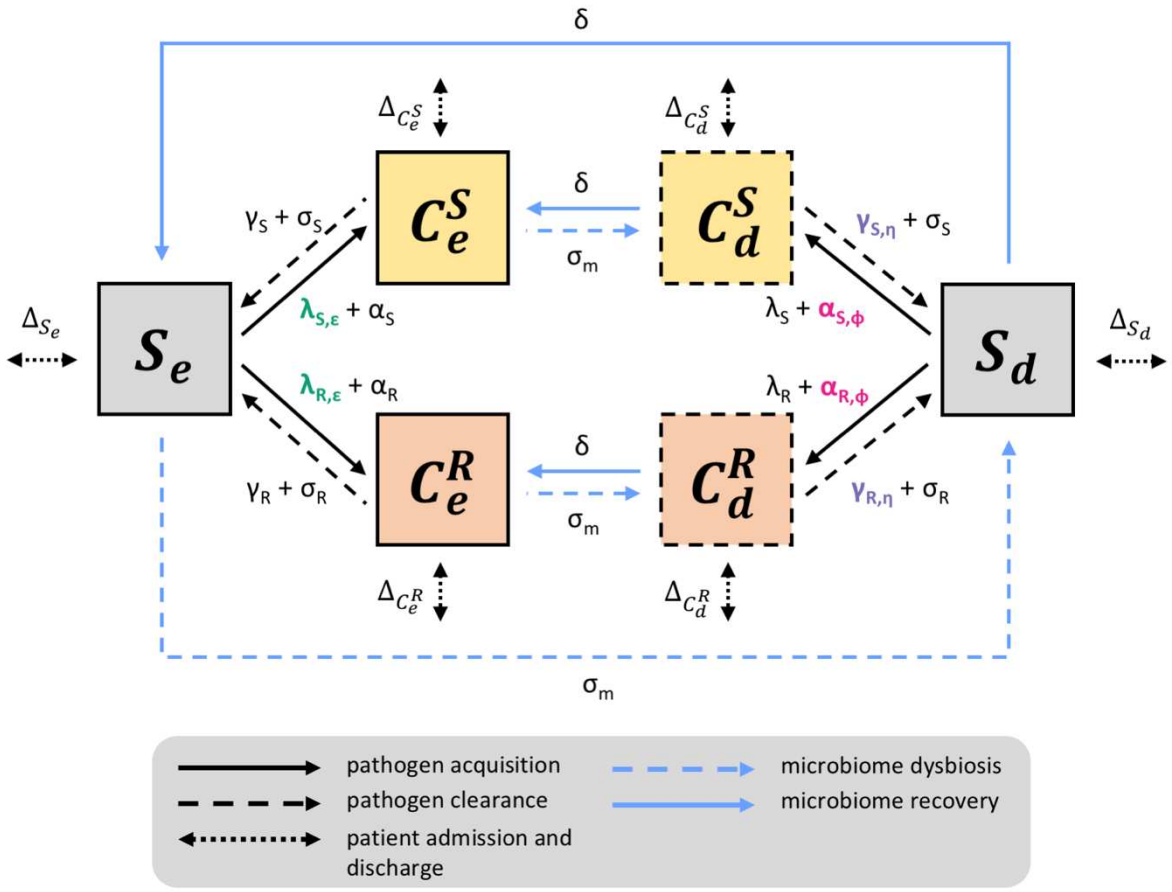

Figure 4.5. Model 4 flow diagram.

4.2.5. Model 5: Introducing interspecific horizontal gene transfer

The final model incorporates interspecific horizontal gene transfer (HGT) of a transmissible resistance gene R into the mixed microbiome-strain competition model. Here, HGT is conceptualized as two-way within-host transfer of the gene R, either from an R-bearing pathogen strain P^R to co-colonizing microbiota, or from R-bearing microbiota to a co-colonizing drug-sensitive pathogen strain P^S. Simplifying assumptions underlying this process include: (i) a symmetric rate of HGT (χ) from each donor, (ii) no loss of resistance upon donation, (iii) no accumulation of resistance (e.g. plasmid copy number dependence), (iv) that all patients bear microbiota capable of receiving and transferring R, (v) that dysbiosis can accelerate the rate of transfer ($\chi_d \geq \chi_e$), (vi) no impact of R on rates of microbiome dysbiosis and recovery, (vii) that a proportion f_ω of patients are admitted to hospital with microbiota bearing R, and lastly (viii) that microbiota of a proportion ω of patients can spontaneously acquire R subsequent to dysbiosis. The latter assumption was

made to reflect increased expression of antibiotic resistance genes among host microbiota following antibiotic therapy, and can be interpreted as a corollary to endogenous pathogen acquisition.(Ruppé et al., 2019) The resulting system of ODEs (**Figure 4.6**) is written as

$$\frac{dS_{e,s}}{dt} = -S_{e,s} \times \left(\lambda_{S,\varepsilon} + \lambda_{R,\varepsilon} + \alpha_S + \alpha_R + \sigma_m\right) + S_{d,s} \times \delta + C^S_{e,s} \times (\gamma_S + \sigma_S) + C^R_{e,s} \times (\gamma_R + \sigma_R) + \Delta_{S_{e,s}}$$

$$\frac{dS_{e,r}}{dt} = -S_{e,r} \times \left(\lambda_{S,\varepsilon} + \lambda_{R,\varepsilon} + \alpha_S + \alpha_R + \sigma_m\right) + S_{d,r} \times \delta + C^S_{e,r} \times (\gamma_S + \sigma_S) + C^R_{e,r} \times (\gamma_R + \sigma_R) + \Delta_{S_{e,r}}$$

$$\frac{dS_{d,s}}{dt} = S_{e,s} \times ((1-\omega) \times \sigma_m) - S_{d,s} \times \left(\lambda_S + \lambda_R + \alpha_{S,\phi} + \alpha_{R,\phi} + \delta\right) + C^S_{d,s} \times \left(\gamma_{S,\eta} + \sigma_S\right) + C^R_{d,s} \times \left(\gamma_{R,\eta} + \sigma_R\right) + \Delta_{S_{d,s}}$$

$$\frac{dS_{d,r}}{dt} = S_{e,s} \times (\omega \times \sigma_m) + S_{e,r} \times \sigma_m - S_{d,r} \times \left(\lambda_S + \lambda_R + \alpha_{S,\phi} + \alpha_{R,\phi} + \delta\right) + C^S_{d,r} \times \left(\gamma_{S,\eta} + \sigma_S\right) + C^R_{d,r} \times \left(\gamma_{R,\eta} + \sigma_R\right) + \Delta_{S_{d,r}}$$

$$\frac{dC^S_{e,s}}{dt} = S_{e,s} \times \left(\lambda_{S,\varepsilon} + \alpha_S\right) - C^S_{e,s} \times (\gamma_S + \sigma_S + \sigma_m) + C^S_{d,s} \times \delta + \Delta_{C^S_{e,s}}$$

$$\frac{dC^S_{e,r}}{dt} = S_{e,r} \times \left(\lambda_{S,\varepsilon} + \alpha_S\right) - C^S_{e,r} \times (\gamma_S + \sigma_S + \sigma_m + \chi_e) + C^S_{d,r} \times \delta + \Delta_{C^S_{e,r}}$$

$$\frac{dC^S_{d,s}}{dt} = S_{d,s} \times \left(\lambda_S + \alpha_{S,\phi}\right) + C^S_{e,s} \times \left((1-\omega) \times \sigma_m\right) - C^S_{d,s} \times (\gamma_{S,\eta} + \sigma_S + \delta) + \Delta_{C^S_{d,s}}$$

$$\frac{dC^S_{d,r}}{dt} = S_{d,r} \times \left(\lambda_S + \alpha_{S,\phi}\right) + C^S_{e,s} \times (\omega \times \sigma_m) + C^S_{e,r} \times \sigma_m - C^S_{d,r} \times (\gamma_{S,\eta} + \sigma_S + \delta + \chi_d) + \Delta_{C^S_{d,r}}$$

$$\frac{dC^R_{e,s}}{dt} = S_{e,s} \times \left(\lambda_{R,\varepsilon} + \alpha_R\right) - C^R_{e,s} \times (\gamma_R + \sigma_R + \sigma_m + \chi_e) + C^R_{d,s} \times \delta + \Delta_{C^R_{e,s}}$$

$$\frac{dC^R_{e,r}}{dt} = S_{e,r} \times \left(\lambda_{R,\varepsilon} + \alpha_R\right) + C^S_{e,r} \times \chi_e + C^R_{e,s} \times \chi_e - C^R_{e,r} \times (\gamma_R + \sigma_R + \sigma_m) + C^R_{d,r} \times \delta + \Delta_{C^R_{e,r}}$$

$$\frac{dC^R_{d,s}}{dt} = S_{d,s} \times \left(\lambda_R + \alpha_{R,\phi}\right) + C^R_{e,s} \times \left((1-\omega) \times \sigma_m\right) - C^R_{d,s} \times (\gamma_{R,\eta} + \sigma_R + \delta + \chi_d) + \Delta_{C^R_{d,s}}$$

$$\frac{dC^R_{d,r}}{dt} = S_{d,r} \times \left(\lambda_R + \alpha_{R,\phi}\right) + C^S_{d,r} \times \chi_d + C^R_{e,s} \times (\omega \times \sigma_m) + C^R_{e,r} \times \sigma_m + C^R_{d,s} \times \chi_d - C^R_{d,r} \times (\gamma_{R,\eta} + \sigma_R + \delta) + \Delta_{C^R_{d,r}}$$

(eq. 4.17)

which describes epidemiological colonization dynamics of a bacterial pathogen among host classes $H_{j,k}$ corresponding to patients of pathogen colonization status H (S, C^S, C^R), microbiome status j (*e*, equilibrium; or *d*, dysbiosis) and microbiome resistance profile k (*s*, not bearing R; *r*, bearing R). In this model, demography terms Δ_i expand to

$$\Delta_{S_{e,s}} = \mu \times \left((1 - f_C) \times (1 - f_d) \times (1 - f_\omega) - S_{e,s}\right)$$

$$\Delta_{S_{e,r}} = \mu \times \left((1 - f_C) \times (1 - f_d) \times f_\omega - S_{e,r}\right)$$

$$\Delta_{S_{d,s}} = \mu \times \left((1 - f_C) \times f_d \times (1 - f_\omega) - S_{d,s}\right)$$

$$\Delta_{S_{d,r}} = \mu \times \left((1 - f_C) \times f_d \times f_\omega - S_{d,r}\right)$$

$$\Delta_{C^S_{e,s}} = \mu \times \left(f_C \times (1 - f_R) \times (1 - f_d) \times (1 - f_\omega) - C^S_{e,s}\right)$$

$$\Delta_{C^S_{e,r}} = \mu \times \left(f_C \times (1 - f_R) \times (1 - f_d) \times f_\omega - C^S_{e,r}\right)$$

$$\Delta_{C^S_{d,s}} = \mu \times \left(f_C \times (1 - f_R) \times f_d \times (1 - f_\omega) - C^S_{d,s}\right)$$

$$\Delta_{C^S_{d,r}} = \mu \times \left(f_C \times (1 - f_R) \times f_d \times f_\omega - C^S_{d,r}\right)$$

$$\Delta_{C^R_{e,s}} = \mu \times \left(f_C \times f_R \times (1 - f_d) \times (1 - f_\omega) - C^R_{e,s}\right)$$

$$\Delta_{C^R_{e,r}} = \mu \times \left(f_C \times f_R \times (1 - f_d) \times f_\omega - C^R_{e,r}\right)$$

$$\Delta_{C^R_{d,s}} = \mu \times \left(f_C \times f_R \times f_d \times (1 - f_\omega) - C^R_{d,s}\right)$$

$$\Delta_{C^R_{d,r}} = \mu \times (f_C \times f_R \times f_d \times f_\omega - C^R_{d,r}$$

(eq. 4.18)

Model 5:

Microbiome-strain competition with HGT

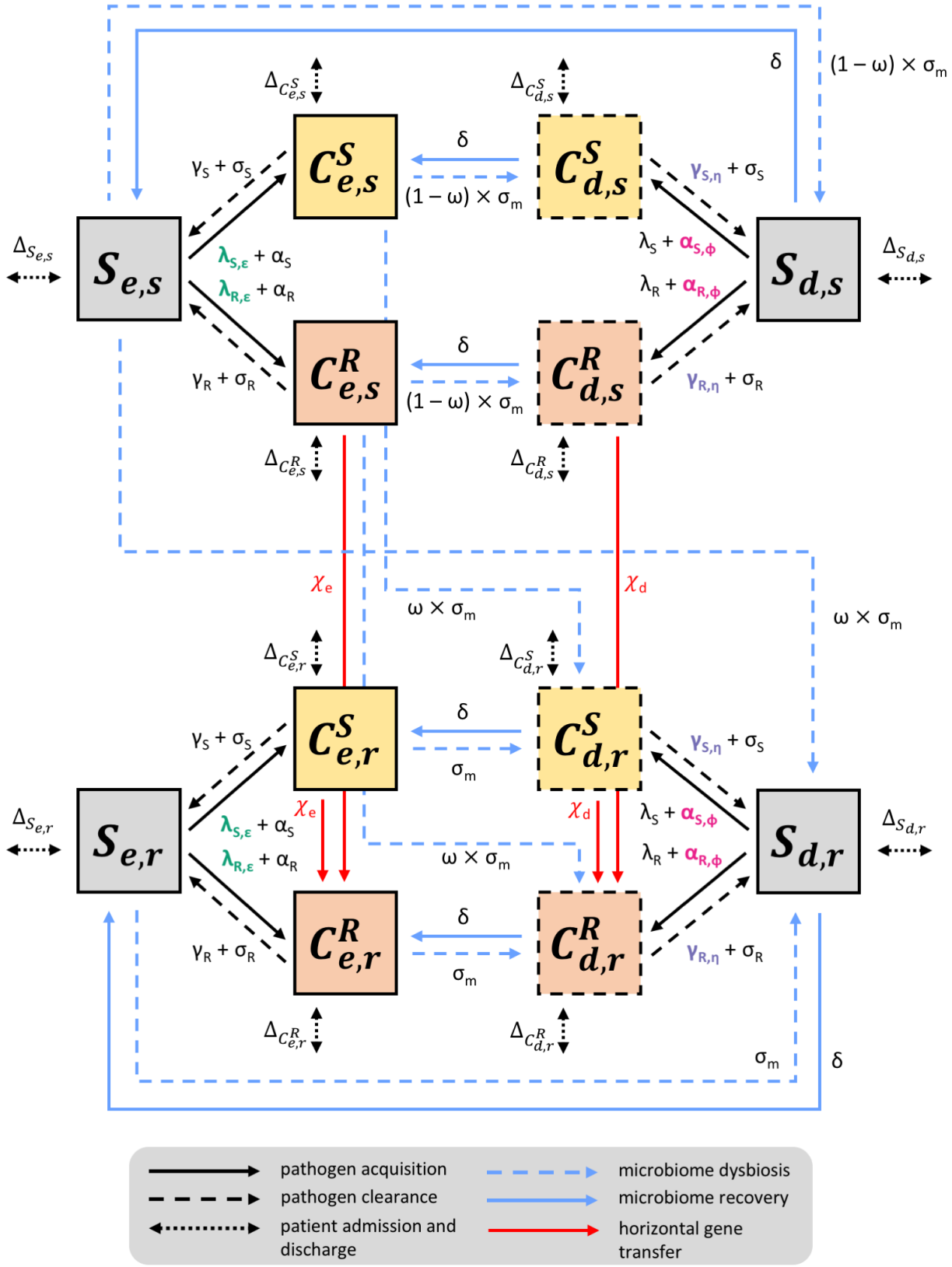

Figure 4.6. Model 5 flow diagram.

4.2.6. Numerical solutions

4.2.6.1. Numerical integration

For each model, ODEs were integrated numerically to calculate steady-state epidemiological outcomes. Integration was conducted by substituting a corresponding vector of numerical parameter values Ω and solving ODE systems using the lsoda method of the function *ode* from the package *deSolve* in R (version 3.6.0). To find steady-state solutions, integration was conducted until there was no change in state variables between times *t* and *t* + 1. Equilibria were corroborated by integrating the same ODE systems in Mathematica using the function NSolve, while restricting all solutions X to $0 \leq X \leq 1$.

4.2.6.2. Epidemiological outcomes

Three epidemiological outcomes were calculated from equilibrium ODE solutions for each Ω:

1. **Colonization prevalence**: the proportion of hospital patients colonized by (i) the drug-sensitive pathogen strain (C^S), (ii) the drug-resistant strain (C^R), or (iii) either strain ($C^S + C^R$) at population dynamic equilibrium
2. **Colonization incidence**: the daily rate of colonization acquisition within the hospital, calculated separately for each route of acquisition (patient-to-patient transmission, endogenous acquisition, HGT). Daily incidence was calculated at population dynamic equilibrium by solving ODE systems numerically for each Ω as described above, then using resulting equilibria as initial values for subsequent numerical integration from time *t* to *t* +1. For P^R in the final 12-compartment model, this is expressed as:

$$inc_\beta = \int_t^{t+1} \lambda_{R,\varepsilon} \times \left(S_{e,s} + S_{e,r}\right) + \lambda_R \times \left(S_{d,s} + S_{d,r}\right) dt$$

$$inc_\alpha = \int_t^{t+1} \alpha_R \times \left(S_{e,s} + S_{e,r}\right) + \alpha_{R,\phi} \times \left(S_{d,s} + S_{d,r}\right) dt$$

$$inc_\chi = \int_t^{t+1} \chi_e \times C_{e,r}^S + \chi_d \times C_{d,r}^S \, dt$$

(eq. 4.19)

3. **The resistance rate**: the proportion of patients colonized with the focal resistant strain P^R relative to the sensitive strain P^S, calculated using equilibrium prevalence values as $C^R/(C^S + C^R)$.

4.2.7. R_0 expressions

R_0 was calculated for P^R across Models 1, 2, 3 and 4, and was interpreted as the expected number of secondary patients colonized by an index patient in a fully susceptible (uncolonized) hospital population (i.e. at *disease-free equilibrium*, DFE, as indicated by the symbol ^ above state variables). To reflect this epidemiological context, two additional assumptions were made specifically for R_0 calculations: no P^R input from the community ($f_R = 0$), and that the rate of endogenous acquisition α_R scales linearly with its current colonization prevalence C^R. R_0 expressions were derived following van den Driessche.(van den Driessche, 2017)

For the susceptible-colonized model (Model 1),

$$R_0 = \hat{S}\frac{\beta + \alpha_R}{\gamma_R + \sigma_R + \mu} \quad \text{(eq. 4.20)}$$

where $\hat{S} = 1$, such that P^R has higher R_0 with increasing rates of transmission (β) or endogenous acquisition (α_R), but lower R_0 with an increasing rate of natural clearance (γ_R). Higher rates of effective antibiotic treatment (σ_R) and patient admission and discharge (μ) also reduce R_0.

For the strain competition model (Model 2), R_0 is derived for P^R assuming that P^S is at endemic equilibrium with input from the community ($f_C > 0$, $f_R = 0$). In this context, the same R_0 expression was found as for the susceptible-colonized model (equation 4.20), except R_0 is reduced because of a lower equilibrium prevalence of susceptible hosts when P^S is endemic ($\hat{S} < 1$). DFE were not found analytically for models with strain competition and were solved numerically (details below).

For the microbiome model (Model 3), R_0 was calculated using next-generation theory as the spectral radius of the next-generation matrix (NGM),

$$R_0 = \rho(\mathbf{NGM}) \quad \text{(eq. 4.21)}$$

where NGM is the product of the transmission matrix **F** (describing the rates at which existing colonies cause colonization in new hosts) and the inverse transition matrix **V** (describing the rates at which colonized hosts shift between colonized classes or are

removed). These are given by

$$\mathbf{F} = \begin{pmatrix} (\alpha_R + (1-\varepsilon)\times\beta)\times\hat{S}_e & (\alpha_R + (1-\varepsilon)\times\beta)\times\hat{S}_e \\ (\alpha_R\times\phi+\beta)\times\hat{S}_d & (\alpha_R\times\phi+\beta)\times\hat{S}_d \end{pmatrix}$$

(eq. 4.22)

and

$$\mathbf{V} = \begin{pmatrix} \gamma_R+\sigma_R+\sigma_m+\mu & -\delta \\ -\sigma_m & \delta+(1-\eta)\times\gamma_R+\sigma_R+\mu \end{pmatrix}$$

(eq. 4.23)

which give

$$R_0 = \frac{\hat{S}_e\times(\alpha_R+(1-\varepsilon)\times\beta)(\delta+(1-\eta)\times\gamma_R+\sigma_m+\sigma_R+\mu)+\hat{S}_d\times(\alpha_R\times\phi+\beta)(\delta+\gamma_R+\sigma_m+\sigma_R+\mu)}{(\sigma_R+\mu)(\delta+\sigma_m+\sigma_R+\mu)+\big(\delta+\sigma_R+\mu+(1-\eta)\times(\sigma_m+\sigma_R+\mu)\big)\times\gamma_R+(1-\eta)\times\gamma_R^2}$$

(eq. 4.24)

where the two terms in the numerator correspond to P^R acquisition, respectively, in hosts with a stable microbiome and in those undergoing dysbiosis. Antibiotic-induced dysbiosis (σ_m) and treatment (σ_R) are found in both numerator and denominator.

When assuming no microbiome-pathogen interactions ($\varepsilon=0,\eta=0,\phi=1$), DFE is

$$\{\hat{S}_e,\hat{S}_d,\hat{C}_e,\hat{C}_d\} = \left\{\frac{\mu\times(1-f_d)+\delta}{\sigma_m+\mu+\delta},\frac{\mu\times f_d+\sigma_m}{\sigma_m+\mu+\delta},0,0\right\}$$

(eq. 4.25)

and R_0 reduces to the same expression as given by the susceptible-colonized model

$$R_0 = \frac{\beta+\alpha_R}{\gamma_R+\sigma_R+\mu}$$

(eq. 4.26)

Finally, for the microbiome-strain competition model (Model 4), the same R_0 expression is found for P^R, but when P^S is endemic,

$$\hat{S}_e+\hat{S}_d<1$$

(eq. 4.27)

so strain competition dampens R_0 relative to the single-strain microbiome competition

model, all else being equal.

4.2.8. Parameterization and analysis

All models were parameterized to represent the same generic antibiotic-resistant pathogen (P^R), varying only its ecological interactions with other bacteria from one model to the next (parameter values in **Table 4.1**; note that not all parameters are present in all models). Univariate and bivariate analysis were conducted to evaluate how key parameters affected epidemiological outcomes (prevalence, incidence, resistance rate, R_0), with a focus on impacts of the patient population's antibiotic exposure prevalence ($\mathbf{a}$), rates of antibiotic-induced pathogen clearance (θ_C) and microbiome dysbiosis (θ_m), the focal pathogen strain's intrinsic antibiotic resistance level (r_R), and mediating impacts of microbiome-pathogen interactions (ε, η, ϕ) and horizontal gene transfer (χ_e, χ_d).

Table 4.1. Parameter values for a theoretical nosocomial pathogen.

Parameter values and ranges for a generic pathogen P circulating in a hospital population, evaluated across five different colonization models. For endogenous acquisition and microbiome recovery, rates presented are assumed rates in untreated hosts, represented by the ' (prime) symbol. Model 1: susceptible-colonized model (equation 4.1); Model 2: strain competition model (equation 4.5); Model 3: microbiome competition model (equation 4.11); Model 4: microbiome-strain competition model (equation 4.15); Model 5: microbiome-strain competition model with HGT (equation 4.17).

Symbol	Parameter	Unit	Value {Range}	Model 1	2	3	4	5
Pathogen colonization								
β	transmission rate	day^{-1}	0.2	X	X	X	X	X
α'	endogenous acquisition rate	day^{-1}	0.01	X	X	X	X	X
γ	natural clearance rate	day^{-1}	0.03	X	X	X	X	X
c	fitness cost of resistance	/	1	X	X	X	X	X
Patient demography								
μ	admission / discharge rate	day^{-1}	0.1	X	X	X	X	X
f_C	admission fraction (colonized)	/	0.1	X	X	X	X	X
f_R	admission fraction (bearing resistant strain)	/	0.5	X	X	X	X	X
f_d	admission fraction (dysbiosis)	/	0			X	X	X
f_ω	admission fraction (microbiota bearing resistance gene)	/	0					X
Antibiotics								
a	antibiotic exposure prevalence	/	0.2 {0 – 1}	X	X	X	X	X
r_R	antibiotic resistance level (P^R)	/	0.8 {0 – 1}	X	X	X	X	X
r_S	antibiotic resistance level (P^S)		0		X		X	X
θ_c	antibiotic-induced pathogen clearance rate	day^{-1}	0.2	X	X	X	X	X
θ_m	antibiotic-induced microbiome dysbiosis rate	day^{-1}	1			X	X	X
Microbiome ecology								
ε	colonization resistance	/	0.5 {0.2 – 0.8}			X	X	X
η	resource competition	/	0.5 {0.2 – 0.8}			X	X	X
ϕ	ecological release	/	5 {2 – 8}			X	X	X
χ_e	HGT rate (equilibrium)	day^{-1}	{0, 0.01, 0.1}					X
χ_d	HGT rate (dysbiosis)	day^{-1}	$\chi_e \times 10$					X
δ'	microbiome recovery rate	day^{-1}	0.143			X	X	X
ω	proportion of patients whose microbiota acquire the resistance gene following antibiotic exposure	/	0.01					X

4.2.9. Modelling antibiotic stewardship interventions

Finally, theoretical antibiotic stewardship interventions were implemented to evaluate their impacts on epidemiological dynamics of endemic P^R in the context of co-circulating P^S and different microbiome-pathogen interactions. Three interventions were conceptualized:

1. **Targeted local prescribing:** avoiding antibiotics that are ineffective against C^R, with no change in impact on C^S or microbiome stability (halving r_R from 0.8 to 0.4)
2. **Microbiome protection:** prioritizing antibiotics that have a lower impact on microbiome dysbiosis, with no change in impact on pathogen colonization (halving θ_m from 1.0 to 0.5)
3. **Judicious prescribing:** reducing overall antibiotic exposure prevalence, with no change in the distribution of antibiotics used (halving **a** from 0.2 to 0.1)

In the context of these interventions, the same generic pathogen P^R described above was simulated across distinct scenarios: (i) in the absence of any microbiome-pathogen competition, (ii) including each microbiome-pathogen competition coefficient (ε, η, ϕ) separately, and lastly (iii) combining all three coefficients. Interventions were implemented sequentially to evaluate their successive impacts on colonization dynamics over a one-year period. ODEs were solved using numerical integration, as described above, with interventions introduced at day 90 (intervention 1), day 180 (intervention 2), and day 270 (intervention 3).

4.3. Results: impacts of within-host ecological interactions on pathogen colonization dynamics

4.3.1. No interactions (Model 1)

In the absence of within-host ecological interactions in the single-strain pathogen colonization Model 1, antibiotic consumption does not select for the epidemiological spread of resistance. When assuming complete antibiotic resistance (r_R = 1.0; **Figure 4.7B**), all antibiotic-related terms drop out of equation 4.1, and antibiotic use has no impact on C^R (colonization prevalence of the focal strain P^R). When assuming incomplete antibiotic resistance (r_R < 1.0; **Figure 4.7A**), antibiotic-induced pathogen clearance is maintained, resulting in decreasing C^R with increasing **a**. This is consistent with the R_0 expression for this model, in which ineffective antibiotic treatment (r_R = 1.0) has no impact, in which effective antibiotic treatment (r_R < 1.0) reduces R_0, and in which there are no positive relationships between **a** and any terms in the numerator. As a result, R_0 decreases with increasing **a**, or remains static if C^R is perfectly antibiotic-resistant (**Figure 4.8A**).

4.3.2. Strain competition (Model 2)

With the introduction of strain competition (Model 2), increasing antibiotic consumption can favour the epidemiological spread of resistance. When P^R is resistant to all antibiotics (r_R = 1), its prevalence C^R increases monotonically with increasing antibiotic exposure (**a**), due to increased clearance of the drug-sensitive strain P^S and its subsequent replacement by P^R (**Figure 4.7E**). When resistance is partial – when P^R is still cleared by antibiotics, but at a lower rate than P^S (r_S < r_R < 1) – C^R is maximized at intermediate antibiotic exposure, owing to a trade-off in how antibiotics both clear P^R through effective antibiotic treatment, and facilitate P^R through preferential clearance of P^S (**Figure 4.7B**). As such, R_0 for P^R tends to increase with antibiotic use when P^R is highly resistant to antibiotics (high r_R), but decrease when still largely sensitive (low r_R) (**Figure 4.8B**). In this way, antibiotic selection for the epidemiological spread of resistance depends on how antibiotics affect both drug-sensitive and drug-resistant strains.

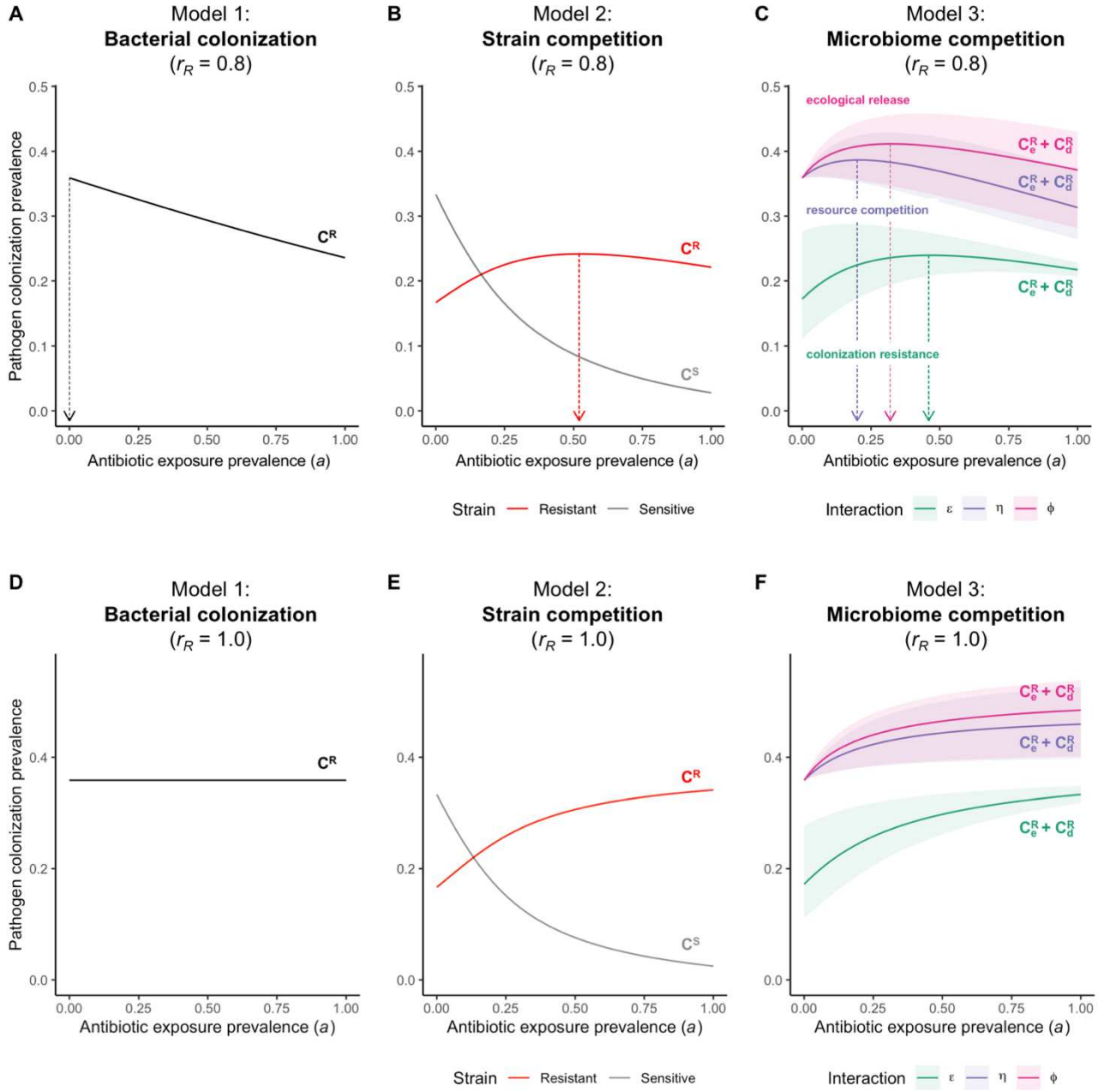

Figure 4.7. Antibiotic selection for resistance.

In contrast to predictions from a model with no ecological competition (**A**, **D**), models including strain competition (**B**, **E**) or microbiome competition (**C**, **F**) can explain how antibiotics select for the epidemiological spread of antibiotic-resistant bacteria. Equilibrium pathogen prevalence is shown as a function of antibiotic exposure prevalence (**a**), assuming partial antibiotic resistance for the top panels **A**, **B** and **C** (r_R = 0.8), and complete antibiotic resistance for the bottom panels **D**, **E** and **F** (r_R = 1.0). For **B** and **E**, P^S and P^R circulate simultaneously, assuming strain-specific differences in antibiotic resistance (r_S = 0, r_R = {0.8, 1.0}), natural clearance (γ_S = 0.03 day^{-1}, γ_R = 0.06 day^{-1}) and transmission ($\lambda_S = \beta \times C^S/N$, $\lambda_R = \beta \times C^R/N$). For **C** and **F**, epidemiological dynamics are evaluated independently for each interaction and superimposed (ε = colonization resistance; η = resource competition; ϕ = ecological release); shaded intervals represent outcomes across the range of values considered for each interaction (see **Figure 4.3**); and antibiotics are assumed to induce dysbiosis after 1 day (θ_m = 1 day^{-1}), from which microbiome stability recovers after 7 days (δ = 1/7 day^{-1}). Dashed vertical arrows denote the levels of antibiotic use that maximize C^R (colonization prevalence of P^R), and are omitted from **D**, **E** and **F**, as C^R is always maximized at **a** = 1.0 when the pathogen is completely drug-resistant. ODEs are integrated numerically using the same parameter values representing a generic nosocomial pathogen P (see **Table 4.1**).

4.3.3. Microbiome-pathogen competition (Model 3)

Independent of strain competition, microbiome-pathogen interactions (Model 3) can also explain antibiotic selection for the spread of resistance. Included microbiome-pathogen interactions are all mechanisms by which increasing antibiotic consumption can favour P^R colonization. Like strain competition, microbiome competition was found to underlie a selection trade-off: C^R and R_0 increase monotonically with antibiotic exposure when P^R is completely antibiotic-resistant (r_R = 1) (**Figure 4.7F**), but can peak at intermediate antibiotic exposure when resistance is partial (0 < r_R < 1) (**Figure 4.7C**). This is because, in this scenario, antibiotics simultaneously clear P^R colonization and induce greater host susceptibility to P^R colonization through dysbiosis. Each individual microbiome-pathogen interaction results in different epidemiological responses to antibiotic use, and in distinct selection trade-offs, hence predicting different levels of antibiotic exposure that maximize C^R (**Figure 4.7C**).

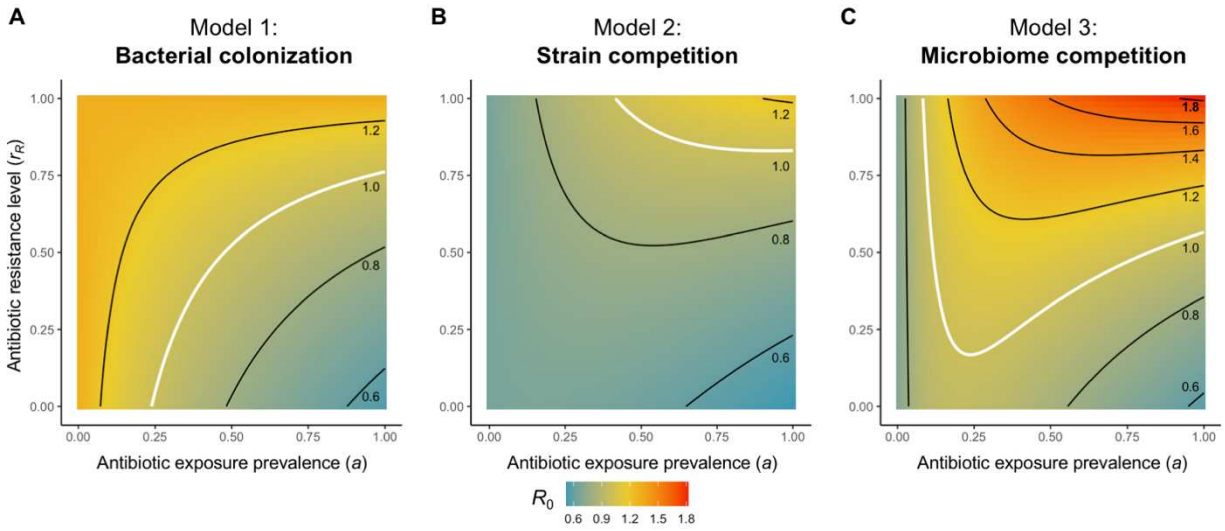

Figure 4.8. R_0 evaluation for Models 1, 2 and 3.

Numerical evaluation of the basic reproduction number (R_0) of P^R as a function of **a** and r_R for Models 1 to 3. White contour lines indicate R_0 = 1, above which a single colonized patient admitted to a naïve hospital population is expected to trigger an outbreak. For **C**, all three microbiome-pathogen interactions are applied simultaneously.

Like in the strain competition model, R_0 for P^R in the microbiome competition model tends to increase with antibiotic use when P^R is highly resistant to antibiotics (high r_R); however, impacts of antibiotics are more heterogeneous when P^R is largely antibiotic-sensitive (low r_R) (**Figure 4.8C**). When multiple microbiome-pathogen interactions are combined, this antibiotic selection trade-off becomes more pronounced. This is seen in **Figure 4.9**, where

R_0 is evaluated in the context of each microbiome-pathogen interaction separately, and in concert, over a range of assumed values. Colonization resistance (ε) is found to dampen R_0 of P^R, while resource competition (η) and ecological release (ϕ) augment it. When microbiota simultaneously limit multiple colonization processes (transmission, emergence, persistence), patients with stable microbiota are more protected from pathogen colonization, but increasing antibiotic use selects more strongly for P^R spread. Taken together, strong microbiome-pathogen interactions can protect patients from P^R colonization in some conditions (e.g. at low **a**), while predisposing them to P^R colonization in others (high **a** and r_R).

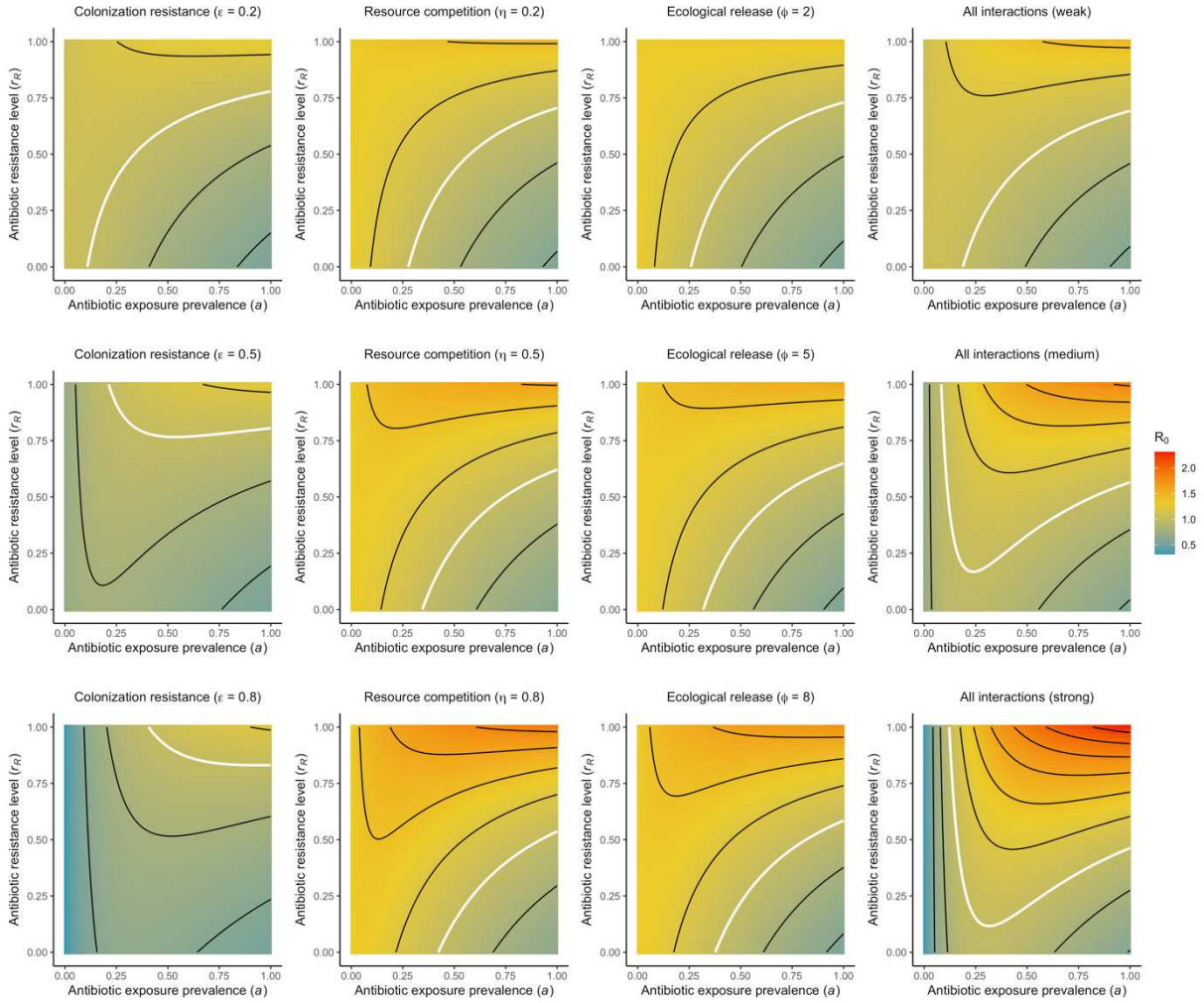

Figure 4.9. R_0 evaluation across microbiome-pathogen interactions.

Different microbiome-pathogen interactions of different strengths (figure titles) mediate how antibiotic use (**a**, x-axis) and resistance (r_R, y-axis) drive R_0 for P^R (z-axis, colour) in Model 3 (equation 4.11). White contour lines indicate R_0=1, and each successive black contour line represents an incremental change of 0.2. Microbiome-pathogen interactions are included separately (columns 1, 2, 3) and together (column 4), and their strengths are varied from low (top row) to medium (middle row) to high (bottom row) using values from the illustration in **Figure 4.3**. See **Table 4.1** for parameter values.

4.3.4. Microbiome-strain competition (Model 4)

Introducing a drug-sensitive strain P^S to the microbiome model dampens R_0 of the focal strain P^R, because fewer patients are susceptible to colonization when the competing strain co-circulates in the population (evaluated numerically in **Figure 4.10**). However, antibiotic use makes way for P^R not only through preferential clearance of P^S, but remaining P^R also benefit preferentially from increased host susceptibility to colonization when antibiotics cause dysbiosis. Accordingly, antibiotics that both disrupt host microbiota and clear drug-sensitive pathogen strains tend to select more strongly for the spread of resistant strains than antibiotics that only target one or the other (**Figure 4.11**).

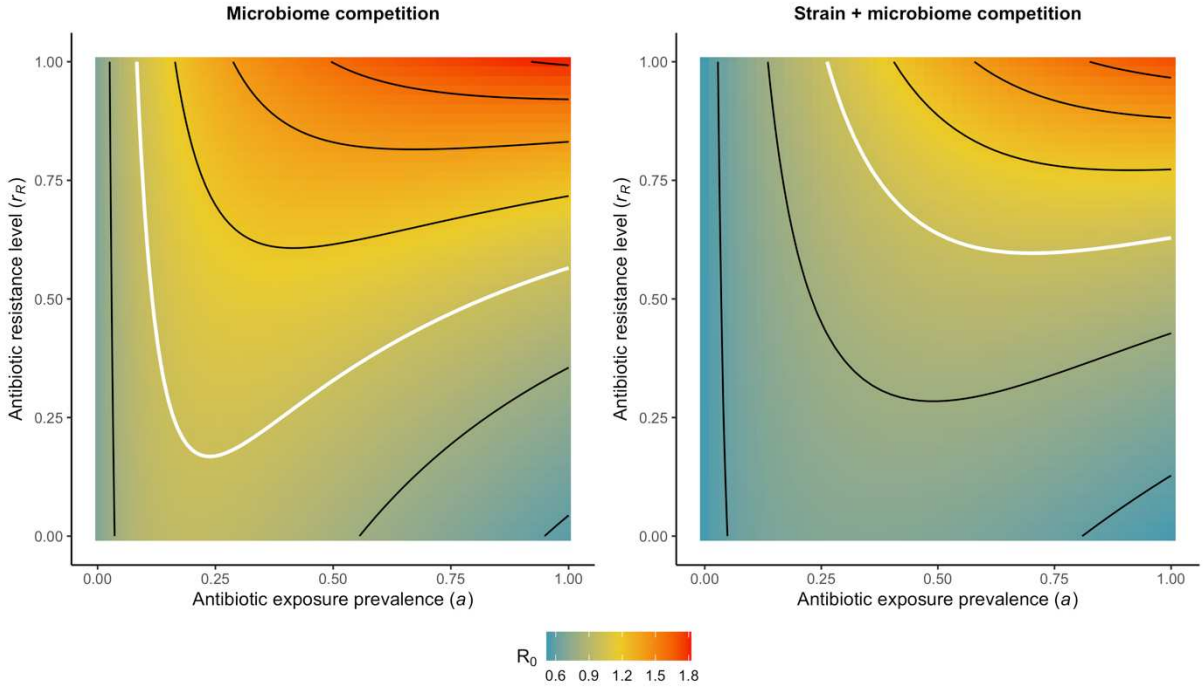

Figure 4.10. R_0 evaluation for microbiome-strain competition.

Introducing strain competition to the microbiome competition model reduces R_0 for P^R. Over the whole parameter space, the focal strain P^R of a two-strain microbiome competition model (right, Model 4) has a lower R_0 than the same pathogen evaluated in the absence of strain competition (left, Model 3). The competing strain P^S is at endemic equilibrium and is completely sensitive to antibiotics (r_S=0). White contour lines indicate R_0=1, and each successive black contour line represents an incremental change of 0.2. See **Table 4.1** for parameter values.

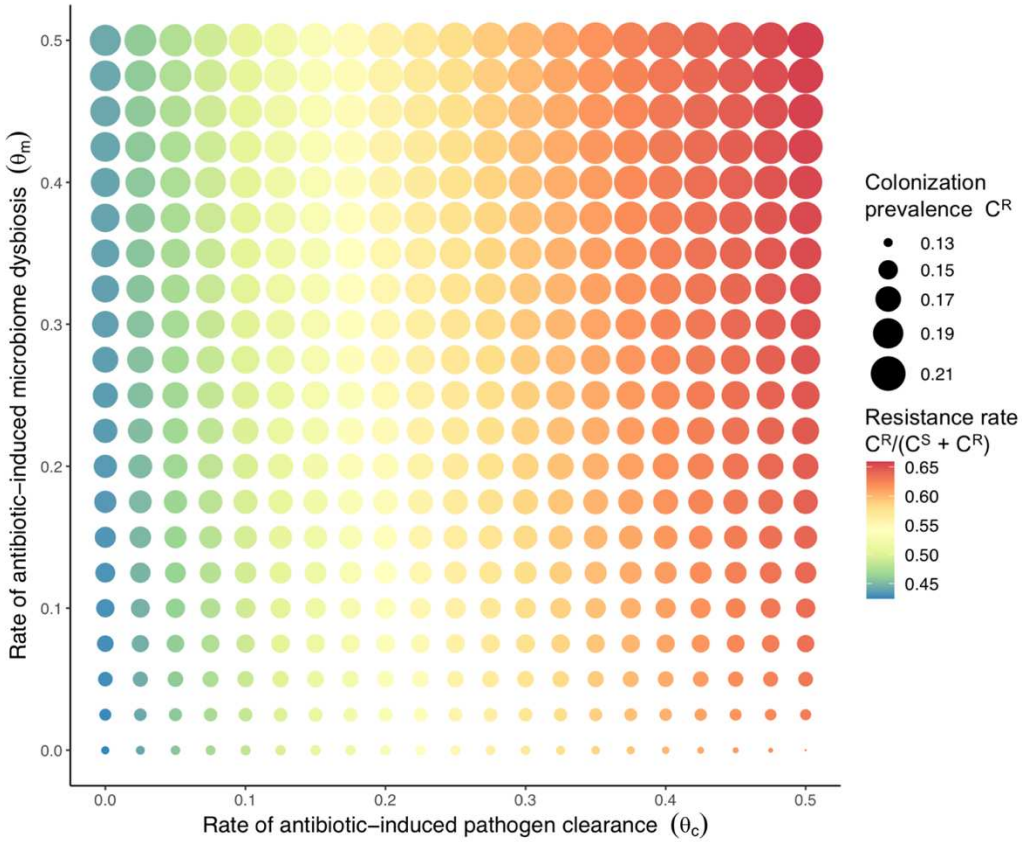

Figure 4.11. Heterogeneous antibiotic impacts across indicators (1/2).

Strain competition and microbiome competition as simultaneous forces of antibiotic selection for resistance. In a mixed microbiome-strain competition model (Model 4), prevalence of P^R (C^R, circle size) and the pathogen's resistance rate (colour) depend on the relative rates at which antibiotics disrupt microbiota (θ_m) and clear pathogen colonization (θ_C). Antibiotics with a stronger effect on pathogen clearance (higher θ_C) increase the resistance rate, while antibiotics that cause more dysbiosis (higher θ_m) increase prevalence.

Overall, links between antibiotic consumption and different indicators of P^R colonization (prevalence, resistance rate) are heterogeneous in the context of different microbiome-pathogen interactions (ε, η, ϕ), different levels of antibiotic resistance (r_R), and asymmetric impacts of antibiotics on microbiome dysbiosis and pathogen clearance (θ_m, θ_C). Antibiotics with stronger impacts on pathogen clearance (higher θ_C) led to increased resistance rates, while impacts on prevalence of the resistant strain were modest and depended on potential interactions with the microbiome. Conversely, antibiotics with stronger impacts on microbiome stability (higher θ_m) led to higher prevalence of the resistant strain, with modest impacts on resistance rates (**Figure 4.11**). Further, impacts of antibiotic treatment on resistance rates were greater when P^R resisted a greater share of antibiotics (higher r_R), while impacts on prevalence were greater when microbiome-pathogen interactions were stronger (higher ε, η, ϕ) (**Figure 4.12**).

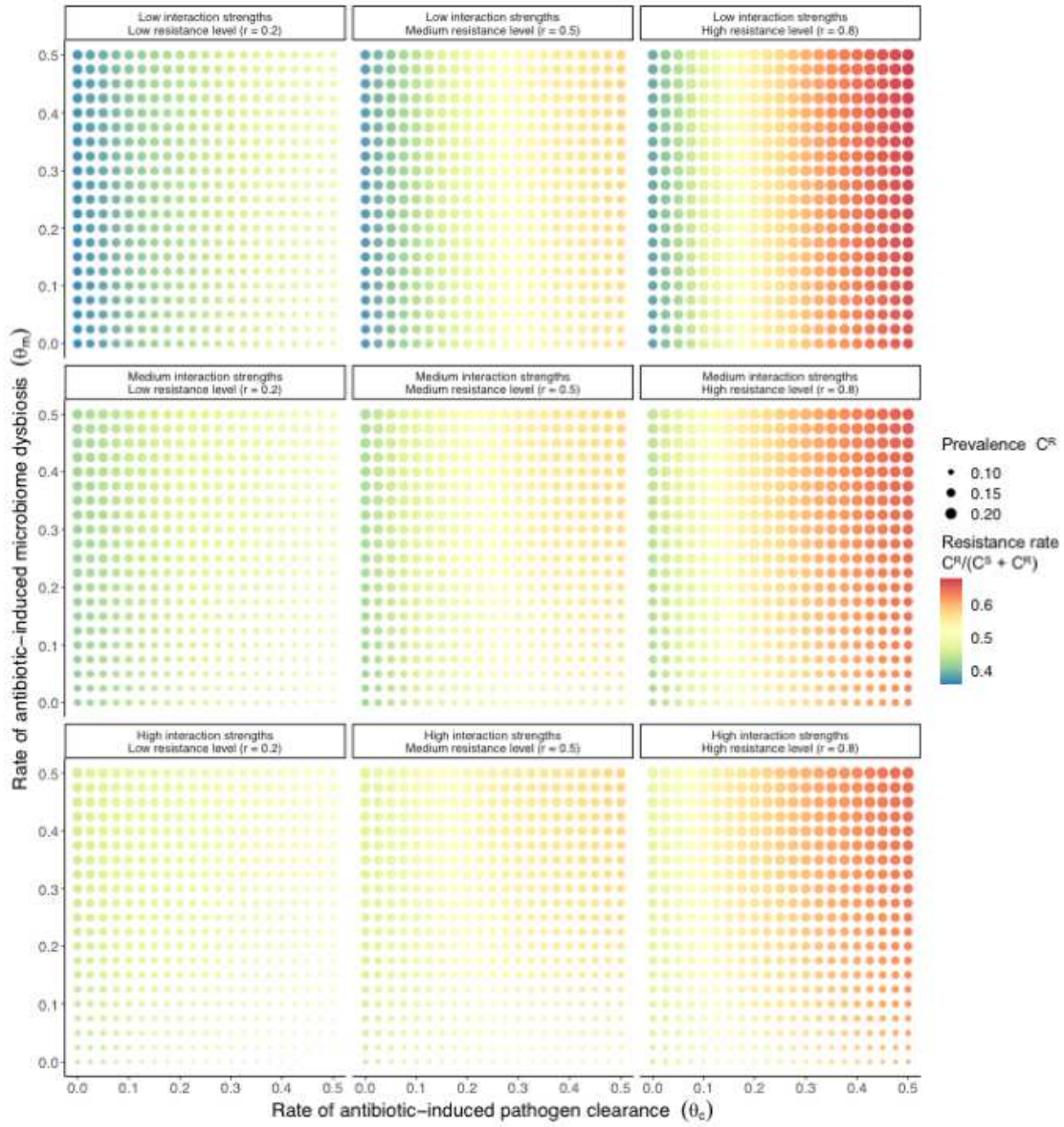

Figure 4.12. Heterogeneous antibiotic impacts across indicators (2/2).

Antibiotic selection for the spread of an antibiotic-resistant pathogen strain P^R depends on the strength of its interactions with microbiota (rows) and its level of resistance to antibiotics r_R (columns). Complete antibiotic sensitivity is assumed for P^S (r_S = 0), and low, medium and high interactions strengths correspond to values in the illustration in **Figure 4.3** ({ε = 0.2, η = 0.2, ϕ = 2}, {ε = 0.5, η = 0.5, ϕ = 5} and {ε = 0.8, η = 0.8, ϕ = 8}, respectively). See **Table 4.1** for parameter values.

4.3.5. Horizontal gene transfer (Model 5)

Overall, an increasing rate of within-host HGT (χ) was found to increase the spread of P^R, regardless of other microbiome-pathogen interactions and across indicators (incidence, prevalence and resistance rate; **Figure 4.13**). Impacts of HGT on C^R colonization (the difference between the solid lines and dotted/dashed lines in **Figure 4.13**) were greatest at intermediate antibiotic exposure (**a**). Under the present modelling assumptions, HGT-driven gains in C^R result from symmetric declines in C^S, such that HGT's potential to drive P^R colonization dynamics depends on the presence of both sufficient resistance donors

and sufficient recipients. This results in non-linear feedbacks between HGT and other processes that drive strain prevalence. In particular, high **a** affords a selective advantage to the strain P^R bearing the transmissible resistance gene, increasing the potential impact of HGT on C^R; but high **a** also reduces the pool of recipient P^S, ultimately limiting HGT's ability to contribute to increases in C^R.

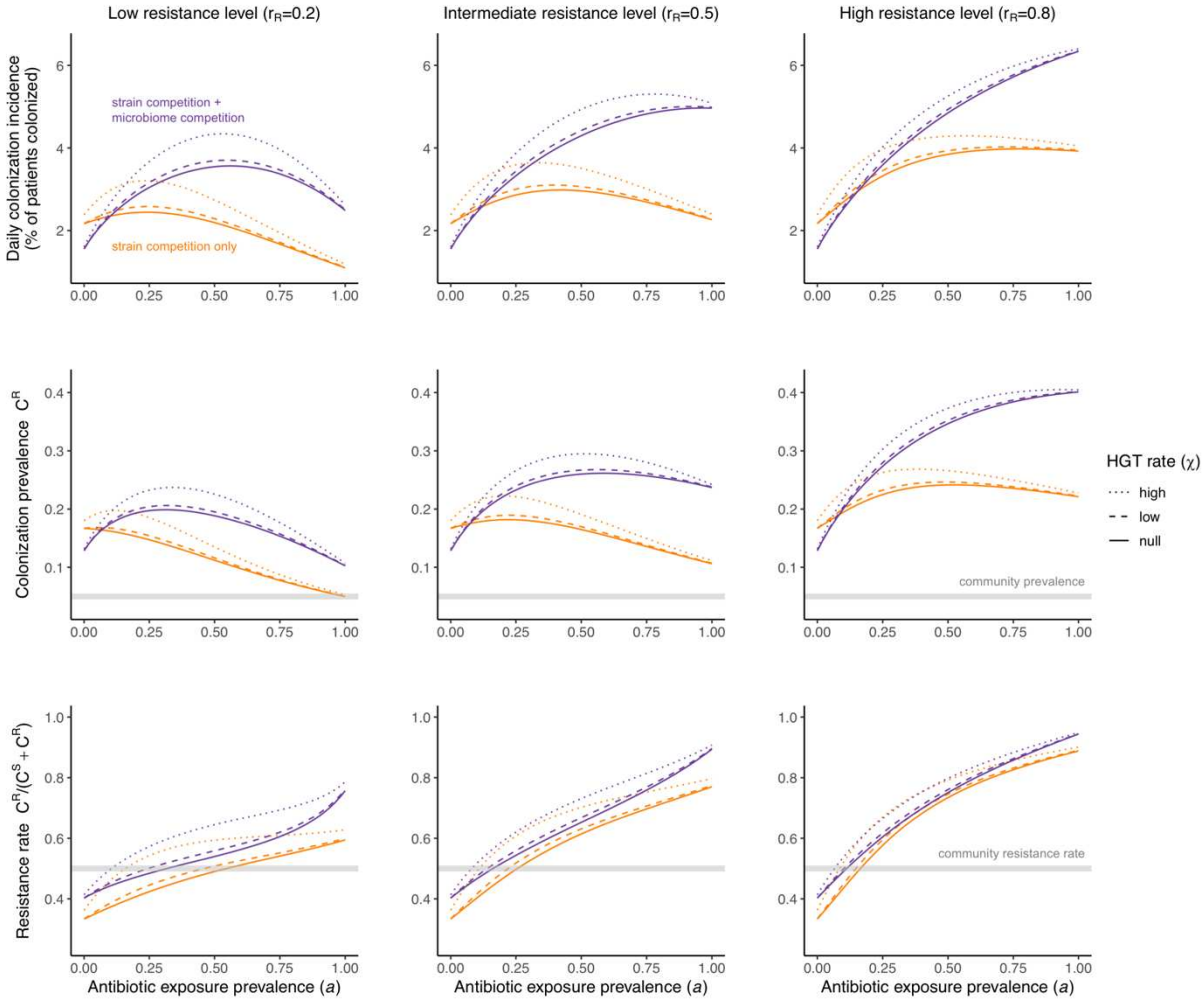

Figure 4.13. Impacts of HGT on model dynamics.

Impacts of horizontal gene transfer (HGT) on antibiotic selection for resistance. Allowing a resistance gene to transfer horizontally increases colonization incidence of the strain P^R that bears the gene (top row), its colonization prevalence C^R (middle row), as well as the pathogen's resistance rate (bottom row). The relative impact of HGT depends on the gene's rate of transfer (χ, line type), antibiotic exposure prevalence (**a**, x-axis), competitive interactions between pathogen strains and host microbiota (colours; purple = microbiome-strain competition; orange = only strain competition), and the level of resistance conferred by the gene (r_R, columns). It is assumed that $\chi_d/\chi_e = 10$, such that the low HGT rate corresponds to $\{\chi_e=0.01, \chi_d=0.1\}$ and the high rate to $\{\chi_e=0.1, \chi_d=1\}$. Alternative HGT assumptions are explored in **Figure 4.14**.

Overall impacts of HGT on C^R were positively associated with other parameters that tend to increase C^R (β, α, ϕ, ω, f_ω) and negatively associated with parameters that tend to decrease C^R (ε, η, δ) (**Figure 4.14A**). Increasing the rate of HGT in hosts undergoing

dysbiosis (χ_d), while holding the rate constant in hosts with stable microbiota (χ_e), augmented HGT's impact but did not substantively shift the level of antibiotic exposure that maximizes C^R prevalence (**Figure 4.14B**). Finally, effects of HGT depended on costs of the resistance gene being transmitted (**Figure 4.14C**). For instance, a metabolically costly but highly drug-resistant gene R (c = 2, r_R = 0.8) was potentially disadvantageous for the pathogen species as a whole at low antibiotic use (reducing total prevalence, $C^S + C^R$) but advantageous at high antibiotic use (increasing $C^S + C^R$).

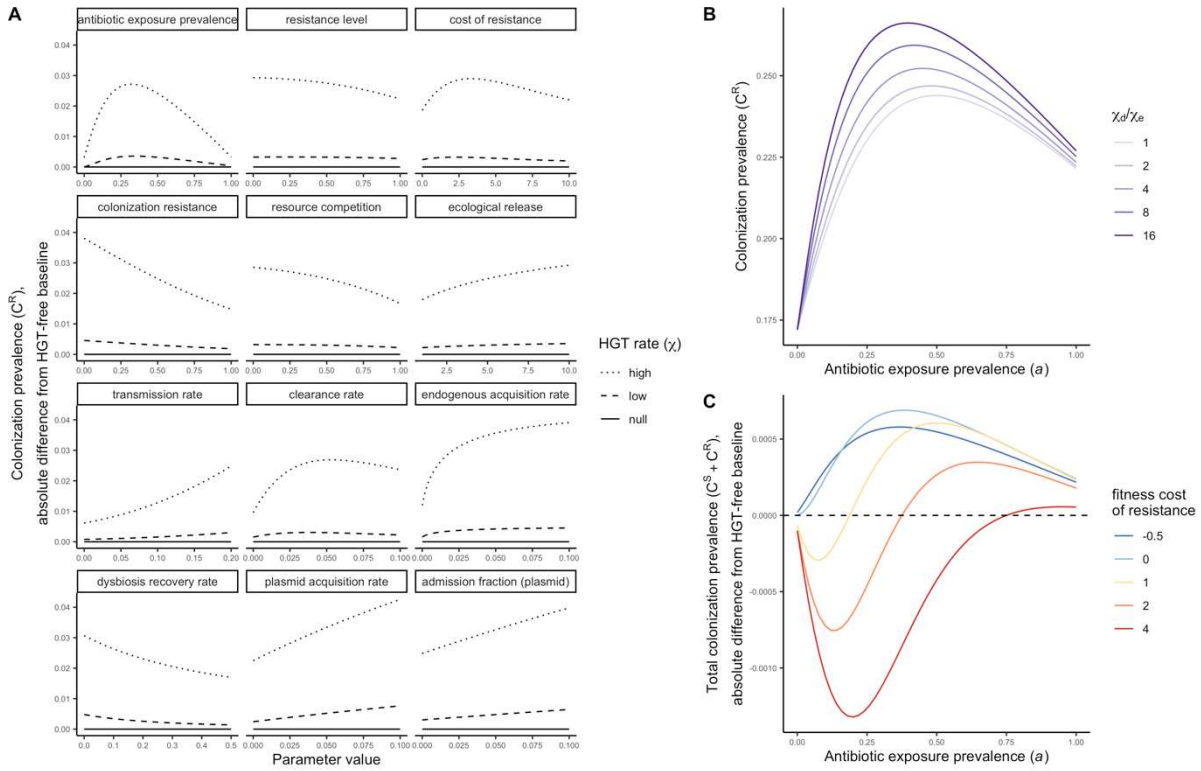

Figure 4.14. Sensitivity analyses for HGT impacts.

Impacts of HGT on pathogen colonization dynamics are tied to other parameters that mediate the prevalence of competing pathogen strains. **(A)** The absolute difference in C^R (dashed and dotted lines) compared to prevalence in the absence of HGT (solid horizontal line) depends on assumed values of other parameters (panels) that drive colonization dynamics. For brevity, ω is referred to as the plasmid acquisition rate, and f_ω as the plasmid admission fraction. **(B)** Assuming a higher rate of HGT in patients undergoing dysbiosis (χ_d) than in patients with stable microbiota (χ_e) has a modest impact on C^R. Here, χ_e is held constant at χ_e=0.05, such that changes in the fraction χ_d/χ_e result from corresponding increases in χ_d. **(C)** Impacts of HGT on total pathogen prevalence ($C^S + C^R$) depend on how selectively (dis)advantageous the resistance gene R is for the pathogen bearing it. Here, total prevalence ($C^S + C^R$) is shown as proportional to a model assuming the same parameter values but excluding HGT (dashed horizontal line). Colours represent different fitness costs of resistance c, demonstrating that HGT not only changes the relative frequency of competing strains, but can feed forward to alter total prevalence of all strains, tending to increase total prevalence when R has little metabolic cost (low c), but decrease prevalence when R is costly (high c). See **Table 4.1** for parameter values.

4.3.6. Impacts of antibiotic stewardship interventions

Lastly, different microbiome-pathogen interactions were found to underlie distinct dynamic responses to theoretical public health interventions (**Figure 4.15**). For the same generic pathogen P^R, interventions generally, but not always prevented against colonization, with predictions depending on the ecological interactions in effect (e.g. strain competition, microbiome competition), the impact of the intervention (e.g. reduced microbiome disruption, reduced overall prescribing), and the epidemiological outcome considered (e.g. prevalence, resistance rate). For instance, intervention 1 (using antibiotics more effective against C^R, holding all else constant) led to substantial declines in both prevalence and the resistance rate, while intervention 3 (reducing antibiotic exposure prevalence, holding all else constant) further reduced the resistance rate but with heterogeneous impacts on prevalence, in some instances increasing C^R relative to pre-intervention levels.

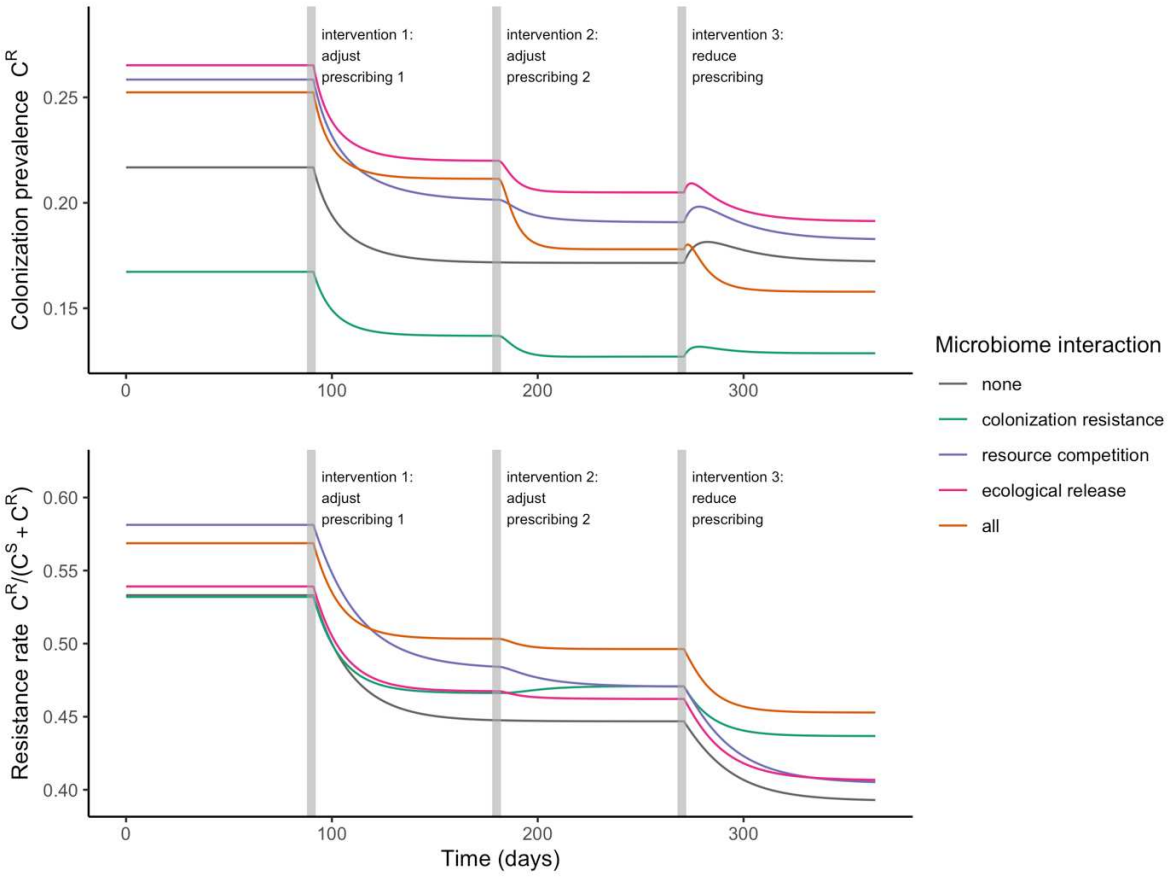

Figure 4.15. Epidemiological impacts of antibiotic stewardship interventions.

Antibiotic prescribing interventions have mixed impacts on colonization dynamics, depending on the microbiome interactions in effect (colours) and the epidemiological outcomes considered (top: P^R's colonization prevalence; bottom: the pathogen's resistance rate). ODEs were integrated numerically, introducing interventions at 3, 6 and 9 months. Interventions represent changes to parameter values corresponding to presumed changes in antibiotic consumption: for intervention 1, the C^R resistance level r_R was halved from 0.8 to 0.4; for intervention 2, the rate of antibiotic-induced microbiome dysbiosis θ_m was halved from 1 to 0.5; and for intervention 3, the baseline antibiotic exposure prevalence **a** was halved from 0.2 to 0.1. See **Table 4.1** for parameter values.

4.4. Discussion

4.4.1. Summary of model and results

I developed a novel modelling framework for antibiotic resistance epidemiology that includes within-host ecological consequences of antibiotic use in the form of microbiome dysbiosis, incorporating a leading hypothesis for antibiotic selection into a classical mathematical model of antibiotic resistance.(Austin et al., 1997; Lipsitch and Samore, 2002) I formalize three examples of microbiome-pathogen competition, and show how they, either separately or in combination with other forces of selection, help explain how antibiotic use drives the spread of ARB in healthcare settings. I found that antibiotic-induced microbiome dysbiosis has a large impact on incidence but little impact on resistance rates, whereas, conversely, antibiotic-induced pathogen clearance has a large impact on resistance rates but not on incidence. These observations reflect the potential importance of different forces of ecological competition for different epidemiological outcomes: while strain-based competition explains relative ecological dynamics of co-circulating strains, microbiome interactions may better explain how increasing antibiotic use favours ARB incidence, and hence why antimicrobial stewardship interventions limit ARB colonization acquisition.(Baur et al., 2017)

Altering population-level antibiotic exposure from the same baseline level was found to either prevent or promote P^R, depending on how P^R was assumed to interact with other bacteria. This heterogeneity results from the distinct antibiotic selection trade-offs underlying different within-host interactions, and corresponding non-linear dynamic feedbacks between antibiotic use and epidemiological indicators. In this model, antibiotics may clear P^R colonization (assuming that P^R is not completely antibiotic-resistant, i.e. $r_R < 1.0$), but in the context of strain competition they make more hosts available to P^R colonization, in the context of microbiome competition they increase host susceptibility to colonization, and in the context of HGT they increase selection for the transmitted resistance gene R while limiting the prevalence of its potential recipients. Through these trade-offs I demonstrate that, for an otherwise identical pathogen P^R, the intensity of antibiotic use that maximizes colonization prevalence is often intermediate ($0 < \mathbf{a} < 1.0$), but can vary from the lower boundary **a**=0 in certain contexts (e.g. given no microbiome-pathogen interactions, no HGT, and a low antibiotic resistance level), to the upper boundary **a**=1.0 in others (e.g. given microbiome-pathogen interactions, HGT and a high resistance level; see **Figure 4.13**).

4.4.2. Findings in context

4.4.2.1. Antibiotic selection for resistance dissemination

These findings build upon previous theoretical work exploring how antibiotics select for the epidemiological spread of antibiotic-resistant bacteria. Modelling studies often assume that antibiotic exposure is a risk factor for ARB colonization, which can be interpreted as indirectly accounting for microbiome dysbiosis. In transmission models of *Clostridioides difficile*, ESBL-producing *Escherichia coli* and *Pseudomonas aeruginosa*, among others, patients undergoing antibiotic therapy have been assumed to be at greater risk of colonization and/or infection.(Gingras et al., 2016; Hurford et al., 2012; MacFadden et al., 2019) An alternative approach has been to use antibiotic exposure as a coefficient on epidemiological parameters (e.g. transmission, endogenous acquisition), allowing ARB colonization rates to scale with antibiotic use.(Knight et al., 2018) These strategies reflect widespread recognition that antibiotic use favours ARB acquisition, through erosion of colonization resistance or other supposed mechanisms, and independent of potential competition with other strains.

The present work formalizes examples of the microbiome-pathogen interactions that underlie these assumptions, demonstrating their relevance to various epidemiological outcomes, explicitly distinguishing them from traditional strain-based selection and providing a framework for their application. In doing so, this framework simplifies into accessible epidemiological parameters what are in reality highly complex ecological systems, comprising a staggering diversity of microbes and interactions among them. This work ultimately demonstrates that accounting for at least some of this ecological complexity may help to explain how antibiotics select for the epidemiological spread of resistance.

4.4.2.2. Antibiotic selection trade-offs

These findings further build upon previous work demonstrating how different assumptions about within-host ecology can shape antibiotic selection trade-offs. At the cellular level, intermediate levels of antimicrobial exposure intensity are predicted to select most strongly for resistance evolution. The *mutant selection window* describes the range of antimicrobial concentrations that select for drug-resistance mutations, and is specific to each pathogen and antimicrobial compound.(Drlica, 2003) Its lower bound is the minimum inhibitory concentration (MIC) for a drug-sensitive wild-type pathogen strain, below which the

antimicrobial has no impact on any strain, while its upper bound is the MIC for the drug-resistant mutant strain, above which the antimicrobial clears all strains. The resulting peak in emergence of antibiotic resistance at intermediate antibiotic concentrations – the so-called “inverted U” of antibiotic selection – has been demonstrated empirically for bacteria including *Streptococcus pneumoniae*,(Croisier et al., 2004; Etienne et al., 2004; Negri et al., 1994; Zinner et al., 2003) *Staphylococcus aureus*,(Cui et al., 2006; Firsov et al., 2006, 2004, 2003; Zhu et al., 2012) *Mycobacterium tuberculosis*,(Gumbo et al., 2007, 2004) *P. aeruginosa*,(Jumbe et al., 2003; Tam et al., 2005b, 2005a) *Enterococcus faecalis*,(Bourgeois-Nicolaos et al., 2007) *Enterobacter cloacae*,(Goessens et al., 2007; Stearne et al., 2007) and *Klebsiella pneumoniae*.(Tam et al., 2007)

In a review, Kouyos *et al*. discuss how simultaneous ecological impacts of antimicrobials can lead to selection trade-offs that favour such an inverted U.(Kouyos et al., 2014) They illustrate conceptually that increasing treatment intensity decreases pathogen density (and hence the rate of resistance mutation), but releases resistant bacteria from competition with drug-sensitive strains, hence maximizing rates of resistance emergence at intermediate treatment intensity. Day & Read extended this trade-off into a general modelling framework for resistance evolution at the within-host level, demonstrating mathematically that intermediate treatment intensity is worst from an evolutionary perspective, with either the largest tolerable dose or the smallest clinically effective dose minimizing the risk of treatment-associated resistance emergence.(Day and Read, 2016) Which dose is best, however, was found to be highly sensitive to model assumptions and parameterization, and hence to different microbes and their particular treatment options. A range of other studies across different hosts, pathogens and treatment types have presented conditions in which either aggressive treatment intensity,(de Roode et al., 2004; Gullberg et al., 2011; Hansen et al., 2020; Huijben et al., 2013; Read et al., 2011) or moderate intensity,(Ankomah and Levin, 2014; Kim et al., 2014; Knudsen et al., 2003; Tam et al., 2005a) is predicted to select most strongly for antimicrobial-resistant infections.

Building on this classic trade-off and extending it to the population level, Colijn et al. developed a mixed within- and between-host co-colonization model, and showed that the degree of competition between co-circulating drug-sensitive and drug-resistant strains governs whether low or high intensities of antibiotic use most favour the spread of resistance through a host population.(Colijn and Cohen, 2015) Sciré et al. used a similar approach, developing a nested strain competition model to show that treatment strategies

that are more beneficial for infection recovery may promote the spread of resistance at the population level, and vice-versa.(Scire et al., 2019)

The present findings suggest that, in addition to intra-specific competition, inter-specific microbiome-pathogen competition and HGT can further shape such antibiotic selection trade-offs, and that the characteristics and strengths of these interactions can determine whether low, medium, or high intensities of antibiotic treatment most favour the spread of a particular drug-resistant pathogen at the epidemiological level. This is exemplified by simulations of theoretical antibiotic stewardship interventions, in which the otherwise identical pathogen P^R experienced diverse, and sometimes opposing responses to different interventions in the context of different microbiome-pathogen interactions, and different epidemiological indicators. However, antibiotic use in the present work reflects bystander exposure among facultative bacterial pathogens, whereas the studies cited above largely focus on antibiotic selection for resistance in actively treated infections. Clinically, it remains unclear if and to what extent antibiotic selection trade-offs result from bystander antibiotic exposure.

A range of other antibiotic selection trade-offs beyond the scope of this work but evaluated elsewhere can further shape the relationship between antibiotic use and selection for resistance, including synergistic interactions between antimicrobials (where increasing synergy may increase treatment efficacy but favour resistance),(Michel et al., 2008) delays to initiation of treatment (where longer delays can shift the dosing strategy that maximizes resistance selection),(Gjini et al., 2020) and delays to antibiotic switching upon identification of drug-resistant organisms (where shorter delays increase treatment efficacy but favour emergence of multidrug-resistance).(Wang and Lipsitch, 2006)

4.4.3. Parsimonious microbiome modelling assumptions

Under a traditional strain competition modelling framework, pathogen colonization is assumed to be limited by closely related strains sharing an ecological niche, with the same approximate epidemiological profile and transmission characteristics. In this context, competition against ARB is assumed to depend on the epidemic spread of competing strains, and removal of drug-sensitive strains from the population necessarily releases antibiotic selection for resistance. By contrast, microbiome population structure is inherently stable, and depends less on the epidemiological transmission of particular taxa, and more on host factors such as diet, maternal inheritance, genetics and antibiotic

exposure.(Brito and Alm, 2016) Despite great inter-individual diversity in microbiome composition, there is functional redundancy from one host to the next, such that colonization resistance and other forms of microbiome competition are shared across healthy individuals, even if colonized with different taxa.(Bashan et al., 2016; Kim et al., 2017) For these reasons, microbiome stability is modelled here as a host trait reflecting the functional ecology of the microbiome in different population dynamic states, as opposed to a more traditional bacterial colonization process governed by rates of acquisition and clearance. This is clearly an oversimplification of real microbiome dynamics and complexity,(Hooks and O'Malley, 2017) but is a useful approximation for the needs of epidemiological modelling, particularly in the absence of data, and reflects the universality of both human microbiome function and of the ecological impacts that antibiotics have on microbiome stability.(Bashan et al., 2016)

4.4.4. Limitations

The modelling framework presented in this Chapter has a number of limitations. First, hospitals and healthcare settings are heterogeneous environments with non-random contact patterns and relatively small population sizes. Stochastic, individual-based models that account for these factors reproduce more realistic nosocomial transmission dynamics than deterministic ODE simulations. Nonetheless, the goal of this work was to study how ecological mechanisms impact average epidemiological outcomes in the context of different modelling assumptions and parameter uncertainty, and in this context ODE modelling was the most appropriate tool. Further insights could certainly be gained by accounting for additional complexity and heterogeneity in future work, from within-host spatial organization,(Estrela et al., 2015) to patient and staff contact behaviour,(Duval et al., 2019a) to inter-institutional or inter-ward meta-population dynamics.(Shapiro et al., 2020)

Second, evaluation of strain competition was limited to a classic exclusive colonization model, the most widely used approach (only an estimated 12% of published strain competition models allow co-colonization or -infection).(Niewiadomska et al., 2019) Yet alternative models predict unique impacts on resistance dynamics,(Spicknall et al., 2013) and explicit consideration of higher-resolution within-host population dynamics has been shown to better reproduce empirical results in previous work.(Davies et al., 2019) Third, the chosen exclusive colonization approach precluded assessment of intraspecific HGT, which may have different impacts on resistance dynamics than interspecific HGT.

4.4.5. Future directions

Although epidemiological data are limited, insights from experiments and within-host models support that antibiotic disruption of microbiome-pathogen competition is a key driver of selection for resistance.(Baumgartner et al., 2020; Estrela and Brown, 2018; O'Brien et al., 2021; Shaw et al., 2019; Stein et al., 2013; Tepekule et al., 2019) The present work highlights the importance of extending these within-host concepts to the population level. Magnitudes of within-host microbiome interactions are difficult to quantify,(Zimmermann-Kogadeeva, 2021) but this theoretical framework generates hypothesis for future study, demonstrating potential consequences of microbiome-pathogen interactions on antibiotic selection for ARB spread, and highlighting that resistance epidemiology is highly sensitive to model parameterization in this context. A clear next step is thus to apply this framework to particular bacterial pathogens circulating among particular patient populations exposed to particular antibiotics, and hence to characterize the magnitudes of within-host competition and antibiotic-induced microbiome dysbiosis that are expected to occur in real clinical settings. Natural candidates for model application include bacterial pathogens known to have strong interactions with the host microbiome, like *C. difficile*, and bacteria known to transfer resistance genes inter-specifically to and from host microbiota, including ESBL-producing Enterobacteriaceae.

Chapter 5. Simulating impacts of microbiome interactions on the efficacy of public health interventions for nosocomial pathogen control

5.1. Introduction

Within-host interactions with the host microbiome can drive the epidemiological dynamics of bacterial pathogens.(Bäumler and Sperandio, 2016; Buffie and Pamer, 2013; Johanesen et al., 2015) This is perhaps best exemplified by the canonical nosocomial pathogen *Clostridioides difficile*: growth within the intestine is inhibited by secondary metabolites of commensal gut bacteria, protecting colonized patients from disease and limiting propagation of the infectious spores that drive between-host transmission.(Kamada et al., 2013a; Pamer, 2016) The human microbiome is purported to play a similar defensive role against a range of nosocomial pathogens, including emerging high-priority multidrug-resistant bacteria like ESBL-producing Enterobacteriaceae.(Kim et al., 2017; Lerminiaux and Cameron, 2019; Pilmis et al., 2020) However, although the epidemiological relevance of microbiome-pathogen interactions is increasingly recognized, quantification of the links between within-host microbiome ecology and nosocomial pathogen epidemiology are scarce, and consequences for the efficacy of public health interventions are poorly understood. Nonetheless, the role of the host microbiome in protecting against colonization and infection with ARB has motivated a need for public health interventions that minimize or reverse harm to patient microbiota, from antibiotic stewardship, to probiotics, to faecal microbiota transplantation, to microbiome protective therapies like DAV132 (a colon-targeted antibiotic adsorbent).(de Gunzburg et al., 2018; Relman and Lipsitch, 2018)

In the previous Chapter, I developed a modelling framework describing colonization dynamics of antibiotic-resistant bacteria in the healthcare setting, and evaluated epidemiological consequences of a range of theoretical within-host microbiome-pathogen interactions. Here, I apply this framework to four specific high-risk nosocomial ARB: *C. difficile*, methicillin-resistant *S. aureus* (MRSA), ESBL-producing *Escherichia coli* (ESBL-EC) and carbapenemase-producing *Klebsiella pneumoniae* (CP-KP). By simulating a range of public health interventions, I demonstrate the theoretical importance of

microbiome-pathogen interactions as mediators of ARB epidemiology in healthcare settings, and determining factors in the control of resistance dissemination.

5.2. Methods

The modelling framework introduced in Chapter 4 was extended through eight key steps to assess the impact of microbiome-pathogen interactions on the epidemiological efficacy of control interventions for selected ARB. First, the model population was parameterized to represent patients in an acute care hospital in France. Second, the ecological impacts of antibiotic consumption on different pathogen strains and on the host microbiome were characterized. Third, the model was adapted to each of the four considered ARB (*C. difficile*, MRSA, ESBL-EC, CP-KP), using parameter estimates from the literature. Fourth, expert elicitation interviews were conducted to characterize the relevance of microbiome dysbiosis for the colonization dynamics of each ARB, and to quantify interaction coefficients with uncertainty. Fifth, epidemiological outcomes were simulated for each ARB, using Monte Carlo sampling methods to account for epistemic uncertainty. Sixth, multivariate sensitivity analyses were conducted to quantify impacts of uncertainty on model outcomes. Seventh, a range of public health interventions were incorporated into model ODEs. Finally, calculations for evaluation of intervention efficacy across distinct epidemiological indicators were conducted.

5.2.1. Characterizing the hospital inpatient population

Model 5 from Chapter 4 (equation 4.17) was parameterized to represent a population of hospital inpatients in France, prioritizing studies from the French acute care setting where available and accounting for parameter uncertainty (**Table 5.1**). Estimates include a mean 8-day (95% CI: 3 – 13 day) hospital length of stay, a mean 19.5% (15.7 – 23.3%) antibiotic exposure prevalence, and a mean 28-day (7 – 49 day) recovery to microbiome equilibrium for hospital patients undergoing microbiome dysbiosis.

Table 5.1. Hospital parameters.

Parameters and probability distributions for baseline hospital inpatient parameters applied across all ARB.

Symbol	Parameter	Unit	Distribution	Reference	Setting	Notes
μ	admission / discharge rate	day^{-1}	1 / Normal (8, 2.55)	(Touat et al., 2019)	French hospitals	/
f_d	admission fraction (dysbiosis)	/	Normal (0.0756, 0.0190)	(Bernier et al., 2014)	French community	taken as proportion of the French community exposed to antibiotics in previous 28 days, extrapolating weekly reimbursed antibiotic prescriptions/1000 inhabitants (18.9, 9.6 – 28.3) to 4 weeks and assuming independent prescriptions =75.6 (38.4 – 113.2) prescriptions/1000 inhabitants
a	antibiotic exposure prevalence	/	Normal (0.195, 0.0195)	(Alfandari et al., 2015)	314 French hospitals	/

θ_c	antibiotic-induced pathogen clearance rate	day^{-1}	1 / Uniform (1, 10)	(Tepekule et al., 2017)	Simulation study	/
θ_m	antibiotic-induced microbiome dysbiosis rate	day^{-1}	1 / Normal (2, 0.4)	(Bhalodi et al., 2019)	Mixed	circumstantial evidence of same-day microbiome disruption following antibiotic therapy; assumed an average minimum 12 hours to disruption
δ'	microbiome recovery rate	day^{-1}	1 / Normal (28, 10.71)	(Burdet et al., 2019; Rafii et al., 2008)	Mixed; French hospital	across studies in a review of antibiotic-induced microbiome disruption, intestinal microflora were observed to "return to normal" 1-49 days after antibiotic cessation; in a French hospital, two measures of microbiome diversity were observed to "return to normal" after 16-21 days.

5.2.2. Modelling ecological impacts of antibiotic exposure

5.2.2.1. Distribution of antibiotics used

Antibiotic exposure prevalence was quantified at the level of antibiotic class using nationally representative antibiotic consumption data from French hospitals in 2016.(Agence nationale de sécurité du médicament et des produits de santé, 2017) A study from American hospitals in 2006-2012 was used to further stratify antibiotics with ATC code J01F into J01FA and J01FF, J01X into J01XA and J01XD, and J01DD+DE into J01DD and J01DE.(Baggs et al., 2016) Final antibiotic consumption data are presented in **Table 5.2**.

Table 5.2. Antibiotic parameters.

Antibiotic classes, their contribution to total hospital antibiotic consumption, their spectrum, and their relative rate of inducing microbiome dysbiosis. Consumption data come from the French Agence nationale de sécurité du médicament et des produits de santé and are supplemented with data from Baggs et al. (Agence nationale de sécurité du médicament et des produits de santé, 2017; Baggs et al., 2016) The literature was used to classify antibiotic classes in terms of their spectrum,(Abbara et al., 2020; Tan et al., 2017) and relative rate of causing microbiome dysbiosis.(Baggs et al., 2018; Brown et al., 2013) The percentage column does not total to 100 due to rounding error.

Antibiotic class	ACT code	% of consumption	Spectrum	Rate of inducing dysbiosis
Amoxicillin and beta-lactamase inhibitor	J01CR02	32.4	Broad	High
Penicillins with extended spectrum	J01CA	21.9	Narrow	Medium
Quinolones	J01M	11.0	Broad	High
C3G	J01DD	8.2	Broad	Very high
C1G	J01DB	3.7	Narrow	High
Macrolides	J01FA	3.4	Narrow	Medium
Imidazole	J01XD	2.9	Narrow	Medium
Piperacillin and beta-lactamase inhibitor	J01CR05	2.3	Broad	High

Aminoglycosides	J01G	2.3	Narrow	Low
Tetracyclines	J01A	2.0	Narrow	Low
Sulfonamides, trimethoprim	J01E	1.8	Narrow	Medium
Glycopeptides	J01XA	1.8	Narrow	Very high
Lincosamides	J01FF	1.6	Broad	Very high
Carbapenems	J01DH	1.5	Broad	High
Penicillins (other)	J01C_other	1.4	Narrow	Medium
C2G	J01DC	0.9	Narrow	High
C4G	J01DE	0.6	Broad	Very high
Other	Other	2.1	Narrow	Medium

5.2.2.2. Antibiotic-induced microbiome dysbiosis

To simulate class-specific rates of microbiome dysbiosis, a previously developed four-point log-linear scale of intestinal microbiome disruption was used.(Brown et al., 2013) For interpretation, antibiotic classes are presented as inducing dysbiosis at a high, medium, low, or very low rate. This scale was supplemented with data for additional antibiotic classes from Baggs et al.(Baggs et al., 2018) As applied here, the cumulative rate that antibiotic treatment induces dysbiosis (σ_m) is given by

$$\sigma_m = \mathrm{a} \times \theta_m \times \sum_{k=0}^{3} (\mathrm{a}_k \times e^{-k})$$

(eq. 5.1)

where $\mathbf{a}_k$ is the proportion of antibiotics consumed of each group k, and where the most ecologically disruptive group ($k = 0$, i.e. 3rd and 4th generation cephalosporins, glycopeptides and lincosamides) causes dysbiosis a mean 12 hours after antibiotic exposure ($\theta_m = 2\ \mathrm{day}^{-1}$), with classes in less disruptive groups ($k = 1,2,3$) causing dysbiosis at successively slower rates (**Figure 5.1C**). Further, it was assumed that microbiota can still recover among patients exposed to aminoglycosides and tetracyclines, the antibiotic classes inducing microbiome dysbiosis at the lowest rate ($k = 3$), such that

$$\delta = \delta' \times (1 - \mathrm{a} \times (1 - \mathrm{a}_{k=3}))$$

(eq. 5.2)

5.2.2.3. Antibiotic-induced pathogen clearance

To characterize class-specific effects on pathogen clearance for each ARB, each strain *i*

was classified as sensitive ($r_{i,j} = 0$), of intermediate sensitivity ($0 < r_{i,j} < 1$), or resistant ($r_{i,j} = 1$) to each antibiotic class j. Overall, the rate that antibiotic treatment clears each strain is given by

$$\sigma_i = \mathrm{a} \times \theta_C \times \sum_{j=1}^{18} (\mathrm{a}_j \times (1 - r_{i,j}))$$

(eq. 5.3)

across the 18 included classes.

5.2.3. Characterizing pathogen epidemiology

For all ARB, data from the literature were used to define epidemiological parameters with uncertainty, again prioritizing studies from French clinical settings where available (**Tables 5.3 – 5.6**). **Figure 5.1B** further illustrates the ways in which the model was parameterized to represent different ARB. Estimates include: higher daily transmission rates for *S. aureus* (0.057, 2.5% – 97.5% quantiles: 0.046 – 0.068) and *K. pneumoniae* (0.029, 0.012 – 0.046) than for *E. coli* (0.0078, 0.0013 – 0.014) and *C. difficile* (0.0056, 0.0037 – 0.0074); and a shorter natural duration of colonization (in the absence of antibiotic treatment) for *C. difficile* (84 days, 66– 117 days) than for *S. aureus* (287 days, 252 – 322 days), *E. coli* (372 days, 321 – 411 days) and *K. pneumoniae* (375 days, 303 – 491 days).

Different types of within-host interactions were considered for different ARB (**Figure 5.1A**). *C. difficile*, MRSA, ESBL-EC and CP-KP were all assumed to compete with host microbiota. MRSA, ESBL-EC and CP-KP were assumed to also compete intra-specifically with non-focal strains. For model application, the focal pathogen was taken as the "drug-resistant" strain C^R, while the "drug-sensitive" strain C^S was taken to represent all other co-circulating strains of the same species, for simplicity characterized, respectively, as methicillin-sensitive *S. aureus* (MSSA), *E. coli* (EC) and *K. pneumoniae* (KP). Finally, both ESBL resistance and carbapenem resistance were assumed to be borne by plasmids capable of horizontal transfer between patient microbiota and, respectively, EC and KP. These structural assumptions were informed using expert opinion (described below).

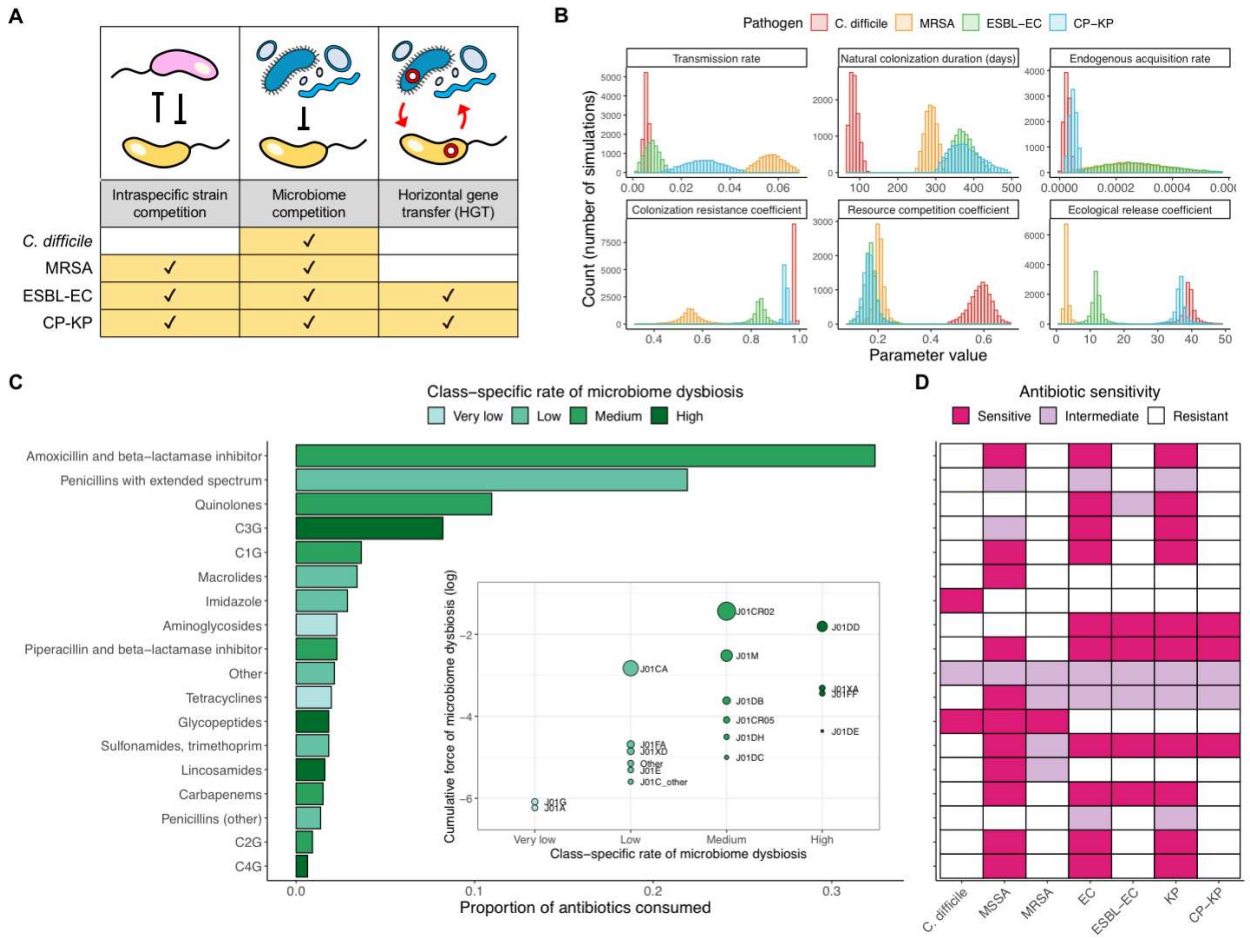

Figure 5.1. Model parameterization across ARB.

Characterizing the species-specific ecology of four selected antibiotic-resistant bacterial pathogens in the hospital setting. (A) Model structure: the within-host ecological interactions assumed for each pathogen. (B) Simulation inputs: 95% distributions for selected model parameters drawn stochastically over 10,000 runs. See **Tables 5.3 – 5.6** for all parameter distributions for all ARB. (C) The distribution of antibiotic classes consumed in French hospitals in 2016,(Agence nationale de sécurité du médicament et des produits de santé, 2017) shaded by their assumed impact on intestinal microbiome dysbiosis. Inset: the cumulative impact of each antibiotic class (given as ATC codes, see **Table 5.2** for corresponding names) on dysbiosis ($a_j \times e^{-k}$); circle size represents each class's contribution to exposure prevalence (a_j). (D) Assumed antibiograms for each pathogen strain and antibiotic class.

For species subject to intra-specific strain competition, strain-specific rates of natural clearance are assumed (resulting from the fitness cost of resistance *c*, as in equation 4.6) and endogenous acquisition. For the latter, in order to prevent rare strains (e.g. CP-KP) from emerging endogenously at the same rate as common strains (KP), rates for each strain were scaled by the prevalence of that strain in the community,

$$\alpha_S = \alpha' \times (1 - a \times (1 - r_S)) \times (1 - f_R)$$
$$\alpha_R = \alpha' \times (1 - a \times (1 - r_R)) \times f_R$$

(eq. 5.4)

Characteristic antibiograms informing antibiotic resistance levels for all strains were

adapted from an online compendium from the Therapeutics Education Collaboration (**Figure 5.1D**).(McCormack and Lalji, 2015) Under these assumptions, MRSA was resistant to the greatest proportion of antibiotics consumed in French hospitals (median r_R = 94.5%), followed by *C. difficile* (94.3%), CP-KP (91.7%) and ESBL-EC (84.8%); co-circulating "drug-sensitive" strains were considerably less antibiotic-resistant (median r_S = 33.0% for MSSA and 23.0% for both *E. coli* and *K. pneumoniae*).

Table 5.3. *C. difficile* parameters.

Symbol	Parameter	Unit	Distribution	Reference	Setting	Notes
β	transmission rate	day^{-1}	Normal (0.00555, 0.000944)	(van Kleef et al., 2016)	English hospitals (modelling study)	mean of point estimates of the daily probability of transmission from colonized patients (0.0037) and infected patients (0.0074)
α'	endogenous acquisition rate	day^{-1}	Normal (0.0000253, 0.0000114)	(Durham et al., 2016)	USA hospitals (modelling study)	proxy measure: the estimated daily rate of progression from colonization to infection in hospital patients, divided by the relative risk of progression in patients exposed to antibiotics
γ	natural clearance rate	day^{-1}	Normal (0.0119, 0.00170)	(Simor et al., 1993)	Canadian care home	fit longitudinal colonization data using exponential decay model
f_C	admission fraction (colonized)	/	Binomial (229, 0.048) / 229	(Barbut, 1996)	11 French hospitals	stool prevalence among asymptomatic patients
r	antibiotic resistance level	/	median 94.3%, (range 93.3–95.4%)	estimated	/	cumulative resistance level across simulated antibiotic consumption data and assumed antibiograms
ε	colonization resistance	/	1 – 1 / Cauchy (52.85, 1.62)	estimated	/	from expert opinion
η	resource competition	/	$(1/\gamma)/(1/\gamma$ + Cauchy (121.11, 4.85))	estimated	/	from expert opinion
ϕ	ecological release	/	Cauchy (39.22 0.922)	estimated	/	from expert opinion

Table 5.4. *S. aureus* parameters.

Symbol	Parameter	Unit	Distribution	Reference	Setting	Notes
β	transmission rate	day^{-1}	Normal (0.057, 0.0057)	(Di Ruscio et al., 2019)	Norwegian hospitals (modelling study)	/
α'	endogenous acquisition rate	day^{-1}	Normal (0.0016, 0.0008)	(Coello et al., 1997; Di Ruscio et al., 2019)	Spanish hospital	proxy measure: the estimated daily rate of progression from colonization to infection in hospital patients
γ	natural clearance rate	day^{-1}	1 / Normal (287, 17.9)	(Shenoy et al., 2014)	Mixed	/
c	fitness cost of resistance	/	Normal (0.2, 0.02)	(Kouyos et al., 2013; Laurent et al., 2001)	French hospitals	growth cultures showed 20% fitness benefit to MSSA over MRSA strains
f_C	admission fraction (colonized)	/	Normal (0.0757, 0.00364)	(Cravo Oliveira Hashiguchi et al., 2019; Scanvic et al., 2001)	French hospitals	estimated as the proportion of patients arriving to a French hospital with MRSA colonization, divided by the estimated proportion of *S. aureus* strains that are methicillin-resistant in France
f_R	admission fraction	/	Normal (0.16, 0.016)	(Cravo Oliveira	France	/

	(bearing resistant strain)			Hashiguchi et al., 2019)		
r_S	antibiotic resistance level (MSSA)	/	median 33.1% (range 17.2–48.9%)	estimated	/	cumulative resistance level across simulated antibiotic consumption data and assumed antibiograms
r_R	antibiotic resistance level (MRSA)	/	median 94.5% (range 90.8–98.2%)	estimated	/	cumulative resistance level across simulated antibiotic consumption data and assumed antibiograms
ε	colonization resistance	/	1 – 1 / Cauchy (2.21, 0.15)	estimated	/	from expert opinion
η	resource competition	/	$(1/\gamma)$ / $(1/\gamma$ + Cauchy (73.09, 3.09))	estimated	/	from expert opinion
ϕ	ecological release	/	Cauchy (2.97, 0.28)	estimated	/	from expert opinion

Table 5.5. *E. coli* parameters.

Symbol	Parameter	Unit	Distribution	Reference	Setting	Notes
β	transmission rate	day^{-1}	Normal (0.0078, 0.00334)	(Gurieva et al., 2018)	13 European ICUs	/
α'	endogenous acquisition rate	day^{-1}	Normal (0.0024, 0.000663)	(Gurieva et al., 2018)	13 European ICUs	/
γ	natural clearance rate	day^{-1}	Normal (0.00269, 0.000216)	(Bar-Yoseph et al., 2016)	Mixed	fit longitudinal colonization data using exponential decay model
c	fitness cost of resistance	/	Normal (0.2, 0.02)	/	/	in absence of data for ESBL resistance, used same distribution as for MRSA
f_C	admission fraction (colonized)	/	Normal (0.275, 0.0140)	(Ebrahimi et al., 2016; Gurieva et al., 2018)	Mixed	estimated as the proportion of patients arriving to 13 European ICUs with ESBL-EC carriage, divided by the estimated proportion of *E. coli* that are ESBL-producing in a Hungarian hospital
f_R	admission fraction (bearing resistant strain)	/	Normal (0.119, 0.0413)	(Ebrahimi et al., 2016)	Hungarian hospital	proportion of fecal *E. coli* that were ESBL-producing from a non-outbreak setting
f_ω	admission fraction (microbiota bearing ESBL gene)		Binomial(857, 0.0665)/857	(Pilmis et al., 2018; Vidal-Navarro et al., 2010)	2 French hospitals	estimated by pooling 857 samples from two studies reporting fecal carriage of ESBL-producing species other than *E. coli*
r_S	antibiotic resistance level (EC)	/	median 23.1% (range 9.6–36.5%)	Estimated	/	cumulative resistance level across simulated antibiotic consumption data and assumed antibiograms
r_R	antibiotic resistance level (ESBL-EC)	/	median 84.9% (range 77.4–92.2%)	Estimated	/	cumulative resistance level across simulated antibiotic consumption data and assumed antibiograms
ε	colonization resistance	/	1-1/Cauchy (6.06, 0.64)	Estimated	/	from expert opinion
η	resource competition	/	$(1/\gamma)/(1/\gamma$ + Cauchy(76.38, 5.35))	Estimated	/	from expert opinion
ϕ	ecological release	/	Cauchy(11.80, 0.80)	Estimated	/	from expert opinion
χ_e	HGT rate (equilibrium)	day^{-1}	χ_d/Log-Normal (1.36, 0.81)	Estimated	/	from expert opinion
χ_d	HGT rate (dysbiosis)	day^{-1}	-log(1-Weibull (0.94, 0.11)) /10	Estimated	/	from expert opinion
ω	proportion of patients whose microbiota acquire ESBL gene following antibiotic exposure	/	Binomial(132, 18/132)/132 × 0.382	(Agence nationale de sécurité du médicament et des produits de santé, 2017; Bar-Yoseph et al., 2016)	Mixed	the proportion of patients in a meta-analysis who, subsequent to treatment, express resistance to the antibiotic with which treated (18/132), multiplied by the proportion of ESBLs among antibiotics consumed in French hospitals (38.2%)

Table 5.6. *K. pneumoniae* parameters.

Symbol	Parameter	Unit	Distribution	Reference	Setting	Notes
β	transmission rate	day^{-1}	Normal (0.029, 0.00842)	(Gurieva et al., 2018)	13 European ICUs	estimate for non-*E. coli* Enterobacteriaceae
α'	endogenous acquisition rate	day^{-1}	Normal (0.0048, 0.00133)	(Gurieva et al., 2018)	13 European ICUs	estimate for non-*E. coli* Enterobacteriaceae
γ	natural clearance rate	day^{-1}	Normal (0.00267, 0.000324)	(Bar-Yoseph et al., 2016)	Meta-analysis	fit longitudinal colonization data using exponential decay model
c	fitness cost of resistance	/	Normal (0.2, 0.02)	/	/	in absence of data for CP resistance, used same distribution as for MRSA
f_C	admission fraction (colonized)	/	Binomial (11420, (928 / 11420)) / 11420	(Cravo Oliveira Hashiguchi et al., 2019; Gurieva et al., 2018)	Mixed	the proportion of patients arriving to 13 European ICUs with CP-KP carriage, divided by the estimated proportion of K. *pneumoniae* that produce carbapenemase in France
f_R	admission fraction (bearing resistant strain)	/	Normal (0.01,0.001)	(Cravo Oliveira Hashiguchi et al., 2019)	France	/
f_ω	admission fraction (microbiota bearing CP gene)		Binomial(1135, 0.00441) / 1135	(Pantel et al., 2015)	7 French hospitals	rectal carriage of carbapenemase-producing bacteria
r_S	antibiotic resistance level (KP)	/	median 23.1% (range 9.6–36.5%)	estimated	/	cumulative resistance level across simulated antibiotic consumption data and assumed antibiograms
r_R	antibiotic resistance level (CP-KP)	/	median 91.7% (range 89.7–93.7%)	estimated	/	cumulative resistance level across simulated antibiotic consumption data and assumed antibiograms
ε	colonization resistance	/	1 - 1 / Cauchy (17.16, 0.97)	estimated	/	from expert opinion
η	resource competition	/	$(1/\gamma)$ / $(1/\gamma$ + Cauchy (74.93, 4.03))	estimated	/	from expert opinion
ϕ	ecological release	/	Cauchy (36.63, 0.82)	estimated	/	from expert opinion
χ_e	HGT rate (equilibrium)	day^{-1}	χ_d / Gamma (2.01,0.36)	estimated	/	from expert opinion
χ_d	HGT rate (dysbiosis)	day^{-1}	-log(1-Gamma(0.54, 3.67))/10	estimated	/	from expert opinion
ω	proportion of patients whose microbiota acquire CP gene following antibiotic exposure		Binomial (132, 0.1363) / 132 $\times$ 0.0151	estimated from (Agence nationale de sécurité du médicament et des produits de santé, 2017; Bar-Yoseph et al., 2016)	Mixed	the proportion of patients in a meta-analysis who, subsequent to treatment, express resistance to the antibiotic with which treated (18/132), multiplied by the proportion of carbapenems among antibiotics consumed in French hospitals (1.5%)

5.2.4. Expert elicitation

5.2.4.1. Context

Expert elicitation is a scientific consensus methodology involving the estimation of unknown parameter values from subject-matter experts. Elicitation methodologies for estimation of clinical parameter values have been developed, and are increasingly used to

inform epidemiological studies.(Johnson et al., 2010a, 2010b) The relevance of different within-host ecological interactions (intraspecific strain competition, microbiome competition, HGT) for different ARB in the hospital environment are not well-defined, and quantitative data linking microbiome interactions with epidemiological parameters are scarce. Expert elicitation was thus used to inform model structure and quantify parameter distributions for microbiome-pathogen interactions for each ARB.

5.2.4.2. Protocol

A standardized expert elicitation protocol was designed following a computer-guided 'chips and bins' methodology validated previously for estimation of quantitative parameters for patient outcomes in clinical settings.(Johnson et al., 2010b) First, the scientific context of the study was introduced, including the potential epidemiological relevance of microbiome-pathogen interactions, and potential roles for intraspecific strain competition and microbiome dysbiosis in explaining how antibiotics select for resistance. Second, the MATCH Uncertainty Elicitation Tool was presented, a computer software designed to facilitate quantitative parameter estimation. Third, the 'chips and bins' method of parameter estimation was explained. This method allows experts to set minimum and maximum values for each parameter and ARB, and to build distributions (histograms) visually by pointing and clicking using MATCH.(Morris et al., 2014) Fourth, potential cognitive biases were reviewed and tips for reliable parameter estimation were provided. Finally, experts were asked to respond to elicitation questions and quantify their beliefs (described below). For parameter quantification, it was stressed that the goal was not to characterize precise numerical estimates of particular mechanistic interactions, but rather to quantify the relative impact of microbiome dysbiosis on different colonization outcomes in the hospital setting.

5.2.4.3. Inclusion criteria and solicitation

Expert inclusion criteria included having a PhD degree, a current academic appointment, and subject-matter expertise in medical microbiology and/or the clinical epidemiology of antibiotic resistance. Experts were initially identified through a review of authors of relevant publications in the field. At the end of each interview, experts were further asked to refer us to additional experts in the form of snowball sampling. Of 23 invited experts, ten ultimately participated in elicitation interviews (acceptance rate 43.5%). Their specialties include bacteriology, internal medicine, intensive care, infectious disease epidemiology and clinical microbiology. Elicitation results are reported anonymously, but all experts

agreed to their acknowledgment in this work, and I thank them sincerely for their participation: Antoine Andremont, Christian Brun-Buisson, Aurélien Dinh, Stephan Harbarth, Jean-Louis Herrmann, Solen Kernéis, Alban Le Monnier, Benoît Pilmis, Etienne Ruppé and Paul-Louis Woerther.

5.2.4.4. Content

Experts were asked a total of six questions, each stratified by the four included ARB (*C. difficile*, MRSA, ESBL-EC, CP-KP). The first question asked about the influence of strain competition on the colonization dynamics of each ARB. Subsequent questions 2 to 6 asked about microbiome-pathogen interactions. To facilitate more reliable parameter interpretation, interaction coefficients were translated into clinical parameters, which experts were asked to assess and quantify. An example is translation of the ecological release coefficient into the relative risk of pathogen outgrowth among hospital patients undergoing microbiome dysbiosis (relative to patients with stable microbiota). Model parameters, the clinical parameters that experts were asked to estimate, and assumed links between them are provided in **Table 5.7**. For each parameter, experts were first asked to describe qualitatively whether microbiome dysbiosis influences that parameter (by answering *yes*, *no*, *partially* or *don't know*). Then, if answering *partially* or *yes*, experts were asked to estimate quantitative parameter estimates using the protocol as described above.

5.2.4.5. Interviews

Experts were consulted individually in the form of one-on-one interviews, and the elicitation protocol was followed systematically to ensure uniformity across experts. Interviews were approximately one hour in length and took place in each expert's office, with the exception of one interview conducted via an online video call.

Table 5.7. Expert elicitation parameters.

Relationship between model parameters and the clinical parameters estimated by experts.

Model parameter		Clinical parameter		Assumed relationship between model and clinical parameters
Name	**Symbol**	**Description**	**Symbol**	
colonization resistance	ε	relative risk of acquiring colonization among patients experiencing microbiome dysbiosis	RR_β	$\varepsilon = 1 - \frac{1}{RR_\beta}$
resource competition	η	excess duration of colonization among patients experiencing microbiome dysbiosis	d	$\eta = \frac{\frac{1}{\gamma}}{\frac{1}{\gamma} + d}$
ecological release	ϕ	relative risk of pathogen outgrowth among patients experiencing microbiome dysbiosis	RR_α	$\phi = RR_\alpha$
HGT rate (dysbiosis)	χ_d	proportion of antibiotic-exposed patients colonized with the specified species that acquire the specified resistance via HGT during their hospital stay	p_{χ_d}	$p_{\chi_d} = 1 - e^{-\chi_d \times \frac{1}{\mu}}$
HGT rate (equilibrium)	χ_e	relative risk of acquiring the specified resistance via HGT among patients experiencing microbiome dysbiosis	RR_χ	$RR_\chi = \frac{\chi_d}{\chi_e}$

5.2.4.6. Analysis of data and generation of parameter distributions

For qualitative questions, expert responses were tallied (**Figure 5.2**). For quantitative questions, parameter distributions were generated by pooling the individual distributions estimated by each expert. For each expert *k*, outcome *i* and ARB *j*, expert histograms generated using MATCH were saved as a vector $x_{i,j,k}$. Scales for different parameters varied substantially across experts (see raw data in **Figure 5.3**). However, for each parameter, estimates were made for each ARB consecutively, such that distributions for each ARB were ranked relative to one another. Friedman's tests were conducted to determine whether the rank order across ARB for each parameter was randomly distributed (the median of each expert's distribution was used to determine rank, considering species as groups and experts as blocks). To preserve rank order when combining expert estimates $x_{i,j,k}$ to form pooled histograms, distributions were centred by the mean relative distance $z_{i,j}$ between each *j* and the reference ARB (taken as MRSA) over all experts *k* (see re-scaled data in **Figure 5.4**). For *C. difficile* and MRSA, HGT was excluded from simulations and pooled distributions were not re-centred. Pooled histograms were fit to six candidate distributions (normal, log-normal, Weibull, Cauchy, exponential and gamma), and the final distribution was selected as the distribution giving the lowest Akaike Information Criterion (using the function fitdist from the R package fitdistrplus). Each expert distribution was weighted equally, contributing to 10% of the final pooled distribution for each species and parameter.

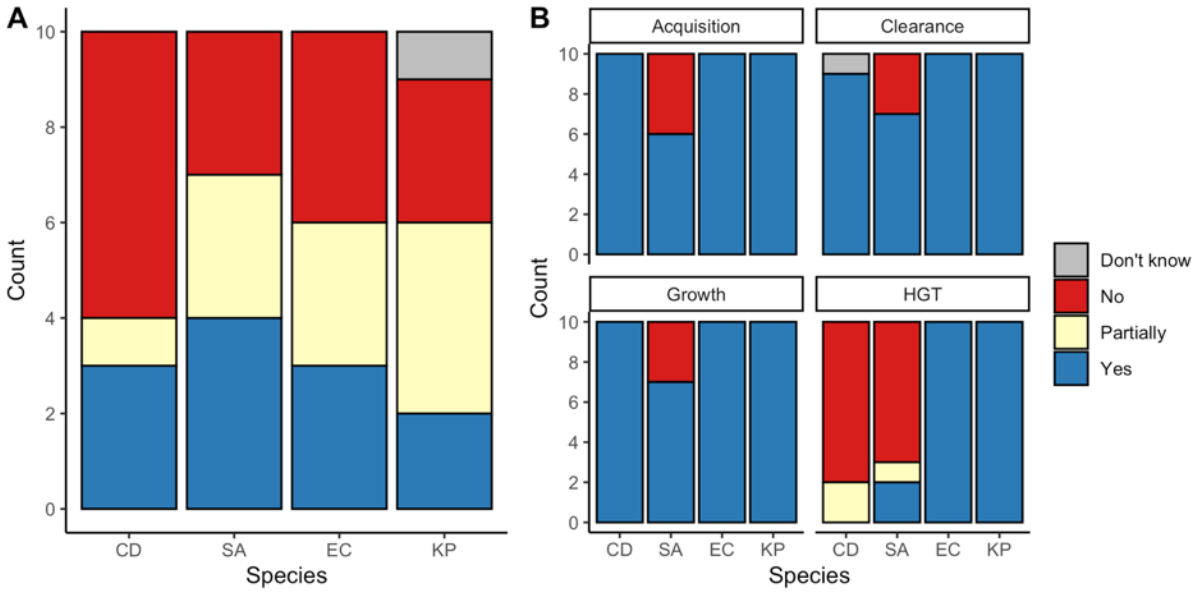

Figure 5.2. Qualitative expert elicitation results.

Expert belief about which mechanisms drive epidemiological dynamics of bacterial pathogens. **(A)** Expert belief in whether or not intraspecific strain competition influences nosocomial colonization dynamics for each pathogen. **(B)** Expert belief in whether or not each of the given colonization processes is affected by microbiome dysbiosis, and for HGT, whether or not this process is relevant in clinical settings. CD: *C. difficile*; SA: *Staphylococcus aureus*; EC: *Escherichia coli*; KP: *Klebsiella pneumoniae*; HGT: horizontal gene transfer.

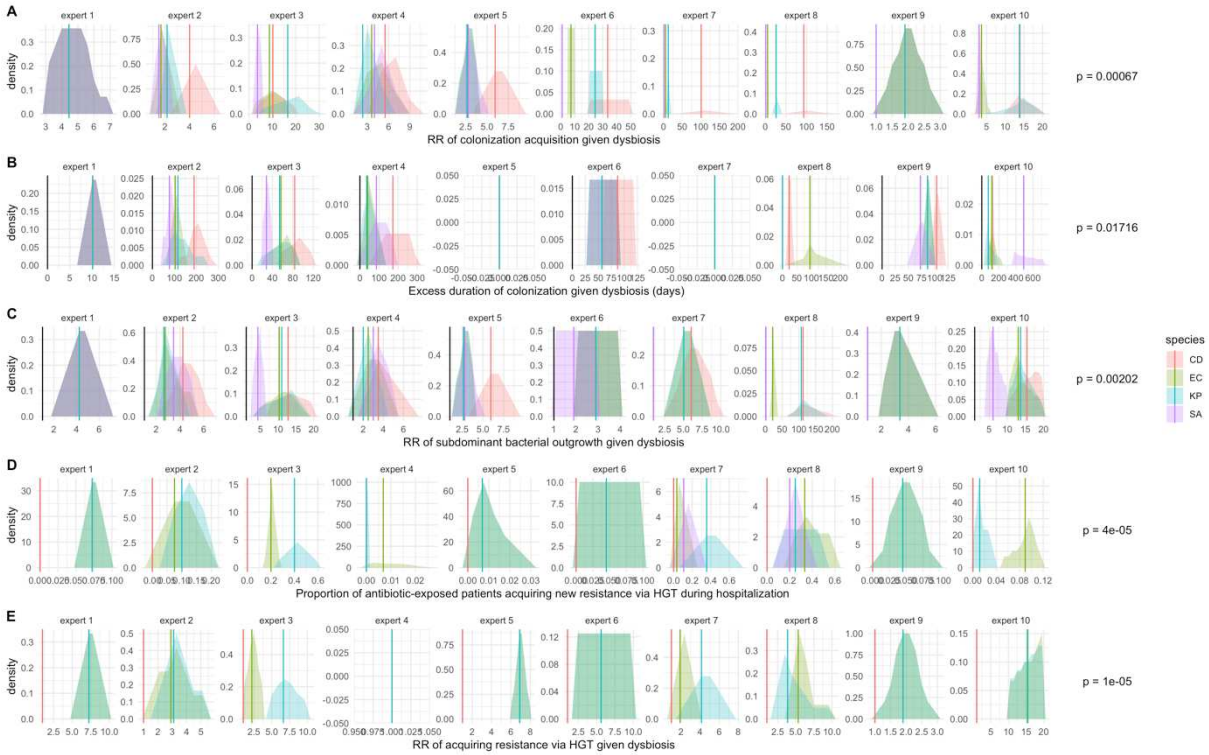

Figure 5.3. Quantitative expert elicitation results (raw data).

Expert belief and uncertainty about the impact of microbiome dysbiosis on nosocomial colonization dynamics of included bacterial pathogens (colours). Rows A through E represent, respectively, responses to questions 2 through 6 from the expert elicitation protocol (see clinical parameters in **Table 5.7**). Distributions were generated during expert interviews using the MATCH Uncertainty Elicitation Tool with the chips and bins method.(Morris et al., 2014) Experts are anonymized and represented by different columns. Vertical bars represent medians of each distribution to visualize the rank order for each

pathogen as estimated by each expert. p-values represent results of Friedman's tests for distribution medians, considering species as groups and experts as blocks for each question; when $p<0.05$, the species rank order across experts is interpreted as non-random.

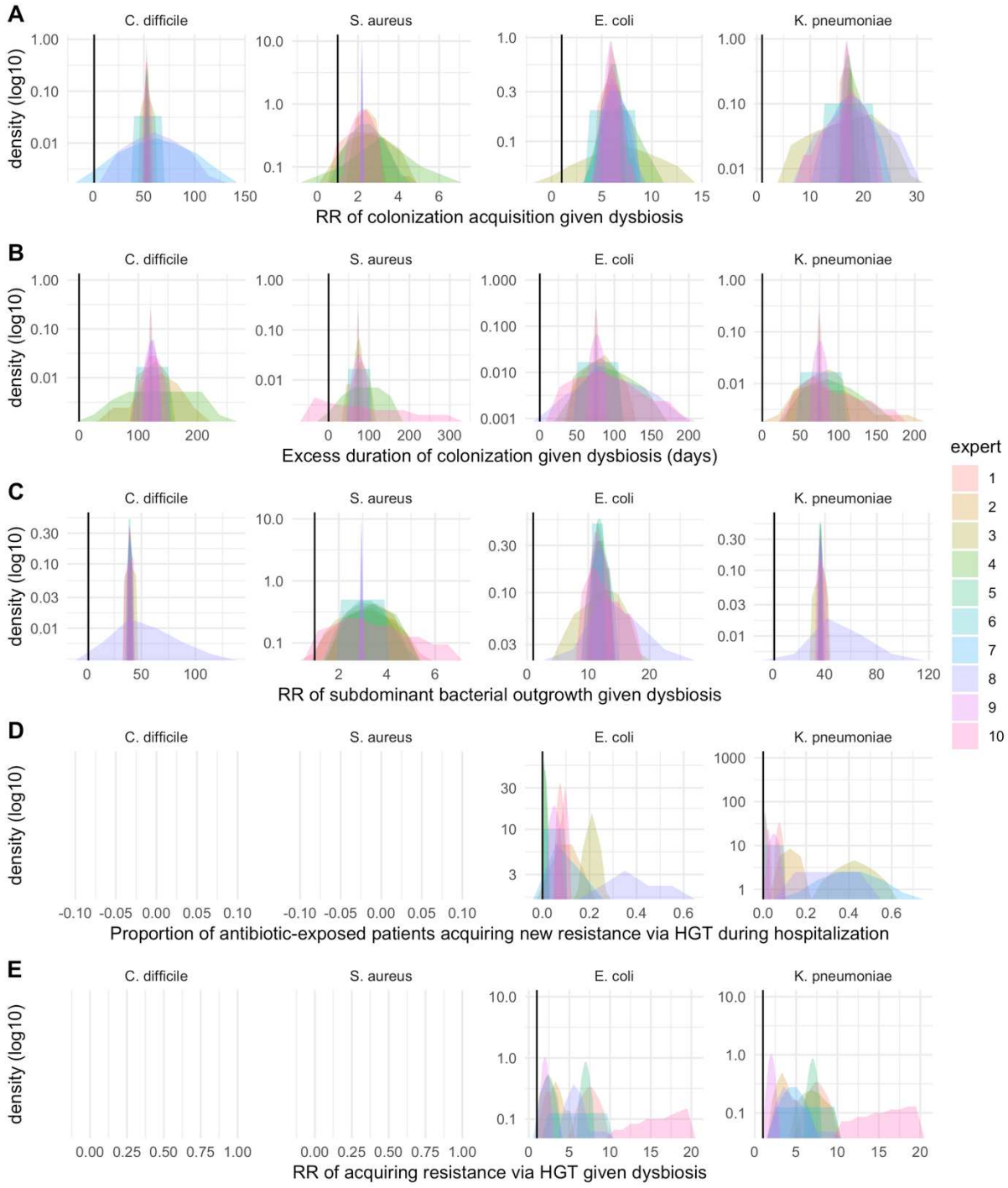

Figure 5.4. Quantitative expert elicitation results (re-centred data)

Expert elicitation results: expert belief and uncertainty about the impact of microbiome dysbiosis on nosocomial colonization dynamics of included bacterial pathogens. Distributions were generated during expert interviews using the MATCH Uncertainty Elicitation Tool with the chips and bins method.(Morris et al., 2014) Experts are anonymized and represented by different colours. Rows A through E represent, respectively, responses to questions 2 through 6 from the expert elicitation protocol (see clinical parameters in **Table 5.7**).

5.2.5. Simulating colonization dynamics using Monte Carlo sampling

Using the model characterizations and parameter values described above, colonization dynamics for each ARB were simulated. Monte Carlo sampling methods were used to account for parameter uncertainty. Specifically, 10,000 unique parameter vectors Ω were created by drawing random values for each parameter from its respective probability distribution. For each Ω, steady-state epidemiological outcomes (prevalence, resistance rate, daily incidence) were calculated through numerical ODE integration as described in section 4.2.6. Final outcome distributions are reported as the median and 95% uncertainty interval, i.e. the 50th (2.5th–97.5th) percentiles across all simulations.

5.2.6. Sensitivity analyses

To evaluate the impact of microbiome competition on model outcomes, a second lot of "single-species simulations" was run after removing microbiome-pathogen interactions from all Ω ($\varepsilon = 0$, $\eta = 0$, $\phi = 1$, $\chi = 0$).

To quantify the impact of parameter uncertainty on model outcomes, multivariate sensitivity analyses were conducted. For each pathogen, model parameter values were re-sampled from their distributions (**Tables 5.1, 5.3 – 5.6**) using Latin Hypercube Sampling over 10,000 iterations. For each parameter set, epidemiological outcomes were re-calculated at population dynamic equilibrium, and partial rank correlation coefficients (PRCCs) were calculated between each parameter and (i) C^R prevalence and (ii) the pathogen resistance rate (using the R package *pse*).(Chalom and Prado, 2013)

5.2.7. Incorporating public health interventions

Three public health interventions τ were incorporated into ODE models (equation 4.17) to evaluate their impact on epidemiological outcomes for each ARB.

5.2.7.1. Contact precautions

Contact precautions were assumed to represent physical or behavioural barriers that block opportunities for transmission, reducing transmission rates by the same fraction τ_{ipc} across all pathogens relative to baseline. This is given by

$$\beta_{ipc} = (1 - \tau_{ipc}) \times \beta \qquad \text{(eq. 5.5)}$$

5.2.7.2. Antibiotic stewardship

Antibiotic stewardship programmes were assumed to alter antibiotic consumption patterns in the hospital. Two main types were considered: antibiotic reduction, which limits overall antibiotic prescribing by a fraction τ_{asp}, given by

$$\mathrm{a}_{asp} = (1 - \tau_{asp}) \times \mathrm{a} \quad \text{(eq. 5.6)}$$

and antibiotic restriction, which adjusts the distribution of antibiotic classes consumed in the hospital. Two types of restriction were considered, the first favouring narrow-spectrum antibiotics (e.g. macrolides) over broad-spectrum (e.g. quinolones), and the second favouring antibiotics that cause dysbiosis at very low or low rates (k={3,2}) over those causing dysbiosis at medium or high rates (k={1,0}) (see **Table 5.2** for antibiotic classification). For both, the proportion of antibiotics in the restricted group ($p_{restrict}$) was reduced by the same fraction τ_{asp} without adjusting the distribution of antibiotics consumed within that group, given by

$$p_{restrict|asp} = p_{restrict} - \tau_{asp} \quad \text{(eq. 5.7)}$$

and the proportion of non-restricted antibiotics was increased symmetrically. With this structure, τ_{asp} alters antibiotic consumption for the same proportion of hospital patients across all three stewardship interventions. In all simulations, $p_{restrict} > \tau_{asp}$.

5.2.7.3. Microbiome recovery therapy

Microbiome recovery therapy was assumed to trigger recovery at rate 0.5 day^{-1} and was apportioned to the fraction τ_{pbt} of patients, such that the overall rate of microbiome recovery when including these interventions (δ_{pbt}) is given by

$$\delta_{pbt} = \delta + 0.5 \times \tau_{pbt} \quad \text{(eq. 5.8)}$$

For simplicity, different values assumed for intervention parameters ($\tau_{ipc} \in \{0.2, 0.35, 0.5\}$, $\tau_{asp} \in \{0.2, 0.35, 0.5\}$, $\tau_{pbt} \in \{0.1, 0.3, 0.5\}$) are interpreted as different levels of compliance to respective interventions.

5.2.8. Calculating intervention efficacy

Intervention efficacy was calculated using two outcomes:

1. Reduction in colonization incidence, 1 – IRR (where IRR is the incidence rate ratio of post-intervention to pre-intervention incidence).
2. Reduction in the resistance rate, 1 – RRR (where RRR is the resistance rate ratio, the ratio of the post-intervention to pre-intervention resistance rate).

Outcomes were matched across Monte Carlo simulations, such that IRRs and RRRs were calculated for each intervention and compliance level for each Ω. The distribution of outcomes is expressed as the median and 95% uncertainty interval. For each intervention, outcomes are compared from simulations that include microbiome-pathogen interactions and dysbiosis ("microbiome simulations") and simulations that exclude them ("single-species simulations"). Unless stated otherwise, results presented are for microbiome simulations.

To validate simulations with data from the literature, antibiotic stewardship results were compared to findings from a systematic review and meta-analysis of hospital antibiotic stewardship interventions.(Baur et al., 2017) They included interventional studies published worldwide describing incidence of bacterial colonization or infection among hospital inpatients (Jan 1960–May 2016). Stewardship interventions were heterogeneous, including audits, antibiotic restriction, antibiotic cycling, antibiotic mixing, feedback, guideline implementation and education. No evidence of publication bias or small study effects were found. Their analysis included 32 studies over 9 million patient-days, though stewardship interventions were co-implemented with other infection control measures (e.g. hand hygiene, patient isolation) in 31% of studies. When limited to stewardship, patients were still significantly less likely to experience colonization and infection (IRR=0.81, 0.67-0.97), but species-specific estimates were not made. When excluding studies that included non-stewardship interventions, ten studies remained for MRSA, seven for *C. difficile*, two for ESBL-*E. coli*, and one for CP-*K. pneumoniae*. For ESBL-*E.* coli, studies of ESBL-producing Enterobacteriaceae and Gram-negative bacteria were considered. Using methodology from Baur et al., incidence risk ratios (IRR) were calculated using the standard inverse-variance method, and pooled IRRs across species using mixed-effects meta-analysis models (R package *metafor*).

5.3. Results

5.3.1. Expert characterization of different nosocomial pathogens

During elicitation interviews, experts highlighted (i) uncertainty about an influence of strain competition on hospital colonization dynamics for all ARB, with the majority of experts believing strain competition was irrelevant for *C. difficile* but at least partially relevant for other ARB, (ii) unanimous certainty about a role for antibiotic-induced microbiome dysbiosis as a driver of colonization for *C. difficile*, ESBL-EC and CP-KP, with somewhat less certainty for MRSA, and (iii) certainty about a role for horizontal gene transfer (HGT) for ESBL-EC and CP-KP (**Figure 5.2**). These findings informed the different ecological interactions included for each ARB (**Figure 5.1A**).

Overall, experts differed substantially in estimated ranges of different parameters, but Friedman's tests suggested that the species rank order was conserved across experts, with *C. difficile* generally having the strongest estimated microbiome-pathogen interaction coefficients, and MRSA the weakest (**Figure 5.3**). For this reason, re-scaled data were used when pooling expert distributions (**Figure 5.4**). Final fitted distributions for each parameter and ARB are given in **Tables 5.3 – 5.6**, and for select parameters in **Figure 5.1B**.

5.3.2. ARB-specific colonization dynamics

Figure 5.5 depicts the baseline steady-state epidemiological outcomes for each ARB (colonization prevalence, colonization incidence and the resistance rate). Across simulations, *C. difficile* was the most prevalent pathogen (**Figure 5.5A**), MRSA had the highest resistance rate (**Figure 5.5B**), and ESBL-EC had the highest rate of incidence within the hospital (**Figure 5.5C**). CP-KP had the lowest prevalence, resistance rate and incidence, consistent with its much low burden in the community. Patient-to-patient transmission was the primary route of MRSA acquisition, while endogenous acquisition was the primary route for the enteric pathogens *C. difficile*, ESBL-EC and CP-KP (**Figure 5.5C**). HGT played a potentially important but highly uncertain role for ESBL-EC and CP-KP, accounting for 8.7% (<0.01–49.7%) and 2.1% (<0.01–22.8%) of acquisition events, respectively.

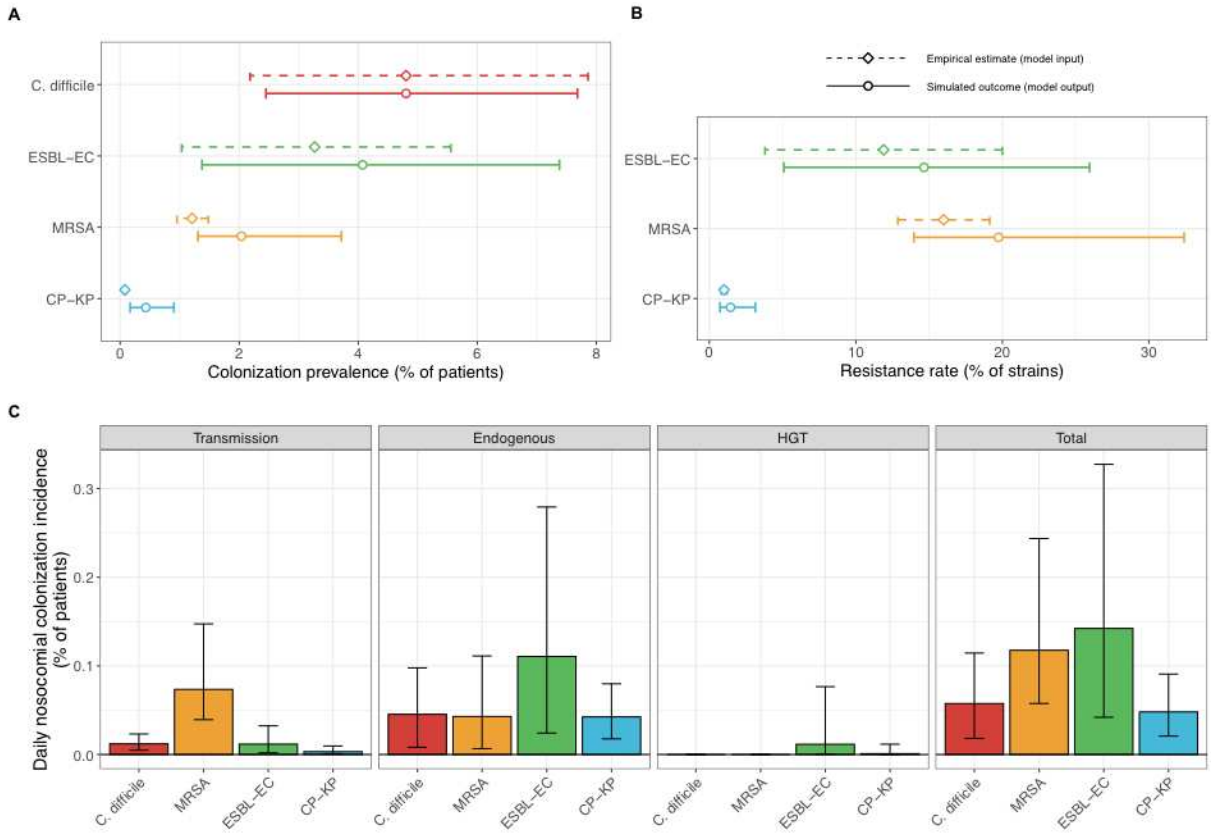

Figure 5.5. Baseline epidemiological outcomes (microbiome simulations).

Baseline steady-state colonization outcomes for each ARB in **microbiome simulations**. **(A)** Colonization prevalence, the percentage of patients colonized with the focal strain. Dashed lines (model inputs) represent assumed community prevalence, i.e. the proportion of patients already colonized upon hospital admission (see **Tables 5.3 – 5.6**). Solid lines represent simulated prevalence within the hospital. **(B)** Resistance rates, the proportion of methicillin-resistant *S. aureus* strains, ESBL-producing *E. coli* strains, and carbapenemase-producing *K. pneumoniae* strains. Dashed lines (model inputs) represent assumed community resistance rates, i.e. resistance rates upon hospital admission (see **Tables 5.3 – 5.6**). Solid lines represent simulated resistance rates within the hospital. **(C)** Pathogen incidence (daily rate of within-hospital colonization acquisition), stratified by route of acquisition. Points (A and B) and bar height (C) represent medians, and error bars represent 95% uncertainty intervals across 10,000 Monte Carlo simulations. For comparison, the same information for single-species simulations excluding the microbiome is presented in **Figure 5.6**.

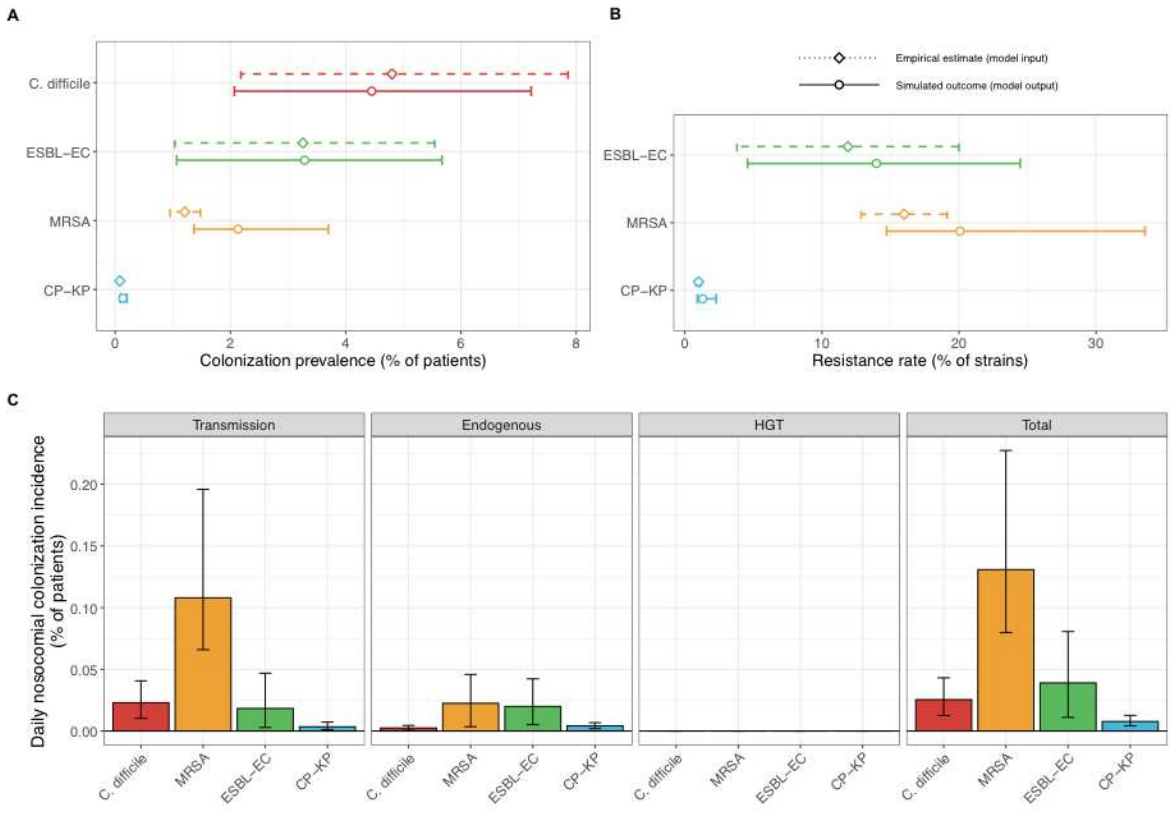

Figure 5.6. Baseline epidemiological outcomes (single-species simulations).

Baseline steady-state colonization outcomes for each ARB in **single-species simulations**. **(A)** Colonization prevalence, the percentage of patients colonized with the focal strain. Dashed lines (model inputs) represent assumed community prevalence, i.e. the proportion of patients already colonized upon hospital admission (see **Tables 5.3 – 5.6**). Solid lines represent simulated prevalence within the hospital. **(B)** Resistance rates, the proportion of methicillin-resistant *S. aureus* strains, ESBL-producing *E. coli* strains, and carbapenemase-producing *K. pneumoniae* strains. Dashed lines (model inputs) represent assumed community resistance rates, i.e. resistance rates upon hospital admission (see **Tables 5.3 – 5.6**). Solid lines represent simulated resistance rates within the hospital. **(C)** Pathogen incidence (daily rate of within-hospital colonization acquisition), stratified by route of acquisition. Points (A and B) and bar height (C) represent medians, and error bars represent 95% uncertainty intervals across 10,000 Monte Carlo simulations.

Figure 5.7 shows how simulated colonization outcomes (prevalence and resistance rates among hospital inpatients) compare to baseline model inputs (assumed prevalence and resistance rates among patients upon admission from the community). Overall, the hospital environment tended to amplify ARB colonization relative to the community. In microbiome simulations, colonization prevalence was greater in the hospital than in the community for MRSA, ESBL-EC and CP-KP, but not *C. difficile*. CP-KP was the pathogen most favoured by the hospital environment, its prevalence increasing by approximately 5.4-fold (95% uncertainty interval: 2.1–10.9) within the hospital relative to baseline prevalence in the community (**Figure 5.7A**). In single-species simulations, CP-KP prevalence increased in hospital but to a lesser degree than in microbiome simulations, while *C. difficile* prevalence decreased in the hospital relative to the community, and

ESBL-EC prevalence was stable. Only for MRSA were nosocomial colonization prevalence ratios approximately equal across microbiome and single-species simulations. For pathogens subject to intraspecific strain competition, resistance rates in the hospital also tended to exceed rates in the community, with similar estimates across single-species and microbiome simulations (**Figure 5.7B**).

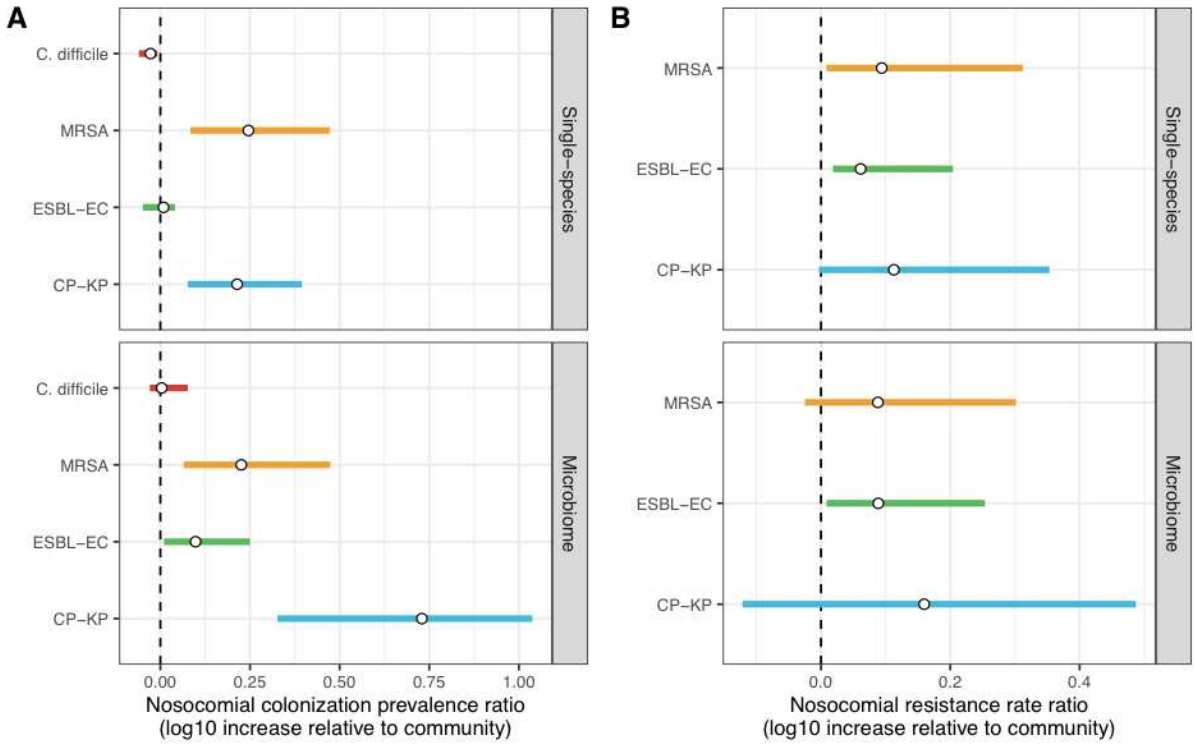

Figure 5.7. Nosocomial ARB amplification.

Change in ARB colonization outcomes in the hospital relative to the community (log_{10} scale), comparing single-species and microbiome simulations. **(A)** The ratio of colonization prevalence among hospital patients relative to baseline colonization prevalence in the community. **(B)** The ratio of resistance rates in the hospital relative to baseline resistance rates in the community. Points represent medians and error bars represent 95% uncertainty intervals across 10,000 Monte Carlo simulations.

5.3.3. Multivariate sensitivity analyses

Results of multivariate sensitivity analyses are provided in **Figure 5.8**. Though each pathogen varied somewhat in which parameters drove colonization dynamics, community prevalence (f_C for *C. difficile*; f_R for MRSA, ESBL-EC and CP-KP) and rates of endogenous acquisition (α_R) were overall most strongly positively correlated with both hospital prevalence and resistance rates across ARB. Ecological release (ϕ) and antibiotic-induced microbiome dysbiosis (θ_m) were also positively associated with prevalence across pathogens, as well as the HGT rate during dysbiosis (χ_d) for ESBL-EC and CP-KP. Rates of hospital admission/discharge (μ) and microbiome recovery (δ) were generally negatively correlated with prevalence across ARB. Conversely, microbiome parameters (ε, η, ϕ, δ,

σ_m, χ_e) were minimally correlated with resistance rates, with the exception of χ_d.

Figure 5.8. Partial rank correlation coefficients.

Multivariate sensitivity analysis describing partial rank correlation coefficients (PRCC) between model parameters and epidemiological outcomes evaluated at population dynamic equilibrium: in panel A, colonization prevalence of each ARB (focal strain C^R); in panel B, the resistance rate.

5.3.4. Intervention efficacy

Epidemiological impacts of simulated public health interventions are presented in **Figures**

5.9 – 5.12 for all species and interventions, and comparing single-species and microbiome simulations. **Figure 5.9** shows efficacy of interventions for reducing colonization incidence. **Figure 5.10** shows efficacy of interventions for reducing pathogen resistance rates. **Figure 5.11** shows how intervention efficacy for reduction of colonization incidence varied across different acquisition routes (patient-to-patient transmission, endogenous acquisition and HGT). Finally, **Figure 5.12** shows how each antibiotic stewardship intervention varied in its efficacy for reducing colonization incidence.

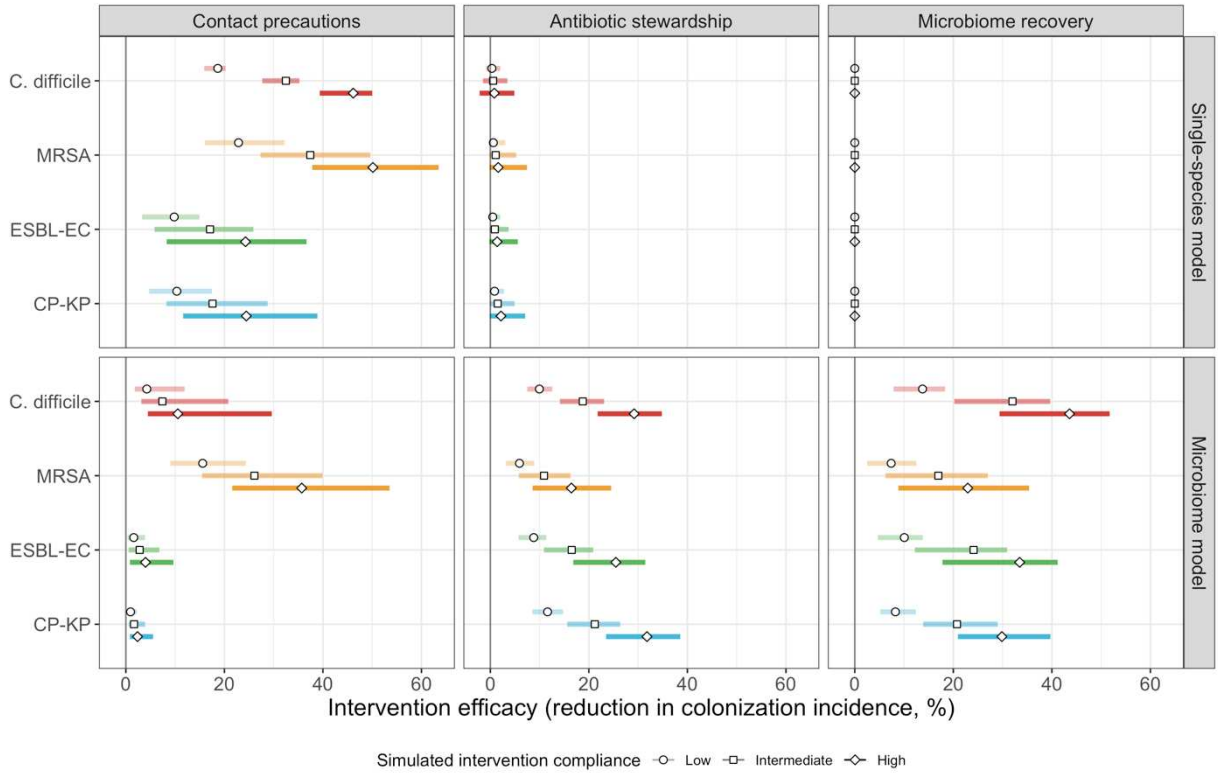

Figure 5.9. Intervention efficacy (colonization incidence).

The microbiome drove pathogen-specific responses to simulated public health interventions (left panels, contact precautions; middle, antibiotic stewardship; right, microbiome recovery therapy). Top panels show results from simulations using classical 'single-species models' that only accounted for the focal pathogen species (including intraspecific strain competition for MRSA, ESBL-EC and CP-KP); bottom panels show simulation results when models also included microbiome-pathogen interactions and antibiotic-induced microbiome dysbiosis. For each intervention, three levels of intervention compliance (shading) were simulated. For antibiotic stewardship, simulation results were pooled across three different types of stewardship (see **Figure 5.12**). Points correspond to medians, and bars to 95% uncertainty intervals across 10,000 Monte Carlo simulations.

5.3.4.1. Contact precautions

Intervention efficacy for colonization prevention varied considerably by pathogen and type of intervention (**Figure 5.9**). Contact precautions were highly effective for reducing MRSA incidence, of intermediate efficacy for *C. difficile*, and minimally effective for ESBL-EC and CP-KP. Contact precautions had comparatively little impact on resistance rates, with a

median 2–4% reduction across simulations and compliance levels for MRSA, 0–2% for CP-KP and negligible impact for ESBL-EC (**Figure 5.10**). These interventions were overall less effective in microbiome simulations, which tended to limit the role of between-host transmission (via colonization resistance) and favour the role of endogenous acquisition (via ecological release) in the hospital environment when compared to single-species simulations (see **Figures 5.5, 5.6**).

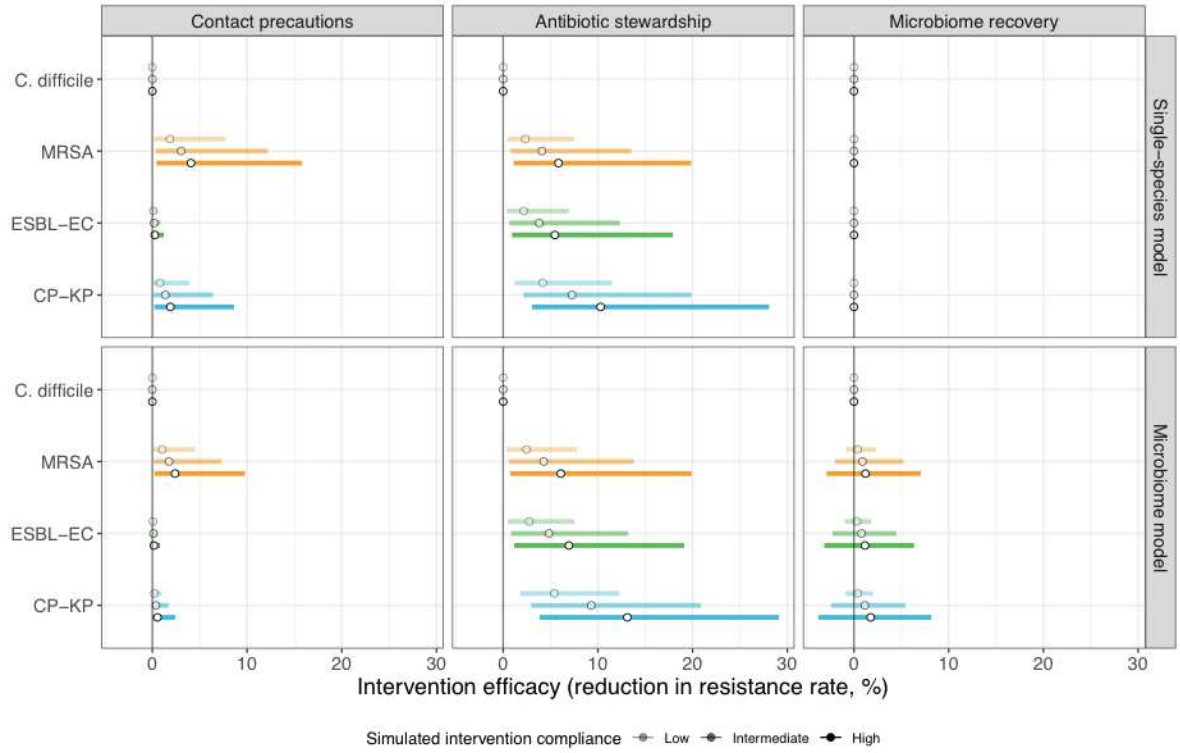

Figure 5.10. Intervention efficacy (resistance rates).

Compared to pathogen incidence, strain dynamic responses to public health interventions were similar across single-species and microbiome simulations (left panels, contact precautions; middle, antibiotic stewardship; right, microbiome recovery interventions). Top panels show results from simulations using 'single-species models' that only accounted for the focal pathogen species (including intraspecific strain competition for MRSA, ESBL-EC and CP-KP); bottom panels show simulation results when models also included microbiome-pathogen interactions and antibiotic-induced microbiome dysbiosis. For each intervention, three levels of intervention compliance (shading) were simulated. Points correspond to medians, and bars to 95% uncertainty intervals across 10,000 Monte Carlo simulations.

5.3.4.2. Antibiotic stewardship

Antibiotic stewardship interventions led to substantial reductions in nosocomial incidence for all pathogens, but only when the microbiome was taken into account (**Figure 5.9**). Unlike contact precautions, which only reduced incidence via transmission, stewardship reduced incidence through all acquisition routes (**Figure 5.11**). Overall efficacy estimates and species-specific responses were similar across three types of stewardship considered (**Figure 5.12**). Pooling these together under intermediate compliance, colonization

incidence was reduced by a median 20% for CP-KP, 18% for C. difficile, 15% for ESBL-EC and 10% for MRSA. Single-species simulations excluding microbiome competition predicted negligible efficacy of all stewardship interventions for reducing incidence, and non-efficacy for *C. difficile*. Stewardship interventions also had a substantial impact on resistance rates, with overall greater reductions for CP-KP than MRSA and ESBL-EC, and similar outcomes across microbiome and single-species simulations (**Figure 5.10**).

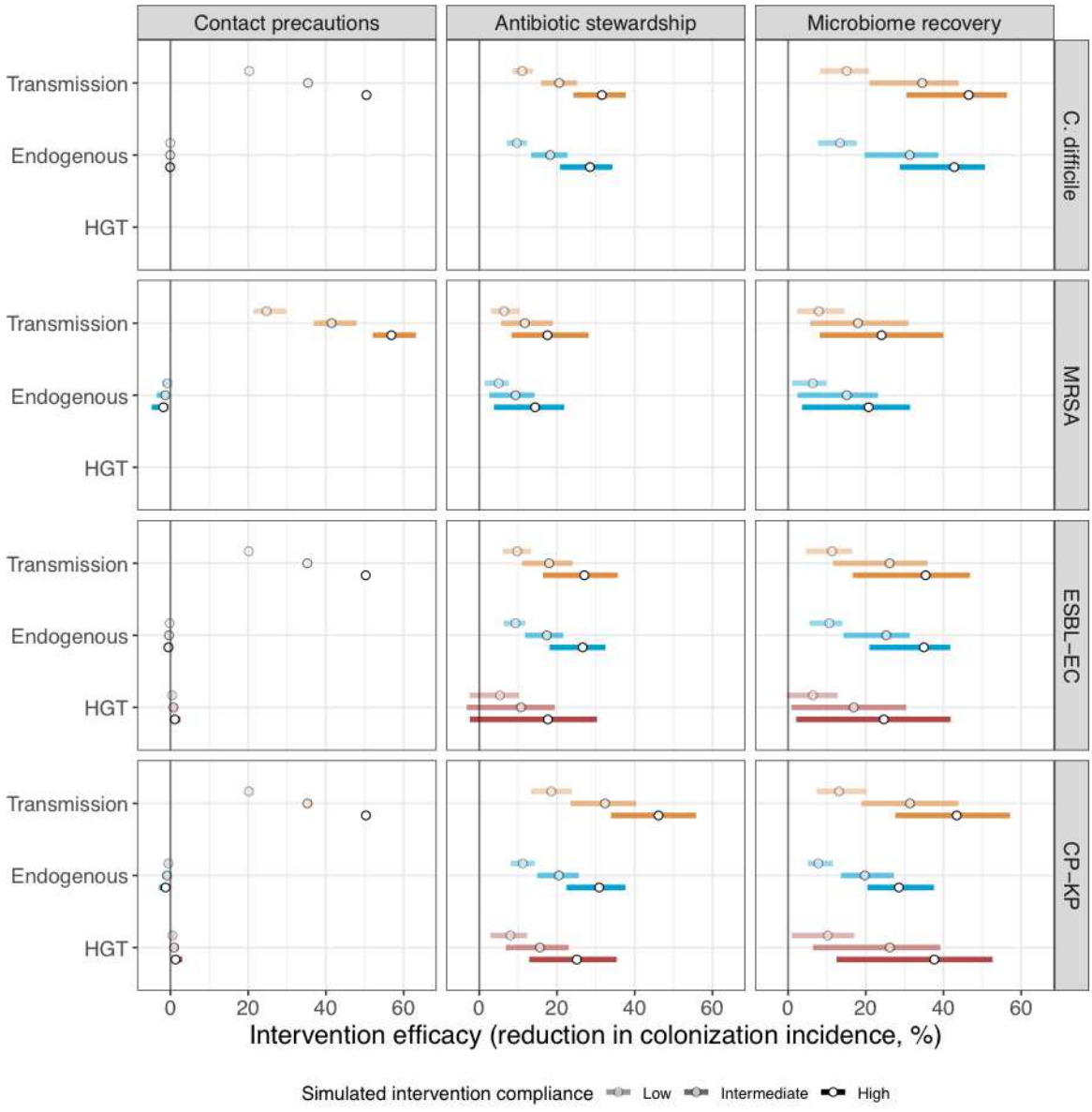

Figure 5.11. Intervention efficacy (acquisition routes).

Interventions acted on different routes of colonization acquisition in **microbiome simulations**. Intervention efficacy (x-axis) for reducing colonization incidence via different routes of colonization acquisition (colours) for different interventions (columns) and ARB (rows). Unlike contact precautions, which only reduced incidence via transmission, antibiotic stewardship and microbiome recovery interventions reduced colonization incidence through all considered routes. Points correspond to medians, and bars to 95% uncertainty intervals across 10,000 Monte Carlo simulations.

5.3.4.3. Microbiome recovery therapy

Lastly, microbiome recovery therapy was potentially highly effective for limiting pathogen incidence, but efficacy varied greatly across different levels of intervention compliance (**Figure 5.9**). This intervention was most effective against *C. difficile*, of similar efficacy against ESBL-EC and CP-KP, and comparatively least effective against MRSA. Across pathogens, microbiome recovery therapy reduced incidence through all acquisition routes (**Figure 5.11**), but had no clear impact on resistance rates (**Figure 5.10**).

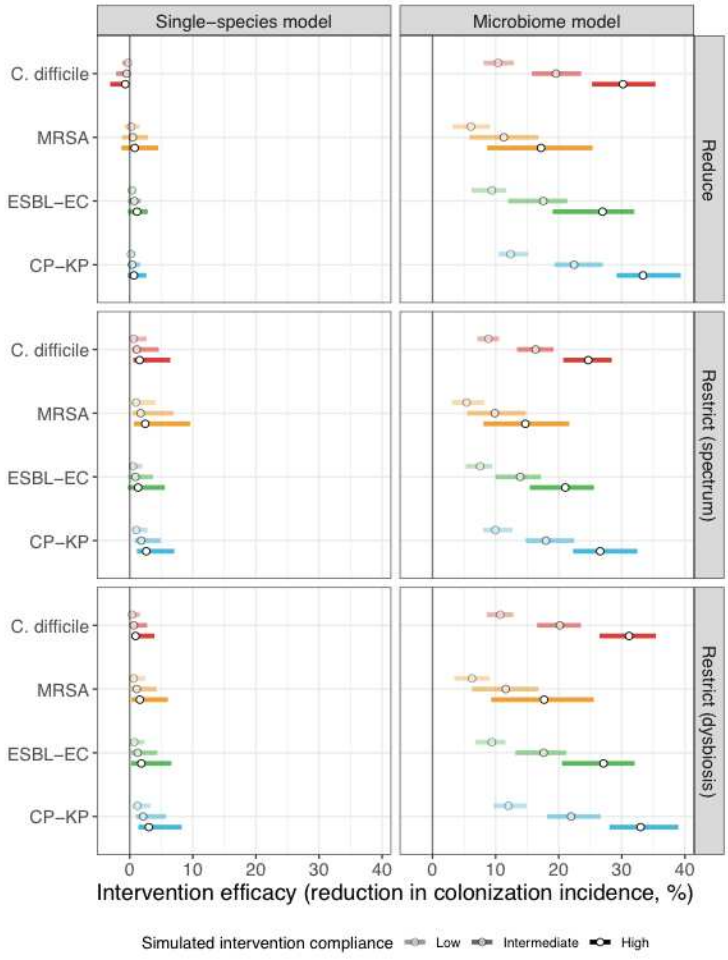

Figure 5.12. Antibiotic stewardship efficacy (colonization incidence).

Intervention efficacy (reduction in colonization incidence) for three considered types of antibiotic stewardship: (i) reducing overall antibiotic prescribing, (ii) restricting broad-spectrum antibiotics in favour of narrow-spectrum antibiotics; and (iii) restricting antibiotics categorized as inducing microbiome dysbiosis at high or very high rates in favour of those that induce dysbiosis at medium or low rates. In microbiome simulations, restricting antibiotics that induce dysbiosis at a high rate was approximately as effective as reducing overall antibiotic prescribing. In single-species simulations, all stewardship interventions were of limited, if any efficacy. Points correspond to medians, and bars to 95% uncertainty intervals across 10,000 Monte Carlo simulations.

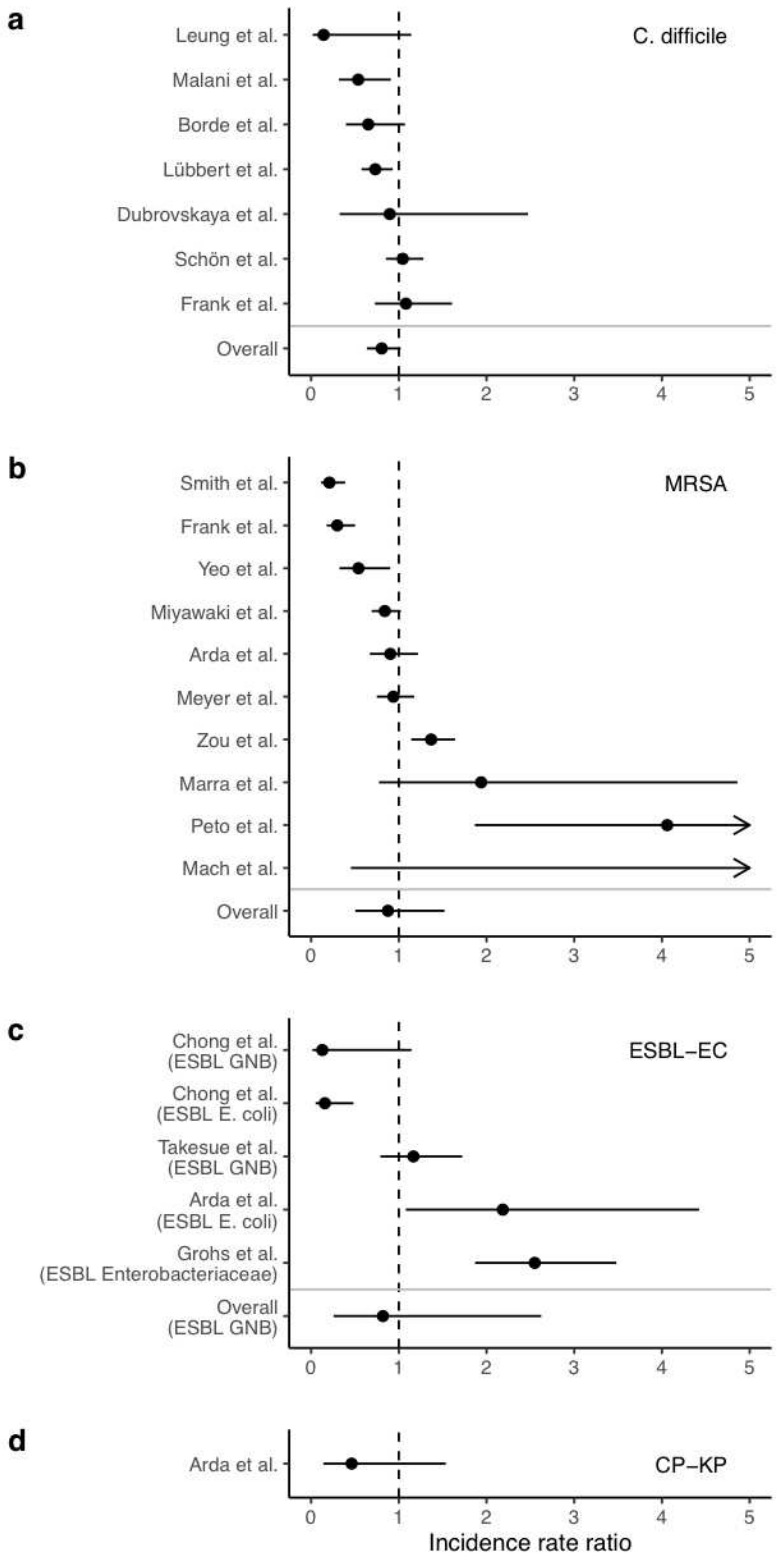

Figure 5.13. Antibiotic stewardship efficacy (meta-analysis).

Incidence rate ratios (IRRs) for ARB colonization and infection among hospital inpatients exposed to antibiotic stewardship interventions. IRRs were calculated using data presented in Baur *et al*.(Baur et al., 2017) Results are stratified by four pathogens: **(a)** *C. difficile*, **(b)** methicillin-resistant *S. aureus*, **(c)** ESBL-producing *E. coli* (and here also including ESBL-producing Enterobacteriaceae or Gram-negative bacteria), and **(d)** carbapenemase-producing *K. pneumoniae*. Points represent means and bars represent 95% confidence intervals.

5.4. Discussion

5.4.1. Summary of model and results

This work has demonstrated the utility of a microbiome-oriented approach for modelling the nosocomial epidemiology of antibiotic-resistant bacterial pathogens. The included pathogens MRSA, *C. difficile* and ESBL- and carbapenemase-producing Enterobacteriaceae are all leading causes of antibiotic-resistant and healthcare-associated infection, but the mechanistic drivers of their epidemiological dynamics remain relatively poorly understood, and developing strategies for their control is a leading public health priority.(Cassini et al., 2019; Jernigan et al., 2020; Miller et al., 2011; Rodríguez-Baño et al., 2018) Model simulations from this Chapter have helped to provide insights into how these ARB spread in healthcare settings, and why particular interventions may be more or less effective than others for colonization prevention.

5.4.1.1. Acquisition routes

Microbiome-pathogen interactions had large impacts on epidemiological dynamics of included pathogens. When microbiota were excluded, patient-to-patient transmission was the cause of most nosocomial ARB acquisition, and MRSA had on average higher incidence than all other ARB combined. By contrast, when microbiome interactions were included, ESBL-EC was the most incident ARB, endogenous acquisition was overall the leading cause of colonization acquisition across ARB, and HGT played a less important role than patient-to-patient transmission but nonetheless contributed to colonization acquisition for multidrug-resistant Enterobacteriaceae. Endogenous acquisition is known to be a major source of ARB colonization – in particular for gut-residing bacteria like *C. difficile* and multidrug-resistant Enterobacteriaceae – and the present findings demonstrate that microbiome-pathogen interactions may help explain high rates of nosocomial colonization incidence for certain ARB in the context of antibiotic use, despite relatively low rates of person-to-person transmission.

5.4.1.2. Intervention efficacy

Microbiome-pathogen interactions also had large impacts on the efficacy of different control interventions for preventing ARB acquisition. When microbiota were excluded, contact precautions were the only interventions capable of reducing ARB colonization incidence, and were effective against all ARB. By contrast, when microbiome interactions were included, contact precautions were effective for reducing incidence of MRSA and to a

lesser extent *C. difficile*, but not Enterobacteriaceae; antibiotic stewardship interventions were broadly effective across all ARB for reducing colonization incidence, in particular for CP-KP; and theoretical microbiome recovery therapy interventions were potentially highly effective for reducing colonization incidence, in particular for *C. difficile*. Overall, these findings suggest that preservation of host microbiota may explain how antibiotic stewardship works to reduce ARB colonization incidence, that interventions favouring healthy microbiome function hold promise to help mitigate the epidemiological burden of antibiotic resistance, and more broadly that patient microbiota may play a significant role in determining the epidemiological impacts of public health interventions.

5.4.2. Findings in context

5.4.2.1. Comparison of results

Microbiome simulations predicted colonization dynamics that are broadly consistent with previous findings from the literature. Modelling studies have estimated that input from the community is the main driver of hospital prevalence, and that both prevalence and resistance rates tend to increase in the hospital relative to the community (Knight et al., 2018; MacFadden et al., 2019). High rates of between-host transmission for MRSA have been observed clinically,(Khader et al., 2019; Nadimpalli et al., 2020) while comparatively high rates of endogenous acquisition for *C. difficile* and antibiotic-resistant Enterobacteriaceae have been estimated elsewhere (Bootsma et al., 2007; Gurieva et al., 2018; Martin et al., 2016). Genomic data also suggest that, for gut-residing ARB like *C. difficile* and ESBL-producing *E. coli*, person-to-person transmission may explain only a minority of nosocomial acquisition events.(Caroff et al., 2017; Ludden et al., 2021)

Estimates of intervention efficacy were also more consistent with findings from the literature when microbiome interactions were taken into account. Clinical trials and modelling estimates have found that contact precautions are effective for reducing incidence of MRSA and to a lesser extent *C. difficile*, but that impact against ESBL-producing Enterobacterales is limited.(Khader et al., 2021; Kluytmans-van den Bergh et al., 2019; Luangasanatip et al., 2015; Maechler et al., 2020; World Health Organization, 2014) By contrast, findings from the updated meta-analysis of clinical trials suggest that hospital antibiotic stewardship interventions may be broadly effective for reducing nosocomial incidence of colonization and infection with all included ARB (**Figure 5.13**). The meta-analysis predicted the same rank order of efficacy across included ARB, and similar mean efficacy for *C. difficile* (19% from n=7 studies, vs. 18% under intermediate

compliance in simulations), ESBL-EC (18% from n=4 studies, vs. 15%) and MRSA (12% from n=10 studies, vs. 10%), but higher efficacy for CP-KP (54% from n=1 study, vs. 20%). However, many of the underlying empirical results were associated with high levels of uncertainty across heterogeneous interventions, and low methodological quality.

When excluding microbiome interactions, simulations predicted negligible efficacy of antibiotic stewardship interventions for controlling ARB incidence. Previous models in the literature have predicted efficacy using predominantly strain-based approaches, but often focus on resistance rates as the primary outcome, and in many cases assume that patient-to-patient transmission is the only route of colonization acquisition.(Niewiadomska et al., 2019) In present simulations, microbiome interactions had a large impact on incidence but little impact on resistance rates, for which stewardship interventions were of similar efficacy across single-species and microbiome simulations (**Figure 5.9** vs. **Figure 5.10**). Consistent with findings in the previous Chapter, this reflects the potential importance of different forces of antibiotic selection for different epidemiological indicators: while intraspecific competition is a key force of antibiotic selection for many ARB, driving the spread of drug-resistant vs. drug-sensitive strains, microbiome interactions may be highly relevant drivers of colonization acquisition, particularly in healthcare settings where risks of antibiotic exposure and microbiome dysbiosis are high.

5.4.2.2. Linking within-host bacterial ecology to between-host dynamics

Studies focusing on within-host microbiome and pathogen dynamics have reached similar conclusions to those found in the present work. Insights from both experiments and mathematical models suggest that antibiotic disruption of microbiome-pathogen competition is a key driver of selection for resistance evolution and dissemination within the host.(Baumgartner et al., 2020; Estrela and Brown, 2018; O'Brien et al., 2021; Shaw et al., 2019; Stein et al., 2013; Tepekule et al., 2019) Modelling has also been used previously to evaluate impacts of microbiome-oriented interventions at the within-host level, suggesting promise for preventing dysbiosis and in turn limiting the proliferation of antibiotic-resistant bacteria.(Guittar et al., 2021; Guk et al., 2021) However, knock-on impacts of these within-host processes on ARB transmission dynamics and epidemiological burden have not been evaluated previously, with the exception of a number of studies describing the epidemiological impacts of HGT.

Although HGT modelling has largely been limited to studies of within-host or within-culture

bacterial population dynamics,(Leclerc et al., 2019; Lerminiaux and Cameron, 2019) its connections to bacterial epidemiology are beginning to come to light. Most notably, Lehtinen et al. analyzed *S. pneumoniae* isolates from infants at a refugee camp in South-East Asia, estimating a low impact of resistance acquisition via HGT relative to selection acting upon standing genetic variation.(Lehtinen et al., 2020) Further, using genomic surveillance data from a UK hospital, Ludden et al. found little evidence for plasmid-mediated transmission of ESBL-encoding genes.(Ludden et al., 2021) By contrast, Evans et al. found evidence for plasmid transfer between distantly-related genera in longitudinal samples of hospital patients in the USA; and León-Sampedro et al. found pervasive within-host transfer of a carbapenemase-encoding plasmid (pOXA-48) among gut microbiota of patients in a hospital in Spain.(D. R. Evans et al., 2020; León-Sampedro et al., 2021) Altogether, these findings suggest an unclear impact of HGT on epidemiological dynamics of antibiotic resistance in healthcare settings, consistent with substantial uncertainty among expert beliefs and HGT-related outcomes in the present work.

5.4.3. Limitations

Simulations were limited by the availability of species-specific model parameters from the literature, in some instances necessitating use of previous modelling results, approximations, or estimates from small studies in particular locations, making the generalizability of findings across healthcare settings unclear. For instance, previous modelling studies have estimated a 4-fold difference in MRSA transmission rates between hospitals and nursing homes.(Khader et al., 2019) Such differences could have a substantial impact on dynamics and estimated intervention efficacy, with higher transmission rates favouring use of contact precautions, and higher rates of endogenous acquisition favouring antibiotic stewardship (in the context of a high estimated ecological release coefficient). Overall, uncertainty in parameter inputs translated to uncertainty in model outputs, reflecting the knowledge gaps underlying simulations (**Figure 5.8**). Uncertainty in endogenous acquisition rates may have been particularly important: direct estimates from the literature were not available for *C. difficile* and MRSA, yet in multivariate sensitivity analyses this parameter emerged as a key driver of both colonization prevalence and resistance rates across all ARB (**Figure 5.8**).

In light of its outsized role in driving outcome uncertainty, it is important to highlight the epistemic uncertainty surrounding endogenous acquisition. In Chapter 4, it was highlighted that this parameter represents acquisition not resulting from person-to-person transmission

(e.g. translocation). However, in reality, what appears to be endogenous acquisition may actually be delayed detection of transmission. A transmitted pathogen can establish a colony without becoming detectable in clinical specimens, but this same colony may later become detectable, for instance after antibiotic exposure. In this case, transmission and endogenous outgrowth may simultaneously drive increased resistance burden and risk of onward transmission. This level of complexity was not explicitly captured in this work, and future modelling studies accounting for hosts with sub-dominant (i.e. clinically undetectable) colonization, and not just dominant (detectable) colonization, may help to disentangle and better quantify the true epidemiological impacts of different routes of acquisition. Similarly, better understanding of endogenous emergence of resistance among microbiota is needed. Here, microbiota could acquire resistance subsequent to microbiome dysbiosis, motivated by empirical work demonstrating increased abundance of antibiotic resistance determinants subsequent to chronic antibiotic therapy, but in reality these mechanisms are poorly understood, and endogenous resistance emergence in the absence of microbiome dysbiosis may also occur.

Further, the nature of microbiome-pathogen interactions and their epidemiological consequences remain poorly understood and largely unquantified. I show in theory why these interactions matter, but it was not possible to inform their parameterization using empirical data. Instead, microbiome-pathogen competition coefficients were translated into clinical parameters, and I designed an expert elicitation exercise allowing subject-matter experts to quantify their beliefs and uncertainty. Although these estimates are subject to substantial bias and uncertainty, they facilitated species-specific characterization of the epidemiological impact of microbiome dysbiosis, and represent useful proxy measures in the absence of clinical data.

More broadly, model characterizations of microbiome-pathogen interactions were conceptual, and were mapped mechanistically to particular colonization processes (transmission, clearance, endogenous acquisition). However, in other contexts, terms like *colonization resistance, resource competition* and *ecological release* may map to specific biochemical processes that could affect epidemiological parameters in different ways. Further, data used to estimate class-specific rates of microbiome dysbiosis are specific to the gut; class-specific data for dysbiosis of the skin, the preferred niche of *S. aureus*, were not available, potentially over-estimating impacts of dysbiosis on MRSA colonization dynamics. Finally, although *C. difficile*, MRSA and ESBL-EC are widely endemic and

arguably well-represented by the average behaviour predicted by ODE integration, stochastic models would allow for more realistic epidemiological dynamics, and could account for the likely important impacts of stochastic uncertainty on intervention efficacy. This may be particularly true for CP-KP, which remains a rare outbreak pathogen in many regions.

5.4.4. Future directions

The view that preservation of the host microbiome is central to the control of antibiotic-resistant bacteria in clinical settings is not new,(Papanicolas et al., 2020) but interactions between bacterial pathogens and the host microbiome are nonetheless rarely considered in the mathematical modelling literature.(Knight et al., 2019) Findings from this Chapter suggest that simultaneous impacts of antibiotics on competing commensal and pathogenic bacteria can drive antibiotic-driven selection for high-risk ARB, with important consequences for their epidemiological dynamics and the efficacy of public health interventions. Although these simulations were limited to a select few ARB, this modelling framework and its findings likely have relevance for other bacteria known to interact with the microbiome, including vancomycin-resistant Enterococci and other multidrug-resistant Enterobacteriaceae.(B Davido et al., 2019; Stecher et al., 2013) Another extension could be to explore impacts of the microbiome on epidemiological dynamics of antibiotic resistance in the community or other healthcare settings.

In light of the present findings, future clinical and modelling studies investigating the nosocomial epidemiology of antibiotic resistance should account for impacts of host microbiota on the growth and spread of ARB where possible. In particular, studies are needed that describe ecological impacts of antibiotic exposure on microbiome population structure across control and treatment groups, with longitudinal follow-up evaluating subsequent nosocomial ARB colonization risk. Studies are also needed that evaluate the epidemiological impacts of interventions that effectively restore microbiome stability and associated colonization resistance as a means to control ARB spread. Increasing availability and synthesis of high-quality within-host microbiological data into the future should facilitate improved characterization of the ecology of microbiome-pathogen interactions, and of the epidemiological consequences of microbiome dysbiosis across host populations, pathogen species and healthcare settings.

Chapter 6. Simulating SARS-CoV-2 outbreaks in the long-term care setting using individual-based modelling

6.1. The COVID-19 pandemic

On December 31st 2019, a cluster of patients with viral pneumonia of unknown aetiology was reported in Wuhan, China.(ProMED: International Society for Infectious Diseases, 2019) On January 9th 2020, a novel coronavirus was identified as the cause of the outbreak,(World Health Organization, 2020a) and on January 11th its first officially recognized fatality was announced.(World Health Organization, 2020b) Two days later, Thailand's Ministry of Public Health reported the first case outside of China,(World Health Organization, 2020c) and on January 24th the first European cases were reported in France, among three travelers hospitalized after returning from Wuhan.(World Health Organization Regional Office for Europe, 2020) Shortly thereafter, on January 30th, WHO's Director-General Dr. Tedros Adhanom Ghebreyesus declared a public health emergency of international concern.(World Health Organization, 2020d) Finally, on March 11th 2020, with more than 118,000 confirmed cases and 4,291 deaths across 114 countries, WHO declared a global pandemic of *coronavirus disease 2019* (COVID-19), caused by *severe acute respiratory syndrome coronavirus 2* (SARS-CoV-2).(World Health Organization, 2020e)

This "first wave" of the COVID-19 pandemic has been succeeded by various subsequent waves, which have ebbed and flowed asynchronously across the globe, affecting nearly every inhabited region on Earth. As of August 9th 2021, the COVID-19 Dashboard administered by Johns Hopkins University estimates that there have been 203 million confirmed cases of COVID-19 and 4.3 million deaths worldwide,(Center for System Science and Engineering at Johns Hopkins University, 2020) although official figures are widely believed to be underestimated.(Kung et al., 2021; Pullano et al., 2021) For instance, in a meta-analysis of seroprevalence studies, Rostami et al. extrapolated globally to estimate that over 260 million individuals had already been exposed to or infected by SARS-CoV-2 as of August 2020.(Rostami et al., 2021) Yet the public health impacts of the COVID-19 pandemic extend far beyond SARS-CoV-2 infection. Disruptions to food security and global trade are just two examples of how COVID-19 has shocked world

economies,(Guan et al., 2020; Swinnen and McDermott, 2020) while one setting in particular has been nearly universally burdened across cities, countries and continents: the healthcare setting.

6.1.1. Pandemic impacts on healthcare facilities

The COVID-19 pandemic has had vast impacts on healthcare facilities and the provisioning of health services. Exponential growth in COVID-19 hospitalizations over various pandemic waves has overwhelmed hospitals worldwide, with the number of patients requiring hospital beds, intensive care and mechanical ventilation often outnumbering local capacity.(Condes et al., 2021; Grasselli et al., 2020; L. Li et al., 2020) This has compromised care pathways and clinical outcomes for COVID-19 patients and non-COVID-19 patients alike.(Bersano et al., 2020; Olivas-Martínez et al., 2021; Richter et al., 2021) In many regions, healthcare centres have been restructured to accommodate surges in COVID-19 patients at the expense of other services, resulting in cancelled surgical operations, delayed emergency care, missed oncological consultations, and other deleterious impacts across care sectors.(Bonalumi et al., 2020; Søreide et al., 2020; Stöß et al., 2020; Y. Wei et al., 2020) Various other complicating factors have exacerbated conditions for both patients and staff, from high rates of healthcare worker sick leave and burn-out, to scarce or compromised infection prevention and control resources, to medication shortages, to surges in hazardous waste disposal, to heightened hospital security needs.(Alquézar-Arbé et al., 2020; Peiffer-Smadja et al., 2020; Siow et al., 2020) Yet one of the most significant impacts of the COVID-19 pandemic on healthcare facilities, and the focus of subsequent Chapters of this thesis, is that they became epicentres for SARS-CoV-2 transmission.

6.1.2. Nosocomial SARS-CoV-2 transmission

During the initial outbreak in Wuhan, nosocomial transmission was determined to be an important driver of SARS-CoV-2 spread, with identified risk factors for HCW infection including limited PPE, sustained exposure to infected patients, and inadequate training.(Sun et al., 2020; J. Wang et al., 2020; X. Wang et al., 2020) The WHO-China Joint Mission – a 9-day visit of 25 international experts to investigate the emerging outbreak – reported 2,055 laboratory-confirmed cases of COVID-19 among Chinese HCWs in February 2020.(World Health Organization, 2020f) By March, nosocomial outbreaks had been reported in, among other locations, a paediatric ward in South Korea,(Jung et al., 2020) a geriatric unit in France,(Vanhems et al., 2020) a university

hospital in Germany,(Correa-Martínez et al., 2020) an orthopaedic surgery department in Spain,(Lakhani et al., 2020) a rehabilitation clinic in Switzerland,(Mohamed Abbas et al., 2021a) and a university medical centre in the United States.(Bays et al., 2020) In the absence of high-resolution epidemiological or genomic data, particularly early in the pandemic and in the context of exponential growth in the community, it has often been difficult to determine whether SARS-CoV-2 infections among patients and healthcare workers are truly a result of nosocomial acquisition.(Mohamed Abbas et al., 2021b) However, a wide number of studies have now observed, characterized and quantified the transmission of SARS-CoV-2 in healthcare settings.

Using mixed epidemiological and genetic data, Meredith et al. estimated that 15% of 374 hospitalized COVID-19 patients across the East of England up to April 2020 likely acquired their infection in hospital.(Meredith et al., 2020) This is broadly consistent with findings from Evans et al., who used a mathematical modelling approach to estimate that 20% of infections in hospital inpatients and 73% in healthcare workers resulted from nosocomial transmission during the first pandemic wave in England.(S. Evans et al., 2020) Later, between November 2020 and January 2021 in four Oxfordshire hospitals, Lumley et al. used whole genome sequencing to estimate a similar rate of nosocomial infection (14%), and found that approximately 80% of nosocomial transmission occurred during super-spreading events.(Lumley et al., 2021) A key role for super-spreading in driving nosocomial transmission has also been identified elsewhere, for instance using detailed contact tracing data from a tertiary hospital in Taiwan,(Huang et al., 2021) and using phylogenetic analysis in a skilled nursing facility in Massachusetts,(Lemieux et al., 2021), a general ward of a hospital in Hong Kong,(Cheng et al., 2021) and a hospital in England.(Illingworth et al., 2021) There is now an extensive literature describing healthcare-associated COVID-19 infection, and nosocomial outbreak risk has been found to depend on a range of factors, including the type of healthcare facility and the characteristics of the underlying patient and staff populations.(M Abbas et al., 2021; Rovers et al., 2020; Q. Zhou et al., 2020)

6.1.3. COVID-19 in long-term care settings

From care homes to rehabilitation centres, long-term care facilities (LTCFs) are uniquely vulnerable to COVID-19. The reasons for this are severalfold. LTCF patients and residents require continuing care, live in close proximity to one another, and are typically elderly and multimorbid, placing them at elevated risk of both acquiring SARS-CoV-2 and suffering

severe outcomes from COVID-19.(D'Adamo et al., 2020; Salcher-Konrad et al., 2020; F. Zhou et al., 2020) High rates of inter-individual contact in certain types of LTCF, including rehabilitation centres and nursing homes, may be a particularly important driver of outbreak risk.(Temime et al., 2021) For instance, some LTCFs permit visitors, allow social gatherings and organize group activities for residents, which are likely to favour transmission to and from patients.

Carers and other HCWs in LTCFs are also susceptible to infection and, amidst imperfect hygiene and infection prevention measures, potentially acquire and transmit the virus through necessary daily interactions with both residents and staff.(Mohamed Abbas et al., 2021a; Gross et al., 2021; Louie et al., 2021) Other occupational hazards, including staff shortages, constrained IPC resources and limited training, likely also contribute to nosocomial transmission.

In a policy brief from WHO, a range of structural issues predisposing LTCFs to SARS-CoV-2 outbreaks were also identified, including underfunding, the sharing of underemployed and undervalued staff across facilities, and fragmentation between long-term care and other health service sectors.(World Health Organization, 2020g) This vulnerability has entailed stark epidemiological realities. In a characteristic outbreak in early 2020 in a skilled nursing facility in Washington, USA, there were a reported 167 infections and 34 deaths within just three weeks of identification of an initial index case.(McMichael et al., 2020) Myriad similar outbreaks have since been reported worldwide, and although the full extent of the ongoing pandemic is unclear and ever-evolving, LTCFs have and continue to bear a disproportionate burden of SARS-CoV-2 infection and COVID-19 mortality.(D. Fisman et al., 2020; D. N. Fisman et al., 2020; Salcher-Konrad et al., 2020) Across Europe, for instance, LTCFs accounted for an estimated 30-60% of all COVID-19 deaths as of June 2020.(ECDC Public Health Emergency Team et al., 2020)

6.2. Mobilizing public health research on COVID-19

The profound and far-reaching consequences of the pandemic have led to an unprecedented groundswell of support from scientific research teams, who re-organized or postponed existing research projects *en masse* to address the imminent threat of COVID-19. Our research group was among those mobilized to contribute to COVID-19 research, particularly in the context of our expertise in epidemiological modelling and nosocomial infection control. Prior to the pandemic, the next step in my thesis was to extend concepts from previous Chapters by simulating within-host microbiome-pathogen interactions in LTCF settings using *CTCmodeler*, a previously developed individual-based pathogen transmission model. However, in light of the urgency of the public health challenges posed by the pandemic, we instead adapted CTCmodeler to simulate SARS-CoV-2 outbreaks, in order to evaluate the efficacy and efficiency of public health interventions for nosocomial COVID-19 control. Below, I describe CTCmodeler and how we adapted it to simulate SARS-CoV-2 epidemics in the LTCF setting.

6.3. CTCmodeler : an individual-based pathogen transmission model

CTCmodeler ('the model') is a stochastic, individual-based pathogen transmission model programmed in C++ using the repast HPC library 2.2.0. It was developed and coded by Audrey Duval, a former PhD student in our research group, as part of her thesis work on nosocomial pathogen control.(Duval, 2019) A detailed description of the model program has been published previously.(Duval et al., 2019b) Briefly, the model simulates (i) dynamic inter-individual contacts among patients and staff in a long-term care facility setting, (ii) pathogen transmission along resulting contact networks, and (iii) disease progression among infected individuals. The model can be flexibly adapted to represent any pathogen by varying underlying epidemiological parameters like the transmission rate, duration of infection and probability of presenting with symptoms. The underlying LTCF population structure and inter-individual contact behaviour were informed using epidemiological data from the Individual-Based Investigation of Resistance Dissemination (i-Bird) study, a longitudinal observational study summarized below, and described in detail elsewhere.(Duval et al., 2018; Obadia et al., 2015)

6.3.1. Demographic and close-proximity interaction data from the i-Bird study

The i-Bird study was an epidemiological investigation led by Professor Didier Guillemot as part of the MOSAR project (Mastering hOSpital Antimicrobial Resistance and its spread into the community) funded by the European Commission. It was conducted between May and November 2009 at Berck-sur-Mer rehabilitation hospital in northern France, and provided detailed demographic data about all individuals in the LTCF over this period. There are five wards in this facility corresponding to different medical specialties: three neurology rehabilitation wards, one geriatric rehabilitation ward, and one nutrition care ward. Patients and staff were associated with specific wards, although some *transversal* staff worked across multiple wards. Patients were potentially admitted or discharged over the course of the study period, with an average length of stay of 7 weeks, and a median 2 (range 0 - 11) new patient admissions per day. Staff were classified across 13 categories of employment, grouped here as HCWs (caregiver, nurse, physiotherapist, occupational therapist, nurse trainee, physician, and hospital porter) and ancillary staff (hospital services, administration, other rehabilitation staff, management, logistical staff, and activity coordinator/hairdresser). A diagram of this LTCF and the average number of patients and staff found in each ward per week is given in **Figure 6.1**.

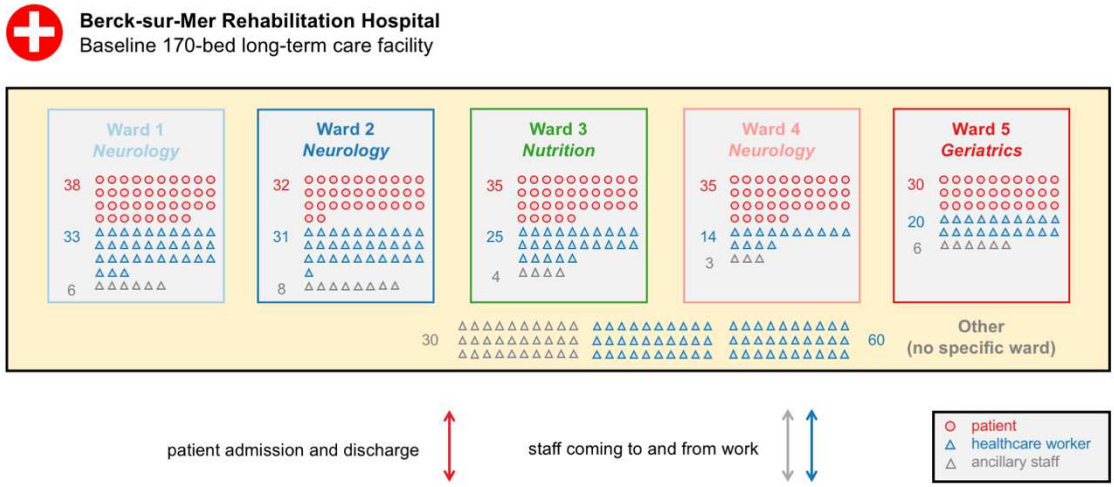

Figure 6.1. LTCF diagram.

A diagram of Berck-sur-Mer rehabilitation hospital, showing the average weekly number of patients and staff in each ward. The ward 'Other' accounts for staff not affiliated with any one particular ward, including those who work in the back office or regularly move between wards.

During the study period, all patients and staff in the LTCF were recruited to wear Radio-Frequency Identification Devices (RFIDs) on their person at all times. RFIDs are sensors capable of detecting proximity to other RFIDs at a high spatio-temporal resolution. In this study, RFIDs detected every 30s whether any other RFIDs were within a proximity of 1.5m at that time. All RFID-RFID pairings were recorded and interpreted as *close-proximity interactions* (CPIs) between the individuals wearing each respective RFID. A statistical analysis of these CPIs has been published previously.(Duval et al., 2018) Briefly, across nearly 2.7 million CPIs recorded among 318 patients and 262 staff over a 17-week period, distinct contact patterns were identified in each ward, reflecting behaviours particular to patients and different types of staff in this LTCF. For instance, patients typically spent 24 hours per day in the facility and had higher rates of contact with HCWs during mornings and afternoons, but with other patients in evenings. Staff were present according to their respective working hours, and had fewer overall contacts during evenings and weekends. HCWs had more distinct contacts with other individuals (on average 14.3 CPIs/day) than patients (11.2 CPIs/day), but had a shorter cumulative duration of time spent in contact with others (15 minutes/day) than patients (32 minutes/day). Compared to other wards, contacts were fewest (8.6 distinct CPIs/day) and longest (47 cumulative minutes/day) in the geriatric ward. In contrast to a contact network observed using similar methods in an acute care setting, patient-patient CPIs were particularly frequent and numerous in this LTCF, reflecting the group meals, art classes and other social activities that took place

over the data collection period in this pre-pandemic LTCF.(Duval et al., 2018; Vanhems et al., 2013)

6.3.2. Simulating dynamic contact networks

Demographic data from iBird were used directly as model inputs to describe the patient and staff populations simulated by CTCmodeler. Real patient admission and staff timesheet data were used to determine who was present in the LTCF on any given day: over each 7-day period, there were a mean 170 patients and 240 staff present each week (as visualized in **Figure 6.1**, and stratified further by type of individual in **Table 6.1**).

Table 6.1. LTCF demography.

Demographic breakdown of patients and staff present in each ward of the simulated baseline LTCF. Staff were grouped as healthcare workers (HCWs) or ancillary staff. The ward 'Other' accounts for staff not affiliated with any one particular ward, including those who work in the back office or regularly move between wards.

Type of individual		Average number present per week per ward (% of all individuals present per ward)						
		Ward 1	Ward 2	Ward 3	Ward 4	Ward 5	Other	All
Patient	Patient	38 (49%)	32 (45%)	35 (55%)	35 (67%)	30 (54%)	0 (0%)	170 (41%)
HCW	Caregiver	20 (26%)	19 (27%)	14 (21%)	7 (13%)	10 (18%)	21 (23%)	92 (22%)
	Nurse	11 (14%)	7 (10%)	8 (13%)	6 (11%)	7 (13%)	12 (13%)	51 (12%)
	Physiotherapist	0 (0%)	0 (0%)	0 (0%)	0 (0%)	0 (0%)	12 (13%)	12 (3%)
	Nurse trainee	1 (1%)	3 (5%)	2 (3%)	0 (0%)	2 (3%)	2 (2%)	10 (2%)
	Occupational Therapist	0 (0%)	0 (0%)	0 (0%)	0 (0%)	0 (0%)	7 (8%)	7 (2%)
	Physician	1 (1%)	2 (3%)	1 (2%)	1 (2%)	1 (2%)	0 (0%)	6 (1%)
	Hospital porter	0 (0%)	0 (0%)	0 (0%)	0 (0%)	0 (0%)	6 (6%)	6 (1%)
Ancillary staff	Hospital services staff	4 (5%)	4 (6%)	3 (5%)	2 (4%)	3 (5%)	0 (0%)	16 (4%)
	Logistical staff	0 (0%)	0 (0%)	0 (0%)	0 (0%)	0 (0%)	16 (18%)	16 (4%)
	Other rehabilitation staff	1 (1%)	3 (4%)	0 (0%)	0 (0%)	2 (4%)	2 (2%)	8 (2%)
	Administrative staff	0 (0%)	0 (0%)	0 (0%)	0 (0%)	0 (0%)	8 (9%)	8 (2%)
	Management	1 (1%)	1 (1%)	1 (2%)	1 (2%)	1 (2%)	2 (2%)	7 (2%)
	Activity coordinator/ hairdresser	0 (0%)	0 (0%)	0 (0%)	0 (0%)	0 (0%)	2 (2%)	2 (0%)
Total (100%)		**78**	**72**	**63**	**53**	**55**	**90**	**410**

CPI data from iBird were also used as model inputs to inform inter-individual contact behaviour. However, to account for missing data resulting from imperfect sensor compliance in the raw network, novel contact networks were simulated. The probability of coming into contact with another individual at each time-step (30 seconds) was estimated from the raw contact data. These contact probabilities were stratified by hour of the day (e.g. 8:00:00-8:59:30, 9:00:00-9:59:30), day of the week (weekday vs. weekend), ward and type of individual. At each time-step, new contacts were simulated based on these probabilities, and contact durations were drawn stochastically from log-normal distributions fit to raw contact duration data and stratified by the same variables. The final simulated contact network aggregated over one randomly selected day is provided in **Figure 6.2**.

Contact behaviours were found to be comparable between the raw and simulated networks, and fidelity of the simulated network has been validated previously by its ability to reproduce transmission dynamics from a real outbreak of methicillin-resistant *Staphylococcus aureus* in this LTCF.(Duval, 2019; Obadia et al., 2015)

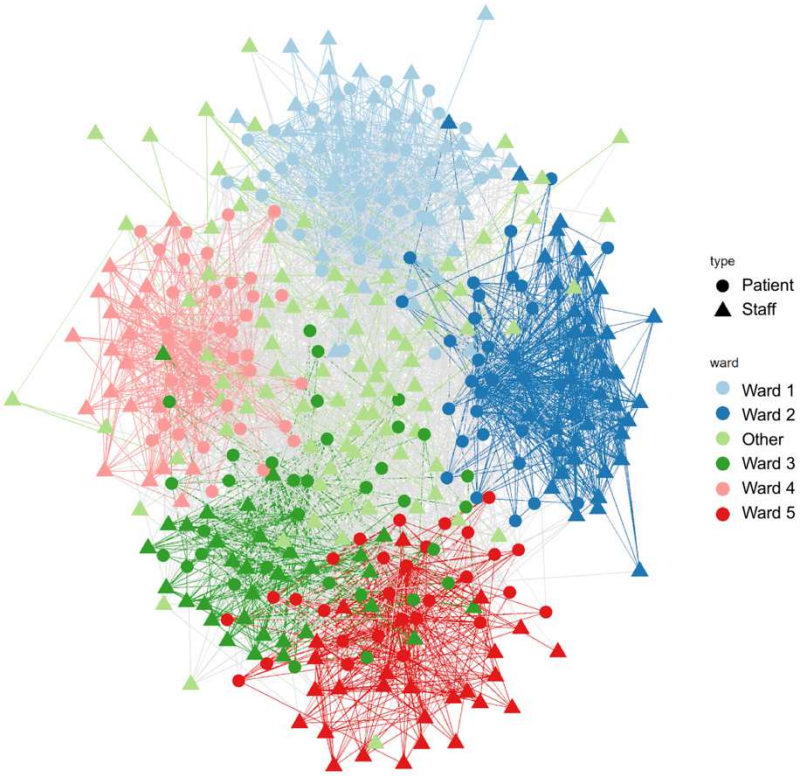

Figure 6.2. Simulated contact network.

A snapshot of the dynamic contact network simulated by CTCmodeler, showing all patients (circles) and staff (triangles) present in the baseline LTCF as nodes, and inter-individual contacts aggregated over one randomly selected day as edges. Nodes and edges are coloured by ward, with grey edges representing contacts across wards. [Rendered by Audrey Duval.]

6.4. Applying CTCmodeler to SARS-CoV-2 and COVID-19

I worked collaboratively with Audrey Duval to apply her model to simulate SARS-CoV-2 outbreaks. Together, we conceptualized how CTCmodeler could be applied to this system, using available literature to inform model parameters and epidemiological scenarios. Audrey updated the program code and launched simulations, while I was responsible for all analysis and calculation of epidemiological outcomes from raw simulation data.

To apply CTCmodeler, three key modeling assumptions were made. First, SARS-CoV-2 was assumed to be introduced into the LTCF through either newly admitted patients or staff members infected in the community. Second, infection followed a modified Susceptible-Exposed-Infected-Recovered process, including pre-symptomatic and asymptomatic infection, with stochastic progression through infection stages. Third, transmission could occur during contacts between infectious and susceptible individuals, with transmission probability scaling linearly with contact duration. These assumptions are detailed further below.

6.4.1. SARS-CoV-2 introductions from the community

We distinguish between SARS-CoV-2 index cases and SARS-CoV-2 introductions. Index cases were defined as patients and staff infected with SARS-CoV-2 upon simulation outset, who were thus assumed to have acquired infection prior to the simulation period. Introductions were defined as subsequent cases of SARS-CoV-2 infection introduced into the LTCF from the community over the course of simulation time, limited to staff members (assumed to contact individuals in the community outside work hours) and newly admitted patients (assumed to potentially carry the virus upon LTCF entry). Different sets of assumptions about index cases and introductions represent different epidemiological scenarios reflecting variable COVID-19 burden in the community, and are defined accordingly in subsequent Chapters.

6.4.2. Characterizing COVID-19 infection

Clinical progression of COVID-19 was characterized by a modified SEIR (Susceptible-Exposed-Infectious-Recovered) process using parameter estimates from the literature (**Figure 6.3**). We assumed: (i) a non-infectious exposed period of 2-5 days, (ii) an infectious pre-symptomatic period of 1-3 days, (iii) an on-average 7-day infectious "symptomatic" period with three levels of symptom severity (severe, mild or

asymptomatic), and (iv) eventual recovery with full immunity. Together, (i) and (ii) amount to an incubation period of 3-8 days including a 1-3 day window of pre-symptomatic transmission, consistent with estimates used elsewhere.(Lauer et al., 2020; Tindale et al., 2020; Zhang et al., 2020) For (iii), we assumed that 70% of infected individuals develop clinical symptoms,(Buitrago-Garcia et al., 2020; Mizumoto et al., 2020; Nishiura et al., 2020) 20% of which develop severe/critical symptoms.(Wu and McGoogan, 2020) Model parameters are provided in **Table 6.3**, at the end of this Chapter.

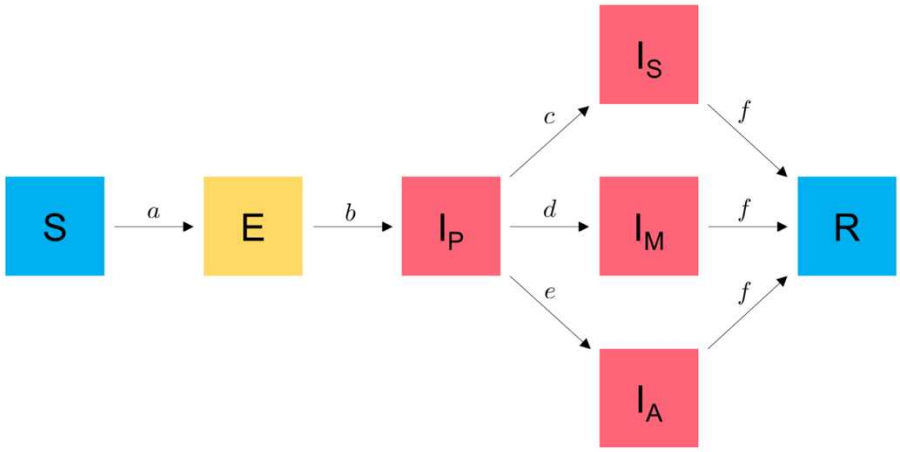

Figure 6.3. SARS-CoV-2 infection flow diagram.

A diagram of the modified SEIR process used to characterize SARS-CoV-2 infection (S = susceptible, E = exposed, I_P = infectious pre-symptomatic, I_A = infectious asymptomatic, I_M = infectious with mild symptoms, I_S = infectious with severe symptoms, R = recovered), with transitions between states *a* to *f* (see **Table 6.2**).

For each individual infection in the model, durations for each stage of infection were drawn probabilistically from their respective distributions. We assumed no difference in average time to symptom onset for mild symptomatic and severe symptomatic cases, nor any difference in symptom duration. As outbreaks were simulated over short time periods to evaluate different epidemiological surveillance strategies, death and potential long-term clinical outcomes were not explicitly simulated. Unlike the bacterial colonization processes modelled using ODEs in Chapters 4 and 5, this COVID-19 infection process is applied to an individual-based model, so transitions between state variables are described algorithmically (**Table 6.2**).

Table 6.2. SARS-CoV-2 infection state transitions.

State transitions for the SEIR infection process. Numerical values are drawn probabilistically for each transition for each individual in the model. Durations were taken as integer values, corresponding to days (parameter values in **Table 6.3**).

Symbol	Name	Transition	Description
a	Infection	S → E	After a contact with an Infectious individual, Susceptible individuals become infected and enter Exposed class with probability: ($p \times$ *duration of contact*)
b	Infectiousness onset (pre-smptomatic)	E → I_P	Exposed individuals become Infectious (but do not yet show symptoms) after duration d_E
c	Sympton onset (severe)	I_P → I_S	Pre-symptomatic individuals progress to the next stage of infectiousness after duration d_p; a proportion (s_{MS}) × (s_S) develop severe symptoms
d	Symptom onset (mild)	I_P → I_M	Pre-symptomatic individuals progress to the next stage of infectiousness after duration d_p; a proportion (s_{MS}) – ($s_{MS} \times s_S$) develop mild symptoms
e	Symptom onset (asymptomatic)	I_P → I_A	Pre-symptomatic individuals progress to the next stage of infectiousness after duration d_p,; a proportion (1 – s_{MS}) are asymptomatic and never develop symptoms
f	Recovery	(I_S or I_M or I_A) → R	Individuals progress to a Recovered state (non-infectious, non-symptomatic, non-susceptible to re-infection) after duration d_S

6.4.3. Characterizing SARS-CoV-2 transmission

Parameter estimates from the literature were used to characterize SARS-CoV-2 transmission (**Table 6.3**). *Susceptible* patients and staff *j* could become infected with SARS-CoV-2 if in direct contact with an *Infectious* individual *i*. We assumed that the probability of transmission per infectious contact, $P_{i,j}$, depends on the transmission probability per time spent in contact, *p*, and the duration of that contact, $D_{i,j}$ (limited to intervals of 30 seconds, the discrete time-step for the transmission model). This is expressed as

$$P_{i \to j} = p \times D_{i,j}$$

(eq. 6.1)

To apply this specifically to SARS-CoV-2, as discussed in Temime et al., the transmission probability parameter *p* was computed as follows.(Temime et al., 2021) Assuming homogeneous mixing among individuals and independent contacts, the basic reproduction number (R_0) of a pathogen can be approximated as

$$R_0 = p \times n \times d \times \tau$$

(eq. 6.2)

where *n* is the average number of daily contacts per individual; *d* is the average duration of these contacts; and τ is the duration of the infectious period. Owing to a lack of data from healthcare settings, these parameters were estimated using epidemiological data from the

French community prior to lockdown in March 2020 (R_0=3),(Salje et al., 2020) and a detailed survey of inter-individual contacts in the general community prior to the pandemic (*n* = 8 contacts/days, d = 30 minutes).(Béraud et al., 2015) Assuming an infectious period of τ = 9 days for COVID-19, we calculated a transmission probability of *p* = 0.14% per minute spent in contact with a *Susceptible* individual. We further set a saturation threshold at one hour of contact, such that the per-contact transmission probability was at most 8.3% per contact between any two individuals. Under baseline assumptions in the simulated LTCF, this estimate for *p* resulted in a mean R_0=4.04 (**Figure 6.4**). Compared to the assumed R_0=3.0 in the community, this is consistent with the finding that, for any given value of *p*, R_0 is expected to vary between community and healthcare settings because of fundamental differences in inter-individual contact behaviour.(Temime et al., 2021)

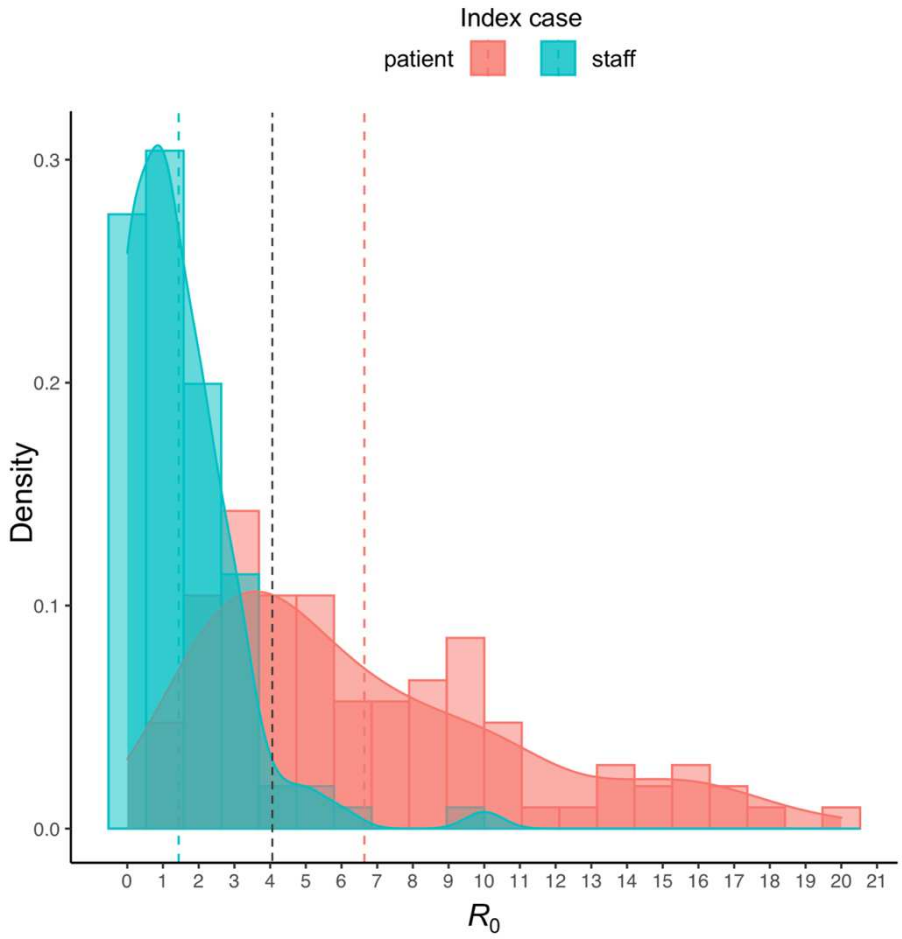

Figure 6.4. R_0 distribution.

Distributions of the basic reproduction number (R_0), the number of secondary infections caused by an initial index case introduced at the beginning of 200 independent stochastic simulations in the simulated LTCF under baseline assumptions (*p*=0.14%). The index case was a patient in 100 simulations (red) and a member of staff in the other 100 (blue). R_0 varied from 0 to 20 across all simulations, with a mean value of R_0=4.04 (dashed black line). However, R_0 was greater when index cases were patients (mean R_0=6.64) than staff (mean R_0=1.44). [Rendered by Audrey Duval.]

Table 6.3. Model parameter estimates.

Parameter	Value (distribution)	Source
Parameters for estimation of SARS-CoV-2 transmission rate per minute of contact		
SARS-CoV-2 basic reproduction number (R_0) in the general community prior to lockdown	3.0	(Salje et al., 2020)
Average infectious period of SARS-CoV-2 (τ)	9 days	(He et al., 2020)
Average number of contacts per day per individual prior to lockdown (n)	8	(Béraud et al., 2015)
Average duration per contact prior to lockdown (d)	30 minutes	(Béraud et al., 2015)
Epidemiological and clinical parameters		
SARS-CoV-2 transmission rate per minute of contact (p)	0.00139	Estimated
Duration of exposed period (latency) (d_E)	2-5 days (uniform)	(Lauer et al., 2020; W. E. Wei et al., 2020)
Duration of pre-symptomatic period (d_P)	1-3 days (uniform)	(Lauer et al., 2020; W. E. Wei et al., 2020)
Duration of symptomatic period (whether asymptomatic, mild symptomatic or severe symptomatic) (d_S)	7 days (log-normal, $\sigma^2 = 7$)	(He et al., 2020)
Proportion of COVID-19 infections presenting any symptoms (s_{MS})	0.7	(Buitrago-Garcia et al., 2020)
Proportion of symptomatic COVID-19 infections with severe symptoms (s_S)	0.2	(Wu and McGoogan, 2020)

It is important to highlight potential limitations of using these pre-pandemic contact data to simulate SARS-CoV-2 outbreaks. First, one assumption underlying CTCmodeler is that inter-individual contacts relevant for transmission are those occurring within a proximity of 1.5m. However, SARS-CoV-2 is viable in aerosol samples, and overdispersion in transmission (i.e. superspreading) may result from aerosol-based rather than droplet-based transmission facilitating spread at longer distances.(Greenhalgh et al., 2021; van Doremalen et al., 2020) Further, these pre-pandemic contact data clearly represent a facility with no social distancing measures or behavioural interventions in place. However, such interventions were widely implemented through early 2020 in response to the pandemic. Conversely, visitors were excluded from CTCmodeler due to lack of data, which is consistent with policies barring guests from LTCFs early in the pandemic.

6.5. Using simulated SARS-CoV-2 outbreaks to evaluate public health interventions

This updated version of CTCmodeler was used to simulate SARS-CoV-2 outbreaks. I then calculated epidemiological indicators describing outbreak dynamics, and developed computational algorithms to quantify the effectiveness and efficiency of surveillance and control interventions through evaluation of simulated outbreak data. These studies and their findings are presented in subsequent Chapters. In **Chapter 7** I describe evaluation of testing strategies for detection of emerging SARS-CoV-2 outbreaks, in an early pandemic context with limited availability of reverse-transcriptase polymerase chain reaction (RT-PCR) testing resources. In **Chapter 8** I describe evaluation of surveillance and control strategies for prevention of nosocomial SARS-CoV-2 transmission, in a later pandemic context with availability of both RT-PCR and antigen rapid diagnostic testing (Ag-RDT), and in the context of reactive surveillance following a surge in SARS-CoV-2 importation risk from the community.

Chapter 7. Optimizing limited testing resources for nosocomial SARS-CoV-2 surveillance

7.1. Introduction

Effective nosocomial COVID-19 surveillance is essential for timely outbreak detection and implementation of public health interventions that limit transmission, including contact tracing, case isolation, and targeted infection prevention measures.(Bakaev et al., 2020; Iritani et al., 2020; Sanchez et al., 2020) The "gold-standard" diagnostic test for active SARS-CoV-2 infection is RT-PCR, typically performed on clinical specimens from nasopharyngeal swabs.(Böger et al., 2021) Though sensitive and highly specific, laboratory-based RT-PCR is relatively expensive and resource intensive, and must be outsourced for institutions lacking on-site infrastructure. Early in the pandemic, shortages of swabs and testing kits, logistical challenges and overwhelmed laboratories together resulted in insufficient testing capacity and delays to test results in healthcare settings worldwide.(Akst, 2020; Beaudevin et al., 2021; Hadaya et al., 2020; Péré et al., 2020) In a survey of 283 heads of emergency departments of Spanish hospitals, 55% reported that diagnostic testing resources were "often" or "very often" scarce over March and April 2020, more than any other medical resource.(Alquézar-Arbé et al., 2020) Although global testing capacity has since been dramatically scaled-up in many regions, in practice COVID-19 surveillance is still limited by available testing capacity and health-economic resources, particularly for institutions in low- and middle-income settings.(Mukhtar and Khogali, 2021; Wachholz and Jacinto, 2020)

In the context of limited testing resources, a common practice in LTCFs in France, the Netherlands, the UK, the USA and elsewhere has been to restrict testing to individuals presenting with characteristic COVID-19 symptoms.(D'Adamo et al., 2020; Department of Health & Social Care, 2020; Ministère des solidarités et de la santé, 2020; Rijksinstituut voor Volksgezondheid en Milieu, 2020) Yet symptomatic infections represent just the tip of the iceberg: many infections cause no or only mild symptoms, produce high quantities of virus in the absence of symptoms, and experience relatively long delays until symptom onset.(Arons et al., 2020; Lauer et al., 2020; W. Li et al., 2020; Tindale et al., 2020) Silent transmission from asymptomatic and pre-symptomatic infections is a known driver of SARS-CoV-2 outbreaks,(Huff and Singh, 2020; Moghadas et al., 2020) and non-

symptomatic cases can act as Trojan Horses, unknowingly introducing the virus into healthcare institutions and triggering nosocomial spread.(Asad et al., 2020; ECDC Public Health Emergency Team et al., 2020; Kimball et al., 2020)

Insufficient surveillance systems, including those lacking testing capacity or relying only on symptoms as indications for testing, have been identified as aggravating factors for SARS-CoV-2 outbreaks in LTCFs.(Arons et al., 2020; Bigelow et al., 2021; Blackman et al., 2020; ECDC Public Health Emergency Team et al., 2020; Gandhi et al., 2020; Louie et al., 2021) Various surveillance strategies have been proposed to optimize limited RT-PCR testing while accounting for the particular transmission dynamics of SARS-CoV-2, including randomly testing HCWs, testing all patients upon admission, and universal or serial testing.(Black et al., 2020; Escobar et al., 2021; Goldberg et al., 2021) Group testing (sample pooling, combining clinical specimens from multiple individuals into a single biological sample for a single RT-PCR test) has also garnered attention as a potentially diagnostically sensitive and resource-efficient alternative to individual-based testing.(Eberhardt et al., 2020; Hogan et al., 2020; Mallapaty, 2020; Narayanan et al., 2020; Pouwels et al., 2020; Yelin et al., 2020)

In order to mitigate and prevent future nosocomial outbreaks, there is an urgent need to optimize COVID-19 surveillance in long-term care settings, taking into account both the unique epidemiological characteristics of SARS-CoV-2 and limited availability of testing resources.(World Health Organization, 2020g) In this Chapter, I investigate the efficacy, timeliness and resource efficiency of a range of RT-PCR surveillance strategies for detection of emerging SARS-CoV-2 outbreaks in the long-term care setting.

7.2. Methods

7.2.1. SARS-CoV-2 outbreak simulations in the long-term care setting

Nosocomial SARS-CoV-2 outbreaks were simulated by Audrey Duval using CTCmodeler, the dynamic, stochastic, individual-based transmission model presented in **Chapter 6**. To represent a vulnerable LTCF at the beginning of the COVID-19 pandemic, we assumed that all patients and staff in the facility were *susceptible*, and that no specific COVID-19 containment measures (e.g. social distancing, vaccination) were in place. SARS-CoV-2 was introduced into the facility under a range of importation scenarios, described below. For each scenario, 100 stochastic outbreak simulations were run for 12 weeks using identical initialization conditions. Accordingly, within-scenario variability in outbreaks resulted only from stochasticity inherent to the SARS-CoV-2 transmission process and COVID-19 infection progression.

7.2.1.1. Importation scenarios

All simulations began with the random introduction of a single non-symptomatic index case from the community into the LTCF on the first day of simulation (t=0), with equal probability of index cases being *exposed*, *pre-symptomatic* or *asymptomatic*. Introductions from the community were limited to staff or new patient admissions, with the latter conceptualized as transfers from other healthcare facilities. Five distinct importation scenarios were considered, each describing a different source and frequency of SARS-CoV-2 introduction(s) into the LTCF:

1. Scenario 1 (*weekly patient or staff*) [baseline scenario]:
    a. an identical 50% probability that index cases were patients or staff
    b. in addition to the initial case at t_0, other community-onset cases were randomly introduced on average once weekly
2. Scenario 2 (*single patient transfer*):
    a. only one infected patient admitted at t_0
3. Scenario 3 (*weekly patient transfer*):
    a. a different infected patient admitted once weekly
4. Scenario 4 (*single infected staff)* :
    a. only one staff member infected in the community at t_0
5. Scenario 5 (*weekly infected staff*) :
    a. a different staff member infected in the community once weekly

7.2.1.2. Sensitivity analyses

Two principal sensitivity analyses for outbreak simulations were included. First, to reflect uncertainty in the estimated transmissibility of SARS-CoV-2 per minute spent in infectious contact (p=0.14% probability / minute), extreme estimates for COVID-19 epidemicity in the community were considered (R_0=1.5, 6), which translated to lower and higher transmission rates, respectively (p=0.07%, 0.28% probability / minute). Second, to account for potential epidemiological impacts of LTCF size and structure, a smaller LTCF geared towards elder care was simulated by restricting simulations to patients and staff from the 30-bed geriatric ward 5 (including 'other' transversal staff). For this, a distinct contact network was simulated, as described for the baseline LTCF in the previous Chapter, and was interpreted as representing a **nursing home**. There were a mean 8.0 daily patient-patient contacts and 8.3 daily patient-staff contacts in this nursing home contact network, which compares to patterns reported previously by Assab & Temime in a nursing home in Paris, France (5.0 daily patient-patient contacts, 6.3 daily patient-staff contacts).(Assab and Temime, 2016) The five SARS-CoV-2 importation scenarios described above were also run for this second LTCF.

7.2.2. Simulation outputs and epidemiological outcomes

Final outputs from each outbreak simulation were summarized in an infection file, describing the infection status (susceptible, exposed, etc.) of each unique individual in the LTCF on each day of simulation time. These outputs were used to calculate four primary epidemiological outcomes:

1. **Infection incidence**: the daily acquisition rate of SARS-CoV-2 infection
2. **Infection prevalenc**e: the number of individuals in each stage of infection on each day
3. **Final outbreak size**: the cumulative number of infections after 12 weeks of unmitigated transmission
4. **Case distribution**: the proportion of infections among patients, HCWs and ancillary staff

Note that the terms **SARS-CoV-2 infection** and **COVID-19** are used interchangeably. Among simulations that resulted in outbreaks (defined as simulations with ≥1 case of nosocomial SARS-CoV-2 transmission within 21 days of the initial index case), two

additional secondary outcomes were calculated: (i) **lag until COVID-19 symptom onset**, the number of days until someone with COVID-19 presented with symptoms in the LTCF; and (ii) **outbreak size upon first presentation of COVID-19 symptoms**. These outcomes are reported as median values across simulations, with uncertainties expressed as 95% uncertainty intervals, i.e. outcomes from the 2.5th and 97.5th percentiles.

7.2.3. Surveillance interventions

Surveillance was applied retrospectively to output data from outbreak simulations, under assumptions of imperfect diagnostic sensitivity and limited capacity of RT-PCR testing. The primary goal was to evaluate the timeliness and resource-efficiency of a range of surveillance interventions for SARS-CoV-2 outbreak detection.

7.2.3.1. Included surveillance interventions

Four types of surveillance were evaluated, each describing different use of RT-PCR tests:

1. Indication-based testing
2. Random testing
3. Testing cascades
4. Group testing

Each was further subdivided into distinct surveillance strategies, listed in **Table 7.1**. For **indication-based testing**, three indications were considered: presentation of severe COVID-like symptoms (reference strategy), presentation of any COVID-like symptoms, or new admission to the LTCF. For **random testing**, tests were randomly distributed among patients, HCWs, or all patients and staff present in the LTCF on the day of testing.

In contrast to these first two types of surveillance, testing cascades and group testing were conceived as hierarchical testing protocols, in which individuals presenting with severe COVID-like symptoms were always tested first to reflect their clinical priority. Remaining tests were subsequently allocated via cascades or as a single group test.

Testing cascades were conceived as mixed testing strategies combining indications and random testing, in which multiple indications were considered simultaneously but ordered according to their perceived clinical priority. If there were more tests available than individuals indicated for testing, remaining tests were distributed randomly among

remaining patients, such that cascades always maximized daily testing capacity.

For **group testing**, clinical specimens from individual swabs were pooled together and tested as one group test, up to a maximum of 32 swabs per test in the baseline analysis (but ranging from 2 to 64 swabs in sensitivity analysis). A simple two-stage 'Dorfman' protocol was used, which does not require additional investment or infrastructure, but which requires all individuals included in the initial group test to be re-swabbed and re-tested individually upon a positive group test result, in order to determine which individual(s) is (are) infected.(Dorfman, 1943; Mallapaty, 2020) Various studies have demonstrated the efficacy of group testing for SARS-CoV-2 detection, with sufficient diagnostic accuracy to detect a single SARS-CoV-2-positive specimen pooled with 30+ negative specimens.(Lohse et al., 2020; World Health Organization, 2020h; Yelin et al., 2020) Yet diluting positive specimens nonetheless reduces the concentration of viral RNA in the sample, which reduces sensitivity of a group test compared to an individual test of the same positive specimen.(Lee et al., 2020) Detailed assumptions for RT-PCR test sensitivity for both individual and group testing are provided below.

Table 7.1. Surveillance strategies.

Surveillance strategies evaluated for detection of SARS-CoV-2 outbreaks in a LTCF. Strategies differ in how swabs and tests were apportioned to patients and staff. Arrows (→) indicate order of priority for testing cascades. Test = RT-PCR test; swab = nasopharyngeal swab; symptoms = COVID-like symptoms; admission = transfer of new patient to the LTCF.

Surveillance type	Description	Surveillance strategy	Daily testing capacity always reached?
Single indication	Administer tests to any individuals indicated for testing, up to the daily testing capacity. If the number of individuals indicated exceeds the number of tests available, select randomly among them.	Symptoms (severe) *[reference strategy]*	No
		Symptoms (any)	No
		Admission	No
Random	Each day, randomly administer tests to individuals in a particular demographic group.	Random (patients)	Yes
		Random (HCWs)	Yes
		Random (all: patients, HCWs and ancillary staff)	Yes
Cascade	A combination of indications and random testing. First, use indications to administer tests according to a given order of priority. Then, if any tests remain, distribute them randomly among patients not otherwise indicated for testing.	Symptoms (severe) → Symptoms (mild) → Random (patients)	Yes
		Symptoms (severe) → Symptoms (mild) → Admission → Random (patients)	Yes
		Symptoms (severe) → Admission → Random (patients)	Yes
		Symptoms (severe) → Admission → Symptoms (mild) → Random (patients)	Yes
Group testing	Classic two-stage Dorfman sample pooling, modified to account for clinical urgency of severe COVID-19. First, administer individual tests to any patients or staff presenting with severe symptoms. Then, if at least one test remains, pool clinical specimens together and run one test across this group sample. If the test result is positive, individually re-swab and re-test all included individuals to identify cases. The maximum number of samples per group test was varied from 2 to 64.	Symptoms (any)	No
		Admission	No
		Random (patients) (always maximizes number of specimens per group test)	No
		Random (HCWs) (always maximizes number of specimens per group test)	No

7.2.4. Diagnostic sensitivity of RT-PCR

7.2.4.1. Individual testing

RT-PCR sensitivity varies over the course of infection, depending on the density of virus in the clinical sample. In a meta-analysis, Kucirka et al. estimated the false-negative rate (FNR) of RT-PCR for detection of SARS-CoV-2 in nasopharyngeal samples as a function of time since infection.(Kucirka et al., 2020) On the first and second days after infection, FNR was 100%, falling to 67% by four days, reaching a minimum of 20% by eight days, and increasing gradually thereafter. These estimates were calculated until 21 days after

infection; the curve was extrapolated linearly until it reached 100% FNR at 28 days (**Figure 7.1**). Here, for a swab administered to an individual infected *t* days prior, the corresponding test result was determined using a stochastic binomial process, in which the probability of a positive test result was calculated as 1-FNR_t.

For individuals infected within the LTCF, duration of infection upon swab administration was calculated directly from simulation output data. For community-onset infections, duration of infection was generated stochastically depending on the stage of infection upon LTCF introduction: 1 day if exposed, $\sim U(2,5) + 1$ days if pre-symptomatic infectious, and $\sim U(2,5) + \sim U(1,3) + 1$ days if asymptomatic. In a **sensitivity analysis**, higher and more stable RT-PCR sensitivity was considered: instead of varying by time since infection, sensitivity was fixed at 30% during the exposed stage of infection (E), and 90% across all infectious stages (I_P, I_A, I_M, I_S).

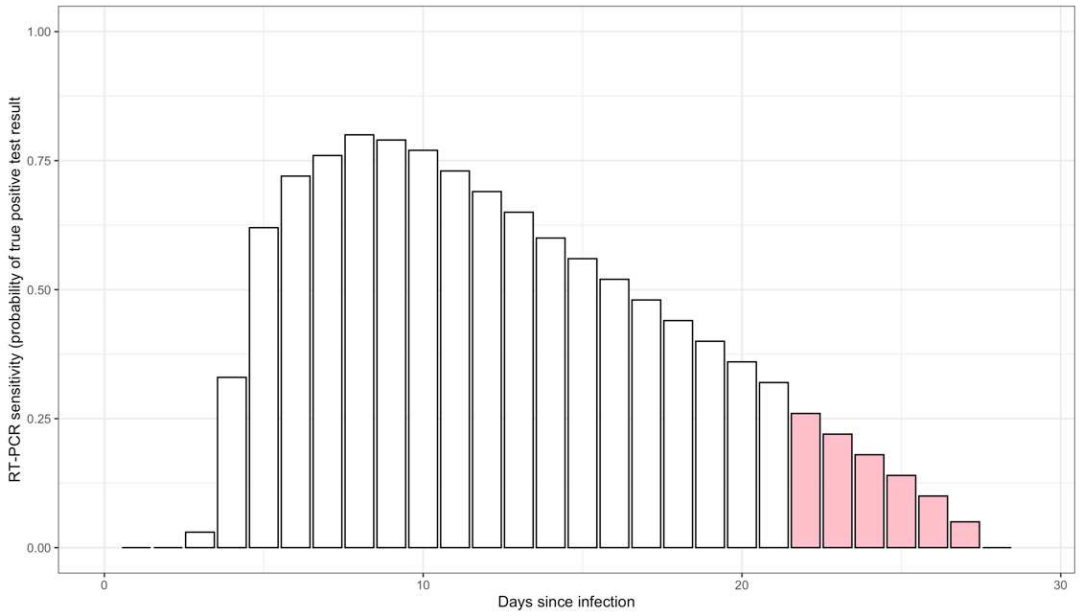

Figure 7.1. RT-PCR sensitivity (individual test).

Diagnostic sensitivity of RT-PCR for detection of SARS-CoV-2 as a function of time since infection. Values were calculated from the RT-PCR false negative rate for detection of SARS-CoV-2 using upper respiratory samples, as estimated for up to 21 days in a meta-analysis.(Kucirka et al., 2020) Pink bars were extrapolated linearly from the data to complete the distribution.

7.2.4.2. Group testing (single positive sample)

Diagnostic sensitivity of RT-PCR is reduced when a pathogen-positive sample is diluted with negative samples and/or less concentrated positive samples. In an experimental study, Yelin et al. combined individual SARS-CoV-2-positive samples with between 1 and 63 negative samples, and evaluated the Cycle threshold (Ct) at which RT-PCR detected

SARS-CoV-2 in each group sample (fluorescence threshold=300).(Yelin et al., 2020) To define RT-PCR test results from these data, a default diagnostic threshold was defined for the main analysis (positive SARS-CoV-2 test result if fluorescence >300 at Ct=40) and a stricter threshold for sensitivity analysis (Ct=35). Using these criteria, the proportion of true positive test results (diagnostic sensitivity) was calculated for each sample size S (the total number of samples included per group sample), and group test sensitivity (s_g) was defined as a function of the number of negative samples included in the group sample (S-1). A linear relationship was assumed,

$$s_g = s_0 - r \times (S - 1) \quad \text{(eq. 7.1)}$$

where *r* is the discounting rate per additional negative sample added to the group sample. In this experimental context, the intercept s_0 is fixed at 1 since the positive sample is a known true-positive. Linear regression was used to estimate the discounting rate for both diagnostic cut-offs, finding *r*=0.690% at Ct=40 and *r*=1.271% at Ct=35 (**Figure 7.2**). These findings are broadly consistent with empirical data: in a large Spanish study evaluating 3,519 nasopharyngeal samples in ten-sample pools, group test sensitivity was estimated at 97.1% when accounting for only major discrepancies between individual and group test results, and 85.5% when accounting for both major and minor discrepancies.(de Salazar et al., 2020) However, this formula does not account for group tests containing multiple true-positive samples.

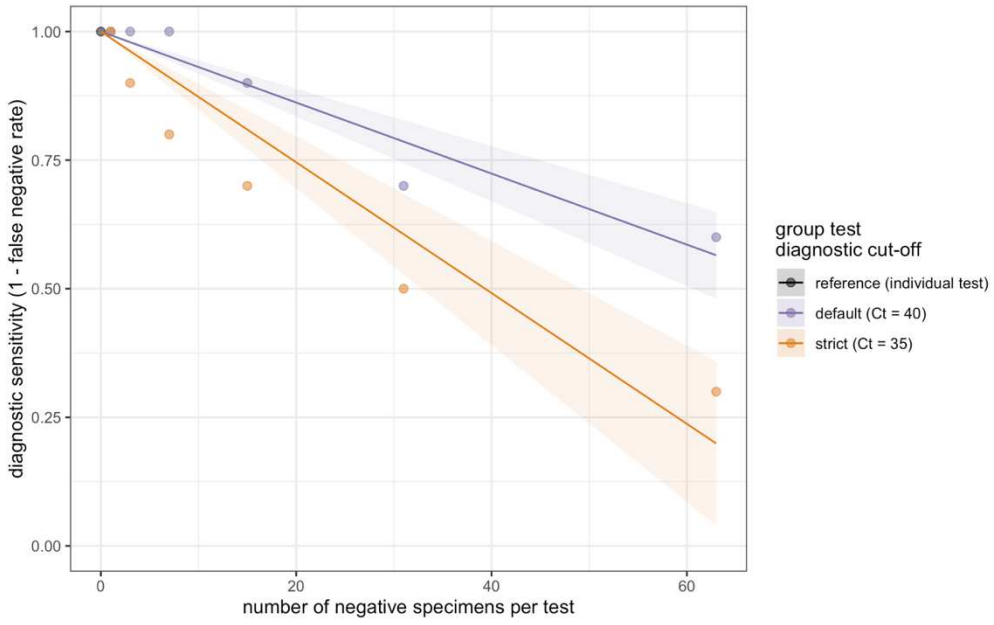

Figure 7.2. Group test sensitivity (single positive specimen).

Diagnostic sensitivity of RT-PCR for detecting SARS-CoV-2 in a group sample declines as additional

negative specimens are added to the group sample. Using data from Yelin et al. (circles), linear regression (lines) was used to estimate *r*, the discounting rate per additional negative specimen added to the sample.(Yelin et al., 2020) A rate *r*=0.006904 was found for the diagnostic cut-off used in the baseline analysis (Ct=40) and *r*=0.01271 for the stricter cut-off used in sensitivity analysis (Ct=35). Here, there is only one individual positive sample included per group sample, regardless of the number of negative samples included.

7.2.4.3. Group testing (multiple positive samples)

Methods have recently been proposed for using detailed virological data to calculate diagnostic sensitivity for a group sample containing multiple positive specimens.(Nguyen et al., 2019) In absence of such data, it was necessary to estimate diagnostic sensitivity for multi-positive group tests given only the number of specimens included, and the diagnostic sensitivity of each positive specimen when tested individually.

For a group sample consisting of multiple potentially detectable positive samples *P* and a set total number of samples *S*, the density of viral particles is necessarily less than the most concentrated sample P_{max}, but more than the density given by a group sample with the same *S* but containing only P_{max} and no other *P*. In this sense, the theoretical sensitivity of RT-PCR for a multi-positive group sample is bounded by s_{max} (sensitivity for P_{max} when tested individually) and $s_{S\text{-}1}$ (sensitivity for P_{max} when diluted with S-1 negative samples, i.e. with no other *P*). By extension, when RT-PCR sensitivity is known for each individual sample s_i, I propose that sensitivity for a group test can be approximated by using equation 1 to estimate sensitivity for P_{max} alone, and then modifying this by the relative individual sensitivities s_i of all other *P* included in the sample. This is given by

$$s_g = s_{max} - r \times (S - P')$$

(eq. 7.2)

where the relative contribution of each *P* (excluding P_1, which gives s_{max}) to s_g is

$$P' = \sum_{i=2}^{P} \frac{s_i}{s_{max}}$$

(eq. 7.3)

This equation is demonstrated in **Figure 7.3** using seven hypothetical examples of group samples, each composed of *S* individual samples, of which *P* are potentially detectable SARS-CoV-2-positive samples. The figure shows s_i (triangles, the diagnostic sensitivity for each *P* when tested individually) and s_g (circles, corresponding diagnostic sensitivity for the group test), and illustrates the theoretical range of s_g (grey shaded area) as a function

of *S* for a given s_{max} and *r*.

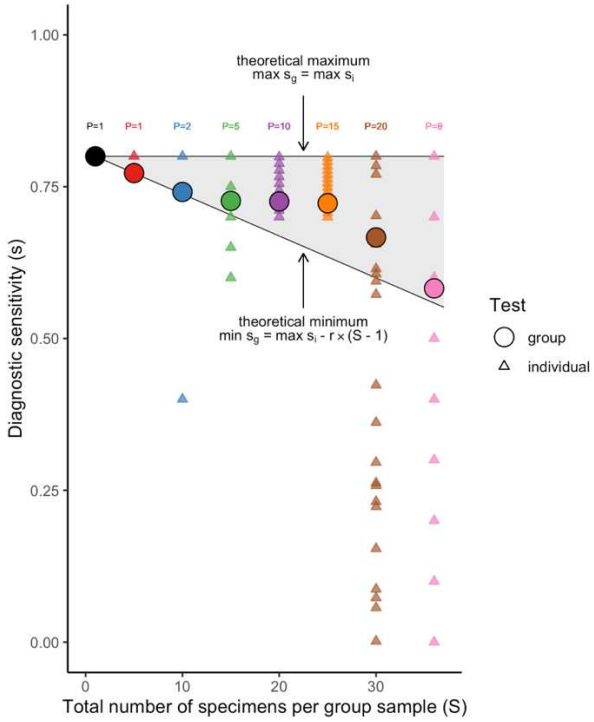

Figure 7.3. Group test sensitivity (multiple positive specimens).

RT-PCR diagnostic sensitivity for a mixed group sample (s_g, circles) was modelled as a function of sensitivity for each individual specimen in that sample (s_i, triangles). Each colour corresponds to a different group. Only positive samples P are shown; negative and undetectable individual samples (s_i = 0) are excluded from the plot. The shaded grey area gives the full theoretical range of s_g (here, given s_{max}=0.7 and *r*=0.006904).

7.2.5. A stochastic algorithm for COVID-19 surveillance

To implement and evaluate surveillance interventions, I developed a stochastic algorithm that reads output files from outbreak simulations to identify on each day:

1. Which individuals were present in the LTCF
2. Which patients were newly admitted to the LTCF over the previous 24 hours
3. Who was actively infected with SARS-CoV-2
4. Who was experiencing COVID-19 symptoms

Using these data, the algorithm could then:

1. Identify which individuals were to be tested, according to the surveillance strategies described above (**Table 7.1**)
2. Administer nasopharyngeal swabs and RT-PCR tests to selected individuals, with

testing capacity ranging from 1 to 32 tests/day

3. Stochastically determine test results, assuming perfect specificity and using the sensitivity curves described above (equation 7.2)
4. Count the cumulative number of swabs and tests used

If on a given day there were more individuals indicated for testing than there were tests available, then tests were distributed randomly among them. It was assumed that no individuals refused testing, and a 24-hour lag from swab to test result was implemented. All parameters used by the surveillance algorithm are provided in **Table 7.2**.

Table 7.2. Surveillance algorithm parameters.

Parameter	Value (distribution)	Source
Daily incidence rate of non-COVID but COVID-like symptoms	0.011	Estimated from OSCOUR data, described in (Fouillet et al., 2015)
Proportion of non-COVID but COVID-like symptoms with signs of severity	0.2	Assumed
Delay from test to test result	1 day	Assumed
RT-PCR specificity	100%	(Böger et al., 2021)
RT-PCR sensitivity	Up to 80% (**Figure 7.1**)	(Kucirka et al., 2020)
Daily testing capacity (tests/day)	1, 2, 4, 8, 16, 32	Assumed
Maximum number of specimens per group test	2, 4, 8, 16, 32, 64	Assumed
RT-PCR sensitivity discounting rate per additional true-negative specimen	0.7% (1.3% in sensitivity analysis)	Estimated from (Yelin et al., 2020)

7.2.5.1. COVID-19-like symptoms

Clinically, COVID-19 can resemble other common acute respiratory infections, such that individuals not infected with SARS-CoV-2 can nonetheless present with COVID-19-like symptoms and be indicated for symptom-based testing.(Borges do Nascimento et al., 2020) Influenza-like illness was used as a proxy for COVID-like symptoms of aetiologies other than SARS-CoV-2. This was calculated using data from 2008-2017 from French emergency departments (OSCOUR network) as the daily incidence rate of influenza-like illness among older adults (50-99 years).(Fouillet et al., 2015) As with COVID-19, it was assumed that 20% of these individuals also present with “severe” symptoms. Actual COVID-19 symptoms were taken directly from simulation output files, so were identical across each run of surveillance for any given outbreak, while COVID-19-like symptoms of other aetiologies were simulated randomly for each run. Hence, within each simulated outbreak, variation in surveillance outcomes resulted from stochasticity in test results and

in the incidence of COVID-19-like symptoms of other aetiologies.

7.2.5.2. Outbreak detection

For each stochastic run of the algorithm, surveillance began on the first day of outbreak simulation (t_0) and continued until the first positive test result was returned. The date of the first positive test was interpreted as corresponding to **outbreak detection**, the primary surveillance endpoint used in evaluation of surveillance efficacy and efficiency. A maximum lag to outbreak detection was defined at 22 days (corresponding to the average epidemic peak across outbreaks), after which all outbreaks were assumed to be detected regardless of the surveillance strategy used.

7.2.6. Surveillance outcome measures

7.2.6.1. Measures of efficacy

Efficacy of surveillance strategies for detection of emerging nosocomial SARS-CoV-2 outbreaks was described using three primary outcome measures. First, **detection lag**, the delay in days from the initial index case to outbreak detection (first positive test result, as described above). For group testing, this was taken as the date of the first positive group test result (first round of testing) and not the date of subsequent case identification (second round). Second, **outbreak size upon detection**, the cumulative number of SARS-CoV-2 infections in the LTCF upon first positive test result. Third, the **probability of detecting an outbreak** (i) at any time t from the index case at t=0, (ii) prior to any secondary cases (interpreted as the probability of detecting the index case before any nosocomial transmission), and (iii) prior to first presentation of COVID-19 symptoms.

7.2.6.2. Measures of efficiency

From a health-economic perspective, an efficient use of healthcare resources is one that yields better health outcomes than alternative uses of the same resources.(Palmer and Torgerson, 1999) Efficiency can be measured using incremental analysis, in which the additional cost of a particular intervention compared to a reference baseline is scaled by its additional health benefit.(Shiell et al., 2002) This is traditionally expressed as the incremental cost-effectiveness ratio using monetary costs and standardized units of health benefit (e.g., quality-adjusted life-years gained). To report on efficiency in terms of the surveillance cost and benefit outcomes measured in this study, a similar metric was defined, the **incremental efficiency ratio** (IER),

$$IER = \frac{(surveillance\ resource\ use)_S - (surveillance\ resource\ use)_R}{(surveillance\ outcome)_S - (surveillance\ outcome)_R}$$

(eq. 7.4)

for each surveillance strategy S relative to the reference R. Efficiency results were calculated using the IER as the number of additional swabs and tests required per 1-case reduction in outbreak size upon detection (for simplicity, reported as **mean additional swabs and tests used per case averted**). The perspective taken was that of an LTCF with a reference strategy of only testing individuals with severe COVID-like symptoms. Here, for group testing, efficiency does account for the second round of testing, i.e. resources required to individually re-swab and re-test all individuals included in the initial positive group test.

7.2.6.3. Outcome uncertainty

Surveillance outcomes were only evaluated for model simulations that resulted in nosocomial outbreaks (as defined above, simulations with ≥1 case of nosocomial transmission within 21 days of the initial index case). For each outbreak simulation, the surveillance algorithm was run 100 times across six testing capacities (1, 2, 4, 8, 16 or 32 RT-PCR tests/day), for a total 60,000 stochastic simulations for each surveillance strategy in the baseline scenario. Outcome measures are reported as medians across all simulations, with uncertainties expressed as 95% uncertainty intervals, i.e. outcomes from the 2.5th and 97.5th percentiles.

7.3. Results

7.3.1. Nosocomial transmission dynamics

7.3.1.1. Prevalence

Introductions of SARS-CoV-2 into the LTCF from the community led to nosocomial outbreaks with exponential growth in infection prevalence. **Figure 7.4** shows the **prevalence** of COVID-19 over time for four example simulations (**left panels**), as well as the **median prevalence** across all 100 outbreaks simulated (**right panel**) for the baseline scenario of weekly patient or staff introductions. Prevalence curves are stratified by infection status (colours), demonstrating lags until first onset of COVID-19 symptoms. Although it was assumed in the model that 70% of infections eventually develop COVID-19 symptoms, this figure demonstrates that symptomatic cases represent a small minority of infections in nascent outbreaks, as a result of: (i) lags to symptom onset due to infection incubation, and (ii) accumulation of non-symptomatic cases due to pre-symptomatic transmission.

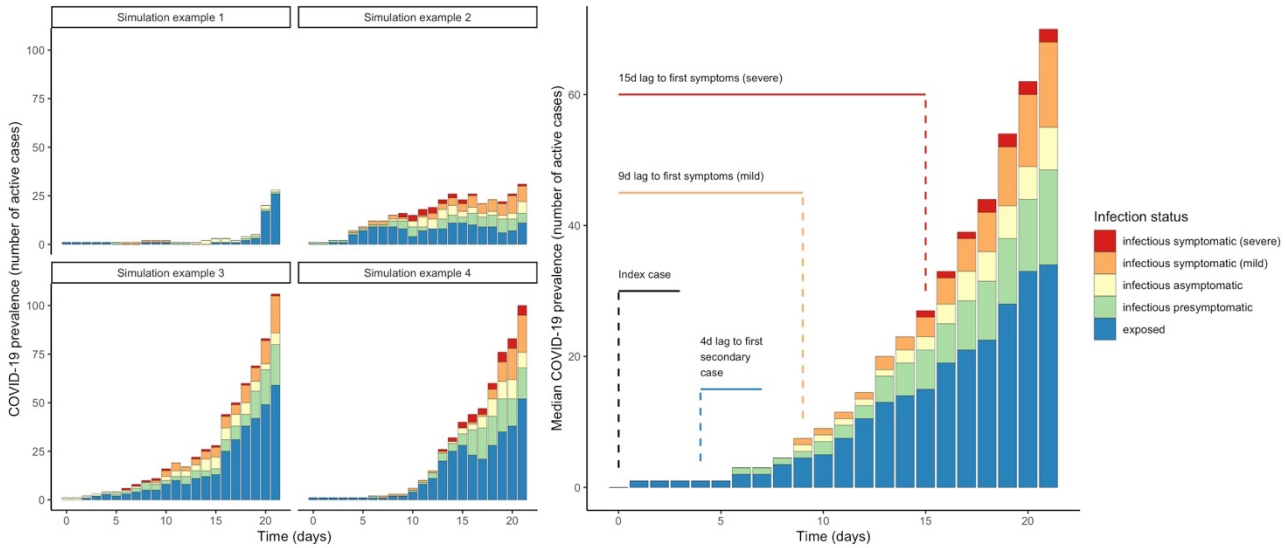

Figure 7.4. Simulated COVID-19 prevalence.

Prevalence curves of COVID-19 cases resulting from random introductions of SARS-CoV-2 into the baseline 170-bed LTCF. **Left:** Four examples of stochastic outbreak simulations. **Right:** The median epidemic curve across all 100 simulations for the baseline scenario, with dotted lines demarcating median time lags to selected events. Bars represent the median number of individuals in each infection class over time, and do not necessarily total to the median number infected (e.g. there is a median 1 infection at *t*=0 but a median 0 infections in each class, as each index case had an equal 1/3 probability of being *exposed*, *pre-symptomatic* or *asymptomatic*).

7.3.1.2. Incidence

Incidence of COVID-19 also increased exponentially upon outbreak onset. **Figure 7.5** shows infection incidence across different epidemiological scenarios (columns) and

indicators (rows). **Figure 7.5A** shows the **daily incidence** of new COVID-19 cases for each simulation (coloured lines) as well as the median across all simulations (black lines). **Figure 7.5B** shows the distribution of the **cumulative incidence** at 12 weeks across all 100 simulations for each scenario; **Figure 7.5C** shows the **case distribution** of the cumulative incidence at 12 weeks, stratified by type of individual infected. From these figures, it can be seen that SARS-CoV-2 spread quickly, but with a great degree of stochasticity upon its introduction into the LTCF. For the baseline importation scenario of weekly patient or staff introductions, after three weeks of unmitigated transmission there were a cumulative 86 (95% uncertainty interval: 6-224) individuals infected, predominantly other patients (median 72%), followed by HCWs (25%) and ancillary staff (3%). Among HCWs, most infections were among caregivers, followed by nurses.

By 12 weeks, most outbreaks had gone extinct, with a median incidence of zero cases across all importation scenarios over the final week of simulation. Epidemiological dynamics were similar across importation scenarios, except for introductions caused by a single member of staff (scenario 4), who did not transmit their infection to anyone else in the facility in 36% of simulations, resulting in no outbreak.

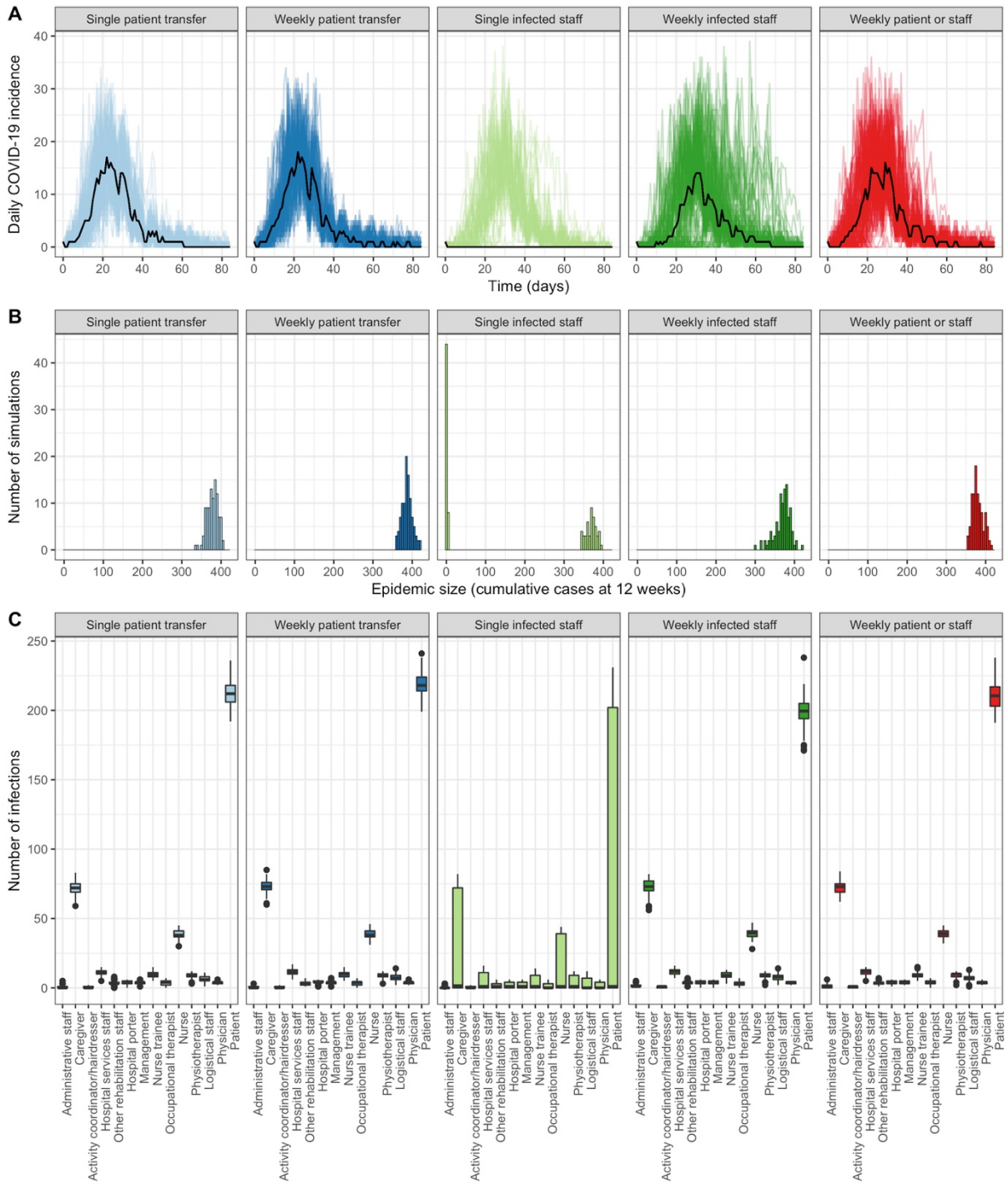

Figure 7.5. Simulated COVID-19 incidence.

Simulated COVID-19 incidence, comparing different epidemiological outcomes (rows) and scenarios of SARS-CoV-2 introduction into the LTCF (columns, with the baseline scenario in red). **(A)** Daily COVID-19 incidence among all patients and staff, with each coloured line representing an individual outbreak simulation. Black lines represent the median daily incidence across 100 simulations. **(B)** Histograms of cumulative incidence at 12 weeks (the final epidemic size). NB: data are naturally censured by the 12-week simulation period. **(C)** Boxplots of case distributions, the cumulative incidence at 12 weeks stratified among the fourteen different categories of individual present in the LTCF.

7.3.1.3. Outbreak dynamics in different facilities

Table 7.3 compares the cumulative incidence of infection over time for the baseline 170-

bed LTCF, and for the smaller 30-bed geriatric LTCF that was simulated as a sensitivity analysis. Cumulative incidence was of course reduced in the smaller LTCF, but overall epidemiological dynamics were similar, with rapid SARS-CoV-2 transmission, particularly among patients, and significantly reduced outbreak risk in scenarios where staff, and not patients introduce the virus.

Table 7.3. Cumulative incidence across facilities.

Cumulative COVID-19 incidence over time, stratified by epidemiological scenario, LTCF, and type of individual. Only simulations resulting in outbreaks were included (for LTCF 1, 64% of simulations from scenario 4, 100% from other scenarios; for LTCF 2, 96% from scenario 2, 24% from scenario 4, 100% from other scenarios).

Scenario	Type of individual	Median cumulative number infected per outbreak by time *t* (95% UI)					
		LTCF 1: Rehabilitation hospital (170 beds)			LTCF 2: Geriatric LTCF (30 beds)		
		1 week (*t*=7)	2 weeks (*t*=14)	3 weeks (*t*=21)	1 week (*t*=7)	2 weeks (*t*=14)	3 weeks (*t*=21)
Scenario 1: Weekly patient or staff	Patient	3 (0 - 16)	21 (0 - 84)	64 (2 - 142)	1 (0 - 10)	7 (0 - 27)	24 (0 - 31)
	HCW	1 (0 - 5)	5 (0 - 25)	22 (1 - 77)	1 (0 - 2)	2 (0 - 12)	8 (1 - 18)
	Ancillary staff	0 (0 - 1)	1 (0 - 5)	3 (0 - 13)	0 (0 - 1)	1 (0 - 3)	2 (0 - 5)
	Total	**4 (1 - 20)**	**30 (2 - 100)**	**86 (6 - 224)**	**2 (1 - 12)**	**10 (2 - 39)**	**34 (3 - 52)**
Scenario 2: Single patient transfer	Patient	7 (2 - 19)	30 (9 - 86)	96 (33 - 145)	3 (1 - 11)	19 (1 - 26)	27 (3 - 31)
	HCW	1 (0 - 5)	8 (1 - 25)	32 (7 - 68)	0 (0 - 3)	5 (0 - 11)	12 (1 - 17)
	Ancillary staff	0 (0 - 2)	1 (0 - 4)	4 (0 - 11)	0 (0 - 1)	0 (0 - 2)	2 (0 - 5)
	Total	**9 (2 - 23)**	**40 (10 - 111)**	**133 (39 - 221)**	**4 (1 - 13)**	**25 (2 - 36)**	**40 (7 - 49)**
Scenario 3: Weekly patient transfer	Patient	7 (2 - 19)	37 (11 - 93)	109 (43 - 148)	4 (1 - 11)	17 (2 - 26)	28 (12 - 32)
	HCW	1 (0 - 4)	9 (2 - 28)	36 (11 - 76)	0 (0 - 4)	4 (0 - 12)	11 (1 - 18)
	Ancillary staff	0 (0 - 2)	1 (0 - 4)	5 (0 - 12)	0 (0 - 1)	0 (0 - 3)	2 (0 - 5)
	Total	**9 (2 - 21)**	**48 (15 - 116)**	**150 (62 - 227)**	**4 (1 - 13)**	**23 (3 - 38)**	**42 (13 - 51)**
Scenario 4: Single infected staff	Patient	0 (0 - 6)	3 (0 - 41)	25 (0 - 97)	0 (0 - 4)	4 (0 - 22)	18 (0 - 29)
	HCW	1 (0 - 4)	3 (1 - 14)	8 (1 - 43)	1 (0 - 2)	2 (1 - 7)	6 (2 - 13)
	Ancillary staff	0 (0 - 1)	0 (0 - 3)	1 (0 - 6)	0 (0 - 1)	0 (0 - 1)	1 (0 - 3)
	Total	**2 (1 - 9)**	**6 (2 - 57)**	**36 (2 - 146)**	**2 (1 - 6)**	**6 (2 - 29)**	**26 (2 - 44)**
Scenario 5: Weekly infected staff	Patient	0 (0 - 11)	2 (0 - 48)	20 (0 - 108)	0 (0 - 4)	0 (0 - 19)	0 (0 - 29)
	HCW	1 (0 - 4)	3 (1 - 15)	10 (1 - 40)	1 (0 - 2)	2 (0 - 7)	3 (1 - 13)
	Ancillary staff	0 (0 - 1)	1 (0 - 3)	1 (0 - 6)	0 (0 - 1)	1 (0 - 2)	1 (0 - 4)
	Total	**2 (1 - 13)**	**6 (2 - 64)**	**34 (3 - 150)**	**1 (1 - 6)**	**2 (2 - 25)**	**4 (3 - 44)**

7.3.1.4. Lags until symptom onset

In the baseline scenario, SARS-CoV-2 outbreaks were characterized by a median lag of 9 (2-24) days between the non-symptomatic index case entering the LTCF and first presentation of mild COVID-19 symptoms among any patient or staff in the facility (**Table 7.4**). By the time symptoms emerged, an additional 5 (0-29) individuals had acquired SARS-CoV-2 but were not (yet) showing symptoms (**Table 7.5**). Lags were longer for first presentation of severe COVID-19 symptoms (15 days from index case, 4-28), coinciding with a greater cumulative number of secondary infections (25, 0-101). These findings underlie potential challenges to relying on symptoms to inform COVID-19 surveillance.

Table 7.4. Lags to first symptom onset.

Lags between introduction of the index case and first presentation of mild and severe COVID-19 symptoms. Results are stratified by epidemiological scenario and LTCF. Only simulations resulting in outbreaks were included (for LTCF 1, 64% of simulations from scenario 4, 100% from other scenarios; for LTCF 2, 96% from scenario 2, 24% from scenario 4, 100% from other scenarios). Lags for outbreaks in which certain symptoms never appeared are indicated as 'never'.

Scenario	Lag until first symptom onset, days (95% CI)			
	LTCF 1: Rehabilitation hospital		LTCF 2: Nursing home	
	Mild symptoms	Severe symptoms	Mild symptoms	Severe symptoms
Scenario 1: Weekly patient or staff	9 (2-24)	15 (4-28)	9 (2-28)	18 (2 - never)
Scenario 2: Single patient transfer	7 (2-15)	12 (4-21)	9 (2-24)	15 (3 - never)
Scenario 3: Weekly patient transfer	7 (2-13)	10 (4-23)	8 (2-19)	14 (3 - never)
Scenario 4: Single infected staff	8 (2-never)	20 (3-never)	17 (2-never)	27 (3 - never)
Scenario 5: Weekly infected staff	10 (2-37)	21 (4-never)	9 (2-28)	never (3 - never)

Table 7.5. Outbreak size upon first symptom onset.

The cumulative number of individuals infected on the day that COVID-19 symptoms first appeared among anyone present in the LTCF (outbreak size upon first symptom onset). Results are stratified by epidemiological scenario and LTCF. Only simulations resulting in outbreaks were included (for LTCF 1, 64% of simulations from scenario 4, 100% from other scenarios; for LTCF 2, 96% from scenario 2, 24% from scenario 4, 100% from other scenarios), and outbreaks were excluded if no symptoms ever occurred over the course of the outbreak.

Scenario	Outbreak size upon first symptom onset (95% UI)			
	LTCF 1: Rehabilitation hospital		LTCF 2: Nursing home	
	Any symptoms	Severe symptoms	Any symptoms	Severe symptoms
Scenario 1: Weekly patient or staff	6 (1-30)	26 (1-102)	3 (1-24)	24 (1-49)
Scenario 2: Single patient transfer	8 (1-25)	26 (3-100)	7 (1-22)	25 (3-42)
Scenario 3: Weekly patient transfer	7 (1-24)	23 (4-97)	5 (1-19)	24 (1-45)
Scenario 4: Single infected staff	2 (1-20)	18 (1-115)	2 (1-9)	22 (2-43)
Scenario 5: Weekly infected staff	2 (1-23)	26 (1-89)	2 (1-20)	20 (1-44)

7.3.2. Surveillance efficacy over time

Figure 7.6 shows the cumulative probability over time of different surveillance strategies detecting emerging SARS-CoV-2 outbreaks, demonstrated in the context of a maximum of 1 test/day using the same example simulations (left panels) and median outbreak prevalence (right panels) as shown in **Figure 7.4**. Different surveillance strategies varied substantially in their ability to detect emerging SARS-CoV-2 outbreaks, with group testing strategies generally having the highest probability of outbreak detection, and random or admission-based strategies the lowest probability. Example simulations (left panels of **Figure 7.6**) demonstrate how surveillance efficacy depended on the stochastic nature of outbreaks, including how many, and which types of individuals became infected over time. Since outbreaks tended to grow exponentially at their outset, delaying outbreak detection by just one or two days potentially coincided with tens more infections occurring.

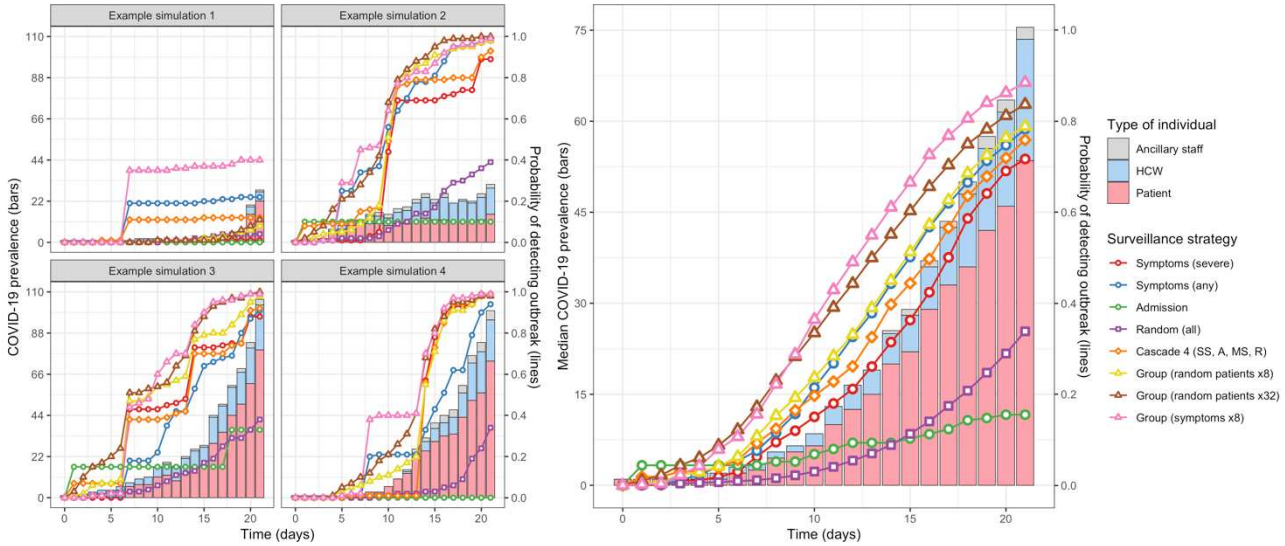

Figure 7.6. Probability of outbreak detection over time (baseline).

Prevalence curves of COVID-19 cases (bars, coloured by type of individual infected; left y-axis) overlayed with the cumulative probability of outbreak detection for various surveillance strategies (points and lines, coloured by surveillance strategy; right y-axis). **Left panels:** the same simulation examples used in **Figure 7.4**. **Right panels:** median outcomes. Plots reflect the baseline scenario (weekly patient or staff introductions) and low testing capacity (1 test/day).

Importantly, surveillance efficacy varied depending on the epidemiological scenario considered and the available testing capacity. Similar to the right panel in **Figure 7.6**, **Figure 7.7** shows median infection prevalence (bars) and median cumulative probability of outbreak detection (lines), stratified across three epidemiological scenarios (columns) and daily RT-PCR testing capacities (rows). Scenarios resulting in smaller outbreaks corresponded with lower probabilities of outbreak detection. Surveillance strategies favouring patient testing were comparatively less effective in scenarios where cases were

only introduced into the LTCF by staff. Conversely, strategies favouring testing at admission were only potentially effective in scenarios with patients introducing the virus into the LTCF. Overall, the strategies most likely to detect outbreaks varied depending on testing capacity: at low capacity, group testing strategies generally had the highest probability of outbreak detection; at high capacity, cascades had highest probabilities.

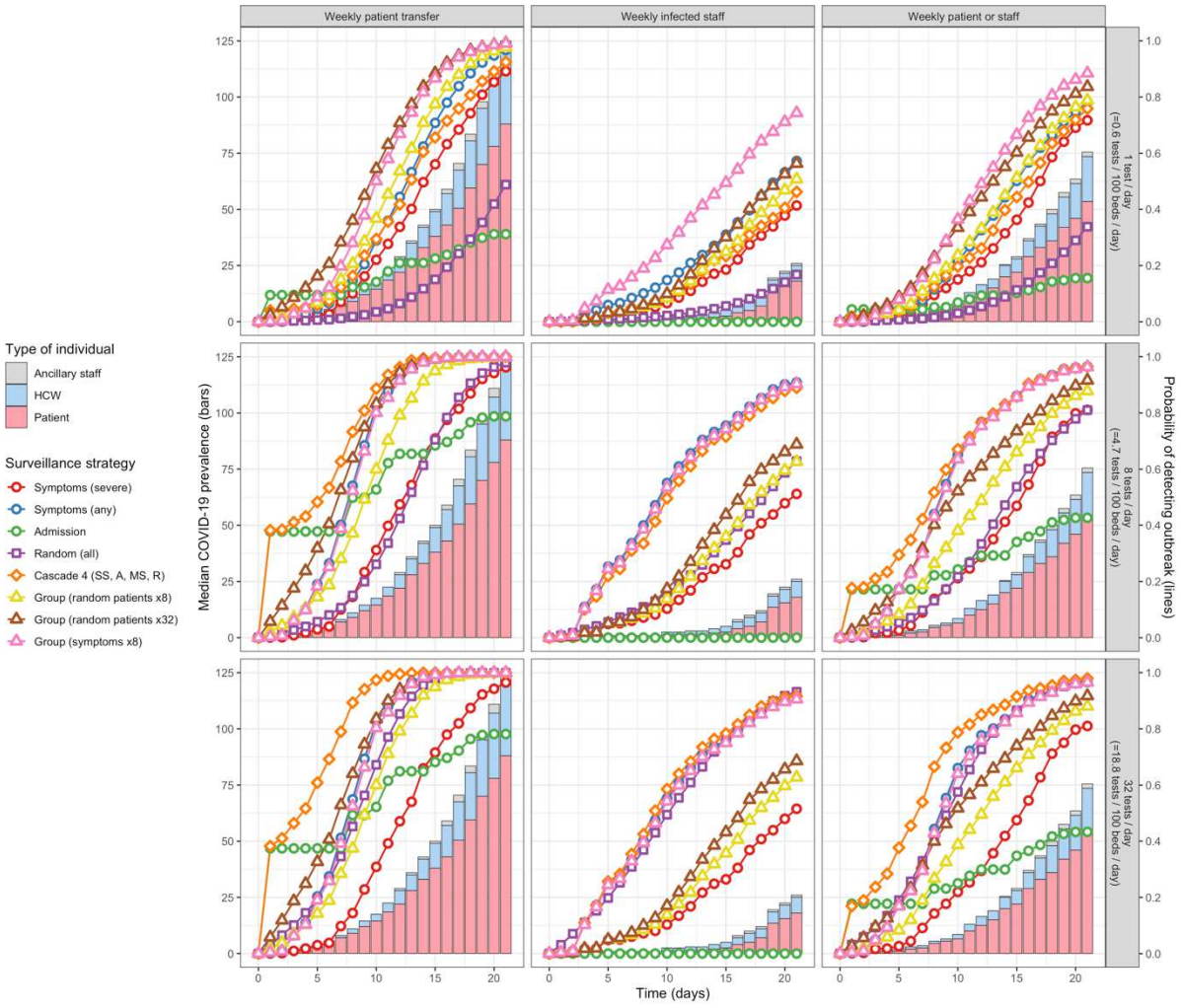

Figure 7.7. Probability of outbreak detection over time (across scenarios).

COVID-19 prevalence varied over time (coloured vertical bars) across selected SARS-CoV-2 importation scenarios (columns). Consequently, the probability of detecting outbreaks over time using different surveillance strategies (coloured lines) varied as a result of differences in how many, and which types of individuals became infected over time across importation scenarios, as well as on daily testing capacity (rows).

7.3.3. Surveillance efficacy as a function of daily testing capacity

Figure 7.8 shows two surveillance efficacy outcomes (**detection lag** and **outbreak size upon detection**) as a function of daily testing capacity for all included surveillance strategies. **Figure 7.9** shows three additional surveillance outcomes (probability of outbreak detection prior to any **secondary cases**, prior to any **mild COVID-19**

symptoms, and prior to any **severe COVID-19 symptoms**), also stratified by testing capacity across selected surveillance strategies.

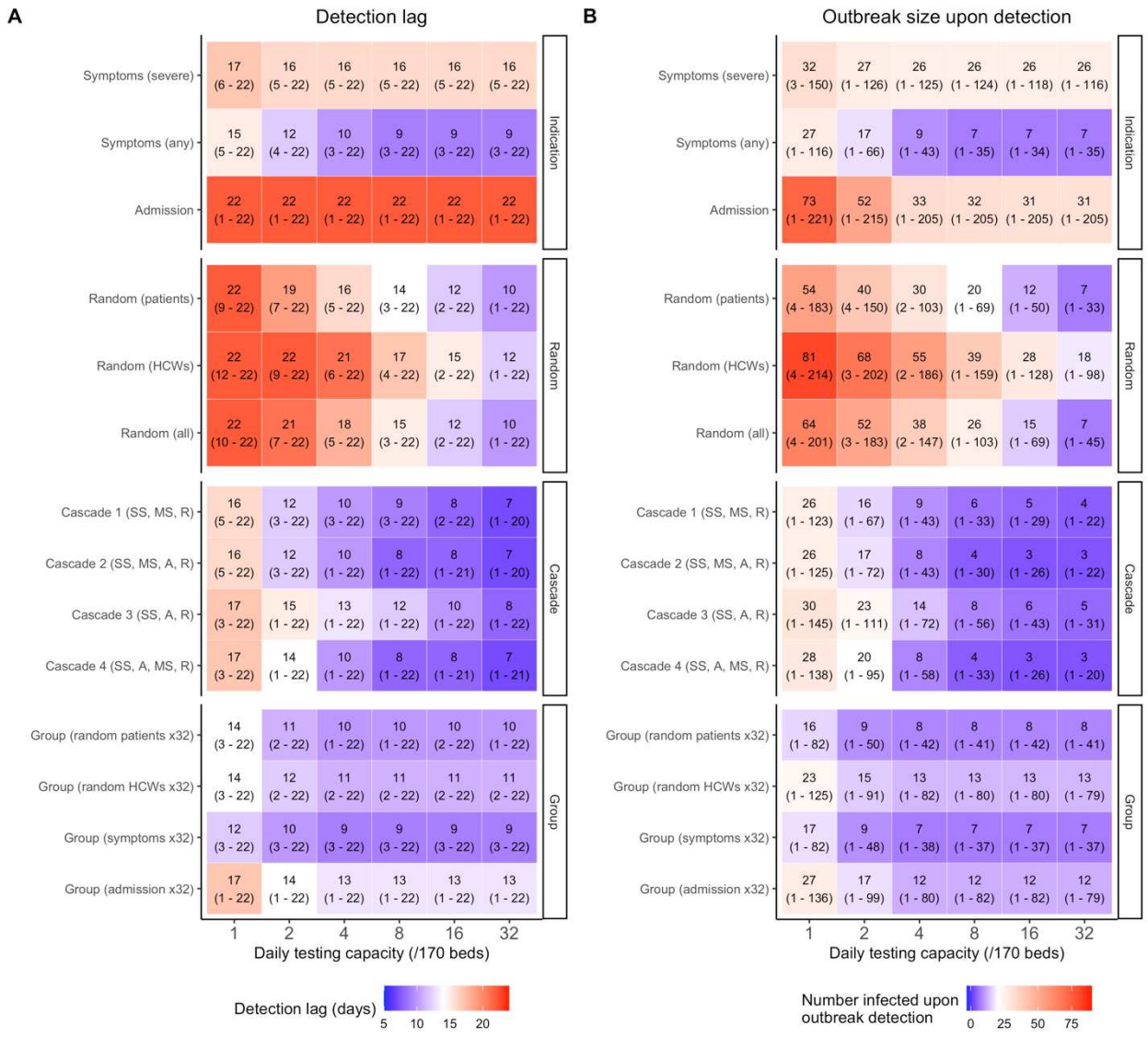

Figure 7.8. Surveillance efficacy (1/2).

For the baseline scenario (weekly patient or staff introductions), surveillance efficacy of different surveillance strategies (y-axis) as a function of the daily RT-PCR testing capacity (x-axis) reported using two outcomes: **(A)** median lag to outbreak detection (95% uncertainty interval) and **(B)** corresponding median outbreak sizes upon outbreak detection (95% uncertainty interval). Group testing strategies included a maximum of 32 swabs per test. For both cascades and group testing, individual tests were always reserved for individuals with severe COVID-19-like symptoms; remaining tests were then distributed according to cascades or as a single group test. SS = severe symptoms; MS = mild symptoms; A = admission; R = random patients.

7.3.3.1. Overall surveillance efficacy across testing capacities

Across all testing capacities, only testing individuals with severe COVID-19-like symptoms was among the least effective surveillance strategies considered (**Figure 7.8**). This "reference" strategy took 16-17 days (range of medians) to detect outbreaks, and had a 2-4% probability of detecting the initial index case prior to any secondary cases (**Figure 7.9**).

Instead of only severe symptoms, testing individuals with any COVID-19-like symptoms was more effective, taking 9-15 days to detect outbreaks, with a 3-14% probability of detecting index cases prior to any secondary cases. Only testing patients at admission was overall ineffective by right of detecting neither staff index cases nor ongoing outbreaks already underway in the LTCF, resulting in long median delays to outbreak detection despite comparatively high probabilities of detecting COVID-19 prior to any secondary cases (10-33%). In the scenario where only new patients introduced SARS-CoV-2 into the LTCF, there was a 34% probability of detecting the index case when testing all patients upon admission, or 66% in the sensitivity analysis considering higher and more stable RT-PCR sensitivity. For random testing strategies, surveillance was highly ineffective when few tests were available, but increasingly effective at higher testing capacities (**Figure 7.8**). Conversely, for indication-based strategies, efficacy plateaued when capacity exceeded the number of individuals potentially indicated for testing (**Figure 7.9**).

7.3.3.2. Optimal surveillance at high testing capacity

At high testing capacity (16-32 tests/day, ≈9-19 tests/100 beds/day), testing cascades were the most effective surveillance strategies (**Figure 7.8**). The four cascades considered detected outbreaks within a median 7-10 days (range of medians), coinciding with just 3-6 COVID-19 infections among all patients and staff. Cascades had a 19-36% chance of detecting outbreaks prior to any secondary cases, a 26-46% chance prior to the emergence of any COVID-19 symptoms, and a 64-85% chance prior to severe COVID-19 symptoms (**Figure 7.9**). Cascades that included both new patient admission and presentation of any COVID-19-like symptoms as indications for testing were most effective.

7.3.3.3. Optimal surveillance at low testing capacity

At low testing capacity (1 or 2 tests/day, ≈0.6-1.2 tests/100 beds/day), group testing was the most effective form of surveillance considered. Compared to the reference (16-17 days) and cascades (16-17 days), outbreaks were detected within 11-14 days (coinciding with a cumulative 9-16 infections) when pooling random patients, or 12-14 days (15-23 infections) when pooling random HCWs (**Figure 7.8**). At this low capacity, it was also more effective to pool symptomatic individuals in group tests (10-12 days, 9-17 infections) than to test them individually (12-15 days, 17-27 infections) because individuals with non-COVID-19 but COVID-19-like symptoms were also “in competition” for limited tests. Compared to the baseline protocol, which assumed a maximum of 32 swabs/test, group

testing was less effective given fewer swabs per test, despite potentially higher test sensitivity. For example, when pooling randomly selected patients in daily group tests, outbreaks were detected within 11-14 days at 32 swabs/test (range of medians across all testing capacities), 12-15 days at 8-16 swabs/test, and 14-17 days at 2-4 swabs/test.

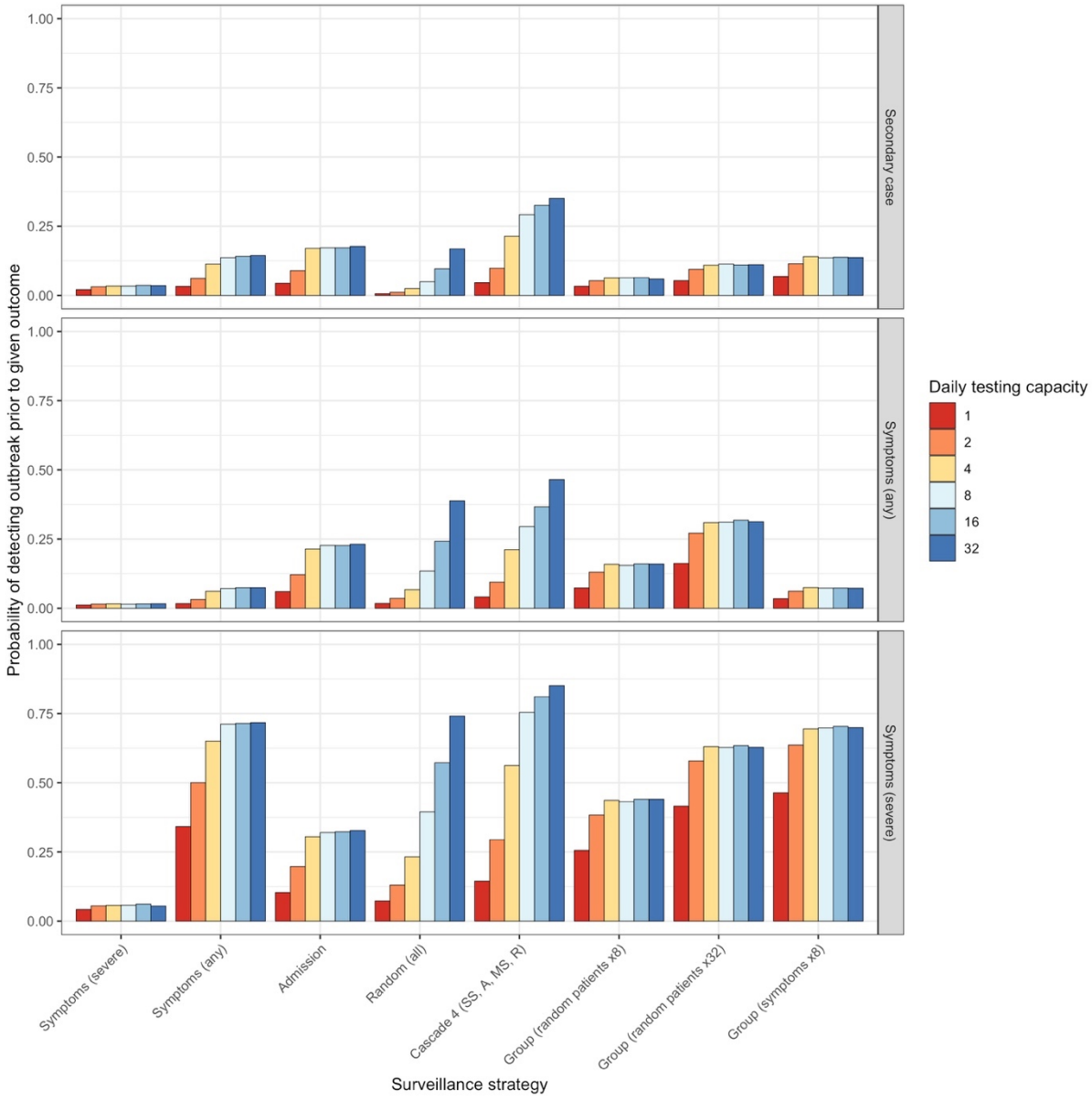

Figure 7.9. Surveillance efficacy (2/2).

For selected surveillance strategies (x-axis), the probability of detecting COVID-19 outbreaks (y-axis) before any secondary cases (top panel), before the onset of any COVID-19 symptoms (middle panel), and before the onset of any severe COVID-19 symptoms (bottom panel), under baseline modelling assumptions. Probabilities depended on the daily testing capacity (colours), and saturate at high testing capacity for all but random and cascade strategies.

7.3.3.4. Surveillance efficacy sensitivity analyses

7.3.3.4.1. RT-PCR cycle threshold

Figure 7.10 shows the efficacy of the four included group testing interventions as reported using the same indicators as in **Figure 7.8** (detection lag in top panels, and outbreak size upon outbreak detection in bottom panels) but comparing results for a high baseline RT-PCR diagnostic threshold (**Ct = 40**) and a lower diagnostic threshold considered in sensitivity analysis (**Ct = 35**). At the high threshold, group testing remained highly effective up to 64 samples per test, but at the low threshold group testing was most effective given 16-32 samples per test, with efficacy declining greatly when 64 samples were included.

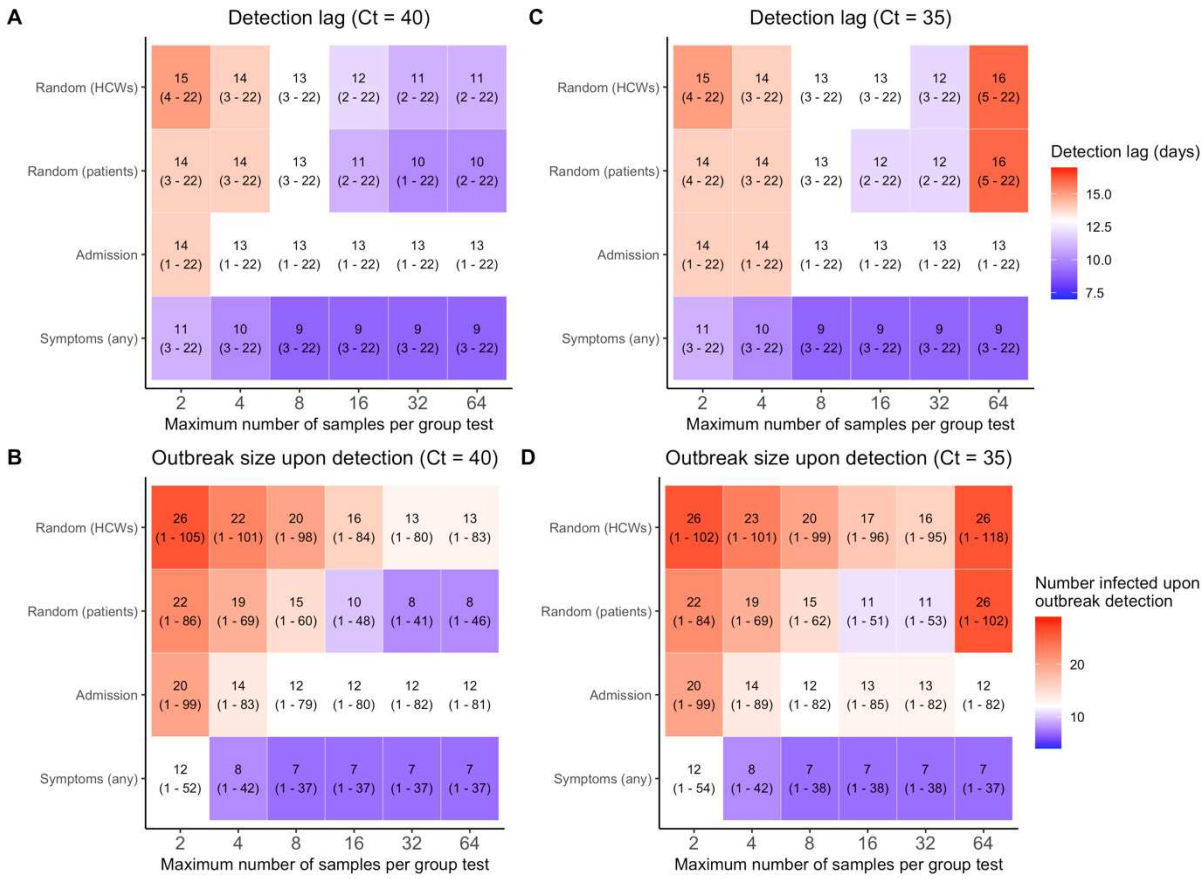

Figure 7.10. Surveillance efficacy sensitivity analysis: cycle threshold value.

Efficacy of group testing depended on which individuals were included in group samples (y-axis) and the maximum number of individual samples included per group sample (x-axis). Efficacy is visualized as a heat map where each tile corresponds to the median outcome (95% uncertainty intervals in parentheses) for two outcomes (detection lag, top panels; outbreak size upon detection, bottom panels) and for baseline modelling assumptions. Two Cycle thresholds (Ct) are considered, which correspond to diagnostic thresholds for RT-PCR testing. **(A)** Detection lag and **(B)** outbreak size upon detection for the baseline Cycle threshold value used in the main analysis (Ct=40). **(C)** Detection lag and **(D)** outbreak size upon detection for the stricter threshold used in sensitivity analysis (Ct=35). The baseline epidemiological scenario is assumed (weekly patient or staff introductions).

7.3.3.4.2. Transmission rates

Figure 7.11 shows surveillance efficacy in a sensitivity analysis where a lower SARS-CoV-2 transmission rate was assumed (p=0.07% probability/minute). Outbreaks were smaller compared to the baseline analysis, resulting in longer lags to outbreak detection, but smaller outbreak sizes when outbreaks were detected. Conversely, **Figure 7.12** shows surveillance efficacy in a sensitivity analysis with a higher SARS-CoV-2 transmission rate (p=0.28% probability/minute), in which larger outbreaks translated to more rapid outbreak detection, but larger outbreak sizes upon detection. Despite these differences, qualitative surveillance conclusions are unchanged from the baseline analysis: group testing was overall most effective when testing resources were limited, while cascades were overall most effective given high testing capacity.

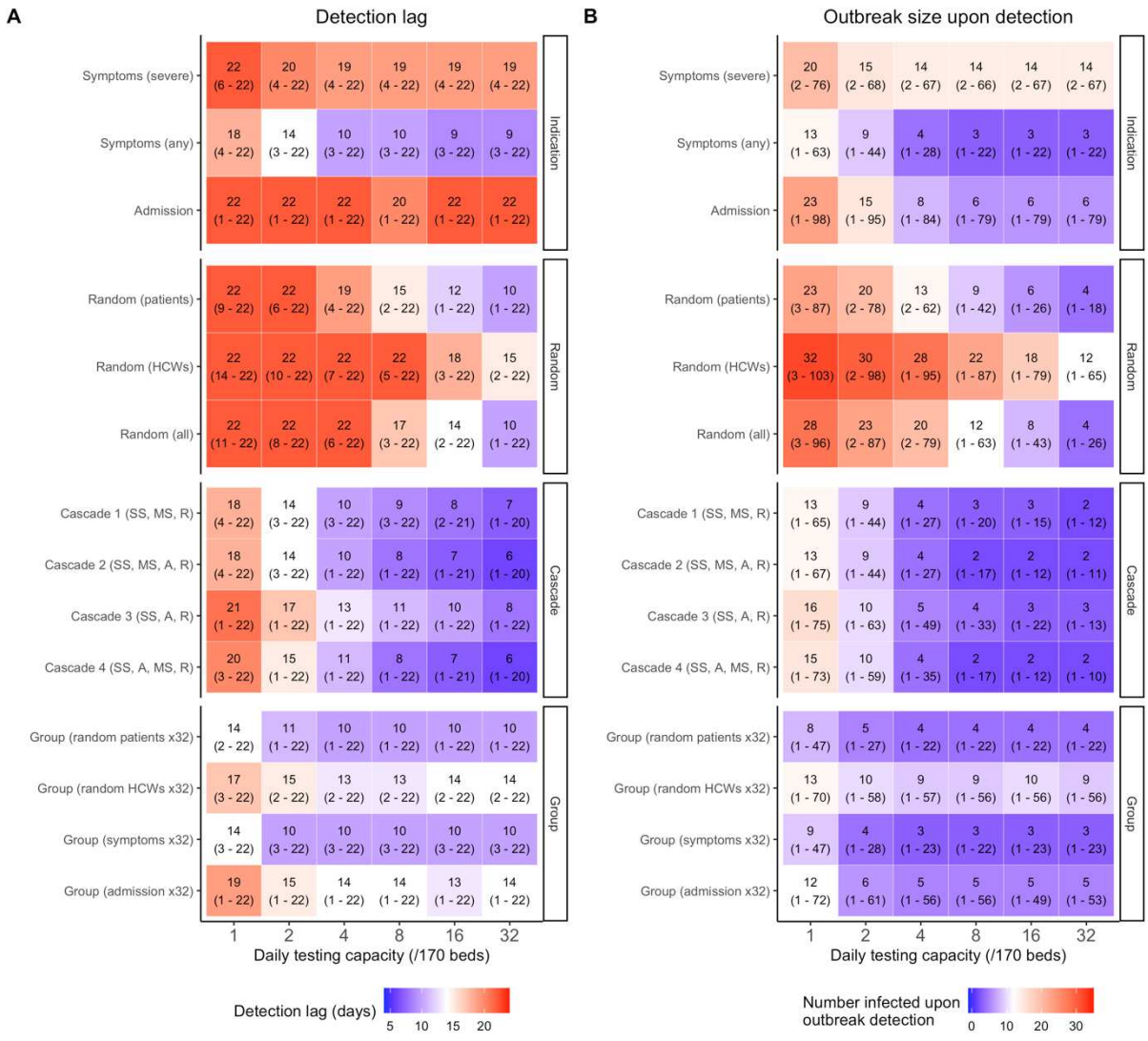

Figure 7.11. Surveillance efficacy sensitivity analysis: low transmission rate.

For simulations in the baseline LTCF with a low transmission rate (*p*=0.07%), **(A)** median lags to outbreak

detection (95% uncertainty interval) and **(B)** corresponding outbreak sizes upon detection are shown for each surveillance strategy (y-axis) as a function of the daily testing capacity (x-axis). Group testing strategies assume a maximum of 32 swabs per test. The baseline epidemiological scenario is assumed (weekly patient or staff introductions).

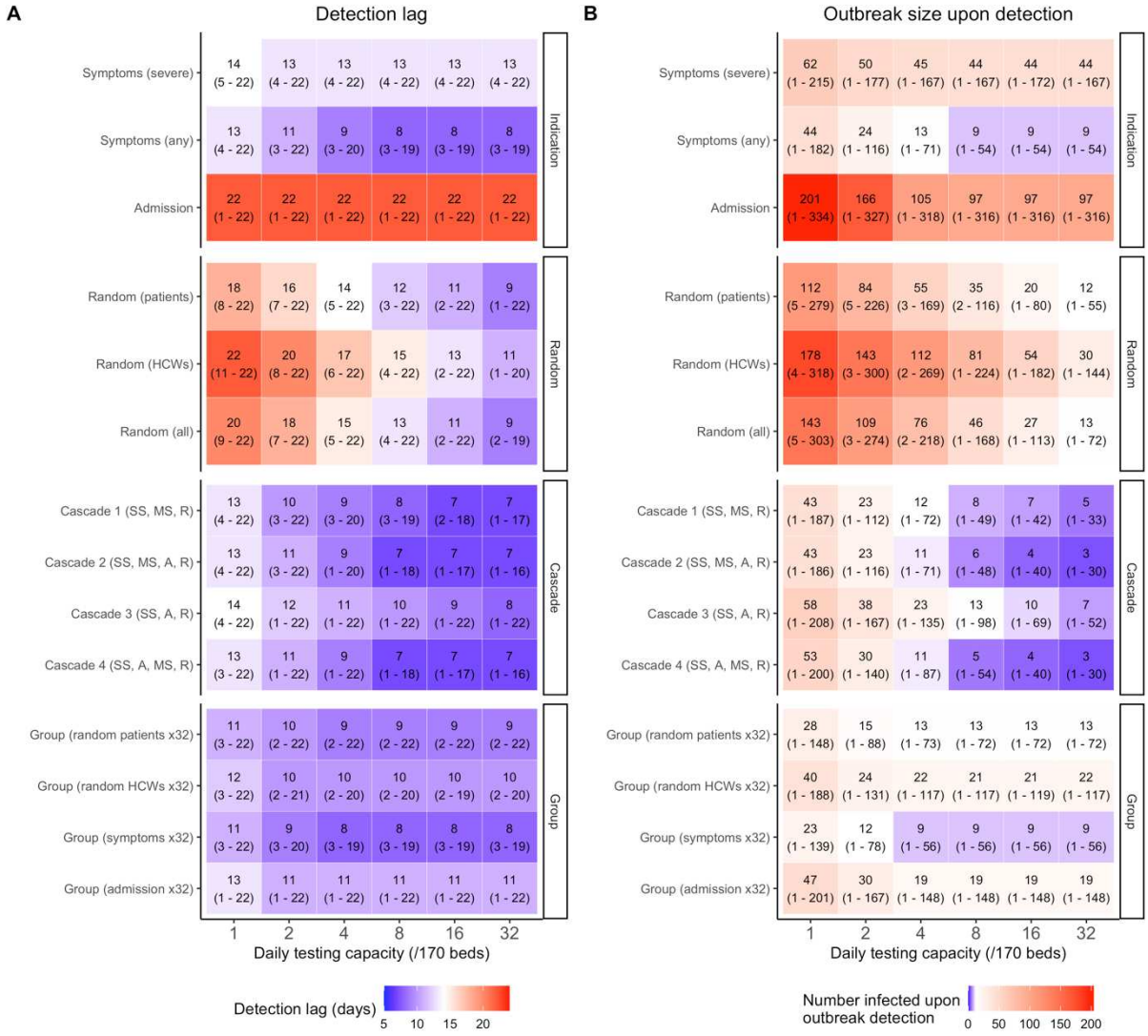

Figure 7.12. Surveillance efficacy sensitivity analysis: high transmission rate.

For simulations in the baseline LTCF with a high transmission rate (p=0.28%), (A) median lags to outbreak detection (95% uncertainty interval) and (B) corresponding outbreak sizes upon detection are shown for each surveillance strategy (y-axis) as a function of the daily testing capacity (x-axis). Group testing strategies assume a maximum of 32 swabs per test. The baseline epidemiological scenario is assumed (weekly patient or staff introductions).

7.3.3.4.3. Smaller geriatric LTCF

Figure 7.13 shows surveillance efficacy in a sensitivity analysis where a smaller, 30-bed nursing home LTCF was simulated. In this analysis, high testing and swabbing capacities approximated universal testing strategies, in which large proportions of individuals were routinely tested several times per week. This explains why randomly testing among all individuals was among the most effective strategies at highest testing capacity, and why pooling even relatively small numbers of randomly selected individuals was a particularly

efficient strategy in this setting (results not shown). Otherwise, qualitative surveillance conclusions were the same as for the baseline LTCF.

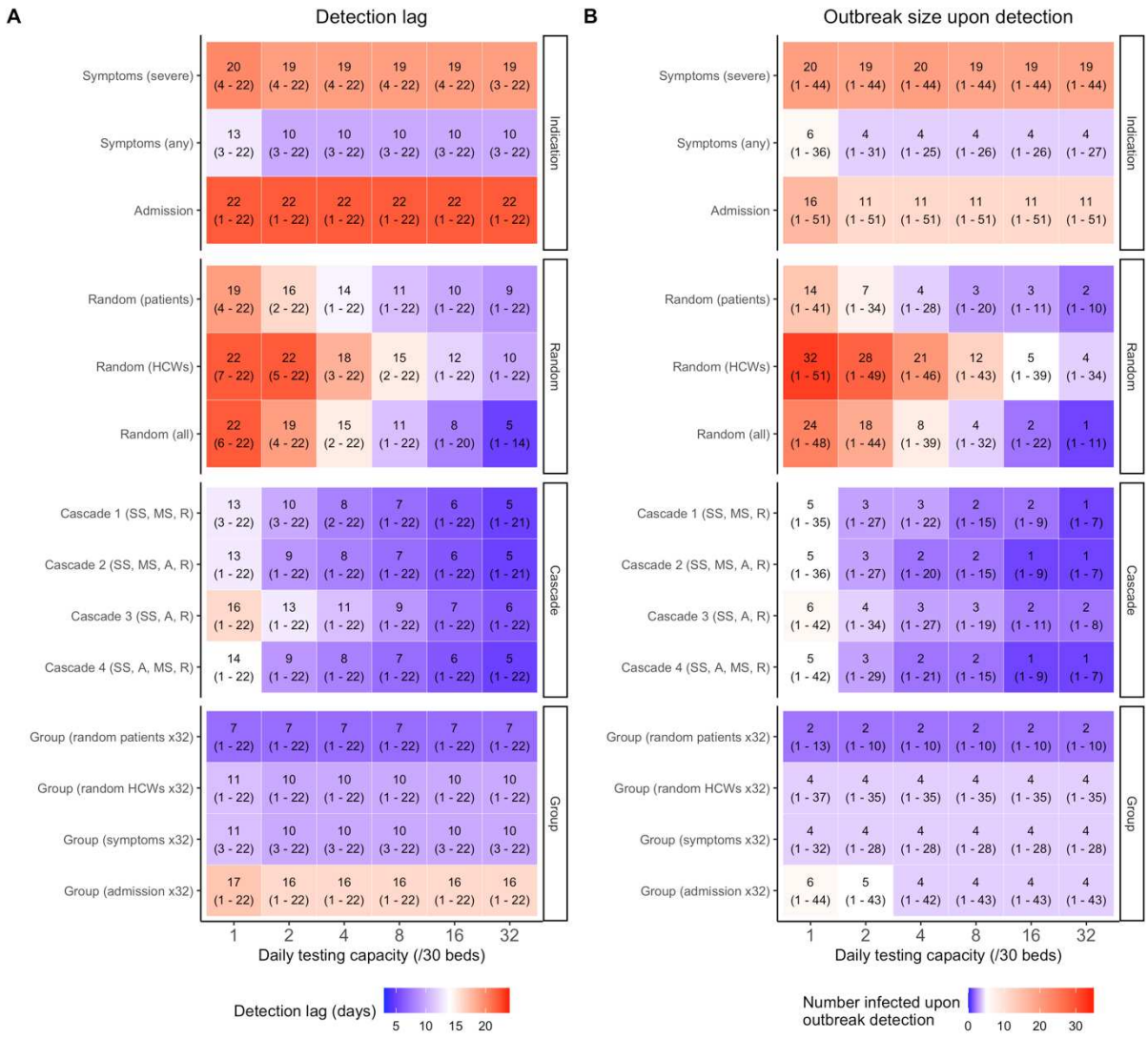

Figure 7.13. Surveillance efficacy sensitivity analysis: nursing home.

For simulations in the 30-bed geriatric LTCF, (A) median lags to outbreak detection (95% uncertainty interval) and (B) corresponding outbreak sizes upon detection are shown for each surveillance strategy (y-axis) as a function of the daily testing capacity (x-axis). Group testing strategies assume a maximum of 32 swabs per test. The baseline epidemiological scenario is assumed (weekly patient or staff introductions).

7.3.4. Surveillance efficiency

Figure 7.14 shows **efficiency plots** depicting how surveillance resource use (number of tests and swabs, x-axes) scales with the efficacy of that surveillance strategy (outbreak detection lag, y-axis). The reference strategy (only testing individuals with severe COVID-19-like symptoms) used the fewest swabs and tests, on average <1/day regardless of the assumed daily testing capacity, owing to a low daily incidence of severe COVID-like

symptoms. At low testing capacity, group testing strategies detected outbreaks earliest while using similar numbers of tests compared to other strategies (although group testing randomly selected patients or staff required extensive swabbing effort). At high capacity, cascades detected outbreaks earliest but used hundreds more tests than indication-based or group testing strategies, while random testing strategies were both less effective and more resource-intensive than cascades.

Figure 7.15 shows **incremental efficiency plots**, depicting, relative to the reference strategy, the incremental benefits of other strategies (in terms of reduction in outbreak size upon detection) scaled against their incremental resource costs (increase in the numbers of tests and swabs used). This plot compares a scenario with low daily testing capacity (2 tests/day) and high capacity (32 tests/day).

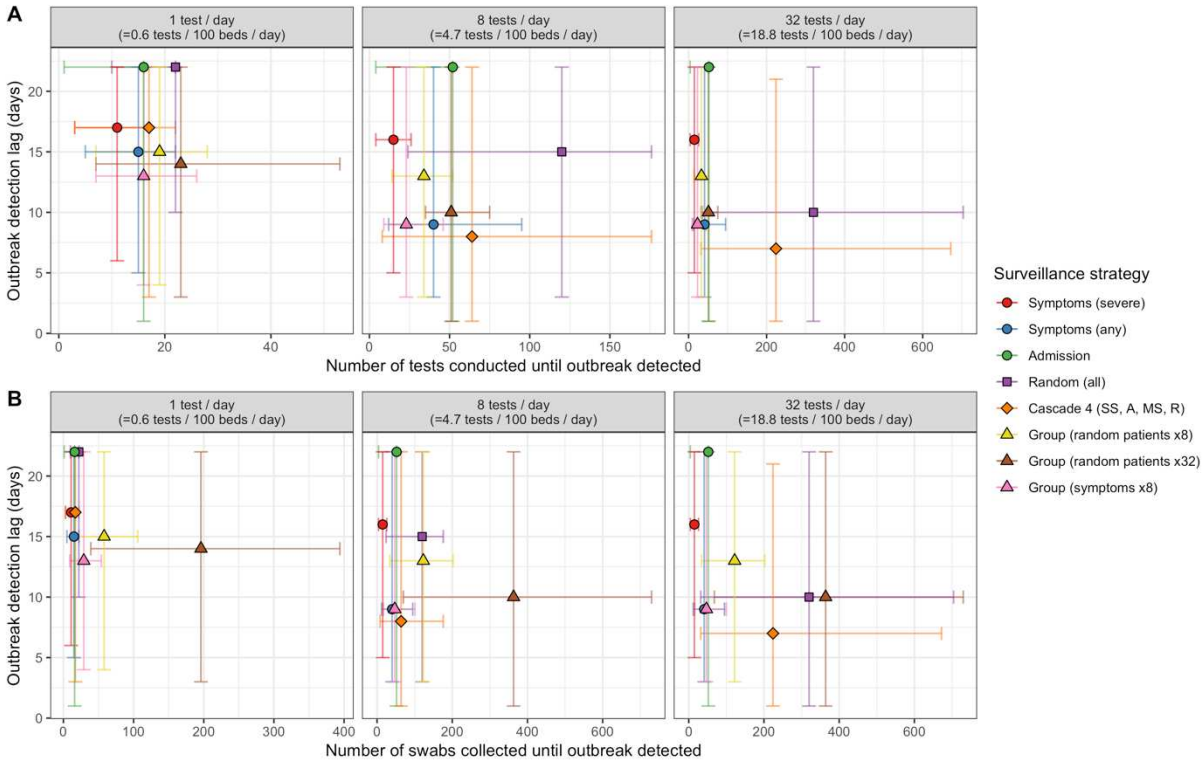

Figure 7.14. Efficiency plots.

Efficiency plots for selected surveillance strategies given baseline modelling assumptions, comparing the efficacy (y-axis) and resource use (x-axis) in terms of the number of tests used (top row) and swabs collected (bottom row) until outbreaks were detected. The assumed daily testing capacity varies across columns. Symbols represent medians and error bars represent 95% uncertainty intervals across all outbreak simulations. For cascades: SS=severe symptoms, MS=mild symptoms, A=admission, R=random (patients).

7.3.4.1. Cascade efficiency

At high testing capacity (16-32 tests/day), the high incremental efficacy of cascades (outbreak detection a mean 5-8 days earlier than the reference, prior to 22-27 additional infections) resulted from extensive resource use (104-276 additional tests and swabs), for mean incremental efficiencies of 4.0-11.2 additional swabs and tests per case averted. Although simply testing all patients and staff with any COVID-19-like symptoms was less effective than using testing cascades, it was a more efficient means to improve surveillance (mean 1.3 additional tests per case averted).

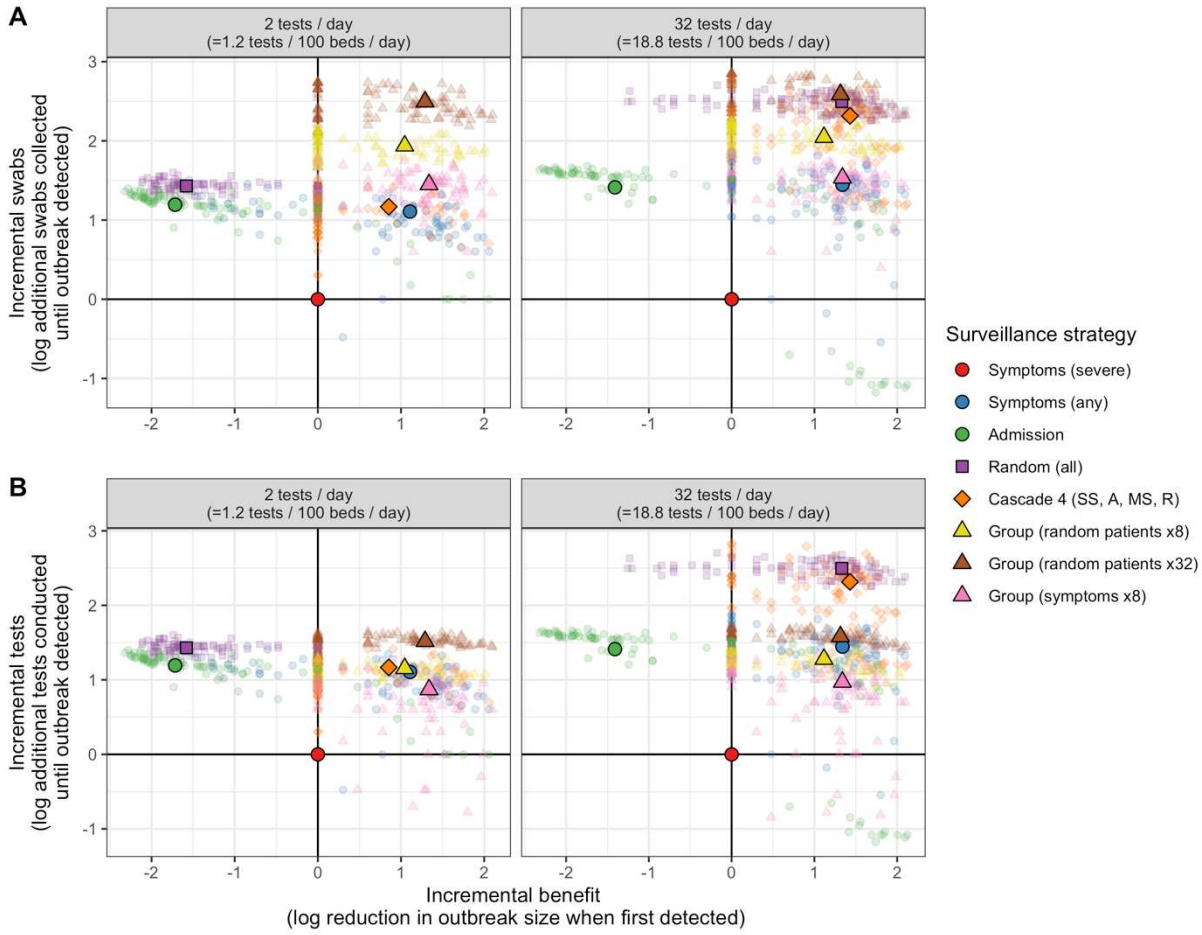

Figure 7.15. Incremental efficiency plots.

Log_{10}-transformed incremental efficiency plots for simulations under baseline modelling assumptions, comparing incremental resource-use in terms of **(A)** nasopharyngeal swabs used and **(B)** RT-PCR tests conducted, and varying testing capacity from 2 tests/day (left panels) to 32 tests/day (right panels). Small translucent points represent median outcomes across 100 surveillance simulations for each simulated outbreak, and larger opaque points represent the mean of all medians.

7.3.4.1. Group testing efficiency

Group testing strategies were generally efficient with respect to tests, but used highly variable numbers of swabs to detect outbreaks. At high swabbing capacity (16-32 swabs/group test, ≈9-19 swabs/100 beds/day) and across all testing capacities, pooling randomly selected patients used a mean 11-38 excess tests to detect outbreaks 2-4 days earlier and prior to 14-21 additional infections (0.8-1.8 additional tests per case averted), but a median 94-384 additional swabs (6.7-18.7 additional swabs per case averted). Pooling the same number of randomly selected HCWs was less efficient than pooling patients (detection=1-4 days earlier, prior to 6-14 infections; efficiency=1.3-2.8 additional tests and 15.9-27.5 additional swabs per case averted).

By contrast, for all scenarios and testing capacities considered, pooling individuals with any COVID-like symptoms was among the most efficient strategies in terms of both swabs and tests. In the most resource-limited scenarios (1-2 tests, ≈0.6-1.2 tests/100 beds/day; 2-8 swabs per group test, ≈1-5 swabs/100 beds/day), this was both the most effective means to detect COVID-19 outbreaks and the most efficient means to improve surveillance from the reference (detection=1-6 days earlier, prior to 11-22 additional infections; efficiency=0.3-0.6 additional tests and 1.0-1.3 additional swabs per case averted).

7.4. Discussion

7.4.1. Summary of model and results

In this Chapter I analyzed outbreak simulations from a high-resolution individual-based model adapted to COVID-19, demonstrating a range of known challenges associated with nosocomial SARS-CoV-2 surveillance in long-term care settings. Challenges include introductions of the virus from the community via non-symptomatic individuals, its rapid and often silent transmission among patients and staff, and lags to or absence of COVID-19 symptoms among a substantial proportion of the population. I then used a stochastic algorithm to evaluate efficacy and efficiency of testing interventions in the context of key surveillance limitations, including imperfect and time-varying diagnostic sensitivity, and limited testing capacity. Findings have ultimately provided evidence for how healthcare institutions can optimize COVID-19 surveillance in the context of high nosocomial outbreak risk and limited RT-PCR tests.

7.4.1.2. Cascades optimize surveillance at high testing capacity

Findings suggest that vulnerable LTCFs can detect emerging COVID-19 outbreaks most quickly by using testing cascades, provided that they have substantial daily testing capacity (on the order of at least 1 test/10 beds/day). The most effective cascades considered multiple indications, including both COVID-19-like symptoms and patient admission, and detected outbreaks days ahead of traditional symptom-based screening and prior to the accumulation of additional infections. By extension, cascades had the greatest probability of identifying non-symptomatic cases, a known challenge for COVID-19 surveillance in real LTCF settings.(World Health Organization, 2020g) These findings held in sensitivity analyses considering outbreaks in a smaller, 30-bed geriatric LTCF, as well as when halving or doubling SARS-CoV-2 transmissibility. Although only a select few indications were considered in the present study, LTCFs may consider a wider range of known risk factors for SARS-CoV-2 acquisition in their own cascades to maximize the probability of detecting emerging outbreaks before widespread transmission.

7.4.1.2. Group testing optimizes surveillance at low testing capacity

COVID-19 surveillance was less effective in resource-limited settings because of an inability to regularly test large numbers of patients and staff. In this analysis, group testing was the most effective COVID-19 surveillance strategy under limited testing capacity, and across all epidemiological scenarios and capacities was the most resource-efficient means

to improve surveillance with respect to a “bare minimum” reference of only testing individuals with severe COVID-like symptoms. Even when assuming stricter diagnostic cut-offs in sensitivity analysis (Ct=35 instead of 40), group testing strategies remained effective up to a maximum of 32 swabs per test. This broadly agrees with previous modeling results suggesting that group testing could be cost-effective for screening in large populations, as well as empirical evidence for the efficiency of group testing for COVID-19 surveillance in nursing homes.(Ben-Ami et al., 2020; Narayanan et al., 2020) As with cascades, LTCFs that conduct group testing may consider a wider range of indications than was possible to include in this study, in order to maximize the probability of including potentially infected patients and staff in routine group tests.

These findings reinforce current guidance from WHO, endorsing sample pooling to increase COVID-19 diagnostic capacity when testing demand outstrips supply, but cautioning against its use for contact tracing or in high-prevalence settings.(World Health Organization, 2020h) This is consistent with its implementation in the present study, as a means of surveillance in resource-limited long-term care settings without known active cases, but which are nonetheless vulnerable to outbreaks.

7.4.2. Findings in context

7.4.2.1. Explosive nosocomial outbreaks

This study, initiated in March 2020, was among the first to simulate SARS-CoV-2 outbreaks in the healthcare setting. Simulations suggest that silent introductions of SARS-CoV-2 lead to large outbreaks in the absence of specific control strategies, consistent with explosive outbreaks observed in LTCFs worldwide early in the pandemic.(Arons et al., 2020; ECDC Public Health Emergency Team et al., 2020; D. Fisman et al., 2020; Iritani et al., 2020; McMichael et al., 2020) Simulations further predicted that larger proportions of patients became infected than staff, consistent with evidence of higher SARS-CoV-2 incidence in patients than staff across LTCF settings globally.(ECDC Public Health Emergency Team et al., 2020; Salcher-Konrad et al., 2020) Larger outbreaks and more rapid dissemination were also predicted when SARS-CoV-2 was introduced through admission of an infected patient, rather than through a member of staff infected in the community, with important implications for surveillance efficacy. This is likely due to the nature of human interactions in the LTCF upon which CTCmodeler is based (patient-patient contacts were particularly long and numerous compared to other settings).(Duval et al., 2018) Overall, these findings reinforce both (i) a need to screen incoming patients

potentially exposed to or infected with SARS-CoV-2,(Gaur et al., 2020) and (ii) the importance of interventions to limit contact between patients (e.g. social distancing among retirement home residents), as already widely recommended for affected facilities in the current pandemic context.(D'Adamo et al., 2020)

7.4.2.2. Silent transmission

Simulated outbreaks were further characterized by delays between silent introduction of SARS-CoV-2 and first onset of COVID-19 symptoms, during which time new infections not (yet) showing symptoms accumulated. This is consistent with reported transmission dynamics of SARS-CoV-2. Modelling studies from early in the pandemic estimated that 30-57% of secondary infections among identified transmission pairs resulted from pre-symptomatic transmission,(He et al., 2020) and that, in outbreaks in Singapore and Tianjin, pre-symptomatic transmission accounted for at least 65% of all transmission events.(Tindale et al., 2020) This is also consistent with reports from various LTCF outbreaks identifying important roles for pre-symptomatic and asymptomatic transmission.(Arons et al., 2020; Bigelow et al., 2021; Black et al., 2020; Escobar et al., 2021; Louie et al., 2021; McMichael et al., 2020; Moghadas et al., 2020) The often silent nature of SARS-CoV-2 transmission highlights epidemiological challenges associated with screening for emerging outbreaks using symptoms alone. In addition to the strategies highlighted above, it was found that testing patients and healthcare workers with any, and not only severe COVID-like symptoms can substantially improve outbreak detection, supporting recommendations to expand testing criteria in LTCFs to include individuals with atypical signs and symptoms of COVID-19, such as muscle aches, sore throat and chest pain.(Gaur et al., 2020)

7.4.2.3. Outbreak detection: a specific epidemiological context

Previous studies of COVID-19 surveillance have largely focused on the ability of testing strategies to mitigate ongoing SARS-CoV-2 transmission in active outbreak settings.(Grassly et al., 2020) In particular, contact tracing has been identified as a highly effective form of surveillance, by targeting testing and isolation interventions to individuals at high risk of infection.(Ferretti et al., 2020; Kucharski et al., 2020) However, these findings have limited relevance for emerging outbreaks, where active SARS-CoV-2 infection and ongoing transmission are not yet known. For healthcare facilities vulnerable to SARS-CoV-2 introductions, specific surveillance strategies are required for initial outbreak detection, in order to alert healthcare professionals and decision-makers to the

presence of the virus in their institutions. Only then can proven measures like contact tracing and case isolation be implemented. By targeting this important epidemiological context, these findings complement an existing evidence base that has until now largely focused on how to control outbreaks that are already detected and well underway.

7.4.2.4. Considerations for implementing group testing

This analysis was limited to classical two-stage group testing, initially proposed by Dorfman in 1943 for syphilis screening among World War II soldiers,(Dorfman, 1943) in which all individuals in a positive group test are individually re-tested to determine who is infected. This is regarded as the most straightforward approach,(Mallapaty, 2020) and I conservatively assumed re-swabbing in addition to re-testing of all individuals in a positive group test to account for potential logistical challenges of storing and maintaining large numbers of swabs for re-testing. Various alternative group testing strategies have been proposed and implemented elsewhere, including the use of simultaneous multi-pool samples, non-adaptive pooling schemes, and others.(Eberhardt et al., 2020; Ghosh et al., 2020; Mallapaty, 2020; Täufer, 2020) These have the advantage of not requiring separate re-testing of all individuals in a positive group test, and are hence more efficient in terms of the number of tests required for case identification. However, these strategies may also require additional testing infrastructure and expertise, which may be cost-prohibitive for the resource-limited settings that may benefit most from group testing in the first place. Decision-makers must consider trade-offs between the various costs and benefits of different group testing technologies, including how many individuals to include per test, how many stages of testing to conduct, and other potential operational obstacles.(World Health Organization, 2020h)

7.4.3. Limitations

This work has several limitations. First, LTCFs represent a diverse range of healthcare institutions, each with unique specializations, patient populations and living conditions, and the generalizability of findings across settings is not clear. However, in simulations there was nonetheless consistency in surveillance outcomes across the baseline 170-bed facility and the 30-bed geriatric facility.

Second, there were substantial uncertainties about the epidemiological characteristics of SARS-CoV-2 infection when this study was conducted. Although already well established that various COVID-19 outcomes vary with age, comorbidity and frailty,(Ma et al., 2020;

Petrilli et al., 2020; Zheng et al., 2020) quantitative descriptions of these associations were and remain incomplete. It was thus not possible to reliably integrate such individual-level variation into the transmission model. For one example, it remains unclear to what extent rates of asymptomatic infection may be expected to vary among LTCF residents and staff. An outbreak investigation across six London care homes experiencing COVID-19 outbreaks estimated similar rates of asymptomatic infection in patients and staff, and found no association with age,(Ladhani et al., 2020) while the meta-analysis used to inform asymptomatic infection in this work highlighted poor reporting of age in included studies, precluding quantification of its relationship to COVID-19 symptom risk.(Buitrago-Garcia et al., 2020) Nonetheless, calibrating model parameters to individual-level risk factors would facilitate more realistic simulations, and accounting for potentially higher rates of severe infection among older and frailer individuals could result in improved performance of symptom-based surveillance, including corresponding cascades and group testing strategies. This distinction may be particularly relevant for hospices, nursing homes, and other LTCFs with particularly frail populations; however, patients in the present rehabilitation hospital population were relatively young (median 58 years, IQR 47-72), limiting potential impacts of age-stratified disease progression in this study.

Other epidemiological uncertainties that were unable to be accounted for include temporal variability in SARS-CoV-2 transmissibility over the infectious period, individual-level variation in transmissibility, and a potential role for environmental acquisition or healthcare workers acting as transient vectors.(Nelson et al., 2021; van Doremalen et al., 2020) Sensitivity analyses considering unusually high and low SARS-CoV-2 transmission rates may in part reflect overall impacts of such assumptions on nosocomial outbreak risk. Although SARS-CoV-2 spread more or less quickly in these analyses, the relative efficacies of surveillance strategies were largely unchanged, resulting in the same conclusions for optimizing use of limited testing resources to detect nascent COVID-19 outbreaks. Nonetheless, there are clear links between viral load, transmissibility and Ct values, such that infections more likely to transmit are also more likely to be detected. Accounting for this in future refinements of our model – for instance, by simulating a proxy for viremia at the individual-level and correlating it with both transmissibility and test sensitivity – would not only be more realistic, but could have important consequences for estimation of surveillance efficacy.

7.4.4. Future work

These findings add to a growing evidence base for optimizing surveillance interventions to control SARS-CoV-2 spread, which has been a central focus of epidemiological modelling studies since COVID-19 first emerged. However, the epidemiological situation continues to evolve apace. There is now substantial worldwide population immunity to SARS-CoV-2, and most LTCFs now have varying degrees of COVID-19 containment measures in place, from social distancing, to use of personal protective equipment, to vaccination, which should altogether reduce transmission rates compared to early in the pandemic. Conversely, the emergence of highly transmissible variants of concern capable of escaping host immune responses may to some extent have the opposite effect. New surveillance technologies also continue to become available, such as antigen rapid diagnostic testing (Ag-RDT), and global RT-PCR capacity has been extensively scaled up since March 2020. In this context, new evidence is needed to understand how LTCFs can continue to adapt and optimize available surveillance technologies in order to protect themselves from COVID-19 as the pandemic rages on.

Chapter 8. Rapid antigen testing as a reactive public health response to surges in nosocomial outbreak risk

8.1. Introduction

A growing number of vaccines have proven safe and effective for prevention of SARS-CoV-2 infection and severe COVID-19, protecting patients and staff from disease and offering hope towards an end to the pandemic.(Dagan et al., 2021; Heath et al., 2021; Pritchard et al., 2021) Yet hospitals and LTCFs remain vulnerable to nosocomial outbreaks despite high vaccination rates.(Bergwerk et al., 2021) LTCFs globally report instances of breakthrough infection and ensuing transmission among immunized staff and residents, notably due to variants of concern like B.1.1.7 (Alpha) and B.1.351 (Beta), which may partly escape vaccine-induced immunity relative to wild type.(Bailly et al., 2021; Tober-Lau et al., 2021; Vanker et al., 2021) This suggests that testing and screening interventions will remain important tools for detecting and isolating SARS-CoV-2 infections in healthcare facilities, even in settings with high vaccine coverage.

However, while repeated screening may be an effective tool for nosocomial transmission prevention,(Holmdahl et al., 2021; Rosello et al., 2021) it also imposes substantial economic cost and occupational burden on healthcare staff.(Buckle et al., 2021; Kierkegaard et al., 2021) For potentially vulnerable, resource-limited facilities, a key challenge is knowing if, when and how to implement SARS-CoV-2 surveillance interventions.(Barker et al., 2021) When outbreak risk is low – perhaps in a highly immunized LTCF around low community incidence and few variants of concern – screening at frequent intervals is probably an inefficient use of limited health-economic resources. Yet outbreak risk is in constant flux, and is sometimes predictable. Festive holidays, for instance, draw individuals from distant places into close contact for prolonged periods, and have been associated with surges in SARS-CoV-2 epidemic risk in China, Israel, and elsewhere.(Chen et al., 2020; Klausner et al., 2020) Into autumn 2021, widespread post-holiday, inter-generational population movement in the context of variants like B.1.617.2 (Delta) and C.37 (Lambda) may pose similar concerns. In such a context where local knowledge or epidemiological data indicate a suspected spike in epidemic risk,

or where identification of a new case or exposed contact within a healthcare facility indicates potential for a nosocomial outbreak, reactive use of antigen rapid diagnostic testing (Ag-RDT) may be an efficient public health response.

Here, to help determine the best surveillance strategies for control of SARS-CoV-2 transmission in healthcare facilities, I evaluated the epidemiological efficacy and health-economic efficiency of single or repeated Ag-RDT screening conducted in response to surges in nosocomial outbreak risk in the long-term care setting.

8.2. Methods

8.2.1. Simulating SARS-CoV-2 outbreaks using CTCmodeler

In **Chapter 6**, I presented CTCmodeler as a tool to simulate SARS-CoV-2 outbreaks in the long-term care setting. In **Chapter 7**, I used this model to evaluate efficacy and efficiency of RT-PCR testing strategies for timely detection of emerging SARS-CoV-2 outbreaks in the context of limited testing resources. In this Chapter, I expand upon this work, using simulated outbreaks from CTCmodeler to evaluate the efficacy and efficiency of testing and screening interventions for prevention of SARS-CoV-2 transmission, in the context of a surge in nosocomial outbreak risk. R code for the surveillance analyses described below is available online at https://github.com/drmsmith/agrdt.

8.2.2. Modelling context

Model simulations were initialized to include a surge in SARS-CoV-2 introductions from the community. This was motivated by lived experiences of colleagues in French long-term care facilities over Christmas 2020. The festive holidays were associated with increased inter-generational contact between individuals in the community and those residing in LTCFs. Accordingly, a surge in nosocomial SARS-CoV-2 outbreaks was anticipated and ultimately detected after the holiday period.(Smith et al., 2020)

Simulation outset was interpreted as coinciding with initial SARS-CoV-2 outbreak detection within the LTCF, triggering implementation of reactive surveillance interventions (introduced below). Accordingly, this modelling context follows naturally from evaluation of surveillance interventions for outbreak detection in the previous Chapter. Here, I evaluate efficiency of surveillance interventions for transmission prevention, once a potential outbreak has been detected.

8.2.3. Transmission model updates

Nine new assumptions were integrated into CTCmodeler to reflect the evolving epidemiology of COVID-19 and present research context. These include:

1. Index cases acquired during a surge in community SARS-CoV-2 circulation
2. Heterogeneous SARS-CoV-2 introductions from the community reflecting local infection burden
3. Variable transmissibility between symptomatic and asymptomatic infections

4. Immediate isolation of patients with severe COVID-19 symptoms
5. Sick-leave and shift replacement for staff with severe COVID-19 symptoms
6. A risk of healthcare workers acting as transient SARS-CoV-2 vectors
7. Initialization conditions reflecting an updated pandemic context
8. Storing SARS-CoV-2 transmission chains
9. Implementation of public health interventions ("COVID-19 containment measures").

These assumptions are detailed below, and corresponding model parameters are provided in **Table 8.1**.

8.2.3.1. Index cases acquired during a surge in community SARS-CoV-2 circulation

As in previous Chapters, I distinguish between SARS-CoV-2 index cases and SARS-CoV-2 introductions. Index cases were defined as patients and staff infected with SARS-CoV-2 upon simulation outset, who were thus assumed to have acquired infection prior to the simulation period. These infections were conceptualized as resulting from inter-generational mixing in the community over festive holidays during the week prior to simulation outset, leading to an increase in nosocomial outbreak risk within the LTCF. Upon simulation initialization, it was assumed that 50% of patients (n=85) and 100% of staff (n=240) had contacts in the community over the previous week, with a 1.2% probability of acquiring SARS-CoV-2 (calibrated to French epidemiological data from Santé Publique France from January 2021). This translated to 1 index patient and 3 index members of staff infected with SARS-CoV-2 at simulation outset, randomly selected among all patients and staff present in the LTCF. Index cases were assumed to be in any infection stage except *severe symptomatic*. Calibrated using model transition parameters (**Table 8.1**), it was assumed that 28.0% of index cases were *exposed*, 4.8% *pre-asymptomatic*, 16.8% *asymptomatic*, 11.2% *pre-symptomatic* and 39.2% *mild symptomatic*.

8.2.3.2. Heterogeneous SARS-CoV-2 introductions reflecting community burden

Introductions were defined as subsequent cases of SARS-CoV-2 infection introduced into the LTCF from the community over the course of simulation time, limited to staff members (assumed to contact individuals in the community outside work hours) and newly admitted patients (assumed to potentially carry the virus upon LTCF entry).

It was assumed that staff introductions were new infections (in the *exposed* stage)

acquired in the previous 24 hours. This reflects infection resulting from community contacts since that individual's previous shift. Community SARS-CoV-2 infection incidence was used to calculate the daily probability of any working member of staff becoming infected with the virus and introducing it to the LTCF. Using French epidemiological data from late January 2021 (daily incidence of 26,676 cases among a population of 67.1 million individuals), a daily community incidence rate of 0.04% was estimated. In a "high incidence" sensitivity analysis, a rate of under-reporting of 90.8% was assumed (as estimated elsewhere by Anand et al.), translating to an incidence rate of 0.37%.(Anand et al., 2020)

For patient introductions, it was assumed that infection is acquired at any time prior to LTCF admission. Community SARS-CoV-2 prevalence was used to estimate the probability that a new patient entering the LTCF is already infected. Using the incidence data above and assuming an infection duration of 12.5 days (the mean duration under present modelling assumptions), a community SARS-CoV-2 infection prevalence of 0.50% was estimated, or 4.57% in the "high incidence" sensitivity analysis. Patient introductions could be in any infection stage, using the same stage-specific probabilities as for index cases (above).

Combining patient and staff introductions, there were a mean 0.08 introductions/day in the baseline "low incidence" scenario, and a mean 0.8 introductions/day in a "high incidence" sensitivity analysis.

8.2.3.3. Variable transmissibility according to symptom status

In CTCmodeler, the probability of SARS-CoV-2 transmission from an infectious individual to a susceptible individual depends on the duration of their contact (see equation 6.1). Previously, using epidemiological data from the community in France, we estimated a SARS-CoV-2 transmission rate per minute of infectious contact p=0.14% (see equation 6.2). Here, we now assume that SARS-CoV-2 infectivity varies between *symptomatic* (including *pre-symptomatic*) and *asymptomatic* (including *pre-asymptomatic*) infections. In a systematic review and meta-analysis, Buitrago-Garcia et al. estimated the secondary attack rate among contacts of asymptomatic infections to be 35% relative to symptomatic infections, and that approximately 30% of all infections remained asymptomatic.(Buitrago-Garcia et al., 2020) Using these data, we stratified p to estimate distinct transmission rates from *symptomatic* (p_{sym}) and *asymptomatic* (p_{asym}) individuals as

$$0.7 \times p_{sym} + 0.3 \times p_{asym} = 0.14\%$$

(eq. 8.1)

where

$$p_{asym} = 0.35 \times p_{sym}$$

(eq. 8.2)

Solving these equations, p_{sym} = 0.174% and p_{asym} = 0.061%.

8.2.3.4. Patients with severe COVID-19 symptoms: isolation

We assumed that patients with severe COVID-19 symptoms are automatically isolated (independent of retrospective surveillance and isolation interventions introduced and evaluated later). We assumed a lag from symptom onset to isolation (24 hours), 100% isolation efficacy for transmission prevention ($p_{sym,isolated}$ = 0, $p_{asym,isolated}$ = 0), and an isolation duration equivalent to the remaining duration of infection (i.e. duration of symptoms), drawn from log-normal(7,7) distribution.

8.2.3.5. Staff with severe COVID-19 symptoms: sick-leave and replacement

We assumed that staff with severe COVID-19 symptoms immediately go on sick leave, with a duration equivalent to symptom duration (drawn from log-normal(7,7) distribution), after which they return to the LTCF *recovered*. During sick-leave, staff were replaced with a temporary member of staff who executes the same functions within the LTCF, and hence with no change to the underlying contact network. Probability of SARS-CoV-2 infection among newly arrived temporary replacement staff is calculated using community prevalence data (as for patient introductions, see above).

8.2.3.6. Healthcare workers as transient SARS-CoV-2 vectors

We allowed members of staff to act as transient vectors for SARS-CoV-2 after contact with infectious patients.(Choi et al., 2021) Transient vectors were assumed to physically “carry” SARS-CoV-2, and could transmit the virus to subsequent patients visited in quick succession (within 60 minutes), infecting those patients without themselves becoming infected. The probability of a member of staff *i* becoming a vector (P_v) was assumed to depend on the duration of their contact with the infectious patient *j*, $D_{i,j}$. This is given by

$$P_v = p_{carriage} \times D_{i,j} \times (1 - P_{protection})$$

(eq. 8.3)

and the probability of this transient vector *i* then infecting a susceptible patient *k* ($P_{i \to k}$) during a subsequent contact relies on transmission rate *p* (using *p* to represent either p_{sym} or p_{asym}), thus taking the same form as standard host-to-host transmission, given by

$$P_{i \to k} = p \times D_{i,k}$$

(eq. 8.4)

but limited to 60 minutes from the end of contact with *j*, after which time *i* loses transient carriage and is no longer a vector.

Here, $p_{carriage}$ is the per-minute probability of a member of staff acquiring transient SARS-CoV-2 carriage. We set a saturation threshold at 80% such that transient carriage is not inevitable subsequent to long infectious contacts. Similar to transmission rates p_{sym} and p_{asym} (see above), we assumed that $p_{carriage}$ varies between *symptomatic* and *asymptomatic* patients, such that $p_{carriage\_asym} = 0.35 \times p_{carriage\_sym}$. Finally, $P_{protection}$ describes the degree to which staff protect themselves during interactions with patients. The latter reflects an assumed asymmetry in patient-staff interactions, in which staff take measures to protect themselves from perceived risk of acquiring the virus when caring for patients, but take less care to protect patients from virus potentially lingering on their clothing or equipment.

8.2.3.7. Initialization conditions for an updated pandemic context

In addition to the index cases introduced above, we updated two key initialization conditions for outbreak simulation to reflect the ongoing pandemic context of COVID-19. First, we assumed a baseline immunizing seroprevalence of 20% among patients and staff. For each individual in each outbreak simulation, initial infection status was determined stochastically, with a 20% probability of entering the simulation already *recovered*. Second, we assumed that baseline rates of infection prevention and control were improved relative to pre-pandemic baseline. This reflects observed increases in compliance to hygiene and infection prevention measures in healthcare institutions worldwide since the beginning of the COVID-19 pandemic.(Moore et al., 2021; Roshan et al., 2020; Wong et al., 2020) For this, we introduced the parameter P_{IPC}, which modifies rates of transmission ($P_{i \to j,IPC}$) and transient carriage acquisition ($P_{v,IPC}$) across all patients and staff, given by:

$$P_{i \to j,IPC} = P_{i \to j} \times (1 - P_{IPC})$$

(eq. 8.5)

and

$$P_{v,IPC} = P_v \times (1 - P_{IPC})$$

(eq. 8.6)

Using data from a clinical trial across 33 Dutch nursing homes, we assumed a baseline 36% compliance to IPC measures in such an intervention context (P_{IPC} = 0.36).(Teesing et al., 2020)

8.2.3.8. Storing SARS-CoV-2 transmission chains

In addition to the simulation output data described in the previous Chapter (a list of introductions from the community, daily infection status), a list of all nosocomial transmission events was saved throughout simulation, including donor and recipient IDs and mode of transmission, i.e. from an infected individual or transient vector. This facilitated evaluation of surveillance interventions for prevention of SARS-CoV-2 transmission.

8.2.3.9. COVID-19 containment measures

Three different COVID-19 *containment measures* were included in outbreak simulations.

8.2.3.9.1 Patient social distancing

First, a patient social distancing intervention was considered, interpreted as cancellation of all social activities occurring in the baseline pre-pandemic contact network. This was modelled by removing all contacts involving ≥3 patients simultaneously. Impacts of this intervention on dynamic contact behaviours simulated by CTCmodeler are visualized in **Figure 8.1**. We did not impose staff social distancing, under the assumption that staff contacts are necessary for provisioning of care.

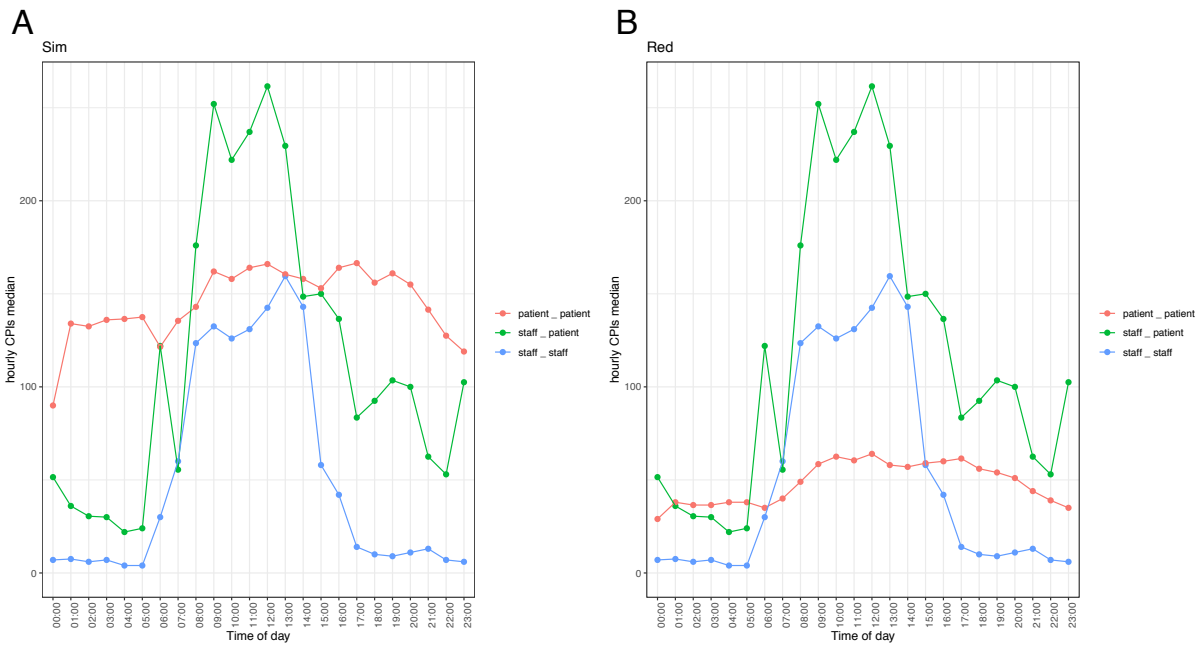

Figure 8.1. Behavioural impacts of the patient social distancing intervention.

Over the course of one day (x-axis), the median hourly number of close-proximity interactions (CPIs, y-axis) is shown. Patient-patient contacts vary considerably across (**A**) the baseline LTCF and (**B**) the LTCF with the patient social distancing intervention in place, while patient-staff and staff-staff contacts are unchanged. [Rendered by Audrey Duval.]

8.2.3.9.2. Mandatory face mask policy

Second, a mandatory face mask policy among all patients and staff was considered. In a systematic review and meta-analysis, Liang et al. estimated an 80% reduction in risk of respiratory virus transmission through wearing of face masks.(Liang et al., 2020) This was modelled here by setting P_{IPC} = 0.8, reducing rates of transmission and transient carriage acquisition across patients and staff.

8.2.3.9.3. Vaccination intervention

Third, a vaccination intervention was considered, in which an assumed 50% of individuals had immunizing seroprevalence at simulation outset (relative to 20% baseline). This could be interpreted in different ways, for instance as 100% vaccine coverage for a vaccine providing 50% protection from infection with the locally circulating strain (in the absence of any further effect of naturally-acquired immunity), 75% vaccine coverage for a vaccine providing 75% protection from infection, etc.

Table 8.1. Transmission model parameter estimates.

COVID-19 infection parameters are unchanged from Chapter 7; all other parameters are new or updated. SA = sensitivity analysis.

Parameter	Value [distribution]	Source
COVID-19 infection parameters		
Duration of exposed period (latency)	2-5 days [uniform]	(Lauer et al., 2020; W. E. Wei et al., 2020)
Duration of pre-symptomatic or pre-asymptomatic period	1-3 days [uniform]	(Lauer et al., 2020; W. E. Wei et al., 2020)
Duration of symptomatic period (whether asymptomatic, mild symptomatic or severe symptomatic)	7 days [log-normal, $\sigma^2 = 7$]	(He et al., 2020)
Proportion of COVID-19 infections presenting any symptoms	0.7	(Buitrago-Garcia et al., 2020)
Proportion of symptomatic COVID-19 infections with severe symptoms	0.2	(Wu and McGoogan, 2020)
Daily incidence proportion of COVID-19-like symptoms	0.011	Estimated from OSCOUR (Fouillet et al., 2015)
SARS-CoV-2 transmission parameters		
SARS-CoV-2 transmission rate per minute of contact, *pre-symptomatic* and *symptomatic* infection (p_{sym})	0.001739	Previous estimate (Chapter 6) scaled using data from (Buitrago-Garcia et al., 2020)
SARS-CoV-2 transmission rate per minute of contact, *pre-asymptomatic* and a*symptomatic* infection (p_{asym})	0.000609	Previous estimate (Chapter 6) scaled using data from (Buitrago-Garcia et al., 2020)
Staff SARS-CoV-2 transient carriage acquisition rate per minute of contact with *symptomatic* or *pre-symptomatic* patients ($p_{carriage\_sym}$)	0.1	Assumed
Staff SARS-CoV-2 transient carriage acquisition rate per minute of contact with *asymptomatic* or *pre-asymptomatic* patients ($p_{carriage\_asym}$)	0.035	Assumed
Degree of patient and staff compliance to infection prevention and control interventions (P_{IPC})	0.36 (0.80 with face mask intervention)	(Liang et al., 2020; Teesing et al., 2020)
Degree to which staff protect themselves (but not patients) from high-risk contacts potentially leading to SARS-CoV-2 transmission ($P_{protection}$)	0.80	Assumed
SARS-CoV-2 introductions from the community		
Daily probability of SARS-CoV-2 introduction from staff	0.03976% (0.366% in SA)	Calibrated to incidence in France in January 2021 (Santé publique France, 2021b)
Probability of SARS-CoV-2 introduction per new patient admission	0.497% (4.57% in SA)	Calibrated to incidence in France in January 2021 (Santé publique France, 2021b)
Probability of SARS-CoV-2 introduction per replacement staff	0.497% (4.57% in SA)	Calibrated to incidence in France in January 2021 (Santé publique France, 2021b)
Probability *exposed* (patient admissions, replacement staff)	0.28	From infection parameters
Probability *pre-asymptomatic* (patient admissions, replacement staff)	0.048	From infection parameters
Probability *asymptomatic* (patient admissions, replacement staff)	0.168	From infection parameters
Probability *pre-symptomatic* (patient admissions, replacement staff)	0.112	From infection parameters
Probability *symptomatic mild* (patient admissions, replacement staff)	0.392	From infection parameters

8.2.4. Simulating one LTCF with three levels of COVID-19 control

Three distinct combinations of the containment measures introduced above were applied to the baseline LTCF, to represent variable degrees of investment in COVID-19 prevention. These are presented as:

1. **Low-control LTCF 1**: no explicit measures in place
2. **Moderate-control LTCF 2**: patient social distancing
3. **High-control LTCF 3**: patient social distancing, face masks and vaccination

For each LTCF, 100 outbreaks were simulated stochastically with otherwise identical initialization conditions, each for a period of two weeks, in order to evaluate short-term outbreak risk and immediate health-economic benefits of surveillance interventions.

8.2.5. Surveillance interventions

Surveillance interventions were implemented in response to the identified surge in nosocomial outbreak risk at simulation outset. As in Chapter 7, surveillance was applied retrospectively to simulated outbreak data using a stochastic algorithm, detailed below. I distinguish between two types of surveillance:

1. **Routine testing**: the targeted use of RT-PCR upon onset of COVID-19-like symptoms or admission of new patients into the LTCF
2. **Screening**: the mass testing of entire populations (e.g. patients, staff) on selected dates

I assessed a total of 27 surveillance interventions grouped into four categories:

1. Routine testing
2. 1-round screening
3. Routine testing + 1-round screening
4. Routine testing + 2-round screening

The latter two categories are defined as *multi-level surveillance interventions* that combine both screening and testing. See the full list of interventions and corresponding assumptions in **Table 8.2**.

Table 8.2. Surveillance interventions.

List of surveillance interventions considered. Screening timing refers to the number of days since initial detection of the surge in outbreak risk upon simulation outset. Sensitivity curves for RT-PCR, Ag-RDT (A) and Ag-RDT (B) are provided in **Figure 8.2**.

#	Surveillance category	Screening timing	Test used	Test target
1	Routine testing	/	RT-PCR	Individuals with COVID-like symptoms and new patient admissions
2	1-round screening	Day 1	Ag-RDT (A) *In sensitivity analysis:* Ag-RDT (B), RT-PCR	Patients & staff *In sensitivity analysis:* only patients, only staff
3		Day 2		
4		Day 3		
5		Day 4		
6		Day 5		
7		Day 6		
8		Day 7		
9		Day 8		
10		Day 9		
11	Routine testing + 1-round screening	Day 1	*For routine testing:* RT-PCR *For screening:* Ag-RDT (A) *For screening in sensitivity analysis:* Ag-RDT (B), RT-PCR	*For routine testing:* individuals with COVID-like symptoms and new patient admissions *For screening:* patients & staff *For screening in sensitivity analysis:* only patients, only staff
12		Day 2		
13		Day 3		
14		Day 4		
15		Day 5		
16		Day 6		
17		Day 7		
18		Day 8		
19		Day 9		
20	Routine testing + 2-round screening	Days 1 & 2	*For routine testing:* RT-PCR *For screening:* Ag-RDT (A) *For screening in sensitivity analysis:* Ag-RDT (B), RT-PCR	*For routine testing:* individuals with COVID-like symptoms and new patient admissions *For screening:* patients & staff *For screening in sensitivity analysis:* only patients, only staff
21		Days 1 & 3		
22		Days 1 & 4		
23		Days 1 & 5		
24		Days 1 & 6		
25		Days 1 & 7		
26		Days 1 & 8		
27		Days 1 & 9		

8.2.6. Diagnostic sensitivity of RT-PCR and Ag-RDT

As in Chapter 7, test sensitivity (probability of positive diagnosis for a true infection) was assumed to depend on infection age *t* (i.e. time since SARS-CoV-2 exposure, as calculated previously), expressed as $s_{PCR}(t)$ for RT-PCR and $s_{RDT}(t)$ for Ag-RDT. Data from Kucirka et al. were again used to inform $s_{PCR}(t)$, and the curve was extrapolated beyond *t*=20 using an exponential function fit to days 11-20 (pink line in **Figure 8.2**).(Kucirka et al., 2020) For diagnostic specificity, 99.7% was assumed for Ag-RDT and 99.9% for RT-PCR.(Brümmer et al., 2021)

Literature estimates for Ag-RDT sensitivity (α) are typically expressed as relative to RT-PCR sensitivity, given here by $s_{RDT}(t) = \alpha \times s_{PCR}(t)$, such that absolute Ag-RDT sensitivity $s_{RDT}(t)$ varies in time with $s_{PCR}(t)$. In a meta-analysis of 73 clinical data sets and 31,202

samples, Brümmer et al. estimated Ag-RDT to be $\alpha = 73.8\%$ as sensitive as RT-PCR,(Brümmer et al., 2021) which when crossed with the data from Kucirka et al. corresponds to a peak absolute Ag-RDT sensitivity of $s_{RDT} = 59.7\%$ at $t = 8$ days. However, they also estimated greater relative Ag-RDT sensitivity up to one week from symptom onset ($\alpha = 87.5\%$) and lower relative sensitivity thereafter ($\alpha = 64.1\%$). Relative Ag-RDT sensitivity was adjusted accordingly using two shape parameters γ and β, and depending on time since peak RT-PCR sensitivity ($\tau = t - 8$), such that:

$$\alpha(t, \beta, \gamma) = (1 - \gamma) \times e^{-\beta \times \tau^2}$$

(eq. 8.7)

where sensitivity of Ag-RDT relative to RT-PCR varies with time, decreasing exponentially with increasing τ. Values of γ and β were estimated by minimizing the sum of three squared distance functions

$$\arg\min((d_1)^2 + (d_2)^2 + (d_3)^2)$$

(eq. 8.8)

using the R function optim. Assuming a 5-day incubation period, these correspond to distances of the target sensitivity function to estimates from Brümmer et al. for, respectively, sensitivity over all t (d_1), up to $t \leq 11$ days from SARS-CoV-2 exposure (d_2), and $t > 11$ days from SARS-CoV-2 exposure (d_3). These are given by:

$$d_1 = 0.738 - \sum_{t=1}^{t_{max}} \frac{\alpha(t, \beta, \gamma)}{s_{RDT}(t)}$$

$$d_2 = 0.875 - \sum_{t=1}^{11} \frac{\alpha(t, \beta, \gamma)}{s_{RDT}(t)}$$

$$d_3 = 0.641 - \sum_{t=12}^{t_{max}} \frac{\alpha(t, \beta, \gamma)}{s_{RDT}(t)}$$

(eq. 8.9)

Solving $\alpha(t, \beta, \gamma)$ over all t using the shape parameters estimated from the minimized sum of squared distances ($\beta = 0.001998$, $\gamma = 0.1172$) reproduced summary estimates from Brümmer et al. to within 0.3%: $\alpha_{t \leq 11} = 87.5\%$, $\alpha_{t > 11} = 64.1\%$, and $\alpha_{t \geq 1} = 73.5\%$. This function was used to determine the probability of a positive test result for Ag-RDT testing as conducted in the main analysis (black line in **Figure 8.2**).

Alternative assumptions for RT-PCR and Ag-RDT diagnostic sensitivity considered in sensitivity analyses were: (i) uniform Ag-RDT sensitivity relative to time-varying RT-PCR ($\alpha = 73.8\%$, green line in **Figure 8.2**), (ii) uniform absolute sensitivity regardless of time since exposure for both RT-PCR ($s_{PCR} = 70\%$) and Ag-RDT ($s_{RDT} = 54\%$), and (iii) perfect absolute sensitivity for both ($s_{PCR} = s_{RDT} = 100\%$).

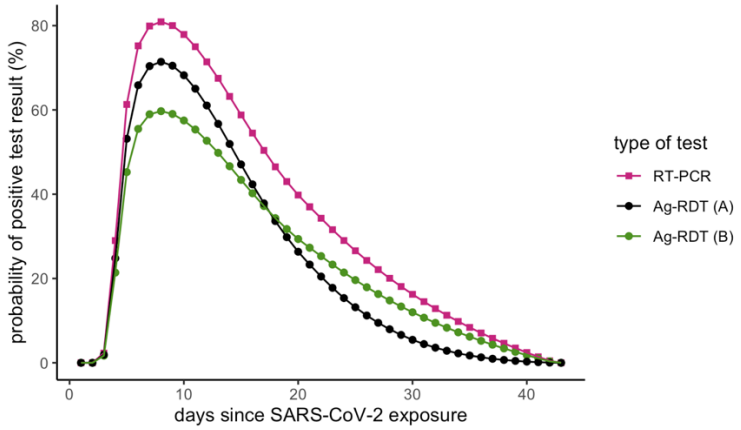

Figure 8.2. Test sensitivity.

Test sensitivity as a function of time since infection, estimated by crossing data from meta-analyses by Kucirka et al. for RT-PCR (pink) and Brümmer et al. for Ag-RDT, considering time-varying Ag-RDT sensitivity relative to RT-PCR (black, for baseline analysis) and uniform relative sensitivity (green, for sensitivity analysis).

8.2.7. Simulating counterfactual scenarios

The surveillance algorithm developed in the previous Chapter was developed further here to account for the updated surveillance interventions described above, to retrospectively apply them to daily outbreak data, and to simulate impacts of testing and isolation on transmission prevention.

Each "run" of the surveillance algorithm was conducted in five steps:

1. The algorithm was applied to each outbreak to determine who to test for SARS-CoV-2 infection and when, and using which type of test, according to the surveillance strategies described in **Table 8.2**
2. Test results were determined stochastically, with probability of SARS-CoV-2 detection depending on test sensitivity s(*t*), as described in **Figure 8.2**
3. Individuals were retrospectively "isolated" upon SARS-CoV-2 diagnosis (positive test result), assuming immediate isolation for Ag-RDT but a 24-hour lag for RT-PCR (reflecting a lag between sample and result)

4. *Counterfactual scenarios* were simulated by pruning transmission events occurring subsequent to isolation, i.e. removing all transmission chains originating from isolated individuals (illustrated in **Figure 8.3A**)
5. Nosocomial incidence was re-calculated subsequent to transmission pruning (change in incidence illustrated in **Figure 8.3B**)

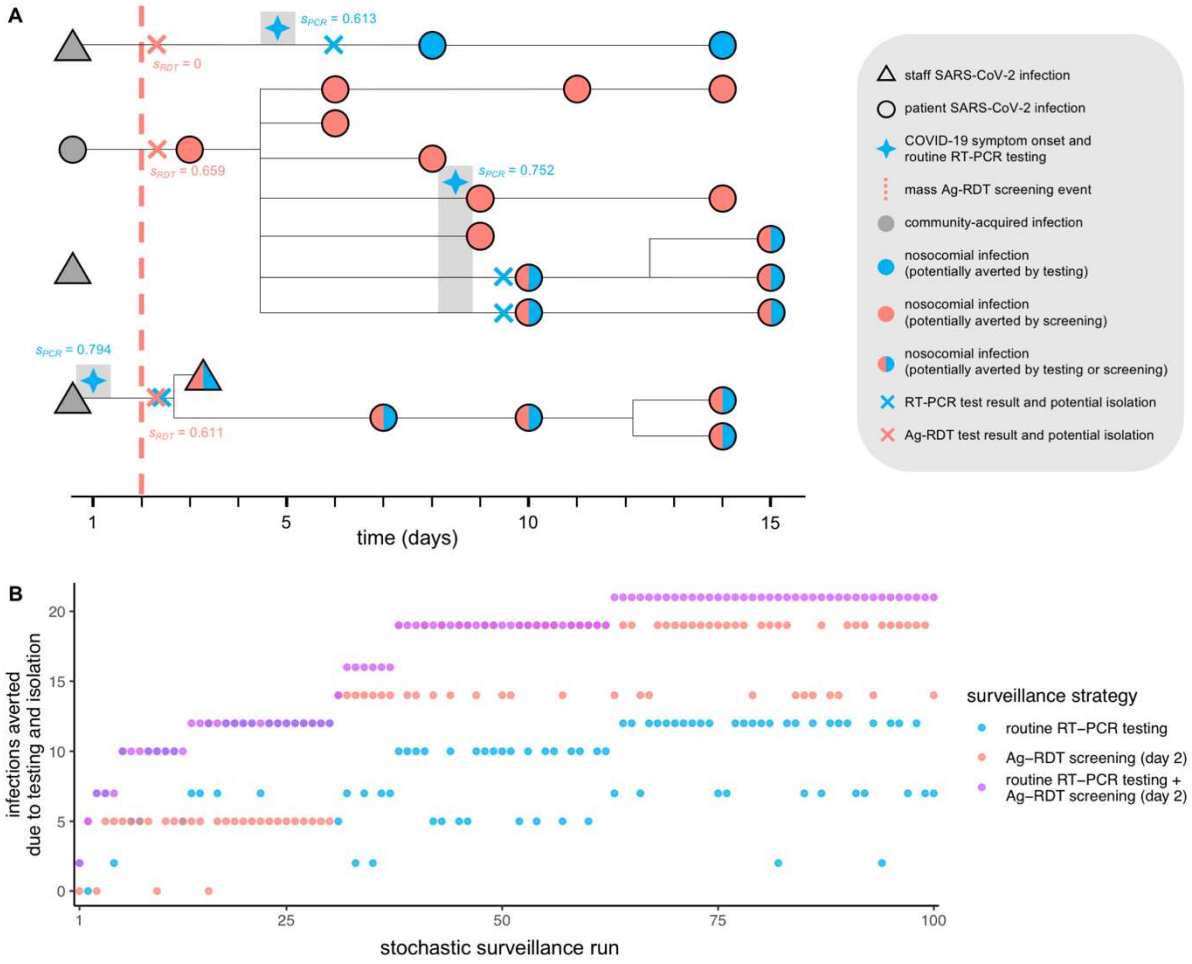

Figure 8.3. Example of counterfactual scenario simulation.

Surveillance interventions were applied retrospectively to simulated SARS-CoV-2 outbreaks, illustrated here using data from outbreak simulation #22 from LTCF 1. **(A)** The SARS-CoV-2 transmission chain, with infections (shapes) transmitted from left to right following black lines. Of four community-onset infections (grey shapes) at simulation outset, three transmitted to other individuals in the LTCF, triggering a nosocomial outbreak. Routine RT-PCR testing was conducted upon COVID-19 symptom onset (blue four-pointed stars), with results and case isolation 24-hours later (blue crosses). A population-wide Ag-RDT screening event was conducted on day 2 (red dashed line) with immediate results and isolation (red crosses). Test sensitivity – the probability of a positive test result and subsequent isolation – is given by *s* adjacent to each test, as determined by infection age *t* at the time of each test (see **Figure 8.2**). Nosocomial infections are coloured blue if potentially averted by routine testing, red if by screening, or both if by either. **(B)** Corresponding surveillance results from three selected surveillance interventions evaluated over 100 stochastic surveillance runs. The multi-level testing + screening intervention always averted at least as many infections as either individual intervention in the same run, demonstrating matching of "controlled" and "uncontrolled" epidemics across interventions, and its relevance for calculation of marginal benefits of multi-level interventions.

With these methods, in each run of surveillance, “uncontrolled” epidemics with no surveillance were matched to “controlled” counterfactual scenarios with surveillance. This methodology is adapted from **single-world counterfactual analysis** (see Kaminsky et al.), and facilitates precise estimation of intervention efficacy by overcoming the strong stochastic effects inherent to outbreaks in small populations, as in the present simulations.(Kaminsky et al., 2019) Single-world matching also facilitated estimation of marginal benefits of multi-level surveillance interventions (interventions 11 to 27), which introduced screening against a backdrop of a facility already conducting routine testing. For these calculations, routine testing was simulated first, with downstream transmission chains pruned as described above; second, screening was applied, with potential only to prune remaining transmission chains not already pruned by routine testing; and third, if conducting a second round of screening, the only chains potentially pruned were those not already pruned by routine testing and the first round of screening. In this way, infections averted by subsequent levels of surveillance did not double-count infections already averted by previous levels (as in **Figure 8.3B**).

This surveillance algorithm was run 100 times per outbreak, across all interventions and factors resulting in a total 43.7 million simulations of nosocomial incidence and surveillance resource use. These outputs were used to calculate surveillance efficacy, efficiency and cost-effectiveness.

8.2.8. Surveillance outcomes

For each outbreak simulation, cumulative nosocomial incidence I was re-calculated for each surveillance simulation after transmission chain pruning.

Surveillance **efficacy** was reported as reduction in I, given by

$$efficacy = 1 - \frac{(I|surveillance)}{(I|no\ surveillance)} \quad \text{(eq. 8.10)}$$

Three measures of efficiency were also calculated.

First, **apparent efficiency** was defined as perceived operational efficiency, calculated using the per-test number of detected infections *D* as

$$apparent\ efficiency = \frac{(D|surveillance)}{n} \times 1{,}000$$

(eq. 8.11)

where *n* is the number of tests used.

Second, **real efficiency** was defined as the relative health benefit resulting from intervention, calculated using the per-test number of infections averted as

$$real\ efficiency = \frac{(I|no\ surveillance)\ -\ (I|surveillance)}{n} \times 1{,}000$$

(eq. 8.12)

For multi-level interventions combining routine testing and screening, marginal real efficiency of screening was calculated by excluding infections already averted and tests already used due to routine testing ("testing"), given by

$$marginal\ real\ efficiency_{screening} = \frac{(I|testing) - (I|testing + screening)}{n_{screening}} \times 1{,}000$$

(eq. 8.13)

Third, **cost-effectiveness** was defined as total surveillance costs per case averted, accounting for unit costs *c* of routine testing ($c_{testing}$) and screening ($c_{screening}$),

$$cost\ effectiveness = \frac{n_{testing} \times c_{testing} + n_{screening} \times c_{screening}}{(I|no\ surveillance) - (I|surveillance)}$$

(eq. 8.14)

Testing unit costs were varied over a wide range to determine impact on cost effectiveness. Under baseline assumptions, RT-PCR for routine testing was assumed to cost €50/test, and Ag-RDT for screening cost €5/test, similar to previous cost estimates for France and the UK.(Assurance maladie française, 2021; Torjesen, 2021)

Other outcomes evaluated to assess performance of testing and screening interventions were true-positive rate (TPR), true-negative rate (TNR), negative predictive value (NPV) and positive predictive value (PPV).

8.2.9. Outcome uncertainty

Figure 8.4 demonstrates how uncertainty in surveillance outcomes was quantified. Distributions of intervention efficacy (the proportion of infections averted) were largely bimodal (**Figures 8.4A, 8.4B**). This reflects the exponential nature of outbreak prevention,

whereby effective isolation of a single index case can prevent entire chains of downstream infection, while missing that case can allow an entire outbreak to result (see **Figure 8.3A**). As a result, outcome distribution quantiles were relatively uninformative (**Figure 8.4B**). Instead, outcomes are reported as means across 10,000 simulations (100 outbreaks × 100 surveillance runs / outbreak). Confidence intervals for means were calculated using bootstrap resampling with 100 replicates and normal approximation using the R package *boot* (increasing the number of replicates was found to have marginal impact, see **Figure 8.4C**).

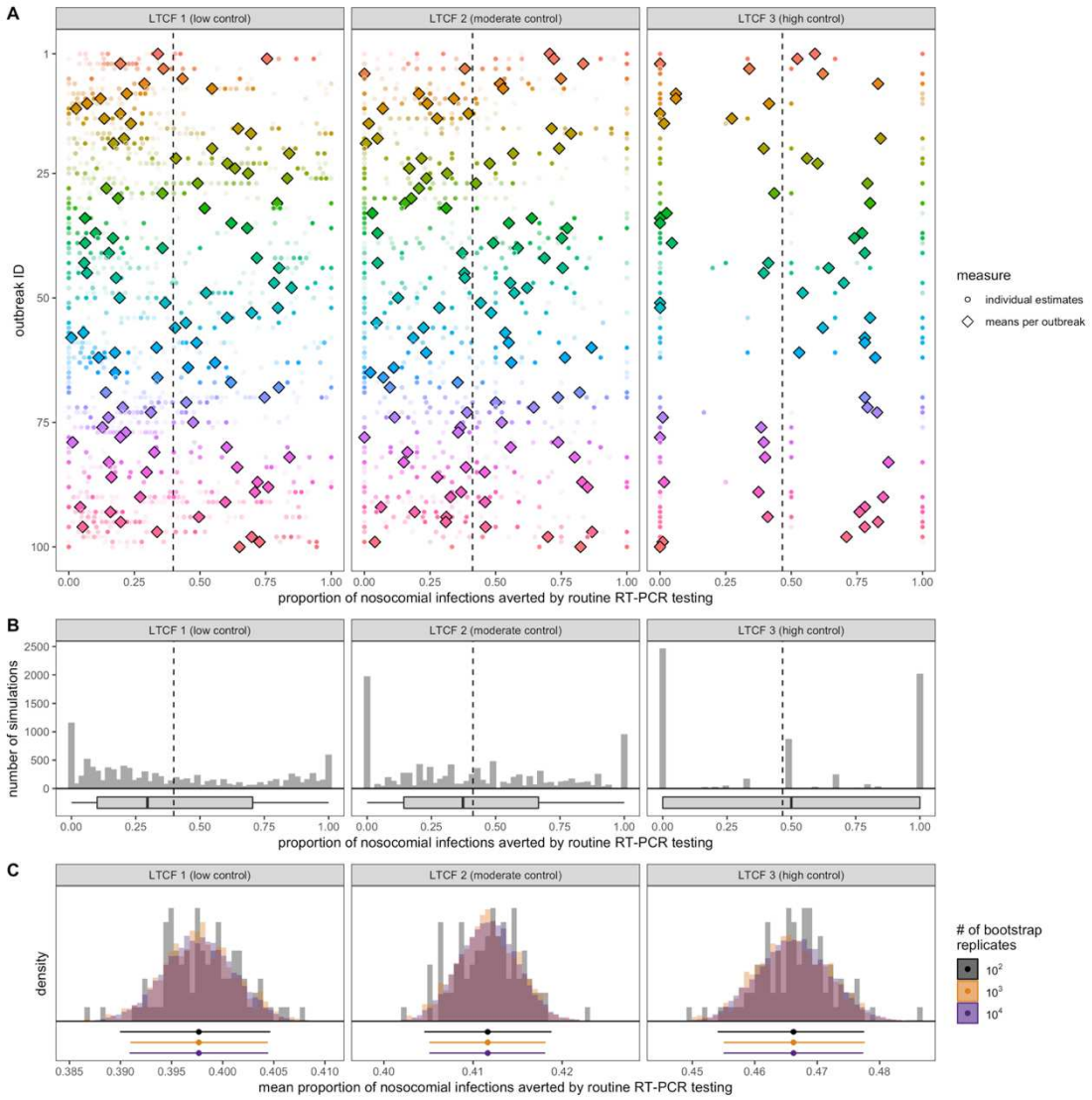

Figure 8.4. Quantifying outcome uncertainty.

Estimation of outcome uncertainty, demonstrated here for efficacy of routine RT-PCR testing (intervention #1). **(A)** Raw surveillance data: for each outbreak simulation (y-axis), each small transparent circle is the proportion of infections averted by routine testing – intervention *efficacy* – for each counterfactual scenario, as simulated by the surveillance algorithm. Opaque diamonds are the means across all 100 counterfactual scenarios for each outbreak. **(B)** The efficacy distribution from A as a histogram (top) and boxplot (bottom), pooling all outbreaks together. In both A and B, the vertical dotted line is the mean across all 10,000 counterfactual scenarios. **(C)** Estimated mean efficacy and 95% confidence intervals using bootstrap resampling, comparing three different numbers of bootstrap replicates (colours).

8.3. Results

8.3.1. Nosocomial outbreak dynamics

8.3.1.1. Outbreak risk and size

Following the surge in SARS-CoV-2 importations at simulation outset, nosocomial incidence varied across LTCFs depending on the COVID-19 containment measures in place (**Figure 8.5**). The low-control LTCF 1 experienced exponential epidemic growth driven by patient-dominated clusters, with a mean 28.9 (range 0–82) nosocomial infections over two weeks. With patient social distancing in the moderate-control LTCF 2, epidemic growth was linear, and nosocomial incidence was reduced by a mean 62.2% to 10.9 (0–34) infections at two weeks, more evenly split among patients and staff. Finally, with 50% immunization, mandatory face masks and social distancing combined in the high-control LTCF 3, outbreaks tended towards extinction, with a cumulative 1.1 (0–6) infections at two weeks, a mean 96.2% reduction in incidence relative to LTCF 1. In this latter LTCF, staff members infected in the community represented the majority of cases, and rarely transmitted. See **Figure 8.6** for cumulative incidence stratified by infection onset and type of individual.

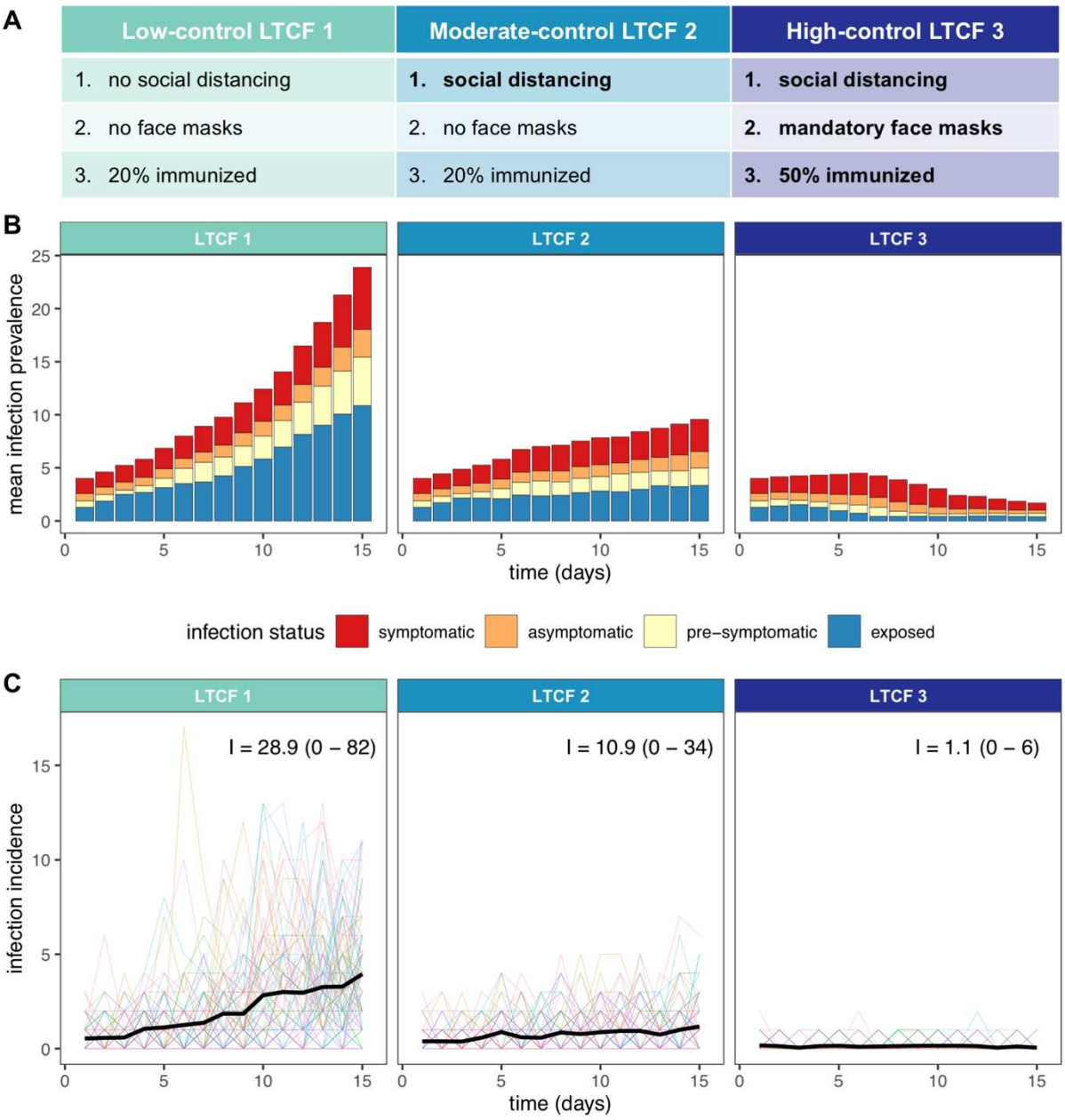

Figure 8.5. Outbreak context.

Modelling context: simulating SARS-CoV-2 outbreaks in a long-term care facility (LTCF) with three different levels of COVID-19 control. **(A)** A list of the COVID-19 containment measures in place across low-control LTCF 1, moderate-control LTCF 2, and high-control LTCF 3. **(B)** Daily infection **prevalence**, the mean number of individuals in each infection stage (colours) over time. Pre-symptomatic infection combines pre-symptomatic and pre-asymptomatic infection, and symptomatic infection combines mild symptomatic and severe symptomatic infection. **(C)** Daily nosocomial infection **incidence**, the number of new SARS-CoV-2 infections acquired within the LTCF each day. Thin coloured lines are individual simulations; the thick black line is the mean across 100 simulations. In text, the mean (range) cumulative nosocomial incidence, I, over two weeks.

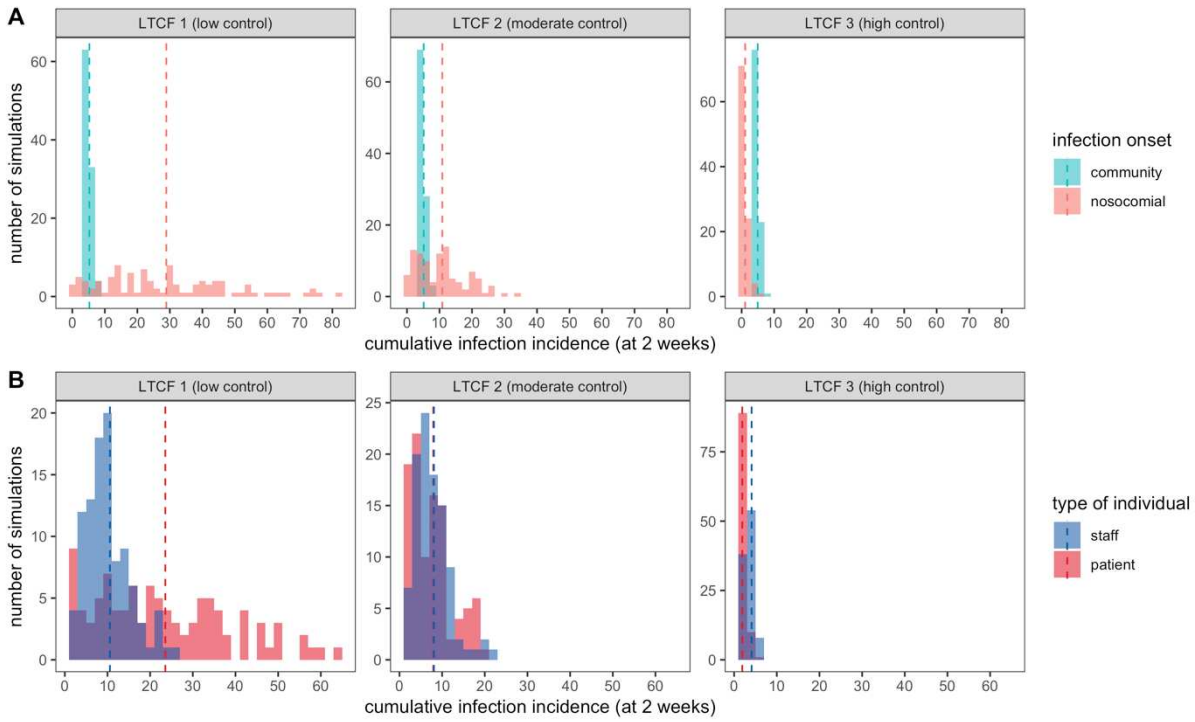

Figure 8.6. Infection distributions by onset and type of individual.

Across LTCFs (columns), the distributions of cumulative SARS-CoV-2 infection incidence at two weeks, stratified by **(A)** location of infection onset, and **(B)** type of individual infected. Dashed vertical lines represent means across 100 outbreak simulations. Note that community-onset infection combines index cases at simulation outset and subsequent introductions over the simulation period.

8.3.1.2. Transmission heterogeneity and super-spreading

Figure 8.7 shows heterogeneity in the number of transmission events caused by different individuals in the LTCF. Super-spreaders (defined as individuals transmitting to ≥3 individuals in the LTCF) drove high incidence in low-control LTCF 1, representing a mean 5.5% of infected individuals but responsible for a mean 47.3% of all nosocomial infections, versus just 0.2% of infected individuals and 1.1% of nosocomial infections in the high-control LTCF 3. The proportion of infected individuals who never transmitted was higher in LTCF 3 (mean 77.7%) than in LTCFs 1 (69.4%) or 2 (67.0%).

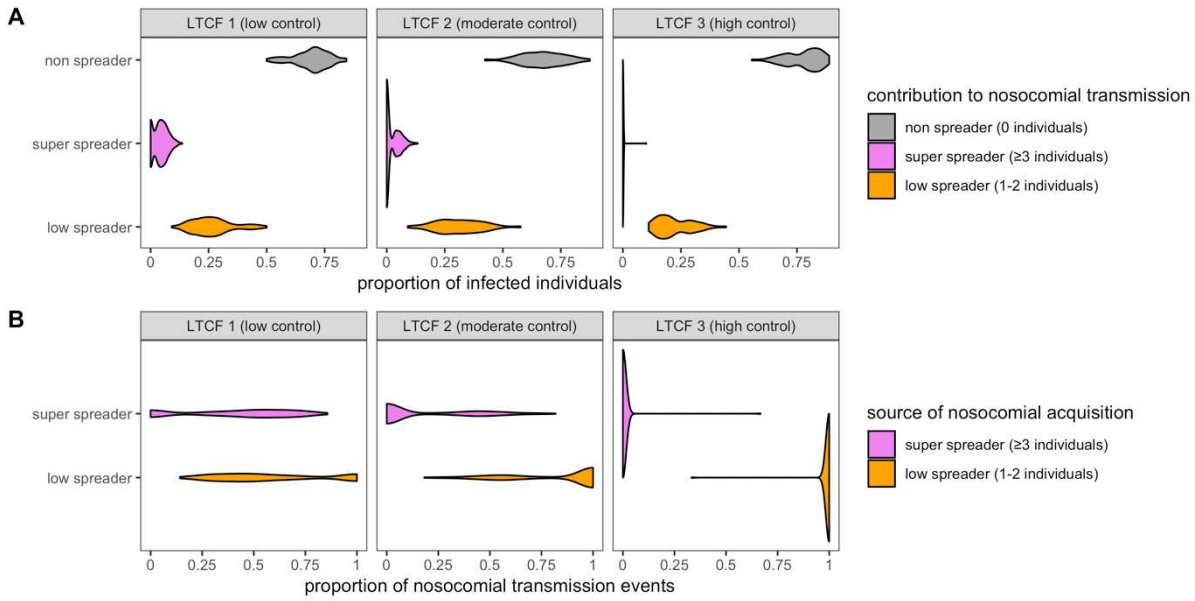

Figure 8.7. Transmission heterogeneity.

Impact of super-spreading on nosocomial SARS-CoV-2 outbreaks. **(A)** Contribution of super-spreading to nosocomial transmission: across simulated outbreaks, the distribution of the proportions of individuals that were super-spreaders (transmitted to ≥3 individuals, pink), low-spreaders (1-2 individuals, orange), and non-spreaders (0 individuals, grey). **(B)** Contribution of super-spreading to nosocomial acquisition: across outbreaks, the distribution of the proportions of acquisitions that resulted from super-spreaders (pink) versus low-spreaders (orange).

8.3.2. Surveillance efficacy

8.3.2.1. Routine RT-PCR testing

Figure 8.8 shows distributions of outbreak sizes (cumulative nosocomial incidence at two weeks) with and without a routine RT-PCR testing intervention (intervention #1 in **Table 8.2**) in place. Routine RT-PCR testing significantly reduced incidence of hospital-acquired SARS-CoV-2 infection, by a mean 39.8% in LTCF 1, 41.2% in LTCF 2, and 46.6% in LTCF 3. Greater relative efficacy in higher-control LTCFs was consistent with a higher average probability of positive test results, a consequence of fewer new, as-yet undetectable infections in scenarios with fewer transmission events and smaller outbreaks (**Figure 8.9**). In terms of absolute efficacy, routine RT-PCR testing translated to a mean 11.9 infections averted in LTCF 1, 4.8 in LTCF 2, and 0.51 in LTCF 3. Greater absolute efficacy in lower control LTCFs is consistent with larger outbreaks, and a greater number of infections to potentially avert through intervention.

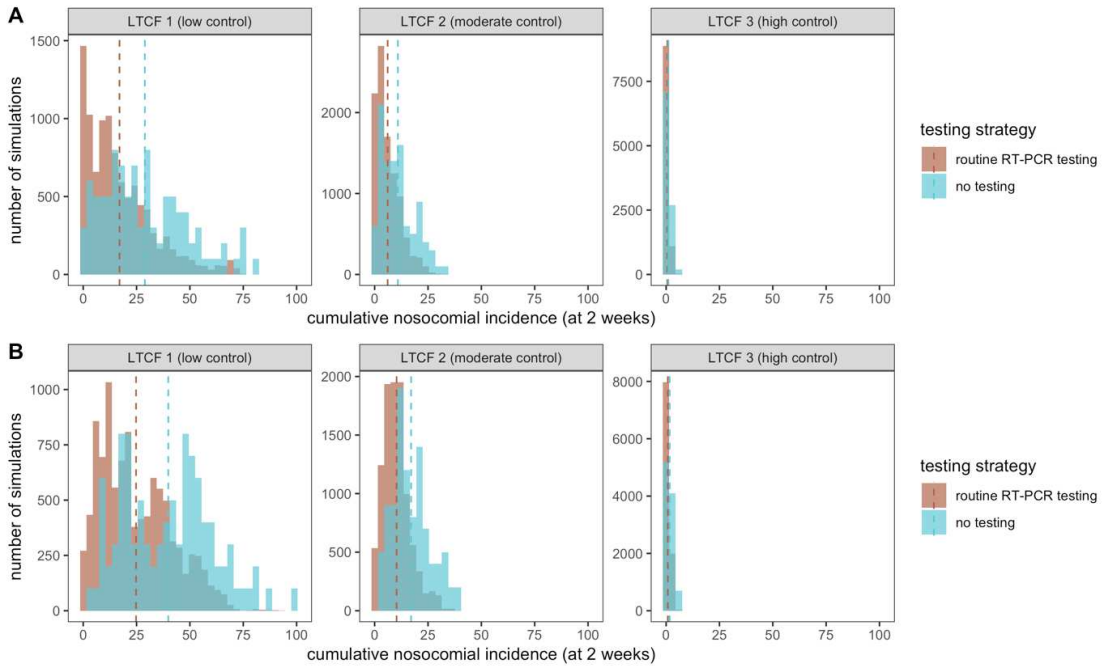

Figure 8.8. Efficacy of routine RT-PCR testing.

Compared to the baseline scenario with no surveillance (blue), counterfactual scenarios with routine RT-PCR testing (brown) had reduced cumulative nosocomial incidence (x-axis, with means as vertical dashed lines) due to pruning of transmission chains. For each LTCF (panels), relative efficacy (% reduction in incidence) was similar whether in **(A)** the baseline scenario of low community SARS-CoV-2 incidence, with a mean 1.1 new community-onset infections over two weeks subsequent to the initial surge; and **(B)** the high community incidence scenario, with a mean 10.6 new community-onset infections over two weeks.

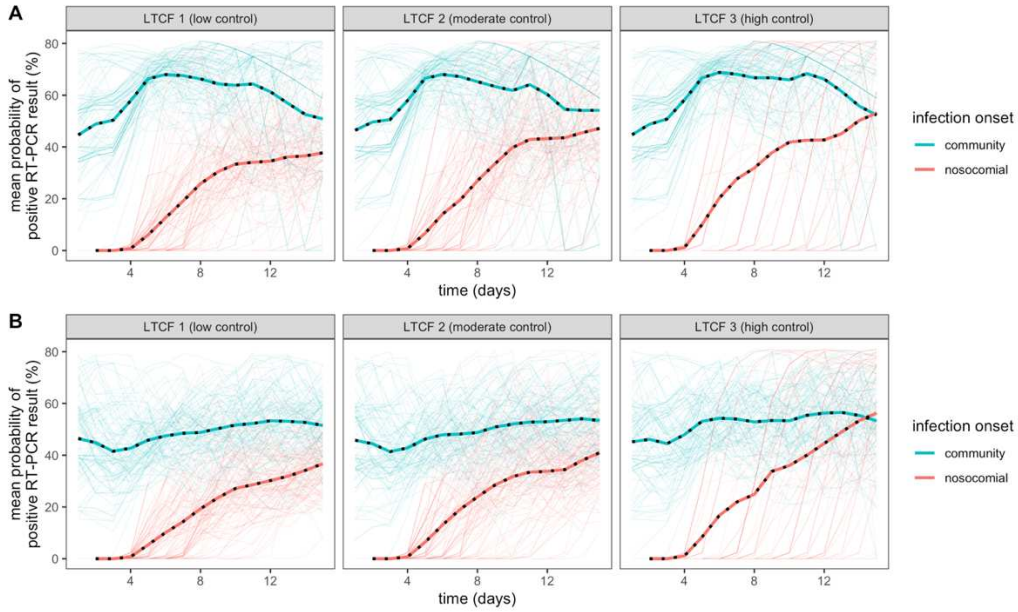

Figure 8.9. Temporal dynamics of RT-PCR sensitivity.

Temporal dynamics of RT-PCR true-positive rate (TPR), in a hypothetical scenario of testing every infected individual every day. TPR is stratified by individuals who acquired infection in the community (blue) versus within the LTCF (red). Note that community-onset infection combines index cases at simulation outset and subsequent introductions over the simulation period. Sensitivity dynamics are shown for **(A)** the baseline low community incidence scenario, with its average 1.1 new community-onset introductions over the two weeks of simulation and **(B)** the high community incidence scenario, with its average 10.6 introductions.

8.3.2.2. One-round Ag-RDT screening

Figure 8.10 compares the relative efficacy (proportion of nosocomial infections averted) of all screening interventions from **Table 8.2**, and **Figure 8.11** compares their absolute efficacy (number of nosocomial infections averted). On its own, 1-round Ag-RDT screening was less effective than routine testing, reducing incidence of hospital-acquired SARS-CoV-2 infection by up to 31.2-37.5% (range of means across LTCFs). For 1-round Ag-RDT screening in combination with routine testing, nosocomial incidence was reduced by 58.4-63.5%. Among infections not prevented by routine testing, this represents a 30.5-32.4% reduction in remaining incidence due to Ag-RDT screening. Whether paired with routine testing or conducted independently, 1-round Ag-RDT screening was most effective if conducted immediately upon outbreak detection.

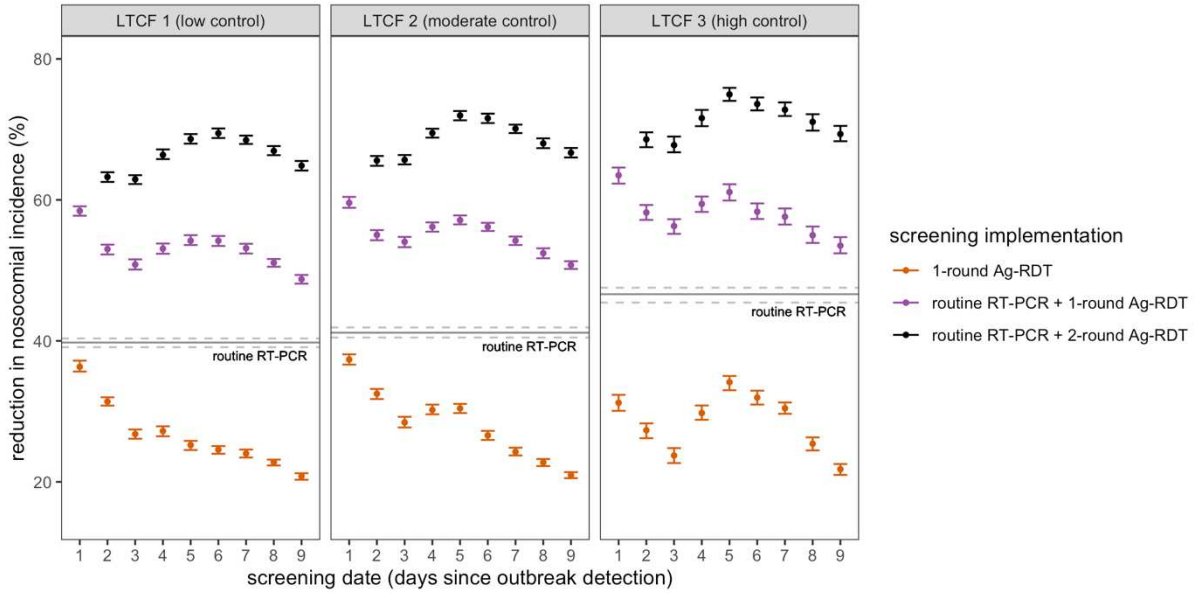

Figure 8.10. Relative surveillance efficacy

Relative efficacy of Ag-RDT screening interventions for reducing nosocomial SARS-CoV-2 incidence. Points represent mean efficacy (across 10,000 simulations) for each of 26 screening interventions, arranged by timing of the screening intervention (days since initial outbreak detection, x-axis) and coloured by screening implementation (either as 1-round screening with no other testing, orange; as 1-round screening in combination with routine RT-PCR testing, purple; or as 2-round screening with routine RT-PCR testing, black). For 2-round screening, the first round was conducted on day 1, with points arranged according to the date of the second round (days 2 to 9). The solid horizontal line represents mean efficacy of routine RT-PCR testing in absence of screening, which is conducted continuously over time and does not correspond to a specific date. Relative reductions in incidence were similar across LTCFs, but there was significant variation in the number of infections averted (**Figure 8.11**). Error bars (dashed lines for routine testing) represent 95% confidence intervals estimated by bootstrap resampling. Baseline assumptions underlying simulations include: "low" community SARS-CoV-2 incidence; time-varying Ag-RDT sensitivity relative to RT-PCR (Ag-RDT A); and screening interventions that target all patients and staff in the LTCF.

8.3.2.3. Two-round Ag-RDT screening

Two-round screening – conducting a first round of screening immediately upon outbreak

detection, and an additional second round over the following days – increased overall surveillance efficacy. Nosocomial incidence was reduced by up to 69.4%-75.0% across LTCFs with well-timed 2-round screening (**Figure 8.10**). This represents a reduction of 48.1%-52.8% among remaining infections not averted by routine testing alone. Optimal timing for the second round of screening was on days 5-6 (4-5 days after the first round of screening).

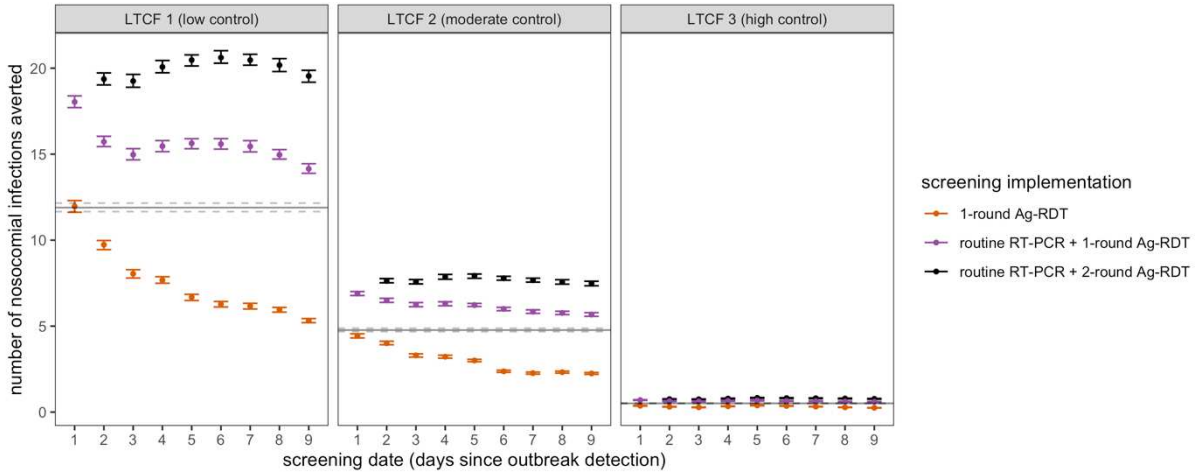

Figure 8.11. Absolute surveillance efficacy.

The total number of nosocomial SARS-CoV-2 infections averted by testing and screening interventions. This contrasts to relative reductions in incidence, as in **Figure 8.10**. Points and error bars correspond to bootstrap means and 95% confidence intervals (for routine RT-PCR testing, the solid horizontal line and dashed lines, respectively). Baseline assumptions underlying simulations include: "low" community SARS-CoV-2 incidence; time-varying Ag-RDT sensitivity relative to RT-PCR (Ag-RDT A); and screening interventions that target all patients and staff in the LTCF.

8.3.2.4. Sensitivity analyses

Figure 8.12. shows how estimated surveillance efficacy varied across a range of sensitivity analyses.

8.3.2.4.1. Screening targets

Targeting both patients and staff for screening was always more effective than only targeting one or the other (**Figure 8.12A**). Targeting only patients was substantially more effective than staff for LTCF 1, consistent with its large patient-led outbreaks. This difference was less pronounced in LTCF 2, while in LTCF 3 screening efficacy was nearly identical whether targeting patients or staff.

8.3.2.4.2. Test types

Use of RT-PCR instead of Ag-RDT was considered for screening interventions,

maintaining its higher diagnostic sensitivity and longer turnaround time (24h) (**Figure 8.12B**). For all screening interventions considered (1-round, 1-round with routine testing, 2-round with routine testing), Ag-RDT screening led to greater reductions in incidence than RT-PCR screening. This suggests that the assumed benefits of using Ag-RDT (faster turn-around time) outweigh its assumed costs (reduced diagnostic sensitivity). This finding was robust to a sensitivity analysis considering the alternative Ag-RDT (B) diagnostic sensitivity curve, which generally resulted in lower efficacy estimates than Ag-RDT (A) but greater efficacy than predicted for RT-PCR screening.

8.3.2.4.3. Community incidence

In an alternative scenario of higher community incidence and more frequent introductions of SARS-CoV-2 into the LTCF, screening was overall less effective for transmission prevention than in the baseline scenario (**Figure 8.12C**). Optimal timing for second-round screening was also delayed further in LTCFs 2 and 3. When incidence is high, delaying the second round of screening allows for considerably more community-onset SARS-CoV-2 infections introduced into the LTCF over the course of simulations to be tested and ultimately detected.

8.3.2.4.4. Sensitivity functions

Alternative diagnostic sensitivity functions that do not vary over time were also considered (**Figure 8.12D**). When assuming uniform but imperfect diagnostic sensitivity over the course of infection (70% for RT-PCR, 54% for Ag-RDT; turquoise points), the second round of screening was more effective the sooner it was conducted. This suggests that, if test sensitivity does not vary over time, it is better to conduct screening rounds consecutively in order to increase probability of detecting infections before transmission occurs. Alternatively, assuming 100% diagnostic sensitivity for both RT-PCR and Ag-RDT (brown points), longer delays to second-round screening resulted in higher efficacy, with nosocomial incidence reduced by up to 98.6-99.2% when second-round screening was conducted 8 days after the first round (the longest interval considered). This suggests that, if tests are perfectly sensitive, it is better to delay second-round screening in order to increase the number of community-onset infections included for testing in the second round. Altogether, this analysis suggests that the time-varying nature of test sensitivity is what drives optimal efficacy of two-round screening at an intermediate screening lag.

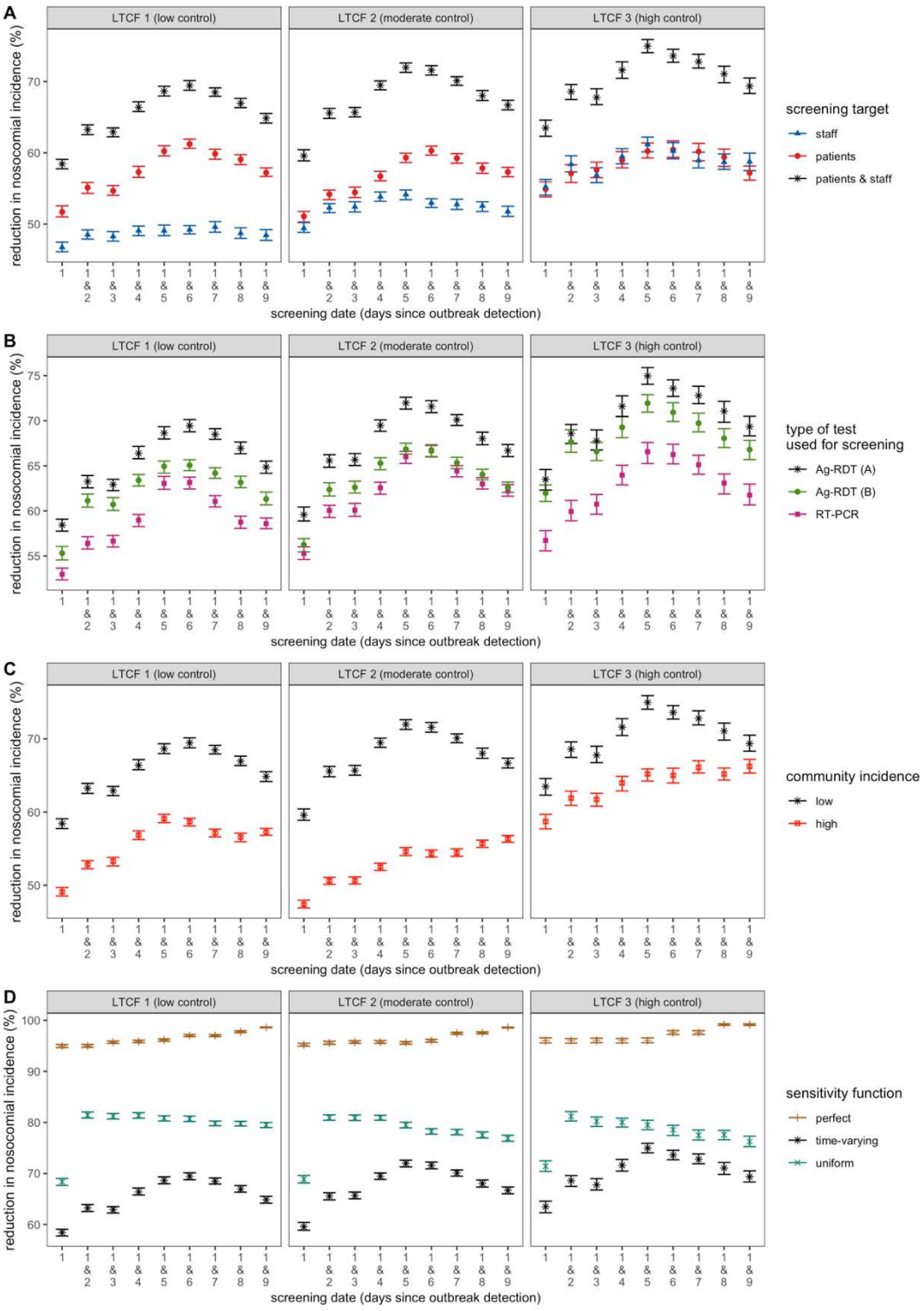

Figure 8.12. Surveillance efficacy sensitivity analyses.

Impacts of alternative modelling assumptions on efficacy of screening interventions. Points and error bars correspond to bootstrap means and 95% confidence intervals. For all panels, black asterisks represent the assumption used in baseline analyses, unless specified otherwise. **(A)** Comparison of targeting patients and/or staff in screening interventions. **(B)** Comparison of using Ag-RDT or RT-PCR for screening, assuming immediate results for Ag-RDT and a 24-hour delay for RT-PCR. Two sensitivity curves for Ag-RDT are considered (see **Figure 8.2**). **(C)** Comparison of screening efficacy in the baseline low incidence scenario, and the alternative high incidence scenario. **(D)** Comparison of alternative sensitivity functions for both RT-PCR and Ag-RDT.

8.3.3. Surveillance performance and efficiency

8.3.3.1. Routine RT-PCR testing

Figure 8.13 shows how various performance measures of routine RT-PCR testing vary across LTCFs. In particular, TPR and NPV were substantially lower in LTCF 1 than in other LTCFs, while PPV was higher. **Figure 8.13** also reveals how efficiency varies across scenarios. Mean apparent efficiency ranged from 28-65 infections detected/1,000 RT-PCR tests across LTCFs, while mean real efficiency ranged from 5-105 infections averted/1,000 RT-PCR tests.

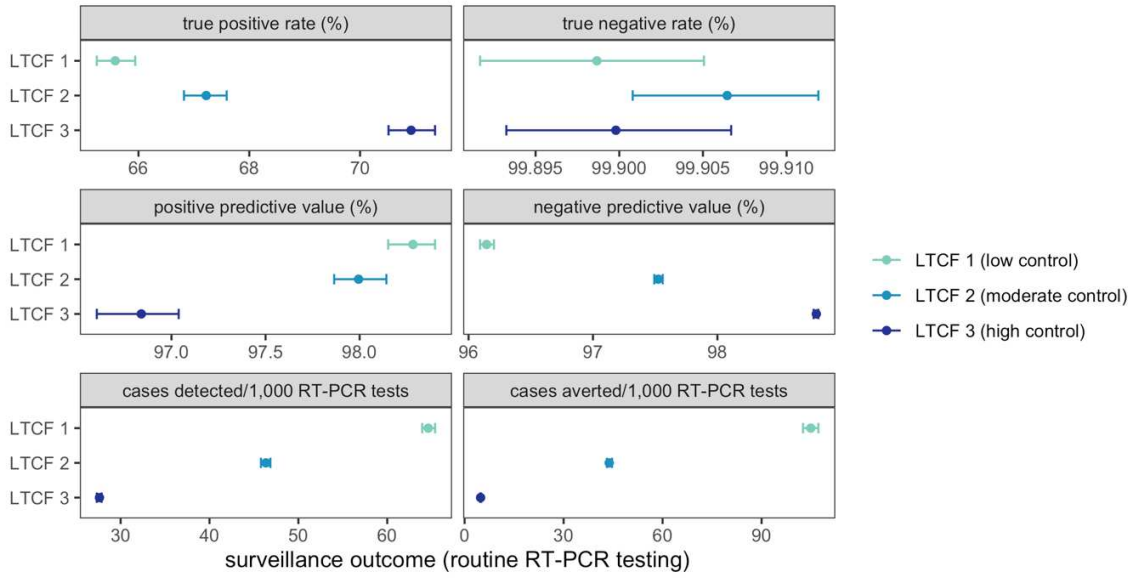

Figure 8.13. Performance of routine RT-PCR testing.

Performance of routine RT-PCR testing across LTCFs (y-axis, colours) and various surveillance outcomes (panels). Points and error bars correspond to bootstrap means and 95% confidence intervals.

8.3.3.2. Ag-RDT screening

Figure 8.14 compares the apparent efficiency (left) and real marginal efficiency (right) of Ag-RDT screening in the context of the most effective overall surveillance intervention evaluated (routine RT-PCR testing + two-round Ag-RDT screening on days 1 and 5). Efficiency estimates are presented as different colours for screening interventions that target all patients (red), all staff (blue), or all individuals in the LTCF (orange).

Apparent efficiency of Ag-RDT screening was nearly identical across LTCFs. This reflects that, despite substantial differences in outbreak size, screening detected similar numbers of infections in each LTCF relative to the large number of screening tests used. However, marginal real efficiency varied greatly across LTCFs. Beyond the infections already averted due to routine RT-PCR testing, this well-timed patient Ag-RDT screening

intervention averted approximately 20 cases/1,000 Ag-RDT tests in LTCF 1, compared to 5 cases/1,000 Ag-RDT tests in LTCF 2, and just 0.5 cases/1,000 Ag-RDT tests in the high control LTCF 3 (**Figure 8.14**).

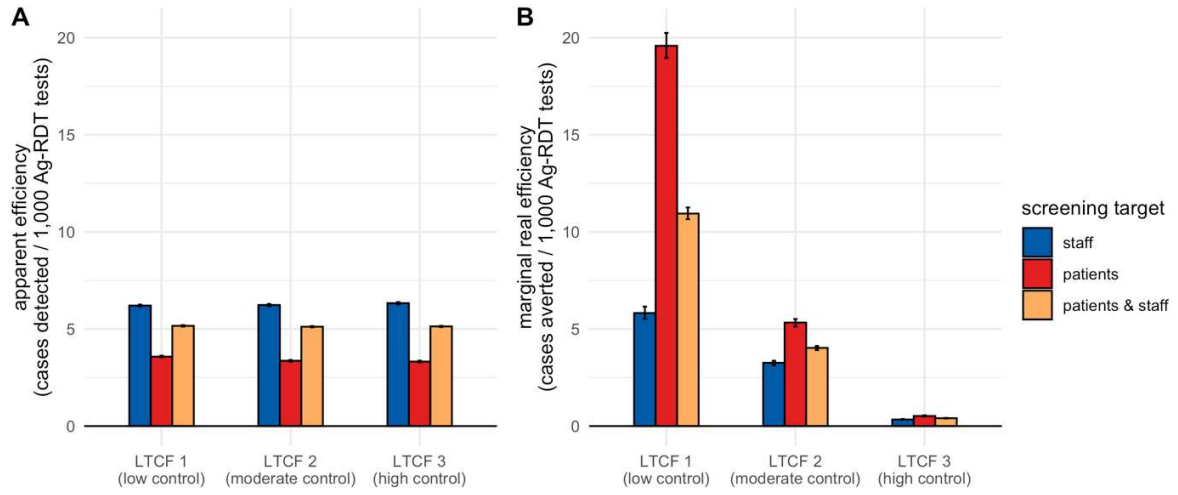

Figure 8.14. Apparent vs. real surveillance efficiency.

Efficiency of Ag-RDT screening in the context of a highly effective surveillance intervention (routine RT-PCR + 2-round Ag-RDT screening on days 1 and 5), comparing (A) apparent screening efficiency with (B) marginal real screening efficiency. Marginal real screening efficiency describes efficiency of Ag-RDT screening for prevention of remaining nosocomial SARS-CoV-2 infections not already averted by routine RT-PCR testing. Screening interventions targeted either all members of staff (blue), all patients (red), or all individuals in the LTCF (orange). Baseline assumptions underlying simulations include: "low" community SARS-CoV-2 incidence and time-varying Ag-RDT sensitivity relative to RT-PCR (Ag-RDT A).

Figure 8.15 shows various performance indicators for Ag-RDT screening interventions, including TPR, TNR, PPV and NPV, and again comparing screening interventions that target only patients (red), only staff (blue), or everyone in the LTCF (orange). TPR was substantially lower in lower control LTCFs, while TNR was indistinguishable across facilities. For 2-round screening interventions, PPV tended to increase when second-round screening was conducted later, while NPV tended to decrease. Overall, targeting staff tended to result in higher screening performance indicator estimates than targeting patients. This reflects that staff infections were more likely to be community-onset, and tended to have higher probabilities of being detected due to an older infection age when screening interventions were conducted, while patient infections were more likely to be nascent nosocomial infections with lower probability of being detected. **Figure 8.15** further builds on **Figure 8.14** by demonstrating, across a range of screening interventions, that apparent efficiency is highly similar across LTCFs, while real marginal efficiency is consistently more than an order of magnitude greater in low control LTCF 1 than in high control LTCF 3.

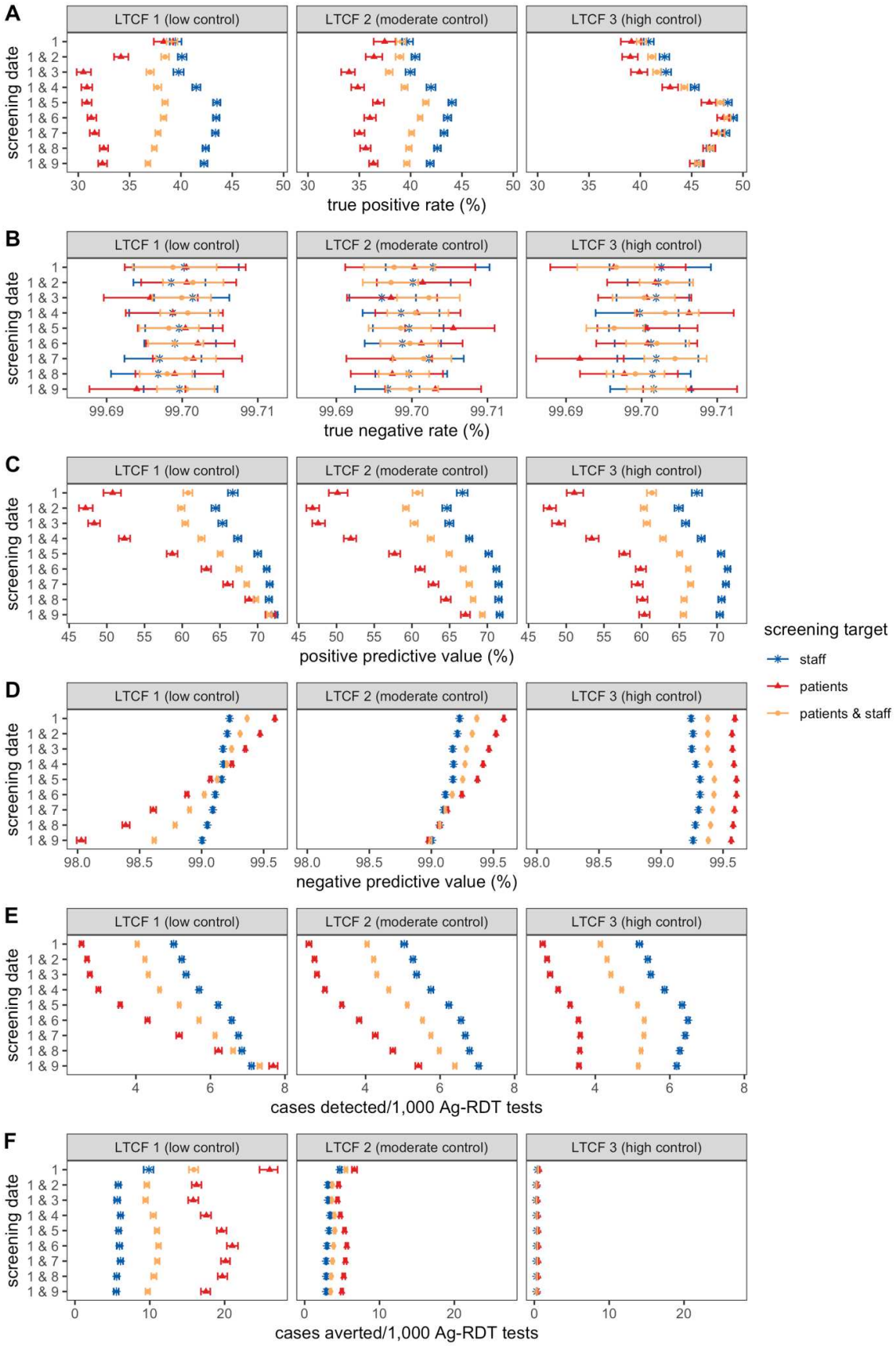

Figure 8.15. Ag-RDT screening performance indicators.

Performance of Ag-RDT screening interventions paired with routine RT-PCR testing (interventions 11 and 20 to 27 from **Table 8.2**) across various surveillance outcomes (rows). For **(F)**, note that efficacy reflects marginal cases averted: cases averted by Ag-RDT screening exclude cases already averted by routine RT-PCR testing. Points and error bars correspond to bootstrap means and 95% confidence intervals

8.3.4. Surveillance cost-effectiveness

Figure 8.16 shows cost-effectiveness estimates for four selected surveillance interventions (colours) across LTCFs and while varying testing unit costs. Similar to real marginal efficiency, cost-effectiveness of different surveillance interventions varied by orders of magnitude across LTCFs.

In LTCF 1, assuming baseline costs of €50/RT-PCR test and €5/Ag-RDT test, routine RT-PCR testing + 1-round Ag-RDT screening cost €422 (€413-€431)/case averted, with similar estimates for 2-round screening. In LTCF 2, the same intervention cost €1,070 (€1,051-€1,088)/case averted, and in LTCF 3 it cost €10,263 (€9,963-€10,583)/case averted.

Cost-effectiveness estimates were highly sensitive to testing unit costs. Above €50/RT-PCR test, routine testing was overall more cost-effective when coupled with Ag-RDT screening. Conversely, above €5/Ag-RDT test, routine testing was overall less cost-effective when coupled with Ag-RDT screening. Although combined testing and screening strategies were much more epidemiologically effective than screening on its own (**Figure 8.10**), they were generally less cost-effective (**Figure 8.16**).

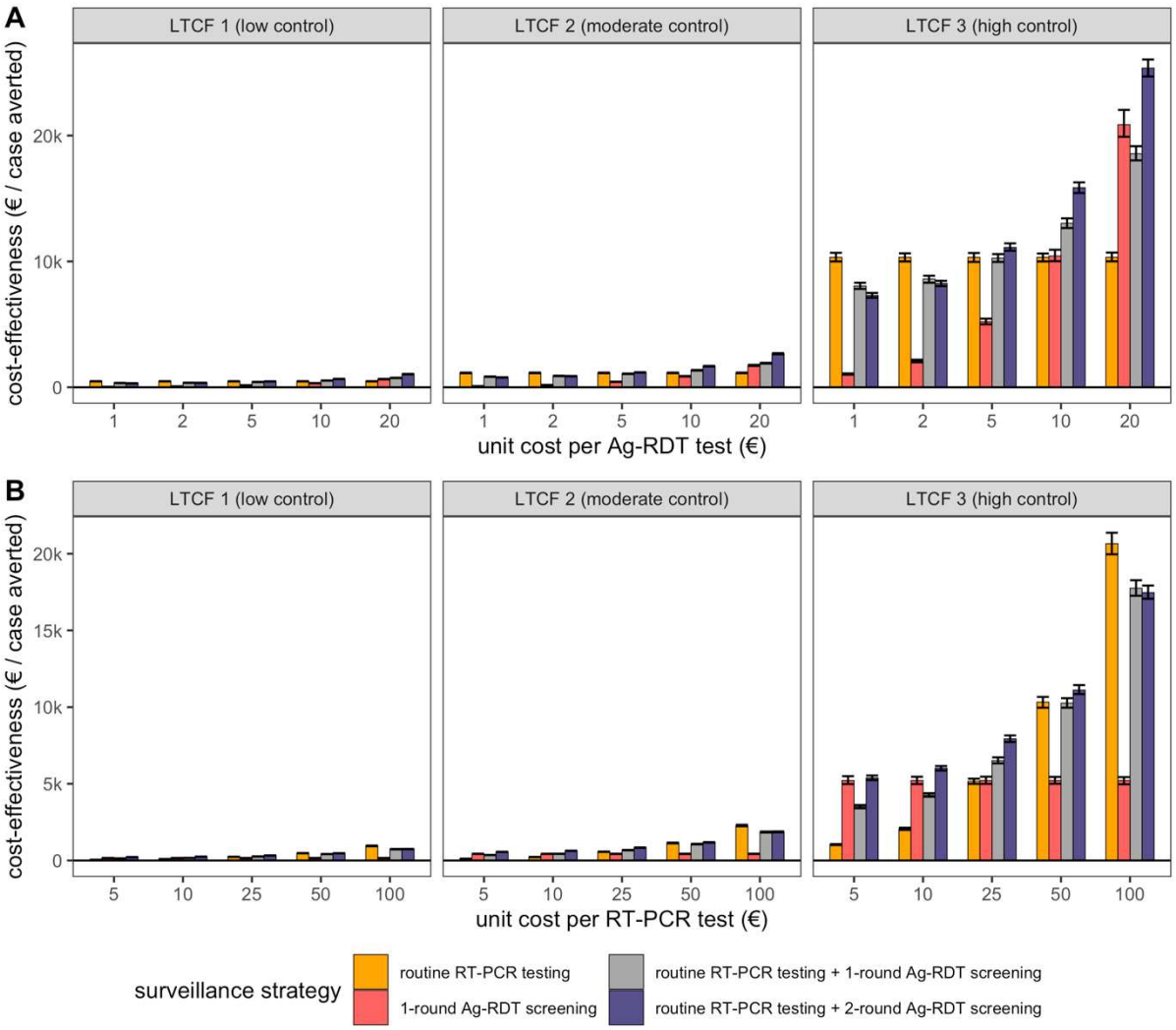

Figure 8.16. Surveillance cost-effectiveness.

Cost-effectiveness of four surveillance interventions (colours), estimated as surveillance unit costs per case averted. Cost-effectiveness was estimated while varying either **(A)** the unit cost per Ag-RDT test (at a fixed €50/RT-PCR test), or **(B)** the unit cost per RT-PCR test (at a fixed €5/Ag-RDT test). One-round screening was conducted on day 1 (strategies 2 and 11 in **Table 8.2**), and 2-round screening on days 1 and 5 (strategy 23). Baseline assumptions underlying simulations include: "low" community SARS-CoV-2 incidence; time-varying Ag-RDT sensitivity relative to RT-PCR (Ag-RDT A); and screening interventions that target all patients and staff in the LTCF.

8.4. Discussion

8.4.1. Summary of model and results

Surges in nosocomial SARS-CoV-2 importation or outbreak risk are often predictable, resulting from phenomena like local emergence of a highly transmissible variant, seasonal or festive gatherings that increase population mixing, and the identification of index cases or exposed contacts within a healthcare facility. When such risks are known, implementing reactive surveillance may help to identify and isolate asymptomatic and pre-symptomatic infections, limiting onward nosocomial transmission. Using simulation modelling, I demonstrate how reactive Ag-RDT screening complements routine RT-PCR testing in reducing nosocomial SARS-CoV-2 incidence following a known surge in outbreak risk.

In simulations, with two rounds of well-timed Ag-RDT screening, up to 75% of infections were prevented, compared to 64% with a single round of screening, or 47% with routine RT-PCR testing alone. A lag of 4-5 days between the first and second rounds of screening was found to be optimal for transmission prevention, as a result of the time-varying nature of test sensitivity (in a sensitivity analysis assuming imperfect but time-invariant sensitivity, an immediate second round of screening was optimal). Underlying outbreak risk was the greatest driver of screening efficiency, more important than screening timing (immediate vs. delayed), test type (Ag-RDT vs. RT-PCR) or target (patients vs. staff). I estimated that a vulnerable LTCF gains between one and two orders of magnitude more health-economic benefit (>10 infections averted/1,000 Ag-RDT tests used for combined routine testing and 2-round screening interventions) than a resilient LTCF with alternative COVID-19 control measures already in place (<1 infection averted/1,000 Ag-RDT tests). This translated to similar cost-effectiveness conclusions, whereby the highest-control LTCF 3 paid over €10,000 in surveillance unit costs per infection averted, compared to approximately €400/infection averted for identical interventions in the lowest-control LTCF 1.

8.4.2. Findings in context

Ag-RDT screening is widely used in healthcare settings, but there is limited empirical evidence demonstrating efficacy for SARS-CoV-2 transmission prevention.(Tulloch et al., 2021) Despite a range of studies reporting efficacy for case identification,(Kernéis et al., 2021; McKay et al., 2021; Wagenhäuser et al., 2021) interventional trials are needed to understand impacts on nosocomial spread. The present comparison of apparent and real screening efficiency demonstrates why case identification may be a poor proxy measure

for actual health and economic benefit. In the absence of empirical data, mathematical models have been useful tools to evaluate performance of SARS-CoV-2 screening interventions in healthcare settings. Most studies have simulated use of routine screening at regular intervals (e.g. weekly, biweekly), finding that more frequent screening reduces outbreak probability, that targeting patients versus staff can significantly impact effectiveness, and that faster diagnostic turn-around time of Ag-RDT tends to outweigh reduced sensitivity relative to RT-PCR.(Chin et al., 2020; Hellewell et al., 2021; Holmdahl et al., 2021; Kahn et al., 2021; Kendall et al., 2021; L. L. K. Nguyen et al., 2020; Pham et al., 2021; Rosello et al., 2021; Vilches et al., 2021; Zhang et al., 2021) These conclusions were all recapitulated in this work.

Despite potential to reduce transmission, routine screening is an economic and occupational burden with uncertain suitability for low-risk healthcare settings.(Buckle et al., 2021; Kierkegaard et al., 2021) These considerations have generally been neglected in previous work. A few modelling studies have estimated cost-effectiveness of nosocomial screening interventions in specific use cases, including for hospital patients admitted with respiratory symptoms,(Ricks et al., 2021) patients admitted to German emergency rooms,(Diel and Nienhaus, 2021) and routine staff and resident testing in English nursing homes.(Stevenson et al., 2021) However, key impacts of stochastic transmission dynamics, screening heterogeneity, and other concomitant COVID-19 containment measures have rarely been accounted for. Further, no studies have evaluated efficacy and efficiency of reactive, as opposed to routine screening, although findings from See et al. suggest greater efficiency of testing in outbreak versus non-outbreak settings.(See et al., 2021) Overall, the present use of high-resolution, stochastic, individual-based modelling complements previous studies in demonstrating how epidemiological and health-economic benefits of reactive screening scale with test sensitivity, screening timing, test type, population targets, and – most critically – underlying nosocomial outbreak risk.

8.4.3. Limitations

Findings should be interpreted in the context of several methodological limitations. First, some results may reflect specificities of the rehabilitation hospital contact network underlying CTCmodeler. Greater efficiency was estimated for screening patients relative to staff, but the opposite result may be expected in settings where staff have higher rates of contact than patients. Second, use of retrospective counterfactual analysis facilitated precise estimation of intervention efficacy, but precluded consideration of how surveillance

interventions might impact human behaviour. For instance, healthcare workers that conduct screening inevitably come into contact with many individuals, potentially creating new opportunities for transmission. This limitation does not hold if results are interpreted in the context of self-administered auto-tests, which may be a cost-effective intervention in the context of at-home testing in the community.(Paltiel et al., 2021) However, auto-testing may be less feasible for patients or residents than staff, particularly in certain high-risk settings.(Würstle et al., 2021)

Third, transmission chain pruning did not account for the possibility of case isolation delaying, rather than preventing infection. For instance, a healthcare worker whose infection was averted due to isolation of an infectious patient could nonetheless become infected by a subsequent contact with a different infectious individual. This effect was likely negligible in higher-control LTCFs, where multiple acquisition routes are unlikely in the context of low nosocomial incidence, but may have resulted in overestimation of intervention efficacy in lower-control LTCFs. However, this effect should not have qualitatively changed any conclusions, as transmission chain pruning was conducted identically across interventions (e.g. testing vs. screening), tests (RT-PCR vs. Ag-RDT) and targets (patients vs. staff).

Fourth, cost-effectiveness estimates only considered testing unit costs, but decision-makers must consider a range of other implementation costs, from human resources, to logistical coordination, to opportunity costs of false-positive isolation. Decision-makers may also have a wide variety of specific tests and manufacturers to choose from, including tests with heterogeneous sampling techniques (e.g. nasopharyngeal swabs vs. saliva or pharynx gargle samples), with potential consequences for surveillance costs, efficacy and occupational burden. (Note that the RT-PCR and Ag-RDT sensitivity curves used in the present work represent average results across a range of different tests used on upper respiratory specimens.) Finally, this analysis was limited to the two weeks following intervention implementation, under the assumption that LTCFs came to control nosocomial transmission at the same time. Findings thus do not capture potential downstream exponential benefits of preventing infections, including those that go on to seed transmission in the community.

8.4.4. Future directions

Since its widespread uptake as a SARS-CoV-2 surveillance intervention, there has been

substantial debate about whether the potential health-economic efficiency of Ag-RDT justifies an elevated risk of false-negative diagnosis.(Deeks and Raffle, 2020; Mina and Andersen, 2021) The present findings are consistent with the view that Ag-RDT is on its own insufficient to eliminate nosocomial SARS-CoV-2 outbreak risk, but that it is nonetheless an effective component of multi-modal infection prevention strategies.(Dinnes, 2021) I demonstrate that reactive Ag-RDT screening is a potentially efficient public health response to surges in outbreak risk in the LTCF setting, but that its health and economic benefits scale by orders of magnitude depending on other epidemiological risk factors, including the facility's inter-individual contact patterns, infection prevention measures, and vaccine coverage. This suggests that healthcare institutions should carefully evaluate their vulnerability to COVID-19 – and hence potential returns on investment – before implementation of Ag-RDT screening interventions. Such decision-making may be guided by local indicators, including the burden of SARS-CoV-2 infection in the local community, levels of SARS-CoV-2 immunity among patients and staff, the immune escape properties of locally circulating variants, and other factors that underlie nosocomial outbreak risk.

Chapter 9. Contributions, perspectives and conclusion

9.1. Synthesis of contributions

The main objectives of this thesis were to develop novel mathematical models to better understand the aetiology and transmission risks of diverse nosocomial pathogens, and to provide evidence for improvement of HCAI surveillance and control interventions. These objectives were met through two principal bodies of work. First, the study of how within-host microbiome-pathogen interactions drive nosocomial dissemination of ARB and determine the efficacy of public health interventions for colonization prevention in the hospital setting. Second, the study of how systematic surveillance and isolation interventions can be optimized to detect and prevent SARS-CoV-2 outbreaks in the long-term care setting. Here, these works are discussed in the context of their broader contributions to the study of the transmission, surveillance and control of HCAI.

9.1.1. How do antibiotics select for the spread of resistance?

This thesis has provided a theoretical framework explaining how antibiotic use in the context of **microbiome-pathogen competition** can drive the epidemiological spread of ARB. This offers an alternative selection mechanism to intraspecific strain competition – the classic modelling framework – for how antibiotics select for resistance dissemination. Through this work, two novel mechanistic **antibiotic selection trade-offs** were identified, whereby intermediate antibiotic use tends to select most strongly for the spread of ARB in the context of either microbiome dysbiosis (due to antibiotics both clearing ARB and increasing host susceptibility to colonization) or interspecific HGT (due to antibiotics both selecting for bacteria bearing an antibiotic-resistance gene and clearing potential HGT recipients).

This work also demonstrated how different colonization **acquisition routes** (including person-to-person transmission, endogenous acquisition, horizontal gene transfer) and within-host **competitive interactions** (colonization resistance, resource competition, ecological release) combine to drive the colonization dynamics of distinct ARB. In particular, high estimated ecological release coefficients for *C. difficile*, ESBL-EC and CP-

KP were found to drive high rates of endogenous colonization acquisition. However, despite large impacts on pathogen prevalence and incidence, microbiome-pathogen interactions had little impact on resistance rates, suggesting that the ecological forces that drive antibiotic selection for ARB dissemination may vary across levels of biological organization (e.g. bacterial strains vs. species) and epidemiological indicators (e.g. resistance isolation rates vs. colonization prevalence).

9.1.2. Which control interventions for which ARB?

Variation in within-host ecology and acquisition routes was found to underlie variation in the efficacy of public health interventions for the control of distinct nosocomial pathogens. **Contact precautions** were highly effective for reducing colonization incidence of MRSA (which was primarily acquired through person-to-person transmission), but had limited impact on incidence of enteric ARB (primarily acquired endogenously). Conversely, **antibiotic stewardship** interventions were broadly effective for colonization prevention across all ARB (with highest efficacy for CP-KP and lowest efficacy for MRSA), as well as for reducing resistance rates (again with highest efficacy for CP-KP). Stewardship interventions were found not only to limit endogenous outgrowth of subdominant ARB, but also to reduce acquisition through HGT and person-to-person transmission, hinting as to why stewardship may be broadly effective across ecologically distinct ARB (as observed empirically). Through similar mechanisms, this work also demonstrated benefits of **microbiome-targeted therapies** that protect microbiome stability and/or diversity as a tool to limit acquisition of HCAI-causing ARB (with highest efficacy for *C. difficile* prevention, and lowest for MRSA prevention), but not to limit resistance rates.

9.1.3. What makes LTCFs vulnerable to SARS-CoV-2 outbreaks?

Through detailed analysis of the *in silico* transmission of SARS-CoV-2 along high-resolution inter-individual contact networks simulated using data from a real long-term care hospital setting, this thesis demonstrated several factors that make LTCFs vulnerable to SARS-CoV-2 outbreaks. First, simulations highlighted how **contact patterns** can shape differential infection risk among patients and staff. As expected, high rates of patient-to-patient contact in the baseline contact network entailed high rates of patient-to-patient transmission, while a simple patient social distancing intervention more than halved nosocomial incidence. Second, high incidence was primarily driven by **super-spreaders**, but only in the absence of control measures: super-spreaders accounted for approximately half of transmission events in a low-control LTCF, but just 1% when combined COVID-19

control measures (social distancing, masks and vaccination) were in place. Third, the introduction of non-symptomatic infections from the community in the context of **symptom-based surveillance** was associated with outbreak vulnerability: routine symptomatic RT-PCR testing entailed longer delays to outbreak detection than other strategies, and prevented on average fewer than half of infections across three simulated LTCFs.

9.1.4. How can SARS-CoV-2 surveillance be optimized?

This thesis demonstrated that optimal surveillance strategies for SARS-CoV-2 outbreak detection and transmission prevention vary depending on the types of tests or combinations of tests used, their diagnostic sensitivity, available testing capacity, testing timeliness, testing targets, and underlying nosocomial outbreak risk. In the context of outbreak detection, SARS-CoV-2 **group testing** (sample pooling) was found to be highly effective and efficient in the context of limited RT-PCR testing capacity (<1 test/100 beds/day), while testing cascades were the most effective strategy when tests were more readily available (>10 tests/100 beds/day), and in particular when cascades included a range of indications, including new patient admission and presentation of any COVID-19-like symptoms among all patients and staff. I also showed that **mass screening** using rapid point-of-care tests may be an effective surveillance intervention for transmission prevention in the context of a surge in SARS-CoV-2 introductions from the community. Screening was always more effective the earlier it was conducted relative to the detected surge in outbreak risk, but two-round screening was optimized by allowing a delay of 4 to 5 days between the first and second rounds. Screening interventions were generally more effective for transmission prevention when using Ag-RDT as opposed to RT-PCR (assuming a 24-hour delay to RT-PCR results), and when targeting patients rather than staff (in the context of a facility with high underlying rates of patient-patient contact). However, the number of infections averted per test used scaled by over an order of magnitude depending on the other COVID-19 control measures in place, demonstrating that health-economic benefits of surveillance depend principally on underlying nosocomial outbreak risk.

9.2. Perspectives for coming years

9.2.1. Bridging scales using nested models

Links between within- and between-host infectious disease dynamics have been widely studied in various contexts, including the evolution of parasite life history and Darwinian selection for antimicrobial resistance, but remain largely absent from epidemiological models of antibiotic resistance.(Birkegård et al., 2018; Day et al., 2011; Niewiadomska et al., 2019; zur Wiesch et al., 2011) The work in this thesis is among the first to mechanistically link microbiome dynamics to the clinical epidemiology of ARB, and to antibiotic selection for resistance dissemination at the population level. However, due to a lack of empirical data to inform more detailed modelling assumptions, within-host dynamics were greatly simplified. A clear extension of the present work is to explicitly account for within-host microbiome and pathogen population dynamics using nested models informed by detailed within- and between-host data.

9.2.2.1. Within-host microbiome dynamics

Impacts of interspecific interactions on within-host microbiome population dynamics and community assembly are increasingly well described. Using different modelling approaches, Levy & Borenstein showed that metabolic competition correlates with microbiome colonization, such that species occupying a similar nutritional niche tend to co-occur,(Levy and Borenstein, 2013) and Coyte et al. showed that inter-specific competition, and not cooperation, best explains the intrinsic population dynamic stability of the microbiome.(Coyte et al., 2015) Competitive interactions between bacteria have also been shown to drive their spatial organization,(Liu et al., 2016) history-dependent species abundance,(Venturelli et al., 2018) and predictability in the taxonomic organization of emergent microbial communities(Friedman et al., 2017).

Other studies have further accounted for antibiotic exposure in this context. Using ecological time-series data, Stein et al. extended a Lotka-Volterra framework to infer competition dynamics and demonstrate that antibiotic exposure can cause catastrophic shifts in microbiome composition.(Stein et al., 2013) Using an alternative stability landscape framework, Shaw et al. modelled the impact of different antibiotic classes on phylogenetic diversity, demonstrating particularly deleterious impacts of clindamycin and ciprofloxacin. Relatively fewer studies have further explored consequences for the emergence of antibiotic resistance. Notably, Tepekule et al. modelled microbiome

population dynamics against a backdrop of ecological competition and antibiotic treatment, and showed how properties of generic antibiotic exposure, including treatment duration and time since last exposure, can explain within-host selection for resistance.(Tepekule et al., 2019) Finally, Guittar et al. used within-host mathematical modelling to show how host-mediated resource competition between mutualistic and pathogenic microorganisms can reproduce a range of empirical observations, including: different infection outcomes among similar hosts exposed to the same pathogen, a non-linear relationship between pathogen inoculum size and colonization duration, use of microbiome recovery therapies to overcome antibiotic-induced dysbiosis, and potential for probiotic therapy to protect against infection.(Guittar et al., 2021)

9.2.2.2. Extensions to between-host dynamics: the missing link

Despite these recent advances in understanding within-host microbiome dynamics, critical links to between-host epidemiological processes are missing. To date, few if any studies have described how impacts of antibiotics on microbiome population dynamics feed forward to impact colonization and/or infection dynamics at the between-host level. Indeed, a lack of data and challenges associated with validating simultaneous within- and between-host outcomes are known barriers to using nested models in the study of infectious disease dynamics.(Restif and Graham, 2015) Yet informative data are not out of reach. In theory, parameters linking within- and between-host processes could be estimated through longitudinal observational studies that simultaneously assess impacts of antibiotic consumption on microbiome dynamics (e.g. estimates of microbiome composition before, during and after antibiotic therapy from metagenomic analysis of stool samples), and subsequent risks of acquisition, clearance and outgrowth of different pathogens in treatment and control groups. With the advent of high-throughput sequencing technologies and advanced methods in genomic epidemiology, future work should be able to more rigorously quantify how indicators of microbiome health and dysbiosis (e.g. species diversity or dynamic stability) map to epidemiological outcomes (e.g. pathogen acquisition risk).

9.2.3. Pathogen-pathogen interactions

Infectious disease models typically consider only one pathogen strain or species at a time. This is a sensible methodological approach in the absence of strong evidence supporting interactions with other co-circulating pathogens, but some pathogen-pathogen interactions may have important epidemiological consequences. Influenza, for example, has been

identified as a key driver of seasonality in invasive pneumococcal disease, such that models of *S. pneumoniae* in isolation may be less likely to correctly represent its epidemiology than models accounting for both *S. pneumoniae* and influenza.(Domenech de Cellès et al., 2019) One possible extension of our microbiome model is to account for co-colonization with and competitive within-host interactions between different nosocomial pathogen species. For instance, Enterobacteriaceae like *E. coli* and *K. pneumoniae* may overlap significantly in their ecological niche and are known to horizontally exchange antibiotic resistance genes,(Mathers et al., 2015) making them hypothetical candidates for such a coinfection model, but data informing if or how such interactions affect their nosocomial epidemiology are scarce.

For COVID-19 patients, **bacterial coinfection** has been a topic of major concern since the beginning of the pandemic. This has been motivated by high rates of mortality due to bacterial coinfection for other respiratory infections (e.g. during the 2009 H1N1 influenza pandemic), resulting in high rates of prophylactic antibiotic prescribing in hospitalized COVID-19 patients.(Knight et al., 2021; MacIntyre et al., 2018) Yet preliminary evidence suggests that bacterial coinfection is relatively rare subsequent to SARS-CoV-2 infection, while coinfection with other respiratory viruses is more common but may be relatively inconsequential (Davis et al., 2020; Langford et al., 2020; Lansbury et al., 2020; Le Hingrat et al., 2021; Rawson et al., 2020) For instance, there was no evidence from extensive UK surveillance data that SARS-CoV-2 infection was associated with increased rates of invasive pneumococcal disease (*S. pneumoniae* was the most common coinfecting bacteria during the H1N1 pandemic).(Amin-Chowdhury et al., 2021; MacIntyre et al., 2018) However, such findings must also be interpreted in the context of global declines in incidence of respiratory bacterial disease coincident with lockdowns during the first wave of the COVID-19 pandemic.(Brueggemann et al., 2021) Indeed, transmission dynamics of diverse pathogen species can be driven by the same host or environmental factors, and limited by the same public health interventions. A critical research question that has thus emerged since early 2020 is: how has the COVID-19 pandemic and its associated control interventions impacted the transmission, surveillance and control of other nosocomial pathogens?

9.2.4. Impacts of the COVID-19 pandemic on other healthcare-associated infections

The overall impact of the COVID-19 pandemic on HCAI epidemiology remains largely

uncertain, but emerging literature suggests that its effects have been heterogeneous across geographical regions, healthcare facilities, types of care, types of infection and pathogen species. In a literature review, O'Toole identified increased rates of carbapenem-resistant Enterobacterales and *A. baumanii*, but reduced rates of MRSA and VRE as compared with pre-pandemic rates; and in a commentary, McMullen et al. suggest that the COVID-19 pandemic may be expected to lead to increased central line-associated bloodstream infection (BSI) and catheter-associated urinary tract infection (UTI), but reduced surgical site infection (SSI).(McMullen et al., 2020; O'Toole, 2021)

9.2.4.1. Increased HCAI burden due to COVID-19

9.2.4.1.1. Mechanisms

There are a number of hypotheses as to why the COVID-19 pandemic may have exacerbated HCAI burden.(McMullen et al., 2020; O'Toole, 2021) These include: disorganization of the workplace, resulting in reduced adherence to standard infection prevention and control practices and to antimicrobial stewardship; healthcare worker absenteeism due to COVID-19 infection or pandemic burnout, resulting in higher patient-to-staff ratios; high rates of prophylactic antibiotic prescribing among COVID-19 patients, resulting in background selection for resistant bacteria; increased use of invasive devices like central lines and mechanical ventilators for treatment of severe COVID-19 infections; and fewer elective hospital admissions, shifting the denominator of patient populations towards more vulnerable individuals, and increasing per-capita HCAI rates.

9.2.4.1.2. Evidence

One of the largest reports of increased HCAI rates during the COVID-19 pandemic comes from an analysis of data from 148 USA hospitals by Baker et al. They reported a 23–108% increase in incidence of central line-associated BSI, and an 8–90% increase for catheter-associated UTI. They also reported increases in MRSA, VRE and multidrug-resistant Gram-negative bacteria, but no change in *C. difficile* infection, and observed that clusters of hospital-onset pathogens were associated with surges in COVID-19 cases.(Baker et al., 2021) A similar increase of central-line associated BSI was reported in Michigan, and of device-associated HCAI in Italy.(Baccolini et al., 2021; LeRose et al., 2021) In ICUs in France, Buetti et al. reported higher rates of BSI among COVID-19 patients than non-COVID-19 patients;(Buetti et al., 2021) and in a COVID-19-dedicated ICU in Germany, two VRE clusters emerged despite intensification of infection prevention measures due to the pandemic.(Kampmeier et al., 2020) In separate hospitals in Florida and Italy,

dissemination of highly drug-resistant *C. auris* was potentially exacerbated by the COVID-19 pandemic, with nosocomial transmission occurring in COVID-19-dedicated wards.(Di Pilato et al., 2021; Prestel et al., 2021) Finally, in a case-control series from Italy, higher rates of multidrug-resistant bacterial infections were reported in COVID-19 versus non-COVID-19 wards, with the greatest difference reported for ESBL-producing *K. pneumoniae*. However, across all wards, they found a significant decrease in the incidence of multidrug-resistant bacterial infections during the pandemic compared to pre-pandemic years (2017-2019).(Bentivegna et al., 2021)

9.2.4.2. Decreased HCAI burden due to COVID-19

9.2.4.2.1. Mechanisms

There are also a number of hypotheses as to why the COVID-19 pandemic may have indirectly helped to reduce HCAI burden.(McMullen et al., 2020; O'Toole, 2021; Smith and Opatowski, 2021) These include: reduced transmission of nosocomial pathogens due to COVID-19 prevention measures, including contact precautions, universal masking, hand hygiene and personal protective equipment; fewer total admissions and hence reduced patient density; fewer surgical operations; reduced pathogen carriage in the community due to decreased population mixing, increased hand hygiene and other pandemic control measures, resulting in fewer introductions into healthcare settings; and reduced hospital and community circulation of potential co-infecting pathogens that predispose patients to severe infection (e.g. reduced influenza incidence resulting in lower rates of invasive disease due to *S. pneumoniae*).

9.2.4.2.2. Evidence

Healthcare facilities worldwide have and continue to report reduced rates of HCAI coincident with implementation of COVID-19 containment measures. In a retrospective cross-sectional study in four California hospitals, overall rates of healthcare-onset MDR bacteria were reduced by 35%, including a 21% decrease in "ESBL" (organism not defined), 41% decrease in MRSA and 80% decrease in VRE. These decreases were concomitant with a 25% increase in hand sanitizer and hand soap usage.(Cole and Barnard, 2021) In a tertiary-care hospital in Madrid, there was a 70% reduction in *C. difficile* infection despite a slight increase in antibiotic use.(Ponce-Alonso et al., 2021) In neurological units in a hospital in Rome, hospitalization from March to May 2020 (as compared to 2019) was independently associated with both reduced antibiotic prescribing and reduced HCAI incidence.(Cerulli Irelli et al., 2020) In another Italian hospital, rates of

SSI during the COVID-19 period in 2020 (as compared to 2018 and 2019) were significantly lower (3.3% during COVID-19 vs. 8.4% in baseline), including significantly lower proportions of patients developing either superficial SSI (0.8% vs. 3.4%) or deep SSI (0% vs. 3.4%). Measures to reduce nosocomial SARS-CoV-2 transmission were independently associated with reduced SSI.(Losurdo et al., 2020)

Significant reductions have also been reported for respiratory viral HCAIs. In a healthcare network in Hong Kong with high compliance of masking among staff (100%) and patients (76%), there were no cases of nosocomial influenza A, influenza B, and RSV infection in early 2020. This was significantly lower than the same period from 2017 to 2019, which had on average 5, 2 and 3 cases of influenza A, influenza B and RSV per month.(Wong et al., 2021) In Singapore's largest hospital system, a multimodal IPC intervention put in place for COVID-19 prevention corresponded with a major decrease in healthcare-associated respiratory virus infection (IRR 0.05–0.13), in addition to reduced MRSA acquisition rates (IRR 0.46–0.64) and CA-BSI rates (IRR 0.07–0.57).(Wee et al., 2021) Finally, in a separate study of adenovirus infection from the same setting, Wee et al. reported reduced incidence of healthcare-associated infection subsequent to COVID-19 containment measures (0.03 cases / 10,000 patient days) compared to the pre-pandemic period (0.40 cases / 10,000 patient-days), despite higher rates of community-onset adenovirus infection at pandemic onset.(Wee et al., 2020)

9.2.4.3. Pandemic impacts on the microbiome

The COVID-19 pandemic may also be associated with important consequences for human microbiota. First, high rates of prophylactic antibiotic prescribing among COVID-19 patients can be expected to increase risks of dysbiosis and *C. difficile* infection.(Kullar et al., 2021) Second, in a review of the causes and consequences of gastrointestinal symptoms associated with COVID-19, Trottein & Sokol describe mechanisms by which SARS-CoV-2 infection may itself trigger gut dysbiosis, and suggest that targeting gut microbiota to limit or prevent dysbiosis may help to control COVID-19 pathogenesis.(Trottein and Sokol, 2020) Evidence for microbiome-targeted interventions remains limited, but one trial of probiotic therapy in COVID-19 patients demonstrated effectiveness for resolution of COVID-19-associated diarrhea compared to controls, and reduced rates of ICU transfer and mortality.(d'Ettorre et al., 2020) In light of findings from this thesis, microbiome-targeted interventions may have the additional downstream benefits of reducing subsequent risk of ARB colonization and HCAI in hospitalized COVID-

19 patients.

COVID-19 containment measures may also have impacted the transmission and composition of human microbiota. For instance, in a cohort of acute myeloid leukemia patients in the USA who provided stool samples longitudinally over pre- and post-pandemic periods, implementation of COVID-19 containment measures left a clear imprint on microbiome composition, including reduced abundance of *Pseudomonas* spp. and *Akkermansia* spp.(Rashidi et al., 2021) In both community and healthcare settings, measures like social distancing, sedentary lifestyles, extensive antimicrobial hygiene practices and travel restrictions may indirectly favour loss of microbial diversity and limit reinoculation with commensal symbionts, with potential deleterious consequences for protection against infectious disease.(Finlay et al., 2021)

9.2.5. Future work

A planned extension of the work from this thesis is to build a hospital model that simultaneously accounts for ARB carriage, SARS-CoV-2 infection and patient microbiota, in order to better understand impacts of the COVID-19 pandemic on the epidemiology of ARB in French hospitals. This project, in partnership with Santé Publique France, will synthesize three sources of surveillance data from hospitals across each of France's 13 metropolitan regions: the daily prevalence of hospitalized COVID-19 patients, the daily incidence of ARB isolation from clinical samples (including MRSA, VRE and ESBL-producing Enterobacteriaceae), and monthly antibiotic consumption data. Together, these data will be fit to mechanistic models to quantify potential impacts of the COVID-19 pandemic – including control interventions like the implementation of contact precautions, and unintended consequences like increased antibiotic prescribing – on the nosocomial dynamics of antibiotic resistance.

9.3. Mathematical modelling for the betterment of public health

Over the last several decades, mathematical modelling has emerged as an indispensable tool in infectious disease epidemiology and HCAI control, but not without its skeptics. In an essay about which types of information ought to be used to inform responses to the COVID-19 pandemic, philosopher of medicine Jonathan Fuller distinguished between public health epidemiologists, who synthesize diverse sources of data to build models and make predictions, and clinical epidemiologists, who eschew such predictions in favour of hard evidence from controlled trials.(Fuller, 2020) Although this binary distinction is perhaps somewhat caricatural,(Lipsitch, 2020) it evokes an older debate about the ultimate purpose of epidemiology.

9.3.1. Contribution of modelling to epidemiology

Epidemiology is traditionally defined as the study of the causes and distributions of diseases in human populations, in order to identify ways to prevent and control disease.(Last, 1993) Inevitably, no one study can address all relevant questions, and much epidemiological research is constrained to respond to either one axis of this definition (aetiology) or the other (intervention). Yet contemporary epidemiological methods are largely built upon causal formalism, and introductory epidemiology textbooks are overwhelming devoted to understanding the causes and distributions of disease, and not optimal means to control them.(Gordis, 2008; Merrill, 2019; Webb et al., 2016) In 2013, epidemiologist Sandro Galea argued for a move towards consequentialism in epidemiology – an approach oriented towards maximizing desired outcomes, i.e. population health – and hence putting greater emphasis on the study of disease prevention and control.(Galea, 2013)

A great strength of mathematical models is that they can be used to address both of these axes. The same model can simultaneously assess how micro-level changes in an exposure translate into macro-level changes in population health (**aetiology**, e.g. how antibiotics select for the spread of ARB, or how different inter-individual contact patterns affect SARS-CoV-2 outbreak risk), and equally how a control measure targeting that exposure feeds forward to impact public health outcomes (**intervention**, e.g. how antibiotic stewardship prevents ARB colonization incidence, or how screening and isolation interventions limit nosocomial SARS-CoV-2 transmission).(Auchincloss and Diez Roux, 2008) Overall, the work in this thesis has provided examples why, in the absence of data

from randomized controlled trials, mathematical modelling is a useful tool both to understand HCAI aetiology and to inform consequentialist public health decision-making.

9.4. Conclusion

Over the course of this thesis, I have used various mathematical modelling approaches to study the transmission, surveillance and control of human pathogens in the healthcare setting. I developed a novel ODE modelling framework to better understand how antibiotic-resistant bacteria spread in hospitals, and used a detailed individual-based model to simulate transmission dynamics of SARS-CoV-2 in long-term care facilities. Both models were applied to evaluate the epidemiological impacts of surveillance and control interventions, helping to elucidate how within-host ecology can impact intervention efficacy, and how imperfect surveillance interventions can be optimized in the context of limited health-economic resources. These findings are readily applicable to hospital infection control programmes, and demonstrate the utility of mathematical modelling for understanding the mechanistic aetiology of HCAI, and for informing public health decision-making in the face of infectious threats, be they bacterial or viral, drug-resistant or -susceptible, ancient or newly discovered.

Bibliography

Abbara, S., Cazanave, C., Dubée, V., D'humières, C., Jauréguiberry, S., Kernéis, S., Lefort, A., Lepeule, R., Pilmis, B., Nguyen, L.L., 2020. Classement pragmatique des antibiotiques en fonction de leur spectre et de leur impact écologique à des fins éducatives : résultats d'une enquête Delphi pour le jeu éducatif « Dawaa ». Médecine et Maladies Infectieuses 50, S60. doi:10.1016/j.medmal.2020.06.115

Abbas, Mohamed, Nunes, T.R., Cori, A., Cordey, S., Laubscher, F., Baggio, S., Jombart, T., Iten, A., Vieux, L., Teixeira, D., Perez, M., Pittet, D., Frangos, E., Graf, C.E., Zingg, W., Harbarth, S., 2021a. Explosive nosocomial outbreak of SARS-CoV-2 in a rehabilitation clinic: the limits of genomics for outbreak reconstruction. J. Hosp. Infect. doi:10.1016/j.jhin.2021.07.013

Abbas, Mohamed, Robalo Nunes, T., Martischang, R., Zingg, W., Iten, A., Pittet, D., Harbarth, S., 2021b. Nosocomial transmission and outbreaks of coronavirus disease 2019: the need to protect both patients and healthcare workers. Antimicrob. Resist. Infect. Control 10, 7. doi:10.1186/s13756-020-00875-7

Abbas, M, Zhu, N.J., Mookerjee, S., Bolt, F., Otter, J.A., Holmes, A.H., Price, J.R., 2021. Hospital-onset COVID-19 infection surveillance systems: a systematic review. J. Hosp. Infect. 115, 44–50. doi:10.1016/j.jhin.2021.05.016

Abraham, E.P., Chain, E., 1988. An enzyme from bacteria able to destroy penicillin. 1940. Rev Infect Dis 10, 677–678.

Agence nationale de sécurité du médicament et des produits de santé, 2017. La consommation d'antibiotiques en France en 2016. Agence nationale de sécurité du médicament et des produits de santé.

Akst, J., 2020. RNA Extraction Kits for COVID-19 Tests Are in Short Supply in US [WWW Document]. The Scientist. URL https://www.the-scientist.com/news-opinion/rna-extraction-kits-for-covid-19-tests-are-in-short-supply-in-us-67250 (accessed 8.12.21).

Alemu, A.Y., Endalamaw, A., Bayih, W.A., 2020. The burden of healthcare-associated infection in Ethiopia: a systematic review and meta-analysis. Trop. Med. Health 48, 77. doi:10.1186/s41182-020-00263-2

Alfandari, S., Robert, J., Péan, Y., Rabaud, C., Bedos, J.P., Varon, E., Lepape, A., Bru, J.P., Gauzit, R., French Infectious Diseases Society (French acronym SPILF), the French National Observatory for Epidemiology of Bacterial Resistance to Antibiotics (ONERBA), and the SPA2 group, 2015. Antibiotic use and good practice in 314 French hospitals: The 2010 SPA2 prevalence study. Med Mal Infect 45, 475–480. doi:10.1016/j.medmal.2015.10.001

Ali, S., Birhane, M., Bekele, S., Kibru, G., Teshager, L., Yilma, Y., Ahmed, Y., Fentahun, N., Assefa, H., Gashaw, M., Gudina, E.K., 2018. Healthcare associated infection and its risk factors among patients admitted to a tertiary hospital in Ethiopia: longitudinal study. Antimicrob. Resist. Infect. Control 7, 2. doi:10.1186/s13756-017-0298-5

Allegranzi, B., Nejad, S.B., Pittet, D., 2017. The Burden of Healthcare-Associated Infection, in: Pittet, D., Boyce, J.M., Allegranzi, B. (Eds.), Hand Hygiene: A Handbook for Medical Professionals. John Wiley & Sons, Inc., Hoboken, NJ, USA, pp. 1–7. doi:10.1002/9781118846810.ch1

Allegranzi, B., Pittet, D., 2009. Role of hand hygiene in healthcare-associated infection prevention. J. Hosp. Infect. 73, 305–315. doi:10.1016/j.jhin.2009.04.019

Allen, L.J.S., 2017. A primer on stochastic epidemic models: Formulation, numerical simulation, and analysis. Infect. Dis. Model. 2, 128–142. doi:10.1016/j.idm.2017.03.001

Alquézar-Arbé, A., Piñera, P., Jacob, J., Martín, A., Jiménez, S., Llorens, P., Martín-Sánchez, F.J., Burillo-Putze, G., García-Lamberechts, E.J., González Del Castillo, J., Rizzi, M., Agudo Villa, T., Haro, A., Martín Díaz, N., Miró, Ò., 2020. Impact of the COVID-19 pandemic on hospital emergency departments: results of a survey of departments in 2020 - the Spanish ENCOVUR study. Emergencias 32, 320–331.

Amin-Chowdhury, Z., Aiano, F., Mensah, A., Sheppard, C.L., Litt, D., Fry, N.K., Andrews, N., Ramsay, M.E., Ladhani, S.N., 2021. Impact of the Coronavirus Disease 2019 (COVID-19) Pandemic on Invasive Pneumococcal Disease and Risk of Pneumococcal Coinfection With Severe Acute Respiratory Syndrome Coronavirus 2 (SARS-CoV-2): Prospective National Cohort Study, England. Clin. Infect. Dis. 72, e65–e75. doi:10.1093/cid/ciaa1728

Anand, S., Montez-Rath, M., Han, J., Bozeman, J., Kerschmann, R., Beyer, P., Parsonnet, J., Chertow, G.M., 2020. Prevalence of SARS-CoV-2 antibodies in a large nationwide sample of patients on dialysis in the USA: a cross-sectional study. Lancet.

doi:10.1016/S0140-6736(20)32009-2

Ani, C., Farshidpanah, S., Bellinghausen Stewart, A., Nguyen, H.B., 2015. Variations in organism-specific severe sepsis mortality in the United States: 1999-2008. Crit. Care Med. 43, 65–77. doi:10.1097/CCM.0000000000000555

Ankomah, P., Levin, B.R., 2014. Exploring the collaboration between antibiotics and the immune response in the treatment of acute, self-limiting infections. Proc. Natl. Acad. Sci. USA 111, 8331–8338. doi:10.1073/pnas.1400352111

Antunes, L.C.S., Visca, P., Towner, K.J., 2014. Acinetobacter baumannii: evolution of a global pathogen. Pathog Dis 71, 292–301. doi:10.1111/2049-632X.12125

Archambaud, C., Derré-Bobillot, A., Lapaque, N., Rigottier-Gois, L., Serror, P., 2019. Intestinal translocation of enterococci requires a threshold level of enterococcal overgrowth in the lumen. Sci. Rep. 9, 8926. doi:10.1038/s41598-019-45441-3

Arons, M.M., Hatfield, K.M., Reddy, S.C., Kimball, A., James, A., Jacobs, J.R., Taylor, J., Spicer, K., Bardossy, A.C., Oakley, L.P., Tanwar, S., Dyal, J.W., Harney, J., Chisty, Z., Bell, J.M., Methner, M., Paul, P., Carlson, C.M., McLaughlin, H.P., Thornburg, N., Tong, S., Tamin, A., Tao, Y., Uehara, A., Harcourt, J., Clark, S., Brostrom-Smith, C., Page, L.C., Kay, M., Lewis, J., Montgomery, P., Stone, N.D., Clark, T.A., Honein, M.A., Duchin, J.S., Jernigan, J.A., Public Health–Seattle and King County and CDC COVID-19 Investigation Team, 2020. Presymptomatic SARS-CoV-2 Infections and Transmission in a Skilled Nursing Facility. N. Engl. J. Med. 382, 2081–2090. doi:10.1056/NEJMoa2008457

Asad, H., Johnston, C., Blyth, I., Holborow, A., Bone, A., Porter, L., Tidswell, P., Healy, B., 2020. Health Care Workers and Patients as Trojan Horses: a COVID19 ward outbreak. Infection Prevention in Practice 100073. doi:10.1016/j.infpip.2020.100073

Asante, J., Noreddin, A., El Zowalaty, M.E., 2019. Systematic review of important bacterial zoonoses in africa in the last decade in light of the “one health” concept. Pathogens 8. doi:10.3390/pathogens8020050

Assab, R., Nekkab, N., Crépey, P., Astagneau, P., Guillemot, D., Opatowski, L., Temime, L., 2017. Mathematical models of infection transmission in healthcare settings: recent advances from the use of network structured data. Curr Opin Infect Dis 30, 410–418. doi:10.1097/QCO.0000000000000390

Assab, R., Temime, L., 2016. The role of hand hygiene in controlling norovirus spread in nursing homes. BMC Infect. Dis. 16, 395. doi:10.1186/s12879-016-1702-0

Assurance maladie française, 2021. Évolution de la tarification des tests de dépistage RT-PCR [WWW Document]. URL https://www.ameli.fr/paris/laboratoire-danalyses-medicales/actualites/evolution-de-la-tarification-des-tests-de-depistage-rt-pcr (accessed 8.11.21).

Atmar, R.L., Opekun, A.R., Gilger, M.A., Estes, M.K., Crawford, S.E., Neill, F.H., Ramani, S., Hill, H., Ferreira, J., Graham, D.Y., 2014. Determination of the 50% human infectious dose for Norwalk virus. J. Infect. Dis. 209, 1016–1022. doi:10.1093/infdis/jit620

Auchincloss, A.H., Diez Roux, A.V., 2008. A new tool for epidemiology: the usefulness of dynamic-agent models in understanding place effects on health. Am. J. Epidemiol. 168, 1–8. doi:10.1093/aje/kwn118

Austin, D.J., Kakehashi, M., Anderson, R.M., 1997. The transmission dynamics of antibiotic-resistant bacteria: the relationship between resistance in commensal organisms and antibiotic consumption. Proc. Biol. Sci. 264, 1629–1638. doi:10.1098/rspb.1997.0227

Ayliffe, G.A., Babb, J.R., Collins, B.J., Lowbury, E.J., Newsom, S.W., 1974. Pseudomonas aeruginosa in hospital sinks. Lancet 2, 578–581. doi:10.1016/s0140-6736(74)91893-5

Babad, H.R., Nokes, D.J., Gay, N.J., Miller, E., Morgan-Capner, P., Anderson, R.M., 1995. Predicting the impact of measles vaccination in England and Wales: model validation and analysis of policy options. Epidemiol. Infect. 114, 319–344. doi:10.1017/s0950268800057976

Baccolini, V., Migliara, G., Isonne, C., Dorelli, B., Barone, L.C., Giannini, D., Marotta, D., Marte, M., Mazzalai, E., Alessandri, F., Pugliese, F., Ceccarelli, G., De Vito, C., Marzuillo, C., De Giusti, M., Villari, P., 2021. The impact of the COVID-19 pandemic on healthcare-associated infections in intensive care unit patients: a retrospective cohort study. Antimicrob. Resist. Infect. Control 10, 87. doi:10.1186/s13756-021-00959-y

Bäckhed, F., Ley, R.E., Sonnenburg, J.L., Peterson, D.A., Gordon, J.I., 2005. Host-bacterial mutualism in the human intestine. Science 307, 1915–1920. doi:10.1126/science.1104816

Baggs, J., Fridkin, S.K., Pollack, L.A., Srinivasan, A., Jernigan, J.A., 2016. Estimating national trends in inpatient antibiotic use

among US hospitals from 2006 to 2012. JAMA Intern. Med. 176, 1639–1648. doi:10.1001/jamainternmed.2016.5651

Baggs, J., Jernigan, J.A., Halpin, A.L., Epstein, L., Hatfield, K.M., McDonald, L.C., 2018. Risk of subsequent sepsis within 90 days after a hospital stay by type of antibiotic exposure. Clin. Infect. Dis. 66, 1004–1012. doi:10.1093/cid/cix947

Bailly, B., Guilpain, L., Bouiller, K., Chirouze, C., N'Debi, M., Soulier, A., Demontant, V., Pawlotsky, J.-M., Rodriguez, C., Fourati, S., 2021. BNT162b2 mRNA vaccination did not prevent an outbreak of SARS COV-2 variant 501Y.V2 in an elderly nursing home but reduced transmission and disease severity. Clin. Infect. Dis. doi:10.1093/cid/ciab446

Bakaev, I., Retalic, T., Chen, H., 2020. Universal Testing-Based Response to COVID-19 Outbreak by a Long-Term Care and Post-Acute Care Facility. J. Am. Geriatr. Soc. 68, E38–E39. doi:10.1111/jgs.16653

Baker, M.A., Sands, K.E., Huang, S.S., Kleinman, K., Septimus, E.J., Varma, N., Blanchard, J., Poland, R.E., Coady, M.H., Yokoe, D.S., Fraker, S., Froman, A., Moody, J., Goldin, L., Isaacs, A., Kleja, K., Korwek, K.M., Stelling, J., Clark, A., Platt, R., Perlin, J.B., CDC Prevention Epicenters Program, 2021. The Impact of COVID-19 on Healthcare-Associated Infections. Clin. Infect. Dis. doi:10.1093/cid/ciab688

Bansal, S., Grenfell, B.T., Meyers, L.A., 2007. When individual behaviour matters: homogeneous and network models in epidemiology. J. R. Soc. Interface 4, 879–891. doi:10.1098/rsif.2007.1100

Barbut, F., 1996. Prevalence and Pathogenicity of Clostridium difficile in Hospitalized Patients. Arch. Intern. Med. 156, 1449. doi:10.1001/archinte.1996.00440120107012

Barker, R.O., Astle, A., Spilsbury, K., Hanratty, B., 2021. COVID-19 testing during care home outbreaks: the more the better? Age Ageing. doi:10.1093/ageing/afab100

Baron, S.W., Ostrowsky, B.E., Nori, P., Drory, D.Y., Levi, M.H., Szymczak, W.A., Rinke, M.L., Southern, W.N., 2019. Screening of Clostridioides difficile carriers in an urban academic medical center: Understanding implications of disease. Infect. Control Hosp. Epidemiol. 1–5. doi:10.1017/ice.2019.309

Barreiro, B., Dorca, J., Esteban, L., Prats, E., Escribá, J.M., Verdaguer, R., Gudiol, F., Manresa, F., 1995. Risk factors for the development of Haemophilus influenzae pneumonia in hospitalized adults. Eur. Respir. J. 8, 1543–1547.

Bar-Yoseph, H., Hussein, K., Braun, E., Paul, M., 2016. Natural history and decolonization strategies for ESBL/carbapenem-resistant Enterobacteriaceae carriage: systematic review and meta-analysis. J. Antimicrob. Chemother. 71, 2729–2739. doi:10.1093/jac/dkw221

Bashan, A., Gibson, T.E., Friedman, J., Carey, V.J., Weiss, S.T., Hohmann, E.L., Liu, Y.-Y., 2016. Universality of human microbial dynamics. Nature 534, 259–262. doi:10.1038/nature18301

Bassetti, M., Righi, E., Carnelutti, A., 2016. Bloodstream infections in the Intensive Care Unit. Virulence 7, 267–279. doi:10.1080/21505594.2015.1134072

Bates, D.W., Larizgoitia, I., Prasopa-Plaizier, N., Jha, A.K., Research Priority Setting Working Group of the WHO World Alliance for Patient Safety, 2009. Global priorities for patient safety research. BMJ 338, b1775. doi:10.1136/bmj.b1775

Bauch, C.T., Rao, A.S.R.S., Pham, B.Z., Krahn, M., Gilca, V., Duval, B., Chen, M.H., Tricco, A.C., 2007. A dynamic model for assessing universal Hepatitis A vaccination in Canada. Vaccine 25, 1719–1726. doi:10.1016/j.vaccine.2006.11.020

Baumgartner, M., Bayer, F., Pfrunder-Cardozo, K.R., Buckling, A., Hall, A.R., 2020. Resident microbial communities inhibit growth and antibiotic-resistance evolution of Escherichia coli in human gut microbiome samples. PLoS Biol. 18, e3000465. doi:10.1371/journal.pbio.3000465

Bäumler, A.J., Sperandio, V., 2016. Interactions between the microbiota and pathogenic bacteria in the gut. Nature 535, 85–93. doi:10.1038/nature18849

Baur, D., Gladstone, B.P., Burkert, F., Carrara, E., Foschi, F., Döbele, S., Tacconelli, E., 2017. Effect of antibiotic stewardship on the incidence of infection and colonisation with antibiotic-resistant bacteria and Clostridium difficile infection: a systematic review and meta-analysis. Lancet Infect. Dis. 17, 990–1001. doi:10.1016/S1473-3099(17)30325-0

Bays, D.J., Nguyen, M.-V.H., Cohen, S.H., Waldman, S., Martin, C.S., Thompson, G.R., Sandrock, C., Tourtellotte, J., Pugashetti, J.V., Phan, C., Nguyen, H.H., Warner, G.Y., Penn, B.H., 2020. Investigation of Nosocomial SARS-CoV-2 Transmission from Two Patients to Health Care Workers Identifies Close Contact but not Airborne Transmission Events. Infect. Control Hosp. Epidemiol. 1–22. doi:10.1017/ice.2020.321

Beaudevin, C., Berlivet, L., Boudia, S., Bourgain, C., Cassier, M., Gaudillière, J.-P., Löwy, I., 2021. 'Test, Test, Test!': Scarcity,

Tinkering, and Testing Policy Early in the COVID-19 Epidemic in France. MAT 8, 1–31. doi:10.17157/mat.8.2.5116

Becker, K., Heilmann, C., Peters, G., 2014. Coagulase-negative staphylococci. Clin. Microbiol. Rev. 27, 870–926. doi:10.1128/CMR.00109-13

Begon, M., Bennett, M., Bowers, R.G., French, N.P., Hazel, S.M., Turner, J., 2002. A clarification of transmission terms in host-microparasite models: numbers, densities and areas. Epidemiol. Infect. 129, 147–153. doi:10.1017/s0950268802007148

Ben-Ami, R., Klochendler, A., Seidel, M., Sido, T., Gurel-Gurevich, O., Yassour, M., Meshorer, E., Benedek, G., Fogel, I., Oiknine-Djian, E., Gertler, A., Rotstein, Z., Lavi, B., Dor, Y., Wolf, D.G., Salton, M., Drier, Y., Hebrew University-Hadassah COVID-19 Diagnosis Team, 2020. Large-scale implementation of pooled RNA extraction and RT-PCR for SARS-CoV-2 detection. Clin. Microbiol. Infect. 26, 1248–1253. doi:10.1016/j.cmi.2020.06.009

Bennett MD, J.E., Dolin MD, R., Blaser MD, M.J., 2014. Mandell, Douglas, and Bennett's Principles and Practice of Infectious Diseases: 2-Volume Set, 8th ed. Saunders, Philadelphia, PA.

Bentivegna, E., Luciani, M., Arcari, L., Santino, I., Simmaco, M., Martelletti, P., 2021. Reduction of Multidrug-Resistant (MDR) Bacterial Infections during the COVID-19 Pandemic: A Retrospective Study. Int. J. Environ. Res. Public Health 18. doi:10.3390/ijerph18031003

Béraud, G., Kazmercziak, S., Beutels, P., Levy-Bruhl, D., Lenne, X., Mielcarek, N., Yazdanpanah, Y., Boëlle, P.-Y., Hens, N., Dervaux, B., 2015. The French Connection: The First Large Population-Based Contact Survey in France Relevant for the Spread of Infectious Diseases. PLoS One 10, e0133203. doi:10.1371/journal.pone.0133203

Bergwerk, M., Gonen, T., Lustig, Y., Amit, S., Lipsitch, M., Cohen, C., Mandelboim, M., Gal Levin, E., Rubin, C., Indenbaum, V., Tal, I., Zavitan, M., Zuckerman, N., Bar-Chaim, A., Kreiss, Y., Regev-Yochay, G., 2021. Covid-19 Breakthrough Infections in Vaccinated Health Care Workers. N. Engl. J. Med. doi:10.1056/NEJMoa2109072

Bernier, A., Delarocque-Astagneau, E., Ligier, C., Vibet, M.-A., Guillemot, D., Watier, L., 2014. Outpatient antibiotic use in France between 2000 and 2010: after the nationwide campaign, it is time to focus on the elderly. Antimicrob. Agents Chemother. 58, 71–77. doi:10.1128/AAC.01813-13

Bersano, A., Kraemer, M., Touzé, E., Weber, R., Alamowitch, S., Sibon, I., Pantoni, L., 2020. Stroke care during the COVID-19 pandemic: experience from three large European countries. Eur. J. Neurol. 27, 1794–1800. doi:10.1111/ene.14375

Bhalodi, A.A., van Engelen, T.S.R., Virk, H.S., Wiersinga, W.J., 2019. Impact of antimicrobial therapy on the gut microbiome. J. Antimicrob. Chemother. 74, i6–i15. doi:10.1093/jac/dky530

Bi, Q., Goodman, K.E., Kaminsky, J., Lessler, J., 2019. What is machine learning? A primer for the epidemiologist. Am. J. Epidemiol. 188, 2222–2239. doi:10.1093/aje/kwz189

Bigelow, B.F., Tang, O., Barshick, B., Peters, M., Sisson, S.D., Peairs, K.S., Katz, M.J., 2021. Outcomes of Universal COVID-19 Testing Following Detection of Incident Cases in 11 Long-term Care Facilities. JAMA Intern. Med. 181, 127–129. doi:10.1001/jamainternmed.2020.3738

Birkegård, A.C., Halasa, T., Toft, N., Folkesson, A., Græsbøll, K., 2018. Send more data: a systematic review of mathematical models of antimicrobial resistance. Antimicrob. Resist. Infect. Control 7, 117. doi:10.1186/s13756-018-0406-1

Bjørnstad, O.N., Shea, K., Krzywinski, M., Altman, N., 2020. The SEIRS model for infectious disease dynamics. Nat. Methods 17, 557–558. doi:10.1038/s41592-020-0856-2

Black, J.R.M., Bailey, C., Przewrocka, J., Dijkstra, K.K., Swanton, C., 2020. COVID-19: the case for health-care worker screening to prevent hospital transmission. Lancet 395, 1418–1420. doi:10.1016/S0140-6736(20)30917-X

Blackman, C., Farber, S., Feifer, R.A., Mor, V., White, E.M., 2020. An Illustration of SARS-CoV-2 Dissemination Within a Skilled Nursing Facility Using Heat Maps. J. Am. Geriatr. Soc. 68, 2174–2178. doi:10.1111/jgs.16642

Blair, J.M.A., Webber, M.A., Baylay, A.J., Ogbolu, D.O., Piddock, L.J.V., 2015. Molecular mechanisms of antibiotic resistance. Nat. Rev. Microbiol. 13, 42–51. doi:10.1038/nrmicro3380

Blanquart, F., 2019. Evolutionary epidemiology models to predict the dynamics of antibiotic resistance. Evol. Appl. 12, 365–383. doi:10.1111/eva.12753

Blanquart, F., Lehtinen, S., Lipsitch, M., Fraser, C., 2018. The evolution of antibiotic resistance in a structured host population. J. R. Soc. Interface 15. doi:10.1098/rsif.2018.0040

Bo, L., Li, J., Tao, T., Bai, Y., Ye, X., Hotchkiss, R.S., Kollef, M.H., Crooks, N.H., Deng, X., 2014. Probiotics for preventing

ventilator-associated pneumonia. Cochrane Database Syst. Rev. CD009066. doi:10.1002/14651858.CD009066.pub2

Bogaert, D., van Belkum, A., 2018. Antibiotic treatment and stewardship in the era of microbiota-oriented diagnostics. Eur. J. Clin. Microbiol. Infect. Dis. 37, 795–798. doi:10.1007/s10096-018-3198-6

Böger, B., Fachi, M.M., Vilhena, R.O., Cobre, A.F., Tonin, F.S., Pontarolo, R., 2021. Systematic review with meta-analysis of the accuracy of diagnostic tests for COVID-19. Am. J. Infect. Control 49, 21–29. doi:10.1016/j.ajic.2020.07.011

Bonalumi, G., di Mauro, M., Garatti, A., Barili, F., Gerosa, G., Parolari, A., Italian Society for Cardiac Surgery Task Force on COVID-19 Pandemic, 2020. The COVID-19 outbreak and its impact on hospitals in Italy: the model of cardiac surgery. Eur. J. Cardiothorac. Surg. 57, 1025–1028. doi:10.1093/ejcts/ezaa151

Bonneault, M., Andrianoelina, V.H., Herindrainy, P., Rabenandrasana, M.A.N., Garin, B., Breurec, S., Delarocque-Astagneau, E., Guillemot, D., Andrianirina, Z.Z., Collard, J.-M., Huynh, B.-T., Opatowski, L., 2019. Transmission Routes of Extended-Spectrum Beta-Lactamase-Producing Enterobacteriaceae in a Neonatology Ward in Madagascar. Am. J. Trop. Med. Hyg. 100, 1355–1362. doi:10.4269/ajtmh.18-0410

Bootsma, M.C.J., Bonten, M.J.M., Nijssen, S., Fluit, A.C., Diekmann, O., 2007. An algorithm to estimate the importance of bacterial acquisition routes in hospital settings. Am. J. Epidemiol. 166, 841–851. doi:10.1093/aje/kwm149

Borchering, R.K., Gunning, C.E., Gokhale, D.V., Weedop, K.B., Saeidpour, A., Brett, T.S., Rohani, P., 2021. Anomalous influenza seasonality in the United States and the emergence of novel influenza B viruses. Proc. Natl. Acad. Sci. USA 118. doi:10.1073/pnas.2012327118

Borges do Nascimento, I.J., Cacic, N., Abdulazeem, H.M., von Groote, T.C., Jayarajah, U., Weerasekara, I., Esfahani, M.A., Civile, V.T., Marusic, A., Jeroncic, A., Carvas Junior, N., Pericic, T.P., Zakarija-Grkovic, I., Meirelles Guimarães, S.M., Luigi Bragazzi, N., Bjorklund, M., Sofi-Mahmudi, A., Altujjar, M., Tian, M., Arcani, D.M.C., O'Mathúna, D.P., Marcolino, M.S., 2020. Novel Coronavirus Infection (COVID-19) in Humans: A Scoping Review and Meta-Analysis. J Clin Med 9. doi:10.3390/jcm9040941

Bourgeois-Nicolaos, N., Massias, L., Couson, B., Butel, M.-J., Andremont, A., Doucet-Populaire, F., 2007. Dose dependence of emergence of resistance to linezolid in Enterococcus faecalis in vivo. J. Infect. Dis. 195, 1480–1488. doi:10.1086/513876

Brito, I.L., Alm, E.J., 2016. Tracking Strains in the Microbiome: Insights from Metagenomics and Models. Front. Microbiol. 7, 712. doi:10.3389/fmicb.2016.00712

Brown, K.A., Khanafer, N., Daneman, N., Fisman, D.N., 2013. Meta-analysis of antibiotics and the risk of community-associated Clostridium difficile infection. Antimicrob. Agents Chemother. 57, 2326–2332. doi:10.1128/AAC.02176-12

Bruce-Chwatt, L.J., 1974. Transfusion malaria. Bull. World Health Organ. 50, 337–346.

Brueggemann, A.B., Jansen van Rensburg, M.J., Shaw, D., McCarthy, N.D., Jolley, K.A., Maiden, M.C.J., van der Linden, M.P.G., Amin-Chowdhury, Z., Bennett, D.E., Borrow, R., Brandileone, M.-C.C., Broughton, K., Campbell, R., Cao, B., Casanova, C., Choi, E.H., Chu, Y.W., Clark, S.A., Claus, H., Coelho, J., Corcoran, M., Cottrell, S., Cunney, R.J., Dalby, T., Davies, H., de Gouveia, L., Deghmane, A.-E., Demczuk, W., Desmet, S., Drew, R.J., du Plessis, M., Erlendsdottir, H., Fry, N.K., Fuursted, K., Gray, S.J., Henriques-Normark, B., Hale, T., Hilty, M., Hoffmann, S., Humphreys, H., Ip, M., Jacobsson, S., Johnston, J., Kozakova, J., Kristinsson, K.G., Krizova, P., Kuch, A., Ladhani, S.N., Lâm, T.-T., Lebedova, V., Lindholm, L., Litt, D.J., Martin, I., Martiny, D., Mattheus, W., McElligott, M., Meehan, M., Meiring, S., Mölling, P., Morfeldt, E., Morgan, J., Mulhall, R.M., Muñoz-Almagro, C., Murdoch, D.R., Murphy, J., Musilek, M., Mzabi, A., Perez-Argüello, A., Perrin, M., Perry, M., Redin, A., Roberts, R., Roberts, M., Rokney, A., Ron, M., Scott, K.J., Sheppard, C.L., Siira, L., Skoczyńska, A., Sloan, M., Slotved, H.-C., Smith, A.J., Song, J.Y., Taha, M.-K., Toropainen, M., Tsang, D., Vainio, A., van Sorge, N.M., Varon, E., Vlach, J., Vogel, U., Vohrnova, S., von Gottberg, A., Zanella, R.C., Zhou, F., 2021. Changes in the incidence of invasive disease due to Streptococcus pneumoniae, Haemophilus influenzae, and Neisseria meningitidis during the COVID-19 pandemic in 26 countries and territories in the Invasive Respiratory Infection Surveillance Initiative: a prospective analysis of surveillance data. Lancet Digit. Health 3, e360–e370. doi:10.1016/S2589-7500(21)00077-7

Brümmer, L.E., Katzenschlager, S., Gaeddert, M., Erdmann, C., Schmitz, S., Bota, M., Grilli, M., Larmann, J., Weigand, M.A., Pollock, N.R., Carmona, S., Ongarello, S., Sacks, J., Denkinger, C.M., 2021. The accuracy of novel antigen rapid diagnostics for SARS-CoV-2: a living systematic review and meta-analysis. medRxiv. doi:10.1101/2021.02.26.21252546

Buckle, P., Micocci, M., Tulloch, J., Kierkegaard, P., Parvulescu, P., Thompson, C., Spilsbury, K., Allen, A.J., Body, R., Hayward,

G., Buchan, I., Gordon, A.L., 2021. COVID-19 point-of-care testing in care homes: what are the lessons for policy and practice? Age Ageing. doi:10.1093/ageing/afab101

Buetti, N., Ruckly, S., de Montmollin, E., Reignier, J., Terzi, N., Cohen, Y., Siami, S., Dupuis, C., Timsit, J.-F., 2021. COVID-19 increased the risk of ICU-acquired bloodstream infections: a case-cohort study from the multicentric OUTCOMEREA network. Intensive Care Med. 47, 180–187. doi:10.1007/s00134-021-06346-w

Buffie, C.G., Bucci, V., Stein, R.R., McKenney, P.T., Ling, L., Gobourne, A., No, D., Liu, H., Kinnebrew, M., Viale, A., Littmann, E., van den Brink, M.R.M., Jenq, R.R., Taur, Y., Sander, C., Cross, J.R., Toussaint, N.C., Xavier, J.B., Pamer, E.G., 2015. Precision microbiome reconstitution restores bile acid mediated resistance to Clostridium difficile. Nature 517, 205–208. doi:10.1038/nature13828

Buffie, C.G., Pamer, E.G., 2013. Microbiota-mediated colonization resistance against intestinal pathogens. Nat. Rev. Immunol. 13, 790–801. doi:10.1038/nri3535

Buitrago-Garcia, D., Egli-Gany, D., Counotte, M.J., Hossmann, S., Imeri, H., Ipekci, A.M., Salanti, G., Low, N., 2020. Occurrence and transmission potential of asymptomatic and presymptomatic SARS-CoV-2 infections: A living systematic review and meta-analysis. PLoS Med. 17, e1003346. doi:10.1371/journal.pmed.1003346

Burdet, C., Nguyen, T.T., Duval, X., Ferreira, S., Andremont, A., Guedj, J., Mentré, F., DAV132-CL-1002 Study Group, 2019. Impact of antibiotic gut exposure on the temporal changes in microbiome diversity. Antimicrob. Agents Chemother. 63. doi:10.1128/AAC.00820-19

Cai, Y., Venkatachalam, I., Tee, N.W., Tan, T.Y., Kurup, A., Wong, S.Y., Low, C.Y., Wang, Y., Lee, W., Liew, Y.X., Ang, B., Lye, D.C., Chow, A., Ling, M.L., Oh, H.M., Cuvin, C.A., Ooi, S.T., Pada, S.K., Lim, C.H., Tan, J.W.C., Chew, K.L., Nguyen, V.H., Fisher, D.A., Goossens, H., Kwa, A.L., Tambyah, P.A., Hsu, L.Y., Marimuthu, K., 2017. Prevalence of Healthcare-Associated Infections and Antimicrobial Use Among Adult Inpatients in Singapore Acute-Care Hospitals: Results From the First National Point Prevalence Survey. Clin. Infect. Dis. 64, S61–S67. doi:10.1093/cid/cix103

Caneiras, C., Lito, L., Melo-Cristino, J., Duarte, A., 2019. Community- and Hospital-Acquired *Klebsiella pneumoniae* Urinary Tract Infections in Portugal: Virulence and Antibiotic Resistance. Microorganisms 7. doi:10.3390/microorganisms7050138

Caroff, D.A., Yokoe, D.S., Klompas, M., 2017. Evolving Insights Into the Epidemiology and Control of Clostridium difficile in Hospitals. Clin. Infect. Dis. 65, 1232–1238. doi:10.1093/cid/cix456

Carratalà, J., Garcia-Vidal, C., Ortega, L., Fernández-Sabé, N., Clemente, M., Albero, G., López, M., Castellsagué, X., Dorca, J., Verdaguer, R., Martínez-Montauti, J., Manresa, F., Gudiol, F., 2012. Effect of a 3-step critical pathway to reduce duration of intravenous antibiotic therapy and length of stay in community-acquired pneumonia: a randomized controlled trial. Arch. Intern. Med. 172, 922–928. doi:10.1001/archinternmed.2012.1690

Cassini, A., Högberg, L.D., Plachouras, D., Quattrocchi, A., Hoxha, A., Simonsen, G.S., Colomb-Cotinat, M., Kretzschmar, M.E., Devleesschauwer, B., Cecchini, M., Ouakrim, D.A., Oliveira, T.C., Struelens, M.J., Suetens, C., Monnet, D.L., Burden of AMR Collaborative Group, 2019. Attributable deaths and disability-adjusted life-years caused by infections with antibiotic-resistant bacteria in the EU and the European Economic Area in 2015: a population-level modelling analysis. Lancet Infect. Dis. 19, 56–66. doi:10.1016/S1473-3099(18)30605-4

Cassini, A., Plachouras, D., Eckmanns, T., Abu Sin, M., Blank, H.-P., Ducomble, T., Haller, S., Harder, T., Klingeberg, A., Sixtensson, M., Velasco, E., Weiß, B., Kramarz, P., Monnet, D.L., Kretzschmar, M.E., Suetens, C., 2016. Burden of six healthcare-associated infections on European population health: estimating incidence-based disability-adjusted life years through a population prevalence-based modelling study. PLoS Med. 13, e1002150. doi:10.1371/journal.pmed.1002150

Center for System Science and Engineering at Johns Hopkins University, 2020. COVID-19 Dashboard [WWW Document]. URL https://gisanddata.maps.arcgis.com/apps/dashboards/index.html#/bda7594740fd40299423467b48e9ecf6 (accessed 8.9.21).

Centers for Disease Control and Prevention, n.d. Underlying Cause of Death, 1999-2019 [WWW Document]. URL https://wonder.cdc.gov/Deaths-by-Underlying-Cause.html (accessed 8.23.21).

Cerulli Irelli, E., Orlando, B., Cocchi, E., Morano, A., Fattapposta, F., Di Piero, V., Toni, D., Ciardi, M.R., Giallonardo, A.T., Fabbrini, G., Berardelli, A., Di Bonaventura, C., 2020. The potential impact of enhanced hygienic measures during the COVID-19 outbreak on hospital-acquired infections: A pragmatic study in neurological units. J. Neurol. Sci. 418, 117111. doi:10.1016/j.jns.2020.117111

Cesario, S.K., 2009. Designing health care environments: Part I. Basic concepts, principles, and issues related to evidence-based design. J Contin Educ Nurs 40, 280–288. doi:10.3928/00220124-20090522-09

Chalom, A., Prado, P., 2013. pse: parameter space exploration with Latin hypercubes. R package.

Chatterjee, A., Modarai, M., Naylor, N.R., Boyd, S.E., Atun, R., Barlow, J., Holmes, A.H., Johnson, A., Robotham, J.V., 2018. Quantifying drivers of antibiotic resistance in humans: a systematic review. Lancet Infect. Dis. 18, e368–e378. doi:10.1016/S1473-3099(18)30296-2

Chaudhury, H., Mahmood, A., Valente, M., 2009. The effect of environmental design on reducing nursing errors and increasing efficiency in acute care settings. Environ Behav 41, 755–786. doi:10.1177/0013916508330392

Cheadle, W.G., 2006. Risk factors for surgical site infection. Surg Infect (Larchmt) 7 Suppl 1, S7-11. doi:10.1089/sur.2006.7.s1-7

Chen, H.D., Frankel, G., 2005. Enteropathogenic Escherichia coli: unravelling pathogenesis. FEMS Microbiol. Rev. 29, 83–98. doi:10.1016/j.femsre.2004.07.002

Chen, J.R., Tarver, S.A., Alvarez, K.S., Tran, T., Khan, D.A., 2017. A proactive approach to penicillin allergy testing in hospitalized patients. J Allergy Clin Immunol Pract 5, 686–693. doi:10.1016/j.jaip.2016.09.045

Chen, S., Yang, J., Yang, W., Wang, C., Bärnighausen, T., 2020. COVID-19 control in China during mass population movements at New Year. Lancet 395, 764–766. doi:10.1016/S0140-6736(20)30421-9

Chen, Y., Zhao, J.Y., Shan, X., Han, X.L., Tian, S.G., Chen, F.Y., Su, X.T., Sun, Y.S., Huang, L.Y., Han, L., Chinese Group on Point-Prevalence Survey of Healthcare-Associated Infections, 2017. A point-prevalence survey of healthcare-associated infection in fifty-two Chinese hospitals. J. Hosp. Infect. 95, 105–111. doi:10.1016/j.jhin.2016.08.010

Cheng, V.C.-C., Fung, K.S.-C., Siu, G.K.-H., Wong, S.-C., Cheng, L.S.-K., Wong, M.-S., Lee, L.-K., Chan, W.-M., Chau, K.-Y., Leung, J.S.-L., Chu, A.W.-H., Chan, W.-S., Lu, K.K., Tam, K.K.-G., Ip, J.D., Leung, K.S.-S., Lung, D.C., Tse, H., To, K.K.-W., Yuen, K.-Y., 2021. Nosocomial outbreak of COVID-19 by possible airborne transmission leading to a superspreading event. Clin. Infect. Dis. doi:10.1093/cid/ciab313

Chin, E.T., Huynh, B.Q., Chapman, L.A.C., Murrill, M., Basu, S., Lo, N.C., 2020. Frequency of Routine Testing for Coronavirus Disease 2019 (COVID-19) in High-risk Healthcare Environments to Reduce Outbreaks. Clin. Infect. Dis. doi:10.1093/cid/ciaa1383

Choi, H., Chatterjee, P., Coppin, J.D., Martel, J.A., Hwang, M., Jinadatha, C., Sharma, V.K., 2021. Current understanding of the surface contamination and contact transmission of SARS-CoV-2 in healthcare settings. Environ Chem Lett 1–10. doi:10.1007/s10311-021-01186-y

Chowell, G., Dahal, S., Bono, R., Mizumoto, K., 2021. Harnessing testing strategies and public health measures to avert COVID-19 outbreaks during ocean cruises. medRxiv. doi:10.1101/2021.01.24.21250408

Chrysou, K., Zarkotou, O., Kalofolia, S., Papagiannakopoulou, P., Chrysos, G., Themeli-Digalaki, K., Tsakris, A., Pournaras, S., 2018. First-year results of an antibiotic stewardship program in a Greek tertiary care hospital. Eur. J. Clin. Microbiol. Infect. Dis. 37, 333–337. doi:10.1007/s10096-017-3137-y

Cobey, S., Baskerville, E.B., Colijn, C., Hanage, W., Fraser, C., Lipsitch, M., 2017. Host population structure and treatment frequency maintain balancing selection on drug resistance. J. R. Soc. Interface 14. doi:10.1098/rsif.2017.0295

Coello, R., Glynn, J.R., Gaspar, C., Picazo, J.J., Fereres, J., 1997. Risk factors for developing clinical infection with methicillin-resistant Staphylococcus aureus (MRSA) amongst hospital patients initially only colonized with MRSA. J. Hosp. Infect. 37, 39–46. doi:10.1016/s0195-6701(97)90071-2

Cole, J., Barnard, E., 2021. The impact of the COVID-19 pandemic on healthcare acquired infections with multidrug resistant organisms. Am. J. Infect. Control 49, 653–654. doi:10.1016/j.ajic.2020.09.013

Colijn, C., Cohen, T., 2015. How competition governs whether moderate or aggressive treatment minimizes antibiotic resistance. Elife 4. doi:10.7554/eLife.10559

Collins, J.M., Blumberg, H.M., 2020. The blueprint for prevention of nosocomial tuberculosis transmission is clear, but why don't we have the will to follow it? Clin. Microbiol. Infect. 26, 970–972. doi:10.1016/j.cmi.2020.04.015

Condes, E., Arribas, J.R., COVID19 MADRID-S.P.P.M. group, 2021. Impact of COVID-19 on Madrid hospital system. Enfermedades infecciosas y microbiologia clinica (English ed.) 39, 256–257. doi:10.1016/j.eimc.2020.06.005

Conzade, R., Grant, R., Malik, M.R., Elkholy, A., Elhakim, M., Samhouri, D., Ben Embarek, P.K., Van Kerkhove, M.D., 2018.

Reported Direct and Indirect Contact with Dromedary Camels among Laboratory-Confirmed MERS-CoV Cases. Viruses 10. doi:10.3390/v10080425

Correa-Martínez, C.L., Schwierzeck, V., Mellmann, A., Hennies, M., Kampmeier, S., 2020. Healthcare-Associated SARS-CoV-2 Transmission-Experiences from a German University Hospital. Microorganisms 8. doi:10.3390/microorganisms8091378

Costelloe, C., Metcalfe, C., Lovering, A., Mant, D., Hay, A.D., 2010. Effect of antibiotic prescribing in primary care on antimicrobial resistance in individual patients: systematic review and meta-analysis. BMJ 340, c2096. doi:10.1136/bmj.c2096

Cox, G., Wright, G.D., 2013. Intrinsic antibiotic resistance: mechanisms, origins, challenges and solutions. Int. J. Med. Microbiol. 303, 287–292. doi:10.1016/j.ijmm.2013.02.009

Coyte, K.Z., Schluter, J., Foster, K.R., 2015. The ecology of the microbiome: Networks, competition, and stability. Science 350, 663–666. doi:10.1126/science.aad2602

Crabbé, A., Jensen, P.Ø., Bjarnsholt, T., Coenye, T., 2019. Antimicrobial tolerance and metabolic adaptations in microbial biofilms. Trends Microbiol. 27, 850–863. doi:10.1016/j.tim.2019.05.003

Crass, R.L., Dunn, R., Hong, J., Krop, L.C., Pai, M.P., 2018. Dosing vancomycin in the super obese: less is more. J. Antimicrob. Chemother. 73, 3081–3086. doi:10.1093/jac/dky310

Cravo Oliveira Hashiguchi, T., Ait Ouakrim, D., Padget, M., Cassini, A., Cecchini, M., 2019. Resistance proportions for eight priority antibiotic-bacterium combinations in OECD, EU/EEA and G20 countries 2000 to 2030: a modelling study. Euro Surveill. 24. doi:10.2807/1560-7917.ES.2019.24.20.1800445

Croisier, D., Etienne, M., Bergoin, E., Charles, P.-E., Lequeu, C., Piroth, L., Portier, H., Chavanet, P., 2004. Mutant selection window in levofloxacin and moxifloxacin treatments of experimental pneumococcal pneumonia in a rabbit model of human therapy. Antimicrob. Agents Chemother. 48, 1699–1707. doi:10.1128/AAC.48.5.1699-1707.2004

Cui, J., Liu, Y., Wang, R., Tong, W., Drlica, K., Zhao, X., 2006. The mutant selection window in rabbits infected with Staphylococcus aureus. J. Infect. Dis. 194, 1601–1608. doi:10.1086/508752

d'Ettorre, G., Ceccarelli, G., Marazzato, M., Campagna, G., Pinacchio, C., Alessandri, F., Ruberto, F., Rossi, G., Celani, L., Scagnolari, C., Mastropietro, C., Trinchieri, V., Recchia, G.E., Mauro, V., Antonelli, G., Pugliese, F., Mastroianni, C.M., 2020. Challenges in the Management of SARS-CoV2 Infection: The Role of Oral Bacteriotherapy as Complementary Therapeutic Strategy to Avoid the Progression of COVID-19. Front Med (Lausanne) 7, 389. doi:10.3389/fmed.2020.00389

D'Adamo, H., Yoshikawa, T., Ouslander, J.G., 2020. Coronavirus Disease 2019 in Geriatrics and Long-Term Care: The ABCDs of COVID-19. J. Am. Geriatr. Soc. 68, 912–917. doi:10.1111/jgs.16445

Dagan, N., Barda, N., Kepten, E., Miron, O., Perchik, S., Katz, M.A., Hernán, M.A., Lipsitch, M., Reis, B., Balicer, R.D., 2021. BNT162b2 mRNA Covid-19 Vaccine in a Nationwide Mass Vaccination Setting. N. Engl. J. Med. 384, 1412–1423. doi:10.1056/NEJMoa2101765

Dan-Nwafor, C.C., Ipadeola, O., Smout, E., Ilori, E., Adeyemo, A., Umeokonkwo, C., Nwidi, D., Nwachukwu, W., Ukponu, W., Omabe, E., Anaebonam, U., Igwenyi, N., Igbodo, G., Eteng, W., Uzoma, I., Saleh, M., Agboeze, J., Mutbam, S., de Gooyer, T., Short, R., Aniaku, E., Onoh, R., Ogah, E., Nguku, P., Oladejo, J., Peter, C., Ojo, O., Ihekweazu, C., 2019. A cluster of nosocomial Lassa fever cases in a tertiary health facility in Nigeria: Description and lessons learned, 2018. Int. J. Infect. Dis. 83, 88–94. doi:10.1016/j.ijid.2019.03.030

Dassner, A.M., Girotto, J.E., 2018. Evaluation of a Second-Sign Process for Antimicrobial Prior Authorization. J. Pediatric Infect. Dis. Soc. 7, 113–118. doi:10.1093/jpids/pix015

Davey, P., Marwick, C.A., Scott, C.L., Charani, E., McNeil, K., Brown, E., Gould, I.M., Ramsay, C.R., Michie, S., 2017. Interventions to improve antibiotic prescribing practices for hospital inpatients. Cochrane Database Syst. Rev. 2, CD003543. doi:10.1002/14651858.CD003543.pub4

Davido, Benjamin, Batista, R., Dinh, A., de Truchis, P., Terveer, E.M., Roberts, B., Kuijper, E.J., Caballero, S., 2019. Fifty shades of graft: How to improve the efficacy of faecal microbiota transplantation for decolonization of antibiotic-resistant bacteria. Int. J. Antimicrob. Agents 53, 553–556. doi:10.1016/j.ijantimicag.2019.03.008

Davido, B, Batista, R., Fessi, H., Michelon, H., Escaut, L., Lawrence, C., Denis, M., Perronne, C., Salomon, J., Dinh, A., 2019. Fecal microbiota transplantation to eradicate vancomycin-resistant enterococci colonization in case of an outbreak. Med Mal Infect 49, 214–218. doi:10.1016/j.medmal.2018.11.002

Davies, N.G., Flasche, S., Jit, M., Atkins, K.E., 2019. Within-host dynamics shape antibiotic resistance in commensal bacteria. Nat. Ecol. Evol. 3, 440–449. doi:10.1038/s41559-018-0786-x

Davis, B., Rothrock, A.N., Swetland, S., Andris, H., Davis, P., Rothrock, S.G., 2020. Viral and atypical respiratory co-infections in COVID-19: a systematic review and meta-analysis. Journal of the American College of Emergency Physicians Open. doi:10.1002/emp2.12128

Day, T., Alizon, S., Mideo, N., 2011. Bridging scales in the evolution of infectious disease life histories: theory. Evolution 65, 3448–3461. doi:10.1111/j.1558-5646.2011.01394.x

Day, T., Read, A.F., 2016. Does High-Dose Antimicrobial Chemotherapy Prevent the Evolution of Resistance? PLoS Comput. Biol. 12, e1004689. doi:10.1371/journal.pcbi.1004689

D'Costa, V.M., King, C.E., Kalan, L., Morar, M., Sung, W.W.L., Schwarz, C., Froese, D., Zazula, G., Calmels, F., Debruyne, R., Golding, G.B., Poinar, H.N., Wright, G.D., 2011. Antibiotic resistance is ancient. Nature 477, 457–461. doi:10.1038/nature10388

de Gunzburg, J., Ducher, A., Modess, C., Wegner, D., Oswald, S., Dressman, J., Augustin, V., Feger, C., Andremont, A., Weitschies, W., Siegmund, W., 2015. Targeted adsorption of molecules in the colon with the novel adsorbent-based medicinal product, DAV132: A proof of concept study in healthy subjects. J. Clin. Pharmacol. 55, 10–16. doi:10.1002/jcph.359

de Gunzburg, J., Ghozlane, A., Ducher, A., Le Chatelier, E., Duval, X., Ruppé, E., Armand-Lefevre, L., Sablier-Gallis, F., Burdet, C., Alavoine, L., Chachaty, E., Augustin, V., Varastet, M., Levenez, F., Kennedy, S., Pons, N., Mentré, F., Andremont, A., 2018. Protection of the human gut microbiome from antibiotics. J. Infect. Dis. 217, 628–636. doi:10.1093/infdis/jix604

de Roode, J.C., Culleton, R., Bell, A.S., Read, A.F., 2004. Competitive release of drug resistance following drug treatment of mixed Plasmodium chabaudi infections. Malar. J. 3, 33. doi:10.1186/1475-2875-3-33

de Salazar, A., Aguilera, A., Trastoy, R., Fuentes, A., Alados, J.C., Causse, M., Galán, J.C., Moreno, A., Trigo, M., Pérez-Ruiz, M., Roldán, C., José Pena, M., Bernal, S., Serrano-Conde, E., Barbeito, G., Torres, E., Riazzo, C., Cortes-Cuevas, J.L., Chueca, N., Coira, A., Sanchez-Calvo, J.M., Marfil, E., Becerra, F., Gude, M.J., Pallarés, Á., Pérez Del Molino, M.L., García, F., 2020. Sample pooling for SARS-COV-2 RT-PCR screening. Clin. Microbiol. Infect. doi:10.1016/j.cmi.2020.09.008

de Wit, E., van Doremalen, N., Falzarano, D., Munster, V.J., 2016. SARS and MERS: recent insights into emerging coronaviruses. Nat. Rev. Microbiol. 14, 523–534. doi:10.1038/nrmicro.2016.81

de Wit, R., Bouvier, T., 2006. "Everything is everywhere, but, the environment selects"; what did Baas Becking and Beijerinck really say? Environ. Microbiol. 8, 755–758. doi:10.1111/j.1462-2920.2006.01017.x

Deeks, J.J., Raffle, A.E., 2020. Lateral flow tests cannot rule out SARS-CoV-2 infection. BMJ 371, m4787. doi:10.1136/bmj.m4787

Department of Health & Social Care, 2020. Admission and Care of Residents during COVID-19 Incident in a Care Home.

Dethlefsen, L., Relman, D.A., 2011. Incomplete recovery and individualized responses of the human distal gut microbiota to repeated antibiotic perturbation. Proc. Natl. Acad. Sci. USA 108 Suppl 1, 4554–4561. doi:10.1073/pnas.1000087107

Dettenkofer, M., Seegers, S., Antes, G., Motschall, E., Schumacher, M., Daschner, F.D., 2004. Does the architecture of hospital facilities influence nosocomial infection rates? A systematic review. Infect. Control Hosp. Epidemiol. 25, 21–25. doi:10.1086/502286

Devaud, M., Kayser, F.H., Bächi, B., 1982. Transposon-mediated multiple antibiotic resistance in Acinetobacter strains. Antimicrob. Agents Chemother. 22, 323–329. doi:10.1128/AAC.22.2.323

Di Pilato, V., Codda, G., Ball, L., Giacobbe, D.R., Willison, E., Mikulska, M., Magnasco, L., Crea, F., Vena, A., Pelosi, P., Bassetti, M., Marchese, A., 2021. Molecular Epidemiological Investigation of a Nosocomial Cluster of C. auris: Evidence of Recent Emergence in Italy and Ease of Transmission during the COVID-19 Pandemic. J. Fungi (Basel) 7. doi:10.3390/jof7020140

Di Ruscio, F., Guzzetta, G., Bjørnholt, J.V., Leegaard, T.M., Moen, A.E.F., Merler, S., Freiesleben de Blasio, B., 2019. Quantifying the transmission dynamics of MRSA in the community and healthcare settings in a low-prevalence country. Proc. Natl. Acad. Sci. USA 116, 14599–14605. doi:10.1073/pnas.1900959116

DiazGranados, C.A., 2012. Prospective audit for antimicrobial stewardship in intensive care: impact on resistance and clinical outcomes. Am. J. Infect. Control 40, 526–529. doi:10.1016/j.ajic.2011.07.011

Diel, R., Nienhaus, A., 2021. Point-of-care COVID-19 antigen testing in German emergency rooms - a cost-benefit analysis. Pulmonology. doi:10.1016/j.pulmoe.2021.06.009

Dinnes, J., 2021. COVID-19 rapid antigen testing strategies require careful evaluation. EBioMedicine 70, 103491. doi:10.1016/j.ebiom.2021.103491

Doan, T., Hinterwirth, A., Worden, L., Arzika, A.M., Maliki, R., Abdou, A., Kane, S., Zhong, L., Cummings, S.L., Sakar, S., Chen, C., Cook, C., Lebas, E., Chow, E.D., Nachamkin, I., Porco, T.C., Keenan, J.D., Lietman, T.M., 2019. Gut microbiome alteration in MORDOR I: a community-randomized trial of mass azithromycin distribution. Nat. Med. 25, 1370–1376. doi:10.1038/s41591-019-0533-0

Dolejska, M., Villa, L., Poirel, L., Nordmann, P., Carattoli, A., 2013. Complete sequencing of an IncHI1 plasmid encoding the carbapenemase NDM-1, the ArmA 16S RNA methylase and a resistance-nodulation-cell division/multidrug efflux pump. J. Antimicrob. Chemother. 68, 34–39. doi:10.1093/jac/dks357

Domenech de Cellès, M., Arduin, H., Lévy-Bruhl, D., Georges, S., Souty, C., Guillemot, D., Watier, L., Opatowski, L., 2019. Unraveling the seasonal epidemiology of pneumococcus. Proc. Natl. Acad. Sci. USA 116, 1802–1807. doi:10.1073/pnas.1812388116

Domenech de Cellès, M., Opatowski, L., Salomon, J., Varon, E., Carbon, C., Boëlle, P.-Y., Guillemot, D., 2011. Intrinsic epidemicity of Streptococcus pneumoniae depends on strain serotype and antibiotic susceptibility pattern. Antimicrob. Agents Chemother. 55, 5255–5261. doi:10.1128/AAC.00249-11

Domenech de Cellès, M., Zahar, J.-R., Abadie, V., Guillemot, D., 2013. Limits of patient isolation measures to control extended-spectrum beta-lactamase-producing Enterobacteriaceae: model-based analysis of clinical data in a pediatric ward. BMC Infect. Dis. 13, 187. doi:10.1186/1471-2334-13-187

Donker, T., Henderson, K.L., Hopkins, K.L., Dodgson, A.R., Thomas, S., Crook, D.W., Peto, T.E.A., Johnson, A.P., Woodford, N., Walker, A.S., Robotham, J.V., 2017. The relative importance of large problems far away versus small problems closer to home: insights into limiting the spread of antimicrobial resistance in England. BMC Med. 15, 86. doi:10.1186/s12916-017-0844-2

Dorfman, R., 1943. The detection of defective members of large populations. Ann. Math. Statist. 14, 436–440. doi:10.1214/aoms/1177731363

Doron, S., Davidson, L.E., 2011. Antimicrobial stewardship. Mayo Clin. Proc. 86, 1113–1123. doi:10.4065/mcp.2011.0358

Drlica, K., 2003. The mutant selection window and antimicrobial resistance. J. Antimicrob. Chemother. 52, 11–17. doi:10.1093/jac/dkg269

Drzewiecka, D., 2016. Significance and Roles of Proteus spp. Bacteria in Natural Environments. Microb. Ecol. 72, 741–758. doi:10.1007/s00248-015-0720-6

Durham, D.P., Olsen, M.A., Dubberke, E.R., Galvani, A.P., Townsend, J.P., 2016. Quantifying Transmission of Clostridium difficile within and outside Healthcare Settings. Emerging Infect. Dis. 22, 608–616. doi:10.3201/eid2204.150455

Duval, A., 2019. Comprendre et contrôler la transmission des bactéries multirésistantes par l'analyse et la modélisation des réseaux d'interactions interindividuelles en milieu hospitalier (Doctoral dissertation).

Duval, A., Obadia, T., Boëlle, P.-Y., Fleury, E., Herrmann, J.-L., Guillemot, D., Temime, L., Opatowski, L., i-Bird Study group, 2019a. Close proximity interactions support transmission of ESBL-K. pneumoniae but not ESBL-E. coli in healthcare settings. PLoS Comput. Biol. 15, e1006496. doi:10.1371/journal.pcbi.1006496

Duval, A., Obadia, T., Martinet, L., Boëlle, P.-Y., Fleury, E., Guillemot, D., Opatowski, L., Temime, L., I-Bird study group, 2018. Measuring dynamic social contacts in a rehabilitation hospital: effect of wards, patient and staff characteristics. Sci. Rep. 8, 1686. doi:10.1038/s41598-018-20008-w

Duval, A., Smith, D., Guillemot, D., Opatowski, L., Temime, L., 2019b. CTCmodeler: An Agent-Based Framework to Simulate Pathogen Transmission Along an Inter-individual Contact Network in a Hospital, in: Rodrigues, J.M.F., Cardoso, P.J.S., Monteiro, J., Lam, R., Krzhizhanovskaya, V.V., Lees, M.H., Dongarra, J.J., Sloot, P.M.A. (Eds.), Computational Science – ICCS 2019: 19th International Conference, Faro, Portugal, June 12–14, 2019, Proceedings, Part II, Lecture Notes in Computer Science. Springer International Publishing, Cham, pp. 477–487. doi:10.1007/978-3-030-22741-8_34

Dykhuizen, D., 2005. Species numbers in bacteria. Proc. Calif. Acad. Sci. 56, 62–71.

Eberhardt, J.N., Breuckmann, N.P., Eberhardt, C.S., 2020. Multi-Stage Group Testing Improves Efficiency of Large-Scale COVID-19 Screening. J. Clin. Virol. 128, 104382. doi:10.1016/j.jcv.2020.104382

Ebrahimi, F., Mózes, J., Monostori, J., Gorácz, O., Fésűs, A., Majoros, L., Szarka, K., Kardos, G., 2016. Comparison of rates of fecal colonization with extended-spectrum beta-lactamase-producing enterobacteria among patients in different wards, outpatients and medical students. Microbiol. Immunol. 60, 285–294. doi:10.1111/1348-0421.12373

ECDC Public Health Emergency Team, Danis, K., Fonteneau, L., Georges, S., Daniau, C., Bernard-Stoecklin, S., Domegan, L., O'Donnell, J., Hauge, S.H., Dequeker, S., Vandael, E., Van der Heyden, J., Renard, F., Sierra, N.B., Ricchizzi, E., Schweickert, B., Schmidt, N., Abu Sin, M., Eckmanns, T., Paiva, J.-A., Schneider, E., 2020. High impact of COVID-19 in long-term care facilities, suggestion for monitoring in the EU/EEA, May 2020. Euro Surveill. 25. doi:10.2807/1560-7917.ES.2020.25.22.2000956

Elias, J., Health Office in the Rural District Office Wartburgkreis, Claus, H., Frosch, M., Vogel, U., 2006. Evidence for indirect nosocomial transmission of Neisseria meningitidis resulting in two cases of invasive meningococcal disease. J. Clin. Microbiol. 44, 4276–4278. doi:10.1128/JCM.00613-06

Elliott, E.J., 2007. Acute gastroenteritis in children. BMJ 334, 35–40. doi:10.1136/bmj.39036.406169.80

Escobar, D.J., Lanzi, M., Saberi, P., Love, R., Linkin, D.R., Kelly, J.J., Jhala, D., Amorosa, V., Hofmann, M., Doyon, J.B., 2021. Mitigation of a coronavirus disease 2019 outbreak in a nursing home through serial testing of residents and staff. Clin. Infect. Dis. 72, e394–e396. doi:10.1093/cid/ciaa1021

Estrela, S., Brown, S.P., 2018. Community interactions and spatial structure shape selection on antibiotic resistant lineages. PLoS Comput. Biol. 14, e1006179. doi:10.1371/journal.pcbi.1006179

Estrela, S., Whiteley, M., Brown, S.P., 2015. The demographic determinants of human microbiome health. Trends Microbiol. 23, 134–141. doi:10.1016/j.tim.2014.11.005

Etienne, M., Croisier, D., Charles, P.-E., Lequeu, C., Piroth, L., Portier, H., Drlica, K., Chavanet, P., 2004. Effect of low-level resistance on subsequent enrichment of fluoroquinolone-resistant Streptococcus pneumoniae in rabbits. J. Infect. Dis. 190, 1472–1475. doi:10.1086/423853

European Centre for Disease Prevention and Control, 2008. Annual Epidemiological Report on Communicable Diseases in Europe 2008. European Centre for Disease Prevention and Control, Stockholm.

Evans, D.R., Griffith, M.P., Sundermann, A.J., Shutt, K.A., Saul, M.I., Mustapha, M.M., Marsh, J.W., Cooper, V.S., Harrison, L.H., Van Tyne, D., 2020. Systematic detection of horizontal gene transfer across genera among multidrug-resistant bacteria in a single hospital. Elife 9. doi:10.7554/eLife.53886

Evans, S., Agnew, E., Vynnycky, E., Robotham, J.V., 2020. The impact of testing and infection prevention and control strategies on within-hospital transmission dynamics of COVID-19 in English hospitals. medRxiv. doi:10.1101/2020.05.12.20095562

Falagas, M.E., Kasiakou, S.K., 2005. Colistin: the revival of polymyxins for the management of multidrug-resistant gram-negative bacterial infections. Clin. Infect. Dis. 40, 1333–1341. doi:10.1086/429323

Feazel, L.M., Malhotra, A., Perencevich, E.N., Kaboli, P., Diekema, D.J., Schweizer, M.L., 2014. Effect of antibiotic stewardship programmes on Clostridium difficile incidence: a systematic review and meta-analysis. J. Antimicrob. Chemother. 69, 1748–1754. doi:10.1093/jac/dku046

Ferjani, S., Saidani, M., Amine, F.S., Boutiba Ben Boubaker, I., 2015. A comparative study of antimicrobial resistance rates and phylogenetic groups of community-acquired versus hospital-acquired invasive Escherichia coli. Med Mal Infect 45, 133–138. doi:10.1016/j.medmal.2015.01.012

Ferretti, L., Wymant, C., Kendall, M., Zhao, L., Nurtay, A., Abeler-Dörner, L., Parker, M., Bonsall, D., Fraser, C., 2020. Quantifying SARS-CoV-2 transmission suggests epidemic control with digital contact tracing. Science 368. doi:10.1126/science.abb6936

Fey, P.D., Saïd-Salim, B., Rupp, M.E., Hinrichs, S.H., Boxrud, D.J., Davis, C.C., Kreiswirth, B.N., Schlievert, P.M., 2003. Comparative molecular analysis of community- or hospital-acquired methicillin-resistant Staphylococcus aureus. Antimicrob. Agents Chemother. 47, 196–203. doi:10.1128/AAC.47.1.196-203.2003

Finlay, B.B., Amato, K.R., Azad, M., Blaser, M.J., Bosch, T.C.G., Chu, H., Dominguez-Bello, M.G., Ehrlich, S.D., Elinav, E., Geva-Zatorsky, N., Gros, P., Guillemin, K., Keck, F., Korem, T., McFall-Ngai, M.J., Melby, M.K., Nichter, M., Pettersson, S., Poinar, H., Rees, T., Tropini, C., Zhao, L., Giles-Vernick, T., 2021. The hygiene hypothesis, the COVID pandemic, and consequences for the human microbiome. Proc. Natl. Acad. Sci. USA 118. doi:10.1073/pnas.2010217118

Firsov, A.A., Smirnova, M.V., Lubenko, I.Y., Vostrov, S.N., Portnoy, Y.A., Zinner, S.H., 2006. Testing the mutant selection window hypothesis with Staphylococcus aureus exposed to daptomycin and vancomycin in an in vitro dynamic model. J. Antimicrob. Chemother. 58, 1185–1192. doi:10.1093/jac/dkl387

Firsov, A.A., Vostrov, S.N., Lubenko, I.Y., Arzamastsev, A.P., Portnoy, Y.A., Zinner, S.H., 2004. ABT492 and levofloxacin: comparison of their pharmacodynamics and their abilities to prevent the selection of resistant Staphylococcus aureus in an in vitro dynamic model. J. Antimicrob. Chemother. 54, 178–186. doi:10.1093/jac/dkh242

Firsov, A.A., Vostrov, S.N., Lubenko, I.Y., Drlica, K., Portnoy, Y.A., Zinner, S.H., 2003. In vitro pharmacodynamic evaluation of the mutant selection window hypothesis using four fluoroquinolones against Staphylococcus aureus. Antimicrob. Agents Chemother. 47, 1604–1613. doi:10.1128/AAC.47.5.1604-1613.2003

Fisher-Hoch, S.P., 2005. Lessons from nosocomial viral haemorrhagic fever outbreaks. Br Med Bull 73–74, 123–137. doi:10.1093/bmb/ldh054

Fisman, D., Lapointe-Shaw, L., Bogoch, I., McCready, J., Tuite, A., 2020. Failing our Most Vulnerable: COVID-19 and Long-Term Care Facilities in Ontario. medRxiv. doi:10.1101/2020.04.14.20065557

Fisman, D.N., Bogoch, I., Lapointe-Shaw, L., McCready, J., Tuite, A.R., 2020. Risk Factors Associated With Mortality Among Residents With Coronavirus Disease 2019 (COVID-19) in Long-term Care Facilities in Ontario, Canada. JAMA Netw. Open 3, e2015957. doi:10.1001/jamanetworkopen.2020.15957

Fouillet, A., Bousquet, V., Pontais, I., Gallay, A., Caserio- Schönemann, C., 2015. The French Emergency Department OSCOUR Network: Evaluation After a 10-year Existence. Online J. Public Health Inform. 7. doi:10.5210/ojphi.v7i1.5740

Frame, J.D., Baldwin, J.M., Gocke, D.J., Troup, J.M., 1970. Lassa fever, a new virus disease of man from West Africa. I. Clinical description and pathological findings. Am. J. Trop. Med. Hyg. 19, 670–676. doi:10.4269/ajtmh.1970.19.670

Friedman, J., Higgins, L.M., Gore, J., 2017. Community structure follows simple assembly rules in microbial microcosms. Nat. Ecol. Evol. 1, 109. doi:10.1038/s41559-017-0109

Friedman, N.D., Temkin, E., Carmeli, Y., 2016. The negative impact of antibiotic resistance. Clin. Microbiol. Infect. 22, 416–422. doi:10.1016/j.cmi.2015.12.002

Fuller, J., 2020. Models v. Evidence. Boston Review.

Galea, S., 2013. An argument for a consequentialist epidemiology. Am. J. Epidemiol. 178, 1185–1191. doi:10.1093/aje/kwt172

Gandhi, M., Yokoe, D.S., Havlir, D.V., 2020. Asymptomatic Transmission, the Achilles' Heel of Current Strategies to Control Covid-19. N. Engl. J. Med. 382, 2158–2160. doi:10.1056/NEJMe2009758

Gangarosa, R.E., Glass, R.I., Lew, J.F., Boring, J.R., 1992. Hospitalizations involving gastroenteritis in the United States, 1985: the special burden of the disease among the elderly. Am. J. Epidemiol. 135, 281–290. doi:10.1093/oxfordjournals.aje.a116282

Garmendia, J., Frankel, G., Crepin, V.F., 2005. Enteropathogenic and enterohemorrhagic Escherichia coli infections: translocation, translocation, translocation. Infect. Immun. 73, 2573–2585. doi:10.1128/IAI.73.5.2573-2585.2005

Gastmeier, P., Bräuer, H., Sohr, D., Geffers, C., Forster, D.H., Daschner, F., Rüden, H., 2001. Converting incidence and prevalence data of nosocomial infections: results from eight hospitals. Infect. Control Hosp. Epidemiol. 22, 31–34. doi:10.1086/501821

Gaur, S., Dumyati, G., Nace, D.A., Jump, R.L.P., 2020. Unprecedented solutions for extraordinary times: Helping long-term care settings deal with the COVID-19 pandemic. Infect. Control Hosp. Epidemiol. 41, 729–730. doi:10.1017/ice.2020.98

Gear, J.S., Cassel, G.A., Gear, A.J., Trappler, B., Clausen, L., Meyers, A.M., Kew, M.C., Bothwell, T.H., Sher, R., Miller, G.B., Schneider, J., Koornhof, H.J., Gomperts, E.D., Isaäcson, M., Gear, J.H., 1975. Outbreake of Marburg virus disease in Johannesburg. Br. Med. J. 4, 489–493. doi:10.1136/bmj.4.5995.489

Genestet, C., Paret, R., Pichat, C., Berland, J.-L., Jacomo, V., Carret, G., Fredenucci, I., Hodille, E., Rasigade, J.-P., Boisset, S., Carricajo, A., Lina, G., Ronnaux-Baron, A.-S., Mornex, J.-F., Grando, J., Sénéchal, A., Ader, F., Dumitrescu, O., Lyon TB study group, 2020. Routine survey of Mycobacterium tuberculosis isolates reveals nosocomial transmission. Eur. Respir. J. 55. doi:10.1183/13993003.01888-2019

Ghosh, S., Rajwade, A., Krishna, Srikar, Gopalkrishnan, N., Schaus, T.E., Chakravarthy, A., Varahan, S., Appu, V., Ramakrishnan, R., Ch, S., Jindal, M., Bhupathi, V., Gupta, A., Jain, A., Agarwal, R., Pathak, S., Rehan, M.A., Consul, S., Gupta, Y., Gupta, N., Agarwal, P., Goyal, R., Sagar, V., Ramakrishnan, U., Krishna, Sandeep, Yin, P., Palakodeti, D., Gopalkrishnan,

M., 2020. Tapestry: A Single-Round Smart Pooling Technique for COVID-19 Testing. medRxiv. doi:10.1101/2020.04.23.20077727

Gillespie, D.T., 1977. Exact stochastic simulation of coupled chemical reactions. J. Phys. Chem. 81, 2340–2361. doi:10.1021/j100540a008

Gingras, G., Guertin, M.-H., Laprise, J.-F., Drolet, M., Brisson, M., 2016. Mathematical Modeling of the Transmission Dynamics of Clostridium difficile Infection and Colonization in Healthcare Settings: A Systematic Review. PLoS One 11, e0163880. doi:10.1371/journal.pone.0163880

Gjini, E., Paupério, F.F.S., Ganusov, V.V., 2020. Treatment timing shifts the benefits of short and long antibiotic treatment over infection. Evol Med Public Health 2020, 249–263. doi:10.1093/emph/eoaa033

Goessens, W.H.F., Mouton, J.W., ten Kate, M.T., Bijl, A.J., Ott, A., Bakker-Woudenberg, I.A.J.M., 2007. Role of ceftazidime dose regimen on the selection of resistant Enterobacter cloacae in the intestinal flora of rats treated for an experimental pulmonary infection. J. Antimicrob. Chemother. 59, 507–516. doi:10.1093/jac/dkl529

Goldberg, S.A., Lennerz, J., Klompas, M., Mark, E., Pierce, V.M., Thompson, R.W., Pu, C.T., Ritterhouse, L.L., Dighe, A., Rosenberg, E.S., Grabowski, D.C., 2021. Presymptomatic Transmission of Severe Acute Respiratory Syndrome Coronavirus 2 Among Residents and Staff at a Skilled Nursing Facility: Results of Real-time Polymerase Chain Reaction and Serologic Testing. Clin. Infect. Dis. 72, 686–689. doi:10.1093/cid/ciaa991

Gordis, L., 2008. Epidemiology, 4th ed. Saunders, Philadelphia.

Goto, M., Al-Hasan, M.N., 2013. Overall burden of bloodstream infection and nosocomial bloodstream infection in North America and Europe. Clin. Microbiol. Infect. 19, 501–509. doi:10.1111/1469-0691.12195

Graber, C.J., Jones, M.M., Glassman, P.A., Weir, C., Butler, J., Nechodom, K., Kay, C.L., Furman, A.E., Tran, T.T., Foltz, C., Pollack, L.A., Samore, M.H., Goetz, M.B., 2015. Taking an Antibiotic Time-out: Utilization and Usability of a Self-Stewardship Time-out Program for Renewal of Vancomycin and Piperacillin-Tazobactam. Hosp Pharm 50, 1011–1024. doi:10.1310/hpj5011-1011

Grant, R., Malik, M.R., Elkholy, A., Van Kerkhove, M.D., 2019. A review of asymptomatic and subclinical middle east respiratory syndrome coronavirus infections. Epidemiol Rev 41, 69–81. doi:10.1093/epirev/mxz009

Grard, G., Fair, J.N., Lee, D., Slikas, E., Steffen, I., Muyembe, J.-J., Sittler, T., Veeraraghavan, N., Ruby, J.G., Wang, C., Makuwa, M., Mulembakani, P., Tesh, R.B., Mazet, J., Rimoin, A.W., Taylor, T., Schneider, B.S., Simmons, G., Delwart, E., Wolfe, N.D., Chiu, C.Y., Leroy, E.M., 2012. A novel rhabdovirus associated with acute hemorrhagic fever in central Africa. PLoS Pathog. 8, e1002924. doi:10.1371/journal.ppat.1002924

Grasselli, G., Pesenti, A., Cecconi, M., 2020. Critical Care Utilization for the COVID-19 Outbreak in Lombardy, Italy: Early Experience and Forecast During an Emergency Response. JAMA 323, 1545–1546. doi:10.1001/jama.2020.4031

Grassly, N.C., Pons-Salort, M., Parker, E.P.K., White, P.J., Ferguson, N.M., Imperial College COVID-19 Response Team, 2020. Comparison of molecular testing strategies for COVID-19 control: a mathematical modelling study. Lancet Infect. Dis. 20, 1381–1389. doi:10.1016/S1473-3099(20)30630-7

Greenhalgh, T., Jimenez, J.L., Prather, K.A., Tufekci, Z., Fisman, D., Schooley, R., 2021. Ten scientific reasons in support of airborne transmission of SARS-CoV-2. Lancet 397, 1603–1605. doi:10.1016/S0140-6736(21)00869-2

Greig, J.D., Lee, M.B., 2012. A review of nosocomial norovirus outbreaks: infection control interventions found effective. Epidemiol. Infect. 140, 1151–1160. doi:10.1017/S0950268811002731

Greischar, M.A., Beck-Johnson, L.M., Mideo, N., 2019. Partitioning the influence of ecology across scales on parasite evolution. Evolution 73, 2175–2188. doi:10.1111/evo.13840

Gross, J.V., Mohren, J., Erren, T.C., 2021. COVID-19 and healthcare workers: a rapid systematic review into risks and preventive measures. BMJ Open 11, e042270. doi:10.1136/bmjopen-2020-042270

Gruell, H., Hamacher, L., Jennissen, V., Tuchscherer, A., Ostendorf, N., Löffler, T., Hallek, M., Kochanek, M., Tannich, E., Böll, B., Fätkenheuer, G., 2017. On taking a different route: an unlikely case of malaria by nosocomial transmission. Clin. Infect. Dis. 65, 1404–1406. doi:10.1093/cid/cix520

Grundmann, H., Hellriegel, B., 2006. Mathematical modelling: a tool for hospital infection control. Lancet Infect. Dis. 6, 39–45. doi:10.1016/S1473-3099(05)70325-X

Guan, D., Wang, D., Hallegatte, S., Davis, S.J., Huo, J., Li, S., Bai, Y., Lei, T., Xue, Q., Coffman, D., Cheng, D., Chen, P., Liang, X., Xu, B., Lu, X., Wang, S., Hubacek, K., Gong, P., 2020. Global supply-chain effects of COVID-19 control measures. Nat. Hum. Behav. 4, 577–587. doi:10.1038/s41562-020-0896-8

Guittar, J., Koffel, T., Shade, A., Klausmeier, C.A., Litchman, E., 2021. Resource competition and host feedbacks underlie regime shifts in gut microbiota. Am. Nat. 198, 1–12. doi:10.1086/714527

Guk, J., Guedj, J., Burdet, C., Andremont, A., de Gunzburg, J., Ducher, A., Mentré, F., 2021. Modeling the Effect of DAV132, a Novel Colon-Targeted Adsorbent, on Fecal Concentrations of Moxifloxacin and Gut Microbiota Diversity in Healthy Volunteers. Clin. Pharmacol. Ther. 109, 1045–1054. doi:10.1002/cpt.1977

Gullberg, E., Cao, S., Berg, O.G., Ilbäck, C., Sandegren, L., Hughes, D., Andersson, D.I., 2011. Selection of resistant bacteria at very low antibiotic concentrations. PLoS Pathog. 7, e1002158. doi:10.1371/journal.ppat.1002158

Gumbo, T., Louie, A., Deziel, M.R., Liu, W., Parsons, L.M., Salfinger, M., Drusano, G.L., 2007. Concentration-dependent Mycobacterium tuberculosis killing and prevention of resistance by rifampin. Antimicrob. Agents Chemother. 51, 3781–3788. doi:10.1128/AAC.01533-06

Gumbo, T., Louie, A., Deziel, M.R., Parsons, L.M., Salfinger, M., Drusano, G.L., 2004. Selection of a moxifloxacin dose that suppresses drug resistance in Mycobacterium tuberculosis, by use of an in vitro pharmacodynamic infection model and mathematical modeling. J. Infect. Dis. 190, 1642–1651. doi:10.1086/424849

Gupta, S., Mullish, B.H., Allegretti, J.R., 2021. Fecal microbiota transplantation: the evolving risk landscape. Am. J. Gastroenterol. 116, 647–656. doi:10.14309/ajg.0000000000001075

Gurieva, T., Dautzenberg, M.J.D., Gniadkowski, M., Derde, L.P.G., Bonten, M.J.M., Bootsma, M.C.J., 2018. The Transmissibility of Antibiotic-Resistant Enterobacteriaceae in Intensive Care Units. Clin. Infect. Dis. 66, 489–493. doi:10.1093/cid/cix825

Guzman Prieto, A.M., van Schaik, W., Rogers, M.R.C., Coque, T.M., Baquero, F., Corander, J., Willems, R.J.L., 2016. Global emergence and dissemination of enterococci as nosocomial pathogens: attack of the clones? Front. Microbiol. 7, 788. doi:10.3389/fmicb.2016.00788

Hadaya, J., Schumm, M., Livingston, E.H., 2020. Testing Individuals for Coronavirus Disease 2019 (COVID-19). JAMA 323, 1981. doi:10.1001/jama.2020.5388

Han, C., Song, Q., Meng, X., Lv, Y., Hu, D., Jiang, X., Sun, L., 2021. Effects of a 4-year intervention on hand hygiene compliance and incidence of healthcare associated infections: a longitudinal study. Infection. doi:10.1007/s15010-021-01626-5

Hansen, E., Karslake, J., Woods, R.J., Read, A.F., Wood, K.B., 2020. Antibiotics can be used to contain drug-resistant bacteria by maintaining sufficiently large sensitive populations. PLoS Biol. 18, e3000713. doi:10.1371/journal.pbio.3000713

Hauck, L.D., Adler, L.M., Mulla, Z.D., 2004. Clinical pathway care improves outcomes among patients hospitalized for community-acquired pneumonia. Ann Epidemiol 14, 669–675. doi:10.1016/j.annepidem.2004.01.003

Hawksworth, D.L., Lücking, R., 2017. Fungal diversity revisited: 2.2 to 3.8 million species. Microbiol. Spectr. 5. doi:10.1128/microbiolspec.FUNK-0052-2016

He, X., Lau, E.H.Y., Wu, P., Deng, X., Wang, J., Hao, X., Lau, Y.C., Wong, J.Y., Guan, Y., Tan, X., Mo, X., Chen, Y., Liao, B., Chen, W., Hu, F., Zhang, Q., Zhong, M., Wu, Y., Zhao, L., Zhang, F., Cowling, B.J., Li, F., Leung, G.M., 2020. Temporal dynamics in viral shedding and transmissibility of COVID-19. Nat. Med. 26, 672–675. doi:10.1038/s41591-020-0869-5

Heath, P.T., Galiza, E.P., Baxter, D.N., Boffito, M., Browne, D., Burns, F., Chadwick, D.R., Clark, R., Cosgrove, C., Galloway, J., Goodman, A.L., Heer, A., Higham, A., Iyengar, S., Jamal, A., Jeanes, C., Kalra, P.A., Kyriakidou, C., McAuley, D.F., Meyrick, A., Minassian, A.M., Minton, J., Moore, P., Munsoor, I., Nicholls, H., Osanlou, O., Packham, J., Pretswell, C.H., San Francisco Ramos, A., Saralaya, D., Sheridan, R.P., Smith, R., Soiza, R.L., Swift, P.A., Thomson, E.C., Turner, J., Viljoen, M.E., Albert, G., Cho, I., Dubovsky, F., Glenn, G., Rivers, J., Robertson, A., Smith, K., Toback, S., 2019nCoV-302 Study Group, 2021. Safety and Efficacy of NVX-CoV2373 Covid-19 Vaccine. N. Engl. J. Med. doi:10.1056/NEJMoa2107659

Heesterbeek, H., Anderson, R.M., Andreasen, V., Bansal, S., De Angelis, D., Dye, C., Eames, K.T.D., Edmunds, W.J., Frost, S.D.W., Funk, S., Hollingsworth, T.D., House, T., Isham, V., Klepac, P., Lessler, J., Lloyd-Smith, J.O., Metcalf, C.J.E., Mollison, D., Pellis, L., Pulliam, J.R.C., Roberts, M.G., Viboud, C., Isaac Newton Institute IDD Collaboration, 2015. Modeling infectious disease dynamics in the complex landscape of global health. Science 347, aaa4339.

doi:10.1126/science.aaa4339

Hellewell, J., Russell, T.W., SAFER Investigators and Field Study Team, Crick COVID-19 Consortium, CMMID COVID-19 working group, Beale, R., Kelly, G., Houlihan, C., Nastouli, E., Kucharski, A.J., 2021. Estimating the effectiveness of routine asymptomatic PCR testing at different frequencies for the detection of SARS-CoV-2 infections. BMC Med. 19, 106. doi:10.1186/s12916-021-01982-x

Herzig, C.T.A., Reagan, J., Pogorzelska-Maziarz, M., Srinath, D., Stone, P.W., 2015. State-mandated reporting of health care-associated infections in the United States: trends over time. Am. J. Med. Qual. 30, 417–424. doi:10.1177/1062860614540200

Hoeksema, M., Jonker, M.J., Bel, K., Brul, S., Ter Kuile, B.H., 2018. Genome rearrangements in Escherichia coli during de novo acquisition of resistance to a single antibiotic or two antibiotics successively. BMC Genomics 19, 973. doi:10.1186/s12864-018-5353-y

Hoenigl, M., Valentin, T., Zarfel, G., Wuerstl, B., Leitner, E., Salzer, H.J.F., Posch, J., Krause, R., Grisold, A.J., 2012. Nosocomial outbreak of Klebsiella pneumoniae carbapenemase-producing Klebsiella oxytoca in Austria. Antimicrob. Agents Chemother. 56, 2158–2161. doi:10.1128/AAC.05440-11

Hogan, C.A., Sahoo, M.K., Pinsky, B.A., 2020. Sample Pooling as a Strategy to Detect Community Transmission of SARS-CoV-2. JAMA. doi:10.1001/jama.2020.5445

Hojsak, I., Snovak, N., Abdović, S., Szajewska, H., Misak, Z., Kolacek, S., 2010. Lactobacillus GG in the prevention of gastrointestinal and respiratory tract infections in children who attend day care centers: a randomized, double-blind, placebo-controlled trial. Clin. Nutr. 29, 312–316. doi:10.1016/j.clnu.2009.09.008

Hojsak, I., Szajewska, H., Canani, R.B., Guarino, A., Indrio, F., Kolacek, S., Orel, R., Shamir, R., Vandenplas, Y., van Goudoever, J.B., Weizman, Z., ESPGHAN Working Group for Probiotics/Prebiotics, 2018. Probiotics for the prevention of nosocomial diarrhea in children. J. Pediatr. Gastroenterol. Nutr. 66, 3–9. doi:10.1097/MPG.0000000000001637

Holmdahl, I., Kahn, R., Hay, J.A., Buckee, C.O., Mina, M.J., 2021. Estimation of Transmission of COVID-19 in Simulated Nursing Homes With Frequent Testing and Immunity-Based Staffing. JAMA Netw. Open 4, e2110071. doi:10.1001/jamanetworkopen.2021.10071

Holmes, A.H., Moore, L.S.P., Sundsfjord, A., Steinbakk, M., Regmi, S., Karkey, A., Guerin, P.J., Piddock, L.J.V., 2016. Understanding the mechanisms and drivers of antimicrobial resistance. Lancet 387, 176–187. doi:10.1016/S0140-6736(15)00473-0

Hooks, K.B., O'Malley, M.A., 2017. Dysbiosis and its discontents. MBio 8. doi:10.1128/mBio.01492-17

Hooper, L.V., Stappenbeck, T.S., Hong, C.V., Gordon, J.I., 2003. Angiogenins: a new class of microbicidal proteins involved in innate immunity. Nat. Immunol. 4, 269–273. doi:10.1038/ni888

Hotchkiss, R.D., 1951. Transfer of penicillin resistance in pneumococci by the desoxyribonucleate derived from resistant cultures. Cold Spring Harb. Symp. Quant. Biol. 16, 457–461. doi:10.1101/sqb.1951.016.01.032

Hsu, A.J., Carroll, K.C., Milstone, A.M., Avdic, E., Cosgrove, S.E., Vilasoa, M., Tamma, P.D., 2015. The Use of a Combination Antibiogram to Assist with the Selection of Appropriate Antimicrobial Therapy for Carbapenemase-Producing Enterobacteriaceae Infections. Infect. Control Hosp. Epidemiol. 36, 1458–1460. doi:10.1017/ice.2015.196

Huang, P.-Y., Wu, T.-S., Cheng, C.-W., Chen, C.-J., Huang, C.-G., Tsao, K.-C., Lin, C.-S., Chung, T.-Y., Lai, C.-C., Yang, C.-T., Chen, Y.-C., Chiu, C.-H., Infection Control Working Group, 2021. A hospital cluster of COVID-19 associated with a SARS-CoV-2 superspreading event. J Microbiol Immunol Infect. doi:10.1016/j.jmii.2021.07.006

Huddleston, J.R., 2014. Horizontal gene transfer in the human gastrointestinal tract: potential spread of antibiotic resistance genes. Infect. Drug Resist. 7, 167–176. doi:10.2147/IDR.S48820

Huerta-Gutiérrez, R., Braga, L., Camacho-Ortiz, A., Díaz-Ponce, H., García-Mollinedo, L., Guzmán-Blanco, M., Valderrama-Beltrán, S., Landaeta-Nezer, E., Moreno-Espinosa, S., Morfín-Otero, R., Rodríguez-Zulueta, P., Rosado-Buzzo, A., Rosso-Suárez, F., Trindade-Clemente, W., Wiltgen, D., 2019. One-day point prevalence of healthcare-associated infections and antimicrobial use in four countries in Latin America. Int. J. Infect. Dis. 86, 157–166. doi:10.1016/j.ijid.2019.06.016

Huff, H.V., Singh, A., 2020. Asymptomatic transmission during the COVID-19 pandemic and implications for public health strategies. Clin. Infect. Dis. doi:10.1093/cid/ciaa654

Huijben, S., Bell, A.S., Sim, D.G., Tomasello, D., Mideo, N., Day, T., Read, A.F., 2013. Aggressive chemotherapy and the selection of drug resistant pathogens. PLoS Pathog. 9, e1003578. doi:10.1371/journal.ppat.1003578

Hurford, A., Morris, A.M., Fisman, D.N., Wu, J., 2012. Linking antimicrobial prescribing to antimicrobial resistance in the ICU: before and after an antimicrobial stewardship program. Epidemics 4, 203–210. doi:10.1016/j.epidem.2012.12.001

Iacovelli, V., Gaziev, G., Topazio, L., Bove, P., Vespasiani, G., Finazzi Agrò, E., 2014. Nosocomial urinary tract infections: A review. Urologia 81, 222–227. doi:10.5301/uro.5000092

Illingworth, C., Hamilton, W., Warne, B., Routledge, M., Popay, A., jackson, christopher, Fieldman, T., Meredith, L.W., Houldcroft, C.J., Hosmillo, M., Jahun, A.S., Caller, L.G., Caddy, S.L., Yakovleva, A., Hall, G., Khokhar, F.A., Feltwell, T., Pinckert, M.L., Georgana, I., Chaudhry, Y., Curran, M.D., Parmar, S., Sparkes, D., Rivett, L., Jones, N.K., Sridhar, S., Forrest, S., Dymond, T., Grainger, K., Workman, C., Gkrania-Klotsas, E., Brown, N.M., Baker, S., Weekes, M.P., Peacock, S.J., Goodfellow, I., Gouliouris, T., de Angelis, D., Török, E., 2021. Superspreaders drive the largest outbreaks of hospital onset COVID-19 infection. doi:10.31219/osf.io/wmkn3

Institute of Medicine (US) Committee on Quality of Health Care in America, 2000. To Err is Human: Building a Safer Health System. National Academies Press (US), Washington (DC). doi:10.17226/9728

Iritani, O., Okuno, T., Hama, D., Kane, A., Kodera, K., Morigaki, K., Terai, T., Maeno, N., Morimoto, S., 2020. Clusters of COVID-19 in long-term care hospitals and facilities in Japan from 16 January to 9 May 2020. Geriatr Gerontol Int 20, 715–719. doi:10.1111/ggi.13973

Jacobsen, S.M., Stickler, D.J., Mobley, H.L.T., Shirtliff, M.E., 2008. Complicated catheter-associated urinary tract infections due to Escherichia coli and Proteus mirabilis. Clin. Microbiol. Rev. 21, 26–59. doi:10.1128/CMR.00019-07

Jernigan, J.A., Hatfield, K.M., Wolford, H., Nelson, R.E., Olubajo, B., Reddy, S.C., McCarthy, N., Paul, P., McDonald, L.C., Kallen, A., Fiore, A., Craig, M., Baggs, J., 2020. Multidrug-Resistant Bacterial Infections in U.S. Hospitalized Patients, 2012-2017. N. Engl. J. Med. 382, 1309–1319. doi:10.1056/NEJMoa1914433

Jijón, S., Shafie, A.A., Temime, L., Jean, K., Kassas, M.E., EMEA-MESuRS working group on nosocomial SARS-CoV-2 modelling, 2020. Risk of incident SARS-CoV-2 infection among healthcare workers in Egyptian quarantine hospitals. medRxiv. doi:10.1101/2020.12.21.20248594

Johanesen, P.A., Mackin, K.E., Hutton, M.L., Awad, M.M., Larcombe, S., Amy, J.M., Lyras, D., 2015. Disruption of the Gut Microbiome: Clostridium difficile Infection and the Threat of Antibiotic Resistance. Genes (Basel) 6, 1347–1360. doi:10.3390/genes6041347

Johnson, S.R., Tomlinson, G.A., Hawker, G.A., Granton, J.T., Feldman, B.M., 2010a. Methods to elicit beliefs for Bayesian priors: a systematic review. J. Clin. Epidemiol. 63, 355–369. doi:10.1016/j.jclinepi.2009.06.003

Johnson, S.R., Tomlinson, G.A., Hawker, G.A., Granton, J.T., Grosbein, H.A., Feldman, B.M., 2010b. A valid and reliable belief elicitation method for Bayesian priors. J. Clin. Epidemiol. 63, 370–383. doi:10.1016/j.jclinepi.2009.08.005

Jumbe, N., Louie, A., Leary, R., Liu, W., Deziel, M.R., Tam, V.H., Bachhawat, R., Freeman, C., Kahn, J.B., Bush, K., Dudley, M.N., Miller, M.H., Drusano, G.L., 2003. Application of a mathematical model to prevent in vivo amplification of antibiotic-resistant bacterial populations during therapy. J. Clin. Invest. 112, 275–285. doi:10.1172/JCI16814

Jung, J., Hong, M.J., Kim, E.O., Lee, J., Kim, M.N., Kim, S.H., 2020. Investigation of a nosocomial outbreak of coronavirus disease 2019 in a paediatric ward in South Korea: successful control by early detection and extensive contact tracing with testing. Clin. Microbiol. Infect. 26, 1574–1575. doi:10.1016/j.cmi.2020.06.021

Kahn, R., Holmdahl, I., Reddy, S., Jernigan, J., Mina, M.J., Slayton, R.B., 2021. Mathematical modeling to inform vaccination strategies and testing approaches for COVID-19 in nursing homes. Clin. Infect. Dis. doi:10.1093/cid/ciab517

Kamada, N., Chen, G.Y., Inohara, N., Núñez, G., 2013a. Control of pathogens and pathobionts by the gut microbiota. Nat. Immunol. 14, 685–690. doi:10.1038/ni.2608

Kamada, N., Seo, S.-U., Chen, G.Y., Núñez, G., 2013b. Role of the gut microbiota in immunity and inflammatory disease. Nat. Rev. Immunol. 13, 321–335. doi:10.1038/nri3430

Kaminsky, J., Keegan, L.T., Metcalf, C.J.E., Lessler, J., 2019. Perfect counterfactuals for epidemic simulations. Philos. Trans. R. Soc. Lond. B, Biol. Sci. 374, 20180279. doi:10.1098/rstb.2018.0279

Kampmeier, S., Tönnies, H., Correa-Martinez, C.L., Mellmann, A., Schwierzeck, V., 2020. A nosocomial cluster of vancomycin

resistant enterococci among COVID-19 patients in an intensive care unit. Antimicrob. Resist. Infect. Control 9, 154. doi:10.1186/s13756-020-00820-8

Kang, T., Kim, T., Ryoo, S., 2020. Detection of airborne bacteria from patient spaces in tuberculosis hospital. Int. J. Mycobacteriol. 9, 293–295. doi:10.4103/ijmy.ijmy_115_20

Kapoor, G., Saigal, S., Elongavan, A., 2017. Action and resistance mechanisms of antibiotics: A guide for clinicians. J Anaesthesiol Clin Pharmacol 33, 300–305. doi:10.4103/joacp.JOACP_349_15

Karampatakis, T., Antachopoulos, C., Iosifidis, E., Tsakris, A., Roilides, E., 2016. Molecular epidemiology of carbapenem-resistant Klebsiella pneumoniae in Greece. Future Microbiol 11, 809–823. doi:10.2217/fmb-2016-0042

Karanika, S., Paudel, S., Grigoras, C., Kalbasi, A., Mylonakis, E., 2016. Systematic Review and Meta-analysis of Clinical and Economic Outcomes from the Implementation of Hospital-Based Antimicrobial Stewardship Programs. Antimicrob. Agents Chemother. 60, 4840–4852. doi:10.1128/AAC.00825-16

Kardas-Sloma, L., Boëlle, P.Y., Opatowski, L., Brun-Buisson, C., Guillemot, D., Temime, L., 2011. Impact of antibiotic exposure patterns on selection of community-associated methicillin-resistant Staphylococcus aureus in hospital settings. Antimicrob. Agents Chemother. 55, 4888–4895. doi:10.1128/AAC.01626-10

Kardaś-Słoma, L., Lucet, J.-C., Perozziello, A., Pelat, C., Birgand, G., Ruppé, E., Boëlle, P.-Y., Andremont, A., Yazdanpanah, Y., 2017. Universal or targeted approach to prevent the transmission of extended-spectrum beta-lactamase-producing Enterobacteriaceae in intensive care units: a cost-effectiveness analysis. BMJ Open 7, e017402. doi:10.1136/bmjopen-2017-017402

Kassam, Z., Lee, C.H., Yuan, Y., Hunt, R.H., 2013. Fecal microbiota transplantation for Clostridium difficile infection: systematic review and meta-analysis. Am. J. Gastroenterol. 108, 500–508. doi:10.1038/ajg.2013.59

Keeling, M.J., Rohani, P., 2007. Modeling Infectious Diseases in Humans and Animals, Illustrated. ed. Princeton University Press, Princeton.

Kendall, E.A., Arinaminpathy, N., Sacks, J.A., Manabe, Y.C., Dittrich, S., Schumacher, S.G., Dowdy, D.W., 2021. Antigen-based rapid diagnostic testing or alternatives for diagnosis of symptomatic COVID-19: A simulation-based net benefit analysis. Epidemiology. doi:10.1097/EDE.0000000000001400

Kermack, W.O., McKendrick, A.G., 1991a. Contributions to the mathematical theory of epidemics--I. 1927. Bull Math Biol 53, 33–55. doi:10.1007/BF02464423

Kermack, W.O., McKendrick, A.G., 1991b. Contributions to the mathematical theory of epidemics--II. The problem of endemicity.1932. Bull Math Biol 53, 57–87. doi:10.1007/BF02464424

Kermack, W.O., McKendrick, A.G., 1991c. Contributions to the mathematical theory of epidemics--III. Further studies of the problem of endemicity. 1933. Bull Math Biol 53, 89–118. doi:10.1007/BF02464425

Kernéis, S., Elie, C., Fourgeaud, J., Choupeaux, L., Delarue, S.M., Alby, M.-L., Quentin, P., Pavie, J., Brazille, P., Néré, M.L., Minier, M., Gabassi, A., Gibaud, A., Gauthier, S., Leroy, C., Voirin-Mathieu, E., Poyart, C., Vidaud, M., Parfait, B., Delaugerre, C., Tréluyer, J.-M., LeGoff, J., 2021. Accuracy of saliva and nasopharyngeal sampling for detection of SARS-CoV-2 in community screening: a multicentric cohort study. Eur. J. Clin. Microbiol. Infect. Dis. doi:10.1007/s10096-021-04327-x

Khader, K., Thomas, A., Jones, M., Toth, D., Stevens, V., Samore, M.H., CDC Modeling Infectious Diseases in Healthcare Program (MInD-Healthcare), 2019. Variation and trends in transmission dynamics of Methicillin-resistant Staphylococcus aureus in veterans affairs hospitals and nursing homes. Epidemics 28, 100347. doi:10.1016/j.epidem.2019.100347

Khader, K., Thomas, A., Stevens, V., Visnovsky, L., Nevers, M., Toth, D., Keegan, L.T., Jones, M., Rubin, M., Samore, M.H., 2021. Association Between Contact Precautions and Transmission of Methicillin-Resistant Staphylococcus aureus in Veterans Affairs Hospitals. JAMA Netw. Open 4, e210971. doi:10.1001/jamanetworkopen.2021.0971

Khdour, M.R., Hallak, H.O., Aldeyab, M.A., Nasif, M.A., Khalili, A.M., Dallashi, A.A., Khofash, M.B., Scott, M.G., 2018. Impact of antimicrobial stewardship programme on hospitalized patients at the intensive care unit: a prospective audit and feedback study. Br. J. Clin. Pharmacol. 84, 708–715. doi:10.1111/bcp.13486

Kierkegaard, P., Micocci, M., McLister, A., Tulloch, J., Parvulescu, P., Gordon, A., Buckle, P., 2021. Implementing Lateral Flow Devices in Long-Term Care Facilities: Experiences from the Liverpool COVID-19 Community Testing Pilot in Care

Homes - A Qualitative Study. SSRN Journal. doi:10.2139/ssrn.3825945

Kim, S., Covington, A., Pamer, E.G., 2017. The intestinal microbiota: Antibiotics, colonization resistance, and enteric pathogens. Immunol. Rev. 279, 90–105. doi:10.1111/imr.12563

Kim, Y., Escalante, A.A., Schneider, K.A., 2014. A population genetic model for the initial spread of partially resistant malaria parasites under anti-malarial combination therapy and weak intrahost competition. PLoS One 9, e101601. doi:10.1371/journal.pone.0101601

Kimball, A., Hatfield, K.M., Arons, M., James, A., Taylor, J., Spicer, K., Bardossy, A.C., Oakley, L.P., Tanwar, S., Chisty, Z., Bell, J.M., Methner, M., Harney, J., Jacobs, J.R., Carlson, C.M., McLaughlin, H.P., Stone, N., Clark, S., Brostrom-Smith, C., Page, L.C., Kay, M., Lewis, J., Russell, D., Hiatt, B., Gant, J., Duchin, J.S., Clark, T.A., Honein, M.A., Reddy, S.C., Jernigan, J.A., Public Health – Seattle & King County, CDC COVID-19 Investigation Team, 2020. Asymptomatic and Presymptomatic SARS-CoV-2 Infections in Residents of a Long-Term Care Skilled Nursing Facility - King County, Washington, March 2020. MMWR Morb. Mortal. Wkly. Rep. 69, 377–381. doi:10.15585/mmwr.mm6913e1

Kirch, W. (Ed.), 2008a. Direct Costs, in: Encyclopedia of Public Health. Springer Netherlands, Dordrecht, pp. 267–267. doi:10.1007/978-1-4020-5614-7_799

Kirch, W., 2008b. Indirect Costs, in: Kirch, W. (Ed.), Encyclopedia of Public Health. Springer, Dordrecht, pp. 753–753. doi:10.1007/978-1-4020-5614-7_1685

Klausner, Z., Fattal, E., Hirsch, E., Shapira, S.C., 2020. A single holiday was the turning point of the COVID-19 policy of Israel. Int. J. Infect. Dis. 101, 368–373. doi:10.1016/j.ijid.2020.10.016

Klevens, R.M., Edwards, J.R., Richards, C.L., Horan, T.C., Gaynes, R.P., Pollock, D.A., Cardo, D.M., 2007. Estimating health care-associated infections and deaths in U.S. hospitals, 2002. Public Health Rep. 122, 160–166. doi:10.1177/003335490712200205

Kluytmans-van den Bergh, M.F.Q., Bruijning-Verhagen, P.C.J., Vandenbroucke-Grauls, C.M.J.E., de Brauwer, E.I.G.B., Buiting, A.G.M., Diederen, B.M., van Elzakker, E.P.M., Friedrich, A.W., Hopman, J., Al Naiemi, N., Rossen, J.W.A., Ruijs, G.J.H.M., Savelkoul, P.H.M., Verhulst, C., Vos, M.C., Voss, A., Bonten, M.J.M., Kluytmans, J.A.J.W., SoM Study Group, 2019. Contact precautions in single-bed or multiple-bed rooms for patients with extended-spectrum β-lactamase-producing Enterobacteriaceae in Dutch hospitals: a cluster-randomised, crossover, non-inferiority study. Lancet Infect. Dis. 19, 1069–1079. doi:10.1016/S1473-3099(19)30262-2

Knight, G.M., Costelloe, C., Deeny, S.R., Moore, L.S.P., Hopkins, S., Johnson, A.P., Robotham, J.V., Holmes, A.H., 2018. Quantifying where human acquisition of antibiotic resistance occurs: a mathematical modelling study. BMC Med. 16, 137. doi:10.1186/s12916-018-1121-8

Knight, G.M., Davies, N.G., Colijn, C., Coll, F., Donker, T., Gifford, D.R., Glover, R.E., Jit, M., Klemm, E., Lehtinen, S., Lindsay, J.A., Lipsitch, M., Llewelyn, M.J., Mateus, A.L.P., Robotham, J.V., Sharland, M., Stekel, D., Yakob, L., Atkins, K.E., 2019. Mathematical modelling for antibiotic resistance control policy: do we know enough? BMC Infect. Dis. 19, 1011. doi:10.1186/s12879-019-4630-y

Knight, G.M., Glover, R.E., McQuaid, C.F., Olaru, I.D., Gallandat, K., Leclerc, Q.J., Fuller, N.M., Willcocks, S.J., Hasan, R., van Kleef, E., Chandler, C.I., 2021. Antimicrobial resistance and COVID-19: Intersections and implications. Elife 10. doi:10.7554/eLife.64139

Knudsen, J.D., Odenholt, I., Erlendsdottir, H., Gottfredsson, M., Cars, O., Frimodt-Møller, N., Espersen, F., Kristinsson, K.G., Gudmundsson, S., 2003. Selection of resistant Streptococcus pneumoniae during penicillin treatment in vitro and in three animal models. Antimicrob. Agents Chemother. 47, 2499–2506. doi:10.1128/AAC.47.8.2499-2506.2003

Kochanek, K.D., Xu, J., Arias, E., 2020. Mortality in the united states, 2019. NCHS Data Brief 1–8.

Komagamine, J., Yabuki, T., Kobayashi, M., Okabe, T., 2019. Prevalence of antimicrobial use and active healthcare-associated infections in acute care hospitals: a multicentre prevalence survey in Japan. BMJ Open 9, e027604. doi:10.1136/bmjopen-2018-027604

Kontula, K.S.K., Skogberg, K., Ollgren, J., Järvinen, A., Lyytikäinen, O., 2018. The outcome and timing of death of 17,767 nosocomial bloodstream infections in acute care hospitals in Finland during 1999-2014. Eur. J. Clin. Microbiol. Infect. Dis. 37, 945–952. doi:10.1007/s10096-018-3211-0

Koopmans, M., 2008. Progress in understanding norovirus epidemiology. Curr Opin Infect Dis 21, 544–552. doi:10.1097/QCO.0b013e3283108965

Kouyos, R., Klein, E., Grenfell, B., 2013. Hospital-community interactions foster coexistence between methicillin-resistant strains of Staphylococcus aureus. PLoS Pathog. 9, e1003134. doi:10.1371/journal.ppat.1003134

Kouyos, R.D., Metcalf, C.J.E., Birger, R., Klein, E.Y., Abel zur Wiesch, P., Ankomah, P., Arinaminpathy, N., Bogich, T.L., Bonhoeffer, S., Brower, C., Chi-Johnston, G., Cohen, T., Day, T., Greenhouse, B., Huijben, S., Metlay, J., Mideo, N., Pollitt, L.C., Read, A.F., Smith, D.L., Standley, C., Wale, N., Grenfell, B., 2014. The path of least resistance: aggressive or moderate treatment? Proc. Biol. Sci. 281, 20140566. doi:10.1098/rspb.2014.0566

Kretzschmar, M., Mangen, M.-J.J., Pinheiro, P., Jahn, B., Fèvre, E.M., Longhi, S., Lai, T., Havelaar, A.H., Stein, C., Cassini, A., Kramarz, P., BCoDE consortium, 2012. New methodology for estimating the burden of infectious diseases in Europe. PLoS Med. 9, e1001205. doi:10.1371/journal.pmed.1001205

Kretzschmar, M., Wallinga, J., 2010. Mathematical models in infectious disease epidemiology, in: Krämer, A., Kretzschmar, M., Krickeberg, K. (Eds.), Modern Infectious Disease Epidemiology: Concepts, Methods, Mathematical Models, and Public Health, Statistics for Biology and Health. Springer New York, New York, NY, pp. 209–221. doi:10.1007/978-0-387-93835-6_12

Kucharski, A.J., Klepac, P., Conlan, A.J.K., Kissler, S.M., Tang, M.L., Fry, H., Gog, J.R., Edmunds, W.J., CMMID COVID-19 working group, 2020. Effectiveness of isolation, testing, contact tracing, and physical distancing on reducing transmission of SARS-CoV-2 in different settings: a mathematical modelling study. Lancet Infect. Dis. 20, 1151–1160. doi:10.1016/S1473-3099(20)30457-6

Kucirka, L.M., Lauer, S.A., Laeyendecker, O., Boon, D., Lessler, J., 2020. Variation in False-Negative Rate of Reverse Transcriptase Polymerase Chain Reaction-Based SARS-CoV-2 Tests by Time Since Exposure. Ann. Intern. Med. doi:10.7326/M20-1495

Kullar, R., Johnson, S., McFarland, L.V., Goldstein, E.J.C., 2021. Potential Roles for Probiotics in the Treatment of COVID-19 Patients and Prevention of Complications Associated with Increased Antibiotic Use. Antibiotics (Basel) 10. doi:10.3390/antibiotics10040408

Kumar, N., Radhakrishnan, A., Wright, C.C., Chou, T.-H., Lei, H.-T., Bolla, J.R., Tringides, M.L., Rajashankar, K.R., Su, C.-C., Purdy, G.E., Yu, E.W., 2014. Crystal structure of the transcriptional regulator Rv1219c of Mycobacterium tuberculosis. Protein Sci. 23, 423–432. doi:10.1002/pro.2424

Kung, S., Doppen, M., Black, M., Braithwaite, I., Kearns, C., Weatherall, M., Beasley, R., Kearns, N., 2021. Underestimation of COVID-19 mortality during the pandemic. ERJ Open Research 7. doi:10.1183/23120541.00766-2020

Kwok, K.O., Read, J.M., Tang, A., Chen, H., Riley, S., Kam, K.M., 2018. A systematic review of transmission dynamic studies of methicillin-resistant Staphylococcus aureus in non-hospital residential facilities. BMC Infect. Dis. 18, 188. doi:10.1186/s12879-018-3060-6

Labi, A.K., Obeng-Nkrumah, N., Owusu, E., Bjerrum, S., Bediako-Bowan, A., Sunkwa-Mills, G., Akufo, C., Fenny, A.P., Opintan, J.A., Enweronu-Laryea, C., Debrah, S., Damale, N., Bannerman, C., Newman, M.J., 2019. Multi-centre point-prevalence survey of hospital-acquired infections in Ghana. J. Hosp. Infect. 101, 60–68. doi:10.1016/j.jhin.2018.04.019

Ladhani, S.N., Chow, J.Y., Janarthanan, R., Fok, J., Crawley-Boevey, E., Vusirikala, A., Fernandez, E., Perez, M.S., Tang, S., Dun-Campbell, K., Evans, E.W.-, Bell, A., Patel, B., Amin-Chowdhury, Z., Aiano, F., Paranthaman, K., Ma, T., Saavedra-Campos, M., Myers, R., Ellis, J., Lackenby, A., Gopal, R., Patel, M., Brown, C., Chand, M., Brown, K., Ramsay, M.E., Hopkins, S., Shetty, N., Zambon, M., 2020. Investigation of SARS-CoV-2 outbreaks in six care homes in London, April 2020. EClinicalMedicine 100533. doi:10.1016/j.eclinm.2020.100533

Lakhani, K., Minguell, J., Guerra-Farfán, E., Lara, Y., Jambrina, U., Pijoan, J., Núñez, J.H., 2020. Nosocomial infection with SARS-CoV-2 and main outcomes after surgery within an orthopaedic surgery department in a tertiary trauma centre in Spain. Int. Orthop. 44, 2505–2513. doi:10.1007/s00264-020-04798-1

Langford, B.J., So, M., Raybardhan, S., Leung, V., Westwood, D., MacFadden, D.R., Soucy, J.-P.R., Daneman, N., 2020. Bacterial co-infection and secondary infection in patients with COVID-19: a living rapid review and meta-analysis. Clin. Microbiol. Infect. 26, 1622–1629. doi:10.1016/j.cmi.2020.07.016

Lansbury, L., Lim, B., Baskaran, V., Lim, W.S., 2020. Co-infections in people with COVID-19: a systematic review and meta-

analysis. J. Infect. 81, 266–275. doi:10.1016/j.jinf.2020.05.046

Last, J.M., 1993. Dictionary of Epidemiology. CMAJ: Canadian Medical Association Journal.

Lauer, S.A., Grantz, K.H., Bi, Q., Jones, F.K., Zheng, Q., Meredith, H.R., Azman, A.S., Reich, N.G., Lessler, J., 2020. The Incubation Period of Coronavirus Disease 2019 (COVID-19) From Publicly Reported Confirmed Cases: Estimation and Application. Ann. Intern. Med. 172, 577–582. doi:10.7326/M20-0504

Laurent, F., Lelièvre, H., Cornu, M., Vandenesch, F., Carret, G., Etienne, J., Flandrois, J.P., 2001. Fitness and competitive growth advantage of new gentamicin-susceptible MRSA clones spreading in French hospitals. J. Antimicrob. Chemother. 47, 277–283. doi:10.1093/jac/47.3.277

Lavigne, J.-P., Sotto, A., Nicolas-Chanoine, M.-H., Bouziges, N., Pagès, J.-M., Davin-Regli, A., 2013. An adaptive response of Enterobacter aerogenes to imipenem: regulation of porin balance in clinical isolates. Int. J. Antimicrob. Agents 41, 130–136. doi:10.1016/j.ijantimicag.2012.10.010

Lawson, E.H., Hall, B.L., Ko, C.Y., 2013. Risk factors for superficial vs deep/organ-space surgical site infections: implications for quality improvement initiatives. JAMA Surg 148, 849–858. doi:10.1001/jamasurg.2013.2925

Le Hingrat, Q., Bouzid, D., Choquet, C., Laurent, O., Lescure, F.-X., Timsit, J.-F., Houhou-Fidouh, N., Casalino, E., Lucet, J.-C., Descamps, D., Visseaux, B., 2021. Viral epidemiology and SARS-CoV-2 co-infections with other respiratory viruses during the first COVID-19 wave in Paris, France. Influenza Other Respi Viruses 15, 425–428. doi:10.1111/irv.12853

Learned, L.A., Reynolds, M.G., Wassa, D.W., Li, Y., Olson, V.A., Karem, K., Stempora, L.L., Braden, Z.H., Kline, R., Likos, A., Libama, F., Moudzeo, H., Bolanda, J.D., Tarangonia, P., Boumandoki, P., Formenty, P., Harvey, J.M., Damon, I.K., 2005. Extended interhuman transmission of monkeypox in a hospital community in the Republic of the Congo, 2003. Am. J. Trop. Med. Hyg. 73, 428–434. doi:10.4269/ajtmh.2005.73.428

Leclerc, Q.J., Lindsay, J.A., Knight, G.M., 2019. Mathematical modelling to study the horizontal transfer of antimicrobial resistance genes in bacteria: current state of the field and recommendations. J. R. Soc. Interface 16, 20190260. doi:10.1098/rsif.2019.0260

Lee, J., Kim, S.Y., Sung, H., Lee, S.W., Lee, H., Roh, K.H., Yoo, C.K., Hong, K.H., 2020. Challenges and issues of SARS-CoV-2 pool testing. Lancet Infect. Dis. 20, 1232–1233. doi:10.1016/S1473-3099(20)30516-8

Lee, T.C., Frenette, C., Jayaraman, D., Green, L., Pilote, L., 2014. Antibiotic self-stewardship: trainee-led structured antibiotic time-outs to improve antimicrobial use. Ann. Intern. Med. 161, S53-8. doi:10.7326/M13-3016

Lehtinen, S., Blanquart, F., Croucher, N.J., Turner, P., Lipsitch, M., Fraser, C., 2017. Evolution of antibiotic resistance is linked to any genetic mechanism affecting bacterial duration of carriage. Proc. Natl. Acad. Sci. USA 114, 1075–1080. doi:10.1073/pnas.1617849114

Lehtinen, S., Chewapreecha, C., Lees, J., Hanage, W.P., Lipsitch, M., Croucher, N.J., Bentley, S.D., Turner, P., Fraser, C., Mostowy, R.J., 2020. Horizontal gene transfer rate is not the primary determinant of observed antibiotic resistance frequencies in Streptococcus pneumoniae. Sci. Adv. 6, eaaz6137. doi:10.1126/sciadv.aaz6137

Lemieux, J.E., Siddle, K.J., Shaw, B.M., Loreth, C., Schaffner, S.F., Gladden-Young, A., Adams, G., Fink, T., Tomkins-Tinch, C.H., Krasilnikova, L.A., DeRuff, K.C., Rudy, M., Bauer, M.R., Lagerborg, K.A., Normandin, E., Chapman, S.B., Reilly, S.K., Anahtar, M.N., Lin, A.E., Carter, A., Myhrvold, C., Kemball, M.E., Chaluvadi, S., Cusick, C., Flowers, K., Neumann, A., Cerrato, F., Farhat, M., Slater, D., Harris, J.B., Branda, J.A., Hooper, D., Gaeta, J.M., Baggett, T.P., O'Connell, J., Gnirke, A., Lieberman, T.D., Philippakis, A., Burns, M., Brown, C.M., Luban, J., Ryan, E.T., Turbett, S.E., LaRocque, R.C., Hanage, W.P., Gallagher, G.R., Madoff, L.C., Smole, S., Pierce, V.M., Rosenberg, E., Sabeti, P.C., Park, D.J., MacInnis, B.L., 2021. Phylogenetic analysis of SARS-CoV-2 in Boston highlights the impact of superspreading events. Science 371. doi:10.1126/science.abe3261

Lenz, R., Leal, J.R., Church, D.L., Gregson, D.B., Ross, T., Laupland, K.B., 2012. The distinct category of healthcare associated bloodstream infections. BMC Infect. Dis. 12, 85. doi:10.1186/1471-2334-12-85

Leong, G., Wilson, J., Charlett, A., 2006. Duration of operation as a risk factor for surgical site infection: comparison of English and US data. J. Hosp. Infect. 63, 255–262. doi:10.1016/j.jhin.2006.02.007

León-Sampedro, R., DelaFuente, J., Díaz-Agero, C., Crellen, T., Musicha, P., Rodríguez-Beltrán, J., de la Vega, C., Hernández-García, M., R-GNOSIS WP5 Study Group, López-Fresneña, N., Ruiz-Garbajosa, P., Cantón, R., Cooper, B.S., San Millán,

Á., 2021. Pervasive transmission of a carbapenem resistance plasmid in the gut microbiota of hospitalized patients. Nat. Microbiol. doi:10.1038/s41564-021-00879-y

Lerminiaux, N.A., Cameron, A.D.S., 2019. Horizontal transfer of antibiotic resistance genes in clinical environments. Can. J. Microbiol. 65, 34–44. doi:10.1139/cjm-2018-0275

LeRose, J., Sandhu, A., Polistico, J., Ellsworth, J., Cranis, M., Jabbo, L., Cullen, L., Moshos, J., Samavati, L., Chopra, T., 2021. The impact of coronavirus disease 2019 (COVID-19) response on central-line-associated bloodstream infections and blood culture contamination rates at a tertiary-care center in the Greater Detroit area. Infect. Control Hosp. Epidemiol. 42, 997–1000. doi:10.1017/ice.2020.1335

Lettau, L.A., 1991. Nosocomial transmission and infection control aspects of parasitic and ectoparasitic diseases. Part II. Blood and tissue parasites. Infect. Control Hosp. Epidemiol. 12, 111–121. doi:10.1086/646297

Letten, A.D., Baumgartner, M., Pfrunder-Cardozo, K.R., Levine, J.M., Hall, A.R., 2021. Human-associated microbiota suppress invading bacteria even under disruption by antibiotics. ISME J. doi:10.1038/s41396-021-00929-7

Levy, R., Borenstein, E., 2013. Metabolic modeling of species interaction in the human microbiome elucidates community-level assembly rules. Proc. Natl. Acad. Sci. USA 110, 12804–12809. doi:10.1073/pnas.1300926110

Lewis, K., 2013. Platforms for antibiotic discovery. Nat. Rev. Drug Discov. 12, 371–387. doi:10.1038/nrd3975

Li, L., Gong, S., Yan, J., 2020. Covid-19 in China: ten critical issues for intensive care medicine. Crit. Care 24, 124. doi:10.1186/s13054-020-02848-z

Li, W., Su, Y.Y., Zhi, S.S., Huang, J., Zhuang, C.L., Bai, W.Z., Wan, Y., Meng, X.R., Zhang, L., Zhou, Y.B., Luo, Y.Y., Ge, S.X., Chen, Y.K., Ma, Y., 2020. Virus shedding dynamics in asymptomatic and mildly symptomatic patients infected with SARS-CoV-2. Clin. Microbiol. Infect. doi:10.1016/j.cmi.2020.07.008

Li, Y., Huang, X., Yu, I.T.S., Wong, T.W., Qian, H., 2005. Role of air distribution in SARS transmission during the largest nosocomial outbreak in Hong Kong. Indoor Air 15, 83–95. doi:10.1111/j.1600-0668.2004.00317.x

Liang, B., Wheeler, J.S., Blanchette, L.M., 2016. Impact of Combination Antibiogram and Related Education on Inpatient Fluoroquinolone Prescribing Patterns for Patients With Health Care-Associated Pneumonia. Ann. Pharmacother. 50, 172–179. doi:10.1177/1060028015625658

Liang, M., Gao, L., Cheng, C., Zhou, Q., Uy, J.P., Heiner, K., Sun, C., 2020. Efficacy of face mask in preventing respiratory virus transmission: A systematic review and meta-analysis. Travel Med Infect Dis 36, 101751. doi:10.1016/j.tmaid.2020.101751

Lin, M.Y., Hota, B., Khan, Y.M., Woeltje, K.F., Borlawsky, T.B., Doherty, J.A., Stevenson, K.B., Weinstein, R.A., Trick, W.E., CDC Prevention Epicenter Program, 2010. Quality of traditional surveillance for public reporting of nosocomial bloodstream infection rates. JAMA 304, 2035–2041. doi:10.1001/jama.2010.1637

Ling, M.L., Apisarnthanarak, A., Madriaga, G., 2015. The Burden of Healthcare-Associated Infections in Southeast Asia: A Systematic Literature Review and Meta-analysis. Clin. Infect. Dis. 60, 1690–1699. doi:10.1093/cid/civ095

Lipsitch, M., 2020. Good science is good science: we need specialists, not sects. Eur J Epidemiol 35, 519–522. doi:10.1007/s10654-020-00651-2

Lipsitch, M., Samore, M.H., 2002. Antimicrobial use and antimicrobial resistance: a population perspective. Emerging Infect. Dis. 8, 347–354. doi:10.3201/eid0804.010312

Liu, W., Røder, H.L., Madsen, J.S., Bjarnsholt, T., Sørensen, S.J., Burmølle, M., 2016. Interspecific bacterial interactions are reflected in multispecies biofilm spatial organization. Front. Microbiol. 7, 1366. doi:10.3389/fmicb.2016.01366

Lohse, S., Pfuhl, T., Berkó-Göttel, B., Rissland, J., Geißler, T., Gärtner, B., Becker, S.L., Schneitler, S., Smola, S., 2020. Pooling of samples for testing for SARS-CoV-2 in asymptomatic people. Lancet Infect. Dis. doi:10.1016/S1473-3099(20)30362-5

Lone, S.A., Ahmad, A., 2019. Candida auris-the growing menace to global health. Mycoses 62, 620–637. doi:10.1111/myc.12904

Lopman, B.A., Reacher, M.H., Vipond, I.B., Hill, D., Perry, C., Halladay, T., Brown, D.W., Edmunds, W.J., Sarangi, J., 2004. Epidemiology and cost of nosocomial gastroenteritis, Avon, England, 2002-2003. Emerging Infect. Dis. 10, 1827–1834. doi:10.3201/eid1010.030941

Losurdo, P., Paiano, L., Samardzic, N., Germani, P., Bernardi, L., Borelli, M., Pozzetto, B., de Manzini, N., Bortul, M., 2020. Impact of lockdown for SARS-CoV-2 (COVID-19) on surgical site infection rates: a monocentric observational cohort study. Updates Surg. 72, 1263–1271. doi:10.1007/s13304-020-00884-6

Louca, S., Mazel, F., Doebeli, M., Parfrey, L.W., 2019. A census-based estimate of Earth's bacterial and archaeal diversity. PLoS Biol. 17, e3000106. doi:10.1371/journal.pbio.3000106

Louie, J.K., Scott, H.M., DuBois, A., Sturtz, N., Lu, W., Stoltey, J., Masinde, G., Cohen, S., Sachdev, D., Philip, S., Bobba, N., Aragon, T., San Francisco Department of Public Health COVID-19 Skilled Nursing Facility Outbreak Response Team, 2021. Lessons From Mass-Testing for Coronavirus Disease 2019 in Long-Term Care Facilities for the Elderly in San Francisco. Clin. Infect. Dis. 72, 2018–2020. doi:10.1093/cid/ciaa1020

Lozupone, C.A., Stombaugh, J.I., Gordon, J.I., Jansson, J.K., Knight, R., 2012. Diversity, stability and resilience of the human gut microbiota. Nature 489, 220–230. doi:10.1038/nature11550

Luangasanatip, N., Hongsuwan, M., Limmathurotsakul, D., Lubell, Y., Lee, A.S., Harbarth, S., Day, N.P.J., Graves, N., Cooper, B.S., 2015. Comparative efficacy of interventions to promote hand hygiene in hospital: systematic review and network meta-analysis. BMJ 351, h3728. doi:10.1136/bmj.h3728

Ludden, C., Coll, F., Gouliouris, T., Restif, O., Blane, B., Blackwell, G.A., Kumar, N., Naydenova, P., Crawley, C., Brown, N.M., Parkhill, J., Peacock, S.J., 2021. Defining nosocomial transmission of Escherichia coli and antimicrobial resistance genes: a genomic surveillance study. Lancet Microbe 2, e472–e480. doi:10.1016/S2666-5247(21)00117-8

Lukaszewicz Bushen, J., Mehta, J.M., Hamilton, K.W., Shawn Binkley, Timko, D.R., Lautenbach, E., Pegues, D.A., 2017. Impact of Two Different Antimicrobial Stewardship Methods on Frequency of Streamlining Antimicrobial Agents in Patients with Bacteremia. Infect. Control Hosp. Epidemiol. 38, 89–95. doi:10.1017/ice.2016.243

Lumley, S.F., Constantinides, B., Sanderson, N., Rodger, G., Street, T.L., Swann, J., Chau, K.K., O'Donnell, D., Warren, F., Hoosdally, S., Laboratory, O.M., Control Team, O.I.P.A., O'Donnell, A.-M., Walker, T.M., Stoesser, N.E., Butcher, L., Peto, T.E., Crook, D.W., Jeffery, K., Matthews, P.C., Eyre, D.W., 2021. Epidemiological data and genome sequencing reveals that nosocomial transmission of SARS-CoV-2 is underestimated and mostly mediated by a small number of highly infectious individuals. J. Infect. doi:10.1016/j.jinf.2021.07.034

Lynch, S.V., Pedersen, O., 2016. The human intestinal microbiome in health and disease. N. Engl. J. Med. 375, 2369–2379. doi:10.1056/NEJMra1600266

Ma, Y., Hou, L., Yang, Xiufang, Huang, Z., Yang, Xue, Zhao, N., He, M., Shi, Y., Kang, Y., Yue, J., Wu, C., 2020. The association between frailty and severe disease among COVID-19 patients aged over 60 years in China: a prospective cohort study. BMC Med. 18, 274. doi:10.1186/s12916-020-01761-0

MacFadden, D.R., Fisman, D.N., Hanage, W.P., Lipsitch, M., 2019. The Relative Impact of Community and Hospital Antibiotic Use on the Selection of Extended-spectrum Beta-lactamase-producing Escherichia coli. Clin. Infect. Dis. 69, 182–188. doi:10.1093/cid/ciy978

MacIntyre, C.R., Chughtai, A.A., Barnes, M., Ridda, I., Seale, H., Toms, R., Heywood, A., 2018. The role of pneumonia and secondary bacterial infection in fatal and serious outcomes of pandemic influenza a(H1N1)pdm09. BMC Infect. Dis. 18, 637. doi:10.1186/s12879-018-3548-0

Macrae, M.B., Shannon, K.P., Rayner, D.M., Kaiser, A.M., Hoffman, P.N., French, G.L., 2001. A simultaneous outbreak on a neonatal unit of two strains of multiply antibiotic resistant Klebsiella pneumoniae controllable only by ward closure. J. Hosp. Infect. 49, 183–192. doi:10.1053/jhin.2001.1066

Maechler, F., Schwab, F., Hansen, S., Fankhauser, C., Harbarth, S., Huttner, B.D., Diaz-Agero, C., Lopez, N., Canton, R., Ruiz-Garbajosa, P., Blok, H., Bonten, M.J., Kloosterman, F., Schotsman, J., Cooper, B.S., Behnke, M., Golembus, J., Kola, A., Gastmeier, P., R-GNOSIS WP5 study group, 2020. Contact isolation versus standard precautions to decrease acquisition of extended-spectrum β-lactamase-producing Enterobacterales in non-critical care wards: a cluster-randomised crossover trial. Lancet Infect. Dis. 20, 575–584. doi:10.1016/S1473-3099(19)30626-7

Magill, S.S., O'Leary, E., Janelle, S.J., Thompson, D.L., Dumyati, G., Nadle, J., Wilson, L.E., Kainer, M.A., Lynfield, R., Greissman, S., Ray, S.M., Beldavs, Z., Gross, C., Bamberg, W., Sievers, M., Concannon, C., Buhr, N., Warnke, L., Maloney, M., Ocampo, V., Brooks, J., Oyewumi, T., Sharmin, S., Richards, K., Rainbow, J., Samper, M., Hancock, E.B., Leaptrot, D., Scalise, E., Badrun, F., Phelps, R., Edwards, J.R., Emerging Infections Program Hospital Prevalence Survey Team, 2018. Changes in Prevalence of Health Care-Associated Infections in U.S. Hospitals. N. Engl. J. Med. 379, 1732–1744. doi:10.1056/NEJMoa1801550

Mallapaty, S., 2020. The mathematical strategy that could transform coronavirus testing. Nature. doi:10.1038/d41586-020-02053-6

Maltby, R., Leatham-Jensen, M.P., Gibson, T., Cohen, P.S., Conway, T., 2013. Nutritional basis for colonization resistance by human commensal Escherichia coli strains HS and Nissle 1917 against E. coli O157:H7 in the mouse intestine. PLoS One 8, e53957. doi:10.1371/journal.pone.0053957

Maltezou, H.C., 2008. Nosocomial influenza: new concepts and practice. Curr Opin Infect Dis 21, 337–343. doi:10.1097/QCO.0b013e3283013945

Manchal, N., Mohamed, M.R.S., Ting, M., Luetchford, H., Francis, F., Carrucan, J., Norton, R., 2020. Hospital acquired viral respiratory tract infections: An underrecognized nosocomial infection. Infection, Disease & Health 25, 175–180. doi:10.1016/j.idh.2020.02.002

Mangen, M.-J.J., Plass, D., Havelaar, A.H., Gibbons, C.L., Cassini, A., Mühlberger, N., van Lier, A., Haagsma, J.A., Brooke, R.J., Lai, T., de Waure, C., Kramarz, P., Kretzschmar, M.E.E., BCoDE consortium, 2013. The pathogen- and incidence-based DALY approach: an appropriate [corrected] methodology for estimating the burden of infectious diseases. PLoS One 8, e79740. doi:10.1371/journal.pone.0079740

Manoukian, S., Stewart, S., Graves, N., Mason, H., Robertson, C., Kennedy, S., Pan, J., Haahr, L., Dancer, S.J., Cook, B., Reilly, J., 2021a. Evaluating the post-discharge cost of healthcare-associated infection in NHS Scotland. J. Hosp. Infect. 114, 51–58. doi:10.1016/j.jhin.2020.12.026

Manoukian, S., Stewart, S., Graves, N., Mason, H., Robertson, C., Kennedy, S., Pan, J., Kavanagh, K., Haahr, L., Adil, M., Dancer, S.J., Cook, B., Reilly, J., 2021b. Bed-days and costs associated with the inpatient burden of healthcare-associated infection in the UK. J. Hosp. Infect. 114, 43–50. doi:10.1016/j.jhin.2020.12.027

Marchetti, A., Rossiter, R., 2013. Economic burden of healthcare-associated infection in US acute care hospitals: societal perspective. J Med Econ 16, 1399–1404. doi:10.3111/13696998.2013.842922

Marino, S., Hogue, I.B., Ray, C.J., Kirschner, D.E., 2008. A methodology for performing global uncertainty and sensitivity analysis in systems biology. J. Theor. Biol. 254, 178–196. doi:10.1016/j.jtbi.2008.04.011

Martin, J.S.H., Monaghan, T.M., Wilcox, M.H., 2016. Clostridium difficile infection: epidemiology, diagnosis and understanding transmission. Nat. Rev. Gastroenterol. Hepatol. 13, 206–216. doi:10.1038/nrgastro.2016.25

Martinez-Valdebenito, C., Calvo, M., Vial, C., Mansilla, R., Marco, C., Palma, R.E., Vial, P.A., Valdivieso, F., Mertz, G., Ferrés, M., 2014. Person-to-person household and nosocomial transmission of andes hantavirus, Southern Chile, 2011. Emerging Infect. Dis. 20, 1629–1636. doi:10.3201/eid2010.140353

Mathers, A.J., Peirano, G., Pitout, J.D.D., 2015. The role of epidemic resistance plasmids and international high-risk clones in the spread of multidrug-resistant Enterobacteriaceae. Clin. Microbiol. Rev. 28, 565–591. doi:10.1128/CMR.00116-14

McCormack, J., Lalji, F., 2015. Antibiotic Sensitivity Chart [WWW Document]. URL http://therapeuticseducation.org/sites/therapeuticseducation.org/files/Antibiotic_Sensitivity_December_2015.pdf (accessed 11.11.20).

McKay, S.L., Tobolowsky, F.A., Moritz, E.D., Hatfield, K.M., Bhatnagar, A., LaVoie, S.P., Jackson, D.A., Lecy, K.D., Bryant-Genevier, J., Campbell, D., Freeman, B., Gilbert, S.E., Folster, J.M., Medrzycki, M., Shewmaker, P.L., Bankamp, B., Radford, K.W., Anderson, R., Bowen, M.D., Negley, J., Reddy, S.C., Jernigan, J.A., Brown, A.C., McDonald, L.C., Kutty, P.K., CDC Infection Prevention and Control Team and the CDC COVID-19 Surge Laboratory Group, 2021. Performance Evaluation of Serial SARS-CoV-2 Rapid Antigen Testing During a Nursing Home Outbreak. Ann. Intern. Med. 174, 945–951. doi:10.7326/M21-0422

McMichael, T.M., Currie, D.W., Clark, S., Pogosjans, S., Kay, M., Schwartz, N.G., Lewis, J., Baer, A., Kawakami, V., Lukoff, M.D., Ferro, J., Brostrom-Smith, C., Rea, T.D., Sayre, M.R., Riedo, F.X., Russell, D., Hiatt, B., Montgomery, P., Rao, A.K., Chow, E.J., Tobolowsky, F., Hughes, M.J., Bardossy, A.C., Oakley, L.P., Jacobs, J.R., Stone, N.D., Reddy, S.C., Jernigan, J.A., Honein, M.A., Clark, T.A., Duchin, J.S., Public Health–Seattle and King County, EvergreenHealth, and CDC COVID-19 Investigation Team, 2020. Epidemiology of Covid-19 in a Long-Term Care Facility in King County, Washington. N. Engl. J. Med. 382, 2005–2011. doi:10.1056/NEJMoa2005412

McMullen, K.M., Smith, B.A., Rebmann, T., 2020. Impact of SARS-CoV-2 on hospital acquired infection rates in the United States: Predictions and early results. Am. J. Infect. Control 48, 1409–1411. doi:10.1016/j.ajic.2020.06.209

Meakins, S.M., Adak, G.K., Lopman, B.A., O'Brien, S.J., 2003. General outbreaks of infectious intestinal disease (IID) in hospitals, England and Wales, 1992-2000. J. Hosp. Infect. 53, 1–5. doi:10.1053/jhin.2002.1326

Meijs, A.P., Ferreira, J.A., DE Greeff, S.C., Vos, M.C., Koek, M.B.G., 2017. Incidence of surgical site infections cannot be derived reliably from point prevalence survey data in Dutch hospitals. Epidemiol. Infect. 145, 970–980. doi:10.1017/S0950268816003162

Melnyk, A.H., Wong, A., Kassen, R., 2015. The fitness costs of antibiotic resistance mutations. Evol. Appl. 8, 273–283. doi:10.1111/eva.12196

Meredith, L.W., Hamilton, W.L., Warne, B., Houldcroft, C.J., Hosmillo, M., Jahun, A.S., Curran, M.D., Parmar, S., Caller, L.G., Caddy, S.L., Khokhar, F.A., Yakovleva, A., Hall, G., Feltwell, T., Forrest, S., Sridhar, S., Weekes, M.P., Baker, S., Brown, N., Moore, E., Popay, A., Roddick, I., Reacher, M., Gouliouris, T., Peacock, S.J., Dougan, G., Török, M.E., Goodfellow, I., 2020. Rapid implementation of SARS-CoV-2 sequencing to investigate cases of health-care associated COVID-19: a prospective genomic surveillance study. Lancet Infect. Dis. 20, 1263–1271. doi:10.1016/S1473-3099(20)30562-4

Merrill, R.M., 2019. Introduction to Epidemiology, 8th ed. Jones & Bartlett Learning.

Michel, J.-B., Yeh, P.J., Chait, R., Moellering, R.C., Kishony, R., 2008. Drug interactions modulate the potential for evolution of resistance. Proc. Natl. Acad. Sci. USA 105, 14918–14923. doi:10.1073/pnas.0800944105

Mideo, N., Alizon, S., Day, T., 2008. Linking within- and between-host dynamics in the evolutionary epidemiology of infectious diseases. Trends Ecol. Evol. (Amst.) 23, 511–517. doi:10.1016/j.tree.2008.05.009

Miller, B.A., Chen, L.F., Sexton, D.J., Anderson, D.J., 2011. Comparison of the burdens of hospital-onset, healthcare facility-associated Clostridium difficile Infection and of healthcare-associated infection due to methicillin-resistant Staphylococcus aureus in community hospitals. Infect. Control Hosp. Epidemiol. 32, 387–390. doi:10.1086/659156

Mina, M.J., Andersen, K.G., 2021. COVID-19 testing: One size does not fit all. Science 371, 126–127. doi:10.1126/science.abe9187

Ministère des solidarités et de la santé, 2020. Recommandations pour le secteur SSR dans le contexte de l'épidémie COVID-19.

Mitchell, R., Taylor, G., Rudnick, W., Alexandre, S., Bush, K., Forrester, L., Frenette, C., Granfield, B., Gravel-Tropper, D., Happe, J., John, M., Lavallee, C., McGeer, A., Mertz, D., Pelude, L., Science, M., Simor, A., Smith, S., Suh, K.N., Vayalumkal, J., Wong, A., Amaratunga, K., Canadian Nosocomial Infection Surveillance Program, 2019. Trends in health care-associated infections in acute care hospitals in Canada: an analysis of repeated point-prevalence surveys. Can. Med. Assoc. J. 191, E981–E988. doi:10.1503/cmaj.190361

Mizumoto, K., Kagaya, K., Zarebski, A., Chowell, G., 2020. Estimating the asymptomatic proportion of coronavirus disease 2019 (COVID-19) cases on board the Diamond Princess cruise ship, Yokohama, Japan, 2020. Euro Surveill. 25. doi:10.2807/1560-7917.ES.2020.25.10.2000180

Moghadas, S.M., Fitzpatrick, M.C., Sah, P., Pandey, A., Shoukat, A., Singer, B.H., Galvani, A.P., 2020. The implications of silent transmission for the control of COVID-19 outbreaks. Proc. Natl. Acad. Sci. USA.

Mollers, M., Lutgens, S.P., Schoffelen, A.F., Schneeberger, P.M., Suijkerbuijk, A.W.M., 2017. Cost of Nosocomial Outbreak Caused by NDM-1-Containing Klebsiella pneumoniae in the Netherlands, October 2015-January 2016. Emerging Infect. Dis. 23, 1574–1576. doi:10.3201/eid2309.161710

Moore, L.D., Robbins, G., Quinn, J., Arbogast, J.W., 2021. The impact of COVID-19 pandemic on hand hygiene performance in hospitals. Am. J. Infect. Control 49, 30–33. doi:10.1016/j.ajic.2020.08.021

Morris, D.E., Oakley, J.E., Crowe, J.A., 2014. A web-based tool for eliciting probability distributions from experts. Environ. Model. Softw. 52, 1–4. doi:10.1016/j.envsoft.2013.10.010

Mossong, J., Hens, N., Jit, M., Beutels, P., Auranen, K., Mikolajczyk, R., Massari, M., Salmaso, S., Tomba, G.S., Wallinga, J., Heijne, J., Sadkowska-Todys, M., Rosinska, M., Edmunds, W.J., 2008. Social contacts and mixing patterns relevant to the spread of infectious diseases. PLoS Med. 5, e74. doi:10.1371/journal.pmed.0050074

Moussa, Y., Shuster, J., Matte, G., Sullivan, A., Goldstein, R.H., Cunningham, D., Ben-Shoshan, M., Baldini, G., Carli, F., Tsoukas, C., 2018. De-labeling of β-lactam allergy reduces intraoperative time and optimizes choice in antibiotic prophylaxis. Surgery. doi:10.1016/j.surg.2018.03.004

Mukhtar, M.M., Khogali, M., 2021. The accelerating COVID-19 epidemic in Sudan. Nat. Immunol. 22, 797–798. doi:10.1038/s41590-021-00950-0

Mylotte, J.M., 2005. Nursing home-acquired bloodstream infection. Infect. Control Hosp. Epidemiol. 26, 833–837. doi:10.1086/502502

Nadimpalli, G., O'Hara, L.M., Pineles, L., Lebherz, K., Johnson, J.K., Calfee, D.P., Miller, L.G., Morgan, D.J., Harris, A.D., 2020. Patient to healthcare personnel transmission of MRSA in the non-intensive care unit setting. Infect. Control Hosp. Epidemiol. 41, 601–603. doi:10.1017/ice.2020.10

Nakoune, E., Lampaert, E., Ndjapou, S.G., Janssens, C., Zuniga, I., Van Herp, M., Fongbia, J.P., Koyazegbe, T.D., Selekon, B., Komoyo, G.F., Garba-Ouangole, S.M., Manengu, C., Manuguerra, J.-C., Kazanji, M., Gessain, A., Berthet, N., 2017. A nosocomial outbreak of human monkeypox in the central african republic. Open Forum Infect. Dis. 4, ofx168. doi:10.1093/ofid/ofx168

Narayanan, K., Frost, I., Heidarzadeh, A., Tseng, K.K., Banerjee, S., John, J., Laxminarayan, R., 2020. Pooling RT-PCR or NGS samples has the potential to cost-effectively generate estimates of COVID-19 prevalence in resource limited environments. medRxiv. doi:10.1101/2020.04.03.20051995

Negri, M.C., Morosini, M.I., Loza, E., Baquero, F., 1994. In vitro selective antibiotic concentrations of beta-lactams for penicillin-resistant Streptococcus pneumoniae populations. Antimicrob. Agents Chemother. 38, 122–125. doi:10.1128/AAC.38.1.122

Nelson, A., Kassimatis, J., Estoque, J., Yang, C., McKee, G., Bryce, E., Hoang, L., Daly, P., Lysyshyn, M., Hayden, A.S., Harding, J., Boraston, S., Dawar, M., Schwandt, M., 2021. Environmental detection of severe acute respiratory syndrome coronavirus 2 (SARS-CoV-2) from medical equipment in long-term care facilities undergoing COVID-19 outbreaks. Am. J. Infect. Control 49, 265–268. doi:10.1016/j.ajic.2020.07.001

Nelson, R.E., Deka, R., Khader, K., Stevens, V.W., Schweizer, M.L., Rubin, M.A., 2017. Dynamic transmission models for economic analysis applied to health care-associated infections: A review of the literature. Am. J. Infect. Control 45, 1382–1387. doi:10.1016/j.ajic.2017.02.035

Neuman, M.I., Hall, M., Hersh, A.L., Brogan, T.V., Parikh, K., Newland, J.G., Blaschke, A.J., Williams, D.J., Grijalva, C.G., Tyler, A., Shah, S.S., 2012. Influence of hospital guidelines on management of children hospitalized with pneumonia. Pediatrics 130, e823-30. doi:10.1542/peds.2012-1285

Nguyen, L.K.N., Megiddo, I., Howick, S., 2020. Simulation models for transmission of health care-associated infection: A systematic review. Am. J. Infect. Control 48, 810–821. doi:10.1016/j.ajic.2019.11.005

Nguyen, L.L.K., Howick, S., McLafferty, D., Anderson, G.H., Pravinkumar, S.J., Van Der Meer, R., Megiddo, I., 2020. Evaluating intervention strategies in controlling coronavirus disease 2019 (COVID-19) spread in care homes: An agent-based model. Infect. Control Hosp. Epidemiol. 1–11. doi:10.1017/ice.2020.1369

Nguyen, N.T., Aprahamian, H., Bish, E.K., Bish, D.R., 2019. A methodology for deriving the sensitivity of pooled testing, based on viral load progression and pooling dilution. J. Transl. Med. 17, 252. doi:10.1186/s12967-019-1992-2

Niehus, R., van Kleef, E., Mo, Y., Turlej-Rogacka, A., Lammens, C., Carmeli, Y., Goossens, H., Tacconelli, E., Carevic, B., Preotescu, L., Malhotra-Kumar, S., Cooper, B.S., 2020. Quantifying antibiotic impact on within-patient dynamics of extended-spectrum beta-lactamase resistance. Elife 9. doi:10.7554/eLife.49206

Niewiadomska, A.M., Jayabalasingham, B., Seidman, J.C., Willem, L., Grenfell, B., Spiro, D., Viboud, C., 2019. Population-level mathematical modeling of antimicrobial resistance: a systematic review. BMC Med. 17, 81. doi:10.1186/s12916-019-1314-9

Nishiura, H., Kobayashi, T., Miyama, T., Suzuki, A., Jung, S.-M., Hayashi, K., Kinoshita, R., Yang, Y., Yuan, B., Akhmetzhanov, A.R., Linton, N.M., 2020. Estimation of the asymptomatic ratio of novel coronavirus infections (COVID-19). Int. J. Infect. Dis. 94, 154–155. doi:10.1016/j.ijid.2020.03.020

Novais, A., Rodrigues, C., Branquinho, R., Antunes, P., Grosso, F., Boaventura, L., Ribeiro, G., Peixe, L., 2012. Spread of an OmpK36-modified ST15 Klebsiella pneumoniae variant during an outbreak involving multiple carbapenem-resistant Enterobacteriaceae species and clones. Eur. J. Clin. Microbiol. Infect. Dis. 31, 3057–3063. doi:10.1007/s10096-012-1665-z

Obadia, T., Opatowski, L., Temime, L., Herrmann, J.-L., Fleury, É., Boëlle, P.-Y., Guillemot, D., 2015. Interindividual Contacts and Carriage of Methicillin-Resistant Staphylococcus aureus: A Nested Case-Control Study. Infect. Control Hosp. Epidemiol. 36, 922–929. doi:10.1017/ice.2015.89

O'Brien, S., Baumgartner, M., Hall, A.R., 2021. Species interactions drive the spread of ampicillin resistance in human-associated

gut microbiota. Evol Med Public Health. doi:10.1093/emph/eoab020

Ofek Shlomai, N., Rao, S., Patole, S., 2015. Efficacy of interventions to improve hand hygiene compliance in neonatal units: a systematic review and meta-analysis. Eur. J. Clin. Microbiol. Infect. Dis. 34, 887–897. doi:10.1007/s10096-015-2313-1

O'Hara, L.M., Calfee, D.P., Miller, L.G., Pineles, L., Magder, L.S., Johnson, J.K., Morgan, D.J., Harris, A.D., 2019. Optimizing Contact Precautions to Curb the Spread of Antibiotic-resistant Bacteria in Hospitals: A Multicenter Cohort Study to Identify Patient Characteristics and Healthcare Personnel Interactions Associated With Transmission of Methicillin-resistant Staphylococcus aureus. Clin. Infect. Dis. 69, S171–S177. doi:10.1093/cid/ciz621

Olivas-Martínez, A., Cárdenas-Fragoso, J.L., Jiménez, J.V., Lozano-Cruz, O.A., Ortiz-Brizuela, E., Tovar-Méndez, V.H., Medrano-Borromeo, C., Martínez-Valenzuela, A., Román-Montes, C.M., Martínez-Guerra, B., González-Lara, M.F., Hernandez-Gilsoul, T., Herrero, A.G., Tamez-Flores, K.M., Ochoa-Hein, E., Ponce-de-León, A., Galindo-Fraga, A., Kershenobich-Stalnikowitz, D., Sifuentes-Osornio, J., 2021. In-hospital mortality from severe COVID-19 in a tertiary care center in Mexico City; causes of death, risk factors and the impact of hospital saturation. PLoS One 16, e0245772. doi:10.1371/journal.pone.0245772

Opatowski, L., Domenech de Cellès, M., Souissi, S., Kardaś-Słoma, L., Temime, L., Guillemot, D., 2013. Contribution des modèles mathématiques à la compréhension de la dynamique de diffusion des bactéries multi-résistantes à l'hôpital. Journal des Anti-infectieux 15, 193–203. doi:10.1016/j.antinf.2013.09.002

Opatowski, L., Guillemot, D., Boëlle, P.-Y., Temime, L., 2011. Contribution of mathematical modeling to the fight against bacterial antibiotic resistance. Curr Opin Infect Dis 24, 279–287. doi:10.1097/QCO.0b013e3283462362

O'Toole, R.F., 2021. The interface between COVID-19 and bacterial healthcare-associated infections. Clin. Microbiol. Infect. doi:10.1016/j.cmi.2021.06.001

Overcash, M.R., Sehulster, L.M., 2021. Estimated incidence rate of healthcare-associated infections (HAIs) linked to laundered reusable healthcare textiles (HCTs) in the United States and United Kingdom over a 50-year period: Do the data support the efficacy of approved laundry practices? Infect. Control Hosp. Epidemiol. 1–2. doi:10.1017/ice.2021.274

Owens, C.D., Stoessel, K., 2008. Surgical site infections: epidemiology, microbiology and prevention. J. Hosp. Infect. 70 Suppl 2, 3–10. doi:10.1016/S0195-6701(08)60017-1

Pai, M., Kalantri, S., Aggarwal, A.N., Menzies, D., Blumberg, H.M., 2006. Nosocomial tuberculosis in India. Emerging Infect. Dis. 12, 1311–1318. doi:10.3201/eid1209.051663

Palmer, S., Torgerson, D.J., 1999. Economic notes: definitions of efficiency. BMJ 318, 1136. doi:10.1136/bmj.318.7191.1136

Paltiel, A.D., Zheng, A., Sax, P.E., 2021. Clinical and Economic Effects of Widespread Rapid Testing to Decrease SARS-CoV-2 Transmission. Ann. Intern. Med. doi:10.7326/M21-0510

Pamer, E.G., 2016. Resurrecting the intestinal microbiota to combat antibiotic-resistant pathogens. Science 352, 535–538. doi:10.1126/science.aad9382

Pantel, A., Marchandin, H., Prère, M.F., Boutet-Dubois, A., Brieu-Roche, N., Gaschet, A., Davin-Regli, A., Sotto, A., Lavigne, J.P., 2015. Faecal carriage of carbapenemase-producing Gram-negative bacilli in hospital settings in southern France. Eur. J. Clin. Microbiol. Infect. Dis. 34, 899–904. doi:10.1007/s10096-014-2298-1

Papagiannitsis, C.C., Giakkoupi, P., Kotsakis, S.D., Tzelepi, E., Tzouvelekis, L.S., Vatopoulos, A.C., Miriagou, V., 2013. OmpK35 and OmpK36 porin variants associated with specific sequence types of Klebsiella pneumoniae. J Chemother 25, 250–254. doi:10.1179/1973947813Y.0000000075

Papanicolas, L.E., Warner, M., Wesselingh, S.L., Rogers, G.B., 2020. Protect commensal gut bacteria to improve antimicrobial stewardship. Clin. Microbiol. Infect. 26, 814–815. doi:10.1016/j.cmi.2020.03.021

Patel, G., Huprikar, S., Factor, S.H., Jenkins, S.G., Calfee, D.P., 2008. Outcomes of carbapenem-resistant Klebsiella pneumoniae infection and the impact of antimicrobial and adjunctive therapies. Infect. Control Hosp. Epidemiol. 29, 1099–1106. doi:10.1086/592412

Paweska, J.T., Sewlall, N.H., Ksiazek, T.G., Blumberg, L.H., Hale, M.J., Lipkin, W.I., Weyer, J., Nichol, S.T., Rollin, P.E., McMullan, L.K., Paddock, C.D., Briese, T., Mnyaluza, J., Dinh, T.-H., Mukonka, V., Ching, P., Duse, A., Richards, G., de Jong, G., Cohen, C., Ikalafeng, B., Mugero, C., Asomugha, C., Malotle, M.M., Nteo, D.M., Misiani, E., Swanepoel, R., Zaki, S.R., Outbreak Control and Investigation Teams, 2009. Nosocomial outbreak of novel arenavirus infection, southern

Africa. Emerging Infect. Dis. 15, 1598–1602. doi:10.3201/eid1510.090211

Pawlowski, A.C., Wang, W., Koteva, K., Barton, H.A., McArthur, A.G., Wright, G.D., 2016. A diverse intrinsic antibiotic resistome from a cave bacterium. Nat. Commun. 7, 13803. doi:10.1038/ncomms13803

Payne, D.C., Vinjé, J., Szilagyi, P.G., Edwards, K.M., Staat, M.A., Weinberg, G.A., Hall, C.B., Chappell, J., Bernstein, D.I., Curns, A.T., Wikswo, M., Shirley, S.H., Hall, A.J., Lopman, B., Parashar, U.D., 2013. Norovirus and medically attended gastroenteritis in U.S. children. N. Engl. J. Med. 368, 1121–1130. doi:10.1056/NEJMsa1206589

Peiffer-Smadja, N., Lucet, J.C., Bendjelloul, G., Bouadma, L., Gerard, S., Choquet, C., Jacques, S., Khalil, A., Maisani, P., Casalino, E., Descamps, D., Timsit, J.F., Yazdanpanah, Y., Lescure, F.X., 2020. Challenges and issues about organizing a hospital to respond to the COVID-19 outbreak: experience from a French reference centre. Clin. Microbiol. Infect. 26, 669–672. doi:10.1016/j.cmi.2020.04.002

Pelat, C., Kardaś-Słoma, L., Birgand, G., Ruppé, E., Schwarzinger, M., Andremont, A., Lucet, J.-C., Yazdanpanah, Y., 2016. Hand Hygiene, Cohorting, or Antibiotic Restriction to Control Outbreaks of Multidrug-Resistant Enterobacteriaceae. Infect. Control Hosp. Epidemiol. 37, 272–280. doi:10.1017/ice.2015.284

Péré, H., Podglajen, I., Wack, M., Flamarion, E., Mirault, T., Goudot, G., Hauw-Berlemont, C., Le, L., Caudron, E., Carrabin, S., Rodary, J., Ribeyre, T., Bélec, L., Veyer, D., 2020. Nasal Swab Sampling for SARS-CoV-2: a Convenient Alternative in Times of Nasopharyngeal Swab Shortage. J. Clin. Microbiol. 58. doi:10.1128/JCM.00721-20

Peters, C.J., Kuehne, R.W., Mercado, R.R., Le Bow, R.H., Spertzel, R.O., Webb, P.A., 1974. Hemorrhagic fever in Cochabamba, Bolivia, 1971. Am. J. Epidemiol. 99, 425–433. doi:10.1093/oxfordjournals.aje.a121631

Petrilli, C.M., Jones, S.A., Yang, J., Rajagopalan, H., O'Donnell, L., Chernyak, Y., Tobin, K.A., Cerfolio, R.J., Francois, F., Horwitz, L.I., 2020. Factors associated with hospital admission and critical illness among 5279 people with coronavirus disease 2019 in New York City: prospective cohort study. BMJ 369, m1966. doi:10.1136/bmj.m1966

Pham, T.M., Tahir, H., van de Wijgert, J.H.H.M., Van der Roest, B., Ellerbroek, P., Bonten, M.J.M., Bootsma, M.C.J., Kretzschmar, M.E., 2021. Interventions to control nosocomial transmission of SARS-CoV-2: a modelling study. medRxiv. doi:10.1101/2021.02.26.21252327

Pilmis, B., Cattoir, V., Lecointe, D., Limelette, A., Grall, I., Mizrahi, A., Marcade, G., Poilane, I., Guillard, T., Bourgeois Nicolaos, N., Zahar, J.R., Le Monnier, A., 2018. Carriage of ESBL-producing Enterobacteriaceae in French hospitals: the PORTABLSE study. J. Hosp. Infect. 98, 247–252. doi:10.1016/j.jhin.2017.11.022

Pilmis, B., Le Monnier, A., Zahar, J.-R., 2020. Gut microbiota, antibiotic therapy and antimicrobial resistance: A narrative review. Microorganisms 8. doi:10.3390/microorganisms8020269

Pineda-Krch, M., 2008. gillespiessa : implementing the stochastic simulation algorithm in *r*. J. Stat. Softw. 25. doi:10.18637/jss.v025.i12

Pinquier, J.-L., Varastet, M., Meyers, D., Sayah-Jeanne, S., Féger, C., Gaumétou, O., Corbel, T., de Gunzburg, J., Mentré, F., Ducher, A., 2021. A Colon-Targeted Adsorbent (DAV132) Does Not Affect the Pharmacokinetics of Warfarin or Clonazepam in Healthy Subjects. Clin. Pharmacol. Drug Dev. doi:10.1002/cpdd.901

Pitout, J.D., Nordmann, P., Poirel, L., 2015. Carbapenemase-Producing Klebsiella pneumoniae, a Key Pathogen Set for Global Nosocomial Dominance. Antimicrob. Agents Chemother. 59, 5873–5884. doi:10.1128/AAC.01019-15

Pittet, D., Hugonnet, S., Harbarth, S., Mourouga, P., Sauvan, V., Touveneau, S., Perneger, T.V., 2000. Effectiveness of a hospital-wide programme to improve compliance with hand hygiene. Infection Control Programme. Lancet 356, 1307–1312. doi:10.1016/s0140-6736(00)02814-2

Plachouras, D., Kärki, T., Hansen, S., Hopkins, S., Lyytikäinen, O., Moro, M.L., Reilly, J., Zarb, P., Zingg, W., Kinross, P., Weist, K., Monnet, D.L., Suetens, C., The Point Prevalence Survey Study Group, 2018. Antimicrobial use in European acute care hospitals: results from the second point prevalence survey (PPS) of healthcare-associated infections and antimicrobial use, 2016 to 2017. Euro Surveill. 23. doi:10.2807/1560-7917.ES.23.46.1800393

Polso, A.K., Lassiter, J.L., Nagel, J.L., 2014. Impact of hospital guideline for weight-based antimicrobial dosing in morbidly obese adults and comprehensive literature review. J Clin Pharm Ther 39, 584–608. doi:10.1111/jcpt.12200

Ponce-Alonso, M., Sáez de la Fuente, J., Rincón-Carlavilla, A., Moreno-Nunez, P., Martínez-García, L., Escudero-Sánchez, R., Pintor, R., García-Fernández, S., Cobo, J., 2021. Impact of the coronavirus disease 2019 (COVID-19) pandemic on

nosocomial Clostridioides difficile infection. Infect. Control Hosp. Epidemiol. 42, 406–410. doi:10.1017/ice.2020.454

Poulou, A., Voulgari, E., Vrioni, G., Koumaki, V., Xidopoulos, G., Chatzipantazi, V., Markou, F., Tsakris, A., 2013. Outbreak caused by an ertapenem-resistant, CTX-M-15-producing Klebsiella pneumoniae sequence type 101 clone carrying an OmpK36 porin variant. J. Clin. Microbiol. 51, 3176–3182. doi:10.1128/JCM.01244-13

Pouwels, K.B., Roope, L.S.J., Barnett, A., Hunter, D.J., Nolan, T.M., Clarke, P.M., 2020. Group Testing for SARS-CoV-2: Forward to the Past? PharmacoEconomics Open 1–4. doi:10.1007/s41669-020-00217-8

Prescott, H.C., Dickson, R.P., Rogers, M.A.M., Langa, K.M., Iwashyna, T.J., 2015. Hospitalization type and subsequent severe sepsis. Am. J. Respir. Crit. Care Med. 192, 581–588. doi:10.1164/rccm.201503-0483OC

Pressley, J., D'Agata, E.M.C., Webb, G.F., 2010. The effect of co-colonization with community-acquired and hospital-acquired methicillin-resistant Staphylococcus aureus strains on competitive exclusion. J. Theor. Biol. 264, 645–656. doi:10.1016/j.jtbi.2010.03.036

Prestel, C., Anderson, E., Forsberg, K., Lyman, M., de Perio, M.A., Kuhar, D., Edwards, K., Rivera, M., Shugart, A., Walters, M., Dotson, N.Q., 2021. Candida auris Outbreak in a COVID-19 Specialty Care Unit - Florida, July-August 2020. MMWR Morb. Mortal. Wkly. Rep. 70, 56–57. doi:10.15585/mmwr.mm7002e3

Pritchard, E., Matthews, P.C., Stoesser, N., Eyre, D.W., Gethings, O., Vihta, K.-D., Jones, J., House, T., VanSteenHouse, H., Bell, I., Bell, J.I., Newton, J.N., Farrar, J., Diamond, I., Rourke, E., Studley, R., Crook, D., Peto, T.E.A., Walker, A.S., Pouwels, K.B., 2021. Impact of vaccination on new SARS-CoV-2 infections in the United Kingdom. Nat. Med. doi:10.1038/s41591-021-01410-w

ProMED: International Society for Infectious Diseases, 2019. UNDIAGNOSED PNEUMONIA - CHINA (HUBEI): REQUEST FOR INFORMATION [WWW Document]. URL https://promedmail.org/promed-post/?id=6864153%20#COVID19 (accessed 8.9.21).

Pshenichnaya, N.Y., Nenadskaya, S.A., 2015. Probable Crimean-Congo hemorrhagic fever virus transmission occurred after aerosol-generating medical procedures in Russia: nosocomial cluster. Int. J. Infect. Dis. 33, 120–122. doi:10.1016/j.ijid.2014.12.047

Pullano, G., Di Domenico, L., Sabbatini, C.E., Valdano, E., Turbelin, C., Debin, M., Guerrisi, C., Kengne-Kuetche, C., Souty, C., Hanslik, T., Blanchon, T., Boëlle, P.-Y., Figoni, J., Vaux, S., Campèse, C., Bernard-Stoecklin, S., Colizza, V., 2021. Underdetection of cases of COVID-19 in France threatens epidemic control. Nature 590, 134–139. doi:10.1038/s41586-020-03095-6

Qadeer, A., Akhtar, A., Ain, Q.U., Saadat, S., Mansoor, S., Assad, S., Ishtiaq, W., Ilyas, A., Khan, A.Y., Ajam, Y., 2016. Antibiogram of medical intensive care unit at tertiary care hospital setting of pakistan. Cureus 8, e809. doi:10.7759/cureus.809

Rafii, F., Sutherland, J.B., Cerniglia, C.E., 2008. Effects of treatment with antimicrobial agents on the human colonic microflora. Ther Clin Risk Manag 4, 1343–1358. doi:10.2147/TCRM.S4328

Railsback, S.F., Grimm, V., 2011. Agent-Based and Individual-Based Modeling: A Practical Introduction. Princeton University Press.

Ramsay, D.E., Invik, J., Checkley, S.L., Gow, S.P., Osgood, N.D., Waldner, C.L., 2018. Application of dynamic modelling techniques to the problem of antibacterial use and resistance: a scoping review. Epidemiol. Infect. 146, 2014–2027. doi:10.1017/S0950268818002091

Rashidi, A., Ebadi, M., Rehman, T.U., Elhusseini, H., Nalluri, H., Kaiser, T., Holtan, S.G., Khoruts, A., Weisdorf, D.J., Staley, C., 2021. Effect of COVID-19 precautions on the gut microbiota and nosocomial infections. Gut Microbes 13, 1–10. doi:10.1080/19490976.2021.1936378

Ravi, A., Halstead, F.D., Bamford, A., Casey, A., Thomson, N.M., van Schaik, W., Snelson, C., Goulden, R., Foster-Nyarko, E., Savva, G.M., Whitehouse, T., Pallen, M.J., Oppenheim, B.A., 2019. Loss of microbial diversity and pathogen domination of the gut microbiota in critically ill patients. Microb. Genom. 5. doi:10.1099/mgen.0.000293

Rawson, T.M., Moore, L.S.P., Zhu, N., Ranganathan, N., Skolimowska, K., Gilchrist, M., Satta, G., Cooke, G., Holmes, A., 2020. Bacterial and Fungal Coinfection in Individuals With Coronavirus: A Rapid Review To Support COVID-19 Antimicrobial Prescribing. Clin. Infect. Dis. 71, 2459–2468. doi:10.1093/cid/ciaa530

Read, A.F., Day, T., Huijben, S., 2011. The evolution of drug resistance and the curious orthodoxy of aggressive chemotherapy. Proc. Natl. Acad. Sci. USA 108 Suppl 2, 10871–10877. doi:10.1073/pnas.1100299108

Reason, J., 2016. Managing the Risks of Organizational Accidents. Routledge.

Regev-Yochay, G., Raz, M., Dagan, R., Roizin, H., Morag, B., Hetman, S., Ringel, S., Ben-Israel, N., Varon, M., Somekh, E., Rubinstein, E., 2011. Reduction in antibiotic use following a cluster randomized controlled multifaceted intervention: the Israeli judicious antibiotic prescription study. Clin. Infect. Dis. 53, 33–41. doi:10.1093/cid/cir272

Relman, D.A., Lipsitch, M., 2018. Microbiome as a tool and a target in the effort to address antimicrobial resistance. Proc. Natl. Acad. Sci. USA 115, 12902–12910. doi:10.1073/pnas.1717163115

Restif, O., Graham, A.L., 2015. Within-host dynamics of infection: from ecological insights to evolutionary predictions. Philos. Trans. R. Soc. Lond. B, Biol. Sci. 370. doi:10.1098/rstb.2014.0304

Reynolds, M.G., Anh, B.H., Thu, V.H., Montgomery, J.M., Bausch, D.G., Shah, J.J., Maloney, S., Leitmeyer, K.C., Huy, V.Q., Horby, P., Plant, A.Y., Uyeki, T.M., 2006. Factors associated with nosocomial SARS-CoV transmission among healthcare workers in Hanoi, Vietnam, 2003. BMC Public Health 6, 207. doi:10.1186/1471-2458-6-207

Rhame, F.S., Sudderth, W.D., 1981. Incidence and prevalence as used in the analysis of the occurrence of nosocomial infections. Am. J. Epidemiol. 113, 1–11. doi:10.1093/oxfordjournals.aje.a113058

Rhodes, J., Fisher, M.C., 2019. Global epidemiology of emerging Candida auris. Curr. Opin. Microbiol. 52, 84–89. doi:10.1016/j.mib.2019.05.008

Rice, L.B., 2008. Federal funding for the study of antimicrobial resistance in nosocomial pathogens: no ESKAPE. J. Infect. Dis. 197, 1079–1081. doi:10.1086/533452

Richmond, J.K., Baglole, D.J., 2003. Lassa fever: epidemiology, clinical features, and social consequences. BMJ 327, 1271–1275. doi:10.1136/bmj.327.7426.1271

Richter, D., Eyding, J., Weber, R., Bartig, D., Grau, A., Hacke, W., Krogias, C., 2021. Analysis of Nationwide Stroke Patient Care in Times of COVID-19 Pandemic in Germany. Stroke 52, 716–721. doi:10.1161/STROKEAHA.120.033160

Ricks, S., Kendall, E.A., Dowdy, D.W., Sacks, J.A., Schumacher, S.G., Arinaminpathy, N., 2021. Quantifying the potential value of antigen-detection rapid diagnostic tests for COVID-19: a modelling analysis. BMC Med. 19, 75. doi:10.1186/s12916-021-01948-z

Rijksinstituut voor Volksgezondheid en Milieu, 2020. Inzet en testbeleid medewerkers verpleeghuizen, woonzorgcentra en kleinschalige woonvormen.

Rivett, L., Sridhar, S., Sparkes, D., Routledge, M., Jones, N.K., Forrest, S., Young, J., Pereira-Dias, J., Hamilton, W.L., Ferris, M., Torok, M.E., Meredith, L., CITIID-NIHR COVID-19 BioResource Collaboration, Curran, M.D., Fuller, S., Chaudhry, A., Shaw, A., Samworth, R.J., Bradley, J.R., Dougan, G., Smith, K.G., Lehner, P.J., Matheson, N.J., Wright, G., Goodfellow, I.G., Baker, S., Weekes, M.P., 2020. Screening of healthcare workers for SARS-CoV-2 highlights the role of asymptomatic carriage in COVID-19 transmission. Elife 9. doi:10.7554/eLife.58728

Rodríguez-Baño, J., Gutiérrez-Gutiérrez, B., Machuca, I., Pascual, A., 2018. Treatment of Infections Caused by Extended-Spectrum-Beta-Lactamase-, AmpC-, and Carbapenemase-Producing Enterobacteriaceae. Clin. Microbiol. Rev. 31. doi:10.1128/CMR.00079-17

Rodríguez-Baño, J., López-Prieto, M.D., Portillo, M.M., Retamar, P., Natera, C., Nuño, E., Herrero, M., del Arco, A., Muñoz, A., Téllez, F., Torres-Tortosa, M., Martín-Aspas, A., Arroyo, A., Ruiz, A., Moya, R., Corzo, J.E., León, L., Pérez-López, J.A., 2010. Epidemiology and clinical features of community-acquired, healthcare-associated and nosocomial bloodstream infections in tertiary-care and community hospitals. Clin. Microbiol. Infect. 16, 1408–1413. doi:10.1111/j.1469-0691.2010.03089.x

Roig, J., Sabria, M., Pedro-Botet, M.L., 2003. Legionella spp.: community acquired and nosocomial infections. Curr Opin Infect Dis 16, 145–151. doi:10.1097/00001432-200304000-00011

Rosello, A., Barnard, R.C., Smith, D.R.M., Evans, S., Grimm, F., Davies, N.G., Centre for Mathematical Modelling of Infectious Diseases COVID-19 modelling working group, Deeny, S.R., Knight, G.M., Edmunds, W.J., 2021. Impact of non-pharmaceutical interventions on SARS-CoV-2 outbreaks in English care homes: a modelling study. medRxiv. doi:10.1101/2021.05.17.21257315

Rosenberger, L.H., Hranjec, T., Politano, A.D., Swenson, B.R., Metzger, R., Bonatti, H., Sawyer, R.G., 2011. Effective cohorting and "superisolation" in a single intensive care unit in response to an outbreak of diverse multi-drug-resistant organisms. Surg Infect (Larchmt) 12, 345–350. doi:10.1089/sur.2010.076

Roshan, R., Feroz, A.S., Rafique, Z., Virani, N., 2020. Rigorous Hand Hygiene Practices Among Health Care Workers Reduce Hospital-Associated Infections During the COVID-19 Pandemic. J. Prim. Care Community Health 11, 2150132720943331. doi:10.1177/2150132720943331

Rostami, A., Sepidarkish, M., Leeflang, M.M.G., Riahi, S.M., Nourollahpour Shiadeh, M., Esfandyari, S., Mokdad, A.H., Hotez, P.J., Gasser, R.B., 2021. SARS-CoV-2 seroprevalence worldwide: a systematic review and meta-analysis. Clin. Microbiol. Infect. 27, 331–340. doi:10.1016/j.cmi.2020.10.020

Round, J.L., Mazmanian, S.K., 2009. The gut microbiota shapes intestinal immune responses during health and disease. Nat. Rev. Immunol. 9, 313–323. doi:10.1038/nri2515

Rovers, J.J.E., van de Linde, L.S., Kenters, N., Bisseling, E.M., Nieuwenhuijse, D.F., Oude Munnink, B.B., Voss, A., Nabuurs-Franssen, M., 2020. Why psychiatry is different - challenges and difficulties in managing a nosocomial outbreak of coronavirus disease (COVID-19) in hospital care. Antimicrob. Resist. Infect. Control 9, 190. doi:10.1186/s13756-020-00853-z

Roy, S., Trinchieri, G., 2017. Microbiota: a key orchestrator of cancer therapy. Nat. Rev. Cancer 17, 271–285. doi:10.1038/nrc.2017.13

Ruppé, E., Armand-Lefèvre, L., Estellat, C., Consigny, P.-H., El Mniai, A., Boussadia, Y., Goujon, C., Ralaimazava, P., Campa, P., Girard, P.-M., Wyplosz, B., Vittecoq, D., Bouchaud, O., Le Loup, G., Pialoux, G., Perrier, M., Wieder, I., Moussa, N., Esposito-Farèse, M., Hoffmann, I., Coignard, B., Lucet, J.-C., Andremont, A., Matheron, S., 2015. High Rate of Acquisition but Short Duration of Carriage of Multidrug-Resistant Enterobacteriaceae After Travel to the Tropics. Clin. Infect. Dis. 61, 593–600. doi:10.1093/cid/civ333

Ruppé, E., Burdet, C., Grall, N., de Lastours, V., Lescure, F.X., Andremont, A., Armand-Lefèvre, L., 2018. Impact of antibiotics on the intestinal microbiota needs to be re-defined to optimize antibiotic usage. Clin. Microbiol. Infect. 24, 3–5. doi:10.1016/j.cmi.2017.09.017

Ruppé, E., Ghozlane, A., Tap, J., Pons, N., Alvarez, A.-S., Maziers, N., Cuesta, T., Hernando-Amado, S., Clares, I., Martínez, J.L., Coque, T.M., Baquero, F., Lanza, V.F., Máiz, L., Goulenok, T., de Lastours, V., Amor, N., Fantin, B., Wieder, I., Andremont, A., van Schaik, W., Rogers, M., Zhang, X., Willems, R.J.L., de Brevern, A.G., Batto, J.-M., Blottière, H.M., Léonard, P., Léjard, V., Letur, A., Levenez, F., Weiszer, K., Haimet, F., Doré, J., Kennedy, S.P., Ehrlich, S.D., 2019. Prediction of the intestinal resistome by a three-dimensional structure-based method. Nat. Microbiol. 4, 112–123. doi:10.1038/s41564-018-0292-6

Russo, P.L., Stewardson, A.J., Cheng, A.C., Bucknall, T., Mitchell, B.G., 2019. The prevalence of healthcare associated infections among adult inpatients at nineteen large Australian acute-care public hospitals: a point prevalence survey. Antimicrob. Resist. Infect. Control 8, 114. doi:10.1186/s13756-019-0570-y

Saha, S., Tariq, R., Tosh, P.K., Pardi, D.S., Khanna, S., 2019. Faecal microbiota transplantation for eradicating carriage of multidrug-resistant organisms: a systematic review. Clin. Microbiol. Infect. 25, 958–963. doi:10.1016/j.cmi.2019.04.006

Salcher-Konrad, M., Jhass, A., Naci, H., Tan, M., El-Tawil, Y., Comas-Herrera, A., 2020. COVID-19 related mortality and spread of disease in long-term care: a living systematic review of emerging evidence. medRxiv. doi:10.1101/2020.06.09.20125237

Saleem, Z., Hassali, M.A., Godman, B., Hashmi, F.K., Saleem, F., 2019. A multicenter point prevalence survey of healthcare-associated infections in Pakistan: Findings and implications. Am. J. Infect. Control 47, 421–424. doi:10.1016/j.ajic.2018.09.025

Salje, H., Tran Kiem, C., Lefrancq, N., Courtejoie, N., Bosetti, P., Paireau, J., Andronico, A., Hozé, N., Richet, J., Dubost, C.-L., Le Strat, Y., Lessler, J., Levy-Bruhl, D., Fontanet, A., Opatowski, L., Boelle, P.-Y., Cauchemez, S., 2020. Estimating the burden of SARS-CoV-2 in France. Science 369, 208–211. doi:10.1126/science.abc3517

Saltelli, A., Tarantola, S., Campolongo, F., 2000. Sensitivity Analysis as an Ingredient of Modeling. Stat Sci 15, 377–395.

Sanchez, G.V., Biedron, C., Fink, L.R., Hatfield, K.M., Polistico, J.M.F., Meyer, M.P., Noe, R.S., Copen, C.E., Lyons, A.K., Gonzalez, G., Kiama, K., Lebednick, M., Czander, B.K., Agbonze, A., Surma, A.R., Sandhu, A., Mika, V.H., Prentiss, T.,

Zervos, J., Dalal, D.A., Vasquez, A.M., Reddy, S.C., Jernigan, J., Kilgore, P.E., Zervos, M.J., Chopra, T., Bezold, C.P., Rehman, N.K., 2020. Initial and Repeated Point Prevalence Surveys to Inform SARS-CoV-2 Infection Prevention in 26 Skilled Nursing Facilities - Detroit, Michigan, March-May 2020. MMWR Morb. Mortal. Wkly. Rep. 69, 882–886. doi:10.15585/mmwr.mm6927e1

Sánchez-Romero, M.A., Casadesús, J., 2014. Contribution of phenotypic heterogeneity to adaptive antibiotic resistance. Proc. Natl. Acad. Sci. USA 111, 355–360. doi:10.1073/pnas.1316084111

Sandegren, L., Andersson, D.I., 2009. Bacterial gene amplification: implications for the evolution of antibiotic resistance. Nat. Rev. Microbiol. 7, 578–588. doi:10.1038/nrmicro2174

Santé publique France, 2021a. e-SIN: signalement externe des infections nosocomiales [WWW Document]. URL https://www.santepubliquefrance.fr/maladies-et-traumatismes/infections-associees-aux-soins-et-resistance-aux-antibiotiques/infections-associees-aux-soins/articles/e-sin-signalement-externe-des-infections-nosocomiales (accessed 8.30.21).

Santé publique France, 2021b. Coronavirus : chiffres clés et évolution de la COVID-19 en France et dans le Monde [WWW Document]. URL https://www.santepubliquefrance.fr/dossiers/coronavirus-covid-19/coronavirus-chiffres-cles-et-evolution-de-la-covid-19-en-france-et-dans-le-monde (accessed 8.12.21).

Satterfield, J., Miesner, A.R., Percival, K.M., 2020. The role of education in antimicrobial stewardship. J. Hosp. Infect. 105, 130–141. doi:10.1016/j.jhin.2020.03.028

Scanvic, A., Denic, L., Gaillon, S., Giry, P., Andremont, A., Lucet, J.C., 2001. Duration of colonization by methicillin-resistant Staphylococcus aureus after hospital discharge and risk factors for prolonged carriage. Clin. Infect. Dis. 32, 1393–1398. doi:10.1086/320151

Schrader, S.M., Vaubourgeix, J., Nathan, C., 2020. Biology of antimicrobial resistance and approaches to combat it. Sci. Transl. Med. 12. doi:10.1126/scitranslmed.aaz6992

Schreiber, P.W., Sax, H., Wolfensberger, A., Clack, L., Kuster, S.P., Swissnoso, 2018. The preventable proportion of healthcare-associated infections 2005-2016: Systematic review and meta-analysis. Infect. Control Hosp. Epidemiol. 39, 1277–1295. doi:10.1017/ice.2018.183

Schwaber, M.J., Carmeli, Y., 2007. Mortality and delay in effective therapy associated with extended-spectrum beta-lactamase production in Enterobacteriaceae bacteraemia: a systematic review and meta-analysis. J. Antimicrob. Chemother. 60, 913–920. doi:10.1093/jac/dkm318

Scire, J., Hozé, N., Uecker, H., 2019. Aggressive or moderate drug therapy for infectious diseases? Trade-offs between different treatment goals at the individual and population levels. PLoS Comput. Biol. 15, e1007223. doi:10.1371/journal.pcbi.1007223

See, I., Paul, P., Slayton, R.B., Steele, M.K., Stuckey, M.J., Duca, L., Srinivasan, A., Stone, N., Jernigan, J.A., Reddy, S.C., 2021. Modeling effectiveness of testing strategies to prevent COVID-19 in nursing homes -United States, 2020. Clin. Infect. Dis. doi:10.1093/cid/ciab110

Seto, W.H., Conly, J.M., Pessoa-Silva, C.L., Malik, M., Eremin, S., 2013. Infection prevention and control measures for acute respiratory infections in healthcare settings: an update. East Mediterr Health J 19 Suppl 1, S39-47. doi:10.26719/2013.19.supp1.S39

Shao, L., Yao, B., Yang, J., Li, X., Ye, K., Zhang, Y., Wang, C., 2020. Characterization of a multidrug-resistant Klebsiella pneumoniae ST3330 clone responsible for a nosocomial outbreak in a neonatal intensive care unit. Ann. Palliat. Med. 9, 1092–1102. doi:10.21037/apm-20-958

Shapiro, J.T., Leboucher, G., Myard-Dury, A.-F., Girardo, P., Luzzati, A., Mary, M., Sauzon, J.-F., Lafay, B., Dauwalder, O., Laurent, F., Lina, G., Chidiac, C., Couray-Targe, S., Vandenesch, F., Flandrois, J.-P., Rasigade, J.-P., 2020. Metapopulation ecology links antibiotic resistance, consumption, and patient transfers in a network of hospital wards. Elife 9. doi:10.7554/eLife.54795

Shaw, L.P., Bassam, H., Barnes, C.P., Walker, A.S., Klein, N., Balloux, F., 2019. Modelling microbiome recovery after antibiotics using a stability landscape framework. ISME J. 13, 1845–1856. doi:10.1038/s41396-019-0392-1

Shears, P., O'Dempsey, T.J.D., 2015. Ebola virus disease in Africa: epidemiology and nosocomial transmission. J. Hosp. Infect. 90,

1–9. doi:10.1016/j.jhin.2015.01.002

Shen, G.-H., Tsao, T.C.-Y., Kao, S.-J., Lee, J.-J., Chen, Y.-H., Hsieh, W.-C., Hsu, G.-J., Hsu, Y.-T., Huang, C.-T., Lau, Y.-J., Tsao, S.-M., Hsueh, P.-R., 2012. Does empirical treatment of community-acquired pneumonia with fluoroquinolones delay tuberculosis treatment and result in fluoroquinolone resistance in Mycobacterium tuberculosis? Controversies and solutions. Int. J. Antimicrob. Agents 39, 201–205. doi:10.1016/j.ijantimicag.2011.11.014

Shen, N.T., Maw, A., Tmanova, L.L., Pino, A., Ancy, K., Crawford, C.V., Simon, M.S., Evans, A.T., 2017. Timely Use of Probiotics in Hospitalized Adults Prevents Clostridium difficile Infection: A Systematic Review With Meta-Regression Analysis. Gastroenterology 152, 1889–1900.e9. doi:10.1053/j.gastro.2017.02.003

Shenoy, E.S., Paras, M.L., Noubary, F., Walensky, R.P., Hooper, D.C., 2014. Natural history of colonization with methicillin-resistant Staphylococcus aureus (MRSA) and vancomycin-resistant Enterococcus (VRE): a systematic review. BMC Infect. Dis. 14, 177. doi:10.1186/1471-2334-14-177

Shiell, A., Donaldson, C., Mitton, C., Currie, G., 2002. Health economic evaluation. J. Epidemiol. Community Health 56, 85–88. doi:10.1136/jech.56.2.85

Sickbert-Bennett, E.E., DiBiase, L.M., Willis, T.M.S., Wolak, E.S., Weber, D.J., Rutala, W.A., 2016. Reduction of Healthcare-Associated Infections by Exceeding High Compliance with Hand Hygiene Practices. Emerging Infect. Dis. 22, 1628–1630. doi:10.3201/eid2209.151440

Simor, A.E., Yake, S.L., Tsimidis, K., 1993. Infection due to Clostridium difficile among elderly residents of a long-term-care facility. Clin. Infect. Dis. 17, 672–678. doi:10.1093/clinids/17.4.672

Siow, W.T., Tang, S.H., Agrawal, R.V., Tan, A.Y.H., See, K.C., 2020. Essential ICU drug shortages for COVID-19: what can frontline clinicians do? Crit. Care 24, 260. doi:10.1186/s13054-020-02971-x

Smith, D.R.M., Duval, A., Zahar, J.R., Opatowski, L., Temime, L., 2020. Bringing COVID-19 home for Christmas: a need for enhanced testing in healthcare institutions after the holidays. medRxiv. doi:10.1101/2020.12.18.20248460

Smith, D.R.M., Opatowski, L., 2021. COVID-19 containment measures and incidence of invasive bacterial disease. Lancet Digit. Health 3, e331–e332. doi:10.1016/S2589-7500(21)00085-6

Smith, D.R.M., Pouwels, K.B., Hopkins, S., Naylor, N.R., Smieszek, T., Robotham, J.V., 2019. Epidemiology and health-economic burden of urinary-catheter-associated infection in English NHS hospitals: a probabilistic modelling study. J. Hosp. Infect. 103, 44–54. doi:10.1016/j.jhin.2019.04.010

Søgaard, M., Nørgaard, M., Dethlefsen, C., Schønheyder, H.C., 2011. Temporal changes in the incidence and 30-day mortality associated with bacteremia in hospitalized patients from 1992 through 2006: a population-based cohort study. Clin. Infect. Dis. 52, 61–69. doi:10.1093/cid/ciq069

Sorbara, M.T., Pamer, E.G., 2019. Interbacterial mechanisms of colonization resistance and the strategies pathogens use to overcome them. Mucosal Immunol. 12, 1–9. doi:10.1038/s41385-018-0053-0

Søreide, K., Hallet, J., Matthews, J.B., Schnitzbauer, A.A., Line, P.D., Lai, P.B.S., Otero, J., Callegaro, D., Warner, S.G., Baxter, N.N., Teh, C.S.C., Ng-Kamstra, J., Meara, J.G., Hagander, L., Lorenzon, L., 2020. Immediate and long-term impact of the COVID-19 pandemic on delivery of surgical services. Br. J. Surg. 107, 1250–1261. doi:10.1002/bjs.11670

Spackova, M., Altmann, D., Eckmanns, T., Koch, J., Krause, G., 2010. High level of gastrointestinal nosocomial infections in the german surveillance system, 2002-2008. Infect. Control Hosp. Epidemiol. 31, 1273–1278. doi:10.1086/657133

Spicknall, I.H., Foxman, B., Marrs, C.F., Eisenberg, J.N.S., 2013. A modeling framework for the evolution and spread of antibiotic resistance: literature review and model categorization. Am. J. Epidemiol. 178, 508–520. doi:10.1093/aje/kwt017

Stearne, L.E.T., Goessens, W.H.F., Mouton, J.W., Gyssens, I.C., 2007. Effect of dosing and dosing frequency on the efficacy of ceftizoxime and the emergence of ceftizoxime resistance during the early development of murine abscesses caused by Bacteroides fragilis and Enterobacter cloacae mixed infection. Antimicrob. Agents Chemother. 51, 3605–3611. doi:10.1128/AAC.01486-06

Stecher, B., Maier, L., Hardt, W.-D., 2013. “Blooming” in the gut: how dysbiosis might contribute to pathogen evolution. Nat. Rev. Microbiol. 11, 277–284. doi:10.1038/nrmicro2989

Stein, R.R., Bucci, V., Toussaint, N.C., Buffie, C.G., Rätsch, G., Pamer, E.G., Sander, C., Xavier, J.B., 2013. Ecological modeling from time-series inference: insight into dynamics and stability of intestinal microbiota. PLoS Comput. Biol. 9, e1003388.

doi:10.1371/journal.pcbi.1003388

Stevenson, M., Metry, A., Messenger, M., 2021. Modelling of hypothetical SARS-CoV-2 point of care tests for routine testing in residential care homes: rapid cost-effectiveness analysis. Health Technol. Assess. 25, 1–74. doi:10.3310/hta25390

Stewart, S., Robertson, C., Kennedy, S., Kavanagh, K., Haahr, L., Manoukian, S., Mason, H., Dancer, S., Cook, B., Reilly, J., 2021a. Personalized infection prevention and control: identifying patients at risk of healthcare-associated infection. J. Hosp. Infect. 114, 32–42. doi:10.1016/j.jhin.2021.03.032

Stewart, S., Robertson, C., Pan, J., Kennedy, S., Dancer, S., Haahr, L., Manoukian, S., Mason, H., Kavanagh, K., Cook, B., Reilly, J., 2021b. Epidemiology of healthcare-associated infection reported from a hospital-wide incidence study: considerations for infection prevention and control planning. J. Hosp. Infect. 114, 10–22. doi:10.1016/j.jhin.2021.03.031

Stewart, S., Robertson, C., Pan, J., Kennedy, S., Haahr, L., Manoukian, S., Mason, H., Kavanagh, K., Graves, N., Dancer, S.J., Cook, B., Reilly, J., 2021c. Impact of healthcare-associated infection on length of stay. J. Hosp. Infect. 114, 23–31. doi:10.1016/j.jhin.2021.02.026

Stöß, C., Steffani, M., Kohlhaw, K., Rudroff, C., Staib, L., Hartmann, D., Friess, H., Müller, M.W., 2020. The COVID-19 pandemic: impact on surgical departments of non-university hospitals. BMC Surg 20, 313. doi:10.1186/s12893-020-00970-x

Suetens, C., Hopkins, S., Kolman, J., Högberg, L.D., 2013. Point prevalence survey of healthcare-associated infections and antimicrobial use in European acute care hospitals 2011-2012. ECDC.

Suetens, C., Latour, K., Kärki, T., Ricchizzi, E., Kinross, P., Moro, M.L., Jans, B., Hopkins, S., Hansen, S., Lyytikäinen, O., Reilly, J., Deptula, A., Zingg, W., Plachouras, D., Monnet, D.L., The Healthcare-Associated Infections Prevalence Study Group, 2018. Prevalence of healthcare-associated infections, estimated incidence and composite antimicrobial resistance index in acute care hospitals and long-term care facilities: results from two European point prevalence surveys, 2016 to 2017. Euro Surveill. 23. doi:10.2807/1560-7917.ES.2018.23.46.1800516

Sui, W., Zhou, H., Du, P., Wang, L., Qin, T., Wang, M., Ren, H., Huang, Y., Hou, J., Chen, C., Lu, X., 2018. Whole genome sequence revealed the fine transmission map of carbapenem-resistant Klebsiella pneumonia isolates within a nosocomial outbreak. Antimicrob. Resist. Infect. Control 7, 70. doi:10.1186/s13756-018-0363-8

Sukhrie, F.H.A., Teunis, P., Vennema, H., Copra, C., Thijs Beersma, M.F.C., Bogerman, J., Koopmans, M., 2012. Nosocomial transmission of norovirus is mainly caused by symptomatic cases. Clin. Infect. Dis. 54, 931–937. doi:10.1093/cid/cir971

Suleyman, G., Alangaden, G.J., 2016. Nosocomial fungal infections: epidemiology, infection control, and prevention. Infect Dis Clin North Am 30, 1023–1052. doi:10.1016/j.idc.2016.07.008

Sun, H., Lu, M., Chen, S., Cheng, Z., Xiong, Y., Wang, X., 2020. Nosocomial SARS-CoV-2 infection among nurses in Wuhan at a single centre. J. Infect. 80, e41–e42. doi:10.1016/j.jinf.2020.03.036

Sun, L., Klein, E.Y., Laxminarayan, R., 2012. Seasonality and temporal correlation between community antibiotic use and resistance in the United States. Clin. Infect. Dis. 55, 687–694. doi:10.1093/cid/cis509

Swinnen, J., McDermott, J., 2020. Covid-19 and global food security. EuroChoices. doi:10.1111/1746-692X.12288

Tacconelli, E., Carrara, E., Savoldi, A., Harbarth, S., Mendelson, M., Monnet, D.L., Pulcini, C., Kahlmeter, G., Kluytmans, J., Carmeli, Y., Ouellette, M., Outterson, K., Patel, J., Cavaleri, M., Cox, E.M., Houchens, C.R., Grayson, M.L., Hansen, P., Singh, N., Theuretzbacher, U., Magrini, N., WHO Pathogens Priority List Working Group, 2018. Discovery, research, and development of new antibiotics: the WHO priority list of antibiotic-resistant bacteria and tuberculosis. Lancet Infect. Dis. 18, 318–327. doi:10.1016/S1473-3099(17)30753-3

Tam, V.H., Louie, A., Deziel, M.R., Liu, W., Drusano, G.L., 2007. The relationship between quinolone exposures and resistance amplification is characterized by an inverted U: a new paradigm for optimizing pharmacodynamics to counterselect resistance. Antimicrob. Agents Chemother. 51, 744–747. doi:10.1128/AAC.00334-06

Tam, V.H., Louie, A., Deziel, M.R., Liu, W., Leary, R., Drusano, G.L., 2005a. Bacterial-population responses to drug-selective pressure: examination of garenoxacin's effect on Pseudomonas aeruginosa. J. Infect. Dis. 192, 420–428. doi:10.1086/430611

Tam, V.H., Schilling, A.N., Neshat, S., Poole, K., Melnick, D.A., Coyle, E.A., 2005b. Optimization of meropenem minimum concentration/MIC ratio to suppress in vitro resistance of Pseudomonas aeruginosa. Antimicrob. Agents Chemother. 49, 4920–4927. doi:10.1128/AAC.49.12.4920-4927.2005

Tamma, P.D., Avdic, E., Keenan, J.F., Zhao, Y., Anand, G., Cooper, J., Dezube, R., Hsu, S., Cosgrove, S.E., 2017. What is the more effective antibiotic stewardship intervention: preprescription authorization or postprescription review with feedback? Clin. Infect. Dis. 64, 537–543. doi:10.1093/cid/ciw780

Tan, C., Vermeulen, M., Wang, X., Zvonar, R., Garber, G., Daneman, N., 2017. Variability in antibiotic use across Ontario acute care hospitals. J. Antimicrob. Chemother. 72, 554–563. doi:10.1093/jac/dkw454

Tängdén, T., Adler, M., Cars, O., Sandegren, L., Löwdin, E., 2013. Frequent emergence of porin-deficient subpopulations with reduced carbapenem susceptibility in ESBL-producing Escherichia coli during exposure to ertapenem in an in vitro pharmacokinetic model. J. Antimicrob. Chemother. 68, 1319–1326. doi:10.1093/jac/dkt044

Tartari, E., Abbas, M., Pires, D., de Kraker, M.E.A., Pittet, D., 2017. World Health Organization SAVE LIVES: Clean Your Hands global campaign-'Fight antibiotic resistance-it's in your hands'. Clin. Microbiol. Infect. 23, 596–598. doi:10.1016/j.cmi.2017.04.021

Täufer, M., 2020. Rapid, large-scale, and effective detection of COVID-19 via non-adaptive testing. J. Theor. Biol. 506, 110450. doi:10.1016/j.jtbi.2020.110450

Tedijanto, C., Olesen, S.W., Grad, Y.H., Lipsitch, M., 2018. Estimating the proportion of bystander selection for antibiotic resistance among potentially pathogenic bacterial flora. Proc. Natl. Acad. Sci. USA 115, E11988–E11995. doi:10.1073/pnas.1810840115

Teesing, G.R., Erasmus, V., Nieboer, D., Petrignani, M., Koopmans, M.P.G., Vos, M.C., Verduijn-Leenman, A., Schols, J.M.G.A., Richardus, J.H., Voeten, H.A.C.M., 2020. Increased hand hygiene compliance in nursing homes after a multimodal intervention: A cluster randomized controlled trial (HANDSOME). Infect. Control Hosp. Epidemiol. 41, 1169–1177. doi:10.1017/ice.2020.319

Temime, L., Gustin, M.-P., Duval, A., Buetti, N., Crépey, P., Guillemot, D., Thiébaut, R., Vanhems, P., Zahar, J.-R., Smith, D.R.M., Opatowski, L., 2021. A conceptual discussion about the basic reproduction number of severe acute respiratory syndrome coronavirus 2 in healthcare settings. Clin. Infect. Dis. 72, 141–143. doi:10.1093/cid/ciaa682

Tepekule, B., Abel Zur Wiesch, P., Kouyos, R.D., Bonhoeffer, S., 2019. Quantifying the impact of treatment history on plasmid-mediated resistance evolution in human gut microbiota. Proc. Natl. Acad. Sci. USA. doi:10.1073/pnas.1912188116

Tepekule, B., Uecker, H., Derungs, I., Frenoy, A., Bonhoeffer, S., 2017. Modeling antibiotic treatment in hospitals: A systematic approach shows benefits of combination therapy over cycling, mixing, and mono-drug therapies. PLoS Comput. Biol. 13, e1005745. doi:10.1371/journal.pcbi.1005745

Thacker, S.B., Parrish, R.G., Trowbridge, F.L., 1988. A method for evaluating systems of epidemiological surveillance. World Health Stat. Q. 41, 11–18.

The Royal Society, 2020. Reproduction number (R) and growth rate (r) of the COVID-19 epidemic in the UK: methods of estimation, data sources, causes of heterogeneity, and use as a guide in policy formulation. The Royal Society.

Theuretzbacher, U., Outterson, K., Engel, A., Karlén, A., 2020. The global preclinical antibacterial pipeline. Nat. Rev. Microbiol. 18, 275–285. doi:10.1038/s41579-019-0288-0

Thom, K.A., Tamma, P.D., Harris, A.D., Dzintars, K., Morgan, D.J., Li, S., Pineles, L., Srinivasan, A., Avdic, E., Cosgrove, S.E., 2019. Impact of a Prescriber-driven Antibiotic Time-out on Antibiotic Use in Hospitalized Patients. Clin. Infect. Dis. 68, 1581–1584. doi:10.1093/cid/ciy852

Tindale, L.C., Stockdale, J.E., Coombe, M., Garlock, E.S., Lau, W.Y.V., Saraswat, M., Zhang, L., Chen, D., Wallinga, J., Colijn, C., 2020. Evidence for transmission of COVID-19 prior to symptom onset. Elife 9. doi:10.7554/eLife.57149

Tober-Lau, P., Schwarz, T., Hillus, D., Spieckermann, J., Helbig, E.T., Lippert, L.J., Thibeault, C., Koch, W., Bergfeld, L., Niemeyer, D., Mühlemann, B., Conrad, C., Kasper, S., Münn, F., Kunitz, F., Jones, T.C., Suttorp, N., Drosten, C., Sander, L.E., Kurth, F., Corman, V.M., 2021. Outbreak of SARS-CoV-2 B.1.1.7 Lineage after Vaccination in Long-Term Care Facility, Germany, February-March 2021. Emerging Infect. Dis. 27, 2169–2173. doi:10.3201/eid2708.210887

Torjesen, I., 2021. Covid-19: How the UK is using lateral flow tests in the pandemic. BMJ 372, n287. doi:10.1136/bmj.n287

Touat, M., Opatowski, M., Brun-Buisson, C., Cosker, K., Guillemot, D., Salomon, J., Tuppin, P., de Lagasnerie, G., Watier, L., 2019. A Payer Perspective of the Hospital Inpatient Additional Care Costs of Antimicrobial Resistance in France: A Matched Case-Control Study. Appl. Health Econ. Health Policy 17, 381–389. doi:10.1007/s40258-018-0451-1

Trottein, F., Sokol, H., 2020. Potential Causes and Consequences of Gastrointestinal Disorders during a SARS-CoV-2 Infection. Cell Rep. 32, 107915. doi:10.1016/j.celrep.2020.107915

Tulloch, J.S.P., Micocci, M., Buckle, P., Lawrenson, K., Kierkegaard, P., McLister, A., Gordon, A.L., García-Fiñana, M., Peddie, S., Ashton, M., Buchan, I., Parvulescu, P., 2021. Enhanced lateral flow testing strategies in care homes are associated with poor adherence and were insufficient to prevent COVID-19 outbreaks: Results from a mixed methods implementation study. Age Ageing. doi:10.1093/ageing/afab162

Ubukata, K., Konno, M., Fujii, R., 1975. Transduction of drug resistance to tetracycline, chloramphenicol, macrolides, lincomycin and clindamycin with phages induced from Streptococcus pyogenes. J Antibiot 28, 681–688. doi:10.7164/antibiotics.28.681

van Bunnik, B.A.D., Woolhouse, M.E.J., 2017. Modelling the impact of curtailing antibiotic usage in food animals on antibiotic resistance in humans. R. Soc. Open Sci. 4, 161067. doi:10.1098/rsos.161067

van den Driessche, P., 2017. Reproduction numbers of infectious disease models. Infect. Dis. Model. 2, 288–303. doi:10.1016/j.idm.2017.06.002

van Doremalen, N., Bushmaker, T., Morris, D.H., Holbrook, M.G., Gamble, A., Williamson, B.N., Tamin, A., Harcourt, J.L., Thornburg, N.J., Gerber, S.I., Lloyd-Smith, J.O., de Wit, E., Munster, V.J., 2020. Aerosol and surface stability of SARS-CoV-2 as compared with SARS-CoV-1. N. Engl. J. Med. 382, 1564–1567. doi:10.1056/NEJMc2004973

van Kleef, E., Deeny, S.R., Jit, M., Cookson, B., Goldenberg, S.D., Edmunds, W.J., Robotham, J.V., 2016. The projected effectiveness of Clostridium difficile vaccination as part of an integrated infection control strategy. Vaccine 34, 5562–5570. doi:10.1016/j.vaccine.2016.09.046

van Kleef, E., Robotham, J.V., Jit, M., Deeny, S.R., Edmunds, W.J., 2013. Modelling the transmission of healthcare associated infections: a systematic review. BMC Infect. Dis. 13, 294. doi:10.1186/1471-2334-13-294

Vanhems, P., Barrat, A., Cattuto, C., Pinton, J.-F., Khanafer, N., Régis, C., Kim, B., Comte, B., Voirin, N., 2013. Estimating potential infection transmission routes in hospital wards using wearable proximity sensors. PLoS One 8, e73970. doi:10.1371/journal.pone.0073970

Vanhems, P., Bénet, T., Munier-Marion, E., 2016. Nosocomial influenza: encouraging insights and future challenges. Curr Opin Infect Dis 29, 366–372. doi:10.1097/QCO.0000000000000287

Vanhems, P., Saadatian-Elahi, M., Chuzeville, M., Marion, E., Favrelle, L., Hilliquin, D., Martin-Gaujard, G., Gourmelon, R., Noaillon, M., Khanafer, N., COVID-Outcomes-HCL Consortium, 2020. Rapid nosocomial spread of SARS-CoV-2 in a French geriatric unit. Infect. Control Hosp. Epidemiol. 41, 866–867. doi:10.1017/ice.2020.99

VanInsberghe, D., Elsherbini, J.A., Varian, B., Poutahidis, T., Erdman, S., Polz, M.F., 2020. Diarrhoeal events can trigger long-term Clostridium difficile colonization with recurrent blooms. Nat. Microbiol. 5, 642–650. doi:10.1038/s41564-020-0668-2

Vanker, A., McGeer, A., O'Byrne, G., Snyder, E.C.R., Salisbury, D.A., Guthrie, J.L., Patel, S.N., Gubbay, J.B., Morgan, M., 2021. Adverse Outcomes Associated with SARS-CoV-2 variant B.1.351 Infection in Vaccinated Residents of a Long Term Care Home, Ontario, Canada. Clin. Infect. Dis. doi:10.1093/cid/ciab523

Velayati, A.A., Masjedi, M.R., Farnia, P., Tabarsi, P., Ghanavi, J., Ziazarifi, A.H., Hoffner, S.E., 2009. Emergence of new forms of totally drug-resistant tuberculosis bacilli: super extensively drug-resistant tuberculosis or totally drug-resistant strains in iran. Chest 136, 420–425. doi:10.1378/chest.08-2427

Venturelli, O.S., Carr, A.C., Fisher, G., Hsu, R.H., Lau, R., Bowen, B.P., Hromada, S., Northen, T., Arkin, A.P., 2018. Deciphering microbial interactions in synthetic human gut microbiome communities. Mol. Syst. Biol. 14, e8157. doi:10.15252/msb.20178157

Versporten, A., Zarb, P., Caniaux, I., Gros, M.-F., Drapier, N., Miller, M., Jarlier, V., Nathwani, D., Goossens, H., Global-PPS network, 2018. Antimicrobial consumption and resistance in adult hospital inpatients in 53 countries: results of an internet-based global point prevalence survey. Lancet Glob. Health 6, e619–e629. doi:10.1016/S2214-109X(18)30186-4

Vidal-Navarro, L., Pfeiffer, C., Bouziges, N., Sotto, A., Lavigne, J.-P., 2010. Faecal carriage of multidrug-resistant Gram-negative bacilli during a non-outbreak situation in a French university hospital. J. Antimicrob. Chemother. 65, 2455–2458. doi:10.1093/jac/dkq333

Vilches, T.N., Nourbakhsh, S., Zhang, K., Juden-Kelly, L., Cipriano, L.E., Langley, J.M., Sah, P., Galvani, A.P., Moghadas, S.M.,

2021. Multifaceted strategies for the control of COVID-19 outbreaks in long-term care facilities in Ontario, Canada. Prev. Med. 148, 106564. doi:10.1016/j.ypmed.2021.106564

Vincent, J.-L., Rello, J., Marshall, J., Silva, E., Anzueto, A., Martin, C.D., Moreno, R., Lipman, J., Gomersall, C., Sakr, Y., Reinhart, K., EPIC II Group of Investigators, 2009. International study of the prevalence and outcomes of infection in intensive care units. JAMA 302, 2323–2329. doi:10.1001/jama.2009.1754

Viscoli, C., 2016. Bloodstream Infections: The peak of the iceberg. Virulence 7, 248–251. doi:10.1080/21505594.2016.1152440

Vynnycky, E., 2010. An Introduction to Infectious Disease Modelling, Illustrated. ed. Oxford University Press, USA, New York.

Wachholz, P.A., Jacinto, A.F., 2020. Comment on: Coronavirus Disease 2019 in Geriatrics and Long-Term Care: The ABCDs of COVID-19. J. Am. Geriatr. Soc. 68, 1168–1169. doi:10.1111/jgs.16551

Wagenhäuser, I., Knies, K., Rauschenberger, V., Eisenmann, M., McDonogh, M., Petri, N., Andres, O., Flemming, S., Gawlik, M., Papsdorf, M., Taurines, R., Böhm, H., Forster, J., Weismann, D., Weißbrich, B., Dölken, L., Liese, J., Kurzai, O., Vogel, U., Krone, M., 2021. Clinical performance evaluation of SARS-CoV-2 rapid antigen testing in point of care usage in comparison to RT-qPCR. EBioMedicine 69, 103455. doi:10.1016/j.ebiom.2021.103455

Wang, J., Zhou, M., Liu, F., 2020. Reasons for healthcare workers becoming infected with novel coronavirus disease 2019 (COVID-19) in China. J. Hosp. Infect. 105, 100–101. doi:10.1016/j.jhin.2020.03.002

Wang, M., Yan, M., Xu, H., Liang, W., Kan, B., Zheng, B., Chen, H., Zheng, H., Xu, Y., Zhang, E., Wang, H., Ye, J., Li, G., Li, M., Cui, Z., Liu, Y.-F., Guo, R.-T., Liu, X.-N., Zhan, L.-H., Zhou, D.-H., Zhao, A., Hai, R., Yu, D., Guan, Y., Xu, J., 2005. SARS-CoV infection in a restaurant from palm civet. Emerging Infect. Dis. 11, 1860–1865. doi:10.3201/eid1112.041293

Wang, X., Zhou, Q., He, Y., Liu, L., Ma, X., Wei, X., Jiang, Nanchuan, Liang, L., Zheng, Y., Ma, L., Xu, Y., Yang, D., Zhang, J., Yang, B., Jiang, Ning, Deng, T., Zhai, B., Gao, Y., Liu, W., Bai, X., Pan, T., Wang, G., Chang, Y., Zhang, Z., Shi, H., Ma, W.-L., Gao, Z., 2020. Nosocomial outbreak of COVID-19 pneumonia in Wuhan, China. Eur. Respir. J. 55. doi:10.1183/13993003.00544-2020

Wang, Y.C., Lipsitch, M., 2006. Upgrading antibiotic use within a class: tradeoff between resistance and treatment success. Proc. Natl. Acad. Sci. USA 103, 9655–9660. doi:10.1073/pnas.0600636103

Webb, P., Bain, C., Page, A., 2016. Essential Epidemiology: An Introduction for Students and Health Professionals, 3rd ed. Cambridge University Press.

Weber, D.J., Rutala, W.A., 2001. Risks and prevention of nosocomial transmission of rare zoonotic diseases. Clin. Infect. Dis. 32, 446–456. doi:10.1086/318509

Wee, L.E., Conceicao, E.P., Sim, J.X.Y., Aung, M.K., Venkatachalam, I., 2020. Impact of infection prevention precautions on adenoviral infections during the COVID-19 pandemic: experience of a tertiary hospital in Singapore. Infect. Control Hosp. Epidemiol. 1–9. doi:10.1017/ice.2020.1365

Wee, L.E.I., Conceicao, E.P., Tan, J.Y., Magesparan, K.D., Amin, I.B.M., Ismail, B.B.S., Toh, H.X., Jin, P., Zhang, J., Wee, E.G.L., Ong, S.J.M., Lee, G.L.X., Wang, A.E.-M., How, M.K.B., Tan, K.Y., Lee, L.C., Phoon, P.C., Yang, Y., Aung, M.K., Sim, X.Y.J., Venkatachalam, I., Ling, M.L., 2021. Unintended consequences of infection prevention and control measures during COVID-19 pandemic. Am. J. Infect. Control 49, 469–477. doi:10.1016/j.ajic.2020.10.019

Wei, W.E., Li, Z., Chiew, C.J., Yong, S.E., Toh, M.P., Lee, V.J., 2020. Presymptomatic Transmission of SARS-CoV-2 - Singapore, January 23-March 16, 2020. MMWR Morb. Mortal. Wkly. Rep. 69, 411–415. doi:10.15585/mmwr.mm6914e1

Wei, Y., Yu, C., Zhao, T.X., Lin, T., Dawei, H.E., Wu, S., Wei, G.-H., 2020. The impact of the COVID-19 pandemic on pediatric operations: a retrospective study of Chinese children. Ital J Pediatr 46, 155. doi:10.1186/s13052-020-00915-3

Westra, E.R., Sünderhauf, D., Landsberger, M., Buckling, A., 2017. Mechanisms and consequences of diversity-generating immune strategies. Nat. Rev. Immunol. 17, 719–728. doi:10.1038/nri.2017.78

White, A.C., Atmar, R.L., Wilson, J., Cate, T.R., Stager, C.E., Greenberg, S.B., 1997. Effects of requiring prior authorization for selected antimicrobials: expenditures, susceptibilities, and clinical outcomes. Clin. Infect. Dis. 25, 230–239. doi:10.1086/514545

WHO Expert Committee on the Selection and Use of Essential Medicines, 2017. The Selection and Use of Essential Medicines 2017. World Health Organization.

Wikswo, M.E., Kambhampati, A., Shioda, K., Walsh, K.A., Bowen, A., Hall, A.J., Centers for Disease Control and Prevention

(CDC), 2015. Outbreaks of Acute Gastroenteritis Transmitted by Person-to-Person Contact, Environmental Contamination, and Unknown Modes of Transmission--United States, 2009-2013. MMWR Surveill Summ 64, 1–16. doi:10.15585/mmwr.mm6412a1

Wilder-Smith, A., Teleman, M.D., Heng, B.H., Earnest, A., Ling, A.E., Leo, Y.S., 2005. Asymptomatic SARS coronavirus infection among healthcare workers, Singapore. Emerging Infect. Dis. 11, 1142–1145. doi:10.3201/eid1107.041165

Wilkinson, J.E., Franzosa, E.A., Everett, C., Li, C., HCMPH researchers and trainees, HCMPH investigators, Hu, F.B., Wirth, D.F., Song, M., Chan, A.T., Rimm, E., Garrett, W.S., Huttenhower, C., 2021. A framework for microbiome science in public health. Nat. Med. 27, 766–774. doi:10.1038/s41591-021-01258-0

Willem, L., Verelst, F., Bilcke, J., Hens, N., Beutels, P., 2017. Lessons from a decade of individual-based models for infectious disease transmission: a systematic review (2006-2015). BMC Infect. Dis. 17, 612. doi:10.1186/s12879-017-2699-8

Williams, K.J., 2009. The introduction of "chemotherapy" using arsphenamine - the first magic bullet. J. R. Soc. Med. 102, 343–348. doi:10.1258/jrsm.2009.09k036

Wind, C.M., de Vries, E., Schim van der Loeff, M.F., van Rooijen, M.S., van Dam, A.P., Demczuk, W.H.B., Martin, I., de Vries, H.J.C., 2017. Decreased Azithromycin Susceptibility of Neisseria gonorrhoeae Isolates in Patients Recently Treated with Azithromycin. Clin. Infect. Dis. 65, 37–45. doi:10.1093/cid/cix249

Wisplinghoff, H., Bischoff, T., Tallent, S.M., Seifert, H., Wenzel, R.P., Edmond, M.B., 2004. Nosocomial bloodstream infections in US hospitals: analysis of 24,179 cases from a prospective nationwide surveillance study. Clin. Infect. Dis. 39, 309–317. doi:10.1086/421946

Wong, S.C., AuYeung, C.H.Y., Lam, G.K.M., Leung, E.Y.L., Chan, V.W.M., Yuen, K.Y., Cheng, V.C.C., 2020. Is it possible to achieve 100 percent hand hygiene compliance during the coronavirus disease 2019 (COVID-19) pandemic? J. Hosp. Infect. 105, 779–781. doi:10.1016/j.jhin.2020.05.016

Wong, S.-C., Lam, G.K.-M., AuYeung, C.H.-Y., Chan, V.W.-M., Wong, N.L.-D., So, S.Y.-C., Chen, J.H.-K., Hung, I.F.-N., Chan, J.F.-W., Yuen, K.-Y., Cheng, V.C.-C., 2021. Absence of nosocomial influenza and respiratory syncytial virus infection in the coronavirus disease 2019 (COVID-19) era: Implication of universal masking in hospitals. Infect. Control Hosp. Epidemiol. 42, 218–221. doi:10.1017/ice.2020.425

Woolhouse, M., Gowtage-Sequeria, S., Evans, B., 2005. T16: Quantitative analysis of the characteristics of emerging and re-emerging human pathogens. Office of Science and Innovation.

Woolhouse, M., Scott, F., Hudson, Z., Howey, R., Chase-Topping, M., 2012. Human viruses: discovery and emergence. Philos. Trans. R. Soc. Lond. B, Biol. Sci. 367, 2864–2871. doi:10.1098/rstb.2011.0354

World Health Organization, 2002. Prevention of hospital-acquired infections : a practical guide. World Health Organization.

World Health Organization, 2011. Report on the Burden of Endemic Health Care-Associated Infection Worldwide. World Health Organization.

World Health Organization, 2014. Evidence of hand hygiene to reduce transmission and infections by multi-drug resistant organisms in health-care settings. World Health Organization.

World Health Organization, 2015. Ebola Situation Report - 1 July 2015 [WWW Document]. URL https://apps.who.int/ebola/current-situation/ebola-situation-report-1-july-2015 (accessed 8.18.21).

World Health Organization, 2020a. WHO Statement regarding cluster of pneumonia cases in Wuhan, China [WWW Document]. URL https://www.who.int/china/news/detail/09-01-2020-who-statement-regarding-cluster-of-pneumonia-cases-in-wuhan-china (accessed 8.9.21).

World Health Organization, 2020b. Timeline of WHO's response to COVID-19 [WWW Document]. URL https://www.who.int/emergencies/diseases/novel-coronavirus-2019/interactive-timeline (accessed 8.9.21).

World Health Organization, 2020c. WHO statement on novel coronavirus in Thailand [WWW Document]. URL https://www.who.int/news/item/13-01-2020-who-statement-on-novel-coronavirus-in-thailand (accessed 8.9.21).

World Health Organization, 2020d. IHR Emergency Committee on Novel Coronavirus (2019-nCoV) [WWW Document]. URL https://www.who.int/director-general/speeches/detail/who-director-general-s-statement-on-ihr-emergency-committee-on-novel-coronavirus-(2019-ncov) (accessed 8.9.21).

World Health Organization, 2020e. WHO Director-General's opening remarks at the media briefing on COVID-19 - 11 March 2020

[WWW Document]. URL https://www.who.int/director-general/speeches/detail/who-director-general-s-opening-remarks-at-the-media-briefing-on-covid-19---11-march-2020 (accessed 8.9.21).

World Health Organization, 2020f. Report of the WHO-China Joint Mission on Coronavirus Disease 2019 (COVID-19) [WWW Document]. URL https://www.who.int/publications/i/item/report-of-the-who-china-joint-mission-on-coronavirus-disease-2019-(covid-19) (accessed 8.10.21).

World Health Organization, 2020g. Preventing and managing COVID-19 across long-term care services: policy brief. World Health Organization, Geneva.

World Health Organization, 2020h. Diagnostic testing for SARS-CoV-2 (Interim Report No. WHO/2019-nCoV/laboratory/2020.6). World Health Organization.

World Health Organization, 2021a. MERS Situation Update | June 2021 [WWW Document]. URL http://www.emro.who.int/health-topics/mers-cov/mers-outbreaks.html (accessed 8.19.21).

World Health Organization, 2021b. Antimicrobial stewardship interventions: a practical guide. WHO Regional Office for Europe.

World Health Organization Regional Office for Europe, 2020. Health emergencies - 2019-nCoV outbreak: first cases confirmed in Europe [WWW Document]. URL https://www.euro.who.int/en/health-topics/health-emergencies/pages/news/news/2020/01/2019-ncov-outbreak-first-cases-confirmed-in-europe (accessed 8.9.21).

Wu, J., Dhingra, R., Gambhir, M., Remais, J.V., 2013. Sensitivity analysis of infectious disease models: methods, advances and their application. J. R. Soc. Interface 10, 20121018. doi:10.1098/rsif.2012.1018

Wu, Z., McGoogan, J.M., 2020. Characteristics of and Important Lessons From the Coronavirus Disease 2019 (COVID-19) Outbreak in China: Summary of a Report of 72 314 Cases From the Chinese Center for Disease Control and Prevention. JAMA 323, 1239–1242. doi:10.1001/jama.2020.2648

Würstle, S., Spinner, C.D., Voit, F., Hoffmann, D., Hering, S., Weidlich, S., Schneider, J., Zink, A., Treiber, M., Iakoubov, R., Schmid, R.M., Protzer, U., Erber, J., 2021. Self-sampling versus health care professional-guided swab collection for SARS-CoV-2 testing. Infection. doi:10.1007/s15010-021-01614-9

Xiao, X., van Hoek, A.J., Kenward, M.G., Melegaro, A., Jit, M., 2016. Clustering of contacts relevant to the spread of infectious disease. Epidemics 17, 1–9. doi:10.1016/j.epidem.2016.08.001

Yang, S.-C., Lin, C.-H., Aljuffali, I.A., Fang, J.-Y., 2017. Current pathogenic Escherichia coli foodborne outbreak cases and therapy development. Arch. Microbiol. 199, 811–825. doi:10.1007/s00203-017-1393-y

Yelin, I., Aharony, N., Tamar, E.S., Argoetti, A., Messer, E., Berenbaum, D., Shafran, E., Kuzli, A., Gandali, N., Shkedi, O., Hashimshony, T., Mandel-Gutfreund, Y., Halberthal, M., Geffen, Y., Szwarcwort-Cohen, M., Kishony, R., 2020. Evaluation of COVID-19 RT-qPCR Test in Multi sample Pools. Clin. Infect. Dis. 71, 2073–2078. doi:10.1093/cid/ciaa531

Yinka-Ogunleye, A., Aruna, O., Dalhat, M., Ogoina, D., McCollum, A., Disu, Y., Mamadu, I., Akinpelu, A., Ahmad, A., Burga, J., Ndoreraho, A., Nkunzimana, E., Manneh, L., Mohammed, A., Adeoye, O., Tom-Aba, D., Silenou, B., Ipadeola, O., Saleh, M., Adeyemo, A., Nwadiutor, I., Aworabhi, N., Uke, P., John, D., Wakama, P., Reynolds, M., Mauldin, M.R., Doty, J., Wilkins, K., Musa, J., Khalakdina, A., Adedeji, A., Mba, N., Ojo, O., Krause, G., Ihekweazu, C., CDC Monkeypox Outbreak Team, 2019. Outbreak of human monkeypox in Nigeria in 2017-18: a clinical and epidemiological report. Lancet Infect. Dis. 19, 872–879. doi:10.1016/S1473-3099(19)30294-4

Zaragoza, R., Vidal-Cortés, P., Aguilar, G., Borges, M., Diaz, E., Ferrer, R., Maseda, E., Nieto, M., Nuvials, F.X., Ramirez, P., Rodriguez, A., Soriano, C., Veganzones, J., Martín-Loeches, I., 2020. Update of the treatment of nosocomial pneumonia in the ICU. Crit. Care 24, 383. doi:10.1186/s13054-020-03091-2

Zellmer, C., Sater, M.R.A., Huntley, M.H., Osman, M., Olesen, S.W., Ramakrishna, B., 2021. Shiga Toxin-Producing Escherichia coli Transmission via Fecal Microbiota Transplant. Clin. Infect. Dis. 72, e876–e880. doi:10.1093/cid/ciaa1486

Zhang, J., Litvinova, M., Wang, W., Wang, Y., Deng, X., Chen, Xinghui, Li, M., Zheng, W., Yi, L., Chen, Xinhua, Wu, Q., Liang, Y., Wang, X., Yang, J., Sun, K., Longini, I.M., Halloran, M.E., Wu, P., Cowling, B.J., Merler, S., Viboud, C., Vespignani, A., Ajelli, M., Yu, H., 2020. Evolving epidemiology and transmission dynamics of coronavirus disease 2019 outside Hubei province, China: a descriptive and modelling study. Lancet Infect. Dis. 20, 793–802. doi:10.1016/S1473-3099(20)30230-9

Zhang, K., Shoukat, A., Crystal, W., Langley, J.M., Galvani, A.P., Moghadas, S.M., 2021. Routine saliva testing for the identification of silent coronavirus disease 2019 (COVID-19) in healthcare workers. Infect. Control Hosp. Epidemiol. 1–5.

doi:10.1017/ice.2020.1413

Zhang, M., Jiang, Z., Li, D., Jiang, D., Wu, Y., Ren, H., Peng, H., Lai, Y., 2015. Oral antibiotic treatment induces skin microbiota dysbiosis and influences wound healing. Microb. Ecol. 69, 415–421. doi:10.1007/s00248-014-0504-4

Zhang, Q., Lambert, G., Liao, D., Kim, H., Robin, K., Tung, C., Pourmand, N., Austin, R.H., 2011. Acceleration of emergence of bacterial antibiotic resistance in connected microenvironments. Science 333, 1764–1767. doi:10.1126/science.1208747

Zheng, Z., Peng, F., Xu, B., Zhao, J., Liu, H., Peng, J., Li, Q., Jiang, C., Zhou, Y., Liu, S., Ye, C., Zhang, P., Xing, Y., Guo, H., Tang, W., 2020. Risk factors of critical & mortal COVID-19 cases: A systematic literature review and meta-analysis. J. Infect. 81, e16–e25. doi:10.1016/j.jinf.2020.04.021

Zhou, F., Yu, T., Du, R., Fan, G., Liu, Y., Liu, Z., Xiang, J., Wang, Y., Song, B., Gu, X., Guan, L., Wei, Y., Li, H., Wu, X., Xu, J., Tu, S., Zhang, Y., Chen, H., Cao, B., 2020. Clinical course and risk factors for mortality of adult inpatients with COVID-19 in Wuhan, China: a retrospective cohort study. Lancet 395, 1054–1062. doi:10.1016/S0140-6736(20)30566-3

Zhou, Q., Gao, Y., Wang, Xingmei, Liu, R., Du, P., Wang, Xiaoqing, Zhang, X., Lu, S., Wang, Z., Shi, Q., Li, W., Ma, Y., Luo, X., Fukuoka, T., Ahn, H.S., Lee, M.S., Liu, E., Chen, Y., Luo, Z., Yang, K., COVID-19 Evidence and Recommendations Working Group, 2020. Nosocomial infections among patients with COVID-19, SARS and MERS: a rapid review and meta-analysis. Ann Transl Med 8, 629. doi:10.21037/atm-20-3324

Zhu, Y., Hu, L., Mei, Q., Cheng, J., Liu, Y., Ye, Y., Li, J., 2012. Testing the mutant selection window in rabbits infected with methicillin-resistant Staphylococcus aureus exposed to vancomycin. J. Antimicrob. Chemother. 67, 2700–2706. doi:10.1093/jac/dks280

Zimmermann-Kogadeeva, M., 2021. Quantifying host-microbiota interactions. Science 373, 173.2-173. doi:10.1126/science.abi9357

Zinner, S.H., Lubenko, I.Y., Gilbert, D., Simmons, K., Zhao, X., Drlica, K., Firsov, A.A., 2003. Emergence of resistant Streptococcus pneumoniae in an in vitro dynamic model that simulates moxifloxacin concentrations inside and outside the mutant selection window: related changes in susceptibility, resistance frequency and bacterial killing. J. Antimicrob. Chemother. 52, 616–622. doi:10.1093/jac/dkg401

zur Wiesch, P.A., Kouyos, R., Engelstädter, J., Regoes, R.R., Bonhoeffer, S., 2011. Population biological principles of drug-resistance evolution in infectious diseases. Lancet Infect. Dis. 11, 236–247. doi:10.1016/S1473-3099(10)70264-4